

Mahmud, Zobaer Al (2019) *Defining ligand binding modes of the orphan G protein-coupled receptor GPR84*. PhD thesis.

<https://theses.gla.ac.uk/74364/>

Copyright and moral rights for this work are retained by the author

A copy can be downloaded for personal non-commercial research or study, without prior permission or charge

This work cannot be reproduced or quoted extensively from without first obtaining permission in writing from the author

The content must not be changed in any way or sold commercially in any format or medium without the formal permission of the author

When referring to this work, full bibliographic details including the author, title, awarding institution and date of the thesis must be given

Enlighten: Theses

<https://theses.gla.ac.uk/>
research-enlighten@glasgow.ac.uk

Defining ligand binding modes of the orphan G protein-coupled receptor GPR84

Zobaer Al Mahmud

M.Pharm, B.Pharm (Hons)

A thesis submitted
in fulfilment of the requirements for the Degree of
Doctor of Philosophy

Institute of Molecular, Cell and Systems Biology
College of Medical, Veterinary & Life Sciences
University of Glasgow



University
of Glasgow | Institute of Molecular,
Cells & System Biology

July 2019

Abstract

Pro-inflammatory and pro-fibrotic G protein-coupled receptor 84 (GPR84), a member of the rhodopsin-like Class A GPCR family, recently has attracted interest as a potential drug target for chronic inflammation-associated diseases including ulcerative colitis, neuropathic pain, atherosclerosis and fibrosis-associated diseases including idiopathic pulmonary fibrosis. However, GPR84 still remains poorly characterized in terms of its signal transduction pathways and pathophysiological roles and is officially considered as ‘orphan’ receptor as the putative endogenous agonists MCFAs are weak activators of the receptor with a poorly defined mode of interaction with the receptor. The modes of ligand binding and mechanism(s) of action of the currently available pharmacological tool compounds are also very limited which have hindered the target validation process. Herein, the G protein coupling selectivity of GPR84, ligand-GPR84 interactions and modes of action of orthosteric and allosteric GPR84 ligands along with their orthologue selectivity were investigated in an attempt to characterize this enigmatic receptor. Employing a series of BRET-based GPR84 SPASM biosensors, GPR84 activation was found to couple to the $G_{\alpha_{i/o}}$ G protein family with preferential recruitment of $G_{\alpha_{i1/2}}$ and $G_{\alpha_{i3}}$ over G_{α_o} and G_{α_z} G proteins. Based on homology modelling and site-directed mutagenesis studies, integral roles of arginine 172 of extracellular loop 2 in orthosteric ligand recognition and functions were identified wherein this residue acted as the putative charge partner for the carboxylate of MCFAs or the hydrophilic head groups of embelin or embelin-like ligands. Homology modelling, mutational analysis and subsequent docking studies also suggested that phenylalanine 170^{EL2}, phenylalanine 335^{F6.51} and tryptophan 360^{7.43} might be associated with orthosteric ligand detection. 3,3'-diindolylmethane (DIM) and DIM analogue di(5,7-difluoro-1H-indole-3-yl)methane (PSB-16671) were found to bind to a site which is topographically distinct from the orthosteric site as both ligands retained their agonist functions upon mutation of all these residues to alanine where the activity of orthosteric agonists was either lost completely or reduced significantly. Functional studies with GPR84 antagonist compound-107 and radioligand binding studies with a chemically related radiolabelled antagonist, [³H]-G9543 suggested that this class of antagonists bind to a site which is

different from the orthosteric and allosteric binding sites, indicating three spatiotemporally distinct ligand binding sites within GPR84.

Antagonists but not agonists of GPR84 displays significant variation in pharmacology between human and mouse orthologues as evidenced from either loss of activity (compound-837) or markedly reduced potencies at mouse GPR84. GPR84 ligands display similar pharmacology in mouse monocyte-macrophage cell line RAW264.7 as those observed in transfected cells expressing mouse GPR84. DIM, analogue 3a (5,5'-dimethoxy-3,3'-diindolylmethane) and particularly PSB-16671 acted as highly effective positive allosteric modulators (PAM) of the function of orthosteric agonists through a mechanism that includes both affinity and efficacy modulation for embelin and C-10 or predominantly governed by affinity modulation with marginal effect on efficacy for full agonists including compound-1. These ligands display PAM activity in a 'probe-dependent' manner wherein the degree of affinity cooperativity tracks with the orthosteric agonist efficacy although little 'probe-dependence' was observed when net affinity/efficacy cooperativity was considered. DIM but not PSB-16671 showed significant variation in allosteric interactions with orthosteric agonists between human and mouse GPR84. Mathematical analysis of allosteric interactions showed that PSB-16671 binds human GPR84 with 360 and 5-fold higher affinity than decanoic acid and DIM, respectively while compound-1 displays 14-fold higher avidity than PSB-16671. The analysis also showed that the estimated binding affinities of these ligands for mouse GPR84 were equivalent to those observed for the human orthologue. In summary, the research studies presented herein provides new insights into ligand-GPR84 interactions and mode(s) of pharmacological actions of the GPR84 tool compounds which might be useful to accelerate structure-based drug design identifying further improved ligands or for translational studies assessing the therapeutic potential of this receptor.

Table of Contents

| | |
|---|-------|
| Abstract..... | ii |
| List of Tables..... | x |
| List of Figures..... | xi |
| List of Publications..... | xiv |
| Acknowledgement..... | xv |
| Author's Declaration..... | xvii |
| Abbreviations..... | xviii |
| 1 Introduction..... | 1 |
| 1.1 G protein coupled receptors (GPCRs) and drug development | 1 |
| 1.1.1 Brief overview of drug development approaches..... | 1 |
| 1.1.2 Role of GPCRs in therapeutic pharmacology | 3 |
| 1.1.3 Challenges in clinical exploitation of orphan or poorly characterized GPCRs | 5 |
| 1.1.4 GPCRs: structural features and classification | 6 |
| 1.2 Heterotrimeric G proteins..... | 11 |
| 1.3 GPCR-mediated signal transduction pathways | 12 |
| 1.3.1 G-protein dependent pathways..... | 12 |
| 1.3.2 G-protein independent pathways | 17 |
| 1.4 Pharmacology of GPCR ligands | 18 |
| 1.4.1 Pharmacology of orthosteric ligands..... | 18 |
| 1.4.2 Complex pharmacology of allosteric ligands: new opportunities and challenges in drug discovery | 21 |
| 1.5 Free fatty acid receptors (FFARs) as novel targets for drug development against inflammatory and metabolic disorders..... | 25 |
| 1.6 G protein coupled receptor 84 | 28 |
| 1.6.1 Discovery of GPR84 and its basic characteristics | 28 |
| 1.6.2 Tissue and cellular distribution of GPR84 expression | 29 |
| 1.6.3 Putative endogenous agonists of GPR84..... | 30 |
| 1.6.4 Natural product-derived agonists of GPR84: DIM and embelin..... | 34 |
| 1.6.5 Synthetic surrogate agonists of GPR84 | 35 |
| 1.6.6 Synthetic GPR84 antagonists..... | 38 |
| 1.7 GPR84-mediated signal transduction pathways | 40 |
| 1.7.1 G-protein dependent signaling | 40 |
| 1.7.2 G-protein-independent signaling | 43 |
| 1.8 Physiological functions and pathophysiological roles of GPR84 | 44 |
| 1.8.1 Immunostimulatory and pro-inflammatory activities mediated by GPR84 | 44 |
| 1.8.2 GPR84 is a potential novel target for drug development against chronic inflammation-associated diseases | 50 |

| | | |
|--------|--|----|
| 1.8.3 | Potential role of GPR84 in neuro-immune and neuro-inflammatory processes | 52 |
| 1.8.4 | Potential role of GPR84 in promoting insulin resistance under inflammatory conditions | 54 |
| 1.8.5 | GPR84 displays pro-fibrotic activity and represents a potential target for drug development against fibrosis-associated diseases | 56 |
| 1.8.6 | GPR84 regulates osteoclastogenesis and could be a potential drug target for bone-destruction related diseases | 58 |
| 1.8.7 | GPR84-B-catenin axis is associated with development and maintenance of acute myeloid leukemia | 61 |
| 1.9 | Aims and objectives of the project | 62 |
| 2 | Materials and methods | 65 |
| 2.1 | Pharmacological tool compounds | 65 |
| 2.2 | Molecular biology and cloning | 67 |
| 2.2.1 | Preparation of LB (Luria-Bertani) medium and LB agar plates..... | 67 |
| 2.2.2 | Preparation of competent bacteria | 68 |
| 2.2.3 | Transformation of competent cells with plasmid cDNA..... | 68 |
| 2.2.4 | Purification of plasmid DNA from bacterial culture | 69 |
| 2.2.5 | PCR based cloning | 70 |
| 2.2.6 | Site-directed mutagenesis..... | 74 |
| 2.2.7 | Plasmids and DNA constructs | 76 |
| 2.3. | Mammalian cell culture and maintenance | 82 |
| 2.3.1 | HEK293T cells | 82 |
| 2.3.2 | Flp-In™ T-REx™-293 cells | 83 |
| 2.3.3 | Flp-In™ T-REx™-293 stable cell lines expressing GPR84 receptor.... | 83 |
| 2.3.4 | RAW 264.7 cells | 83 |
| 2.3.5 | Thawing of cells | 84 |
| 2.3.6 | Passaging of cells | 84 |
| 2.3.7 | Cryopreservation of cells for long-term storage | 85 |
| 2.4. | Transient transfection..... | 85 |
| 2.4.1 | Transient transfection using PEI..... | 85 |
| 2.4.2 | Transient transfection using lipofectamine..... | 86 |
| 2.5 | Generation of Flp-In T-REx-293 cell lines inducibly expressing GPR84 receptor | 87 |
| 2.6 | Biochemical and functional pharmacological assays | 89 |
| 2.6.1 | Membrane preparations | 89 |
| 2.6.2 | Determination of membrane protein concentration | 90 |
| 2.6.3 | Sodium dodecyl sulphate-polyacrylamide gel electrophoresis (SDS-PAGE) 91 | |
| 2.6.3. | Immunoblotting or western blot | 92 |
| 2.6.5 | [³⁵ S]-GTPγS binding assay | 94 |

| | | |
|--------|---|-----|
| 2.6.6 | HTRF-based cAMP accumulation assay | 95 |
| 2.6.7 | Radioligand saturation binding assays | 97 |
| 2.6.8 | Bioluminescence resonance energy transfer (BRET) assay using SPASM sensor | 98 |
| 2.7. | Structural studies | 100 |
| 2.7.1 | Homology modelling..... | 100 |
| 2.7.2 | Ligand docking | 101 |
| 2.8. | Data analysis and curve fitting..... | 101 |
| 2.8.1 | Analysis of functional agonist and antagonist assays | 101 |
| 2.8.2 | Analysis of radioligand binding data | 102 |
| 2.8.3 | Analysis of ligand co-operativity and other allosteric parameters .. | 103 |
| 2.8.4 | Global Gaddum/Schild EC ₅₀ shift analysis..... | 103 |
| 2.8.5 | Statistical analysis..... | 104 |
| 3 | Investigation of G-protein Selectivity of GPR84 | 105 |
| 3.1. | Introduction..... | 105 |
| 3.2. | Results | 106 |
| 3.2.1. | Characterization of cell lines expressing GPR84 SPASM sensors.. | 106 |
| 3.2.2. | Validation of GPR84 SPASM sensors..... | 107 |
| 3.2.3. | DIM and embelin act as partial agonists and compound-1 and compound-51 act as super-agonists at the hGPR84-SPASM-Gα _{i1/2} sensor ... | 108 |
| 3.2.4. | GPR84 signals through Gα _{i/o} pathway | 110 |
| 3.2.5. | The coupling efficiency of interaction between human GPR84 and individual Gα _{i/o} G proteins | 113 |
| 3.2.6. | 6-OAU, compound-1 and TUG-1765 displayed greater maximal response than decanoic acid at the hGPR84-SpNG-Gα _{i1/2} sensor | 115 |
| 3.3. | Discussion | 116 |
| 3.3.1. | BRET based SPASM biosensors can be employed effectively for the study of GPR84-G protein interactions..... | 116 |
| 3.3.2. | BRET based GPR84 SPASM sensor is an effective strategy to investigate the relative intrinsic activity of GPR84 agonists | 120 |
| 4 | Investigation of modes of binding of ligands to human GPR84 | 122 |
| 4.1. | Introduction..... | 122 |
| 4.2. | Characterization of Flp-In TM T-REx TM - 293 cell lines expressing hGPR84- Gα _{i2} fusion proteins..... | 123 |
| 4.2.1. | Characterization of expression of hGPR84-G protein fusion constructs by Western blot analysis | 123 |
| 4.2.2. | Saturation binding study | 124 |
| 4.2.3. | Functional characterization of Flp-In TM T-REx TM - HEK 293 cell lines expressing FLAG-hGPR84-Gα _{i2} fusion proteins | 126 |
| 4.2.4. | Human GPR84 couples to PTX sensitive Gα _i protein | 128 |

| | | |
|--------|--|-----|
| 4.2.5. | The GPR84-G α_{i2} fusion protein approach enhances coupling efficiency between GPR84 and G α_i protein | 129 |
| 4.2.6. | GPR84 agonists displayed similar activity at the FLAG-hGPR84-G α_{i2} and FLAG-hGPR84-G α_{i2} C352I fusion protein | 132 |
| 4.2.7. | Functional characterization using the cAMP inhibition assay | 134 |
| 4.3. | Investigation of the mode of binding of ligands to hGPR84 | 135 |
| 4.3.1. | Assessment of expression levels of different mutants of hGPR84 | 139 |
| 4.3.2. | Arginine 172 of EL2 is a key molecular determinant of orthosteric ligand binding to hGPR84 | 142 |
| 4.3.3. | Embelin, compound-1 and 6-OAU share a common binding site with MCFAs | 145 |
| 4.3.4. | TUG-1765 and related molecules bind to the orthosteric pocket of hGPR84 | 146 |
| 4.3.5. | Phenylalanine 335 located in TMD VI might be associated with orthosteric ligand recognition | 149 |
| 4.3.6. | Role of Phenylalanine 170 of GPR84 in ligand recognition | 151 |
| 4.3.7. | Assessment of effects of mutation of phenylalanine 101 or tryptophan 360 to alanine on agonist functions of different GPR84 ligands | 154 |
| 4.3.8. | Potential docking poses of orthosteric agonists | 157 |
| 4.3.9. | GPR84 antagonist compound-107 binds to a site on GPR84 which is topographically distinct from the orthosteric and allosteric agonist binding sites | 160 |
| 4.4. | Discussion | 162 |
| 4.4.1. | Arginine 172 of EL2 is integral to orthosteric ligand recognition and functions | 163 |
| 4.4.2. | Phenylalanine 170 and 335 might be associated with ligand recognition | 165 |
| 4.4.3. | Mutational analysis and functional studies suggested multiple distinct binding sites on human GPR84 | 167 |
| 5 | Defining the orthologue selectivity of GPR84 ligands | 169 |
| 5.1. | Introduction | 169 |
| 5.2. | Characterization of cell lines expressing FLAG-mGPR84-G α_{i2} , FLAG-mGPR84-G α_{i2} C352I or FLAG-mGPR84-eYFP constructs | 170 |
| 5.2.1. | Characterization of the expression of FLAG-mGPR84-G α_{i2} or FLAG-mGPR84-G α_{i2} C352I by western blot analysis | 170 |
| 5.2.2. | Characterization of the expression of FLAG-mGPR84-eYFP or FLAG-hGPR84-eYFP in HEK-293 cells | 171 |
| 5.2.3. | Functional characterization using [35 S]-GTP γ S binding assays | 173 |
| 5.2.4. | Mouse GPR84 couples to PTX-sensitive G α_i G proteins | 176 |
| 5.3. | Orthosteric and allosteric agonists display similar activities at human and mouse orthologues of GPR84 | 177 |
| 5.4. | Defining the pharmacology of GPR84 ligands in RAW 264.7 cells | 184 |

| | | |
|--------|---|-----|
| 5.4.1. | Orthosteric and allosteric agonists of GPR84 display similar pharmacology in RAW 264.7 cells to those observed in transfected cells expressing FLAG-mGPR84-eYFP | 184 |
| 5.4.2. | GPR84 antagonists showed reduced potency in RAW 264.7 cells compared to human GPR84 expressing THP-1 cells | 187 |
| 5.4.3. | GLPG1205 displays differential modes of action in antagonizing the effect of compound-1 and PSB-16671 in RAW264.7 cells..... | 190 |
| 5.5. | Antagonist 107 and 104 display reduced potency at mouse GPR84 compared to the human orthologue while antagonist 837 was inactive at mouse GPR84 | 191 |
| 5.6. | Discussion | 196 |
| 5.6.1. | Human and mouse GPR84 can exist as N-glycosylated forms | 196 |
| 5.6.2. | Characterization of orthosteric and allosteric activators of GPR84 in RAW 264.7 cells | 197 |
| 5.6.3. | Antagonists but not agonists of GPR84 display significant variations in pharmacology between human and mouse orthologues..... | 199 |
| 6 | Allosteric modulation of GPR84..... | 202 |
| 6.1. | Introduction..... | 202 |
| 6.2. | DIM analogues 6a and 3a are activators of human GPR84 | 204 |
| 6.3. | DIM is a potent PAM agonist at human GPR84 | 205 |
| 6.3.1. | DIM is a potent PAM of potency and efficacy of decanoic acid... | 205 |
| 6.3.2. | DIM displays strong allosteric interactions with other orthosteric agonists of human GPR84 | 207 |
| 6.3.3. | DIM displays probe dependence in allosteric modulation of potency of orthosteric agonists | 211 |
| 6.3.4. | DIM acts as a moderately potent PAM of potency of compound-1 and C-10 at mouse GPR84 while it behaves as a potent PAM of potency but weak NAM of efficacy of compound-1 in LPS-treated RAW264.7 cells | 212 |
| 6.4. | DIM analogue 3a is a PAM agonist at human GPR84 | 215 |
| 6.4.1. | DIM analogue 3a is a potent PAM of potency of compound-1 and 6-OAU | 215 |
| 6.4.2. | DIM analogue 3a is a moderately potent PAM of potency and efficacy of decanoic acid | 217 |
| 6.4.3. | DIM analogue 3a displays probe dependence in modulating function of GPR84 orthosteric agonists | 218 |
| 6.5. | DIM analogue 6a is a weak NAM of efficacy of compound-1 at human GPR84 | 220 |
| 6.6. | DIM analogues 2b and 3c lack affinity at human GPR84..... | 221 |
| 6.7. | DIM analogue PSB-16671 is a potent PAM agonist at both human and mouse GPR84 | 223 |
| 6.7.1. | PSB-16671 is more effective than DIM in enhancing the potency of decanoic acid | 223 |
| 6.7.2. | PSB-16671 is more effective than DIM in potentiating function of compound-1 and embelin at human GPR84 | 224 |

| | | |
|--------|--|-----|
| 6.7.3. | PSB-16671 displays little probe-dependence in allosteric modulation of orthosteric agonists at human GPR84 | 227 |
| 6.7.4. | PSB-16671 is also a potent PAM of activity of orthosteric agonists at mouse GPR84 | 227 |
| 6.7.5. | PSB-16671 is a potent PAM agonist of the function of orthosteric agonists of mouse GPR84 in RAW 264.7 cells | 231 |
| 6.7.6. | PSB-16671 exhibits probe-dependence in modulating function of orthosteric agonists of GPR84 in RAW264.7 cells..... | 235 |
| 6.8. | Discussions | 236 |
| 6.8.1. | Orthosteric and allosteric ligand act co-operatively to greatly enhance the function of GPR84 which may be a therapeutic strategy to limit atherosclerosis | 236 |
| 6.8.2. | MCFAs may act as endogenous allosteric modulators of GPR84 rather than acting as orthosteric agonists..... | 238 |
| 6.8.3. | The relative contribution of affinity and efficacy modulation to the functional cooperativity between DIM or PSB-16671 and orthosteric GPR84 agonists | 239 |
| 6.8.4. | Probe-dependence of allosteric effects of DIM and DIM analogues 240 | |
| 6.8.5. | Relative to DIM or 3a, PSB-16671 displays markedly higher positive cooperativity with orthosteric GPR84 agonists | 242 |
| 6.8.6. | DIM but not PSB-16671 displays marked variation between human and mouse GPR84 in modulating the function of orthosteric agonists | 243 |
| 6.8.7. | Complex allosterism between DIM and compound-1 in LPS-treated RAW264.7 cells | 244 |
| 6.8.8. | Orthosteric and allosteric ligands bind human and mouse GPR84 with similar affinity..... | 245 |
| 7 | Final discussion..... | 248 |
| | References..... | 256 |
| | Appendices | 294 |

List of Tables

| | |
|--|-----|
| Table 1-1 Brief overview of signalling pathways, physiological functions and clinical trial status of free fatty acid sensing GPCRs..... | 27 |
| Table 1-2 Potential endogenous agonists of GPR84 | 33 |
| Table 1-3 Natural product-derived and synthetic surrogate agonists of GPR84.. | 37 |
| Table 1-4 Synthetic ligands acting as GPR84 antagonists..... | 39 |
| Table 3-1 Potency and relative efficacy of different GPR84 agonists at the FLAG-hGPR84-SPASM-G $\alpha_{i1/2}$ sensor | 110 |
| Table 3-2 Potency and relative efficacy of compound-1 and TUG-1765 at different FLAG-hGPR84-SpNG-G α sensors..... | 115 |
| Table 4-1 Binding affinity of [3 H]-G9543 to the wild type and mutant versions of hGPR84 and corresponding receptor density | 142 |
| Table 4-2 Potency and efficacy of GPR84 ligands at wild type, R172A or R172K GPR84 | 145 |
| Table 4-3 Potency and efficacy of GPR84 agonists at wild type and F335 ^{6.51} A GPR84 in [35 S]-GTP γ S binding assays..... | 151 |
| Table 4-4 Potency and efficacy of GPR84 ligands at wild type and F170A GPR84 | 154 |
| Table 4-5 Potency and efficacy of GPR84 agonists at wild type, F101A and W360A GPR84 in [35 S]-GTP γ S binding assays..... | 156 |
| Table 5-1 Potency of different GPR84 agonists at human and mouse GPR84 observed in transiently transfected HEK-293 cells | 181 |
| Table 5-2 Potency of different agonists at human and mouse GPR84 observed in doxycycline-inducible Flp-In T-REx-293 cells expressing human or mouse GPR84 as fusion protein constructs | 183 |
| Table 5-3 Potencies of GPR84 orthosteric and allosteric agonists in LPS-treated RAW 264.7 cells..... | 187 |
| Table 5-4 Potencies of GPR84 antagonists to inhibit the response to an EC ₈₀ concentration of various agonists at LPS-induced RAW264.7 cells..... | 190 |
| Table 5-5 Potencies of compounds-104, 107 and 837 to inhibit the response to an EC ₈₀ concentration of compound-1 or PSB-16671 at FLAG-hGPR84-G α_{i2} or FLAG mGPR84-G α_{i2} | 195 |
| Table 6-1 Allosteric parameters for the interaction between DIM and C-10 at FLAG-hGPR84-G α_{i2} | 207 |
| Table 6-2 Allosteric parameters for the interactions between DIM and different orthosteric agonists in [35 S]-GTP γ S binding assays at FLAG-hGPR84-G α_{i2} | 211 |
| Table 6-3 Allosteric parameters for the interaction between compound-1/C-10 and DIM at mouse GPR84. | 215 |
| Table 6-4 Operational model parameters of allosteric interactions between 3a and different orthosteric agonists at FLAG-hGPR84-G α_{i2} | 218 |
| Table 6-5 Allosteric parameters for interaction between 6a and compound-1 at FLAG-hGPR84-G α_{i2} | 221 |
| Table 6-6 Operational model parameters of allosteric interactions between PSB-16671 and orthosteric agonists at FLAG-hGPR84-G α_{i2} | 226 |
| Table 6-7 Operational model parameters of allosteric interactions between PSB-16671 and different orthosteric agonists at FLAG-mGPR84-G α_{i2} | 229 |
| Table 6-8 Operational model parameters of allosteric interactions between PSB-16671 and different orthosteric agonists at RAW 264.7 cells. | 234 |

List of Figures

| | |
|---|-----|
| Figure 1.1 Basic characteristic topology of G-protein coupled receptors..... | 7 |
| Figure 1.2 Basic structural motifs of five families of G-protein coupled receptors. | 9 |
| Figure 1.3 GPCR-mediated signal transduction pathways and regulatory mechanisms of signal termination. | 16 |
| Figure 1.4 Different types of orthosteric ligands based on two-state GPCR activation model..... | 20 |
| Figure 1.5 Orthosteric agonism and different phenotypes of positive allosteric modulators (PAMs)..... | 22 |
| Figure 1.6 Various phenotypes of negative allosteric modulators (NAMs) and combined PAM-NAM. | 23 |
| Figure 1.7 Marked upregulation of GPR84 in monocytes/macrophages upon immunostimulation or inflammatory conditions. | 30 |
| Figure 1.8 Proposed GPR84-mediated signaling pathways and associated patho- physiological outcomes in macrophages. | 42 |
| Figure 1.9 GPR84 signaling and its patho-physiological outcomes in neutrophils. | 43 |
| Figure 1.10 Agonist-activated GPR84 signaling generates a pro-inflammatory macrophage phenotype..... | 46 |
| Figure 1.11 GPR84 deficiency in mice leads to Th2 shift and generates an anti- inflammatory macrophage phenotype..... | 48 |
| Figure 1.12 Proposed role of GPR84 in mediating cross-talk between adiposity and diabetes. | 55 |
| Figure 1.13 GPR84 signaling inhibits RANKL-induced osteoclast differentiation by inhibiting NF- κ B and MAPK signaling pathways. | 60 |
| Figure 1.14 GPR84 regulates Wnt- β catenin signaling in pre-leukemic stem cells to develop and maintain MLL leukemia. | 62 |
| Figure 2.1 Structure of GPR84 allosteric agonist DIM and DIM analogues used in the studies..... | 66 |
| Figure 2.2 Chemical structures of a series of compound-1 derivatives..... | 67 |
| Figure 3.1 Schematic diagram of a BRET-based SPASM sensor for GPR84..... | 106 |
| Figure 3.2 Doxycycline-induced expression of FLAG-hGPR84-SPASM-G $\alpha_{i1/2}$ and FLAG-hGPR84-SPASM-NP biosensors in Flp-In T-REx-293 stable cells. | 107 |
| Figure 3.3 A FLAG-hGPR84-SPASM-G $\alpha_{i1/2}$ sensor is functional when expressed in a Flp-In T-REx-293 stable cell line. | 108 |
| Figure 3.4 DIM and embelin act as partial agonists and compound-1 and compound-51 act as super-agonists at the FLAG-hGPR84-SPASM-G $\alpha_{i1/2}$ sensor.. | 109 |
| Figure 3.5 Compound-1-occupied GPR84 adopts G $\alpha_{i/o}$ -coupled active conformations in HEK-293 cells. | 112 |
| Figure 3.6 TUG-1765 stabilizes G $\alpha_{i/o}$ -coupled active conformations of GPR84 in HEK 293 cells. | 113 |
| Figure 3.7 The relative coupling efficiency of interaction between human GPR84 and individual G $\alpha_{i/o}$ G proteins. | 115 |
| Figure 4.1 Immunoblot of FLAG-hGPR84-G α_{i2} WT, FLAG-hGPR84-G α_{i2} C352I and FLAG-hGPR84-G α_{i2} C352G fusion protein constructs probed with anti-FLAG antibody. | 124 |
| Figure 4.2 The radioligand [3 H]-G9543 displayed similar binding properties at FLAG-hGPR84-G α_{i2} and FLAG-hGPR84-G α_{i2} C352I receptor constructs. | 125 |

| | |
|--|-----|
| Figure 4.3 Functional characterization of Flp-In TM T-REx TM -293 stable cell lines expressing either FLAG-hGPR84-Gα _{i2} , FLAG-hGPR84-Gα _{i2} C352I or FLAG-hGPR84-Gα _{i2} C352G fusion constructs. | 128 |
| Figure 4.4 Effects of pertussis toxin (PTX) pre-treatment on DIM-induced [³⁵ S]-GTPγS binding to membranes purified from Flp-In TM T-REx TM -293 stable cell lines expressing either FLAG-hGPR84-Gα _{i2} , FLAG- hGPR84-Gα _{i2} C352I or FLAG-hGPR84-Gα _{i2} C352G..... | 129 |
| Figure 4.5 The GPR84-Gα _{i2} fusion protein approach enhances coupling efficiency between GPR84 and Gα _i protein compared to the eYFP tagged GPR84 construct. | 131 |
| Figure 4.6 Agonists of hGPR84 display similar activity at FLAG-hGPR84-Gα _{i2} and FLAG-hGPR84-Gα _{i2} C352I fusion proteins. | 133 |
| Figure 4.7 Effects of agonist-mediated GPR84 activation on intracellular cAMP accumulation..... | 135 |
| Figure 4.8 Homology model of human GPR84 and the putative ligand-binding cavity..... | 138 |
| Figure 4.9 Primary amino acid sequence of human GPR84 highlighting the residues I have mutated.. | 139 |
| Figure 4.10 Binding properties of [³ H]-G9543 at wild type and mutant versions of human GPR84. | 141 |
| Figure 4.11 Mutation of phenylalanine 101 ^{3,33} or tryptophan 360 ^{7,43} to alanine completely eliminated the ability of the radiolabelled antagonist [³ H]-G9543 to bind to human GPR84. | 142 |
| Figure 4.12 Mutation of arginine 172 of hGPR84 to either alanine or lysine abolishes the agonist function of decanoic acid, embelin, compound-1 and 6-OAU but not of DIM or PSB-16671. | 144 |
| Figure 4.13 Decanoic acid, embelin and compound-1 share a common binding site in hGPR84. | 146 |
| Figure 4.14 A series of compound-1 analogues are orthosteric agonists of human GPR84. | 148 |
| Figure 4.15 Phenylalanine 335 of human GPR84 might be part of the orthosteric ligand binding site. | 150 |
| Figure 4.16 The effect of alteration of phenylalanine 170 to alanine on GPR84 ligand recognition. | 153 |
| Figure 4.17 Effects of mutation of either F101 or W360 to alanine on GPR84 ligand functions..... | 155 |
| Figure 4.18 The putative binding mode of embelin in GPR84. A potential docking pose of embelin is shown..... | 158 |
| Figure 4.19 A potential docking pose of 6-OAU within GPR84. | 159 |
| Figure 4.20 A putative binding mode of compound-1 within GPR84. | 160 |
| Figure 4.21 GPR84 antagonist compound-107 does not bind to the orthosteric or allosteric agonist sites within GPR84. | 161 |
| Figure 5.1 Immunoblot of FLAG-mGPR84-Gα _{i2} and FLAG-mGPR84-Gα _{i2} C352I probed with anti-ICL3-mouse GPR84 antiserum. | 171 |
| Figure 5.2 Immunoblot of FLAG-mGPR84-eYFP and FLAG-hGPR84-eYFP probed with anti-GFP (A) or anti-ICL3-mouse GPR84 antiserum (B). | 173 |
| Figure 5.3 FLAG-mGPR84-Gα _{i2} , FLAG-mGPR84-Gα _{i2} C352I and FLAG-mGPR84-eYFP are functionally active in [³⁵ S]-GTPγS binding assays. | 175 |
| Figure 5.4 Mouse GPR84 couples to pertussis toxin-sensitive Gα _i G proteins.... | 177 |
| Figure 5.5 Agonists of human GPR84 display very similar activity at mouse GPR84. | 179 |
| Figure 5.6 Human and mouse GPR84 showed similar responsiveness to orthosteric and allosteric ligands in HEK-293 cells. | 180 |

| | |
|--|-----|
| Figure 5.7 Mouse GPR84 responds to different GPR84 agonists in a manner very similar to human orthologue..... | 182 |
| Figure 5.8 Comparison of GPR84 agonist functions between human and mouse GPR84. | 183 |
| Figure 5.9 RAW 264.7 cells respond to GPR84 orthosteric and allosteric agonists in a manner equivalent to transfected cells expressing mouse GPR84. | 186 |
| Figure 5.10 GPR84 antagonists compound-104, 107,161 and GLPG1205 but not compound-837 effectively blocked agonist-induced responses in RAW 264.7 cells. | 189 |
| Figure 5.11 GLPG1205 antagonizes effect of compound-1 in a competitive manner while it is non-competitive with PSB-16671 in blocking effect of PSB-16671 in RAW264.7 cells..... | 191 |
| Figure 5.12 Antagonist compounds -104 and 107 are more potent at human GPR84 than the mouse orthologue while compound 837 is inactive at mouse GPR84. | 192 |
| Figure 5.13 Compound-104 and 107 display markedly lower potency at mouse GPR84 compared to the human orthologue while compound-837 is inactive at mouse GPR84..... | 194 |
| Figure 5.14 The radiolabelled antagonist [³ H]-G9543 did not display significant binding to mouse GPR84..... | 195 |
| Figure 6.1 DIM analogues 6a and 3a retain the ability to activate human GPR84 while 2b, 3b and 3c lack agonist function. | 204 |
| Figure 6.2 DIM and C-10 display strong positive cooperativity in modulating function of each other at human GPR84. | 206 |
| Figure 6.3 DIM is a potent PAM of potency of compound-1 and 6-OAU at human GPR84 while it modulates both the potency and efficacy of embelin. | 210 |
| Figure 6.4 Probe dependence of DIM-promoted affinity modulation of different GPR84 orthosteric agonists at FLAG-hGPR84-Gα _{i2} | 212 |
| Figure 6.5 DIM acts as a PAM of potency of compound-1 at FLAG-mGPR84-Gα _{i2} while it behaves as a PAM of affinity and NAM of efficacy of compound-1 at LPS-treated RAW264.7 cells..... | 214 |
| Figure 6.6 DIM analogue 3a is a potent PAM of potency of compound-1 and 6-OAU at human GPR84. | 216 |
| Figure 6.7 DIM analogue 3a is a moderately potent PAM of potency and efficacy of C-10 at human GPR84. | 218 |
| Figure 6.8 DIM analogue 3a exhibits probe-dependence in modulating binding affinity of orthosteric agonists at human GPR84 in [³⁵ S]-GTPγS binding assays. | 219 |
| Figure 6.9 DIM analogue 6a acts as a weak NAM of efficacy of compound-1 at human GPR84. | 220 |
| Figure 6.10 DIM analogues 2b and 3c lack ability to bind human GPR84. | 222 |
| Figure 6.11 PSB-16671 is a PAM of potency of C-10 at human GPR84. | 224 |
| Figure 6.12 PSB-16671 acts as a PAM of potency of compound-1 while it behaves as a strong PAM of potency and efficacy of embelin at human GPR84. | 226 |
| Figure 6.13 PSB-16671 displays strong positive cooperativity with different orthosteric agonists of GPR84 at FLAG-mGPR84-Gα _{i2} | 229 |
| Figure 6.14 PSB-16671 displays high positive cooperativity in modulating function of compound-1, C-10 and embelin in [³⁵ S]-GTPγS binding assays in RAW 264.7 cells. | 233 |

List of Publications

Manuscripts

Mahmud, Z.A., Jenkins, L., Ulven, T., Labéguère, F., Gosmini, R., De Vos, S., Hudson, B.D., Tikhonova, I.G. and Milligan, G. (2017) Three classes of ligands each bind to distinct sites on the orphan G protein-coupled receptor GPR84. *Sci Rep.* 7(1):17953.

Mancini, S.J., Mahmud, Z.A., Jenkins, L., Bolognini, D., Newman, R., Barnes, M., Edye, M.E., McMahon, S.B., Tobin, A.B. and Milligan, G. (2019) On-target and off-target effects of novel orthosteric and allosteric activators of GPR84. *Sci Rep.* 9(1):1861.

Poster Presentation

Mahmud, Z.A., Jenkins, L. and Milligan, G. (2018) 'Allosteric modulation of the orphan G-protein coupled receptor GPR84'
British Pharmacological Society 7th Focused Meeting on Cell Signalling
16-17 April 2018, University of Nottingham, Nottingham, UK

Acknowledgement

I would firstly wish to thank my supervisor Professor Graeme Milligan for his continuous support, guidance, direction and supervision throughout my PhD project. I am really lucky to have such a great scientist like Graeme as my mentor who contributed immensely to develop my research skill and to work independently with generating own ideas. I also highly appreciate his suggestions and critical review of my thesis draft which enhances my writing skill as well.

I am also greatly thankful to Laura Jenkins for her continuous support and guidelines especially for providing technical assistance, training with different pharmacological assays and molecular biology techniques. Laura, without your care, patience and support it would have been challenging for me to do well in the lab. I also want to say a special thanks to Dr Brian Hudson for helping me a lot in planning experiments, analysing data, critiquing my research findings and most importantly for discussing on GPCR that enhanced my theoretical knowledge and understanding. I am also grateful to my assessors, Professor Matthew Dalby and Dr Christopher McInerny for providing valuable feedback, advice and suggestions. I would like to thank Irina G. Tikhonova, School of Pharmacy, Queen's University Belfast, for the homology modelling and ligand docking, to Dorota Maciejewska, Department of Organic Chemistry, Medical University of Warsaw, Poland for providing the analogues of DIM, to Dr. Laurent Saniere (Galapagos NV) for provision of PBS-16671, compound-1, compound-51, compounds 9, 104, 107, 161, 837, GLPG1205 and [³H]-G9543 and to Dr. Trond Ulven, Department of Physics, Chemistry and Pharmacy, University of Southern Denmark, for provision of compound-1 and its derivatives.

I am highly grateful to the Commonwealth Scholarship Commission, UK for financial support. I extend my thanks to Dr. Sheikh Zahir Raihan for introducing me to the lab and helping me to settle in a foreign environment, to Dr. Richard Ward for providing me suggestions and guidelines for conducting molecular cloning and immunoblotting, to Dr. Daniele Bolognini for providing assistance in data analysis, to Dr. Frederike Muskens for helping in drawing chemical structures and to Dr. Sara Marsango for her encouragement and support to do immunoblotting. I also appreciate the encouragement and advice from Dr. John Pediani, Dr. Elisa Alvarez-Curto, Dr. Kenneth Watterson, Dr. Eugenia Sergeev,

Dr. Sara Mancini, Dr. Tezz Quon and Dr. Li-Chiung Lin. I extend this thanks to my fellow PhD student Davide Capoferri for his continuous friendly support. I am also indebted to Dr. Swapan Kumar Sarker and to Md Shahinur Hossain for their companionship, constant laughs and emotional support in Glasgow. Finally, I extend my special thanks to my beloved parents, brothers and sisters for their sacrifices and support during my PhD tenure.

Author's Declaration

I declare that, except where explicit reference is made to the contribution of others, that this thesis is the result of my own work and has not previously been submitted for a degree or diploma at the University of Glasgow or at any other institution.

Signature:

Name: Zobaer Al Mahmud

Date: 27/08/2019

Abbreviations

| | |
|-----------|---|
| 7-TMR | Seven transmembrane receptor |
| ANOVA | Analysis of variance |
| AP-2 | Adaptor protein-2 |
| ATP | Adenosine triphosphate |
| BCA | Bicinchoninic acid |
| BRET | Bioluminescence resonance energy transfer |
| BSA | Bovine serum albumin |
| cAMP | Cyclic adenosine monophosphate |
| cDNA | Complementary deoxyribonucleic acid |
| CHO | Chinese hamster ovary |
| COX-2 | Cyclooxygenase-2 |
| CPM | Counts per minute |
| DAG | Diacylglycerol |
| DMEM | Dulbecco's modified eagle's medium |
| DMSO | Dimethyl sulfoxide |
| DNA | Deoxyribonucleic acid |
| dNTP | Deoxynucleoside triphosphate |
| DPM | Disintegrations per minute |
| ECL | Extracellular loop |
| EDTA | Ethylene diamine tetra acetic acid |
| EL2 | Extracellular loop 2 |
| ERK | Extracellular-signal regulated kinase |
| eYFP | Enhanced yellow fluorescent protein |
| FBS | Foetal bovine serum |
| FFA | Free fatty acid receptor |
| FFA1 | Free fatty acid receptor 1 |
| FFA2 | Free fatty acid receptor 2 |
| FFA3 | Free fatty acid receptor 3 |
| FFA4 | Free fatty acid receptor 4 |
| FRET | Fluorescence resonance energy transfer |
| G protein | Guanine nucleotide-binding protein |
| GABA | γ -Aminobutyric acid |
| GAP | GTPase-activating protein |
| GDP | Guanosine diphosphate |
| GEF | Guanine nucleotide exchange factor |
| GFP | Green fluorescent protein |
| GLP-1 | Glucagon-like peptide-1 |
| GOI | Gene of Interest |
| GPCR | G protein-coupled receptor |
| GRKs | G protein-coupled receptor kinases |

| | |
|---------------|---|
| GTP | Guanosine triphosphate |
| HA | Hemagglutinin |
| HBSS | Hank's balanced salt solution |
| HEK | Human embryonic kidney |
| HRP | Horseradish peroxidase |
| HTRF | Homogenous time resolved fluorescence |
| IBD | Inflammatory bowel disease |
| ICL | Intracellular loop |
| IFN- γ | Interferon gamma |
| IL | Interleukin |
| IP1 | Inositol 1 Phosphate |
| IP3 | Inositol 1,4,5-trisphosphate |
| LB | Luria-Bertani |
| LCFA | Long chain fatty acid |
| LPS | Lipopolysaccharide |
| MAP | Mitogen-activated protein kinase |
| MCFAs | Medium chain fatty acids |
| mRNA | messenger ribonucleic acid |
| NAM | Negative allosteric modulator |
| NLuc | NanoLuc Luciferase |
| PAGE | Polyacrylamide gel electrophoresis |
| PAM | Positive allosteric modulator |
| PAR1 | Protease activated receptor 1 |
| PBS | Phosphate-buffered saline |
| PCR | Polymerase chain reaction |
| PEI | Polyethyleneimine |
| PKA | Protein kinase A |
| PKC | Protein kinase C |
| PLC | Phospholipase C |
| PPAR γ | Peroxisome Proliferator Activated Receptor γ |
| PTX | Bordetella pertussis toxin |
| RGS | Regulators of G protein signalling |
| RNA | Ribonucleic acid |
| RPM | Revolutions per minute |
| SCFAs | Short chain fatty acids |
| SDS | Sodium Dodecyl Sulphate |
| siRNA | Small Interfering Ribonucleic Acid |
| SPASM | Systematic protein affinity strength modulation |
| TM | Transmembrane domain |
| TNF α | Tumor necrosis factor alpha |

1 Introduction

1.1 G protein coupled receptors (GPCRs) and drug development

1.1.1 Brief overview of drug development approaches

Development of highly selective efficacious drugs having no side effects to treat unmet medical needs is the major goal of translational or therapeutic pharmacology. Though historically most of the drugs were discovered and developed to clinical use by applying phenotypic screening-based drug development approach, within the last three decades rational molecular target-based approaches have gained popularity as the predominant drug development approach for both the pharmaceutical industry and academic translational research community thanks to modern developments in recombinant technology and molecular biology techniques along with the human genome projects (Croston, 2017; Eder et al., 2014; Zheng et al., 2013). Though in an analysis performed by Swinney and Anthony, (2011) phenotypic screening-based approaches were found to be more productive than the target-based approach, evident from the fact that 62% of 45 FDA approved small molecule first-in-class drugs were developed within the timeframe of 1999 to 2008 by phenotypic screening-based approaches, Eder et al., (2014) found that after 5 years, target-based approach become the dominant drug development strategy contributing to the development of 70% of FDA approved first-in-class drugs within 1999 to 2013. In the phenotypic screening-based approach, also known as classical pharmacology or forward pharmacology, a disease model is first developed followed by screening of compounds for the desired outcome in cells, tissues, organs or animals without prior knowledge about the molecular target of the compounds (Schenone et al., 2013; Zheng et al., 2013). This screening process results in the identification of lead compounds able to ameliorate the disease phenotype. The molecular target is then identified for the candidate lead compounds which facilitates the lead optimization process. In contrast to this classical approach, rational target-based drug discovery process also known as 'reverse pharmacology' or 'reverse chemical genetics', starts with the identification of the molecular target (proteins, gene or RNA) which is thought to play crucial roles in specific disease progression and modulation of this target

activity either through inhibition or stimulation is proposed to reverse the disease phenotype (Zheng et al., 2013). The proposed pathophysiological role or disease modifying characteristic of the drug target is then validated by several investigations including loss-of-function experiments through genetic elimination of the target gene in animals (studies with knockout animals) or gene knockdown studies either through RNA interference or antisense RNA technology and by studies using highly selective and potent tool compounds (small molecule chemical probes) in *in vitro* cellular or *in vivo* disease models (Hughes et al., 2011; Bunnage et al., 2013). Several biochemical assays are then performed wherein large chemical libraries are tested using high throughput screening in an effort to identify the hits or lead compounds. These lead candidates are then subjected to extensive chemical optimization processes i.e. structure activity relationship (SAR) studies to improve the pharmacodynamics profiles including selectivity, affinity and efficacy as well as to ensure the favourable pharmacokinetic profiles (absorption, distribution, metabolism and excretion, ADME) (Zheng et al., 2013). Mechanism-of-action studies are then conducted using cell-based or animal disease models in an effort to validate the cellular activities of the lead compounds and to investigate the off-target effects which might produce side effects (Schenone et al., 2013). Only a few lead compounds displaying the desired efficacy with defined mechanism of action can pass to the next stages of a drug development program, preclinical toxicity studies and hopefully to the clinical trials in healthy volunteer or patients (Zheng et al., 2013).

Though a target-based drug discovery approach is more advantageous in terms of cost, speed and feasibility of SAR studies over a phenotypic screening-based approach, translation of pharmacology of potential drug candidates observed in recombinant systems to clinical results is challenging as recombinant systems are too simplistic to mimic the complex biology of the whole organism (Croston, 2017). Recent analysis showed that higher rates of withdrawal of drug candidates from phase II or phase III clinical trials are due to lack of efficacy or unintended toxicity, although other factors including lack of correlation between disease animal models and human disease or polymorphisms in patients might be potential causes for failure in translatability (Bunnage et al., 2013; Zheng et al., 2013; Morgan et al., 2012). Such reported lack of efficacy in the late stage of

drug development implies that improper target validation in the early stage drug discovery program is a major contributing factor for high attrition rates of clinical drug candidates in phase II or phase III clinical trials (Jones, 2016; Zheng et al., 2013; Bunnage et al., 2013). Therefore, in the target-based drug discovery approach, effective preclinical target validation is the key to success in translation of pharmacology of drug candidates into clinical effect. As use of low quality pharmacological tool compounds (nonselective and undercharacterized probe without having defined mechanism of action) can lead to incomplete or misleading results regarding the biological function and pathophysiological roles of the target of interest (Clegg et al., 2017), generation of highly selective and potent tool compounds with thorough pharmacological characterization is vital for uncovering the therapeutic potential of the molecular target (Milligan, 2018; Wacker et al., 2017).

1.1.2 Role of GPCRs in therapeutic pharmacology

G protein coupled receptors (GPCRs) are seven transmembrane domain (7TM) containing integral membrane proteins which bind and activate heterotrimeric G-proteins to transduce an extracellular signal to intracellular effector proteins leading to cellular response. As they can also interact with other cytoplasmic signalling proteins including kinases and β -arrestins, seven transmembrane receptors (7TMR) is a more appropriate terminology (Kobilka, 2007). However, the GPCR terminology is widely accepted and hence in this thesis this terminology will be used. The GPCR superfamily comprising about 800 members (Fredriksson and Schioth, 2005) in humans is the largest family of membrane spanning proteins. Among them 400 members are olfactory receptors and rest are nonolfactory/chemosensory receptors i.e. they are responsive to diverse chemicals including ions, neurotransmitters, biogenic amines, small and large peptides, hormones, lipids, intermediate metabolites including ATP, fatty acids etc. and thus regulate almost all physiological processes (Hauser et al., 2017).

Among the various pharmacological targets including GPCRs, ion channels, kinases, nuclear hormone receptors, proteases and transporters, historically GPCRs have been considered as the most successful molecular targets for drug development, and several researchers (Sriram and Insel, 2018; Hauser et al., 2017; Santos et al., 2017; Rask-Andersen et al., 2014; Rask-Andersen et al.,

2011; Overington et al., 2006; Hopkins and Groom, 2002; Menzaghi et al., 2002) highlight that GPCRs are the targets for approximately 30-36% of FDA-approved drugs. Among the 398 nonolfactory GPCRs in human, 134 GPCRs have already been exploited therapeutically, contributing to the development of some 700 FDA approved drugs (Sriram and Insel, 2018) and 66 novel GPCRs are targets for 321 potential drug candidates which are under investigation in clinical trials (Hauser et al., 2017). Still there remain 198 nonolfactory GPCRs that might be potential untapped sources for future drug development. High success in therapeutic exploitation of GPCRs stems from the substantial association of GPCR signalling with diverse human pathophysiological processes and high pharmacological tractability of this superfamily due to the presence of druggable binding sites in the extracellular sides of the receptor which make them more accessible to small molecules (Sriram and Insel, 2018; Milligan, 2018; Rask-Andersen et al., 2014). These druggable binding sites (orthosteric and allosteric sites) on GPCRs possess physicochemical properties required for designing small molecule drugs (molecular weight <900 daltons) having favourable oral bioavailability (Mason et al., 2012; Wacker et al., 2017). Recent developments in structural biology of GPCRs due to the availability of crystal structures of 44 GPCRs and 205 ligand-receptor complexes (Hauser et al., 2017) will revolutionize structure-based drug design as it will facilitate virtual screening-based lead discovery and lead optimization processes. Along with this structural information, therapeutic exploitation of untapped GPCRs will be promoted by the utilization of new modalities of GPCR pharmacology including allosteric modulation and biased signalling (G protein and β -arrestin biased agonism or antagonism or allosteric modulation) leading to enhanced selectivity and specificity of the agent with concomitant improvement in drug safety profile (Hauser et al., 2017; Sriram and Insel, 2018). Moreover, recent discovery of new types of GPCR-targeted biologics including monoclonal antibodies/nanobodies, anti-sense oligonucleotides and gene therapy as well as novel drug delivery systems are likely to accelerate GPCR-based drug discovery programs (Sriram and Insel, 2018).

1.1.3 Challenges in clinical exploitation of orphan or poorly characterized GPCRs

Although more than 350 genes encode for non-olfactory GPCRs (Fredriksson et al., 2003), only 250 of them have been characterized in terms of ligand recognition and there remain over 100 orphan GPCRs i.e. their endogenous ligands are either unexplored or there is a lack of consensus among the scientific community regarding the physiological relevance of proposed endogenous ligands (Milligan, 2018; Davenport et al., 2013; Chung et al., 2008; Geetha et al., 2007; Fredriksson and Schioth, 2005). Orphan GPCRs might be a potential source of therapeutics and several drug candidates which are currently under clinical trials target different orphan receptors. Based on their selective expression profile and association with different disease states, orphan receptors are appreciated to be potential therapeutics for several diseases including diabetes (GPR119), allergic inflammation and cardiovascular diseases such as angiotensin-II induced hypertension and heart failure (GPR35), multiple sclerosis (GPR55), ulcerative colitis (GPR84), gastrointestinal diseases (LGR4 and LGR5), Alzheimer's disease (GPR3), CNS disorders including schizophrenia (GPR88) etc. (Ye et al., 2019; Sriram and Insel, 2018; Hauser et al., 2017; Stockert and Devi, 2015; Fang et al., 2015; Divorty et al., 2015; Divorty et al., 2018). However, there remain a number of challenges to exploit these enigmatic receptors therapeutically. Due to the lack of structural information, designing and identifying selective and potent tool compounds for orphan receptors is difficult which makes understanding of the biological function and pharmacological properties of these undercharacterized receptors more challenging. Even after the receptor has been deorphanized i.e. paired with an endogenous ligand, orphan receptors still remain poorly characterized in terms of their signalling pathways, pharmacological properties and biological functions. As during the deorphanization stage, high throughput screening of a large number of chemicals is performed using assays (internalization assays, β -arrestin recruitment assays, Ca mobilization assays employing chimeric or promiscuous G proteins) in which final readout is independent of specific signalling pathways, one of the initial challenges to uncover therapeutic potential of orphan receptors is to explore which specific G protein(s) is coupled to the receptor and what are the downstream signalling pathways (Hudson et al., 2011). Such information regarding the signal transduction pathways are required for designing/

development of assays to be employed in subsequent target validation processes or in defining the pharmacology of the specific receptor (Hudson et al., 2011). As tool compounds are vital for characterization of the receptor, development of potent and selective pharmacological ligands for an orphan receptor is crucial which can be used confidently to probe receptor functions in both physiological and disease states (Milligan, 2018; Wacker et al., 2017). The paucity of potent and selective chemical probes has been considered to be one of the major obstacles to the proper characterization of enigmatic receptors including GPR35, FFA2 etc. which has been hindering their therapeutic exploitation (Milligan, 2018; Divorty et al., 2015; Holliday et al., 2012). In this context investigation of ligand binding modes i.e. defining which amino acid residues are responsible for the ligand recognition are essential as this information could be subsequently employed in structure based drug design (SBDD) to identify and generate novel selective and potent synthetic ligands having potential to probe receptor functions (Hudson et al., 2011). However in case of orphan receptors structure-based drug design using virtual screening is challenging due to lack of any crystal structures and thus is dependent on constructing high quality homology models using the available crystal structure of other receptors which displays high sequence identity with the target receptor (Ngo et al., 2016). In addition, defining the mode of actions of pharmacological tool compounds along with identifying their potential orthologue selectivity and designing more improved disease models to be used in *in vivo* functions of the receptor are of paramount importance to uncover the therapeutic potential of such poorly characterized receptors (Milligan, 2018; Hauser et al., 2017).

1.1.4 GPCRs: structural features and classification

GPCRs are single polypeptides characterized by common structural features of having a seven transmembrane (TM1-7) hydrophobic α -helices connected by three intracellular loops (ICL1-3) and three extracellular loops (ECL1-3), a variable extracellular N-terminal domain and an intracellular C-terminal domain (Kobilka, 2007)(Figure 1.1). From the extracellular side view, the seven transmembrane helices are oriented in a counter-clockwise manner forming a helical bundle which serves as the structural core of the receptor. While the 7-TM domain displays highest degree of sequence similarity among different classes of GPCRs, the N-terminus, C-terminus and ICL3 are divergent in terms of

structure and sequence (Kobilka, 2007). Extracellular regions contain conserved cysteine residues forming disulphide bonds which confer stability to the structure. For example, most of the GPCRs contain a disulphide bridge connecting ECL2 and TM3 (Venkatakrishnan et al., 2013). Broadly, extracellular regions of the receptor including N-terminus, extracellular loops (especially ECL2) and extracellular sides of the 7-TM domains serve as ligand binding pockets and the signal(s) is transduced to the intracellular effector proteins (G proteins, GRK, arrestin) by conformational rearrangements of TM domains in which the intracellular loops and cytoplasmic sides of TM domains constitute the binding pocket for cytosolic signalling effector proteins (Venkatakrishnan et al., 2013; Katrich et al., 2013). TM3 is considered as the structural and functional hub of the receptor playing crucial roles in ligand binding, signal transmission and G-protein interaction (Venkatakrishnan et al., 2013).

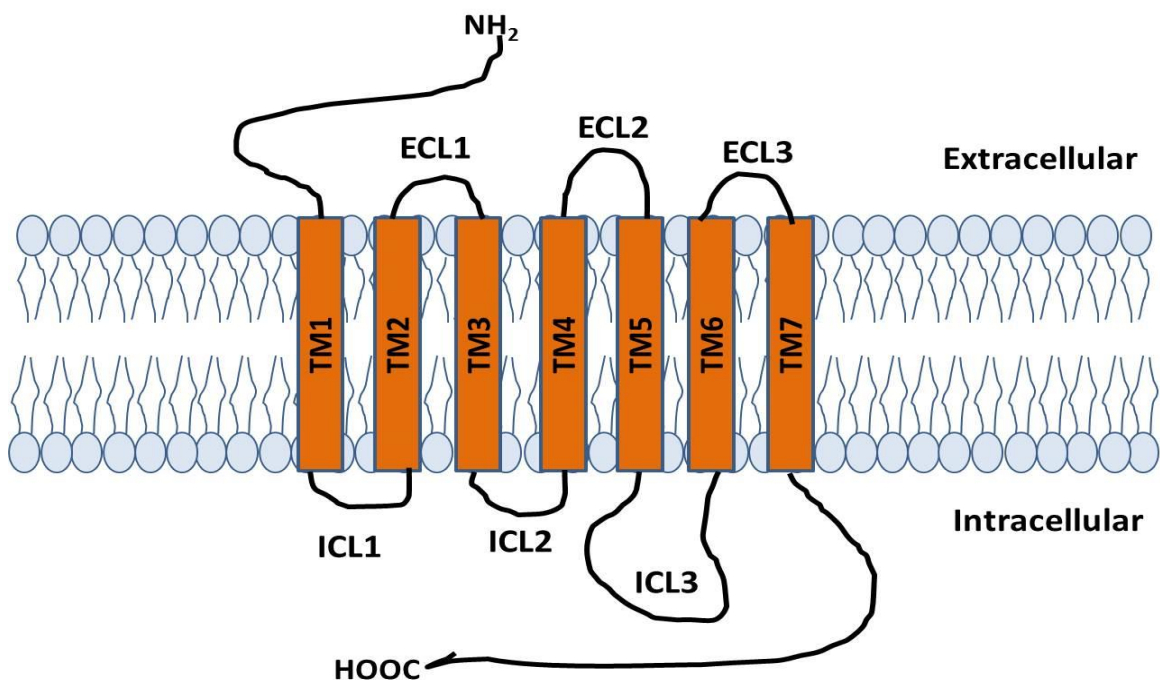


Figure 1.1 Basic characteristic topology of G-protein coupled receptors.

All GPCRs share a common structural motif in which seven hydrophobic α helices traverse the phospholipid bilayer of the plasma membrane which is connected by three extracellular loops (ECL1-3) and three intracellular loops (ICL1-3). Besides these 7-transmembrane domains (TMD), GPCRs also have an extracellular N-terminus and an intracellular C-terminus domain.

Based on phylogenetic criteria, Fredriksson et al., (2003) divided human GPCRs into five main families, glutamate like, rhodopsin like, adhesion, frizzled/taste2 and secretin (Figure 1.2).

1.1.4.1 Rhodopsin like (Class A) family

The rhodopsin like Class A family is the largest family comprising 719 members including aminergic receptors, muscarinic receptors, free fatty acid receptors etc. (Alexander et al., 2017). This class includes the most successfully exploited drug targets. Diverse ranges of small molecule ligands including neurotransmitters, hormones, small peptides, photons etc. bind to the binding pocket created by the seven transmembrane helical bundle of Class A family, though extracellular loops also may play important roles in ligand recognition (Weis and Kobilka, 2018). In contrast to the other four families, Class A family receptors possess a short N-terminus (Lagerstrom and Schioth, 2008) which does not play role in ligand binding (Fredriksson et al., 2003). Class A family receptors contain the highly conserved (E)/DRY motif at the interface between the cytoplasmic end of TM3 and ICL2, and the NPxxY motif in TM7 (Fredriksson et al., 2003) which act as micro-switches stabilizing the inactive conformations and undergo rearrangements in amino acid positions upon GPCR activation (Weis and Kobilka, 2018).

1.1.4.2 Secretin family (Class B)

The secretin family (Class B) comprises 15 GPCRs in human including calcitonin receptor, secretin receptor, vasoactive intestinal peptide receptor etc., and contains a long N-terminal tail (60-80 amino acids) having 6 conserved cysteine residues which form three conserved disulphide bonds imparting stability to the structure as well as serving to dock the C-terminal region of peptide ligands (Fredriksson et al., 2003; Schiöth and Fredriksson, 2005). Conserved cysteine residues are also present in ECL1 and ECL2. Secretin family receptors are responsive to diffusible ligand, large peptides which are accommodated by orthosteric binding sites encompassing both the N-terminus and extracellular loops.

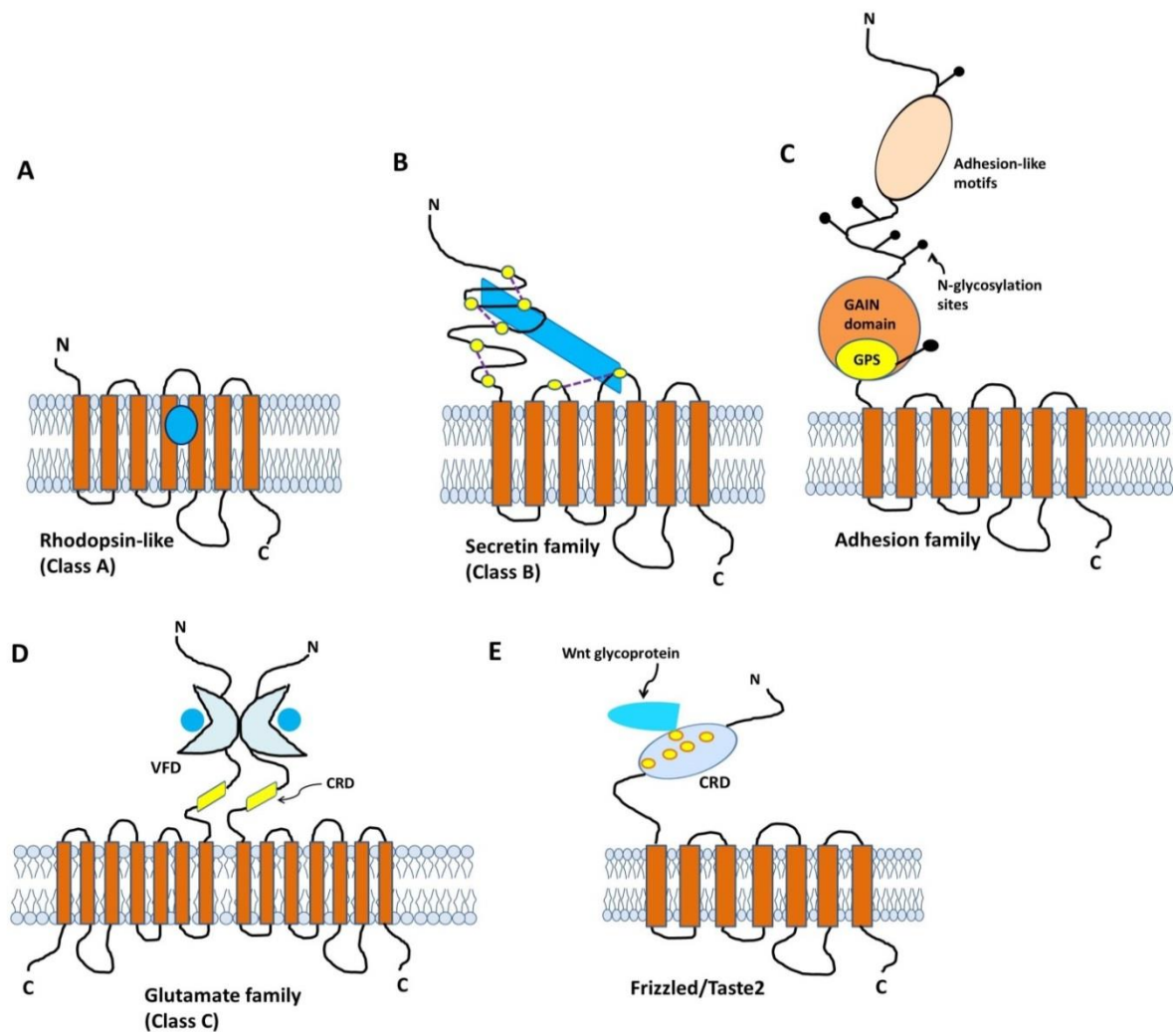


Figure 1.2 Basic structural motifs of five families of G-protein coupled receptors.

The GRAFS classification system divides all the GPCRs of vertebrates into five major classes. Rhodopsin like Class A family receptors contain a short N-terminus (A) while the other four families possess large N-termini with specific conserved domain(s) (B-E). A cysteine rich (cysteine residues are depicted as small yellow circles) hormone binding domain in N-terminus along with the extracellular loops constitutes the orthosteric binding site for Secretin family (B). Adhesion family receptors are characterized by presence of a cysteine rich GPCR proteolysis site (GPS) motif embedded in a conserved GPCR autoproteolysis inducing domain (GAIN) and by adhesion-like motifs responsible for cell-cell and cell-matrix interactions (C). The N-terminus of Class C Glutamate family receptors contains a unique bilobar venus fly trap domain (VFD) and a cysteine rich domain (CRD) (D). The cleft between two lobes of VFD represents the orthosteric binding pocket for orthosteric ligands, shown as blue circles. Frizzled receptors contain a conserved cysteine rich domain (CRD) in the N-terminus to which Wnt glycoproteins bind (E).

1.1.4.3 Glutamate receptor family (Class C)

The glutamate receptor family (Class C) contains 22 members including metabotropic glutamate receptors, calcium sensing receptors (CaSR), GABA_B receptors etc. Class C glutamate like receptors are characterized by long N-terminal tail (280-580 amino acids) containing a bilobar venus fly trap domain (VFD) and a cysteine rich domain in between the helical domain and VFD

(Lagerstrom and Schioth, 2008; Fredriksson et al., 2003). Orthosteric ligands bind to the cleft created by two distinct lobes of VFD while allosteric modulators bind within the helical bundle (Rosenbaum et al., 2009). Class C receptors form homodimers or heterodimers and this dimerization is required for the functional activation of the receptor.

1.1.4.4 Adhesion family

The adhesion family is the second largest family of human GPCRs containing 33 members, most of which are orphan receptors (Lagerstrom and Schioth, 2008). This family is also termed as Class B2 family as the 7TM domain is structurally similar to Class B secretin family. Similar to secretin family, these receptors contain a large N-terminus. In contrast to the secretin family, the N-terminus contains a unique conserved GPCR autoproteolysis inducing domain (GAIN domain) composed of some 320 amino acid residues and specific functional domains/cell adhesion domains (EGF, cadherin, lectin, laminin, immunoglobulin like domain etc.) responsible for ligand-receptor interactions (Lagerstrom and Schioth, 2008; Hamann et al., 2015; Alexander et al., 2015). GAIN domain contains a cysteine rich GPCR proteolysis site (GPS) comprising approximately 40 to 50 amino acid residues (Arc et al., 2012; Hamann et al., 2015). Adhesion family receptors undergo autoproteolysis in the GPS motif resulting in two parts, N-terminal fragment (NTF) and 7TM containing C-terminal fragment (CTF) connected by noncovalent interactions. Adhesion like motifs of functional domains are engaged in cell-cell and cell-matrix adhesion (Yona et al., 2008; Hamann et al., 2015; Fredriksson et al., 2003) which is the basis of the 'adhesion family' nomenclature.

1.1.4.5 Frizzled/taste2 receptors

Frizzled/taste2 receptors, comprising 24 members, are characterized by a large N-terminus (200 amino acids) containing a cysteine rich domain which, along with extracellular loops acts as the binding site for the orthosteric ligand such as secreted lipoglycoproteins/Wnt glycoproteins (Fredriksson et al., 2003; Schulte, 2010). Similar to other GPCRs, frizzled receptors contain conserved cysteine residues on ECL1 and ECL2. (Schulte, 2010). Frizzled receptor-mediated

signalling including Wnt/ β -catenin signalling is associated with developmental processes.

1.2 Heterotrimeric G proteins

Heterotrimeric G proteins are guanine nucleotide binding proteins composed of three subunits (α , β and γ subunits) which act as signal transducers, relaying information from activated cell surface receptors (GPCRs) to intracellular effector proteins including enzymes and ion channels (Simon et al., 1991). $G\alpha$ subunit is composed of a Ras-like GTPase domain and an α -helical domain (Sprang et al., 2007). The guanine nucleotide (GDP or GTP)-binding pocket is located in a deep cleft between these two domains (Gurevich and Gurevich, 2018). In resting condition, GDP is bound to $G\alpha$ subunit, while GDP is displaced by GTP upon G protein activation. $G\beta$ and $G\gamma$ subunits are tightly associated with each other forming a heterodimer which acts as a functional unit. There are 20 isoforms of $G\alpha$ subunit (Sprang et al., 2007), five isoforms of $G\beta$ subunit (β_{1-5}) and twelve isoforms of $G\gamma$ subunits (γ_{1-5} and γ_{7-13}) (Wettschureck and Offermanns, 2005; Milligan and Kostenis, 2006). G proteins are classified based on the variation in $G\alpha$ subunit. On the basis of sequence homology and functional similarities G proteins are divided into four major classes including $G\alpha_s$, $G\alpha_{i/o}$, $G\alpha_{q/11}$ and $G\alpha_{12/13}$ family G proteins (Simon et al., 1991; Syrovatkina et al., 2016), each class contains two or more isotypes. In the case of $G\alpha_s$ family which stimulates adenylyl cyclase enzymes, while the $G\alpha_s$ isotype is ubiquitously expressed, $G\alpha_{olf}$ is expressed largely in olfactory neurons (Syrovatkina et al., 2016; Milligan and Kostenis, 2006). $G\alpha_{i/o}$ family G proteins which inhibit adenylyl cyclase enzymes is the most diverse and largest family containing $G\alpha_{i1}$, $G\alpha_{i2}$, $G\alpha_{i3}$, $G\alpha_{oA}$, $G\alpha_{oB}$, $G\alpha_g$, $G\alpha_{t1}$, $G\alpha_{t2}$ and $G\alpha_z$ isotypes (Syrovatkina et al., 2016). Among them, $G\alpha_{i1}$, $G\alpha_{i2}$ and $G\alpha_{i3}$ are expressed ubiquitously whilst expression of $G\alpha_o$, $G\alpha_t$ and $G\alpha_z$ are highly restricted to neuron and neuroendocrine, retinal rods and cone cells and neuron and platelets, respectively (Syrovatkina et al., 2016; Milligan and Kostenis, 2006). $G\alpha_{q/11}$ family which activates phospholipase CB enzymes contains $G\alpha_q$, $G\alpha_{11}$, $G\alpha_{14}$, $G\alpha_{16}$ or $G\alpha_{15}$ (mouse version of $G\alpha_{16}$) isotypes among which $G\alpha_q$ and $G\alpha_{11}$ are ubiquitous while $G\alpha_{14}$ and $G\alpha_{15/16}$ are found in only hematopoietic cells and kidney, lung or liver, respectively (Syrovatkina et al., 2016). $G\alpha_{12/13}$ family G proteins comprised of $G\alpha_{12}$ and $G\alpha_{13}$ isoforms are expressed in every cell/tissue and are appreciated to regulate

several Rho-GEFs (Syrovatkina et al., 2016; Milligan and Kostenis, 2006; Wettschureck and Offermanns, 2005).

1.3 GPCR-mediated signal transduction pathways

1.3.1 G-protein dependent pathways

1.3.1.1 GPCR activation and G protein recruitment

The fundamental function of a GPCR is to link extracellular signals to intracellular effector proteins which then regulate signalling cascades leading to the generation of a biological response. GPCR activation following agonist binding is the first stage of this complex signalling process. At resting state GPCRs maintain an equilibrium between active and inactive conformational states. Agonist binding to a specific GPCR favours and stabilizes active conformational states which are characterized by structural rearrangements of the cytoplasmic end of TM domains and side chain micro-switches. Comparison of inactive and active state crystal structures of several Class A GPCRs, including rhodopsin, β_2 -adrenergic receptor, M_2 muscarinic receptor, μ opioid receptor and adenosine A_{2A} receptor revealed that agonist-stimulated conformational changes reflect a conserved rotation and outward movement of TM6 by 3.5-14 Å away from the helical bundle with concomitant outward movement of TM5 and inward movement/rearrangements of TM7 (Scheerer et al., 2008; Rasmussen et al., 2011; Lebon et al., 2011; Xu et al., 2011; Kruse et al., 2013; Ring et al., 2013; Huang et al., 2015). Micro-switches including the conserved (E)/DRY motif in TM3 and NPxxY motif in TM7 undergo rotamer conformational changes upon class A GPCR activation (Kruse et al., 2013; Katritch et al., 2013) and these rearrangements of conserved motifs are important for the stabilization of movement of cytoplasmic ends of TM domains (Katritch et al., 2013). For example, disruption of electrostatic interaction or the so called “ionic lock” between Arg^{3.50} of conserved (E)/DRY motif in the cytoplasmic end of TM3 and acidic residues including Glu^{6.30} in TM6 was reported to be associated with conversion from inactive to active state conformations of rhodopsin (Scheerer et al., 2008;), β_2 adrenergic receptor (Kobilka, 2007) and probably for other Class A GPCRs. Breakdown of this ionic lock in rhodopsin and β_2 -adrenergic receptors facilitates outward movement of TM6 away from the core of the helical bundle

(Altenbach et al., 2008; Yao et al., 2006) and thereby leads to stabilization of active conformations of the corresponding receptor. Similarly, the highly conserved Tyr^{7.53} of the NPxxY motif at the cytoplasmic end of TM7 undergoes rotamer conformational changes upon activation of several Class A GPCRs including rhodopsin, adrenergic receptors, adenosine receptors etc. (Labon et al., 2011; Xu et al., 2011; Audet and Bouvier, 2012; Katritch et al., 2013). These conformational rearrangements of TM5, TM6 and TM7 open a crevice lined by amino acid residues from TM3, TM5 and TM6 on the intracellular cytoplasmic sides of the transmembrane domains which serves as the binding pocket for the C-terminal $\alpha 5$ helix of the G α subunit of a heterotrimeric G protein (Weis and Kobilka, 2018; Venkatakrishnan et al., 2013; Hofmann et al., 2009). Similar to Class A GPCRs, activated Class B family receptors including GLP-1R and the calcitonin receptor also display large outward movements (15 and 18Å°, respectively) of TM6 and a small inward movement of TM7 forming a cavity on the cytoplasmic sides of the helical domains to which α helix of Ras-like domain of the G s subunit binds (Zhang et al., 2017; Liang et al., 2017). These studies implied that despite having differences in terms of amino acid sequences, the mechanism of GPCR activation is conserved among different classes of GPCRs. Not only does agonist binding promote G protein binding to the receptor, in a reciprocal way G protein recruitment also enhances agonist affinity for the receptor, which implies that GPCRs act as classic allosteric proteins (Weis and Kobilka, 2018).

Binding of G protein to the agonist-bound activated GPCR triggers a conformational change in the G protein which promotes exchange of GTP for GDP in the cleft between the Ras-like domain and the α -helical domain of G α subunit (Syrovatkina et al., 2016). GTP binding to G α subunit leads to dissociation of the G protein from agonist-bound GPCR as well as dissociation of G α subunit from the G $\beta\gamma$ heterodimer. Both G α subunit and G $\beta\gamma$ dimer can then act as signal transducers stimulating downstream signalling pathways (Syrovatkina et al., 2016), which are described briefly in the following subsection. G protein-dependent signalling is terminated by the inherent GTPase activity of the G α subunit which hydrolyses bound GTP into GDP and inorganic phosphate (Syrovatkina et al., 2016). This inherent GTPase activity is further accelerated by GTPase activating proteins (GAPs) such as regulators of G protein

signalling (RGS) proteins (Ross and Wilkie, 2000). The hydrolysis product GDP-bound $G\alpha$ subunit can then re-associate with $G\beta\gamma$ dimer forming the heterotrimeric G protein which can further bind to agonist-bound activated GPCR to initiate another cycle. This activation-deactivation cycle for G protein is depicted in Figure 1.3 (A, D).

1.3.1.2 $G\alpha$ -mediated signalling

Activated GTP bound $G\alpha$ subunits transduce extracellular signal from activated GPCRs to the intracellular signal effectors generating several second messengers. Activated $G\alpha_s$ (s stands for stimulatory) G protein activates transmembrane adenylyl cyclase (AC) enzymes which catalyse conversion of ATP to cyclic adenosine monophosphate (cAMP) (Gilman, 1987). Elevated intracellular cAMP levels lead to activation of cAMP-dependent protein kinase A (PKA) followed by a phosphorylation-induced cascades of downstream substrates ultimately leading to cellular responses including gene expression, glycogenolysis, lipolysis, hormone secretion etc. (Wettschureck and Offermanns, 2005). In contrast to G_s G protein, activated $G_{i/o}$ family G proteins inhibit adenylyl cyclase activity resulting in decreased intracellular cAMP levels. Active $G_{q/11}$ G proteins activate phospholipase C β which catalyses hydrolysis of phosphatidylinositol 4,5-bisphosphate (PIP₂) into 1,4,5-triphosphate (IP₃) and diacylglycerol (DAG) (Rhee, 2001). IP₃ triggers intracellular calcium mobilization by interacting with the IP₃ receptor on the ligand-gated calcium channel of the endoplasmic reticulum whilst DAG activates protein kinase C (PKC) which triggers downstream phosphorylation cascades (Wettschureck and Offermanns, 2005). Depending on the cell types, these second messengers (IP₃, Ca²⁺, DAG) mediate different cellular processes including smooth muscle contraction, neuronal excitation, platelet activation etc. (Wettschureck and Offermanns, 2005). $G_{12/13}$ family G proteins were reported to mediate cellular signalling pathways which are associated with cytoskeleton rearrangements/cell contraction, cell migration, invasion, platelet activation, cell growth and differentiation (Juneja and Casey, 2009; Suzuki et al., 2009). Both activated G_{12} and G_{13} subunits were reported to activate Rho-specific guanine nucleotide exchange factors such as PDZ-RhoGEF and leukemia-associated RhoGEF (LARG) whilst activity of p115 Rho GEF was enhanced by only G_{13} subunit (Kozasa et al., 1998; Hart et al., 1998; Fukuhara et al., 1999; Fukuhara

et al., 2000; Siehler, 2007; Siehler, 2009; Suzuki et al., 2009). These stimulated Rho GEFs then promote GTP exchange for GDP on monomeric Rho GTPases which activates downstream Rho kinase (ROCK) leading to actin cytoskeleton rearrangements and cellular contraction (Siehler, 2009; Siehler, 2007). Activated $G\alpha_{12}$ has also been shown to stimulate RasGAP-Ras-MEKs and MEK5-ERK5 pathways leading to cellular growth and transformation (Juneja and Casey, 2009) while activated $G\alpha_{13}$ was reported to interact with Hax-1 protein which activates downstream Rac protein leading to cellular migration (Radhika et al., 2004).

1.3.1.3 $G\beta\gamma$ -mediated signalling

$G\beta\gamma$ heterodimer dissociated from the GTP bound $G\alpha$ subunit of activated G protein was shown to mediate many of the signalling pathways that are similar to those stimulated by $G\alpha$ -dependent pathways. For example, $G\beta\gamma$ was reported to activate phospholipase CB2 isoforms (Rhee, 2001) resulting in generation of second messengers IP_3 and DAG from PIP₂, triggering intracellular calcium mobilization and PKC-mediated signalling, respectively. $G\beta\gamma$ also stimulates phosphatidylinositol 3 kinases (β and γ isoforms) leading to activation of the AKT signalling pathway which is associated with cell survival and proliferation (Naor et al., 2000; Khan et al., 2013). While $G\beta\gamma$ was shown to stimulate adenylyl cyclase type II, IV and VII leading to enhanced production of intracellular cAMP level, adenylyl cyclase type I was reported to be inhibited by this transducer (Khan et al., 2013; Milligan and Kostenis, 2006). It is also appreciated that $G\beta\gamma$ dimer activates mitogen activated protein kinase (MAPK) signalling pathways including c-Src-mediated phosphorylation of extracellular signal-regulated kinase1/2 (ERK1/2) (Naor et al., 2000). Finally, $G\beta\gamma$ dimer was also reported to directly interact with ion channels including inwardly rectifying K^+ channel and voltage-dependent Ca^{2+} channel (VDCC) resulting in activation and inhibition of the channels, respectively (Khan et al., 2013). As $G\alpha_i$ G proteins are expressed in cells more abundantly than $G\alpha_s$ or $G\alpha_q$ family G proteins, $G\beta\gamma$ -dependent signalling is usually mediated by the activation of $G\alpha_i$ -coupled receptors (Syrovatkina et al., 2016 Wettschureck and Offermanns, 2005).

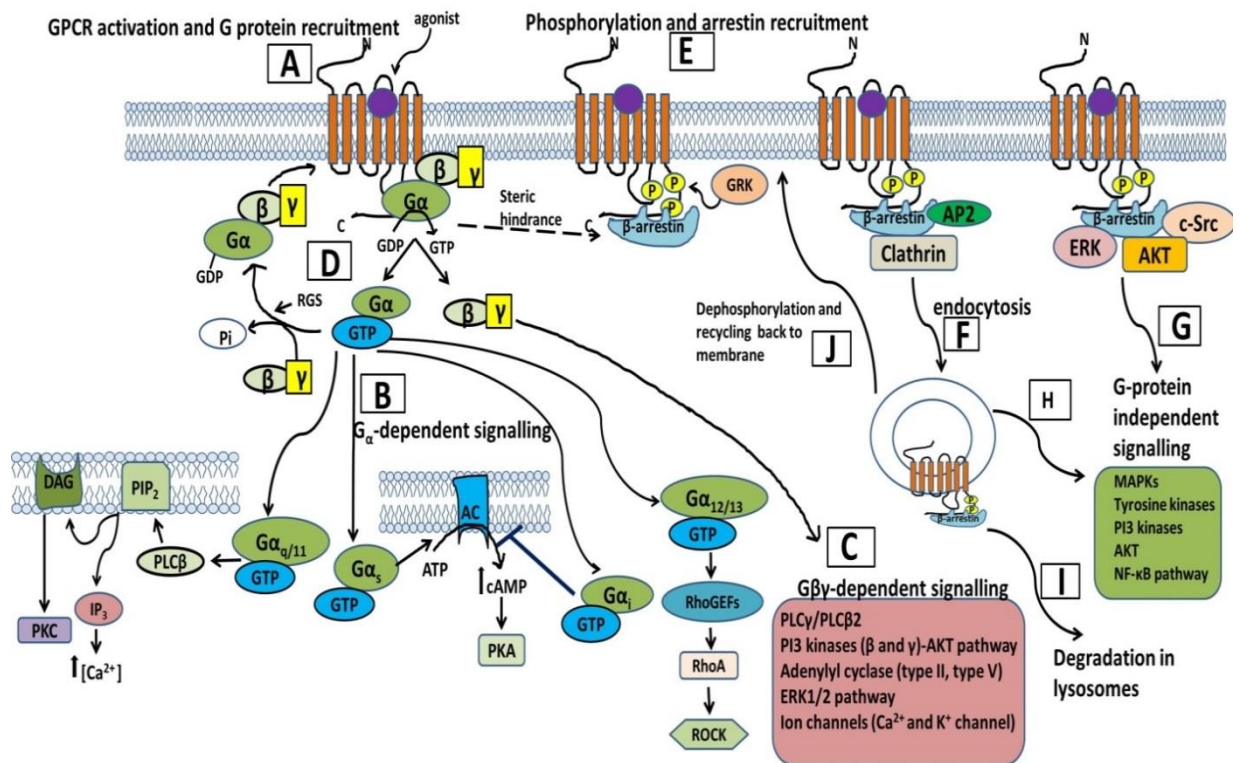


Figure 1.3 GPCR-mediated signal transduction pathways and regulatory mechanisms of signal termination. Upon agonist binding, GPCR changes its conformation by structural rearrangements of cytoplasmic ends opening a pocket for binding of C terminal helix of Gα subunit of heterotrimeric G protein (A). Activated GPCR acts as a guanine nucleotide exchange factor (GEF) to induce exchange of GTP for GDP on Gα subunit. GTP-bound Gα subunit then dissociates from Gβγ dimer and both can act as signal transducer. Gα-dependent signalling pathways are illustrated in (B). While active Gα_s and Gα_i regulate adenylyl cyclase activity resulting in enhanced or reduced intracellular cAMP levels, respectively, activated Gα_{q/11} G proteins stimulate PLCβ-IP₃-Ca signalling pathway. Gα_{12/13} activates Rho guanine nucleotide exchange factors (RhoGEFs) which trigger RhoA/ROCK signalling pathway. G protein activation and subsequent signalling is terminated by inherent GTPase activity of Gα subunit which results in hydrolysis of GTP into GDP and phosphate group followed by re-association of Gα-GDP and Gβγ (D). Regulators of G protein signalling (RGS) acts as GTPase activating protein (GAP) promoting the hydrolysis of GTP into GDP. Gβγ dimer also can activate downstream signalling pathways including stimulation of adenylyl cyclase, PLCγ/PLCβ2, PI3 kinases and ERK1/2 as well as regulates inwardly rectifying K⁺ and Ca²⁺ channels. GPCR signalling is also regulated by phosphorylation of serine-threonine residues on C-terminal tails and ICL3 by G protein-coupled receptor kinases (GRK) and subsequent recruitment of β-arrestin to the phosphorylated active receptor (E) which sterically hinders further G protein coupling to the receptor. β-arrestin acts as a scaffolding protein to recruit clathrin and AP-2 leading to clathrin-mediated endocytosis of the receptor (F). β-arrestin can also stimulate downstream signalling pathways including stimulation of MAPKs pathways (G). Endosomal β-arrestin also can trigger G-protein independent signalling pathways (H). Endocytosed receptor would be then either targeted for degradation in lysosomes (I) leading to downregulation or subjected to dephosphorylation and recycling back to membrane to induce resensitization (J).

1.3.1.4 Regulation of G protein-mediated signalling

To counteract sustained GPCR-mediated signalling some regulatory mechanisms operate in every cell type. G protein-mediated signalling is terminated by a cascade of regulatory processes including GPCR phosphorylation and β-arrestin coupling, endocytosis and downregulation of GPCR by lysosomal degradation (Luttrell and Lefkowitz, 2002). These regulatory processes lead to the

desensitization of GPCR which is defined as the attenuation of response to agonist resulting in decreased generation of second messengers. Serine-threonine residues on the C-terminal tail and ICL3 of agonist-bound activated GPCRs undergo phosphorylation by G-protein coupled receptor kinases (GRKs) which enhances affinity of the regulatory arrestin proteins for the receptor (Shukla et al., 2011). Nonvisual arrestins, β -arrestin 1 and β -arrestin 2 then bind to the phosphorylated agonist-activated GPCR leading to uncoupling of G-proteins due to steric hindrance which attenuates further signalling from activated receptor (Luttrell and Lefkowitz, 2002; Smith and Rajagopal, 2016). β -arrestins act as scaffolding proteins recruiting several trafficking proteins including clathrin, adapter protein 2 (AP-2), NSF etc which trigger endocytosis of the receptor (Lefkowitz and Shenoy, 2005). This internalization of receptor, resulting in reduced number of cell surface receptors might not be essential for receptor desensitization but contributes to the receptor dephosphorylation and re-sensitization (Shenoy and Lefkowitz, 2003). Upon internalization, β -arrestin is released from the agonist-occupied endosomal receptor followed by ligand dissociation and dephosphorylation of the receptor by phosphatases in an acidified vesicle compartment (Luttrell and Lefkowitz, 2002). Endocytosed receptor can then either be targeted for degradation in lysosomes leading to downregulation of GPCR or can be recycled back to the membrane, a process which is known as re-sensitization (Shenoy and Lefkowitz, 2003).

1.3.2 G-protein independent pathways

In addition to playing a crucial role in GPCR desensitization and internalization, β -arrestins are appreciated to behave as signal transducers by acting as scaffolding proteins for recruitment of different signalling molecules to the activated agonist-bound GPCR (Eichel et al., 2016; Shukla et al., 2011; Ma and Pei, 2007; Reiter and Lefkowitz, 2006; Luttrell and Lefkowitz, 2002). β -arrestins are reported to act as adapter proteins recruiting c-Src tyrosine kinase to activated GPCR ultimately leading to ERK1/2 activation (DeWire et al., 2007). β -arrestins were also shown to scaffold ERK1/2 cascades, p38 cascades and JNK3 signalling cascades, leading to activation of the corresponding MAP kinase (Lefkowitz and Shenoy, 2005; Shenoy and Lefkowitz, 2003). β -arrestin - dependent signalling was also shown to regulate activation of PI3K-AKT pathway

and inhibition of NF- κ B pathways (DeWire et al., 2007; Reiter and Lefkowitz, 2006).

1.4 Pharmacology of GPCR ligands

1.4.1 Pharmacology of orthosteric ligands

The pharmacology of a drug is characterized by three parameters, binding affinity for the receptor, target coverage and efficacy of the ligand (Kenakin, 2013). Affinity of the drug for the receptor reflects how strongly the drug can bind with the binding site on the receptor and usually is represented by the equilibrium dissociation constant measured in direct binding assays such as saturation and competition binding assays using a radiolabelled ligand or in fluorescence polarization assays using fluorescent ligands (Rossi and Taylor, 2011). In the case of unavailability of radiolabelled or fluorescent probes, the potency value measured in functional assays using [35 S]-GTP γ S binding assays employing a GPCR-G protein fusion protein or BRET-based β -arrestin recruitment assays have been used as surrogate measures of agonist binding affinity for the receptor as these assay systems provide 1:1:1 stoichiometry of ligand:receptor:readout as G-protein activation or β -arrestin recruitment are immediately downstream of GPCR activation and thus are not subjected to signal amplification (Smith, 2012; Hudson et al., 2014b). Efficacy of a ligand is defined as the property of a drug to trigger measurable physiological or pharmacological responses following binding to the receptor (Kenakin, 2001; Smith et al., 2011a) and is usually defined by the parameter E_{\max} , the maximal response obtained from the concentration-response curve for the ligand conducted in functional assays. The molecular basis of efficacy of a ligand lies in the ligand-stimulated change in conformation of the target receptor which exposes the active sequences on the cytosolic region of the receptor to trigger the binding and/activation of signalling effector proteins such as G-protein/arrestin or other proteins including GRKs leading to cellular response or change in receptor behaviour, respectively (Kenakin, 2002). The least complex model of GPCR activation is presented by the classic two state thermodynamic equilibrium model according to which a GPCR can exist in either an inactive or active state and an equilibrium is maintained between the two states (Leff, 1995; Kobilka and Deupi, 2007; Park et al., 2008). Upon binding to receptor, different ligands

can display preferential affinity for one of the two states and thereby selectively stabilize either of these two states, which forms the basis for the classification of orthosteric ligands into agonist, inverse agonist and neutral antagonist (Figure 1.4). Agonists are further divided into full and partial agonists depending on the extent of receptor activation triggered by them. Full agonists can trigger the receptor activation to the full extent leading to generation of highest maximal response while partial agonists cause partial receptor activation, leading to sub-maximal responses (Kenakin, 2001; Kobilka, 2007). Though the two state model can describe the different functional activities of GPCRs in response to treatment with various ligands having different efficacy, in reality like other proteins, GPCRs can exist in multiple states and always display a cluster of conformations described as an ensemble (Kenakin, 2002; Kenakin, 2013; Kobilka and Deupi, 2007). In basal condition, the unliganded receptor displays a set of conformations among which predominant conformations are inactive basal ensembles which are not related to cellular activity while very few conformations are associated with cellular response (G-protein activation, phosphorylation, arrestin recruitment etc) and are termed as the pharmacologically active ensemble which lead to ligand-independent signalling or constitutive activity (Kenakin, 2013). Ligand binding to the receptor causes a redistribution of such a cluster of conformations in such a way that ligand-stabilized conformations are co-incident with the pharmacologically active ensemble and leads to cellular activation (Kenakin, 2002; Kenakin, 2013). As there are various pharmacologically active ensembles which are related to different responses including G-protein activation, arrestin binding, phosphorylation etc, it is possible that a ligand might have different efficacies in each i.e efficacy is pluridimensional (Kenakin, 2011). The prevalence of these agonist-stabilized ensembles associated with different signalling pathways is determined by the relative stabilization by agonist and will define the strength and preference of activation of a specific signalling pathway (Kenakin, 2013). Some ligand might preferentially activate a specific signalling pathway over other(s) which is termed as agonist bias or functional selectivity (Kenakin, 2011). This signalling bias can be exploited for the development of more selective and safer drug candidates.

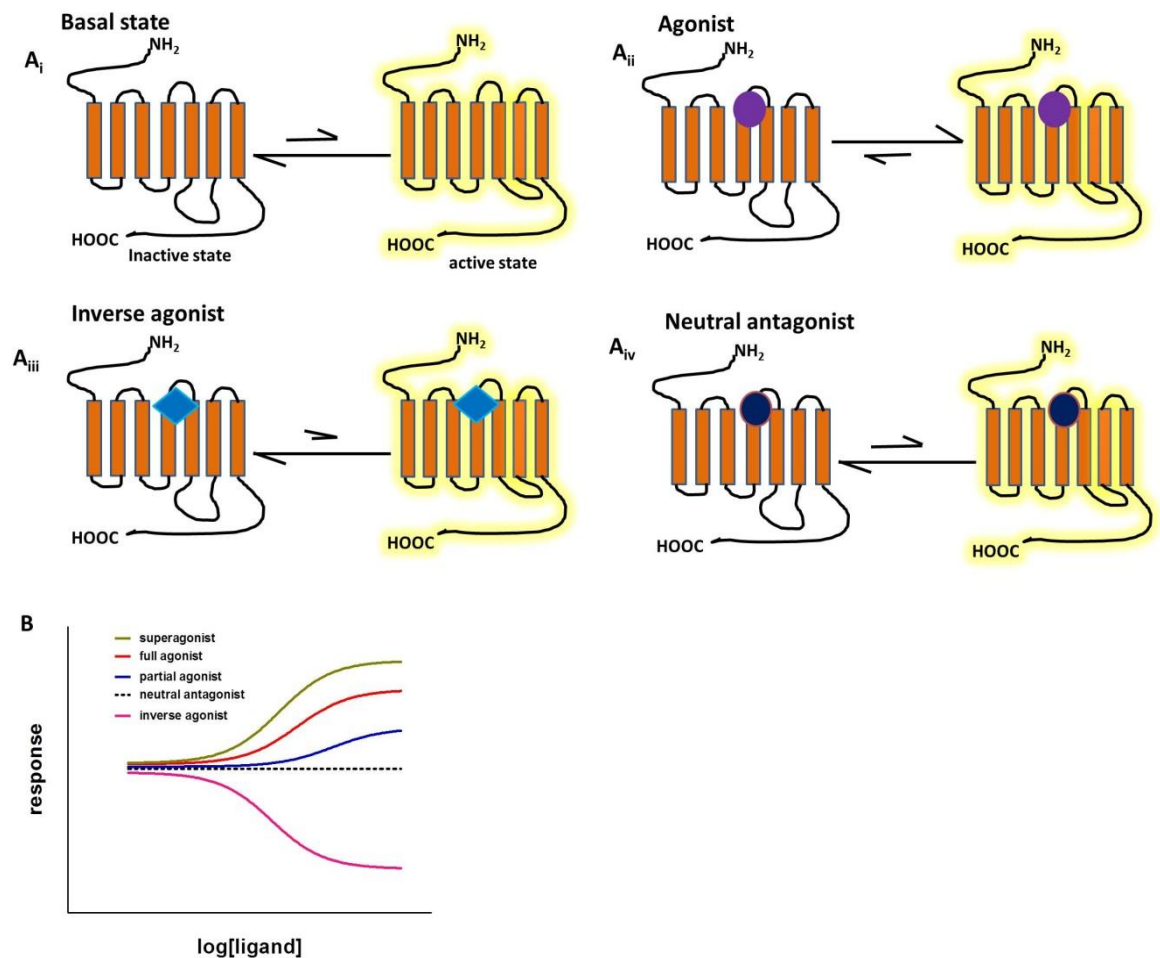


Figure 1.4 Different types of orthosteric ligands based on two-state GPCR activation model.

According to the classic 'two-state model' of GPCR activation, GPCRs can isomerise from the inactive state to active state and ligands are classified based on their ability to shift the equilibrium to these. If a small fraction of total receptors adopt the conformation related to active state while the predominant form are in inactive states, then even in the absence of any ligand, some system response might be found, and this activity is termed ligand-independent signalling or constitutive activity (A_i). Upon binding to the receptor, if a ligand shifts the equilibrium to favour active conformations, then it is termed as an agonist (A_{ii}) whilst ligands that shift the equilibrium toward inactive conformations are classed as inverse agonists (A_{iii}). Neutral antagonists are thought to have similar binding avidity for both the active and inactive conformation of the receptor (A_{iv}) and thus although they can competitively inhibit agonist binding to the receptor, they do not possess any efficacy on their own right. Representative concentration-response curves for different types of orthosteric ligands in a constitutively active GPCR system are shown in (B). Full agonists are endogenous agonists displaying highest maximal response in a specific tissue/system while superagonists are termed as synthetic ligands which share common binding sites with endogenous agonist but exhibit higher maximal response than the full agonist. A partial agonist display sub-maximal response whilst a neutral antagonist does not show any efficacy on its own right. Inverse agonists are ligands which counteract the ligand-independent signalling or constitutive activity in a concentration-dependent manner.

1.4.2 Complex pharmacology of allosteric ligands: new opportunities and challenges in drug discovery

Though historically drug development has been based on targeting the orthosteric site, recently allosteric ligands which bind to sites that are distinct from the orthosteric site, have attracted great interest for the development of drug candidates with sub-type selectivity and higher safety profiles. Moreover, orthosteric sites of Class B, secretin family receptors are not amenable to small molecule drug development as the endogenous ligands are large peptides with diffuse pharmacophores forming several contacts with the large N-terminal domain as well as extracellular loops and thus are difficult to exploit therapeutically (Christopoulos et al., 2014). In this case, targeting allosteric sites might be a good option for therapeutic intervention. Allosteric modulation of a GPCR is a phenomenon in which a ligand, by binding to a site which is topographically different from the binding sites of endogenous ligands, can trigger a distinct change in conformation of the receptor states which results in either an alteration of function of the co-bound orthosteric agonist and or activation of the receptor on its own right in the absence of the agonist probe leading to cellular response (Hudson et al., 2013c). Allosteric modulators which potentiate the function of an orthosteric probe by enhancing the binding affinity for the receptor (affinity modulation which is expressed by a parameter termed as affinity cooperativity factor, α) and/or maximal response of the orthosteric agonist (efficacy modulation expressed by the parameter termed as activation cooperativity factor, β) are called positive allosteric modulators (PAMs) while the modulators which decrease the function of the orthosteric agonist probe by either decreasing the binding affinity and/or efficacy of the co-bound probe are termed as negative allosteric modulators (NAMs) (Kenakin, 2017). Similar to orthosteric agonists, allosteric ligands can also display agonism or inverse agonism in its own right. Combinations of any two properties of these three phenotypes (positive and negative allosteric modulation and allosteric agonism) will lead to generation of more complex allosteric phenotypes including ago-allosteric modulators (or PAM agonist), NAM agonist, PAM/NAM, PAM antagonist etc (for details see Figure 1.5 and 1.6), implying that modes of action of allosteric ligands are more diverse and complex than orthosteric ligands. These diverse modalities of action of allosteric ligands represent a set of potential

options of therapeutic intervention as well as making defining the pharmacology of the allosteric ligand more challenging (Hudson et al., 2013c).

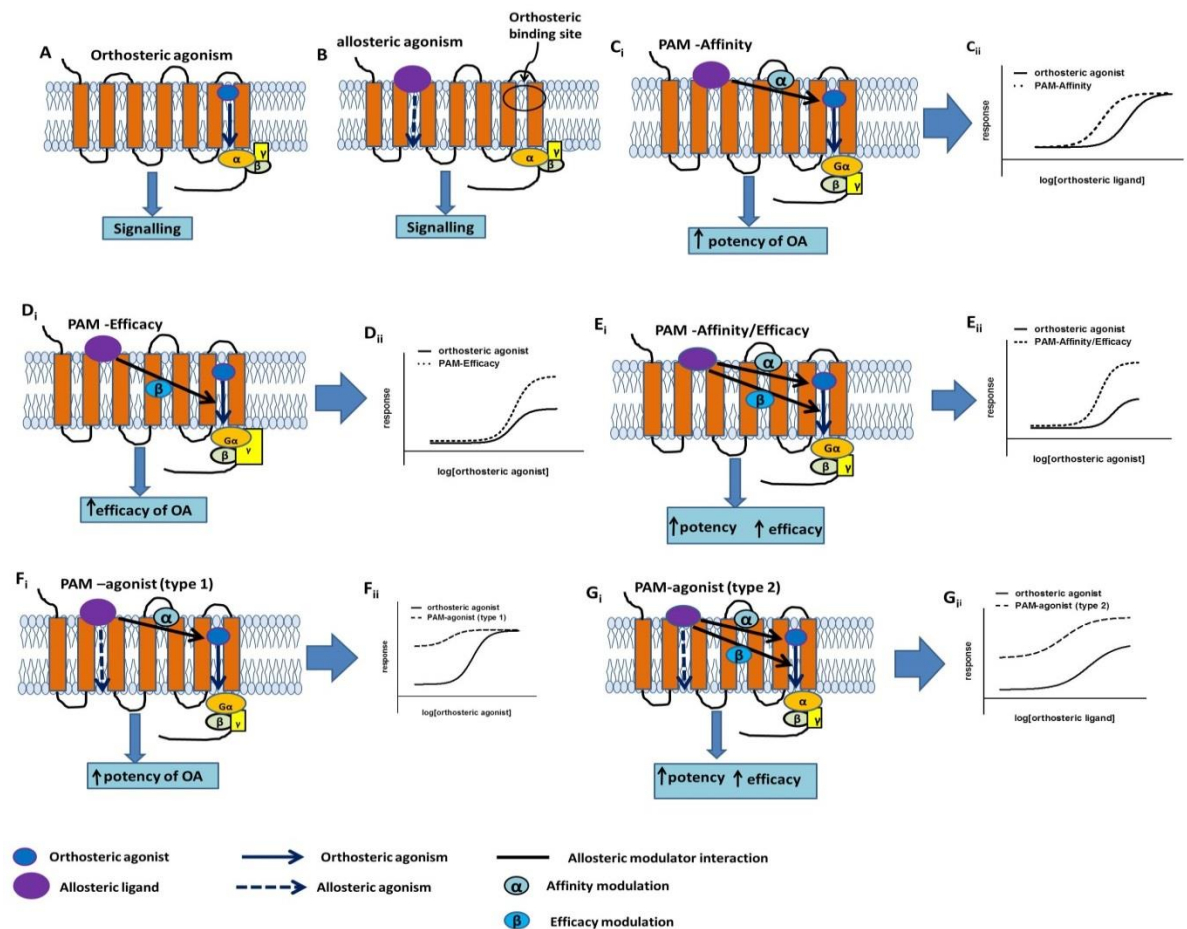


Figure 1.5 Orthosteric agonism and different phenotypes of positive allosteric modulators (PAMs). Binding of orthosteric agonists to a specific GPCR results in conformational change of the receptor which ultimately activates downstream signalling pathways producing pharmacological response (A). Allosteric agonists bind to the receptor on a site which is topographically distinct from the orthosteric binding site and in the absence of orthosteric agonist, allosteric agonist can activate the downstream signalling pathway leading to cellular response on its own right (B). The effect of a PAM of affinity on functional response of the orthosteric agonist is illustrated in (C_i). PAM of affinity enhances the binding affinity of the orthosteric agonist for the receptor and thus enhances the potency of the orthosteric agonist which results in the shifting of the concentration-response curve for orthosteric agonist to the left (C_{ii}) (Hudson et al., 2013c). Co-binding of a PAM of efficacy results in increase in efficacy of the orthosteric agonist while potency of the orthosteric agonist remains unaltered (D_i) (Hudson et al., 2013c) and the resulting concentration-response curve for the orthosteric agonist in the presence of a single concentration of PAM of efficacy is shown in (D_{ii}). Another allosteric phenotype is possible where the allosteric ligand can enhance both the binding affinity and efficacy of the orthosteric agonist (E_i) and this allosteric ligand is termed as PAM of affinity and efficacy; the resulting concentration-response curve for orthosteric agonist in the presence of a single concentration of a PAM-affinity/efficacy is displayed in (E_{ii}). More complex allosteric phenotype is represented as PAM-agonist or ago-allosteric modulator whereas the allosteric ligand can display efficacy on its own right in the absence of the orthosteric agonist and also can potentiate the function of the orthosteric agonist when co-binding the receptor with the orthosteric agonist (F_i and G_i) (Hudson et al., 2013c; Kenakin, 2017). One variant of PAM-agonist increases only the binding affinity of the orthosteric agonist (F_i) resulting in left-ward shifting of the concentration-response curve for agonist probe (F_{ii}) whilst another variant can enhance both the binding affinity and efficacy of the orthosteric agonist (G_i) resulting in left-ward and up-ward displacement of the concentration-response curve for orthosteric agonist (G_{ii}); in both cases the allosteric agonism of the PAM-agonist is reflected as enhanced basal signal in the absent of the orthosteric agonist (F_{ii} and G_{ii}).

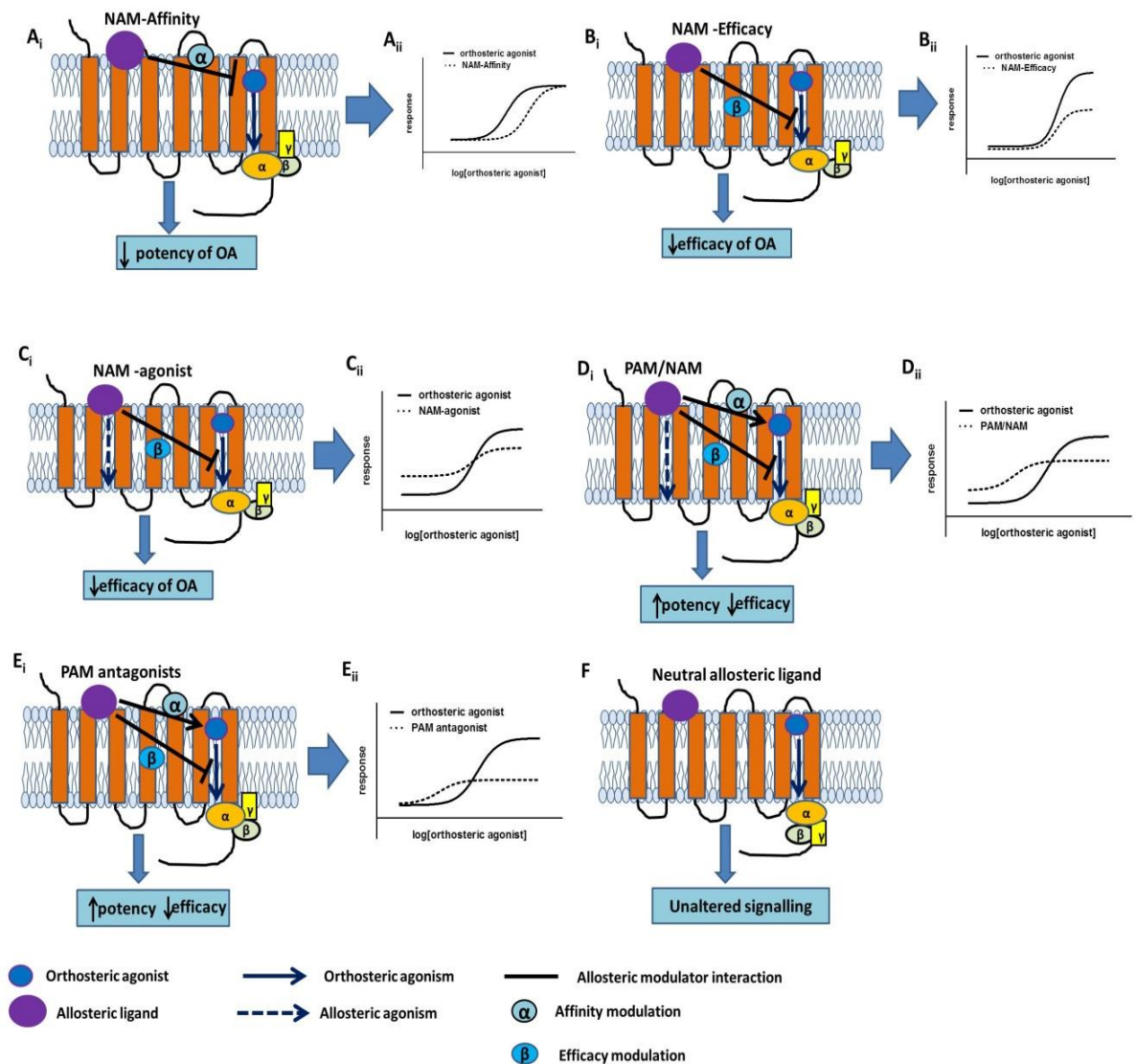


Figure 1.6 Various phenotypes of negative allosteric modulators (NAMs) and combined PAM-NAM. Negative allosteric modulators are allosteric ligands which can decrease the binding affinity of the orthosteric agonist for the receptor (NAM of affinity) (A_i) or the efficacy of the orthosteric agonist (NAM of efficacy) (B_i) resulting in right-ward (A_{ii}) or down-ward (B_{ii}) displacement of the concentration-response curve for the orthosteric agonist, respectively (Hudson et al., 2013c). Another variant of NAM is called NAM-agonist which can activate the receptor on its own right producing pharmacological response in the absence of the orthosteric agonist and also can decrease the efficacy of the orthosteric agonist when co-binding with the receptor (C_i), the resulting concentration-response curve for the orthosteric agonist in the presence of a single concentration of the NAM-agonist displays enhanced basal signal reflecting allosteric agonism and depressed maximal response reflecting NAM property (C_{ii}) (Kenakin, 2017). More complex scenario is represented in (D_i) where the allosteric modulator can enhance the binding affinity of the orthosteric agonist for the receptor with concomitant decrease in the efficacy of the agonist probe i.e. they can act as PAM of affinity but NAM of efficacy ($\alpha\beta > 1$); the resulting sinistral and down-ward displacement of the concentration-response curve for the orthosteric agonist by co-binding of a single concentration of the PAM-NAM is shown in (D_{ii}) (Hudson et al., 2013c). A variant of PAM-NAM profile is termed as PAM-antagonist (E_i) for which the combined affinity/efficacy cooperativity factor ($\alpha\beta$) is lower than 1 (Kenakin, 2017) and the resulting concentration-response curve for the orthosteric agonist in the presence of a single concentration of PAM-antagonist is shown in (E_{ii}). Allosteric ligand which binds to the receptor without affecting the binding affinity and efficacy of the orthosteric agonist is termed as negative allosteric ligand (NAL) or silent allosteric modulator (SAM) (F) (Wooten et al., 2013).

Allosteric modulators display some unique pharmacological properties including selectivity and saturability of the effect, probe dependence, transducer dependence and reciprocity of the effect (Christopoulos, 2014; Keov et al., 2011; May et al., 2007) and each pharmacological property offers distinct advantages in terms of drug development. As allosteric sites are subject to less evolutionary pressure than orthosteric sites which need to accommodate the endogenous ligands, allosteric sites are usually more divergent in amino acid sequences among receptor subtypes compared to the orthosteric sites (Christopoulos, 2014). Therefore targeting the allosteric site(s) might generate sub-type selective drug candidates where orthosteric sites are not amenable to selective drug development due to the very high sequence homology across receptor subtypes such as muscarinic acetylcholine receptors, metabotropic glutamate receptors, dopamine receptors etc (Hudson et al., 2013c; May et al., 2007). Unlike orthosteric agonism/antagonism, allosteric effects mediated by an allosteric ligand on orthosteric ligand affinity/efficacy reaches a saturating point depending on the cooperativity between two ligands which implies that after all the allosteric sites have been occupied by the allosteric ligand, no further allosteric effect will be observed irrespective of the concentration of the allosteric modulator (Keov et al., 2011; Kenakin and Miller, 2010). This property of saturability of allosteric effect would be advantageous as it will be more protective against overdose-mediated on-target toxicity (Wooten et al., 2013; Keov et al., 2011). While allosteric modulators displaying lower and limited cooperativity might be beneficial in terms of safety profile and fine tuning the physiological signalling which is advantageous in cases of a highly regulated physiological system (Keov et al., 2011; Christopoulos and Kenakin, 2002), this will concomitantly make the detection and validation of allosteric ligand pharmacology more challenging (Christopoulos, 2014). Pure PAMs also mimic physiological conditions in a sense that they will maintain the spatiotemporal nature of physiological signalling with concomitant potentiation of function of the endogenous ligand which will be beneficial in the cases of therapies against disorders associated with tightly regulated neurological or endocrine function including Alzheimer's disease, schizophrenia, acute and chronic central nociception etc (Burford et al., 2015; May et al., 2007). Another unique property of allosteric modulation is that the allosteric effect is probe dependent which implies that the magnitude and direction of allosteric effect will vary depending

on the nature of the orthosteric ligand used to probe the receptor function (Keov et al., 2011). Probe dependence implies that for the detection and validation of an allosteric modulator, it is necessary to investigate the allosteric effect of the defined modulator on each of the available endogenous agonists for the receptor. Allosteric modulation is also transducer dependent i.e an allosteric ligand might modulate (either potentiation or inhibition) a specific signalling pathway to the exclusion of others (Christopoulos, 2014). For example, the marketed drug cinacalcet acts as a PAM of calcium function at CaSR in intracellular calcium mobilization assay while it was shown to be a neutral allosteric ligand (NAL) in calcium-induced ERK1/2 phosphorylation (Leach et al., 2013). Finally, reciprocity of the allosteric effect is another unique property of allosterism which implies that the effect of allosteric modulator on binding affinity of an orthosteric agonist will be exactly the same as the effect of the orthosteric ligand on binding affinity of the modulator (May et al., 2007). Though targeting allosteric sites seems to present multiple therapeutic advantages, translation of allosteric pharmacology into therapeutics might face some challenges including potential difficulty in lead optimization process due to steep/flat structure activity relationship (SAR) as well as in preclinical studies due to potential species variation in allosteric effect which might stem from the more divergent allosteric sites across different species (Hudson et al., 2013c; Lindsley et al., 2016; Gentry et al., 2015).

1.5 Free fatty acid receptors (FFARs) as novel targets for drug development against inflammatory and metabolic disorders

Low-grade chronic inflammation plays a pivotal role in the pathogenesis of various chronic diseases (Minihane et al., 2015; Alvarez-Curto and Milligan, 2016) including type-2 diabetes and other metabolic disorders and various autoimmune diseases. The prevalence of these inflammation-associated diseases has been rising globally due to the modern diet containing nutritional overload, stressful and sedentary lifestyle, poor dietary habits etc and has been considered as a growing public health concern worldwide. Limited efficacy and selectivity, along with side effects of current anti-inflammatory agents have led researchers to develop more effective therapies for these disorders. In this regard, it has been suggested that G protein-coupled receptors (GPCRs) responsive to free fatty

acids (FFAs) would be an interesting area of research to develop drugs that can alleviate inflammatory conditions (Talukdar et al., 2011; Oh and Lagakos, 2011) as FFARs are considered to play critical roles in linking metabolism and immune functions (Alvarez-Curto and Milligan, 2016). Though previously free fatty acids were considered only as an energy source or as building blocks of cell membrane with the only intracellular targets being peroxisome proliferator activated receptors (PPARs) (long chain fatty acids) or histone deacetylase (short chain fatty acids), findings from extensive research conducted for the last two decades have established that free fatty acids can also act as signalling molecules by activating several cell surface GPCRs (Milligan et al., 2017b). These include the long chain and medium chain fatty acid sensing FFA1, short chain fatty acid sensing FFA2 and FFA3 and long chain saturated and polyunsaturated fatty acid sensing FFA4 (Milligan et al., 2017a; Milligan et al., 2017b; Husted et al., 2017; Davenport et al., 2013; Hara et al., 2013; Stoddart et al., 2008b; Brown et al., 2003; Hirasawa et al., 2005; Itoh et al., 2003; Le Poul et al., 2003). The signalling pathways, endogenous ligands and patho-physiological functions of these free fatty acid receptors are briefly shown in Table (1.1). FFA1 and FFA4 were shown to regulate insulin secretion and thus considered to be potential drug target for type II diabetes (Watterson et al., 2014; Kaku et al., 2015; Milligan et al., 2017a). B-arrestin-mediated FFA4 signalling in adipocytes and macrophages leads to anti-inflammatory effects (Alvarez-Curto and Milligan, 2016; Holliday et al., 2012) while FFA1 and FFA3 were reported to regulate inflammatory processes in gut and airways, respectively. Exploitation of these pathophysiological roles of FFA receptors might lead to potential drug development against different inflammatory and metabolic disorders (type II diabetes, obesity, inflammatory bowel diseases, ulcerative colitis etc). However, several FFA receptor-targeted agents including TAK-875 (Phase III clinical trial, diabetes) and JTT-851 (Phase II clinical trial, diabetes), AMG-837 and LY2881835 (Phase I, diabetes) and GLPG0974 (Phase II trial, ulcerative colitis) were withdrawn from clinical trials due to either toxicity or lack of efficacy, implying that further research to uncover the basic biology and pharmacology of these receptors are required to fully exploit them therapeutically.

Table 1-1 Brief overview of signalling pathways, physiological functions and clinical trial status of free fatty acid sensing GPCRs

| Receptor | Signalling pathways | Physiological functions | Free fatty acids as activators (carbon chain length) | Clinical trial status |
|----------------------|---|--|--|--|
| FFA1 (GPR40) | Gα _{q/11} * Gα _{i/o} β-arrestin-2 | i) Glucose stimulated insulin secretion (GSIS) from pancreatic β cells ii) Incretin (GLP-1) secretion from enteroendocrine cells iii) Anti-fibrotic activity | LCFA and MCFAs (C6-C22) Saturated, unsaturated | TAK-875 (partial agonist) in type II diabetes; discontinued from Phase III clinical trial due to liver toxicity; AMG-837 and LY2881835 removed from phase I trial (type II diabetes) due to toxicity PBI-4050 in idiopathic pulmonary fibrosis, pulmonary hypertension in heart failure with reduced ejection fraction (in phase II clinical trial, ongoing) |
| FFA2 (GPR43) | Gα _{i/o} * Gα _{q/11} β-arrestin | i) GLP-1 release from enteroendocrine cells ii) Inhibition of lipolysis in adipocytes iii) regulation of GSIS iv) Chemotaxis of neutrophils | SCFA (C1- C6) | GLPG0974 (antagonist) in ulcerative colitis, discontinued from phase II clinical trial due to lack of efficacy |
| FFA3 (GPR41) | Gα _{i/o} | i) Inhibition of GSIS ii) Regulation of inflammatory processes in airways | SCFA (C3-C7) | No clinical candidate yet |
| FFA4 (GPR120) | Gα _{q/11} β-arrestin-2 | i) Anti-inflammatory effects in gut and adipose tissue ii) incretin (GLP-1 and GIP) secretion iii) glucose uptake in adipocytes | LCFAs and MCFAs (C14-C22) Saturated and polyunsaturated FAs | No clinical candidate yet |
| GPR84 | Gα _{i/o} | Pro-inflammatory; Immunostimulatory Pro-fibrotic | MCFAs (C9-C14) (saturated) | GLPG1205 in IPF (Phase II clinical trial, ongoing), withdrawn from phase II clinical trial in ulcerative colitis due to lack of efficacy. PBI-4050 in IPF, type 2 diabetes associated with metabolic syndrome, Alstrom syndrome (phase II trial, ongoing) |

*the principal signalling pathway. This table is a modified version of the table shown in Alvarez-Curto and Milligan, (2016) with input from Watterson et al., (2014) and Milligan et al., (2017b).

1.6 G protein coupled receptor 84

1.6.1 Discovery of GPR84 and its basic characteristics

G-protein coupled receptor 84 (GPR84) (initially known as EX33 receptor) is a member of the seven transmembrane GPCR superfamily and belongs to the rhodopsin-like “Class A” family (Wittenberger et al., 2001). Tikhonova (2017) reported that phylogenetically GPR84 belongs to the prostanoid receptor subfamily of Class A GPCRs. Two groups of researchers independently identified GPR84 in 2001 using either an expressed sequence tag data mining approach (Wittenberger et al., 2001) or degenerate primer RT-PCR cloning from human neutrophils (Yousefi et al., 2001). GPR84 is localized to chromosome 12q13.13 in human and is composed of a single exon of 1191 bp encoding a protein of 396 amino acids (Wittenberger et al., 2001; Yousefi et al., 2001). Murine GPR84 is considered to be the orthologue of GPR84 as it bears 85% identity to human GPR84 in terms of amino acid sequence (Wittenberger et al., 2001). Both human and mouse GPR84 possess a short N-terminus and C-terminus with similar sequence identity while the ICL3 comprising 118 amino acid residues exhibits higher divergence between the two species (Wittenberger et al., 2001). Both these orthologues of GPR84 contain a conserved disulphide bridge between ECL1 and ECL2 (Wittenberger et al., 2001). Though GPR84 displays characteristic structural features similar to the rhodopsin like Class A family GPCRs, it contains G¹¹⁷RY motif in place of the conserved D(E)RY motif in the interface between TM3 and ICL2 (Yousefi et al., 2001; Wittenberger et al., 2001). Wittenberger et al. (2001) and Yousefi et al. (2001) found only slight homology between GPR84 and other well-known GPCRs and grouped it distantly with another orphan receptor, GPR85. GPR84 displays low sequence identity with the four characterized fatty acid sensing receptors (FFA1-4) and exhibits only 20% sequence homology with the well-studied B2-adrenergic receptor (Nikaido et al., 2015; Tikhonova, 2017). Sequence comparisons conducted by Brueggemeier et al. (2005) and Gaidarov et al., (2018) identified 26% homology between GPR84 and human D2 dopamine receptor. However, highest homology (31%) was found with the orexin 1 receptor (Tikhonova, 2017).

1.6.2 Tissue and cellular distribution of GPR84 expression

Using northern blot and Q-RT-PCR analysis, several groups (Wittenberger et al., 2001; Yousefi et al. 2001; Venkataraman and Kuo, 2005; Wang et al., 2006b; Lattin et al., 2008) have shown that in human and mouse, GPR84 expression is restricted primarily to immune-related tissues or cells including bone marrow, lymph nodes, thymus, spleen, lung and peripheral blood leucocytes such as monocytes/macrophage, neutrophils, eosinophils, T and B cells; implying that GPR84 might be associated with immunological functions. Among the immune cells, highest expression was observed in neutrophils followed by macrophages (Yousefi et al. 2001). Although resting expression was low, GPR84 expression was found to be induced strikingly under immunostimulation or inflammatory conditions (Figure 1.7). For example, treatment of monocytes/macrophages with a well-known inflammation inducer, lipopolysaccharide (LPS) resulted in significant enhancement of GPR84 expression (Wang et al., 2006b; Bouchard et al., 2007; Muller et al., 2017, Recio et al., 2018; Mancini et al., 2019). LPS-promoted strong upregulation of GPR84 was shown to be observed in all mouse macrophages including bone-marrow derived macrophages (BMDMs), resident peritoneal macrophages, and also in RAW264.7 cells, mouse microglial cells and human monocyte derived macrophages (hMDMs) (Recio et al., 2018). Microglia of the CNS also express GPR84 markedly in response to TNF- α and IL-1 in different neuro-inflammatory conditions such as endotoxemia and experimental autoimmune encephalomyelitis (EAE) (Bouchard et al., 2007) and based on this finding, it has been postulated by Bouchard and his colleagues that strong GPR84 up-regulation also might be found in CNS in other neuro-immunological disorders including brain injury, infection, cancer, and Alzheimer's disease where TNF- α and IL-1 production are augmented. These findings indicate a link between GPR84 and neuro-inflammatory diseases (Bouchard et al., 2007). However, GPR84 was not found to play any role in the disease progression of endotoxemia or EAE as no alteration in terms of clinical outcome was observed between GPR84 deficient mice and wild type mice (Audoy-Remus et al., 2015). Though basal expression level of GPR84 in adipocytes is very low compared to immune cells (monocytes/macrophages or neutrophils), GPR84 was reported to be upregulated in mouse adipocytes in response to TNF- α or LPS (Nagasaki et al., 2012). TNF α and IL1 β -mediated strong upregulation of GPR84 in human adipocytes was also reported by Muredda et al., (2018). Nagasaki et al., (2012)

proposed that upregulation of GPR84 by TNF- α is mediated by NF- κ B signaling pathways. This hypothesis was based on the observation that pre-treatment of adipocytes with the NF- κ B inhibitors BAY11-7082 or MG132 resulted in effective blockade of TNF α -induced upregulation of GPR84.

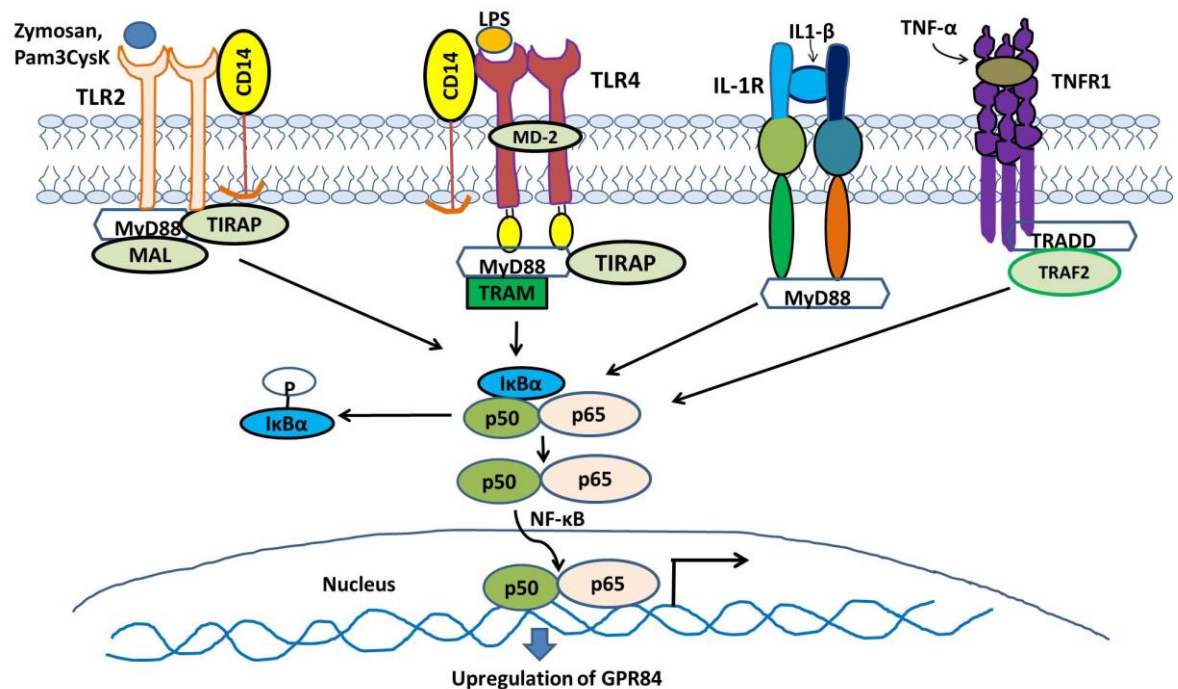


Figure 1.7 Marked upregulation of GPR84 in monocytes/macrophages upon immunostimulation or inflammatory conditions. GPR84 has been reported to be strongly upregulated in response to immunostimulants including the TLR4 agonist LPS, TLR2 agonists Zymosan and Pam3CysK and pro-inflammatory cytokines including IL-1 β and TNF- α . All these stimulants activate their corresponding receptors which signal through NF- κ B signaling pathway.

1.6.3 Putative endogenous agonists of GPR84

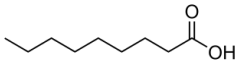
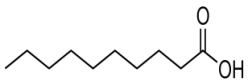
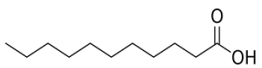
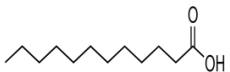
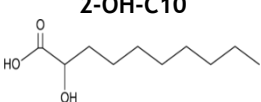
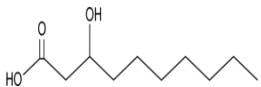
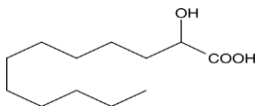
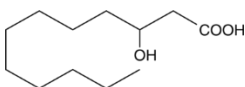
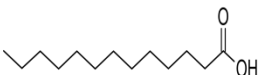

Using both [35 S]-GTP γ S binding and forskolin-stimulated cAMP assays, Wang et al. (2006b) for the first time reported that GPR84 is activated by medium chain fatty acids (MCFAs) with carbon chain lengths of 9 to 14, and among them decanoic acid (C10), undecanoic acid (C11) and lauric acid (C12) were shown to act most potently with EC₅₀ values of 5, 9, and 10 μ M and 4, 8, and 9 μ M, respectively, in the [35 S]-GTP γ S binding and the cAMP assays, respectively (Table 1.2). Suzuki et al. (2013) have shown that 2- and 3-hydroxy MCFAs have better potency than the respective non-hydroxylated fatty acids. Southern et al. (2013) also confirmed the agonism of MCFAs such as decanoic acid and undecanoic acid using a β -arrestin recruitment assay. In contrast, GPR84 does not respond to short-chain or long-chain saturated and unsaturated FFAs while these fatty acids

are agonists for GPR40/41/43/120 (Wang et al., 2006b; Talukdar et al., 2011). However, a patent literature search revealed that eicosa-5,8,11,14-tetraenoic acid and 5S,6R-dihydroxy-eicosa-7,9,11,14-tetraenoic acid also have agonistic activity towards GPR84 (Hakak et al., 2007). Southern et al., (2013) also reported that eicosatetraenoic acid activated GPR84 with higher potency and efficacy than decanoic acid in calcium mobilization assay using CHO cells co-expressing GPR84-HA and a chimeric protein $G\alpha_{qi(5)}$. These findings contradict the previous finding that GPR84 is not activated by long chain fatty acids. Further investigations are required to solve this discrepancy. Complete blockade of inhibition of forskolin-stimulated cAMP generation and [35 S]-GTP γ S binding by pre-treatment with pertussis toxin (PTX) confirmed that GPR84 activation mediated by MCFAs couples with $G_{i/o}$ proteins resulting in adenylyl cyclase inhibition and decreased intracellular cAMP levels (Wang et al., 2006b).

One of the major criteria of orphanization of a receptor is that to be a true endogenous ligand for the receptor, the tissue or circulating concentration of the ligand under physiological conditions should be enough to activate the receptor effectively (Davenport et al., 2013). For example, though the tryptophan derivative, kynurenic acid was proposed to be the endogenous agonist of GPR35 (Wang et al., 2006a), this pairing has been questioned by others (Jenkins et al., 2011; Milligan, 2011; Divorcy et al., 2015) as due to the low potency of this ligand at human GPR35, the circulating concentration of kynurenic acid would not be able to activate hGPR35 effectively. Similarly, MCFAs and hydroxylated-MCFAs should be considered as putative endogenous ligands of GPR84 as it remains uncertain whether these MCFAs are produced at concentrations required for GPR84 activation under physiological or pathological conditions (Suzuki et al., 2013; Mahmud et al., 2017; Recio et al., 2018; Gaidarov et al., 2018); although Wang et al. (2006b) maintained that after fatty meal intake, concentrations of the MCFAs would be increased to a level that could activate GPR84. The putative endogenous agonists MCFAs of carbon chain length 9-14 lack specificity towards GPR84 as they have also been shown to act as ligands for both FFA1(GPR40) and FFA4(GPR120) (Christiansen et al., 2015; Hirasawa et al., 2005; Itoh et al., 2003). Moreover, modes of binding of MCFAs are poorly defined and they possess low potency at GPR84 which suggests that they might act as surrogate agonists at GPR84 rather than the true endogenous

agonists. Due to the unavailability of radioligands developed against the binding sites shared by MCFAs, binding affinities for GPR84 are also lacking and the measured potency values reported by several groups cannot be used as surrogate measures of affinity due to the existence of receptor reserve in recombinant heterologous expression systems. Rapid metabolism of free fatty acids (Holliday et al., 2012) also remains a great challenge for using these compounds as tool compounds due to insufficient availability of the desired concentrations in biological compartments. These limitations (lack of selectivity, lower potency, and rapid metabolism) have made these MCFAs challenging to use as tool compounds for the *in vivo* characterization and elucidation of pharmacological properties of GPR84. Indeed Recio et al., (2018) and Sundqvist et al., (2018) reported that MCFAs generated poor biological responses in macrophages and neutrophils in terms of triggering electrical impedance and oxidative burst, respectively whereas the synthetic agonists 6-OAU and compound-1 were found to be highly effective, respectively.

Table 1-2 Potential endogenous agonists of GPR84

| Agonist | Source | Potency (EC ₅₀) | Comment |
|--|---|--|---|
| C-9  | Tropical oils | 52 μ M (cAMP accumulation assay) 70 μ M ([³⁵ S]-GTP γ S binding assay; Wang et al., 2006b) | Nonselective, also activates GPR40 and GPR120; Lower potency and undefined affinity Rapid metabolism Unsuitable to be used as tool compounds |
| C-10  | Tropical oils | 4.5 μ M (cAMP assay; Wang et al., 2006b) 4.6 μ M ([³⁵ S]-GTP γ S binding assay; Wang et al., 2006b) 15 μ M (biosensor-based BRET assay; Gagnon et al., 2018) 6.1 μ M (β -arrestin recruitment assay; Pillaiyar et al., 2017) | |
| C-11  | Tropical oils | 7.7 μ M (cAMP assay) 8.6 μ M ([³⁵ S]-GTP γ S binding assay; Wang et al., (2006b) | |
| C-12  | Tropical oils | 8.8 μ M (cAMP assay) 10.5 μ M ([³⁵ S]-GTP γ S binding assay; Wang et al., (2006b) | |
| 2-OH-C10  | formed by fatty acid 2-hydroxylase especially in brain | 31 μ M ([³⁵ S]-GTP γ S binding assay; Suzuki et al., 2013) 41 μ M (cAMP assay; Zhang et al., 2016) | |
| 3-OH-C10  | In vivo production by β -oxidation in peroxisomes | 230 μ M([³⁵ S]-GTP γ S binding assay; Suzuki et al., 2013) | |
| 2-OH-C12  | formed by fatty acid 2-hydroxylase mainly in the brain | 9.9 μ M ([³⁵ S]-GTP γ S binding assay) 40 μ M (chemotaxis of macrophages) Suzuki et al., 2013) | |
| 3-OH-C12  | In vivo production by β -oxidation in peroxisomes | 13 μ M ([³⁵ S]-GTP γ S binding assay; Suzuki et al., (2013) 24.2 μ M (chemotaxis of PMN) 40 μ M (chemotaxis of macrophages) 1.3 μ M (cAMP assay; Pillaiyar et al., 2018) 4.4 μ M (β -arrestin assay; Pillaiyar et al., 2018) | |
| C-13  | Tropical oils | 24.8 μ M (cAMP) 21.4 μ M (GTP γ S binding assay) Wang et al., (2006b) | |
| C-14  | Tropical oils | 93 μ M (cAMP) 14.4 μ M (GTP γ S binding assay) Wang et al., (2006b) | |

1.6.4 Natural product-derived agonists of GPR84: DIM and embelin

1.6.4.1 3, 3'-diindolylmethane (DIM)

Using [^{35}S]-GTP γ S binding assay employing a GPR84-G α_{i1} fusion protein, Takeda et al., (2003) for the first time identified that 3,3'-diindolylmethane (DIM), a metabolite of indole-3-carbinol, found in cruciferous vegetables acts as a moderately potent (EC_{50} : 11 μM) agonist of GPR84. DIM also was reported to be an allosteric agonist at GPR84 (Nikaido et al., 2015) and subsequently Pillaiyar et al., (2017) reported that DIM acts as a PAM agonist of C-10 potency and efficacy in cAMP assays in recombinant cells. Though the potency of DIM is greater than MCFAs, it is not highly selective as DIM possesses some off-target effects, displaying partial agonism at the CB2 receptor (Yin et al., 2009) and has been shown to be an activator of aryl hydrocarbon receptor (Yin et al., 2012) and estrogen receptor α (ER α) (Marques et al., 2014). Due to lower potency and off-target effects, DIM could not be used as pharmacological tool compounds to elucidate biological functions of GPR84.

1.6.4.2 Embelin

2,5-dihydroxy-3-undecyl-1,4-benzoquinone (embelin), a natural product obtained from fruits of *Embelia ribes* Burm (Lu et al., 2016) was identified as a GPR84 agonist by Hakak et al., (2007). Embelin has been reported to display moderate potency in a [^{35}S]-GTP γ S binding assay (EC_{50} : 0.54 μM ; Hakak et al., 2007), cAMP inhibition assay (EC_{50} : 0.8 μM ; Pillaiyar et al., 2017), β -arrestin recruitment assay (EC_{50} : 0.4 μM ; Pillaiyar et al., 2017) and in a biosensor-based BRET assay (EC_{50} : 10 μM). By contrast, Gaidarov et al., (2018) reported that embelin exhibited higher potency in forskolin-induced cAMP accumulation assays (EC_{50} : 89 nM) which was further supported by the observation that embelin triggered phosphorylation of ERK1/2 and Akt in IFN γ -primed human macrophages with potency of 3 and 78 nM, respectively. Gagnon et al., (2018) reported that embelin acted as a partial agonist in a G α_{i2} activation biosensor-based BRET assay and ERK1/2 phosphorylation assay compared to C-10. However, similar to DIM and MCFAs, embelin lacks selectivity towards GPR84 as it was reported to be an inhibitor of X-linked inhibitor of apoptosis protein (XIAP) (Nikolovska-Coleska et al., 2004; Mori et al., 2007; Hu et al., 2011; Ahn et al., 2007).

1.6.5 Synthetic surrogate agonists of GPR84

1.6.5.1 PSB-16671

Pillaiyar et al., (2017) developed some DIM analogues showing higher potency at human GPR84, which could be used as pharmacological tool compounds. Among them, di(5,7-difluoro-1H-indole-3-yl)methane or PSB-16671 was reported to be 6-fold more potent than its parent compound, DIM (Pillaiyar et al., 2017). PSB-16671 exhibited 132-fold lower potency in β -arrestin recruitment assays than that displayed in cAMP accumulation assays, suggesting it to be $G\alpha_i$ -pathway biased (Pillaiyar et al., 2017). Similar to DIM, PSB-16671 acts as an ago-allosteric modulator of decanoic acid functions at human GPR84 in forskolin-induced cAMP accumulation assays in recombinant cells. Unlike DIM, PSB-16671 was shown to be inactive at the aryl hydrocarbon receptor (AhR). Unlike MCFAs, PSB-16671 did not display any agonism at FFA1 and FFA4 (Pillaiyar et al., 2017). PSB-16671 was also found to be inactive at the phylogenetically related orphan receptor GPR35 at 10 μ M concentration (Pillaiyar et al., 2017). Due to this selectivity and higher potency than MCFAs and DIM, PSB-16671 could be used as a pharmacological tool compound to explore biological activities of GPR84.

1.6.5.2 6-n-octylaminouracil (6-OAU)

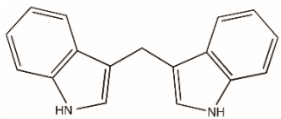
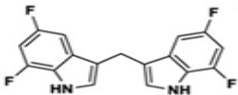
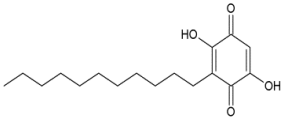
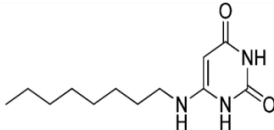
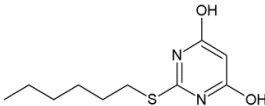
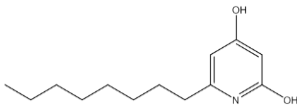
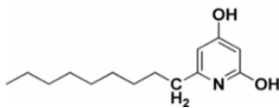
6-OAU was first identified by Suzuki et al., (2013) as a specific surrogate agonist of GPR84 by a high-throughput screening program using a [35 S]-GTP γ S binding assay employing a GPR84- $G\alpha_{i1}$ fusion protein. 6-OAU was reported to display significantly higher potency than the purported endogenous agonist, C-10 and allosteric agonist, DIM in both cAMP assays and [35 S]-GTP γ S binding assays (Suzuki et al., 2013; Zhang et al., 2016; Pillaiyar et al., 2018). 6-OAU has been shown to induce internalization of GPR84-EGFP at 6.25 to 200 μ M (Suzuki et al., 2013) and reported to trigger GPR84 desensitization and β -arrestin recruitment (Zhang et al., 2016). 6-OAU was also reported to inhibit forskolin-induced cAMP production in cultured mouse microglia in a concentration-dependent fashion which was effectively blocked by PTX treatment suggesting, $G\alpha_{i/o}$ -dependency of 6-OAU-mediated GPR84 signaling (Wei et al., 2017). 6-OAU produced robust microglial ruffling and motility in a GPR84-dependent manner which was evidenced from the complete abrogation of 6-OAU-mediated microglial ruffling and motility when microglia isolated from mice lacking functional GPR84 were

used. 6-OAU also displayed higher efficacy in promoting microglial ruffling and motility than C-10 and embelin (Wei et al., 2017). Specificity of 6-OAU was confirmed by Recio et al., (2018) based on the lack of any electrical impedance response representing cytoskeletal rearrangements in LPS-stimulated GPR84 KO macrophages while 6-OAU at 1-10 μ M concentrations produced robust impedance response in LPS-treated mouse BMDMs which was even higher than that produced by C5a. Compared to 6-OAU, the presumed endogenous agonists C-10, C-11 and C-12 were found to either inactive (C-10) or produced very weak impedance responses in mouse macrophages, implying that 6-OAU could be used as tool compound instead of weakly active MCFAs to explore biological functions of GPR84 (Recio et al., 2018).

1.6.5.3 Compound-1, compound-51 and TUG-1765

Using a high-throughput screening (HTS) program employing calcium mobilization assays in HEK293 cells stably expressing GPR84-HA and $G\alpha_{16}$ G-protein, Zhang et al., (2016) identified that 2-(hexylthio)pyrimidine-4,6-diol (ZQ-16 or compound-1) acts as a highly potent and selective agonist at GPR84. Compound-1 displayed similar efficacy but higher potency than 6-OAU in calcium mobilization and cAMP accumulation assays (Liu et al., 2016; Zhang et al., 2016). In an attempt to optimize the potency of compound-1, Liu et al., (2016) synthesized a set of derivatives among them 6-octylpyridine-2,4-diol (compound-50/TUG-1765) and 6-nonylpyridine-2,4-diol (compound-51). These acted as highly potent activators of GPR84 displaying EC_{50} of 1.34 and 0.189 nM, respectively in calcium mobilization assays (Liu et al., 2016). Compound-51 is by far the most potent agonist of GPR84 reported to date. Both compound-1 and compound-51 were reported to be highly selective agonist of GPR84 as both did not display any agonistic activity at other fatty acid sensing receptors, FFA1, FFA3, FFA4 and GPR119 (Zhang et al., 2016; Liu et al., 2016). Due to their high potency and selectivity, these compounds could be used as surrogate agonists for pharmacological and physiological characterization of GPR84.

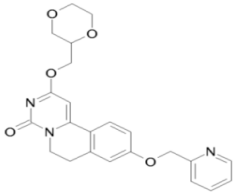
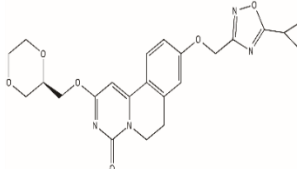
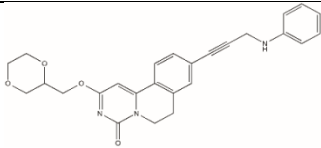
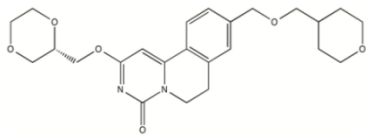
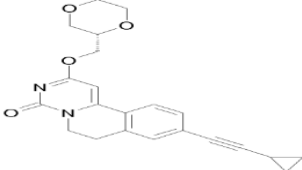
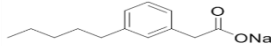
Table 1-3 Natural product-derived and synthetic surrogate agonists of GPR84

| Agonist | Potency (EC ₅₀) | Efficacy | Comments |
|--|---|---|--|
| DIM  | 0.5 μ M ([³⁵ S]-GTP γ S binding assay; Wang et al., 2006b) 1.1 μ M (cAMP assay; Zhang et al., 2016) 1.64 μ M (B-arrestin recruitment assay; Pillaiyar et al., 2017) | Partial agonist in B-arrestin recruitment assay | Non-selective; Off target effect: activator of aryl hydrocarbon receptor and ER α ; Partial agonist at CB2 receptor; Ago-allosteric modulator |
| PSB-16671  | 41.3 nM (cAMP assay; Pillaiyar et al., 2017) 5.47 μ M (B-arrestin recruitment assay; Pillaiyar et al., 2017) | Higher efficacy than C-10 | Selective ago-allosteric modulator; Biased towards G α_i pathway |
| Embelin  | 0.63 μ M ([³⁵ S]-GTP γ S binding assay; Mahmud et al., 2017) 0.8 μ M (cAMP assay; Pillaiyar et al., 2017) 0.4 μ M (B-arrestin assay; Pillaiyar et al., 2017) 10 μ M (biosensor-based BRET assay; Gagnon et al., 2018) | Partial agonist in BRET assay using G α_{i2} biosensor and in ERK1/2 phosphorylation assay | Non-selective Off-target effect: inhibitor of X-linked inhibitor of apoptosis protein (XIAP) |
| 6-OAU  | 512 nM (GTP γ S binding assays; Suzuki et al., 2013) 341 nM (cAMP assay; Zhang et al., 2016) 17 nM (cAMP assay; Pillaiyar et al., 2018) 110 nM (B-arrestin recruitment assay; Pillaiyar et al., 2018) | superagonist | Selective |
| Compound-1/ZQ-16  | 134 nM (cAMP assay; Zhang et al., 2016) 139 nM (Ca mobilization assay; Liu et al., 2016) 78 nM (B-arrestin recruitment assay; Pillaiyar et al., 2018) | superagonist | Selective Orthosteric to MCFAs |
| Compound-50 (TUG-1765)  | 1.34 nM (Ca mobilization assay; Liu et al., 2016) | superagonist | Selective |
| Compound-51  | 0.189 nM (Ca mobilization assay; Liu et al., 2016) 0.35 nM (cAMP assay; Liu et al., 2016) | superagonist | Selective, most potent agonist |

1.6.6 Synthetic GPR84 antagonists

Labeguere et al., (2014) synthesized a series of selective GPR84 antagonists (Table 1.4) which contain dihydropyrimidinoisoquinolinones as the core moiety of their chemical structure. Exemplars of these antagonists, compound-9, 104, 107 and 122 (GLPG1205) (2-([1,4]dioxin-2-ylmethoxy)-9-(pyridine-2-ylmethoxy)-6,7-dihydro-pyrimido[6,1-a]isoquinolin-4-one; 9-(5-cyclopropyl-[1,2,4]oxadiazol-3-ylmethoxy)-2-((R)-1-[1,4]dioxan-2-ylmethoxy)-6,7-dihydro-pyrimido[6,1-a]isoquinolin-4-one; 2-([1,4]dioxan-2-ylmethoxy)-9-(3-phenylamino-prop-1-ynyl)-6,7-dihydro-pyrimido[6,1-a]isoquinolin-4-one; 9-(2-cyclopropylethynyl)-2-[(2S)-1,4-dioxan-2-yl]methoxy]-6,7-dihydropyrimido[6,1-a]isoquinolin-4-one, respectively) were reported to display high potency (EC_{50} : 0.01-100 nM) in inhibiting DIM-induced [^{35}S]-GTP γ S incorporation into membranes of GPR84 expressing cells whilst compound-161 (2-((S)-1-[1,4]dioxan-2-ylmethoxy)-9-(tetrahydro-pyran-4-yl-methoxymethyl)-6,7-dihydro-pyrimido[6,1-a]isoquinolin-4-one) showed moderate potency (EC_{50} : 101-500 nM). All these ligands were shown to effectively antagonize embelin-induced human neutrophil chemotaxis displaying EC_{50} in the range of 0.01 to 100 nM (Labeguere et al., 2014). Compound-104, 107 and 161 were found to antagonize the effect of GPR84 agonist embelin and DIM with nanomolar potency and in a non-competitive manner (Mahmud et al., 2017). Recio et al., (2018) reported that compound-9 effectively blocked 6-OAU mediated GPR84 signaling including cAMP inhibition, cytokine expression, p65 nuclear translocation, phosphorylation of ERK1/2 and Akt etc. Sundqvist et al., (2018) also reported that GLPG1205 acted as highly potent antagonist of GPR84 activity displaying IC_{50} of 15 nM in inhibiting compound-1-mediated superoxide generation in human neutrophils. 3-pentylbenzeneacetic acid sodium (PBI-4050), a synthetic derivative of C-10 was reported to be a GPR84 antagonist/inverse agonist with pIC_{50} of 3.4 ± 0.06 (versus C-10) and 3.68 ± 0.28 (versus embelin) measured in BRET assay using HEK-293 cells transiently transfected with GPR84 and $G\alpha_{i2}$ activation biosensor (Gagnon et al., 2018). PBI-4050 also effectively blocked ERK1/2 phosphorylation induced by C-10 or embelin-mediated GPR84 activation in HEK293 cells expressing GPR84 (Gagnon et al., 2018). PBI-4050 was also found to decrease basal ERK1/2 phosphorylation level in these cells suggesting that it might act as an inverse agonist.

Table 1-4 Synthetic ligands acting as GPR84 antagonists

| GPR84 Antagonist | Structure | Potency (IC ₅₀) | Comment |
|-------------------------|---|---|---|
| Compound-9 |  | 0.01-100 nM([³⁵ S]-GTPγS binding assay, vs DIM; Labeguere et al., 2014) | Selective (Recio et al., 2018) |
| Compound-104 |  | 0.01-100 nM([³⁵ S]-GTPγS binding assay, vs DIM; Labeguere et al., 2014) | Noncompetitive with embelin and DIM (Mahmud et al., 2017) |
| Compound-107 |  | 0.01-100 nM([³⁵ S]-GTPγS binding assay, vs DIM) Labeguere et al., (2014) | Noncompetitive with embelin and DIM (Mahmud et al., 2017) |
| Compound-161 |  | 101-500 nM([³⁵ S]-GTPγS binding assay, vs DIM; Labeguere et al., 2014) | Noncompetitive with embelin and DIM (Mahmud et al., 2017) |
| GLPG1205 (compound-122) |  | 0.01-100 nM([³⁵ S]-GTPγS binding assay, vs DIM; Labeguere et al., 2014) 15 nM (ROS generation in neutrophils, versus compound-1; Sundqvist et al., 2018) | Selective (>1000-fold vs other FFARs) |
| PBI-4050 |  | 200-400 μM (BRET assay; Gagnon et al., (2018) | Very low potency; Might act as an inverse agonist; Nonselective, also agonist for FFA1(GPR40) |

1.7 GPR84-mediated signal transduction pathways

1.7.1 G-protein dependent signaling

Based on aequorin reporter-based calcium mobilization assay using chimeric G proteins in recombinant CHO cells, Wang et al., (2006b) demonstrated that agonist-activated GPR84 couples to PTX sensitive $G\alpha_{i/o}$ proteins but not to G_q , G_s or G_{16} G proteins. Using $G\alpha$ activation biosensors in BRET-based assays in transiently transfected HEK293 cells, Gagnon et al., (2018) also showed that C-10 and embelin-mediated GPR84 activation coupled effectively to $G\alpha_i$ proteins but not to $G\alpha_q$, $G\alpha_s$ or $G\alpha_{13}$. In contrast to the findings revealed by Gagnon et al., (2018), Gaidarov et al., (2018) reported that along with $G\alpha_{i/o}$ G protein, embelin-mediated GPR84 activation also resulted in $G\alpha_{12/13}$ coupling leading to Rho/Rac signaling pathways evidenced from the embelin-induced modest enhancement of intracellular cAMP levels in HEK cells co-transfected with GPR84 and chimeric G protein, $G\alpha_{s-G12(5)}$ or $G\alpha_{s-G13(5)}$ which was further amplified by pre-treatment of cells with $G\alpha_{i/o}$ protein inhibitor, PTX. The $G\alpha_{i/o}$ coupling mediated by agonist-bound GPR84 results in inhibition of adenylyl cyclase leading to reduction in intracellular cAMP levels in recombinant cells which was reported to be blocked completely by PTX treatment (Wang et al., 2006b; Zhang et al., 2016; Mahmud et al., 2017; Gaidarov et al., 2018; Gagnon et al., 2018; Recio et al., 2018). $G\alpha_i$ -mediated inhibition of adenylyl cyclase by GPR84 activation was further supported by the finding that compared to wild type macrophages, mouse GPR84 KO macrophages displayed markedly higher intracellular cAMP levels in response to forskolin induction (Nicol et al., 2015). In contrast to this, Gaidarov et al., (2018) reported that in human macrophages agonist-mediated GPR84 signaling did not lead to $G\alpha_i$ -mediated inhibition of adenylyl cyclase resulting in decreased production of intracellular cAMP, rather GPR84 activation resulted in elevated intracellular cAMP levels in human macrophages which was due to the $G\beta\gamma$ -mediated activation of adenylyl cyclase 4 and/7 along with COX2-dependent PGE_2 release which acted in an autocrine/paracrine fashion to stimulate the G_s -coupled receptor prostaglandin E receptor 2 (EP_2) ultimately enhancing cAMP level by stimulating adenylyl cyclase (Figure 1.8). This prediction was based on the observations that embelin and its derivatives amplified the G_s -coupled receptor agonist-mediated intracellular cAMP

accumulations in IFN γ -primed human macrophages, elevated intracellular cAMP levels on their own in macrophages which was effectively inhibited by pretreatment with COX2 inhibitor indomethacin and G α_i inhibitor PTX and triggered PGE2 release from IFN γ -induced human macrophages in a G α_i and COX2-dependent manner (Gaidarov et al., 2018). This G $\beta\gamma$ -mediated cAMP elevation was shown to be associated with induction of expression of ABCA1 and ABCG1 cholesterol transporters which enhance apo-A1 mediated reverse cholesterol transport in human macrophages (Gaidarov et al., 2018). In macrophages (Figure 1.8), monocytes and neutrophils (Figure 1.9), GPR84 activation also triggers non-canonical G $\beta\gamma$ -mediated PLC β -IP $_3$ -Ca signaling pathway which was evidenced from the concentration-dependent robust increase in intracellular calcium mobilization in IFN γ -primed human macrophages (Gaidarov et al., 2018) and in human neutrophils and monocytes (Sundqvist et al., 2018) following treatment with embelin and compound-1, respectively. Agonist-activated GPR84 was found to induce ERK1/2 phosphorylation in recombinant cells (Gagnon et al., 2018; Zhang et al., 2016). G α_i -mediated ERK1/2 phosphorylation and G $\beta\gamma$ -mediated and PI3-kinase dependent Akt phosphorylation were also induced in human and mouse macrophages following embelin and 6-OAU-mediated GPR84 activation (Gaidarov et al., 2018; Recio et al., 2018). Absence of GPR84-agonist-induced Ca flux, ERK1/2 and Akt phosphorylation in macrophages or neutrophils derived from GPR84 deficient mice (Gaidarov et al., 2018; Recio et al., 2018) and PTX-induced abrogation of ERK1/2 and Akt phosphorylation confirmed the GPR84 dependency of stimulation of these pathways. These patterns of GPR84-mediated signaling are very similar to that displayed by chemotactic receptors. Recio et al., (2018) have shown that 6-OAU-stimulated GPR84 activation resulted in NF- κ B activation in LPS-induced mouse macrophages which was evidenced from the significant increase in nuclear translocation of p65 subunit of NF- κ B heterodimer in wild type BMDM but not in GPR84 deficient macrophages. Recio and colleagues (2018) proposed that activation of NF- κ B pathway by GPR84 signaling resulted in enhanced expression of pro-inflammatory mediators from LPS-induced macrophages. PTX pretreatment blocked the 6-OAU-mediated upregulation of pro-inflammatory cytokines (TNF α , IL-6, IL-12) and chemokines (CCL2, CCL5, CXCL1) in LPS-treated mouse BMDMs which suggests G $_{i/o}$ -dependency of pro-inflammatory effects. Contrary to the finding reported by Recio et al., (2018),

Park et al., (2018) observed down-regulation of RANKL-induced NF- κ B signaling pathway in osteoclast precursor cells, BMDMs.

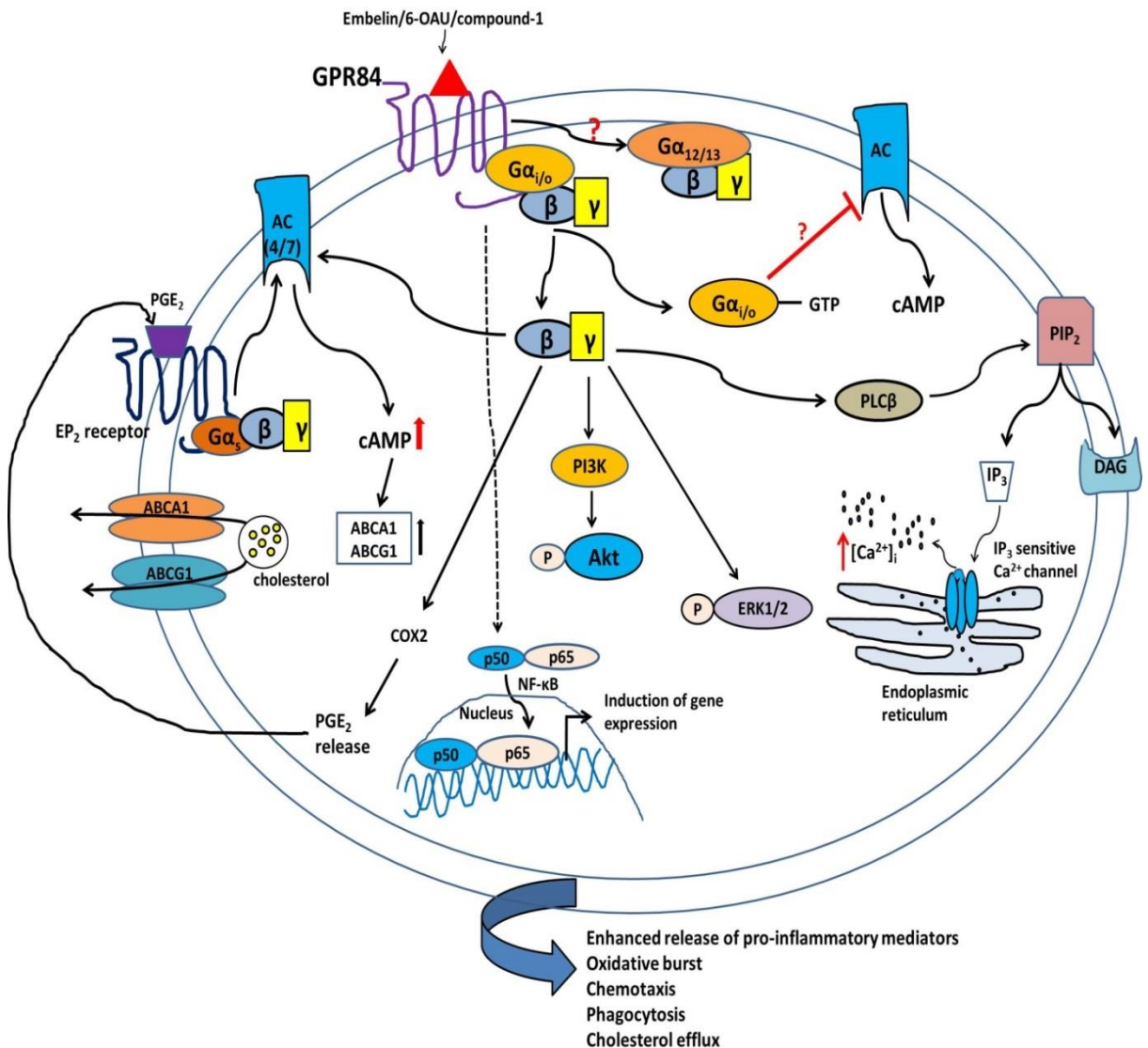


Figure 1.8 Proposed GPR84-mediated signaling pathways and associated patho-physiological outcomes in macrophages. In macrophages, agonist-activated GPR84 couples to Gα_{i/o} G proteins resulting in either Gα_i-mediated adenylyl cyclase inhibition leading to decreased intracellular cAMP production (Nicol et al., 2015) or Gβγ-mediated activation of adenylyl cyclase 4/7 resulting in increased intracellular accumulation of cAMP (Gaidarov et al., 2018). Gβγ also leads to COX2 dependent prostaglandin E2 release which acts in an autocrine manner to activate Gs-coupled EP2 receptor resulting in activation of AC4/7 enzyme ultimately promoting accumulation of cAMP. These elevated cAMP levels result in enhanced expression of ATP binding cassette transporter, ABCA1 and ABCG1 which enhances cholesterol efflux in macrophages. GPR84 activation also triggers Gβγ-mediated phosphorylation of extracellular signal-regulated kinases ERK1/2 and activation of phosphoinositide 3-kinases (PI3K) leading to Akt phosphorylation. Gβγ signaling also includes stimulation of phospholipase Cβ (PLCβ) which catalyzes hydrolysis of phosphatidylinositol 4,5-bisphosphate (PIP₂) into diacylglycerol and inositol 1,4,5-trisphosphate (IP₃). IP₃ triggers calcium mobilization by acting on IP₃-sensitive calcium channel on endoplasmic reticulum. Gα_i coupling was also shown to be engaged in enhanced nuclear translocation of NF- κ B which is associated with enhanced expression of pro-inflammatory mediators in macrophages.

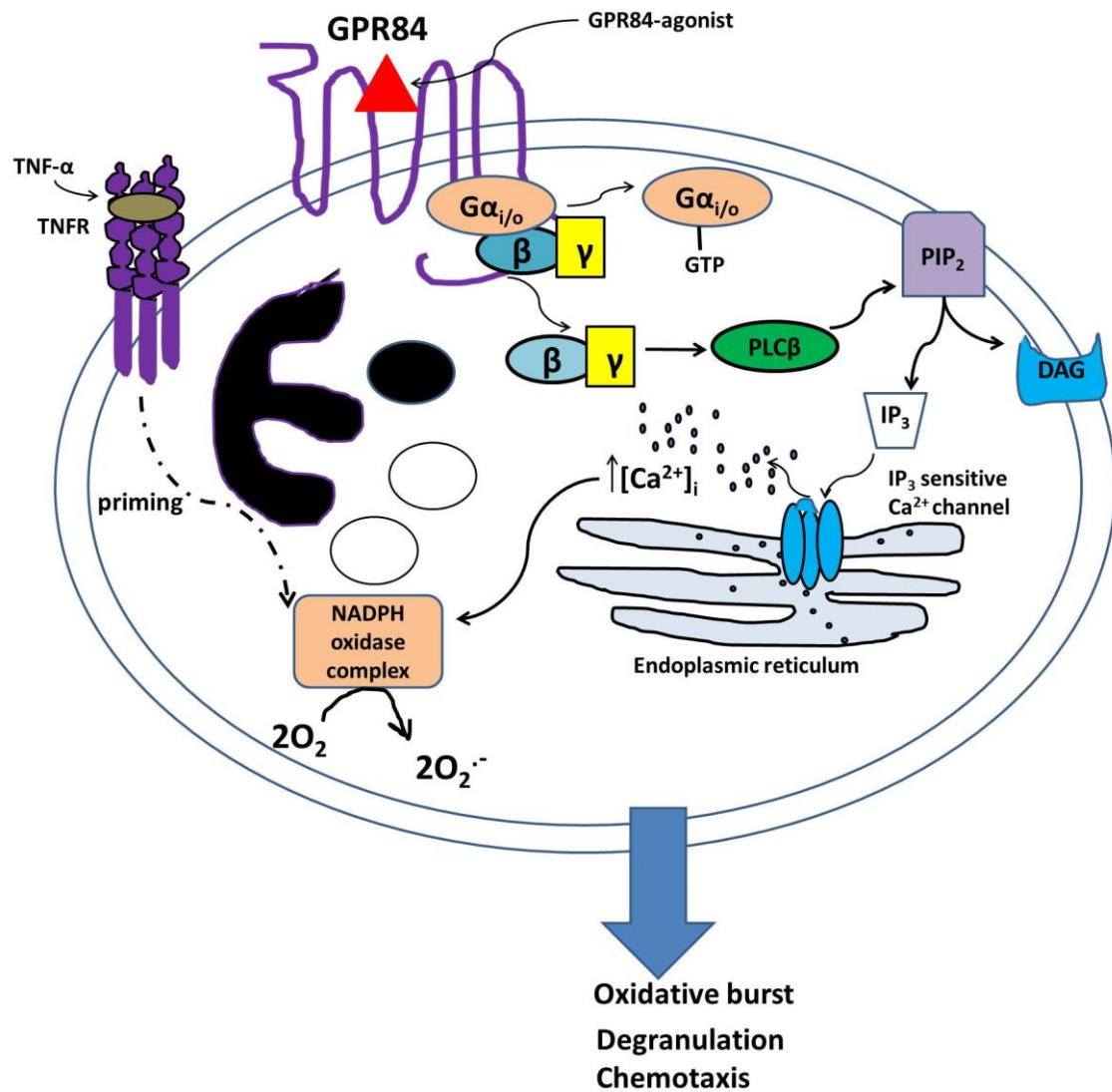


Figure 1.9 GPR84 signaling and its patho-physiological outcomes in neutrophils. In neutrophils agonist-stimulated GPR84 couples to PTX sensitive Gα_{i/o} G proteins and induces Gβγ-mediated activation of PLCβ-IP₃-Ca²⁺ signal transduction pathway resulting in triggering a robust calcium flux which is associated with an increased assembly of NADPH-oxidase on plasma membrane of the phagosome, enhanced granule mobilization and secretion and chemotaxis of neutrophils. Complete abrogation of compound-1-mediated superoxide release from TNF-α or latrunculin treated-human neutrophils following treatment with PTX but not with G_q inhibitor, YM-254890 was indicative of Gα_i dependency of GPR84-induced ROS generation in neutrophils (Sundqvist et al., 2018). Pro-inflammatory cytokine TNF-α amplifies the superoxide release mediated by GPR84 activation.

1.7.2 G-protein-independent signaling

Apart from G-protein-dependent signaling, GPR84 activation was also shown to induce G-protein independent signaling pathways such as β-arrestin recruitment, although details are lacking. Southern et al., (2013) for the first time reported that MCFAs including decanoic acid and undecanoic acid and the natural product-derived embelin induced robust β-arrestin recruitment towards GPR84 in CHO cells. Agonist-mediated β-arrestin recruitment towards GPR84 was then further observed in recombinant cells by other groups (Zhang et al., 2016;

Pillaiyar et al., 2017; Pillaiyar et al., 2018). Recently, Pillaiyar et al., (2017) reported that some DIM analogues including di(7-azaindolyl)methane, 10-ethyl-diindolylmethane, 10-propyl-diindolylmethane and 10-isobutyl-diindolylmethane are absolutely biased toward β -arrestin recruitment over $G\alpha_i$ -mediated adenylyl cyclase inhibition whereas Pillaiyar et al., (2018) identified a $G\alpha_i$ -pathway selective biased GPR84 agonist, PSB-16434, a 6-OAU derivative which displayed a bias factor of 1.9.

6-OAU and compound-1 were shown to produce robust GPR84 internalization and desensitization (Zhang et al., 2016) and authors argued that agonist-mediated internalization and desensitization might be due to β -arrestin2 recruitment to the activated receptor. Until now, detailed mode and regulation of GPR84 internalization and desensitization are not available. However, Sundqvist et al., (2018) reported that desensitization of compound-1-mediated GPR84 signaling is independent of the actin cytoskeleton.

1.8 Physiological functions and pathophysiological roles of GPR84

1.8.1 Immunostimulatory and pro-inflammatory activities mediated by GPR84

Some groups of researchers have demonstrated an association between GPR84 and inflammation indicating a role of GPR84 in the crosstalk between the metabolism of fatty acids and immunological regulation (Figure 1.10). In a study conducted by Wang et al. (2006b), it was found that GPR84 activation by MCFAs and the allosteric modulator DIM significantly and concentration-dependently elevated the secretion of the pro-inflammatory cytokine, IL-12-p40 subunit from RAW264.7 macrophages following immunostimulation such as LPS treatment. The up-regulation of this cytokine is responsible for the promotion of Th1 reactions and inhibition of Th2 reactions and thereby mediates the immune functions of the receptor by eradicating pathogenic microorganisms (Wang et al., 2006b). GPR84 activation mediated by 6-OAU and hydroxylated MCFAs has also been shown to mediate amplification of secretion of other pro-inflammatory mediators such as TNF- α and IL-8 from human macrophages and neutrophils, respectively upon stimulation with LPS (Suzuki et al., 2013). Role of GPR84 in

regulating expression of pro-inflammatory mediators was also supported by the observation that 6-OAU-stimulated GPR84 activation resulted in enhanced upregulation of TNF- α , IL-6, IL-12p40, CCL2, CCL5, CXCL1, FC γ R1 and ICAM-1 in LPS-primed mouse peripheral macrophages but not in GPR84 deficient macrophages and these effects of 6-OAU were completely counteracted by the selective GPR84 antagonist, compound-9 (Recio et al., 2018). GPR84-mediated upregulation of chemokines including CXCL1 was also confirmed by an in vivo study which showed marked increase in blood level of CXCL1 following intravenous injection of 6-OAU into rats (Suzuki et al., 2013). Absence of any upregulation of pro-inflammatory mediators in macrophages which were not pre-stimulated with LPS, suggested that 6-OAU or MCFAs-promoted enhanced expression of pro-inflammatory cytokines and chemokines in macrophages are mediated by GPR84 signaling and LPS acts to upregulate GPR84 expression in these cells (Wang et al., 2006b; Suzuki et al., 2013; Recio et al., 2018).

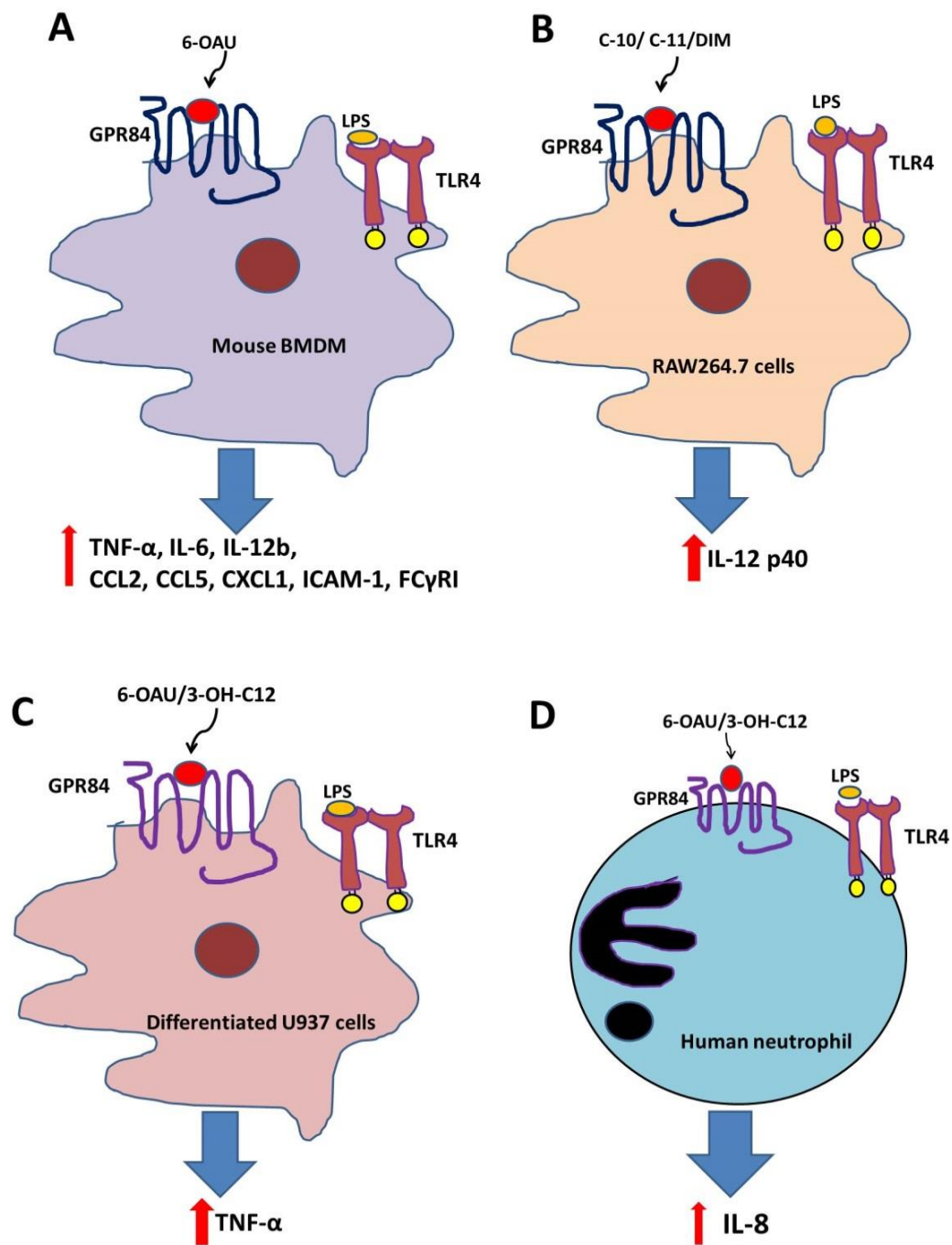


Figure 1.10 Agonist-activated GPR84 signaling generates a pro-inflammatory macrophage phenotype. 6-OAU-mediated GPR84 activation results in enhanced upregulation of pro-inflammatory cytokines TNF- α , IL-6, IL-12b, chemokine CCL2, CCL5 and CXCL1 and adhesion molecule ICAM-1 and scavenger receptor FC γ RI in LPS-treated mouse macrophages (A) (Recio et al., 2018). MCFAs including C-10, C-11 and C-12 and allosteric agonist DIM were reported to amplify upregulation (both mRNA and protein levels) of pro-inflammatory cytokine IL-12p40 in LPS-stimulated RAW264.7 mouse macrophages (B) (Wang et al., 2006b). GPR84 activation mediated by 6-OAU and hydroxylated MCFAs including 3-OH-C12 also results in enhanced secretion of pro-inflammatory cytokine, TNF- α from LPS-treated differentiated U937 cells (C) and IL-8 from LPS-induced human neutrophils (D) (Suzuki et al., 2013).

Gene knockout studies in mice revealed that GPR84 deficiency leads to up-regulation of anti-inflammatory Th2 cytokines and down-regulation of pro-inflammatory cytokines (Figure 1.11). Under neuropathic conditions, compared

to wild type macrophages, LPS-induced GPR84 KO peripheral macrophages displayed lower induction of pro-inflammatory mediators, TNF- α , IL-6, IL-1 β , IL-12 p40, Nos2, Ptges2, CCL2, CCL3 and higher expression of anti-inflammatory cytokine IL-10 (Nicol et al., 2015). In response to nerve injury, compared to wild type macrophages, forskolin-stimulated GPR84 KO macrophages (both BMDM and peritoneal macrophages) also produced significantly higher level of intracellular cAMP levels which is consistent with the fact that GPR84 is coupled to G $\alpha_{i/o}$ proteins (Nicol et al., 2015). Moreover, significantly higher induction of anti-inflammatory arginase-1 and IL-10 were observed in injured sciatic nerve of GPR84 KO mice than that of wild type littermates (Nicol et al., 2015). As the enzyme, arginase-1 (Arg-1) is downstream of cAMP, inhibition of cAMP production by activation of GPR84 leads to decreased activation of Arg-1, resulting in amplification of pro-inflammatory M1 macrophage polarization (Nicol et al., 2015). Based on these findings Nicol et al., (2015) proposed that GPR84 deficiency leads to generation of anti-inflammatory macrophages phenotype (M2 macrophages/alternatively activated) whilst GPR84 activation produces pro-inflammatory macrophage phenotype (M1 macrophages/classically activated). Gaidarov et al., (2018) also reported that GPR84 deletion led to markedly reduced secretion of pro-inflammatory mediators including IL-6, KC-GRO α , VEGF, macrophage-inflammatory protein2 (MIP-2) and neutrophil gelatinase associated lipocalin (NGAL) from LPS-treated peritoneal exudates containing macrophages, neutrophils and B/T cells compared to wild type exudates. Consistent with these findings, anti-CD3-induced secretion of IL-4 from CD4⁺ T cells was strikingly up-regulated in GPR84 KO mice, which is suggestive of a role of GPR84 in the regulation of IL-4 gene expression (Venkataraman and Kuo, 2005). Venkataraman and Kuo (2005) also reported elevated expression of anti-inflammatory Th2 cytokines such as IL-4, IL-5 and IL-13 in Th2 effector cells of GPR84 deficient mice compared to those from WT mice. All these findings suggest that GPR84 may cause disruption in Th1/Th2 balance by promoting Th1 cytokine production and down-regulating Th2 cytokine secretion and thus might be involved in the pathogenesis of Th1 type diseases (Yonezawa et al., 2013). Although Th1 responses are essential for pathogen eradication, excessive Th1 responses may have serious consequences that lead to aggravation of autoimmune diseases and inflammatory disorders such as multiple sclerosis, IBD, rheumatoid arthritis etc (Wang et al., 2006b).

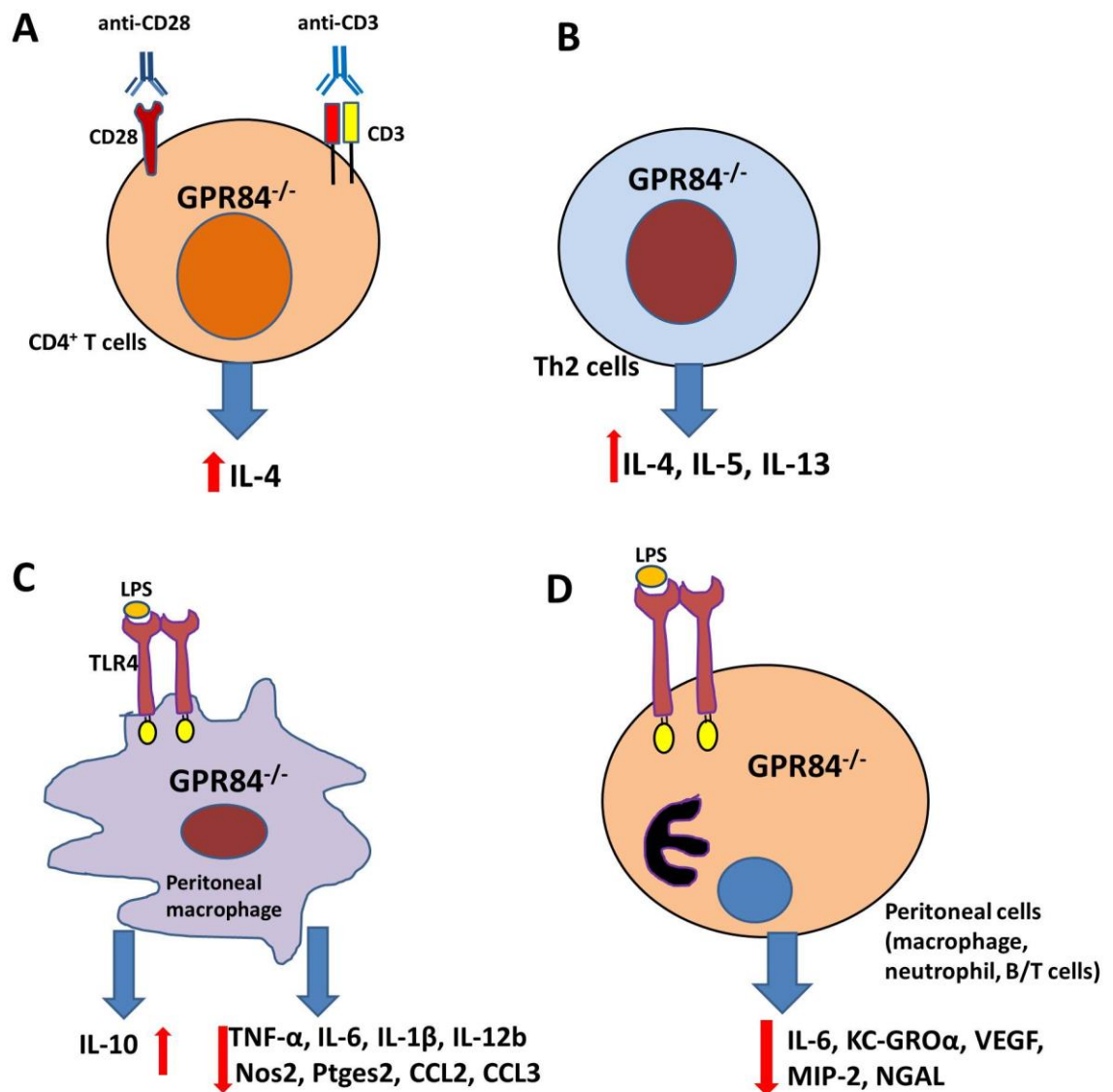


Figure 1.11 GPR84 deficiency in mice leads to Th2 shift and generates an anti-inflammatory macrophage phenotype. Gene knockout studies in mice performed by Venkataraman and Kuo, (2005) revealed that GPR84 deficiency led to amplification of secretion of anti-inflammatory cytokine IL-4 from anti-CD3 and anti-CD28-induced CD4⁺ T lymphocytes (A) and of IL-4, IL-5 and IL-13 from Th2 effector cells (B) compared to those of WT mice. Attenuated expression of pro-inflammatory mediators including TNF-α, IL-1β, IL-6, IL-12b, Nos2, Ptges2, CCL2 and CCL3 and higher expression of anti-inflammatory cytokine, IL-10 in GPR84 deficient macrophages (C) and marked reduction in secretion of pro-inflammatory mediators including IL-6, KC-GROα, VEGF, MIP-2 and NGAL from peritoneal exudates of GPR84 KO mice (D) were reported by Nicol et al., (2015) and Gaidarov et al., (2018), respectively.

The pro-inflammatory activities of GPR84 have also been confirmed by the fact that the surrogate agonist, 6-OAU strongly induces chemotaxis of human neutrophils and macrophages in a GPR84-dependent manner in both the in vitro “Transwell assay” and in vivo rat air pouch model (Suzuki et al., 2013). The patent literature also demonstrates the role of GPR84 in chemotaxis of immune cells including neutrophils, macrophages and dendritic cells and shows that GPR84 antagonists including GLPG1205 prevent this chemotaxis effectively (Brys

and Dupont, 2013). Though Suzuki et al., (2013) reported that 6-OAU and hydroxylated MCFAs including 2-OH-C12 and 3-OH-C12 induced robust chemotaxis of PMA-treated U937 cells (human model macrophages) in a PTX-sensitive $G\alpha_{i/o}$ pathway dependent manner, Recio et al., (2018) did not find any chemotaxis of mouse bone marrow derived macrophages (BMDMs) in response to 6-OAU-mediated GPR84 activation, although 6-OAU was found to significantly amplify C5a-mediated chemotaxis of macrophages. Gaidarov et al., (2018) also reported that embelin-mediated GPR84 activation induced human neutrophil chemotaxis. However, embelin displayed low potency in neutrophil chemotaxis (micromolar range) which is consistent with its low potency in calcium signaling assay.

Consistent with the fact that agonist-mediated GPR84 signaling exacerbates inflammatory responses in macrophages as evidenced from augmented expression of pro-inflammatory cytokine and chemokines, Recio et al., (2018) found that 6-OAU-mediated GPR84 activation resulted in enhanced bacterial adhesion and phagocytosis by macrophages, which confirmed the role of GPR84 in inflammatory and immunostimulatory activities. 6-OAU-mediated promotion of bacterial adhesion to mouse macrophages was absent in GPR84 KO mice and completely blocked by the GPR84 antagonist, compound-9 and Recio and colleagues (2018) argued that this enhanced bacterial adhesion was due to the marked upregulation of FcγR1 in macrophages. Similarly, 6-OAU-promoted marked enhancement of phagocytosis of *E. coli* and opsonized polystyrene beads by macrophages was effectively hindered by pre-treatment of cells with GPR84 antagonist compound-9 and GPR84 KO macrophages were unable to display phagocytosis of *E. coli* and opsonized beads, confirming the GPR84 dependency of these pro-inflammatory activities (Recio et al., 2018). Wang et al., (2019) also reported that zebrafish GPR84 overexpression led to marked enhancement in phagocytosis of *E. coli* and *S. aureus* by RAW264.7 mouse macrophages, confirming the role of GPR84 in immune reactions.

Similar to macrophages, GPR84 also modulates neutrophil biology by promoting immune reactions or exacerbating inflammatory responses in neutrophils which was evidenced from the observations that compound-1-activated GPR84 signaling in neutrophils resulted in enhanced chemotaxis of neutrophils along with enhanced granule mobilization and secretion and ROS generation from

neutrophils, activities associated with immunological processes such as phagocytosis of microorganisms (Sundqvist et al., 2018). Agonist-mediated GPR84 activation was also found to potentiate the fMLP and C5a-mediated ROS generation from neutrophils (Gaidarov et al., 2018). While compound-1-mediated GPR84 activation triggers robust intracellular calcium flux in human neutrophils and monocytes to an extent equivalent to that generated by the formyl peptide receptor1 (FPR1) agonist, fMLP, compared to fMLP, compound-1 displayed significantly lower efficacy in inducing NADPH-oxidase-promoted superoxide production, granule mobilization and secretion and in chemotaxis assay (Sundqvist et al., 2018). These findings imply that though GPR84 mediates degranulation and chemotaxis of human neutrophils and thus acts as a chemoattractant receptor, compared to fMLP-FPR1 system, the GPR84-compound-1 axis acts as a weak secretagogue and chemoattractant for human neutrophils. However, Mancini et al., (2019) reported that the extent of mouse neutrophil chemotaxis triggered by compound-1-mediated GPR84 activation was very similar to that generated by fMLP. Overall, these studies provide strong evidence for the immune functions and pro-inflammatory activities of GPR84 and suggest that GPR84 is an important player in mediating crosstalk between metabolism and immunological processes (immunometabolism).

1.8.2 GPR84 is a potential novel target for drug development against chronic inflammation-associated diseases

Based on the discussions presented in section 1.8.1, it is evident that GPR84 mediates inflammatory responses in macrophages and neutrophils or can exacerbate established inflammation. Therefore, inhibition of GPR84-mediated pro-inflammatory activities might be an effective treatment strategy for chronic inflammation-associated diseases including ulcerative colitis, IBD, rheumatoid arthritis, chronic inflammatory arthritis, atherosclerosis, reflux esophagitis etc (Labeguere et al., 2014; Suzuki et al., 2013; Gaidarov et al., 2018). It is predicted that the highly restricted expression pattern in immune cells and strong up-regulation of GPR84 under inflammatory conditions may lead to the development of more selective and less toxic GPR84 modulators compared to established anti-inflammatory agents (Bouchard et al., 2007).

In a study investigating the pathophysiology of reflux esophagitis, Abdel-Aziz et al. (2016) reported strong upregulation of GPR84 in rat and human esophageal epithelial cells during esophagitis suggesting a causal relationship between GPR84 and esophagitis. Marked upregulation of GPR84 in the areas of macrophage infiltration in synovial tissue in rheumatoid arthritis was reported by Hakak et al., (2007) suggesting the potential role of GPR84 in the pathogenesis of rheumatoid arthritis. These reports of strong upregulation of GPR84 during diseased conditions imply that therapies targeting GPR84 will be advantageous in terms of displaying favorable safety profile.

1.8.2.1 GPR84, a novel target for drug development against ulcerative colitis

Due to the strong upregulation of GPR84 in ulcerative colitis (Dupont et al., 2015) and potential role of GPR84-mediated inflammatory activities including neutrophil chemotaxis in the pathogenesis of ulcerative colitis, recently GPR84 inhibition has attracted considerable interest as a novel therapeutic strategy to develop drugs to treat ulcerative colitis and Galapagos NV, a Belgian pharmaceutical company, performed some preclinical and clinical studies using the GPR84 antagonist, GLPG1205. GLPG1205 was found to effectively prevent disease progression in a chronic DSS (dextran sodium sulfate)-induced mouse colitis model with effective blockade of macrophage and neutrophil chemotaxis (Dupont et al., 2015) and displayed a satisfactory safety profile and target engagement in healthy human volunteers in a Phase I clinical trial (Vanhoutte et al., 2015). However no clinical efficacy was found in a phase II clinical trial in ulcerative colitis patients (Vermiere et al., 2017) suggesting that either GPR84 is not associated with the pathogenesis of ulcerative colitis or further studies are required in terms of physiological and pharmacological characterization of this enigmatic receptor.

1.8.2.2 GPR84 is a potential target for development of drugs against atherosclerosis

Gaidarov et al., (2018) reported that embelin-mediated GPR84 activation resulted in significant upregulation of the cholesterol transporters ABCA1 and ABCG1 in human macrophages which are involved in apolipoproteinA1-mediated cholesterol efflux. Due to this higher expression of cholesterol transporters, the GPR84 agonist embelin was found to promote 4-fold enhancement in reverse

cholesterol transport in human macrophages (Gaidarov et al., 2018). Patent literature also revealed that embelin decreased the atherosclerotic lesions/plaque size in apolipoprotein E KO (ApoE^{-/-}) mice, an animal model of atherosclerosis (Hakak et al., 2007). Hakak et al., (2007) argued that embelin-promoted inhibition of atherogenesis in the animal model was due to the upregulation of ABCA1 and downregulation of MCP-1 in macrophages in response to embelin-stimulated GPR84 activation because decreased expression of ABCA1 and increased expression of MCP-1 were reported to be associated with pathogenesis of atherosclerosis (Dawson et al., 2003; Aiello et al., 1999; Van Eck et al., 2006). These findings suggest that GPR84 stimulation can be exploited therapeutically for the development of anti-atherosclerotic drugs. Recio et al., (2018) observed that under hypercholesterolemia, apolipoprotein E deficient mice (ApoE^{-/-}) displayed significantly higher expression of GPR84 mRNA in aortic tissue and oxidized LDL-treated human monocyte-derived macrophages showed strong upregulation of GPR84. Based on these findings, Recio et al., (2018) predicted that infiltrating macrophages upregulates GPR84 in atherosclerotic lesions which might be associated with the pathogenesis of atherosclerosis. This is contrary to the anti-atherosclerotic properties of GPR84 activation mediated by embelin reported by Gaidarov et al., (2018), and this dichotomy is clearly worthy of further investigation.

1.8.3 Potential role of GPR84 in neuro-immune and neuro-inflammatory processes

1.8.3.1 Role of GPR84 in chronic neuropathic pain

Nicol et al. (2015) explored for the first time whether GPR84 plays an important role in mediating chronic neuropathic nociception and if this could be exploited to develop an effective treatment for chronic neuropathic pain. Significant upregulation of GPR84 in sciatic nerve and spinal cord of wild type mice at 7 and 21 days after peripheral nerve injury indicates the potential role of GPR84 in mediating neuropathic chronic pain, which was further supported by the loss of mechanical and thermal hypersensitivity towards chronic neuropathic pain in GPR84 deficient mice whereas wild type mice displayed elevated hypersensitivity in response to nerve injury (Nicol et al., 2015). Nicol and colleagues (2015) argued that this lack of neuropathic chronic pain in GPR84 KO

mice was due to the marked reduction in peripheral macrophages-mediated inflammatory responses which was evidenced from the observation that GPR84 deletion led to significant attenuation of LPS-induced upregulation of pro-inflammatory mediators including TNF- α , IL-1 β , IL-6, IL-12b, nitric oxide synthase 2 (NOS2), prostaglandin E synthase 2 (PTGES2), CCL2, CCL3 in macrophages compared to wild type mice.

1.8.3.2 Role of GPR84 in regulating microglia biology

Strong upregulation of GPR84 in microglia in response to inflammatory stimulation (TNF- α , IL-1 β) (Bouchard et al., 2007; Bedard et al., 2007) or under pathological conditions including neuronal injury (Wei et al., 2017; Nicol et al., 2015), endotoxemia and experimental autoimmune encephalomyelitis (Bouchard et al., 2007) or Alzheimer's disease (Audoy-Remus et al., 2015) suggests that GPR84 might be a potential mediator of neuroinflammation. In contrast to this prediction, GPR84 was not found to regulate pro-inflammatory responses in microglia (Wei et al., 2017; Nicol et al., 2015). Nicol et al., (2015) observed no alteration between GPR84 KO and wild type mice in terms of microgliosis and microglial activation following peripheral nerve injury. Consistent with this finding, Wei and colleagues (2017) observed that treatment of LPS-induced mouse microglia with GPR84 surrogate agonist 6-OAU did not result in any upregulation of pro-inflammatory mediators such as IL-1 β , IL-6, IL-12p40, TNF- α , iNOS, CXCL1 whereas strong upregulation of these mediators in LPS-stimulated mouse bone marrow-derived macrophages were reported by Recio et al., (2018), suggesting that GPR84 activation did not generate any pro-inflammatory response in microglia. This was further supported by the absence of nuclear translocation of NF- κ B subunit p65 in response to agonist-mediated GPR84 activation in LPS-induced mouse microglia (Wei et al., 2017) whilst Recio et al., (2018) reported 6-OAU-induced strong nuclear translocation of this NF- κ B subunit in LPS-stimulated BMDMs. As NF- κ B transcription factor is thought to be responsible for induction of pro-inflammatory cytokines (Sun and Ye, 2012), lack of activation of this pathway in microglia following treatment with GPR84 agonists (6-OAU, embelin and C-10) is in agreement with the observation that GPR84 is not associated with inflammatory responses mediated by microglia. However, GPR84 activation was found to mediate microglial motility and ruffling in a $G\alpha_{i/o}$ pathway dependent manner as 6-OAU, embelin and C-10, each induced

robust membrane ruffling and motility of mouse microglia and 6-OAU-promoted motility was completely blocked by PTX pre-treatment (Wei et al., 2017). Recently, based on gene knock out studies in a mouse model of Alzheimer's disease, Audoy-Remus et al., (2015) reported a beneficial role of microglial GPR84 in preventing cognitive decline during neurodegenerative disorders. Compared to wild type littermates, GPR84 KO APP/PS1 (mouse model for Alzheimer's disease) mice displayed reduced cognitive performance and microgliosis along with enhanced β -amyloid-stimulated dendritic degeneration (Audoy-Remus et al., 2015). Based on the observations that APP/PS1 mice expressing microglial GPR84 exhibited significantly higher (16-32%) microglial recruitment around amyloid plaques along with 2.5-fold lower dendritic degeneration compared to the mice deficient in GPR84, the authors proposed that GPR84-mediated microglial recruitment prevents cognitive decline and plays a moderate role in dendritic homeostasis.

1.8.4 Potential role of GPR84 in promoting insulin resistance under inflammatory conditions

Chronic inflammation plays a crucial role in the pathogenesis of obesity-related disorders including insulin resistance, type 2 diabetes and metabolic syndrome (Muredda et al., 2018; McArdle et al., 2013; Alvarez-Curto and Milligan, 2016; Nawrocki and Scherer, 2004). Strong upregulation of GPR84 in mouse bone marrow, kidney and brain and in mouse BMDMs in hyperglycemic conditions suggested that GPR84 might be associated with the pathogenesis of diabetes (Recio et al., 2018). Recently, the role of GPR84 in initiating insulin resistance during inflammatory conditions has been proposed by Nagasaki et al. (2012) who showed that GPR84 mRNA expression was significantly augmented in 3T3-L1 adipocytes and in adipose tissue of obese mice, in response to inflammatory cytokine TNF- α secreted from macrophages which migrated to the adipose tissue (Figure 1.12). Although Takeuchi et al. (2006) reported that serum adiponectin level is increased in response to dietary medium-chain triglycerides (MCT), in 3T3-L1 adipocytes, GPR84 activation by MCFAs resulted in amplification of TNF- α -induced down-regulation of adiponectin (Nagasaki et al., 2012). As adiponectin is appreciated to enhance insulin sensitivity (Diez and Iglesias, 2003; McArdle et al., 2013), MCFAs-stimulated suppression of adiponectin expression in TNF- α -induced adipocytes implies that MCFAs-GPR84 axis may initiate insulin resistance

and thus mediate the cross-talk between adiposity and type 2 diabetes. Consistent with the finding reported by Nagasaki et al., (2012), Trayhurn and Denyer, (2012) observed that macrophage-conditioned medium led to significant increase in GPR84 mRNA expression in human adipocytes. Muredda et al., (2018) also reported strong upregulation of GPR84 in human adipocytes upon stimulation with pro-inflammatory cytokines TNF- α or IL1- β . As GPR84 mediates inflammatory responses (see section 1.8.1), significant upregulation of GPR84 in adipocytes upon inflammatory conditions implies that GPR84 can exacerbate the obesity-promoted inflammatory response in adipose tissue and thereby mediates the vicious cycle between obesity and inflammation.

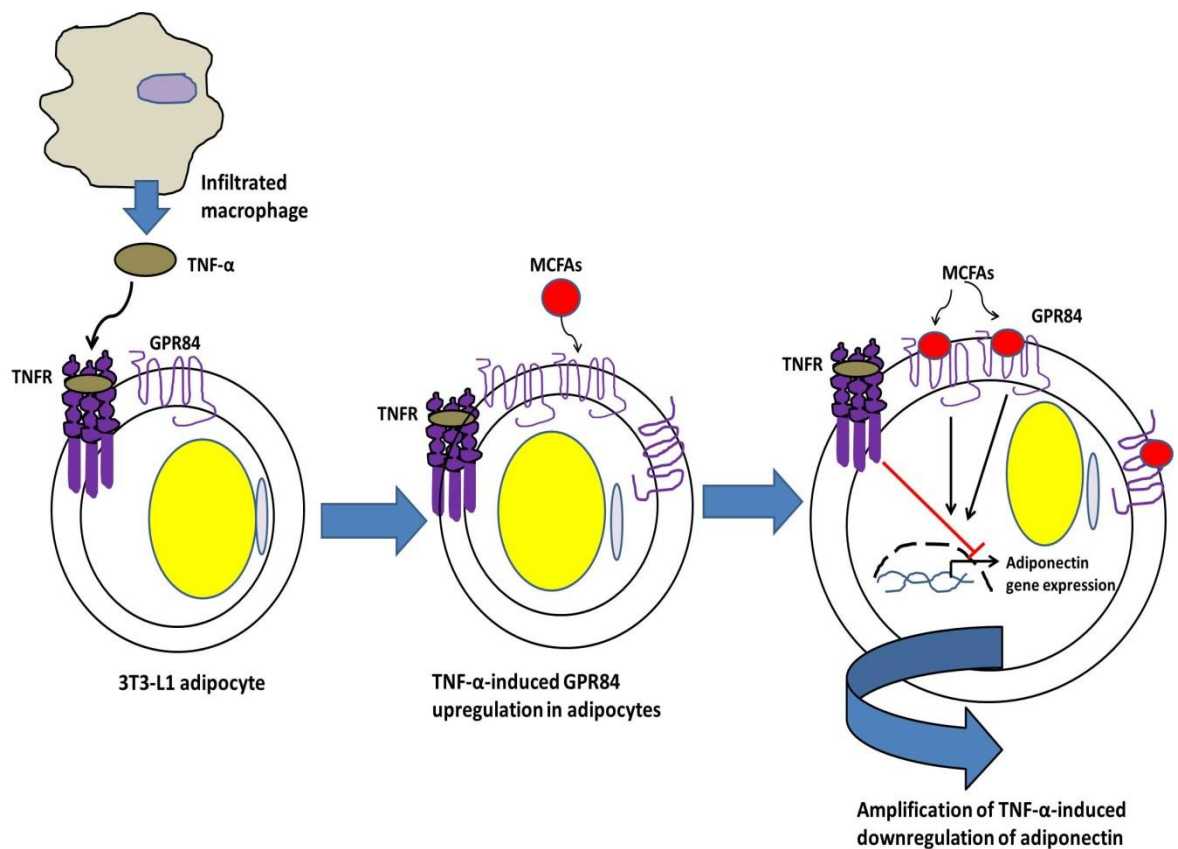


Figure 1.12 Proposed role of GPR84 in mediating cross-talk between adiposity and diabetes. GPR84 is strongly upregulated in adipocytes in response to inflammatory stimuli such as TNF- α secreted from macrophages infiltrated into inflamed adipose tissue. MCFAs-mediated GPR84 signaling amplifies TNF- α -promoted reduction in adiponectin expression in adipocytes which can lead to initiation of insulin resistance exacerbating a vicious cycle between obesity and diabetes.

1.8.5 GPR84 displays pro-fibrotic activity and represents a potential target for drug development against fibrosis-associated diseases

Currently available antifibrotic therapeutics (pirfenidone or nintedanib) for the treatment of idiopathic pulmonary fibrosis (IPF) lead to gastro-intestinal and cardiovascular side effects which markedly decrease patient compliance resulting in significant discontinuation of therapy (Marium et al., 2018). Moreover, both antifibrotics have limited efficacy in preventing underlying disease progression (Khalil et al., 2019) which necessitates novel development of therapeutics for this life-threatening disease. Recently, based on the results obtained from the studies with gene knock out mice and animal models of fibrosis, Gagnon et al., (2018) reported that two fatty acid sensing receptors GPR40 and GPR84 are involved in the pathogenesis of fibrosis in different organs including lung, kidney, heart, pancreas etc and suggested that agonism of GPR40 and antagonism of GPR84 could be novel therapeutic strategies to treat fibrosis-associated diseases such as IPF. Marked upregulation of GPR84 expression in human dermal fibroblasts and podocytes in response to the fibrosis promoting TGF β -1 and inflammatory stimuli including LPS and IFN γ along with the strong upregulation of GPR84 mRNA in different kidney fibrosis models despite very low basal expression in healthy renal tissue suggested a potential role of GPR84 in fibrosis pathophysiology (Gagnon et al., 2018). Consistent with these findings, Saniere et al., (2019) found marked upregulation of GPR84 in bronchial epithelial cells and infiltrated immune cells in both fibrosis mouse models and IPF patients whilst no expression of GPR84 in lung tissues of healthy human volunteers was observed. Genetic elimination of GPR84 in mice resulted in 50% reduction in kidney fibrosis in an adenine-promoted nephropathy model, further supporting role of GPR84 in fibrogenesis (Gagnon et al., 2018). Gagnon et al., (2018) also found that the antifibrotic agent PBI-4050 effectively blocked the TGF β -1-induced upregulation of the myofibroblast marker α -SMA and pro-fibrotic markers CTGF and COL1A1 in human dermal fibroblasts which demonstrated a link between GPR84 activation and fibroblast differentiation and activation in skin fibrosis as no GPR40 expression was found in dermal fibroblasts. Besides this, PBI-4050 treatment also resulted in effective blockade of LPS/IFN γ -promoted upregulation of inflammatory mediators (MCP-1, IL-6, IL-12p40, CCL2) in mouse peritoneal macrophages and inhibition of LPS-stimulated upregulation of IL-6 and

IL-8 in human podocytes (Gagnon et al., 2018). Based on these outcomes the authors maintained that inhibition of GPR84-mediated pro-inflammatory activities might be associated with PBI-4050-mediated prevention of fibrosis in different rodent models. Saniere et al., (2019) also reported that pharmacological inhibition of GPR84-mediated inflammatory responses and oxidative burst was partly responsible for the observed anti-fibrotic action of GLPG1205 in a mouse model of lung fibrosis. As chronic inflammation is associated with initial stages of the pathology of fibrosis-related disorders, combination therapy of an anti-inflammatory GPR84 antagonist with other anti-fibrotics might enhance the efficacy of the clinical therapy.

Li et al., (2018) demonstrated that PBI-4050, an agonist for GPR40 and antagonist/inverse agonist for GPR84 effectively inhibited kidney and pancreatic islet fibrosis and isletitis in a mouse model of diabetic nephropathy associated with type 2 diabetes. They argued that along with the GPR40 agonism which is beneficial in counteracting fibrosis, antagonism of GPR84-mediated macrophage infiltration and oxidative burst in kidney and pancreatic islets were the possible underpinning mechanisms of actions of PBI-4050 in inhibiting disease progression in diabetic nephropathy. Puengel et al., (2018) also reported that inhibition of GPR84-mediated immune cell (neutrophil and macrophages) infiltration into hepatic tissue could be a possible therapeutic strategy to treat non-alcoholic steatohepatitis and in mouse models of acute and chronic liver injury two GPR84 antagonists were found to effectively decrease disease progression as evident from significant reduction in steatohepatitis and fibrosis.

Nguyen et al., (2019) explored that GPR84 antagonism is the potential mode of action of PBI-4050 in inhibiting disease progression of pulmonary hypertension associated with heart failure with reduced ejection fraction (HFrEF). The pathophysiology of this secondary pulmonary hypertension includes macrophage infiltration into lung tissues and lung fibroblast activation and differentiation into pro-fibrotic myofibroblasts resulting in excessive extracellular matrix deposition in the alveolar wall. The authors suggested that agonist-activated GPR84 is associated with ERK1/2 signaling pathway-mediated pro-fibrotic activities and antagonism of GPR84 is partly responsible for PBI-4050-induced inhibition of lung fibrosis in the animal model of heart failure. GPR84 was upregulated significantly in lung tissue of rats with heart failure suggesting a

pathophysiological role of GPR84 in the disease progression. Studies with human lung fibroblasts identified that GPR84 is upregulated in these cells in response to stimulations with TGF- β 1 and endothelin-1, known mediators of pulmonary hypertension and heart failure and this upregulation was blocked by PBI-4050 (Nguyen et al., 2019). The GPR84 agonists compound-1/ZQ-16 and embelin were found to significantly upregulate expression of myofibroblasts markers including α -smooth muscle actin (α -SMA), connective tissue growth factor (CTGF) and COL1A1 and fibroblast activator endothelin-1 (ET-1), suggesting that GPR84 signaling is associated with lung fibrosis by activating and differentiating lung fibroblasts into myofibroblasts (Nguyen et al., 2019). As compound-1 and embelin were reported to induce GPR84-mediated ERK1/2 phosphorylation (Gaidarov et al., 2018; Zhang et al., 2016) and GPR84 antagonist PBI-4050 completely blocked the TGF- β -mediated ERK1/2 phosphorylation in human lung fibroblasts, Nguyen and colleagues (2019) proposed that GPR84-mediated ERK1/2 signaling at least partly contributes to the fibrogenesis and antagonism of this signaling is one of the major mechanisms by which PBI-4050 acts in preventing lung fibrosis in heart failure with pulmonary hypertension.

These promising outcomes obtained in pre-clinical studies suggest that GPR84 antagonism can be exploited therapeutically for drug development against fibrosis-associated diseases and currently the GPR84 antagonist GLPG1205 (<https://www.glp.com/IPF>; Sanier et al., 2019) and PBI-4050 are in phase II and Phase III clinical trials, respectively in patients with idiopathic pulmonary fibrosis (Li et al., 2018). GLPG1205 was found to be effective in preventing disease progression in pre-clinical animal models of IPF (Sanier et al., 2019) and displayed promising safety and tolerability in healthy human volunteers in a Phase I clinical study. Similarly, in a phase II clinical trial, PBI-4050 was found to display promising clinical efficacy and safety profile in patients with either IPF or type 2 diabetes associated with metabolic syndrome (Gagnon et al., 2018; Khalil et al., 2019).

1.8.6 GPR84 regulates osteoclastogenesis and could be a potential drug target for bone-destruction related diseases

Targeting the receptor activator of nuclear factor- κ B ligand (RANKL)-induced signaling pathways which regulate osteoclast differentiation is considered to be

a potential novel strategy for drug development against many diseases related to bone loss including osteoporosis, arthritis and rheumatoid arthritis, cancer metastases etc (Wada et al., 2006). Though fatty acid sensing receptors have mainly attracted interest as potential therapeutics for inflammatory and metabolic disorders, recent findings show that these receptors are also associated with regulation of bone physiology. FFA1 (GPR40) and FFA4 (GPR120) were reported to block RANKL-induced osteoclast differentiation by downregulating the NF- κ B signaling pathway (Kim et al., 2016; Wauquier et al., 2013). Similar to FFA1 and FFA4, GPR84 was also found to downregulate RANKL-stimulated osteoclastogenesis by suppressing NF- κ B and MAPK signaling pathways (Park et al., 2018) (Figure 1.13). Overexpression of GPR84 in osteoclast precursor cells, bone marrow-derived macrophages (BMDM) resulted in significant inhibition of RANKL-induced osteoclast formation whilst GPR84 knock down by small hairpin RNA transfection enhanced RANKL-promoted osteoclast differentiation (Park et al., 2018). GPR84 overexpression in BMDM led to downregulation of c-Fos and NFATc1 (both mRNA and protein levels) and TRAP and cathepsin K, two osteoclast specific genes. In contrast, knock down of GPR84 was found to significantly upregulate expression of c-Fos and NFATc1 as well as TRAP and cathepsin K in BMDM. GPR84 also concentration-dependently suppressed RANKL-induced NF- κ B transcriptional activity as measured by a luciferase reporter assay in RAW264.7 cells (Park et al., 2018). Moreover ectopic expression of GPR84 led to significant reduction in RANKL-promoted phosphorylation of inhibitory κ B α protein (I κ B α) and JNK, p38 and ERK while GPR84 gene silencing enhanced phosphorylation of these signaling mediators. As c-Fos, NF- κ B and NFATc1 were reported to play crucial roles in the gene expression essential for osteoclast differentiation (Kim and Kim, 2014; Asagiri and Takayanagi, 2007; Wada et al., 2006; Takayanagi et al., 2002;), Park et al., (2018) maintained that downregulation of these transcription factors by GPR84 signaling is the underpinning mechanism of GPR84-mediated downregulation of RANKL-induced osteoclast differentiation. These findings showed that GPR84 can be a potential target for drug development against diseases associated with bone disorders including osteoporosis and rheumatoid arthritis.

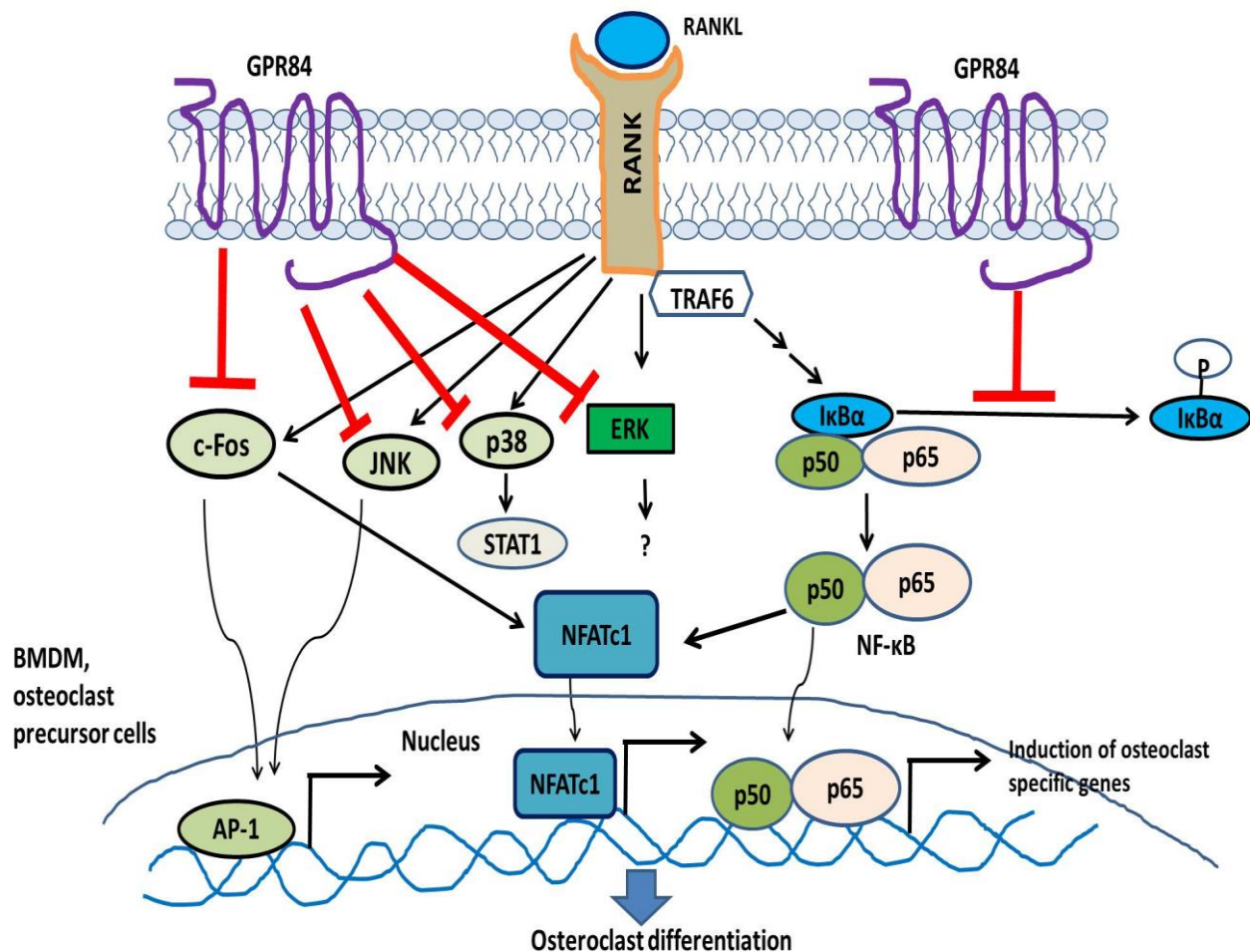


Figure 1.13 GPR84 signaling inhibits RANKL-induced osteoclast differentiation by inhibiting NF-κB and MAPK signaling pathways. Binding of receptor activator of nuclear factor-κB ligand (RANKL) to RANK receptor on bone marrow derived macrophages (BMDM) induces recruitment of adaptor protein TRAF6 to the receptor which activates downstream signaling effectors associated with MAPKs and NF-κB pathways. Phosphorylation of NF-κB inhibitory protein IκBα leads to activation of NF-κB heterodimer (p50/p65) and subsequent nuclear translocation of NF-κB to act as a transcription factor inducing gene expressions related to osteoclast differentiation. Activated NF-κB heterodimer also can activate another transcriptional factor, nuclear factor of activated T cells, cytoplasmic 1 (NFATc1). Recruitment of TRAF6 also activates AP-1 component c-Fos which acts as a transcription factor and an activator for NFATc1. Nuclear translocation of NFATc1 leads to induction of gene expression associated with osteoclast differentiation. GPR84 signaling inhibits c-Fos expression and downregulates RANKL-induced activation of NF-κB pathway by inhibiting phosphorylation of IκBα which ultimately lead to downregulation of NFATc1 activities (Park et al., 2018). GPR84 also prevents RANKL-promoted phosphorylation of three mitogen activated protein kinases (MAPK) including c-Jun N-terminal protein kinase (JNK), p38 and extracellular signal-regulated kinase (ERK) which might be associated with osteoclast specific gene expression (Park et al., 2018).

1.8.7 GPR84- β -catenin axis is associated with development and maintenance of acute myeloid leukemia

Wnt- β -catenin signaling has been implicated in tumorigenesis and thus considered as a novel target for anti-cancer drug development (Krishnamurthy and Kurzrock, 2018; Dorsam and Gutkind, 2007). Recently, Dietrich et al. (2014) proposed that GPR84 acts as a positive regulator of wnt- β -catenin signaling pathway in leukemic stem cells (LSCs) and thereby plays an important role in the development and maintenance of acute myeloid leukemia (AML) (Figure 1.14). GPR84 expression has been shown to be significantly elevated in human and mouse AML LSCs compared to hematopoietic stem cells (HSCs) (Saito et al., 2010; Dietrich et al. 2014) which suggests a potential role of GPR84 in the development of AML leukemia. Strong upregulation of active β -catenin in mouse MLL LSC along with higher expression of GPR84 is indicative of GPR84-induced potentiation of β -catenin expression. Small hairpin mRNA-induced GPR84 knock down in mouse MLL pre-LSCs resulted in significant downregulation of active β -catenin expression with concomitant reduction in growth and proliferation of leukemic cells (Dietrich et al., 2014). These effects of GPR84 gene silencing were fully reversed by transduction of constitutively active form of β -catenin in leukemic cells. Moreover, overexpression of GPR84 in mouse KLS-derived pre-LSC transduced with the oncogenic gene Hoxa9/Meis1a (KLSA9M pre-LSC) led to strong upregulation of β -catenin and transcription factors, TCF7L2 and c-Fos (both mRNA and protein level) with concomitant upregulation of a set of wnt- β -catenin target genes associated with leukemogenesis (Dietrich et al., 2014). These findings suggest that GPR84 is a positive regulator of Wnt- β -catenin signaling pathway and inhibition of the GPR84- β -catenin system might be a novel strategy for drug development for acute myeloid leukemia (AML).

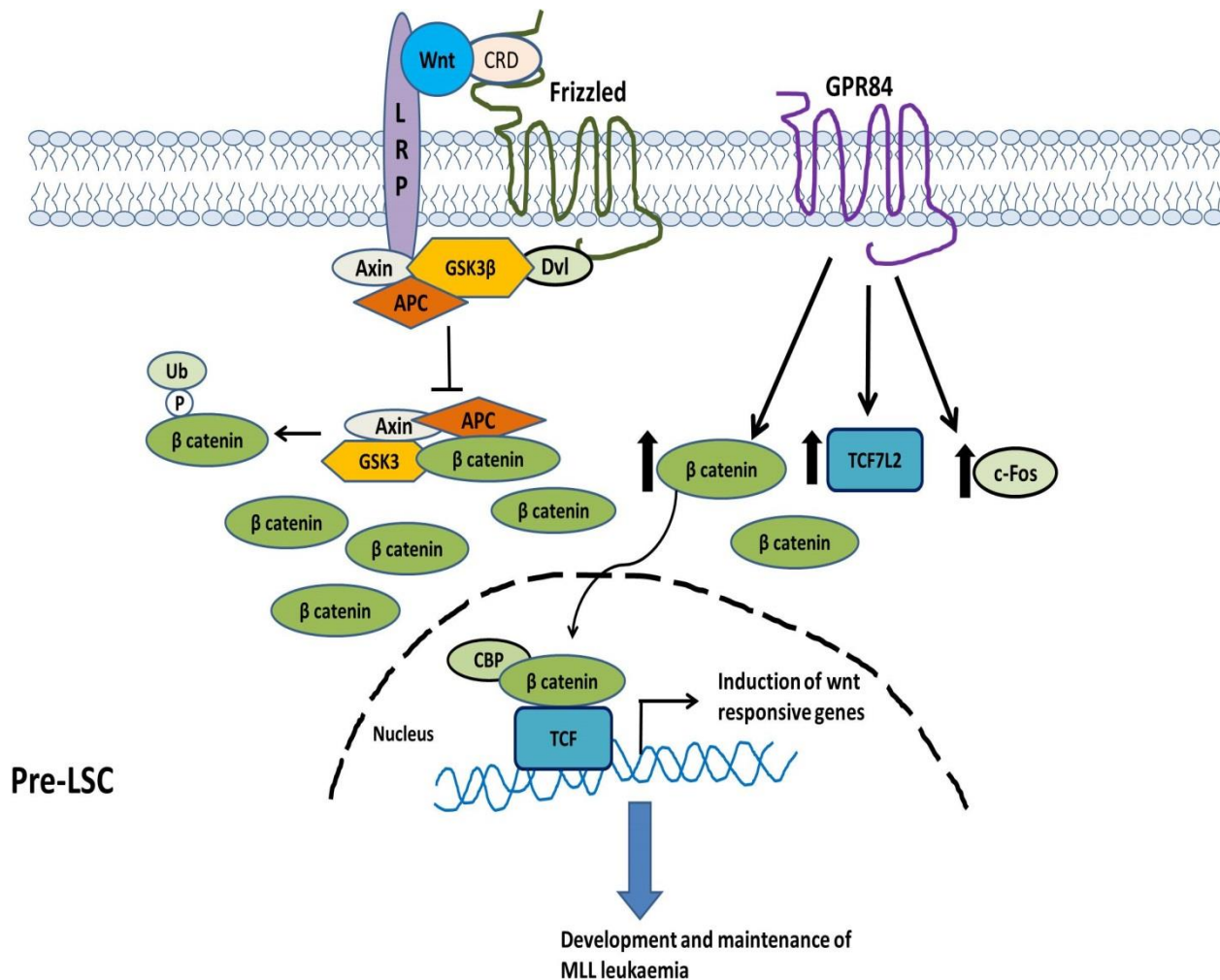


Figure 1.14 GPR84 regulates Wnt-β catenin signaling in pre-leukemic stem cells to develop and maintain MLL leukemia. In the absence of wnt glycoprotein, β-catenin is phosphorylated by glycogen synthetase kinase 3β (GSK3β) of the destruction complex Axin-APC-GSK3 followed by ubiquitination and proteosomal degradation. Wnt glycoprotein ligand binds to the cysteine rich domain (CRD) of 7-TM frizzled receptor and to the low density lipoprotein receptor-related protein (LRP) which activates Disheveled (Dvl) protein followed by recruitment of Axin-APC-GSK3 complex to the receptor (Krishnamurthy and Kurzrock, 2018). This sequestration of cytosolic protein GSK3 inhibits phosphorylation of β-catenin leading to subsequent accumulation of β-catenin in cytoplasm (Dorsam and Gutkind, 2007). β-catenin then translocates to the nucleus to act as a co-activator for transcription factor, T-cell factors (TCFs) which induce expression of Wnt responsive genes. GPR84 is supposed to act as a potentiator of Wnt-β-catenin signaling pathway by upregulating expression of β-catenin and its co-effectors including TCF7L2 and c-Fos which results in enhanced expression of MLL target genes responsible for leukemogenesis (Dietrich et al., 2014).

1.9 Aims and objectives of the project

GPR84 is still officially considered as ‘orphan’ receptor as the putative endogenous agonists MCFAs are weakly potent activators of GPR84 and their mode of binding to GPR84 is poorly defined. Only one study has been done on the mode of decanoic acid binding to GPR84. However Nikaido et al., (2015) failed to identify the charge partner for the carboxylate function of the fatty acids. Although a few articles have been published regarding the signal transduction pathways, physiological functions and pathophysiological roles of

the GPR84, it still remains poorly characterized and details of the mode of action of pharmacological tools are limited. As such its regulation, physiological functions and pathophysiological roles have not yet been clarified; hindering drug development programmes and therefore warrant further research. In this regard, investigation of modes of ligand binding to GPR84 and defining the mode of action of pharmacological tools are required which will aid generation of further improved tool compounds that can be utilized for physiological characterization of the receptor. The aims and objectives of my PhD thesis are as follows:

- 1) **Exploring the G protein selectivity of the receptor** using novel BRET-based GPR84 biosensors developed using a SPASM (systematic protein affinity strength modulation) based approach (Sivaramakrishnan and Spudich, 2011). **(Chapter 3)**
- 2) **Defining the ligand binding pockets of GPR84** by a combination of site directed mutagenesis and molecular modelling. The studies will also define whether reported synthetic ligands act at the same site as the fatty acids or act as allosteric activators. **(Chapter 4)**
- 3) **Defining the ortholog selectivity of GPR84 ligands and characterizing the pharmacology of GPR84 ligands in more physiological settings using RAW264.7 cells:** Though several potent and selective tool compounds have been developed recently, the mechanism of actions of these tool compounds including orthosteric and allosteric ligands are very limited. Moreover detailed orthologue selectivity of these pharmacological tools is unexplored. Exploring the complex pharmacology of these tool compounds is crucial for the characterization of this enigmatic receptor and is thus essential to uncover the therapeutic potential of this receptor. Pharmacological profiles of currently available GPR84 agonists and antagonists along with their potential orthologue selectivity were investigated using transfected cells expressing human and mouse GPR84 as well as the mouse monocyte macrophage cell line RAW264.7 **(Chapter 5)**.
- 4) **Exploring the allosteric modulation of GPR84:** Detailed allosteric interactions between DIM and DIM analogues and orthosteric GPR84 agonists were characterized using transfected cells expressing human and mouse GPR84 and RAW264.7 cells **(Chapter 6)**. The potential orthologue selectivity of DIM and

PSB-16671-mediated allosteric modulation was also investigated using human and mouse GPR84 expressing cell lines.

Overall the studies performed in this project aims at investigating ligand binding modes and characterizing allosteric modulation of GPR84 which will aid drug discovery programmes either through accelerating structure-based drug design, identifying more improved ligands, or exploiting the novel modality of allosteric interaction for development of allosteric therapeutic agent(s).

2 Materials and methods

2.1 Pharmacological tool compounds

Medium chain fatty acids including decanoic acid (C-10), undecanoic acid (C-11), lauric acid (C-12); 3,3'-diindolylmethane (DIM) and 2,5-dihydroxy-3-undecyl-1,4-benzoquinone (embelin) were purchased from Sigma-Aldrich.

DIM analogues 5,5'-diiodo-3,3'-diindolyl-(4-methylphenyl)methane (2b); 5,5'-dimethoxy-3,3'-diindolylmethane (3a); 5,5'-dimethoxy-3,3'-diindolyl-(4-methylphenyl)methane (3b); 5,5'-dimethoxy-3,3'-diindolyl-(3,5-difluorophenyl)methane (3c) and 5,5'-dinitro-3,3'-diindolylmethane (6a) (see Figure 2.1 for structures) were a gift from Dorota Maciejewska, Department of Organic Chemistry, Medical University of Warsaw, Poland.

6-n-octylaminouracil (6-OAU) was purchased from Cayman Chemical (USA) while 2-(hexylthio)pyrimidine-4,6-diol (ZQ-16 or compound-1) was provided by Trond Ulven, University of Copenhagen and Galapagos NV.

A series of compound-1 derivatives including 6-phenylethylpyridine-2,4-diol (TUG-1758); 6-phenylbutylpyridine-2,4-diol (TUG-1759); 2-nonylpyridine (TUG-1760); 2-nonyl-4-pyridone (TUG-1761); 6-undecylpyridine-2,4-diol (TUG-1762); 6-decylpyridine-2,4-diol (TUG-1763); 6-heptylpyridine-2,4-diol (TUG-1764); 6-octylpyridine-2,4-diol (compound-50/TUG-1765) (see Figure 2.2 for structures) were provided by Trond Ulven, University of Copenhagen.

GPR84 agonist 6-nonylpyridine-2,4-diol (compound-51), GPR84 allosteric agonist di(5,7-difluoro-1H-indole-3-yl)methane (PSB-16671) and GPR84 antagonists including compound-9 (2-([1,4]dioxin-2-ylmethoxy)-9-(pyridine-2-ylmethoxy)-6,7-dihydro-pyrimido[6,1-a]isoquinolin-4-one); compound-104 (9-(5-cyclopropyl-[1,2,4]oxadiazol-3-ylmethoxy)-2-((R)-1-[1,4]dioxan-2-ylmethoxy)-6,7-dihydro-pyrimido[6,1-a]isoquinolin-4-one); compound-107 (2-([1,4]dioxan-2-ylmethoxy)-9-(3-phenylamino-prop-1-ynyl)-6,7-dihydro-pyrimido[6,1-a]isoquinolin-4-one); compound-122/GLPG1205 (9-(2-cyclopropylethynyl)-2-[(2S)-1,4-dioxan-2-yl]methoxy)-6,7-dihydropyrimido[6,1-a]isoquinolin-4-one); compound-161 (2-((S)-1-[1,4]dioxan-2-ylmethoxy)-9-(tetrahydro-pyran-4-yl-methoxymethyl)-6,7-

dihydro-pyrimido[6,1-a]isoquinolin-4-one); compound-837 and radioligand [^3H]-G9543 were synthesized and provided by Belgian pharmaceutical company Galapagos NV.

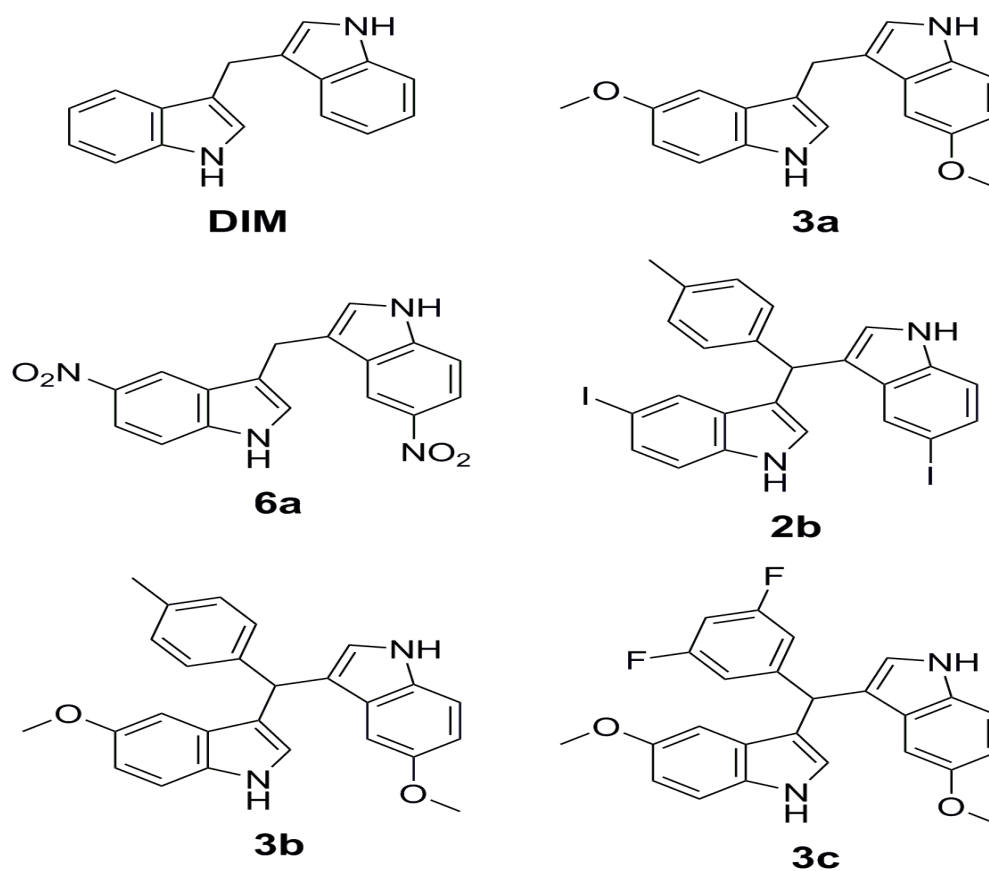


Figure 2.1 Structure of GPR84 allosteric agonist DIM and DIM analogues used in the studies. Chemical structure of DIM and certain DIM analogues including 3a, 6a, 2b, 3b and 3c are shown.

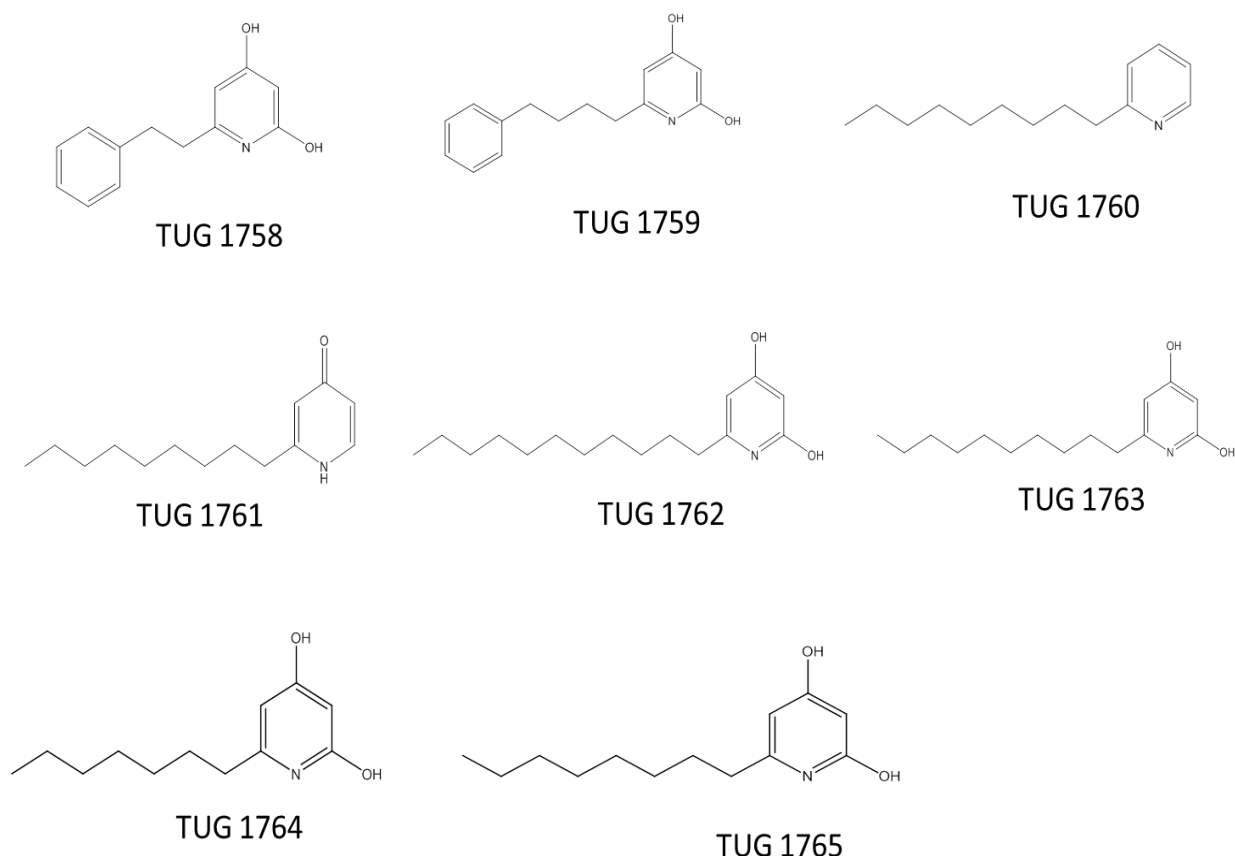


Figure 2.2 Chemical structures of a series of compound-1 derivatives. Chemical structures of a set of compound-1 derivatives used in the screening assay for GPR84 agonism are shown.

2.2 Molecular biology and cloning

2.2.1 Preparation of LB (Luria-Bertani) medium and LB agar plates

10 g tryptone, 5 g yeast extracts and 10 g NaCl were combined and 800 ml deionized, distilled water was added to the dry reagents followed by adjustment of the pH of the solution to 7.0 with NaOH. The volume of the solution was then brought up to 1 liter. The solution was then autoclaved on liquid cycle for 20 minutes at 15 psi. To prepare LB agar plates, LB medium was prepared as above and 15 g of bacto-agar was added per 1L of LB followed by autoclaving at 126°C. After autoclaving, the bottles were allowed to cool to 55°C and an appropriate amount of filter-sterilized antibiotic ampicillin was added at a final concentration of 50-100 µg/ml. The bottle was then swirled to ensure proper mixing of ampicillin with LB agar and approximately 20 ml of agar was poured into a 10 cm petri-dish. The plates were then kept at room temperature for 20 minutes to allow the agar to solidify. After solidified and dried, the plates were inverted and stored at 4°C in the dark.

2.2.2 Preparation of competent bacteria

A stock of XL1-blue cells (Agilent Technologies) stored in -80°C was taken out, thawed on ice and streaked out on an LB agar plate with no antibiotics and grown overnight at 37°C . On the following day, a single colony was picked and grown in 5 ml of LB media (without antibiotic) overnight at 37°C in a shaking incubator at 220 rpm. This 5 ml culture was then sub-cultured into 100 ml of LB media and grown at 37°C in a shaking incubator until the optical density at 600 nm was reached to 0.48. The growth of bacteria was halted by chilling on ice for 5 minutes followed by centrifugation at 1811xg for 10 minutes at 4°C in 50 ml sterile falcon tubes. The resulting bacterial cell pellets from each 50 ml falcon tubes were re-suspended in 20 ml of solution 1 (30 mM CH_3COOK , 10 mM RbCl , 10 mM CaCl_2 , 50 mM MnCl_2 and 15% (v/v) glycerol; pH 5.8; filter sterilized and stored at 4°C) by gentle pipetting followed by chilling on ice for 5 minutes. The chilled pellets were further subjected to centrifugation at 1811xg for 10 minutes at 4°C . The pellets from this 2nd centrifugation was then re-suspended in 2 ml of solution 2 (10 mM 3-morpholinopropane-1-sulfonic acid (MOPS), 10 mM RbCl , 75 mM CaCl_2 , 15% (v/v) glycerol, pH 6.5 with HCl ; filter sterilized and stored at 4°C) by gentle pipetting and chilled on ice for a further 15 minutes. Bacterial cells were then aliquoted in 220 μl volumes in sterile pre-chilled 1.5 ml microcentrifuge tubes and stored at -80°C .

2.2.3 Transformation of competent cells with plasmid cDNA

Chemically competent XL1-blue cells (section 2.2.2) were taken out of -80°C and thawed on ice for 20 minutes. 50 μl of thawed competent cells were aliquoted for each transformation into pre-chilled 1.5 ml microcentrifuge tube followed by addition of 1-5 μl of DNA (10-100 ng) or 5 μl of the ligation reaction mixture to the cells and mixing gently by flicking the bottom of the tube. The competent cell/DNA mixture was then incubated on ice for 15 minutes and subjected to heat shock at 42°C for 90 seconds by placing the tubes on a rack which was placed in a water bath. The tubes were then immediately placed on ice for 2 minutes. 500 μl of LB media without any antibiotics was added to each tube and bacteria were grown in 37°C in a shaking incubator (220 rpm) for 45 seconds to 1 hour allowing bacteria to express antibiotic resistance genes. 50 to 200 μl of transformation was then plated using a sterile spreader onto a pre-warmed 10

cm LB agar plate containing 50 µg/ml ampicillin. The plates were incubated upside down at 37°C overnight. Only the cells containing the transformed plasmid will be able to form colonies in the LB agar ampicillin plate. On the following day, a single colony was picked and grown overnight in 5 ml of LB media containing 50 µg/ml ampicillin at 37°C in a shaking incubator. The resulting cultures were either DNA mini-prep'd or sub-cultured further to make larger volumes of closed circular DNA (cDNA) (mid-prep and maxi-prep).

2.2.4 Purification of plasmid DNA from bacterial culture

Microgram quantities of plasmid DNA were purified from bacterial culture using Wizard® Plus SV Minipreps DNA Purification System (Promega) following the manufacturer's instructions. Briefly, 5 ml of overnight bacterial culture was centrifuged at 3220 x g for 5 minutes and the resulting pellets were thoroughly re-suspended in 250 µl of cell resuspension solution (50 mM Tris-HCl (pH 7.5), 10 mM EDTA, 100 µg/ml RNase A). The bacterial cells were then lysed by adding 250 µl of cell lysis solution (0.2M NaOH, 1% SDS) to each sample and inverting the tube 4 times to ensure proper mixing. To inactivate endonucleases or other proteins, 10 µl of alkaline protease solution was added to each sample with mixing by inverting the tube 4 times followed by incubation at room temperature for 5 minutes. 350 µl of ice-cold neutralization solution (1.32M potassium acetate; pH 4.8) was then added and the tube was inverted 4 times to mix. In this stage, proteins and genomic DNA are precipitated while smaller plasmids are able to renature at lower pH and remain in solution. The mixture was then centrifuged at 17,900 x g for 10 minutes at room temperature and the resulting supernatant (cleared lysate) was carefully decanted into the spin column inserted into a collection tube. The supernatant was centrifuged at 17,900 x g for 1 minute at RT allowing the plasmid DNA to bind the column. The flow-through was discarded and the spin column was re-inserted into the collection tube. The column was washed with 750 µl of column wash solution (80 mM potassium acetate, 8.3 mM Tris-HCl (pH 7.5), 40 µM EDTA, 95% ethanol added [final concentration of ethanol was 55%]) by centrifugation at 17,900 x g for 1 minute at RT. The flow-through was discarded and the column was re-inserted into the collection tube. Column washing was carried out once again with 250 µl of wash solution but this time centrifugation was performed for 2 minutes. The spin column was then transferred to a sterile 1.5 ml

microcentrifuge tube prior to the addition of 100 µl nuclease-free water to the spin column. Plasmid DNA was then eluted by centrifugation at 17,900 x g for 1 minute and stored in -20°C.

Milligram quantities of plasmid DNA was purified from 100 to 200 ml of bacterial culture using QIAGEN® Plasmid Maxi Kit according to the manufacturer's instructions which are very similar to that described above for miniprep preparation with slight modification.

After miniprep or maxiprep, the concentration and purity of the DNA were estimated by reading the absorbance of diluted samples (1:200) at 260 nm and 280 nm using a UV spectrophotometer. The absorbance at 260 nm (A_{260}) reveals the quantity of the DNA while the ratio of absorbance at 260 to that at 280 nm (A_{260}/A_{280}) reflects the purity of the sample with the ratio between 1.8 to 2.0 being considered as highly pure DNA.

2.2.5 PCR based cloning

In polymerase chain reaction (PCR) based cloning, firstly a PCR reaction was performed to amplify the specific DNA fragments along with incorporating restriction sites on the two ends of the open reading frame (ORF) so that the gene of interest could easily be inserted into the recipient plasmid. The PCR amplified product was then purified from other PCR reaction components. This purified PCR product and the recipient plasmid vector were then subjected to double restriction digestion with two restriction endonucleases followed by running gel electrophoresis of restriction digests (both insert and plasmid vector). Gel purification was then performed to isolate and purify the digested insert and vector DNA which were then fused by conducting a DNA ligation reaction with DNA ligase enzyme ultimately leading to the generation of a plasmid construct containing the gene of interest.

2.2.5.1 Polymerase chain reaction (PCR)

In an attempt to incorporate restriction sites or epitope tag (FLAG epitope tag or fluorescent protein tag) on both terminus or single terminus of the gene of interest and to amplify the DNA fragment, a PCR reaction was set up on ice in a total volume of 50 µl in a 500 µl sterile PCR tube with the following components:

- 5 µl of 10x Pfu DNA Polymerase reaction buffer (Promega)
- 1 µl of 10 mM dNTP mix (final concentration: 200 µM of each dATP, dCTP, dGTP and dTTP; Promega)
- 0.5 µM of each sense and antisense oligonucleotide primers
- 50 to 100 ng of DNA template
- 1 µl of (2.5 units/µl) Pfu DNA Polymerase (Promega)
- Nuclease-free water quantity sufficient to 50 µl

The PCR reaction tubes were then transferred to a thermal cycler and subjected to thermal cycling using the following PCR programme:

| Step | Temperature | Time |
|-----------------------------------|---|---|
| 1. Initial denaturation | 95°C | 5 minutes |
| 2. Denaturation | 95°C | 1 minute |
| 3. Annealing | 55 to 65°C depending on the T _m of the primers | 1 minute |
| 4. Extension | 72°C | 1 minute 30 seconds (2 minutes/kb of DNA fragment length) |
| 5. Repeat steps 2-4 for 30 cycles | | |
| 6. Final extension | 72°C | 5-10 minutes |
| 7. Hold | 4°C | indefinite |

After finishing the PCR, 5 µl of the PCR product was run on an agarose gel to check the success of the PCR.

2.2.5.2 PCR purification

The amplified PCR product was purified from other PCR reagents including primers, nucleotides, polymerases and salts using QIAquick PCR Purification Kit (Qiagen) according to the manufacturer's instructions. Briefly, 5 volumes of binding buffer, Buffer PB was added to 1 volume of the PCR sample and mixed well. To bind DNA, the sample was then transferred to the QIAquick spin column inserted into a collection tube followed by centrifugation at 17900 x g for 1 minute. After discarding the flow-through, the spin column was re-inserted back into the collection tube. The column was then washed by adding 750 µl of Buffer PE (absolute ethanol was added previously to buffer PE) to the column and spinning down at 17900 x g for 1 minute. The flow-through was discarded again

and the column was placed back to the collection tube followed by an additional centrifugation for 1 minute to ensure the complete removal of residual ethanol. The spin column was then placed in a sterile 1.5 ml microcentrifuge tube prior to the addition of 30 μ l of sterile nuclease-free water to the centre of the column. The column was incubated at RT for 1 minute and then spun down for 1 minute at 17900 x g to elute the DNA into the microcentrifuge tube.

2.2.5.3 Restriction endonuclease reaction

The purified PCR amplified product and the recipient plasmid DNA (vector) were digested using two restriction endonucleases to generate sticky-end DNA fragments which can subsequently be ligated. The restriction endonuclease digest was set up on ice in a total reaction volume of 50 μ l in a sterile microcentrifuge tube with the following components:

- 5 μ l 10x CutSmart[®] Buffer (New England Biolabs, NEB)
- 500 ng to 1 μ g PCR amplified purified DNA or 2-5 μ g of recipient plasmid DNA
- 1-2 μ l of High-Fidelity (HF[®]) Restriction Endonuclease 1(NEB)
- 1-2 μ l of High-Fidelity (HF[®]) Restriction Endonuclease 2(NEB)
- x μ l dH₂O (to bring the total volume to 50 μ l)

These components were mixed by either flicking the bottom of the tube or pipetting gently up and down followed by centrifugation for a few seconds in a microcentrifuge. The restriction digest reaction was then incubated at 37°C for at least 4 hours or overnight.

2.2.5.4 DNA gel electrophoresis and gel purification using gel extraction kit

The digested DNA fragments (insert and recipient plasmid) were subjected to gel electrophoresis to separate them based on their length in base pairs. Briefly, 0.3 g of agarose was dissolved in 30 ml of TAE buffer (40 mM Tris, 1 mM EDTA (at pH 8) and 20 mM acetic acid) followed by heating in a microwave for 2 minutes with intermittent swirling. The dissolved agarose was allowed to cool to 50°C prior to the addition of SYBR[®] Safe DNA gel stain (Life Technologies) in a final dilution of 1:1000. The melted agarose was then poured into a gel tray with the well comb

in place and allowed to cool for 20 minutes to solidify the gel followed by flooding the gel tank with TAE buffer with approximately 2 mm TAE above the gel. The well comb was removed carefully and 6x DNA gel loading buffer (0.4 mg/mL sucrose, 0.25% (w/v) bromophenol blue) was added to the samples at a ratio of 1:5. 5 µl of 1 kb HyperLadder™ (Bioline Reagents) was then loaded to the first lane of the gel to quantify and determine the size of the DNA samples followed by addition of 5 to 50 µl of samples to other wells. The gel was then run at 125 V for 25-30 minutes.

Following gel electrophoresis, the desired DNA fragments (recipient plasmid and insert) were cut out of the agarose gel and purified using QIAquick Gel Extraction Kit (Qiagen). The gel bands containing the desired DNA fragments were visualized under UV light and excised with a clean sharp razor blade. The excised gel slices were weighed in sterile microcentrifuge tubes and 3 volumes of Buffer QG were added to 1 volume of gel (100 mg gel~100 µl) followed by incubation at 50°C in a heating block for 10 minutes with intermittent vortexing in every 2-3 minutes to ensure the solubilisation of the gel slice. After that, 1 gel volume of isopropanol was added to the sample and mixed well. The sample was then transferred to a QIAquick spin column placed in a 2 ml collection tube and centrifuged for 1 minute at 17,900 x g. After discarding the flow-through, the column was placed back to the collection tube and washed with 750 µl of Buffer PE (suggested amount of 96 to 100% ethanol was added to the buffer) by spinning down at 17,900 x g for 1 minute. Further centrifugation was performed to ensure complete removal of residual ethanol from the column and the column was then placed into a sterile 1.5 ml microcentrifuge tube. 30 µl of nuclease-free water was added to the centre of the column and incubated for 1 minute. DNA was then eluted by centrifuging at 17,900 x g for 1 minute.

The purified DNA (5 µl of the cut insert and recipient plasmid vector) fragments were again subjected to 1% agarose gel electrophoresis to determine the concentration of each DNA fragments in order to set up the ligation reaction. This approximate quantification of DNA was performed by running 5 µl of 1 kb HyperLadder™ in parallel and comparing the intensity of DNA intercalating dyes (imaged using a UV transilluminator) within the gel band of the marker with those of the samples. After estimating the DNA concentrations, the required

amounts of cut vector DNA and insert DNA to reach a molar ratio of 1:3 and 1:5 were determined using the following formula:

$$(ng\ of\ insert) = (molar\ ratio\ of\ \frac{insert}{vector}) \times (\frac{ng\ of\ vector \times kb\ size\ of\ insert}{kb\ size\ of\ vector})$$

2.2.5.5 DNA ligation

In the final stage of generation of a recombinant plasmid, the restriction digested DNA fragment containing the gene of interest was fused to the digested plasmid vector containing compatible sticky ends by performing a ligation reaction using T4 DNA Ligase (Promega). The ligation reaction was set up on ice in a total volume of 20 µl in a sterile tube with the following components:

- 2 µl of 10x T4 DNA ligase reaction buffer(Promega)
- 100 ng of vector plasmid DNA
- x µl of insert DNA (as calculated to reach a molar ratio of 1:3 (vector: insert))
- 1 µl/400 units of T4 DNA ligase (Promega)
- Nuclease-free water to a final volume of 20 µl

Another reaction (vector only control) was set up in which all the above reagents were assembled in another sterile tube except the insert DNA. The ligation reaction tubes were then incubated for 4 hours at room temperature or overnight at 16°C. After that, 5 µl of the ligation reaction was transformed into chemically competent XL1-blue cells (section 2.2.3) and the recombinant plasmid DNA was isolated and purified from bacterial cultures by performing miniprep preparation (section 2.2.4).

2.2.6 Site-directed mutagenesis

Point mutation of interest on DNA sequence was performed by following a QuickChange II Site-Directed Mutagenesis protocol (Stratagene, Cheshire, UK). In this method, a double-stranded mutant plasmid containing the desired mutation is amplified via PCR reaction with two synthetic oligonucleotide primers, each containing the desired mutation utilizing a double-stranded plasmid vector as the template. The two mutagenic oligonucleotide primers, complementary to

each other which contain the desired mutation in the middle of the primer, were designed using the software program, such as Agilent QuikChangell (<https://www.genomics.agilent.com/primerDesignProgram.jsp>). In the case of primer designing, it was ensured that length of the primers was between 25 and 45 bases with higher GC content (40 to 60%) and the melting temperature (T_m) was $\geq 78^\circ\text{C}$. For the amplification of mutant plasmid, a PCR amplification reaction (sample reaction) was set up on ice in a final volume of 50 μl in a sterile PCR tube containing the following components:

- 5 μl of 10x Pfu DNA Polymerase buffer with MgSO_4 (Promega)
- 1 μl of 10 mM dNTP mix (200 μM each dNTP)
- 1.25 μl (125 ng) of forward oligonucleotide primer
- 1.25 μl (125 ng) of reverse oligonucleotide primer
- 50 to 100 ng of dsDNA template
- 1 μl of (2.5 units/ μl) Pfu DNA Polymerase (Promega)
- Nuclease-free water quantity sufficient to 50 μl

Another PCR reaction (control reaction) was set up on ice in another PCR tube containing all the components as mentioned above except the two primers. Employing the following cycling programme both the PCR reaction mixtures (sample reaction and control reaction) were subjected to thermal cycling using an Eppendorf Mastercycler:

| Step | Temperature | Time |
|-----------------------------------|--|---|
| 1. Initial denaturation | 95°C | 5 minutes |
| 2. Denaturation | 95°C | 30 seconds |
| 3. Annealing | 55 to 65°C depending on the T_m of the primers | 1 minute |
| 4. Extension | 72°C | ~16 minutes for 8kb plasmid (2 minutes/kb of plasmid length) |
| 5. Repeat steps 2-4 for 16 cycles | | |
| 6. Hold | 4°C | Indefinite |

Immediately after completion of thermal cycling, 1 μl of (10 units/ μl) of DpnI restriction endonuclease (Promega) was added to both sample and control reaction mixture followed by gentle mixing and spinning down in a microcentrifuge for 1 minute. The reaction mixtures were then incubated at

37°C for 2 hours to digest the parental methylated dsDNA leaving the synthesized mutant plasmid intact. 1 µl of the DpnI-treated DNA from each control and sample reaction was then transformed into separate 50 µl of XL1-blue competent bacteria following the protocol described in section (2.2.3).

2.2.7 Plasmids and DNA constructs

2.2.7.1 Generation of FLAG-hGPR84-Gα_{i2} fusion construct

The FLAG-hGPR84-Gα_{i2} fusion protein was constructed by replacing enhanced yellow fluorescent protein (eYFP) within the FLAG-hGPR84-eYFP-pcDNA5/FRT/TO construct (previously generated in the Milligan Lab; Mahmud et al., 2019) with a sequence corresponding to rat Gα_{i2} using NotI and XhoI restriction enzymes. Rat Not1-Gα_{i2}-Xho1 was amplified by polymerase chain reaction (PCR) using β₂AR-HindIII-Gα_{i2}-Xho1-pcDNA5/FRT/TO as the template and the following forward and reverse primers designed to incorporate a NotI restriction site upstream and XhoI restriction site downstream of the Gα_{i2} sequence.

Forward primer: 5' -GATCGCGGCCGCGGCTGCACCGTCAGCGCCGAGGAC- 3'

Reverse primer: 5' -GATCCTCGAGTCAGAAGAGGCCACAGTCCTTCAG-3'

Restriction digestion of FLAG-hGPR84-eYFP-pcDNA5/FRT/TO plasmid vector and NotI-Gα_{i2}-XhoI PCR amplified product with NotI and XhoI restriction enzymes followed by ligation with T4 DNA ligase led to the generation of FLAG-hGPR84-Gα_{i2} fusion construct. The reading frame and orientation of the construct were then confirmed by DNA sequencing performed by the MRC PPU DNA Sequencing and Services (School of Life Sciences, University of Dundee, Scotland) using an Applied Biosystems 3730 DNA sequencer.

2.2.7.2 Generation of PTX-insensitive mutants of the hGPR84-Gα_{i2} fusion protein

A pertussis toxin (PTX) resistant FLAG-hGPR84-Gα_{i2} C352G mutant construct was prepared via PCR using QuickChange II Site-Directed Mutagenesis protocol (section 2.2.6) using the following primers

C352G Forward primer: 5' -CAACCTGAAGGACCGGTGGCCTCTTCTG-3'

C352G Reverse primer: 5' -CAGAAGAGGCCACCGTCCTTCAGGTTG-3'

Similarly, another PTX-insensitive FLAG-GPR84-G α_{i2} C352I mutant construct was generated through site-directed mutagenesis protocol (section 2.2.6) using the following primers-

C352I Forward primer: 5' -CAA CCTGAAGGACATTTGGCCTCTTCTG-3'

C352I Reverse primer: 5' -CAGAAGAGGCCAATGTCCTTCAGGTTG-3'

In both cases, FLAG-hGPR84-G α_{i2} -pcDNA5/FRT/TO construct was used as the template for the PCR reactions of site-directed mutagenesis protocol.

2.2.2.3 Generation of point mutants of human GPR84

A series of FLAG-hGPR84-G α_{i2} C352I constructs containing point mutation of interest were generated by employing QuickChange II site-directed mutagenesis method (section 2.2.6). The oligonucleotide primers designed for the PCR amplification of mutant plasmid containing specific point mutation are mentioned below:

F101A

Forward primer: 5' GTATTTGGGCTCCTCCTTGCTGCCTCCAATTCTGTCTC 3'

Reverse primer: 5' GAGACAGAATTGGAGGCAGCAAGGAGGAGCCCAAATAC 3'

F170A

Forward primer: 5' GTCTGCACCTGCAGCGCTGACCGCATCCGAGG 3'

Reverse primer: 5' CCTCGGATGCGGTCAGCGCTGCAGGTGCAGAC 3'

R172A

Forward primer: 5' CCTGCAGCTTTGACGCCATCCGAGGCCGGCC 3'

Reverse primer: 5' GGCCGGCCTCGGATGGCGTCAAAGCTGCAGG 3'

R172K

Forward primer: 5' CCTGCAGCTTTGACAAAGATCCGAGGCCGGCC 3'

Reverse primer: 5' GGCCGGCCTCGGATCTTGTCAAAGCTGCAGG 3'

F335A

Forward primer: 5' CCTGAGCTACATCCCCGCCTTGCTGCTCAACATTC 3'

Reverse primer: 5' GAATGTTGAGCAGCAAGGCGGGGATGTAGCTCAGG 3'

W360A

Forward primer: 5' CTTGCTGCCAACCTCACCGGCTCAATGGTTGCATCAAC 3'

Reverse primer: 5' GTTGATGCAACCATTGAGGCGGTGAGGTTGGCAGCAAG 3'

2.2.2.4 Generation of the FLAG-hGPR84-G α_{i3} C351I fusion protein

Using CRF-G α_{i3} C351I plasmid vector as the template, PCR reaction was performed to amplify the sequence corresponding to rat G α_{i3} C351I containing NotI and XhoI restriction sites on the two terminuses. The primers used in the PCR were as follows:

Not1-G α_{i3} Forward primer:

5' -TAAGCAGCGGCCGCGGCTGCACGTTGAGCGCCGAGGACAAG-3'

Xho1-G α_{i3} Reverse primer: 5' -

TAAGCACTCGAGTCAGTAAAGCCCACATTCCTTTAAGTTG-3'

FLAG-hGPR84-G α_{i2} -pcDNA5/FRT/TO plasmid vector and Not1-G α_{i3} C351I-Xho1 PCR amplified product were then restriction digested using both Not1 and Xho1 restriction enzymes and G α_{i3} C351I was inserted between Not1 and Xho1 restriction sites of the plasmid vector by a ligation reaction. The construct was then confirmed by DNA sequencing.

2.2.2.5 Generation of FLAG-hGPR84-SPASM sensor constructs

The fusion fragment of systematic protein affinity strength modulation (SPASM) sensor and G protein peptide, SPASM-G $\alpha_{i1/2}$ composed of mCitrine (BRET acceptor), ER/K α -helix, Nano Luciferase (BRET donor), and G $\alpha_{i1/2}$ C terminus peptide encoding the last 27 amino acids of G $\alpha_{i1/2}$, each element being separated by a flexible linker (Gly-Ser-Gly)₄ residues was PCR amplified using FLAG-HindIII-hCXCR4-KpnI-SPASM-G $\alpha_{i1/2}$ -XhoI-pcDNA5/FRT/TO as the template and the primers used in this PCR reaction were as follows:

Forward primer, Not1-mCitrine:

5'-TAAGCAGCGGCCGCGTGAGCAAGGGCGAGGAGCTGTTC-3'

Rev primer, BGH Rev Primer: 5'-TAGAAGGCACAGTCGAGGCTGATCAGC-3'

The PCR amplified product, SPASM-G $\alpha_{i1/2}$ containing NotI and XhoI sites on its termini was then subcloned in frame between NotI and XhoI restriction sites of FLAG-hGPR84-G α_{i2} -pcDNA5/FRT/TO plasmid. Here, previously constructed FLAG-hGPR84-G α_{i2} -pcDNA5/FRT/TO plasmid and the amplified product SPASM-G $\alpha_{i1/2}$ were restriction digested with NotI and XhoI followed by ligation reaction with T4 DNA ligase. The generated FLAG-hGPR84-SPASM-G $\alpha_{i1/2}$ sensor construct was then confirmed by DNA sequencing.

The FLAG-hGPR84-SPASM-NP sensor which contains a repeating (Gly-Ser-Gly)₄ residues in place of the G protein peptide (last 27 amino acids of C terminus of G protein) was also generated following similar sub-cloning scheme. Here, the SPASM-NP sensor part was PCR amplified using FLAG-HindIII-hCXCR4-KpnI-SPASM-NP-XhoI-pcDNA5/FRT/TO plasmid as the template and the two primers as mentioned above. The resulting amplified product SPASM-NP was then sub-cloned into FLAG-hGPR84-G α_{i2} -pcDNA5/FRT/TO plasmid vector between NotI and XhoI restriction sites.

2.2.2.6 Generation of FLAG-hGPR84-SPASM mNeonGreen sensors

A series of BRET based biosensors, FLAG-hGPR84-SpNG-G $\alpha(x)$ sensors were generated whereas the last 27 amino acids of C-terminus of different G proteins (G $\alpha_{i1/2}$, G α_{i3} , G $\alpha_{o/A}$, G α_z , G α_q , G α_s , G α_{12} , G α_{13} , G α_{14} and G α_{16}) were coupled to the SPASM sensor part of the construct which was incorporated at the C-terminus of the FLAG-tagged human GPR84. Here, the SPASM sensor part is composed of mNeonGreen (BRET acceptor), ER/K α helix and Nano luciferase (NLUC, BRET donor) with each element being separated by a flexible linker, a repeating (Gly-Ser-Gly)₄ residues (Mackenzie et al., 2019).

FLAG-hGPR84-SpNG-G $\alpha(x)$ sensor (where X= i_{1/2}, i₃, o, z, s, q, 12, 13, 14 and 16) was generated by replacing eYFP within the FLAG-hGPR84-eYFP-pcDNA5/FRT/TO construct with a sequence corresponding to SpNG (stands for SPASM mNeonGreen) fused to G $\alpha(x)$ G protein peptide using NotI and XhoI restriction

enzymes. The recipient plasmid FLAG-hGPR84-eYFP-pcDNA5/FRT/TO and the insert containing plasmid hFFA2-SpNG-G α (x)-pcDNA5/FRT/TO (a gift from Dr Brian Hudson) were restriction digested with NotI and XhoI enzymes. Subsequent ligation of restriction fragments SpNG-G α (x) and FLAG-hGPR84-pcDNA5/FRT/TO led to the generation of FLAG-hGPR84-SpNG-G α (x) sensor construct.

The FLAG-hGPR84-SpNG-NP sensor was generated using the same sub-cloning scheme as that of FLAG-hGPR84-SpNG-G α (x) sensor only difference between these two sensors is that NP sensor contains a repeating (Gly-Ser-Gly)₄ residues in the place of G protein peptide. Simply, FLAG-hGPR84-eYFP-pcDNA5/FRT/TO and hFFA2-SpNG-NP-pcDNA5/FRT/TO (a gift from Dr Brian Hudson) were restriction digested with NotI and XhoI enzymes followed by ligation of SpNG-NP and FLAG-hGPR84-pcDNA5/FRT/TO restriction fragments ultimately generating FLAG-hGPR84-SpNG-NP-pcDNA5/FRT/TO construct. The generated SPASM sensor constructs were then confirmed by DNA sequencing.

2.2.2.7 Cloning of mouse GPR84

Mouse GPR84 was cloned from the mouse leukaemic macrophage cell line RAW 264.7. At first, RNA was extracted from RAW 264.7 cells using RNeasy Mini Kit (Qiagen) followed by cDNA synthesis by reverse transcription reaction using QuantiTect Reverse Transcription Kit (Qiagen) according to the manufacturer's instructions.

RNA extraction from RAW264.7 cells

1x10⁶ RAW264.7 cells were harvested by scraping with a cell scraper followed by centrifugation at 8000 x g for 1 minute. The cells pellets were then washed with 1XPBS and subjected to centrifugation again for 15 seconds at 17,900 x g. The supernatant was discarded and cell pellets were disrupted in 350 μ l of buffer RLT and homogenized by passing through a 20 gauge needle fitted to a syringe. 350 μ l of 70% ethanol was added to the homogenized lysate and mixed well by pipetting followed by transferring 700 μ l of the sample to an RNeasy Mini spin column placed in a 2 ml collection tube which was then subjected to centrifugation at 17,900 x g for 15 seconds. The flow-through was discarded and 700 μ l of Buffer RW1 was added to the spin column followed by centrifugation again at 17,900 x g for 15 seconds to wash out the contaminating carbohydrates,

proteins and fatty acids. After discarding flow-through, 500 µl of buffer RPE was added to the column and spun down for 15 seconds at 17900 x g to remove the traces of salts remained in the column. Flow-through was discarded and the column was washed again with 500 µl of RPE buffer by centrifugation at 17,900 x g for 2 minutes. The spin column was then placed on a new 1.5 ml Eppendorf microcentrifuge tube and 30 µl of RNase-free water was added directly to the column followed by incubation at room temperature for 1 minute. The sample was then centrifuged for 1 minute at 17,900 x g to elute RNA. Eluted RNA was immediately placed on ice. After estimating the concentration, RNA was either used for reverse transcription or stored in -80°C.

Mouse cDNA synthesis by reverse transcription reaction

Firstly, genomic DNA was eliminated from the extracted RNA sample. The genomic DNA elimination reaction was set up on the ice. Less than 1 µg of template RNA, 2 µl of 7X gDNA Wipeout buffer and required volume of RNase-free water to make a final volume of 14 µl were added to a nuclease-free microcentrifuge tube, mixed and stored on ice. Genomic DNA was then wiped out by incubating the reaction tube at 42°C for 2 minutes. The reaction mixture was immediately placed on ice. 1 µl of Quantiscript Reverse transcriptase (also contains RNase inhibitor), 4 µl of 5x Quantiscript RT buffer (also contains Mg²⁺ and dNTPs) and 1 µl of RT random primer mix were added to the tube containing the entire genomic DNA elimination reaction volume (14 µl). After mixing, the reaction mix was incubated at 42°C for 3 minutes followed by incubation at 95°C for 3 minutes to inactivate the reverse transcriptase.

Using this cDNA as template, FLAG epitope tag (amino acid sequence DYKDDDDK) was incorporated at the N-terminus of mouse GPR84 by PCR reaction using the following primers:

Mouse GPR84 Forward primer:

5' CATGTTGGATCCGCCACCATGGACTACAAGGACGACGATGATAAGTGGAAACAGCTCAGATGCCAAC 3'

Mouse GPR84 Reverse primer: 5' CAT GTTGCG GCC GCGATGGAAACCGGCGGAAACTCTG 3'

The sequences corresponding to BamHI and NotI sites required for cloning are underlined. The resulting PCR amplified product, FLAG-mouse GPR84 was then subcloned in-frame between the BamHI and NotI sites of an eYFP-pcDNA5/FRT/TO plasmid ultimately generating FLAG-mouse GPR84-eYFP-pcDNA5/FRT/TO construct. The identity of the construct was then confirmed by DNA sequencing.

2.2.2.8 Generation of FLAG-mGPR84-G α_{i2} and FLAG-mGPR84-G α_{i2} C352I fusion constructs

Firstly, the internal BamHI site of G α_{i2} of FLAG-hGPR84-G α_{i2} and FLAG-hGPR84-G α_{i2} C352I was silently mutated by site-directed mutagenesis according to the QuikChange method (section 2.2.6) using the following primers:

C636T G α_{i2} Forward: 5' GAGCGGAAGAAGTGGATTCACTGCTTTGAGGGTG 3'

C636T G α_{i2} Reverse: 5' CACCCTCAAAGCAGTGAATCCACTTCTTCCGCTC 3'

The FLAG-mGPR84-G α_{i2} and pertussis toxin resistant construct FLAG-mGPR84-G α_{i2} C352I fusion proteins were then generated by replacing human GPR84 of FLAG-hGPR84-C636T G α_{i2} -pcDNA5/FRT/TO or FLAG-hGPR84-C636TG α_{i2} C352I-pcDNA5/FRT/TO plasmid, respectively with the sequence corresponding to mouse GPR84 using BamHI and Not1 restriction enzymes.

2.3. Mammalian cell culture and maintenance

Mammalian cell culture and maintenance and transfection processes were performed in a Class II laminar flow biosafety cabinet following proper sterile techniques and guidelines. The cells were incubated in an inCu saFe SANYO humidified incubator supplied with 5% CO₂. All solutions, reagents and equipment which came in contact with the cells were ensured to be sterile. All solutions or reagents used for the cell culture were pre-warmed for 15-30 minutes to 37°C using a water bath.

2.3.1 HEK293T cells

Human embryonic kidney 293 cells expressing SV40 T-antigen (HEK293T), which were employed for the transient heterologous expression of receptor of interest,

were maintained in Dulbecco's modified Eagle's Medium (DMEM) with high glucose (Sigma-Aldrich) supplemented with 10% heat-inactivated fetal bovine serum (FBS, ThermoFisher Scientific), 2 mM L-glutamine (Sigma-Aldrich), 100 units/ml penicillin (ThermoFisher Scientific), 100 µg/ml streptomycin (ThermoFisher Scientific) at 37°C and 5% CO₂ under humidified atmosphere. After the cells have grown to 80% confluency, HEK293T cells were passaged at 1:10 dilution into T75 cm² cell culture flask (Corning).

2.3.2 Flp-In™ T-REx™-293 cells

Parental Flp-In™ T-REx™-293 cells (Invitrogen Life Technologies) employed for the stable transfection of receptor of interest were cultured and maintained in Dulbecco's modified Eagle's medium without sodium pyruvate (Gibco™, ThermoFisher Scientific) supplemented with 10% (v/v) heat-inactivated FBS, 100 units/ml penicillin, 100 µg/ml streptomycin and 10 µg/ml blasticidin (InvivoGen) at 37 °C in a 5% CO₂ humidified atmosphere.

2.3.3 Flp-In™ T-REx™-293 stable cell lines expressing GPR84 receptor

Flp-In™ T-REx™-293 stable cell lines able to inducibly express human or mouse GPR84 were maintained in DMEM without sodium pyruvate (high glucose) supplemented with 10% heat-inactivated FBS, 100 units/ml penicillin, 100 µg/ml streptomycin, 10 µg/ml blasticidin and 200 µg/ml hygromycin B (InvivoGen) at 37°C and 5% CO₂ in humidified atmosphere. These cells were passaged routinely after 80% confluency by splitting cells into 1:10 or 1:20 dilution. The expression of the receptor construct of interest was induced on demand by treating the cells with 100 ng/ml of doxycycline (Sigma-Aldrich) for 24 hours.

2.3.4 RAW 264.7 cells

RAW 264.7 mouse monocyte-macrophages were cultured and maintained in DMEM (with 4.5g/L D-glucose, 0.11 g/L sodium pyruvate) (Gibco™, ThermoFisher Scientific) supplemented with 10% heat-inactivated FBS, 100 units/ml penicillin, 100 µg/ml streptomycin and 2 mM L-glutamine at 37°C and 5% CO₂. These cells were subcultured at 1:10 dilution into 75 cm² or 150 cm² flask. Briefly, the medium was removed followed by addition of 10 ml of media to the flask. Cells

were then dislodged by scraping gently with a sterile cell scraper followed by addition of appropriate aliquots of cell suspension into new cell culture flask. To upregulate GPR84 expression, RAW 264.7 cells were treated with 100 ng/ml of lipopolysaccharide (LPS) (Sigma-Aldrich, Dorset, UK) for 5, 8, 11 or 24 hours prior to membrane preparation.

2.3.5 Thawing of cells

1 vial of cells (HEK293T or Flp-In™ T-REx™-293 stable cell lines) stored in liquid nitrogen were taken out, thawed at 37°C in a water bath and decontaminated with 70% ethanol. After complete thawing, the cells were transferred to a 15 ml sterile falcon tube filled with 10 ml of pre-warmed culture media in the laminar flow hood followed by centrifugation at 201 x g for 4 minutes at room temperature. The cell pellets were then re-suspended with 10 ml of culture media in the hood and transferred to a 75 cm² cell culture flask followed by incubation overnight in 37°C and 5% CO₂. In the next day, the media was aspirated and replaced with fresh media. The cells were checked daily for confluency. In the case of RAW264.7 cells, after thawing the cells at 37°C in a water bath and decontaminating with 70% ethanol, cells were transferred to a 75 cm² flask pre-filled with 12 ml of warmed growth media followed by incubating at 37°C and 5% CO₂ for 4 hours. The media were then aspirated off and replaced with 10 ml of fresh pre-warmed media and incubated overnight.

2.3.6 Passaging of cells

When cells were grown to 80 to 90% confluency (for HEK293T or Flp-In™ T-REx™-293 stable cell lines), all media was aspirated off and washed once with pre-warmed 10 ml of sterile phosphate-buffered saline (PBS) (137 mM NaCl, 2.7 mM KCl, 10 mM Na₂HPO₄, 1.8 mM KH₂PO₄; pH:7.4) to remove excess media and serum. 2 ml of pre-warmed 0.25% trypsin-EDTA solution (Sigma-Aldrich) was then added to the monolayer of cells to detach them from the bottom of the flask and kept at room temperature in the hood for 1 to 3 minutes depending on the adherence of the cells. To ensure cell dissociation completely, the flask was tapped gently. To stop trypsinization and make cell suspension, 8 ml of pre-warmed growth media with serum was added to the flask followed by pipetting up and down to break down the clumps of cells. 1 ml (1:10 dilution) or 0.5 (1:20

dilution) ml of 10 ml cell suspension was then transferred to a new 75 cm² cell culture flask with 9 ml or 9.5 ml of pre-warmed fresh media added, respectively.

2.3.7 Cryopreservation of cells for long-term storage

For long-term storage, cells were preserved in cryovials in liquid nitrogen. After reaching 80% confluency, the media was aspirated off and washed with 1XPBS followed by the addition of 2 ml of 0.25% trypsin-EDTA solution to detach the cells. Cells were then re-suspended with 8 ml media and cells were counted by trypan blue exclusion method using a haemocytometer. The cell suspension was then subjected to centrifugation at 201 x g for 4 minutes at room temperature. Media were carefully aspirated off and cell pellets were re-suspended at a density of 3x10⁶ cells/ml in sterile freezing media (Fetal bovine serum with 10% DMSO for HEK293T or Flp-In[™] T-REx[™]-293 stable cell lines; FBS with 5% DMSO for RAW264.7 cells). 1 ml of cell suspension was then aliquoted into each cryovial followed by storage in -80°C for 24 hours prior to storage in liquid nitrogen.

2.4. Transient transfection

2.4.1 Transient transfection using PEI

For transient expression of receptor of interest, receptor construct was transfected into HEK293T cells using cationic DNA complexing agent, polyethyleneimine (PEI, linear, MW: 25000, Polysciences, Inc.). PEI was dissolved in 150 mM NaCl by gentle shaking and sonicating to make a 1mg/ml stock solution followed by adjusting pH to 7.0 with HCl. PEI solution was then filter sterilized and aliquoted in 1 ml volume and stored in -20°C. The day before transfection, 2X10⁶ HEK293T cells were plated on 10 cm cell culture dishes by splitting (1:4 dilution) 80% confluent cells from T75 flask. On the day of transfection, 5 µg DNA was diluted in 250 µl of 150 mM sterile NaCl (pH 7.4) and 30 µl of 1 µg/µl PEI (1:6 DNA:PEI) was diluted in 250 µl of 150 mM sterile NaCl in two separate sterile 1.5 ml Eppendorf microcentrifuge tubes. This volume of 250 µl for each mixture of DNA and PEI is for one 10 cm dish and volumes can be scaled proportionally for additional dishes. Diluted DNA complexes were then added to diluted PEI tube and the mixture was vortexed for few seconds followed by incubation for 10 to 15 minutes at room temperature. In the meantime media from the 10 cm dish was removed and fresh media was added.

After incubation, DNA/PEI complexes were added to the cells in a dropwise manner (500 μ l/dish). In parallel, as a negative control, pcDNA3.1 or pcDNA5/FRT/TO vector was also transfected to HEK293 cells in another 10 cm dish using the above-mentioned process. Where necessary, this protocol can be scaled down according to the number of cells per preparation for transfection of cells in 6-well plates or 12-well plates. The transfected dishes were then returned to the cell culture incubator. The cells were harvested after 36 to 48 hours of transient transfection for the preparation of the membrane.

2.4.2 Transient transfection using lipofectamine

Cationic lipid-based transfection reagent (Lipofectamine 2000 or lipofectamine 3000 reagents) forms liposomes by complexing with plasmid DNA or siRNA. Positive charges of cationic lipids neutralize negative charges of the phosphate backbone of DNA and impart an overall positive charge to the surface of the liposome in water. These surface positive charges of DNA-liposome complex lead to the fusion of DNA-lipid complex to the negatively charged cell membrane followed by delivery of the DNA to the cytosol of cells by endocytosis. The day before the transfection, HEK293 cells were seeded on 6-well plates/12-well plates/10 cm cell culture dishes so that 70 to 80% confluency would be obtained prior to the transfection. For the 6-well plate, transfection protocol is as follows which can be scaled up or down accordingly for 10 cm dishes or 12-well plates, respectively. One day before transfection, 0.5×10^6 cells were plated in 2 ml of growth medium in each well of the 6-well plates. On the day of transfection, 8 μ l of P3000TM reagent was diluted in 100 μ l of serum-free DMEM medium or Opti-MEM medium in a sterile microcentrifuge tube. 2.0 μ g of plasmid DNA was then added to the diluted P3000 reagent and mixed by vortexing for a few seconds. 4 μ l of LipofectamineTM 3000 reagent (Invitrogen Life Technologies) was diluted in 100 μ l of either serum-free DMEM medium or Opti-MEM medium in another sterile tube. Diluted DNA in P3000 reagent was then mixed well with the diluted Lipofectamine 3000 reagent (1:1 ratio) and vortexed for few seconds followed by incubating the mixture at room temperature for 10 to 15 minutes. After incubation, the DNA-lipid complex was added to cells in a dropwise manner (200 μ l/well). The cells were then incubated in 37°C and 5% CO₂ in an incubator for 24-48 hours until to be used in assays.

Transient transfection using Lipofectamine 2000 reagent (Invitrogen Life Technologies) protocol is identical to that of lipofectamine 3000 reagent protocol. On the day before transfection, 0.5×10^6 HEK293 cells were seeded in 2 ml growth media in each well of the 6 well plates. 2.5 μ g of plasmid DNA was diluted in 100 μ l of serum-free media and 5 μ l of Lipofectamine 2000 reagent (1:2 DNA: Lipofectamine) was diluted in 100 μ l of serum-free media. Diluted plasmid DNA was mixed with diluted lipofectamine 2000 (1:1 ratio) and incubated for 15 minutes at room temperature followed by dropwise addition of the DNA-lipid complex to cells (200 μ l/well). Transfected cells were then incubated in 37°C and 5% CO₂ for 24-48 hours until to be used in assays.

2.5 Generation of Flp-In T-REx-293 cell lines inducibly expressing GPR84 receptor

Doxycycline-inducible Flp-InTM T-RExTM-293 stable cell lines expressing FLAG-hGPR84-G α_{i2} , FLAG-hGPR84-G α_{i2} C352G, FLAG-hGPR84-G α_{i2} C352I, FLAG-hGPR84-G α_{i3} , FLAG-hGPR84-SPASM G $\alpha_{i1/2}$, FLAG-hGPR84-SPASM NP, FLAG-mGPR84-eYFP, FLAG-mGPR84-G α_{i2} or FLAG-mGPR84-G α_{i2} C352I were generated. Another six doxycycline-inducible Flp-In T-REx-293 stable cell lines expressing FLAG-hGPR84 R172A-G α_{i2} C352I, FLAG-hGPR84 R172K-G α_{i2} C352I, FLAG-hGPR84 F170A-G α_{i2} C352I, FLAG-hGPR84 F335A-G α_{i2} C352I, FLAG-hGPR84 F101A-G α_{i2} C352I or FLAG-hGPR84 W360A-G α_{i2} C352I receptor construct were also developed. These stable cell lines were generated by co-transfection of receptor construct of interest subcloned into the pcDNA5/FRT/TO vector and integration plasmid vector pOG44 (1:9 ratio, w/w) into Flp-InTM T-RExTM-293 cells using 1mg/ml of cationic DNA complexing agent, polyethyleneimine (PEI, MW-25000). After successful co-transfection, Flp recombinase expressed from pOG44 plasmid catalyses the homologous recombination of Flp recombination target (FRT) sites on pcDNA5/FRT/TO vector containing gene of interest and host genome and thus receptor of interest is inserted into the genome of the host cells at integrated FRT site (Ward et al., 2011). Flp-InTM T-RExTM-293 cells were cultured in DMEM without sodium pyruvate (Invitrogen) supplemented with 10% FBS, 1% penicillin/streptomycin and 10 μ g/ml blasticidin and were split into 10 cm dishes so that 60 to 80% confluency was attained prior to the transfection. 8 μ g of DNA (0.8 μ g receptor of interest in pcDNA5/FRT/TO vector and 7.2 μ g of pOG44 plasmid vector) was diluted in 250 μ l of 150 mM sterile NaCl (pH 7.4) in a sterile

microcentrifuge tube. Similarly, 48 μ l of PEI (ratio 1:6 DNA/PEI) was diluted in a similar volume of 150 mM sterile NaCl in another sterile tube. Diluted total DNA complexes were then added to diluted PEI and mixed well with slight vortexing for a few seconds. A negative control for transfection was also prepared by mixing empty pcDNA5/FRT/TO vector with pOG44 plasmid vector and PEI, each diluted in 150 mM NaCl. The DNA-PEI complexes were then incubated at room temperature for 10 to 15 minutes followed by addition to the cells in a dropwise manner. 24 hours following transfection, growth media was removed and replaced with fresh growth media. 48 hours after transfection, the transfected cells were split in 1:10 and 1:30 dilution into 10 cm dishes and incubated overnight. On the following day, the medium was removed and replaced with the medium supplemented with 200 μ g/ml of hygromycin B antibiotic to initiate the selection of stably transfected cells. The media was changed every 3-4 days to remove the dead non-transfected cells. After 14 days, several hygromycin-resistant colonies were formed which were collected by trypsinization of cells with 0.25% trypsin-EDTA solution and transferred to a 75 cm² flask to grow. After expanding and passaging the cells for one more time, these stable transfectants were then tested either through western blotting or confocal microscopy to ensure that the receptor of interest was inducible with doxycycline. In resting condition, the tet repressor protein (homodimer) expressed from the host cell binds to the tet operator 2 (TetO₂) sequence of the hybrid promoter, CMV/TetO₂ of the integrated pcDNA5/FRT/TO containing the receptor of interest and thus represses the transcription of gene (Ward et al., 2011). The addition of tetracycline such as doxycycline to culture medium leads to expression of the gene of interest (GOI) by binding with the tet repressor protein followed by dissociation of tet repressor-doxycycline complex allowing induction of transcription of GOI. For long term storage, some cells from early passages were frozen down using FBS with 10% DMSO as freezing medium and subsequently stored in liquid nitrogen.

2.6 Biochemical and functional pharmacological assays

2.6.1 Membrane preparations

Membranes were prepared from Flp-InTM T-RExTM-293 stable cells either untreated or treated with 100 ng/ml doxycycline for 24 hours to express receptor of interest, transiently transfected HEK-293 cells or from RAW264.7 cells either untreated or treated for 5 hours, 8 hours, 11 hours and 24 hours with pure LPS (Enzo Life Sciences; acts as a specific activator of TLR4 and does not activate other form of TLRs including TLR2). After the specific time period of cellular treatment either with doxycycline or LPS/PTX or after 36 to 48 hours following transient transfection, cells were harvested by removing the growth medium, rinsing once with 10 ml of ice-cold phosphate-buffered saline (PBS; pH 7.4) for each dish followed by either pipetting up and down to detach the cells or scraping the cells from the bottom of the dish with cell scraper. The cell suspensions in ice-cold PBS were transferred to a 50 ml falcon tube and were then centrifuged at 1811 x g for 5 min at 4°C. The supernatant was discarded and then rinsed with 20 ml ice-cold PBS followed by re-centrifugation at 1811 x g at 4°C for 5 min. The cell pellets were then stored at -80°C until used. The frozen cell pellets were thawed on ice for 30 minutes and suspended in 5 volumes (1-2 ml) of ice-cold TE membrane buffer (10 mM Tris-HCl, 0.1 mM EDTA, pH 7.5) containing 1xComplete EDTA free protease inhibitor cocktail tablet (Roche Applied Science, West Sussex, UK) (1 tablet per 50 ml of TE buffer). Pellet suspensions were then homogenized with 50 strokes of a ground glass on Teflon homogenizer (5 ml hand-held homogenizer) to rupture the cells. The homogenates were then transferred to a pre-chilled 7 mL bijoux container (Greiner Bio-one) and passed 5 times through a 25 gauge needle fitted to a 2 ml syringe to rupture the cells again. The suspensions were then transferred to a 15 ml falcon tube and centrifuged at 314 x g at 4°C for 5 min to remove the unbroken cells, nuclei or other cellular debris. The supernatant was then transferred to ultracentrifuge glass tubes and centrifuged at 50,000 rpm for 45 minutes at 4°C using OptimaTM TLX Ultracentrifuge (Beckman Coulter) with a TLA100.2 rotor. After the ultra-centrifugation, the supernatant was discarded and each pellet of membrane fractions was re-suspended in 1 ml of ice-cold TE membrane buffer supplemented with protease inhibitor cocktail and passed 10 times through a 2 ml syringe attached to a 25 gauge needle to make the mixture

homogenous. The generated each membrane preparation was then transferred to a pre-chilled 1.5 ml sterile microcentrifuge tube. The total protein concentration of each membrane preparation was measured by bicinchoninic acid (BCA) assay and membranes were aliquoted into 500 μ l sample which were then stored at -80°C until to be used. These stored membrane preparations are usable until 6 months.

2.6.2 Determination of membrane protein concentration

Amount of total proteins in each generated membrane preparation was determined by bicinchoninic acid (BCA) assay using BCA protein assay kit (Pierce, Fisher Scientific, Loughborough, UK). This BCA assay is a colorimetric detection method based on the reduction of Cu^{2+} (from BCA reagent B, 4% cupric sulfate) to Cu^{+} ion by peptide bond in alkaline condition followed by chelation of cuprous ion by the bicinchoninic acid forming a purple-coloured water-soluble complex which displays strong absorbance at 562 nm. Previously a series of standard bovine serum albumin (fatty acid-free) concentrations (0.2, 0.4, 0.6, 0.8, 1.0, 1.2, 1.4, 1.6, 1.8, 2.0 and 2.2 mg/ml) were prepared from 5 mg/ml stock solution by serial dilutions using TE buffer (10 mM Tris-HCl, 0.1 mM EDTA, pH 7.5) and were stored in -20°C . These standard BSA solutions were thawed prior to the BCA assay and 10 μ l of each concentration of the standard was added in triplicate to a 96 well clear flat bottom assay plate (Corning, USA). As a negative control/blank standard, 10 μ l of TE buffer was also added in triplicate to the plate followed by addition of 10 μ l of each membrane preparation in triplicate to the same plate. 1 part of BCA Reagent B (4% cupric sulfate) was added to 49 parts of BCA Reagent A (sodium carbonate, sodium bicarbonate, bicinchoninic acid and sodium tartrate in 0.1M sodium hydroxide) to make the working reagent. 200 μ l of this working reagent was then added to each well of the microplate using an Eppendorf repeater with handheld dispenser. The plate was then covered with a disposable seal (Topseal TM, PerkinElmer) and incubated for 20 minutes in 37°C followed by measuring the absorbance at 562 nm on a microplate reader, PHERAstar FS plate reader (BMG Labtech, Aylesbury, UK). The average absorbance value for the blank standard was then subtracted from the values for BSA standards and unknown samples followed by generation of a standard curve for BSA plotting blank corrected average values against the corresponding concentration of BSA. Using linear regression analysis, the protein

concentration of each unknown membrane preparation was interpolated from the standard curve.

2.6.3 Sodium dodecyl sulphate-polyacrylamide gel electrophoresis (SDS-PAGE)

To investigate the expression of receptor of interest in transfected cells, membranes generated from the cells were subjected to sodium dodecyl sulphate polyacrylamide gel electrophoresis (SDS-PAGE) followed by immunoblotting with a specific antibody. SDS-PAGE resolves the proteins based on their electrophoretic mobility. SDS denatures the protein by breaking the secondary, tertiary and quaternary structure upon binding to the protein as well as imparts an overall negative charge to the protein ultimately converts the proteins into negatively charged linear polypeptide chains which under electric field can mobilize through the acrylamide mesh to the anode according to their molecular weight.

Membrane preparations stored in -80°C were thawed and diluted with TE membrane buffer so that all the samples have identical concentration. To deglycosylate the glycoprotein, membrane preparation was treated with peptide N-glycosidase enzyme (PNGase F; Roche Diagnostics). Briefly, the calculated volume of membrane sample was mixed gently with the required volume of 10X incubation buffer (20 mM potassium phosphate buffer, pH 7.2) and PNGase F at a final concentration of 0.05 unit/ μl followed by heating at 37°C for 2 hours. As a negative control, a similar volume of membrane sample mixed with an equal volume of incubation buffer without adding PNGase F was also heated at 37°C for 2 hours. Each of PNGase F treated and untreated membrane samples was then mixed with equal volume of 2X Laemmli buffer (60 mM Tris, 80 mM sodium dodecyl sulphate (SDS), 50 mM dithiothreitol (DTT), 10% (v/v) glycerol, 0.01% (w/v) bromophenol blue, pH 6.8) followed by heating at 37°C for 15 minutes. DTT disrupts disulphide bonds of proteins and thereby denatures the protein. SDS also acts as a denaturant as discussed above and heating also contribute to the denaturation of the protein. Laemmli buffer also serves as the loading buffer for the samples.

50 ml of 20X Novex Bolt™ MOPS SDS Running Buffer (Life Technologies) was mixed with 950 ml of deionized water. Precast gels, Bolt™ 4-12% Bis-Tris 1.00 mmX10 well (Invitrogen, Thermo Fisher Scientific) stored at 4°C were removed from the fridge and kept at room temperature before running. After removal of the comb and peeling away the tape at the bottom of the gel cassette, the wells of the gel were rinsed with deionized water. Two gel cassettes were then inserted into two chambers of the Bolt™ Mini Gel Tank (Life Technologies) which already have been filled with 1X MOPS SDS running buffer to just above the electrode. It was also ensured that wells were completely filled with buffer. 5 to 8 µl of ECL™ Rainbow™ marker, RPN800E (GE Healthcare, UK) which allow the estimation of protein size of the samples, was then added to the first well of the gel followed by addition of samples containing 10 to 20 µg of proteins to the following wells and any empty well was filled with 1X Laemmli buffer. Gels were then run in MOPS SDS buffer at 165V for 45 minutes until the bromophenol dye front reached just above the edge of the gel.

2.6.3. Immunoblotting or western blot

Following separation of proteins by SDS-PAGE, proteins were electrophoretically transferred from the Bis-Tris gels to Nitrocellulose blotting membrane (GE Healthcare Life Science) in transfer buffer (200 mM glycine, 25 mM Tris, 20% (v/v) methanol) at 30 V for 1 hour using an XCell II™ Blot Module (Life Technologies). Prior to the transfer, filter paper, sponges and nitrocellulose membrane were soaked in 1X transfer buffer. A sandwich of sponge pad, filter paper, electrophoresed Bis-Tris gel, nitrocellulose membrane, filter paper and sponge pad was assembled placing the cathode core on the bottom and any bubbles between layers of the sandwich were removed using a blotting roller. The anode core was then placed on the top of the sandwich and the blot module assembly was closed. This blot module was then inserted into the chamber of the XCell SureLock™ Mini-Cell Electrophoresis System (Life Technologies) followed by addition of 1X transfer buffer to the module core and to the chamber to the level of the electrode. A constant voltage of 30 V was then applied for 1 hour to allow the transfer of proteins from the gel to nitrocellulose membrane. After membrane transfer, the nitrocellulose membrane was placed in a tray and wet for 2 minutes in PBS-T (1X phosphate buffered saline with 0.2% (v/v) Tween 20). To block the nonspecific sites on the membrane, the

nitrocellulose membrane was blocked with 5% (w/v) Marvel powdered skimmed milk in PBS-T for 2 hours at room temperature with gentle shaking, ensuring that sufficient blocking buffer was applied to cover the membrane. Membranes were then incubated overnight with primary antibody at the appropriate dilution (made up in PBS-T with 3% milk) at 4°C with gentle shaking. Mouse monoclonal anti-FLAG M2 antibody (Sigma-Aldrich) was diluted at 1:1,000 while both sheep polyclonal anti-GFP antiserum (produced in-house) and rabbit anti-ICL3-mouse GPR84 antiserum (produced in-house) were diluted at 1: 10,000 in PBS-T with 3% milk. On the following day, the primary antibody solution was poured off and the blot was washed 4 times for 5 minutes in PBS-T with shaking on a platform shaker. Blot was then incubated in diluted horseradish peroxidase (HRP) conjugated secondary antibody (made up in PBS-T with 3% milk) for 2 hours at room temperature with gentle shaking ensuring that blot was protected from light by covering the incubation box with aluminium foil. HRP-labelled anti-mouse IgG secondary antibody (GE Healthcare Life Sciences, Buckinghamshire, UK) (1: 10,000 dilution), anti-goat IgG secondary antibody (1:20,000 dilution) and anti-rabbit IgG secondary antibody (GE Healthcare) (1:20,000 dilution) were used to detect anti-FLAG M2 antibody, anti-GFP antiserum and anti-ICL3-mouse GPR84 antiserum, respectively. The secondary antibody solution was poured off and the blot was then washed 4 times with PBS-T for 5 minutes with shaking on a platform shaker at room temperature. The blot was protected from light during washing.

Proteins on the blot were detected by enhanced chemiluminescent (ECL) detection method which is based on the emission of light from the oxidation of luminol by HRP-conjugated secondary antibody in the presence of peroxide. This luminescence is proportional to the amount of the target protein present on the nitrocellulose membrane and can be detected by CCD cameras capturing a digital image of the western blot or photographic film. Equal parts of the peroxide solution and the luminol/enhancer solution of SuperSignal™ West Pico PLUS chemiluminescent substrate kit (Thermo Scientific, USA) were mixed to prepare the working solution and sufficient volume of this working solution was added to the membrane. The blot being protected from light was then incubated for 5 minutes with gentle shaking on a benchtop shaker. The working solution was then removed and excess reagent was drained. The blot was placed in a

clear plastic coating inside a developing cassette. Air bubbles were removed by smoothing out the plastic coating gently and the blot was then exposed to a Carestream KODAK BioMax Light film (Sigma-Aldrich) in a dark room for a specific period of time which was subsequently processed using a KODAK[®] X-OMAT[®] Film developer.

2.6.5 [³⁵S]-GTPγS binding assay

To assess the G protein activation level of the receptor [³⁵S]-GTPγS binding assay was employed. Upon receptor activation following agonist stimulation, GTP is exchanged for GDP on activated Gα subunit which can be terminated by GTPase activity of the Gα subunit resulting in hydrolysis of GTP into GDP and inorganic phosphate. Similar to intracellular GTP, exogenous [³⁵S]-GTPγS which is a radiolabelled analogue of GTP containing a ³⁵S on the gamma phosphate, can also be exchanged for GDP on Gα subunit of the activated G protein. In contrast to intracellular GTP, this radioligand is resistant to hydrolysis by inherent GTPase activity leading to accumulation of agonist-receptor- [³⁵S]-GTPγS-bound G protein ternary complex (Harrison and Traynor, 2003; Strange, 2010). This bound radioligand can be separated from the unbound form by filtration with washing and the radioactivity can be counted by liquid scintillation spectroscopy. The resultant radioactivity is proportional to the amount of G protein activation level.

[³⁵S]-GTPγS binding assay was performed according to the method described by Milligan (2003). 5 μg of membrane proteins generated from transfected cells expressing receptor of interest or from LPS-induced RAW264.7 cells were pre-incubated with indicated concentrations of ligands for 15 minutes at 25°C in assay buffer (20 mM HEPES, 5 mM MgCl₂, 160 mM NaCl, 1 μM GDP, 0.05% fatty acid-free bovine serum albumin, pH 7.5) in a total assay volume of 500 μl either in glass tubes or in 1.0 ml 96 deep-well plate (Starlab, USA). In case of experiments designed for assessing potential allosteric interactions between DIM or DIM analogues and orthosteric agonists (C-10, embelin, 6-OAU, compound-1) both the potential modulator and orthosteric agonist probe were added to the membranes at the same time. In case of experiments designed to assess the ability of various concentrations of antagonist (compound 9, 104, 107, 161, 837 or GLPG1205) to inhibit the effect of an EC₈₀ concentration of an agonist (C-10,

embelin, DIM or compound-1) or to change the position of concentration-response curves for an agonist (Schild analysis), antagonist was pre-incubated with the membrane protein for 15 minutes at room temperature prior to the addition of agonist concentration(s). [^{35}S]-GTP γ S (50 nCi per reaction) (PerkinElmer Life Sciences) was then added to each tube to initiate the reaction followed by 45 minutes incubation at 30°C in a temperature-controlled water bath. Reactions were then terminated by rapid vacuum filtration through GF/C filters (pre-soaked in cold PBS) using a 24-well Brandel cell harvester (Alpha Biotech, Glasgow, UK). In cases of assays performed in 96 deep-well plates, vacuum filtration was performed through GF/C glass fibre filter fitted in 96-well white microplate (also known as UniFilter plate, PerkinElmer Life Sciences, Beaconsfield, UK) using a UniFilter FilterMate Harvester (PerkinElmer Life Sciences, Beaconsfield, UK). To separate the bound radioligands from unbound forms, GF/C filters were washed three times with ice-cold phosphate buffered saline (pH 7.4). [^{35}S]-GTP γ S bound to the activated GPCR-G protein complex of the membrane was unable to pass through the filter paper while the unbound form of the radioligand was washed away through the filter. Filter papers were kept at room temperature for air drying for a minimum of 2 hours or overnight and then transferred to 6 ml PE Pony Vials (PerkinElmer). 3 ml liquid scintillation fluid (Ultima Gold TM XR scintillation cocktail, PerkinElmer Life Sciences, Beaconsfield, UK) was added to each cut filters. The retained radioactivity was measured using a liquid scintillation counter, Tri-Carb[®] 2910 TR (PerkinElmer). In the case of UniFilter, after air-drying for minimum 2 hours, adhesive BackSeal was applied to each UniFilter plate and 50 μl of scintillation cocktail, MicroScint-20 (PerkinElmer Life Sciences, Beaconsfield, UK) was added to each well of the plate using an Eppendorf Repeater with manual handheld dispenser. Each UniFilter plate was then sealed with TopSealTM (PerkinElmer) and retained radioactivity of the bound radioligand was measured using a microplate scintillation counter, TopCount NXTTM (Packard). The obtained radioactivity of [^{35}S]-GTP γ S in the form of counts per minute (CPM) was then plotted against the ligand concentrations in logarithmic scale.

2.6.6 HTRF-based cAMP accumulation assay

Forskolin-induced cAMP accumulation assay based on the homogeneous time-resolved fluorescence resonance energy transfer (HTRF) was performed using

cAMP dynamic kit (CisBio Bioassays, CisBio, Codolet, France) following the manufacturer's instructions. It is a competitive immunoassay wherein cAMP labelled with d2 dye (FRET acceptor) competes with the unlabelled cAMP produced in the cells or exogenous standard cAMP for the site on the monoclonal antibody, anti-cAMP labelled with Eu^{3+} -Cryptate (FRET donor). FRET occurs when cAMP-d2 conjugate binds with the anti-cAMP-cryptate conjugate. Therefore, intracellular cAMP produced by activation of adenylyl cyclase will displace the cAMP-d2 from the binding site on anti-cAMP-cryptate conjugate leading to no FRET signal, implying that the measured FRET is inversely proportional to the accumulated cAMP in the cells. As GPR84 is a $\text{G}\alpha_i$ -coupled receptor, the ability of agonist-promoted activated GPR84 to inhibit the forskolin-induced cAMP accumulation was assessed by this HTRF-based assay. Flp-InTM T-RExTM-293 stable cells harbouring FLAG-hGPR84- $\text{G}\alpha_{i2}$, FLAG-hGPR84- $\text{G}\alpha_{i2}$ C352I or FLAG-hGPR84- $\text{G}\alpha_{i2}$ C352G treated with 100 ng/ml doxycycline for 24 hours to express the receptor of interest were utilized for this experiment. The cells were dissociated by versene-EDTA solution followed by resuspension with Hank's Balanced Salt Solution (HBSS) (137 mM NaCl, 5.3 mM KCl, 0.34 mM Na_2HPO_4 , 0.44 mM KH_2PO_4 , 4 mM NaHCO_3 , 1.26 mM CaCl_2 , 0.5 mM MgCl_2 and 0.4 mM MgSO_4 at pH 7.3). The cells were then counted by trypan blue exclusion method and 5 μl of cell suspensions in HBSS containing 2000 cells/ μl was plated in 384-well low volume plate and incubated for 30 minutes at room temperature with 5 μl indicated concentrations of agonist/vehicle (nonstimulated cells control) containing 1 μM forskolin. The agonist was prepared using the cell stimulation buffer which contains 0.5 mM 3-isobutyl-1-methylxanthine (IBMX), 1 μM forskolin and HBSS. Forskolin acts as an activator of the enzyme adenylyl cyclase raising the intracellular cAMP level while IBMX was added to the buffer to act as a phosphodiesterase inhibitor and thereby inhibits degradation of cAMP. In parallel, to generate a standard curve, 5 μl of various concentrations ranging from 0.17 to 712 nM of standard cAMP were added to the cells and incubated for 30 minutes with the 5 μl of cell stimulation buffer. After cells has been stimulated, 5 μl of diluted (1:20) cAMP-d2 conjugate in lysis buffer (except in cell negative control and standard negative control) and 5 μl of diluted (1:20) anti-cAMP cryptate conjugate in lysis buffer were added to each well followed by incubation at room temperature for 1 hour in dark. Fluorescence was measured at 620 nm (for Eu^{3+} -Cryptate, FRET donor) and at 665 nm (for d2-dye,

FRET acceptor) using PHERAstar FS plate reader (BMGLabtech, Aylesbury, UK). The 665 nm/ 620 nm fluorescence emission ratio was then calculated and the ability of the agonist to inhibit forskolin-induced production of cAMP was determined. Briefly, the emission ratio (ratio at 665 nm/620 nm) was multiplied by 10,000 and using this ratio for samples or negative control, the Delta F values were calculated using the following formula:

$$\text{Delta } F = \frac{\text{Ratio for standard or sample} - \text{Ratio for negative control}}{\text{Ratio for negative control}} \times 100$$

$$\text{Where } \text{Ratio} = \frac{\text{Fluorescence at 665 nm}}{\text{Fluorescence at 620 nm}} \times 10^4$$

A cAMP standard curve was then drawn by plotting delta F (%) in the y-axis and respective concentrations of standard cAMP in the x-axis. Using this sigmoidal standard curve, the cAMP concentration of the samples was deduced from their respective delta F (%) value.

2.6.7 Radioligand saturation binding assays

[³H]-G9543, an analogue of compounds 104, 107 and 161 with the same characteristic 2-(substituted-alkoxy)-9-substituted-6,7-dihydro-pyrimido[6,1-a]isoquinolin-4-one chemotype (Mahmud et al., 2017) was used for saturation binding assays to measure the expression of the receptor construct in transfected cells. Various concentrations of [³H]-G9543 were incubated with 5 µg of membrane protein expressing the receptor of interest with (non-specific binding) or without (total binding) 1 µM of GPR84 antagonist, 104 for 1 hour at 25°C in assay buffer (phosphate-buffered saline, 0.5% fatty acid free bovine serum albumin, pH 7.4) in a total volume of 500 µl in glass tubes. The reaction was terminated and [³H]-G9543 bound to the receptor construct was isolated from the unbound form by vacuum filtration through GF/C filter papers (Alpha Biotech) using a 24-well Brandel Cell harvester (Alpha Biotech, Glasgow, UK) followed by washing each reaction tube three times with ice-cold PBS (pH 7.4). After drying the filters for at least 2 hours at room temperature, cut filters were transferred to 6 ml PE Pony Vials (PerkinElmer) followed by addition of 3 ml of liquid scintillation fluid, Ultima Gold™ XR (PerkinElmer Life Sciences, Beaconsfield, UK) to each cut filter and then the retained radioactivity was measured by liquid scintillation analyser, Tri-Carb® 2910 TR (PerkinElmer). To

determine the actual concentration of [³H]-G9543 added to tubes, two aliquots of a similar volume of each concentration of [³H]-G9543 used in the assay were added to 6 ml PE vial and radioactivity was quantified after adding 3 ml Ultima Gold™ XR. The concentration of [³H]-G9543 added per tube was calculated using the following formula:

$$\frac{\text{Standard (DPM)}}{\text{Specific activity}(\frac{\text{DPM}}{\text{fmol}})} \times \frac{1}{500(\text{Assay volume})} = \frac{\text{fmol}}{\mu\text{L}} = \frac{\text{nmol}}{\text{L}} = nM$$

Total binding of [³H]-G9543 to the receptor was calculated using the following formula: $\text{Total binding}(\frac{\text{fmol}}{\text{mg}}) = \frac{\text{Total DPM}}{\text{Specific activity}(\frac{\text{DPM}}{\text{fmol}})} \times \frac{1000}{\text{Protein}(\frac{\mu\text{g}}{\text{tube}})}$

Nonspecific binding of the radioligand was calculated using the following

$$\text{formula: } \text{Nonspecific binding}(\frac{\text{fmol}}{\text{mg}}) = \frac{\text{Nonspecific DPM}}{\text{Specific activity}(\frac{\text{DPM}}{\text{fmol}})} \times \frac{1000}{\text{Protein}(\frac{\mu\text{g}}{\text{tube}})}$$

Specific binding was then determined by subtracting nonspecific binding from total binding and plotted against concentrations of [³H]-G9543 to construct saturation binding isotherms.

2.6.8 Bioluminescence resonance energy transfer (BRET) assay using SPASM sensor

G protein specificity of GPR84 was investigated by novel SPASM biosensor-based BRET assays. GPR84 SPASM biosensor is a single polypeptide in which FLAG-tagged human GPR84 is fused at C-terminus with a G protein peptide comprising last 27 amino acids of the α5 helix of G protein flanked by a SPASM sensor part consisting of a BRET acceptor m-Citrine or mNeonGreen and a BRET donor NanoLuc linked by a flexible linker ERK helix. If the α5 helix peptide is of cognate G protein for the receptor, following agonist treatment, this G protein peptide will interact with GPR84 in such a way that the distance between BRET acceptor and donor will be decreased allowing the bioluminescence resonance energy transfer between them. Here NanoLuc luciferase enzyme catalyses the oxidation of a coelenterazine analogue, furimazine into furimamide with concomitant emission of light which can be transferred to mCitrine/mNeonGreen acceptor.

2.6.8.1 BRET assay using mCitrine-based SPASM sensors

Flp-InTM T-RExTM-293 stable cell lines stably harbouring FLAG-hGPR84-SPASM $G\alpha_{i1/2}$ and FLAG-hGPR84-SPASM No-pep sensor construct were used for the BRET assay. Cells were split in 1:4 from 80% confluent T75 flask. On the same day, 96 well white plates with a flat bottom (Greiner Bio-one) were coated with 40 μ l/well (concentration: 50 μ g/ml) of poly D lysine hydrobromide (Sigma-Aldrich) in serum-free DMEM media and incubated overnight at 4°C temperature. Poly D lysine will enhance the cell attachment to the bottom of the plate. On the following day, cells were harvested along with counting by trypan blue exclusion method and 100 μ l of cells were seeded at 50,000 cells per well on poly-D-lysine coated 96 well plates and after 6 hours of incubation in 5% CO₂ and at 37°C, 100 ng/ml of doxycycline was added to induce the expression of the receptor of interest. The plates were incubated for overnight at 37° and 5% CO₂. 24 hours later, media was aspirated from the plate and cells were washed for two times with 100 μ l of pre-warmed (37°C) HBSS (pH 7.4) buffer followed by addition of 80 μ l of HBSS per well. At this point, plates were read to measure the fluorescence intensity of BRET acceptor, mCitrine using a CLARIOstar (BMG Labtech) plate reader to determine the receptor expression. Nano Glo substrate (Promega Corporation, Madison, USA) was diluted from 800x stock to 10x concentration using pre-warmed HBSS buffer and 10 μ l of the diluted substrate was added to each well at the final concentration of 5 μ M. The plates were immediately wrapped with aluminium foil to protect the cells from light and were then incubated for 10 minutes in 37°C followed by addition of 10 μ l indicated 10X concentrations of ligands/vehicle. The plates being protected from light were incubated again for five minutes in 37°C and luminescence at 530 nm (mCitrine emission) and 455 nm (emission from the oxidation of furimazine to furimamide by NanoLuc) was measured by CLARIOstar plate reader using a bandwidth of 50 nm. The BRET ratio was calculated as emission at 530 nm/emission at 455 nm. Net BRET was determined by subtracting the value of the BRET ratio of FLAG-hGPR84-SPASM-No peptide sensor from that of FLAG-hGPR84-SPASM- $G_{i1/2}$ sensor. Multiplication of this value by 1000 gives the mBRET units. Change in BRET, Δ BRET was calculated as follows:

$$\Delta\text{BRET} = \text{BRET}_{\text{ligand}} - \text{BRET}_{\text{buffer}}$$

2.6.8.2 BRET assay using mNeonGreen-based SPASM sensors

FLAG-hGPR84-SpNG-G α (x) sensors (where x= i1/2, i3, o, z, s, q, 12, 13, 14 and 16) or a FLAG-hGPR84-SpNG-NP sensor construct were transfected to HEK-293T cells using Lipofectamine 3000 reagents (see section 2.4.2) and after 24 hours of transfection, cells were seeded at 40,000 cells per well on poly-D-lysine coated 96 well plates. 48 hours following transfection, cells were washed for two times with 100 μ l of HBSS-20 mM HEPES (pH 7.4) buffer and 80 μ l of buffer was added to each well. Fluorescence intensity of mNeonGreen was then measured using CLARIOstar plate reader to determine the relative expression of the sensor constructs. Nano Glo substrate was then added to each well at the final concentration of 5 μ M. The plates wrapped with aluminium foil were then incubated for 10 minutes in 37°C followed by addition of indicated concentrations of ligands or of vehicle buffer. The plates were incubated again for five minutes in 37°C. Using a bandwidth of 50 nm, NLUC and mNeongreen emission signals were then collected at 450 and 525 nm respectively by Clariostar plate reader. The BRET ratio was calculated as the ratio of luminescence at 525 nm to luminescence at 450 nm. Multiplication of this value by 1000 provided the mBRET units.

2.7. Structural studies

2.7.1 Homology modelling

The homology modelling and ligand docking were conducted by Dr. Irina G. Tikhonova, School of Pharmacy, Medical Biology Centre, Queen's University Belfast, Belfast, BT9 7BL, United Kingdom as part of the collaborative work. A hybrid template was generated by assembling the helical bundle of seven transmembrane domains from the OX1 receptor crystal structure (Protein Data Bank code: 4ZJ8) with the 2nd extracellular loop (EL2) from the crystal structure of rhodopsin (PDB code: 2Z73) and based on this combined template a homology model of GPR84 was generated with the Prime 3.8 module of the Schrodinger software (Schrodinger, LLC, New York, 2014) using the default energy-based method (Jacobson et al., 2004). The resulting homology model was then optimized using molecular mechanics and dynamics tools of MacroModel 10.6

module of the Schrodinger software package (Schrodinger, LLC, 2014) (Tikhonova, 2017; Mahmud et al., 2017).

2.7.2 Ligand docking

Using the InducedFit module (Friesner et al., 2006; Sherman et al., 2006) of the Schrodinger software, ligand docking to the constructed GPR84 homology model was performed. Herein, the induced fit docking (IFD) methodology based on glide (ligand sampling) and prime (receptor sampling) program (Friesner et al., 2006) was employed to generate multiple ensembles of docking poses. The receptor grid was defined around Arg172 while the side chain trimming was performed for residues Tyr69 and Phe335 that largely occluded the binding cavity. From the resulting multiple ligand docking poses, the best docking pose was selected based on the docking energy and interactions with Arg172 (Mahmud et al., 2017). Maestro 9.9 of the Schrodinger software package was employed for the generation of figures of the molecular models.

2.8. Data analysis and curve fitting

Data analysis and curve fitting were carried out using the GraphPad Prism software package version 5.0b (GraphPad, San Diego).

2.8.1 Analysis of functional agonist and antagonist assays

The functional concentration-response curve (CRC) for agonist ligand displays a sigmoidal curve with a standard slope factor (Hill slope) of 1. Usually, seven or eleven concentrations of an agonist ligand were plotted in logarithmic scale on X-axis with the vehicle control plotted at 1 log unit lower than the lowest concentration of the ligand. The agonist functional response data were then analysed by non-linear regression analysis with fitting data to a three-parameter sigmoidal curve where Hill slope was constrained to unity and the model for this curve fitting is depicted below:

$$Response(Y) = Bottom + \frac{(Top - Bottom)}{[1 + 10^{(\log EC_{50} - X)}]}$$

Here, Top is the maximal asymptote of the curve reflecting the maximal response (E_{max}) displayed by the agonist ligand while bottom is the response of the vehicle control and logEC₅₀ is the logarithm of the EC₅₀ value. EC₅₀ is the concentration of the agonist required for the generation of half-maximal response while X is the concentration of agonist ligand. The best fit values for the negative logarithm of EC₅₀ (pEC₅₀) were determined from at least three independent experiments and these values were then represented as means±SEM.

In case of inhibition experiments with antagonists wherein the ability of several concentrations (seven) of antagonist to inhibit the response produced by an EC₈₀ concentration of an agonist was assessed, the data were analysed by non-linear regression analysis with data fitted to a three-parameter log (inhibitor) vs response inverse sigmoidal curve where Hill slope was constrained to -1 using the following model:

$$Response(Y) = Bottom + \frac{(Top - Bottom)}{[1 + 10^{(X - \log IC_{50})}]}$$

Here, IC₅₀ is the concentration of the antagonist required for the 50% inhibition of the agonist response. The negative logarithm of IC₅₀ i.e pIC₅₀ was determined from the best-fit value of curve-fitting from at least three individual experiments and was presented as mean±SEM.

2.8.2 Analysis of radioligand binding data

Radioligand saturation binding curve follows the shape of a rectangular hyperbola. In this binding experiment, specific binding of the radioligand to the receptor was first calculated by subtracting the non-specific binding from the total binding and these specific binding data were analysed by non-linear regression by fitting data to a one site specific binding model allowing estimation of radioligand binding affinity (K_d) and total number of receptor binding sites (B_{max}) in the sample.

$$Specific\ binding\ (Y) = \frac{B_{max} \times (X)}{K_d + (X)}$$

Here, K_d is the equilibrium binding constant or the concentration of the radioligand required for binding half of the receptor sites in equilibrium, B_{\max} is the maximum specific binding and X is the concentration of the radioligand.

2.8.3 Analysis of ligand co-operativity and other allosteric parameters

To estimate the magnitude and direction of the allosteric effect, data obtained from allosterism experiments were analysed using an operational model of allosteric modulation described previously (Ehlert, 2005; Keov et al., 2011). The general version of this model can be depicted by the following equation:

$$E = \frac{E_m(\tau_A[A](K_B + \alpha\beta[B]) + \tau_B[B]K_A)^n}{([A]K_B + K_AK_B + [B]K_A + \alpha[A][B]^n + (\tau_A[A](K_B + \alpha\beta[B]) + \tau_B[B]K_A)^n)}$$

Where, E is the pharmacological effect, $[A]$ and $[B]$ are the orthosteric and allosteric compound concentration at equilibrium, respectively; K_A and K_B are the equilibrium dissociation constants of the orthosteric and allosteric ligands respectively, denoting the binding affinities of the two ligands to the receptor; α is the binding cooperativity factor denoting the magnitude and direction of the allosteric effect on binding affinity of the orthosteric agonist to the receptor, β is the activation cooperativity factor representing the measure of the allosteric effect on orthosteric efficacy. τ_A and τ_B represent the intrinsic activity (ability to activate the receptor directly) of the orthosteric and allosteric ligand, respectively. E_m is the maximal possible system response and n denotes the slope factor of the transducer function. In case of global fitting of the allosterism data through this equation, E_m and n values were always constrained to E_{\max} of the experiment and 1, respectively and other parameters (K_A , K_B , α , β , τ_A and τ_B) were estimated.

2.8.4 Global Gaddum/Schild EC_{50} shift analysis

To investigate whether an antagonist interacts with an agonist in a competitive or non-competitive manner, a set of agonist concentration-response assays were performed in the absence or presence of a various fixed concentrations of the antagonist and data were globally fit to the Gaddum/Schild EC_{50} shift analysis which provides estimation of the pA_2 value (the negative logarithm of the

concentration of antagonist needed to shift the agonist concentration-response curve by a factor of 2) and the Schild slope factor. While pA_2 reflects the antagonist affinity for the receptor, the Schild slope factor, S reveals how well the antagonist-promoted shifting of the concentration-response curve corresponds to the competitive interaction between two ligands with the value of 1 reflecting perfect competitive nature of the interaction.

2.8.5 Statistical analysis

All data were presented as mean \pm SEM of three independent experiments. All statistical analysis of data was conducted using the GraphPad Prism software package version 5.0b. Assuming that data were normally distributed, data were analysed either through two-tailed unpaired student's t-test (for two groups) or one-way analysis of variance (ANOVA) (for three or more groups) followed by Tukey's or Dunnett's multiple comparison test to determine the level of significance between treatment vs control groups with the p-value less than 0.05 being considered as statistically significant.

3 Investigation of G-protein Selectivity of GPR84

3.1. Introduction

Elucidation of GPCR-G protein coupling selectivity is crucial for defining the functions and pharmacology of the G-protein coupled receptor (GPCR) of interest. Activation of a GPCR by endogenous and synthetic ligands is generally transduced by heterotrimeric G-proteins which transfer the extracellular signal to intracellular second messengers. So, investigation of G-protein selectivity of any GPCR is of paramount importance as it will link activation of the GPCR to physiological responses. Moreover, exploring the G-protein specificity of any GPCR is crucial as it will help define the downstream intracellular signalling pathway related to specific GPCRs ultimately defining the cellular and biological effects associated with it. This can be exploited for the development of drug screening assays for orphan receptors. Wang et al., (2006b) initially investigated G protein specificity of GPR84 and reported that the chimeric proteins $Gq_{i(9)}$ and $Gq_{o(5)}$ but not $Gq_{s(5)}$ significantly promoted decanoic acid stimulated activation of GPR84 using an aequorin-based calcium assay in Chinese Hamster Ovary (CHO) cells. This suggested that activated GPR84 preferentially adopts $G\alpha_{i/o}$ -coupled conformations. Recently Gaidarov et al., (2018) reported that along with $G\alpha_{i/o}$, embelin-occupied GPR84 also couples to G_{12}/G_{13} mediated signalling pathways in HEK-293 cells. They found that embelin and its analogues promoted intracellular cAMP production in a concentration-dependent fashion in HEK-293 cells co-transfected with GPR84 and $Gs_{13(5)}$ or $Gs_{12(5)}$ chimeric proteins, an effect which was significantly potentiated by pre-treatment of the cells with the $G\alpha_i$ inhibitor, pertussis toxin (PTX). To explore the G-protein selectivity of GPR84 more extensively, I have used novel BRET-based GPR84 sensors developed using a SPASM (systematic protein affinity strength modulation) based approach (Sivaramakrishnan and Spudich, 2011). Firstly, FLAG-hGPR84-SPASM mCitrine- $G\alpha_{i1/2}$ and FLAG-hGPR84-SPASM mCitrine-NP BRET sensor constructs were generated to assess whether this approach could be suitable to explore GPCR-G protein interaction for GPR84. In this construct, FLAG-tagged human GPR84 was fused at the C-terminus to a peptide encoding the last 27 amino acids of the $\alpha 5$ -helix of $G\alpha_{i1/2}$ which was separated by a SPASM sensor (Figure 3.1). The SPASM sensor is composed of a yellow fluorescent protein, mCitrine, acting as BRET acceptor and a Nano Luciferase (NanoLuc) acting as a BRET donor linked by a

flexible sequence. This ER/K α -helix represents a peptide motif encoding a repeated sequence of four glutamic acid (E) residues followed by four residues of either arginine (R) or lysine (K) (Sivaramakrishnan and Spudich, 2011). Each component of the sensor was separated by a linker composed of the (Gly-Ser-Gly)₄ sequence ensuring the flexibility of the fusion protein. The FLAG-hGPR84-SPASM mCitrine-NP sensor was generated using the same molecular cloning scheme with the only difference being that NP sensor did not contain the C-terminus G protein peptide after Nano Luc, rather it contained the (Gly-Ser-Gly)₄ linker. Both the GPR84 SPASM sensors were then subcloned into the multiple cloning sites of pcDNA5/FRT/TO plasmid and doxycycline-inducible Flp-In T-REx-293 cell lines expressing FLAG-hGPR84-SPASM-Gai_{1/2} or FLAG-hGPR84-SPASM-NP constructs were generated.

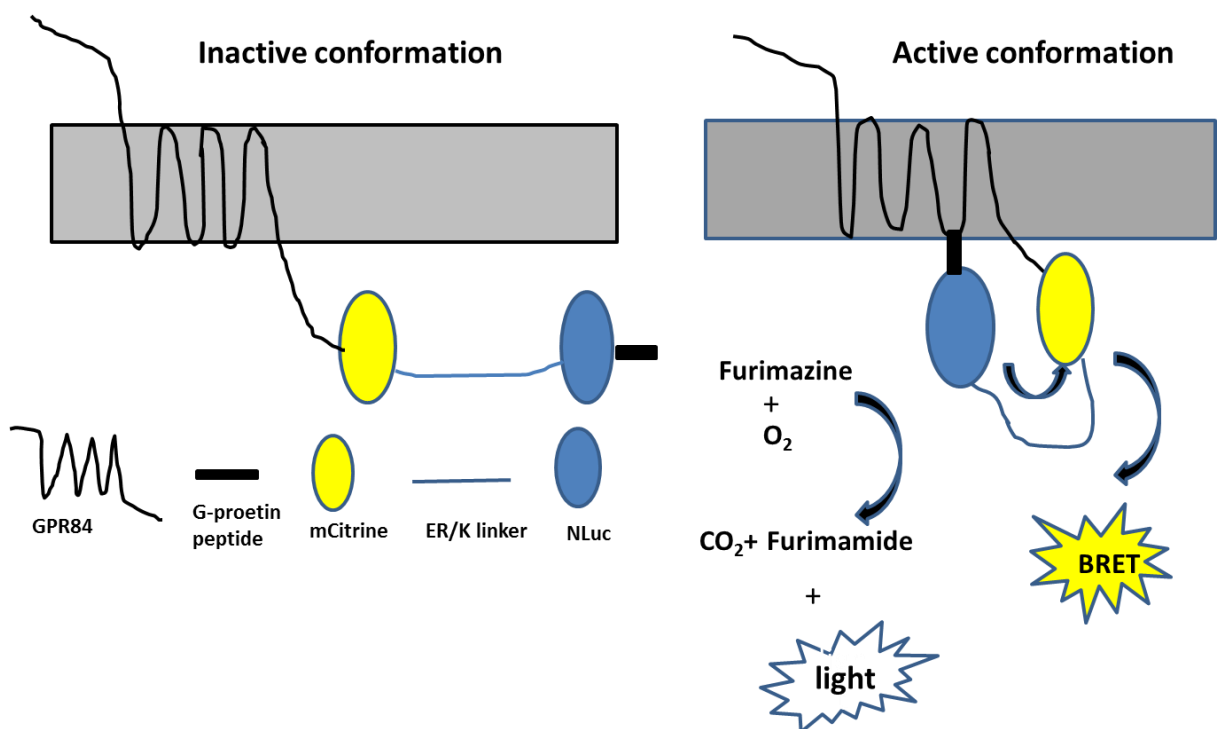


Figure 3.1 Schematic diagram of a BRET-based SPASM sensor for GPR84

3.2. Results

3.2.1. Characterization of cell lines expressing GPR84 SPASM sensors

The expression of the GPR84 SPASM sensor constructs was investigated by western blot analysis using an anti-GFP antiserum which is able to identify the mCitrine component of the expressed sensor. A distinct band of some 104 kDa in

the immunoblot of membranes generated from doxycycline (100 ng/ml for 24 hours) induced Flp-In T-REx-293 cells confirmed the expression of either FLAG-hGPR84-SPASM-G $\alpha_{i1/2}$ or FLAG-hGPR84-SPASM-NP sensor constructs as intact polypeptides in the corresponding stable cell lines (Figure 3.2). No expression of SPASM sensor constructs was detected in membranes generated from untreated cells. Two bands of greater than 225 kDa size detected in both the membrane preparations obtained from doxycycline-treated cells might reflect oligomers or aggregates of the receptor constructs in the membrane. The pre-treatment of the membrane preparations with the N-glycosidase enzyme, PNGase F (0.05 unit/ μ l sample) slightly enhanced the migration of the receptor construct in SDS-PAGE, indicating that GPR84 contains some N-linked oligosaccharides.

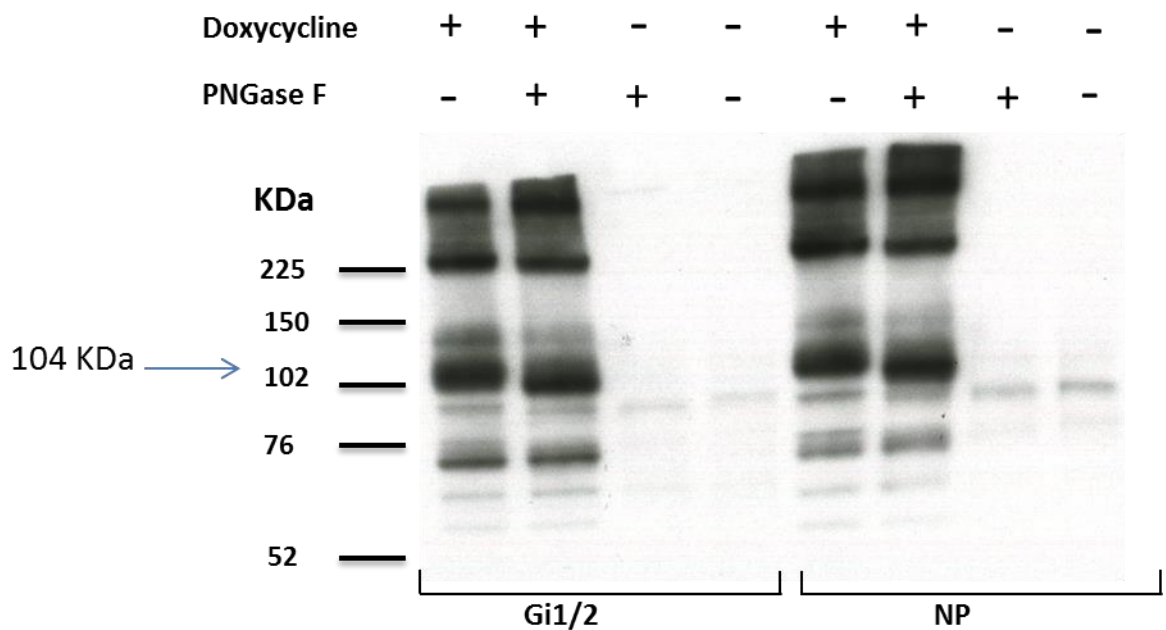


Figure 3.2 Doxycycline-induced expression of FLAG-hGPR84-SPASM-G $\alpha_{i1/2}$ and FLAG-hGPR84-SPASM-NP biosensors in Flp-In T-REx-293 stable cells. Membranes were prepared from treated (100 ng/ml of doxycycline; +dox; duration: 24 hours) or untreated (-dox) Flp-In T-REx-293 cell lines harbouring FLAG-hGPR84-SPASM-G $\alpha_{i1/2}$ or FLAG-hGPR84-SPASM-NP sensor constructs. These membranes were then either untreated (-PNGase F) or treated with the N-glycosidase enzyme, PNGase F (+). Samples containing 5 μ g membrane protein were then resolved by SDS-PAGE and immunoblotted with a goat polyclonal anti-GFP antiserum.

3.2.2. Validation of GPR84 SPASM sensors

To validate SPASM sensor responses, bioluminescence resonance energy transfer (BRET) assays were performed using established GPR84 agonists. In the absence of agonist, it might be expected that there would be no interaction between

GPR84 and G peptide, leading to very low/no BRET signal because the BRET donor and BRET acceptor are separated by the ER/K linker. Agonist treatment of the cells expressing the SPASM sensor is expected to result in enhanced BRET due to the interaction between GPR84 and the C terminus G peptide which brings the BRET donor and acceptor into closer proximity (Figure 3.1).

Compound-1 treatment concentration-dependently induced BRET gain for the hGPR84-SPASM-G $\alpha_{i1/2}$ sensor with pEC₅₀ of 6.84 \pm 0.03 (Figure 3.3) and Δ BRET of 0.16 \pm 0.003 was obtained with 3 μ M compound-1 treatment, which was significantly higher (*P* value <0.001) than that obtained at the NP sensor (Δ BRET: 0.005 \pm 0.001). Similarly, compound-51 stimulation also resulted in increased BRET in a concentration-dependent manner for the hGPR84-SPASM-G $\alpha_{i1/2}$ sensor but not for the hGPR84-SPASM-NP sensor. 100 nM of compound-51 generated a Δ BRET ratio of 0.21 \pm 0.004 for the hGPR84-SPASM-G $\alpha_{i1/2}$ sensor which was significantly higher than that obtained at the NP sensor (Δ BRET: 0.009 \pm 0.002). These results confirmed the functional integrity of the hGPR84-SPASM-G $\alpha_{i1/2}$ sensor.

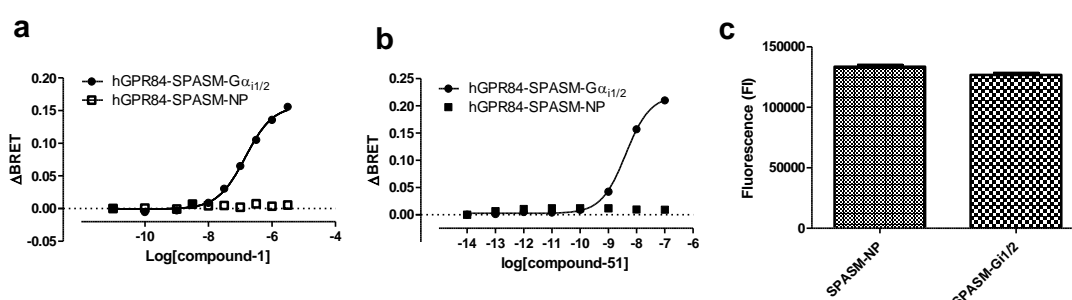


Figure 3.3 A FLAG-hGPR84-SPASM-G $\alpha_{i1/2}$ sensor is functional when expressed in a Flp-In T-REx-293 stable cell line. Flp-In T-REx-293 cells were induced with doxycycline (100 ng/ml) for 24 hours to express either FLAG-hGPR84-SPASM-G $\alpha_{i1/2}$ or FLAG-hGPR84-SPASM-NP sensor and BRET was measured after addition of various concentrations of compound-1 (a) or compound-51 (b). No significant difference in the expression level of the hGPR84-SPASM-G $\alpha_{i1/2}$ sensor and hGPR84-SPASM-NP sensor constructs was observed by measuring the fluorescence intensity of mCitrine following doxycycline treatment (c).

3.2.3. DIM and embelin act as partial agonists and compound-1 and compound-51 act as super-agonists at the hGPR84-SPASM-G $\alpha_{i1/2}$ sensor

Decanoic acid(C-10), DIM, embelin, compound-1 and compound-51 each enhanced BRET in a concentration-dependent fashion with pEC₅₀ of 4.78 \pm 0.03, 6.00 \pm 0.01, 6.28 \pm 0.06, 6.90 \pm 0.07 and 8.40 \pm 0.04, respectively which implies that agonist stimulation promoted the interaction between activated GPR84 and the

C-terminal $G\alpha_{i1/2}$ peptide (Figure 3.4 and Table 3.1). Although potencies of DIM and embelin were significantly ($P<0.001$) higher compared to that of decanoic acid, both agonists showed significantly reduced efficacy (44% and 37%, compared to C-10) compared to decanoic acid, indicating that DIM and embelin acted as partial agonists in this assay. Compound-1, a synthetic agonist of GPR84 exhibited 132-fold higher potency and 6.6-fold higher efficacy compared to the presumed endogenous agonist decanoic acid. Compound-51 was the most potent synthetic agonist and showed 8.5-fold higher efficacy than decanoic acid (Figure 3.4). If the endogenous agonist decanoic acid is considered as a full agonist, then compound-1 and its analogue compound-51 behaved as super-agonists of GPR84 in this SPASM sensor-based assay. The rank order of intrinsic activity of the agonists at the hGPR84-SPASM- $G\alpha_{i1/2}$ sensor was as follows: **Embelin<DIM<C-10<Compound-1<Compound-51**.

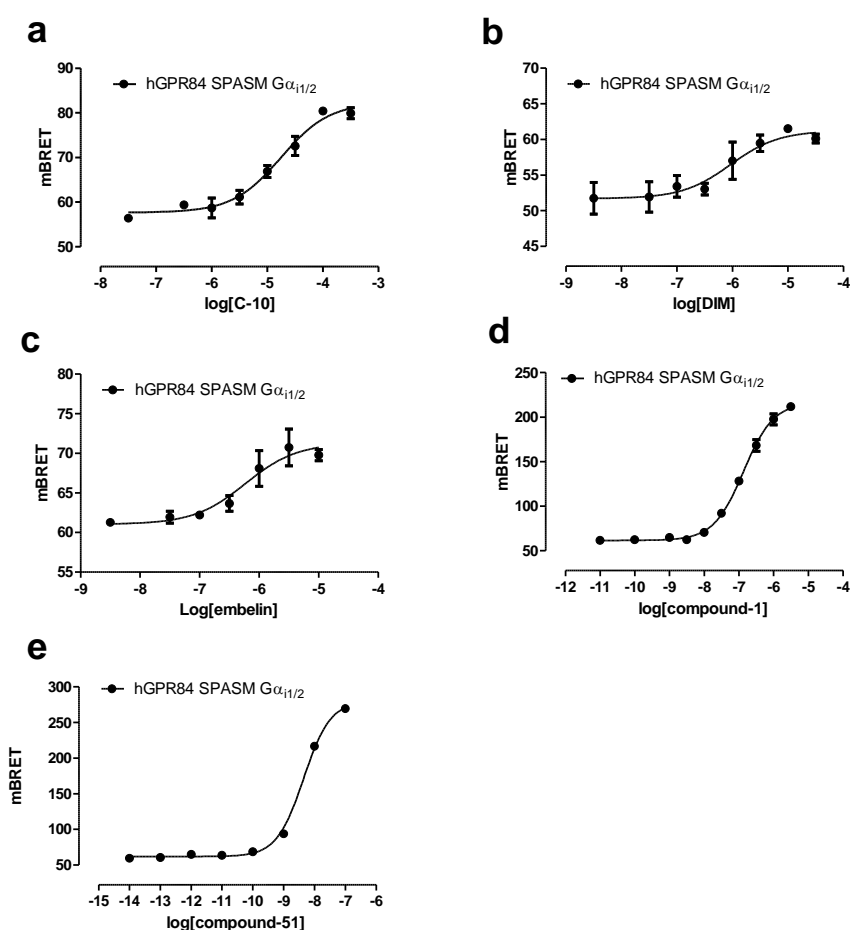


Figure 3.4 DIM and embelin act as partial agonists and compound-1 and compound-51 act as super-agonists at the FLAG-hGPR84-SPASM- $G\alpha_{i1/2}$ sensor. Flp-In T-REx-293 stable cell lines harbouring FLAG-hGPR84-SPASM- $G\alpha_{i1/2}$ were treated with doxycycline (100 ng/ml) for 24 hours to induce the expression of the construct. BRET signals were then measured following treatment of the cells for five minutes with various concentrations of C-10 (a), DIM (b), embelin (c), compound-1 (d) or compound-51 (e).

Table 3-1 Potency and relative efficacy of different GPR84 agonists at the FLAG-hGPR84-SPASM-G $\alpha_{i1/2}$ sensor

| Ligand | pEC ₅₀ , Mean \pm SEM (Efficacy, Emax) ^a |
|-------------|---|
| C-10 | 4.78 \pm 0.03 (100) |
| DIM | 6.0 \pm 0.01*** (44) |
| Embelin | 6.28 \pm 0.06*** (37) |
| Compound-1 | 6.9 \pm 0.07*** (664) |
| Compound-51 | 8.4 \pm 0.04*** (857) |

Potency and efficacy of different GPR84 agonists were measured in BRET assays using FLAG-hGPR84-SPASM-G $\alpha_{i1/2}$ biosensor as described in Figure 3.4.

^aEmax values were normalized to C-10 response; Statistical analysis was performed by one-way analysis of variance (ANOVA) followed by Dunnett's multiple comparison tests using potency value of C-10 as the reference. Statistical significance is denoted by *P<0.05, **P<0.01, ***P<0.001.

3.2.4. GPR84 signals through G $\alpha_{i/o}$ pathway

To explore the G protein selectivity of GPR84, a series of BRET-based SPASM sensor constructs, FLAG-hGPR84-SpNG-G α_x (where x= i_{1/2}, i₃, o, z, s, q, 12, 13, 14, 16 and SpNG stands for SPASM NeonGreen) was generated wherein a peptide composed of the last 27 amino acids of the C-terminus of different G proteins was fused to the C-terminal tail of FLAG-tagged human GPR84 which is linked by a SPASM sensor composed of mNeonGreen (BRET acceptor) and Nano Luciferase enzyme (BRET donor) separated by ER/K α -helix. Though previously mCitrine was used as the BRET acceptor, for this generation of SPASM sensors, mNeonGreen was chosen as it was reported to be the brightest monomeric green or yellow fluorescent protein available (Shaner et al., 2013). Using these GPR84 SPASM sensor constructs, BRET assays were performed to explore the molecular coupling of the receptor. As measured by the fluorescence intensity of mNeonGreen, all the SPASM sensor constructs displayed similar expression levels in transiently transfected HEK-293 cells (Figure 3.5 b). Compound-1 concentration-dependently enhanced BRET with pEC₅₀ of 6.40 \pm 0.04, 6.64 \pm 0.08, 6.10 \pm 0.20 and 5.65 \pm 0.05 for hGPR84-SpNG-G $\alpha_{i1/2}$, hGPR84-SpNG-G α_{i3} , hGPR84-SpNG-G α_o and hGPR84-SpNG-G α_z sensors, respectively (Figure 3.5 a) demonstrating that agonist-stimulated GPR84 can interact with the C-terminus peptide of many G $\alpha_{i/o}$ family G-proteins. No BRET signal was obtained for SPASM sensors containing the C-terminal peptide of Gq, Gs, G₁₂, G₁₃, G₁₄ and G₁₆. These results indicated that GPR84 activation is coupled selectively to G $\alpha_{i/o}$ pathways which is in agreement with results previously reported by Wang et al., (2006b).

Importantly, no BRET signal was detected following the addition of compound-1 to cells expressing a hGPR84-SpNG-NP sensor which lacked the C-terminal peptide sequence, indicating the crucial role of the C-terminus peptide in GPR84-G protein interaction. Similarly, TUG-1765 also promoted a concentration-dependent increase in BRET signal for hGPR84-SpNG-G $\alpha_{i1/2}$, hGPR84-SpNG-G α_{i3} , hGPR84-SpNG-Go and hGPR84-SpNG-Gz sensors affording pEC₅₀ of 8.13 \pm 0.1, 8.5 \pm 0.09, 8.2 \pm 0.4 and 8.1 \pm 0.2, respectively, whilst addition of varying concentrations of TUG-1765 to cells expressing sensors containing Gq, Gs, G₁₂, G₁₃, G₁₄ or G₁₆ C-terminal peptides did not produce any BRET signal (Figure 3.6). These data demonstrated that TUG-1765-occupied GPR84 can signal through G $\alpha_{i/o}$ pathways and did not couple to Gq, Gs, G₁₂, G₁₃, G₁₄ and G₁₆ G-proteins.

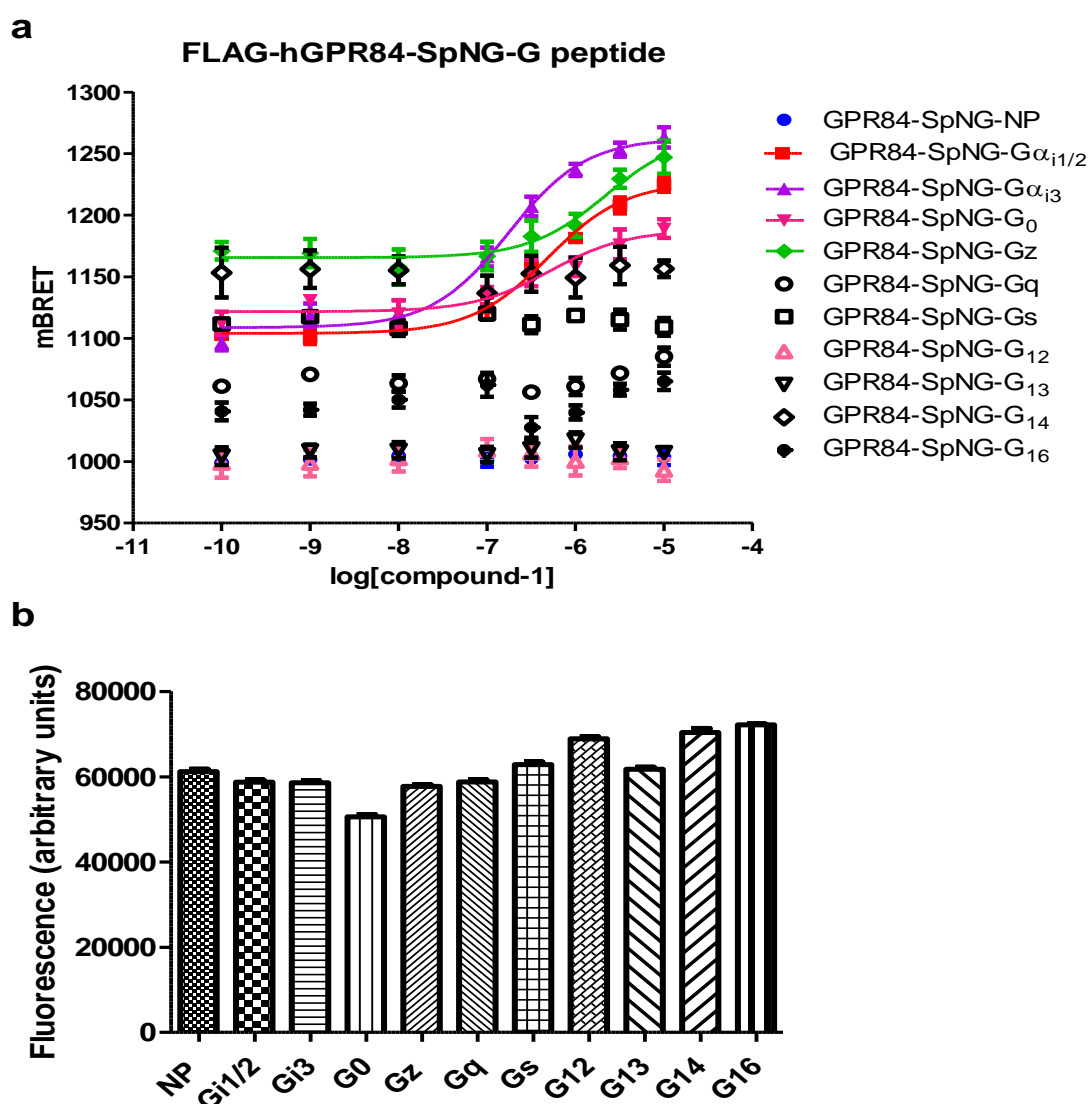


Figure 3.5 Compound-1-occupied GPR84 adopts $G_{\alpha_{i/o}}$ -coupled active conformations in HEK-293 cells. HEK-293 cells were transiently transfected with either FLAG-hGPR84-SpNG- G_{α} (x) sensors (where X= i1/2, i3, o, z, s, q, 12, 13, 14 and 16) or a FLAG-hGPR84-SpNG-NP sensor construct and BRET signals were monitored following treatment of the cells for 5 minutes with varying concentrations of compound-1 (a). The relative expression levels of the SPASM sensor constructs was measured by the fluorescence intensity of mNeonGreen following transient transfection of the sensor constructs into HEK-293 cells (b).

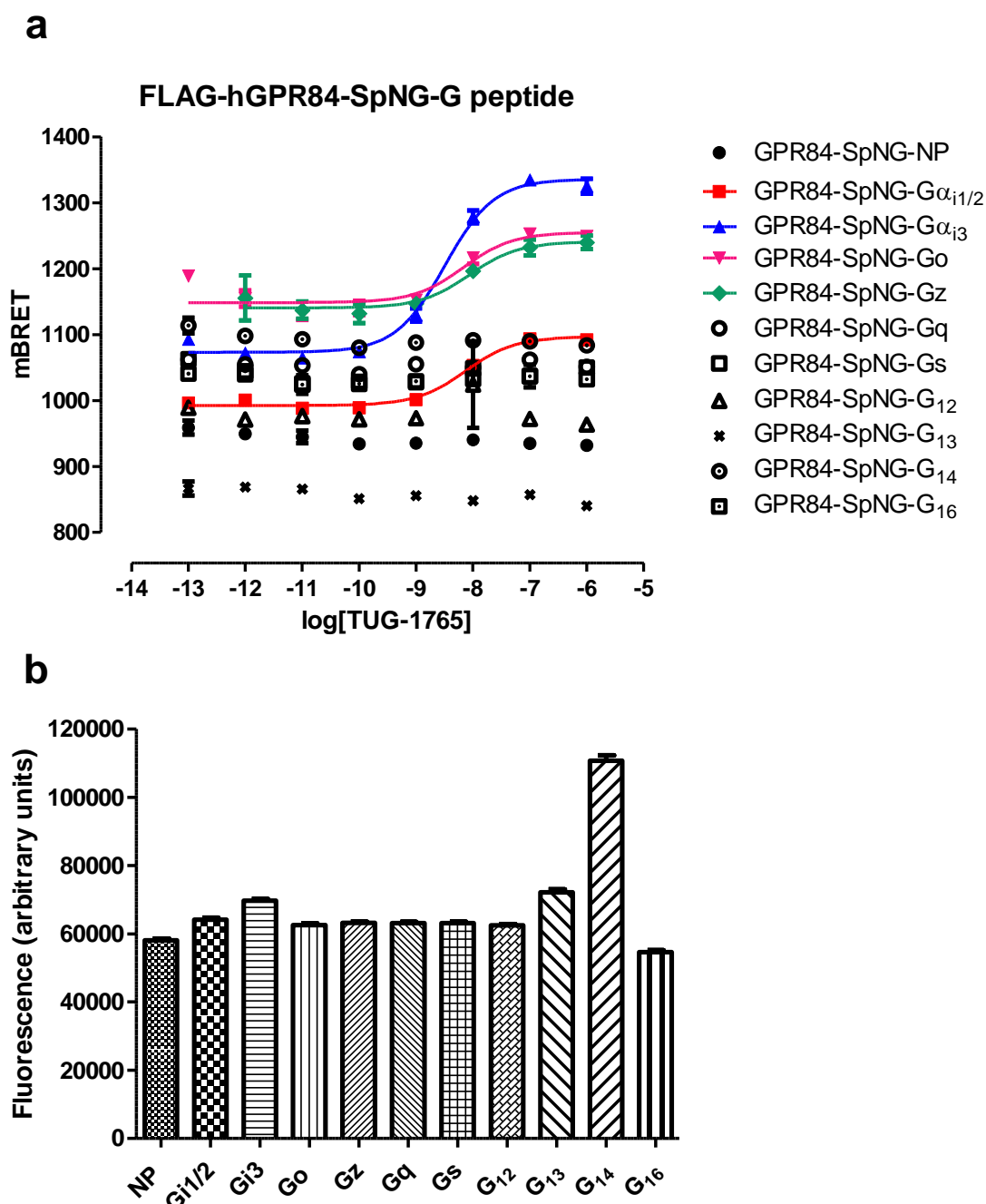


Figure 3.6 TUG-1765 stabilizes $G\alpha_{i/o}$ -coupled active conformations of GPR84 in HEK 293 cells. BRET assays were performed using HEK-293 cells transiently transfected with either FLAG-hGPR84-SpNG- $G\alpha(x)$ sensors (where $X = i1/2, i3, o, z, s, q, 12, 13, 14$ and 16) or a FLAG-hGPR84-SpNG-NP sensor construct. Changes in BRET following treatment of different GPR84-SPASM sensors with varying concentrations of TUG-1765 are shown in (a) and the relative expression levels of the sensors measured by the fluorescence intensity of mNeonGreen following transient transfection of the SPASM sensors into HEK-293 cells are shown in (b). All the GPR84-G peptide SPASM sensor constructs were effectively expressed in HEK-293 cells, with only the G14 sensor being markedly higher than others.

3.2.5. The coupling efficiency of interaction between human GPR84 and individual $G\alpha_{i/o}$ G proteins

In the case of compound-1 mediated GPR84-G protein interactions assessed by BRET using FLAG-hGPR84-SpNG-G peptide sensors, although similar potency

values were obtained for hGPR84-SpNG-G $\alpha_{i1/2}$, hGPR84-SpNG-G α_{i3} and hGPR84-SpNG-Go sensors (Figure 3.7a and Table 3.2), the potency of compound-1 was decreased significantly ($P<0.01$) by 5.6-fold at the hGPR84-SpNG-Gz sensor (pEC_{50} : 5.65 ± 0.05) compared to that displayed at the hGPR84-SpNG-G $\alpha_{i1/2}$ sensor (pEC_{50} : 6.40 ± 0.04). The highest maximal BRET increase was obtained for the hGPR84-SpNG-G α_{i3} sensor (50% higher response than the hGPR84-SpNG-G $\alpha_{i1/2}$ sensor, $P<0.001$) while hGPR84-SpNG-Go and hGPR84-SpNG-Gz sensors displayed significantly ($P<0.001$) lowered maximal response with 40% and 56% reduction in E_{max} values, respectively compared to that for G $\alpha_{i1/2}$ sensor (Figure 3.7a and Table 3.2). These results suggested that compound-1 stimulation preferentially stabilized GPR84 active conformations that interacted with G α_{i3} and G $\alpha_{i1/2}$. The rank order of coupling efficiency of compound-1-stimulated interaction between GPR84 and individual G $\alpha_{i/o}$ protein was as follows: **G α_{i3} > G $\alpha_{i1/2}$ > Go > Gz.**

Contrary to the results obtained with compound-1, TUG-1765-occupied GPR84 coupled equally well to G $\alpha_{i1/2}$ and G α_{i3} which was evident from the fact that the FLAG-hGPR84-SpNG-G α_{i3} sensor displayed similar potency and efficacy to that exhibited by the FLAG-hGPR84-SpNG-G $\alpha_{i1/2}$ sensor (Figure 3.7b and Table 3.2). The efficacy of TUG-1765 was decreased drastically at both FLAG-hGPR84-SpNG-Go and FLAG-hGPR84-SpNG-Gz sensors with 85% and 63% reduction in E_{max} values, respectively compared to that of G $\alpha_{i1/2}$ sensor suggesting reduced coupling efficiency of interaction between GPR84 and Go/Gz G-peptides. The rank order of the relative efficiency of interaction between TUG-1765 stimulated GPR84 and different G protein subunits are as follows: **G $\alpha_{i1/2}$ =G α_{i3} > Gz > Go.**

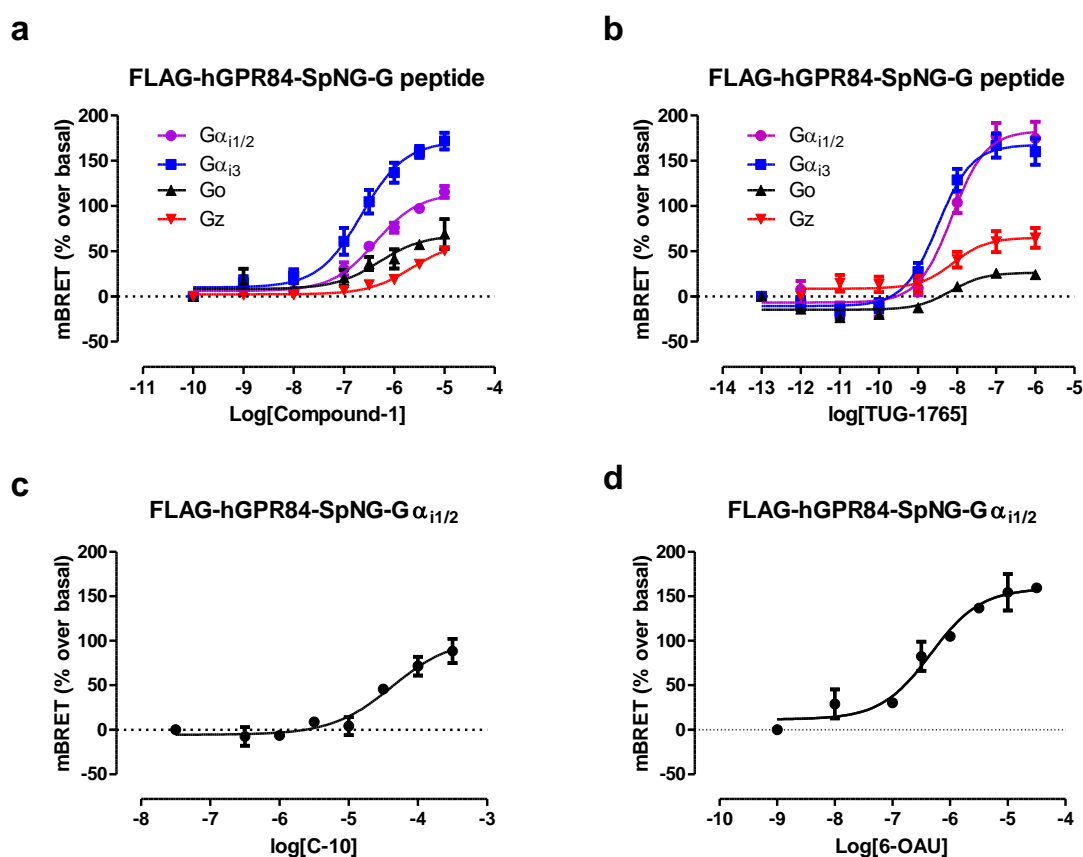


Figure 3.7 The relative coupling efficiency of interaction between human GPR84 and individual G $\alpha_{i/o}$ G proteins. HEK-293 cells were transiently transfected with either FLAG-hGPR84-SpNG-G $\alpha_{i1/2}$, FLAG-hGPR84-SpNG-G α_{i3} , FLAG-hGPR84-SpNG-G α_o , FLAG-hGPR84-SpNG-Gz or FLAG-hGPR84-SpNG-NP sensors and BRET was measured following treatment of these cells for five minutes with various concentrations of either compound-1 (a) or TUG-1765(b). Concentration-response curves are shown for C-10 (c) or 6-OAU (d) in the BRET assay performed using HEK-293 cells transiently transfected with either FLAG-hGPR84-SpNG-G $\alpha_{i1/2}$ or FLAG-hGPR84-SpNG-NP sensors.

Table 3-2 Potency and relative efficacy of compound-1 and TUG-1765 at different FLAG-hGPR84-SpNG-G α sensors

| Ligand | SpNG-G $\alpha_{i1/2}$ | SpNG-G α_{i3} | SpNG-G α_o | SpNG-Gz |
|------------|-------------------------|------------------------------|-------------------------|-------------------------------|
| Compound-1 | 6.4 \pm 0.04 (100) | 6.64 \pm 0.08 (149%)*** | 6.1 \pm 0.2 (60%)* | 5.65 \pm 0.05** (44%)*** |
| TUG-1765 | 8.13 \pm 0.1 (100) | 8.5 \pm 0.09 (95.4) | 8.2 \pm 0.4 (15)** | 8.1 \pm 0.2 (37)** |

Potency values of compound-1 and TUG-1765 measured in BRET assays (as described in Figure 3.7) employing different G $\alpha_{i/o}$ SPASM sensors are represented as mean \pm S.E.M. Emax values were normalized to percent of response displayed at the G $\alpha_{i1/2}$ sensor and are shown in parentheses. One-way analysis of variance (ANOVA) followed by Dunnett's multiple comparison tests was performed to evaluate significance between potency and efficacy of compound-1 or TUG-1765 displayed at the G $\alpha_{i1/2}$ sensor and other G $\alpha_{i/o}$ biosensors with *P<0.05, **P<0.01, ***P<0.001.

3.2.6. 6-OAU, compound-1 and TUG-1765 displayed greater maximal response than decanoic acid at the hGPR84-SpNG-G $\alpha_{i1/2}$ sensor

Concentration-response studies for decanoic acid and 6-OAU were performed in the BRET assay using the FLAG-hGPR84-SpNG-G $\alpha_{i1/2}$ sensor to compare their

relative efficacy. Both decanoic acid and 6-OAU generated concentration-dependent elevation of BRET signals with pEC_{50} of 4.37 ± 0.14 and 6.30 ± 0.13 , respectively (Figure 3.7 c-d). The estimated potency (EC_{50} : 500 nM) of 6-OAU in this assay is fully consistent with those obtained in either [35 S]-GTP γ S binding assay (EC_{50} : 512 nM) or the cAMP accumulation assay (EC_{50} : 438 nM) as reported by Suzuki et al., (2013) and Liu et al., (2016), respectively. 6-OAU displayed greater maximal response than decanoic acid (Figure 3.7) which is in agreement with the finding observed in the β -arrestin recruitment assay (Pillaiyar et al., 2018) but not with that obtained in the cAMP assay where C-10 and 6-OAU showed similar efficacy (Pillaiyar et al., 2018). Similarly, compound-1 and its analogue TUG-1765 showed significantly higher maximal effects than decanoic acid in this SPASM sensor-based BRET assay (Figure 3.7).

3.3. Discussion

3.3.1. BRET based SPASM biosensors can be employed effectively for the study of GPR84-G protein interactions

The GPCR-G protein fusion protein approach has been employed for the study of GPCR-G protein interactions for the last 25 years (Bertin et al., 1994; Seifert et al., 1999; Milligan, 2000). Compared to co-expression of GPCR and G protein as separate signalling moieties, GPCR-G protein fusion proteins offer some benefits. The rate and extent of coupling between GPCR and G protein depend on the relative concentration of these two proteins and on the physical closeness of the G protein to the plasma membrane (Seifert et al., 1999; Milligan, 2002). As expression levels of different endogenous G proteins in particular cells/tissues are different, it is difficult to define G-protein selectivity of a receptor of interest by co-expressing GPCR and G protein as separate polypeptides because the relative density of GPCR and individual G proteins may not be the same. So, the co-expressed system is limited for comparing the relative efficiency of interaction between a GPCR of interest and individual G proteins. To overcome this limitation, the fusion protein approach wherein the N terminus of a G protein α -subunit is fused to the C terminus of the receptor, was developed and employed successfully in the investigation of GPCR-G protein coupling. Fusion proteins ensure 1:1 stoichiometry between GPCR and G protein which makes it a suitable approach for comparing G-protein selectivity of a particular receptor

(Seifert et al., 1999; Wise et al., 1999; Milligan, 2002; Malik et al., 2017). Besides this, the 1:1 stoichiometry and close physical proximity of both proteins will result in enhanced coupling efficiency between them (Seifert et al., 1999). However, in such fusion proteins, GPCR and fused G protein are constrained which may decrease their rotational freedom. Recently GPCR-G protein SPASM sensors have been developed by Malik et al., (2013). These incorporate aspects of the fusion protein approach. Here GPCR and G protein/G peptide are separated by an ER/K α -helical linker ensuring the flexibility of each peptide moiety in the biosensors (Sivaramakrishnan and Spudich, 2011; Malik et al., 2017). Based on this, FRET-based SPASM biosensors for a series of Class A GPCRs have been generated to study ligand-mediated GPCR-G protein coupling (Malik et al., 2013; Semack et al., 2016; Malik et al., 2017). For example, a FRET-based β_2 -AR-SPASM- $G\alpha$ peptide fusion protein was reported by Malik et al., (2013) to be a suitable strategy to detect ligand-activated G-protein selective active conformations of the β_2 -adrenergic receptor in live cells. Applying these SPASM sensors, they found that classical agonist isoproterenol stabilized a G_s -coupled active conformation of the β_2 adrenergic receptor in HEK-293 cells whilst the inverse agonist metoprolol stabilized a G_i -coupled conformation of this receptor. Similarly, by employing the GPCR-G peptide SPASM sensor technique, Semack et al., (2016) found that the $G\alpha$ C terminus peptide is sufficient to detect G protein selectivity of six class A GPCRs, the β_3 -adrenergic receptor, dopamine receptor D1, α_2 -adrenergic receptor, cannabinoid receptor type 1 (CB1), α_1 -adrenergic receptor and vasopressin 1A receptor (V_{1A} R). Using this SPASM-based approach, together with molecular dynamics (MD) simulations, they also explored the molecular determinants of the C-terminal peptide of G_s and G_q subunits which defined the structural basis of G-protein selection bias for the β_2 -adrenergic receptor and V_{1A} R. Mackenzie et al., (2019) recently reported that BRET-based GPR35-G peptide SPASM sensors could be an appropriate system for defining the pharmacology of GPR35 ligands. Using these novel biosensors they explored the molecular basis for the G-protein selectivity of GPR35 and identified that a single amino acid residue (Leucine G.H5.23) located within the α -5 helix of $G\alpha_{13}$ defined the marked $G\alpha_{13}$ selectivity over $G\alpha_{12}$.

Compared to currently available FRET or BRET assays wherein fluorescent protein-tagged GPCR and G protein are co-expressed into cells, FRET/BRET-

based SPASM biosensors also offer similar benefits as that of GPCR-G protein fusion proteins as discussed above which makes it a novel and suitable strategy for the study of GPCR-G protein interactions. In order to investigate the G protein specificity of GPR84, I have employed BRET-based GPR84-G peptide SPASM biosensors where a peptide comprising the last 27 amino acids of the C terminus of the G protein is fused to GPR84 and both the peptides are separated by ER/K linker and BRET probes. The rationale for choosing this length of the C-terminus peptide was to maintain the helical structure of the $\alpha 5$ helix of the $G\alpha$ protein (Malik et al., 2013). It was reported previously that the C-terminus of the $G\alpha$ protein is mainly responsible for binding to the agonist-stimulated active G-protein-coupled receptor (Conklin et al., 1996; Oldham and Hamm, 2008, Semack et al., 2016; Mackenzie et al., 2019). Indeed, here also the $G\alpha$ peptide comprising the last 27 amino acids was found to be sufficient to interact with GPR84, which was evident from the fact that the addition of various concentrations of GPR84 agonists to the cells expressing GPR84-SPASM sensors that contain either $G\alpha_{i1/2}$, $G\alpha_{i3}$, $G\alpha_o$ or G_z G-peptides resulted in enhanced BRET signals, whereas no significant BRET signal was generated by a sensor lacking the C-terminal peptide sequence. Although it was reported that GPR84 couples to $G\alpha_{i/o}$ family G-proteins, (Wang et al., 2006b; Gaidarov et al., 2018) details of G protein specificity within the family were lacking. For example, agonist-mediated preferential coupling to individual $G\alpha_{i/o}$ proteins was not studied extensively. Moreover, both Wang et al., (2006b) and Gaidarov et al., (2018) investigated GPR84-G protein coupling properties by co-expression of chimeric G proteins and GPR84 into recombinant cells which, as discussed earlier is not suitable for defining preferential G protein coupling due to the differential expression profile of individual G proteins in cells/tissues. Consistent with previous findings, here I have found that compound-1 and TUG-1765 stimulated GPR84 coupling to $G\alpha_{i/o}$ family G proteins. Compound-1-occupied GPR84 was found to adopt an active conformation in HEK293 cells which preferentially recruited $G\alpha_{i3}$ and $G\alpha_{i1/2}$ over $G\alpha_o$ and G_z G proteins. Though the potency of compound-1 was similar for the activation of $G\alpha_{i1/2}$ and $G\alpha_{i3}$ G-peptides, the maximal response for the recruitment of $G\alpha_{i3}$ was found to be increased by 1.5-fold compared to $G\alpha_{i1/2}$. On the other hand, TUG-1765-occupied GPR84 coupled equally well to $G\alpha_{i1/2}$ and $G\alpha_{i3}$ as both the measured potency and efficacy of TUG-1765 was very similar for the activation of $G\alpha_{i1/2}$ and $G\alpha_{i3}$. Moreover,

maximal responses for the activation of both $G\alpha_o$ and $G\alpha_z$ protein were much lower following treatment with both compound-1 and TUG-1765. These variations in efficacy of agonists for activation of different $G\alpha$ subunits were not a reflection of differential expression levels of the GPR84-SPASM sensors as all the sensors showed very similar expression levels in HEK-293 cells. Moreover, the assay employed herein relied on the measurement of ratiometric BRET signals which is independent of the expression level of the receptor construct (Mackenzie et al., 2019).

Though Gaidarov et al., (2018) reported that embelin-mediated GPR84 activation was transduced via $G\alpha_{i/o}$ and $G\alpha_{13}/G\alpha_{12}$ G proteins in HEK-293 cells, no interaction between GPR84 and $G\alpha_{12}/G\alpha_{13}$ G proteins was observed following activation by compound-1 or TUG-1765 in the SPASM sensor-based BRET assays. This might be due to the agonist-specific biased signalling. To confirm whether GPR84 also couples to the $G\alpha_{12}/G\alpha_{13}$ -signalling pathway, further investigation using other agonists of GPR84 is required. Though Zhang et al., (2016) reported that agonist-occupied GPR84 interacted with $G\alpha_{16}$ G-protein, no interaction between GPR84 and $G\alpha_{16}$ G-peptide was found in BRET assays using hGPR84-SPASM- $G\alpha_{16}$ biosensor. This might be due to the full length of the G protein rather than the last 27 aa of the C-terminus peptide is essential for $G\alpha_{16}$ coupling.

BRET-based GPR84-G-peptide SPASM sensors could be employed effectively for exploring the pharmacology of GPR84 ligands as the potency values of different GPR84 agonists estimated by this system are consistent with the values reported by other groups. For example, measured potencies of decanoic acid, DIM, embelin and 6-OAU were very similar to those reported in the published literature (Suzuki et al., 2013; Zhang et al., 2016; Liu et al., 2016; Mahmud et al., 2017). The potency (EC_{50} : 125 nM at the hGPR84-SPASM- $G\alpha_{i1/2}$) of compound-1 estimated in this assay was similar to that observed in calcium mobilization assays (EC_{50} : 213 nM or 139 nM) and cAMP assays (EC_{50} : 134 nM or 144 nM) reported by Zhang et al., (2016) and Liu et al., (2016) but was about 125 times lower than that (EC_{50} : 1 nM both in cAMP assays and [35 S]-GTP γ S binding assays) reported by Mahmud et al., (2017). Similarly, the potency of compound-51 (EC_{50} : 4.0 nM) provided by the hGPR84-SPASM- $G\alpha_{i1/2}$ sensor was some 11-fold and 21-fold lower than that observed in cAMP assays (EC_{50} : 0.35 nM) and calcium

mobilization assays (EC_{50} : 0.19 nM), respectively (Liu et al., 2016). The substantially lower potency of compound-51 observed in the SPASM sensor-based BRET assay might be due to the fact that less receptor reserve is obtained for G-protein activation compared to that generated in downstream signalling events like adenylyl cyclase inhibition or IP_3 -sensitive Ca^{2+} channel opening.

3.3.2. BRET based GPR84 SPASM sensor is an effective strategy to investigate the relative intrinsic activity of GPR84 agonists

Investigation of the relative intrinsic activity of ligands of a particular GPCR is limited by the fact that the relative efficacy depends on the expression profile of that GPCR in a specific cellular system which may lead to differential relative densities of GPCR, G protein and effector protein (Milligan, 2000). As the GPCR-G protein fusion approach ensures the 1:1 stoichiometry between GPCR and tethered G protein (Seifert et al., 1999; Milligan, 2002), use of this fusion protein could be an effective strategy for the study of relative efficacies of agonists of the GPCR of interest. Moreover, the BRET-based SPASM biosensor is employed to measure GPCR-G protein interaction which is not/less subject to signalling amplifications and other modulatory effects such as signal convergence/divergence and feedback from other signalling pathways. So, compared to the assays that measure efficacy at downstream signalling events, BRET-based SPASM sensor approaches may be more appropriate for comparing relative efficacies of ligands of a GPCR. In the case of GPR84, though 6-OAU and decanoic acid exhibited similar efficacy in the cAMP assay (Pillaiyar et al., 2018), 6-OAU was found to display higher maximal response than decanoic acid in the SPASM sensor-based BRET assay. In the BRET assay employing the hGPR84-SPASM- $G\alpha_{i1/2}$ sensor, DIM and embelin were found to generate sub-maximal responses i.e they behaved as partial agonists compared to decanoic acid while Pillaiyar et al., (2018) reported that embelin and decanoic acid displayed similar efficacy in cAMP assays as well as in β -arrestin recruitment assays. Another important outcome was that compound-1 and its analogue TUG-1765 were found to activate GPR84 with markedly higher efficacy compared to the putative endogenous agonist, decanoic acid demonstrating that they functioned as super-agonists in this system. Super-agonists could be potential candidates for the development of therapeutics. For example, MK-667, a growth hormone

secretagogue was reported to be a super-agonist at the ghrelin receptor and is considered to be a potential drug for growth hormone deficiency disorders (Smith et al., 2011a). Recently Gaidarov et al., (2018) have explored the anti-atherosclerotic property of GPR84 in macrophages which might be exploited for the development of agonist drugs to treat atherosclerosis. In this regard, super-agonists, compound-1 and its derivatives could be considered as potential therapeutic candidates.

4 Investigation of modes of binding of ligands to human GPR84

4.1. Introduction

Investigation of GPCR-ligand interaction is important for structure-based drug design (SBDD) programmes as well as for the development of pharmacological tool compounds which can be utilized for the physiological characterization of the receptor. In the case of GPR84, although some potent and selective agonists such as 6-n-octylaminouracil (6-OAU), 2-hexylthiopyrimidine-4, 6-diol (compound-1), 6-nonylpyridine-2, 4-diol (compound-51) have been developed, their modes of binding to GPR84 are still unknown. Even very little is known regarding the binding mode of the putative endogenous agonists, medium chain fatty acids (MCFAs). Only one study has been performed (Nikaido et al., 2015) in an effort to identify the molecular determinants of GPR84-decanoic acid interactions. As GPR84 still remains a very poorly characterized receptor, pharmacological tool compounds need to be generated for the elucidation of biological functions of this receptor. Besides this, though GPR84 has been considered to be a potential drug target, drug development programmes are hindered by the paucity of structural information on this receptor. In this regard, investigation of ligand binding modes to GPR84 is essential as it will aid the lead optimization process and thereby will accelerate drug development. Although the crystal structure of a GPCR complexed with the specific ligand is required for the elucidation of molecular determinants of ligand binding, computational techniques such as homology modelling can predict the theoretical structure of the GPCR of interest in the absence of high-resolution atomic level structure (Costanzi, 2013; Tikhonova, 2017). This predicted model structure could be then assessed by mutagenesis studies in which effects of mutation of specific amino acid residues on the potency and efficacy of the ligands are investigated. Based on input from mutagenesis studies, the docking of the ligands into the constructed homology model can be performed to predict the binding poses of the ligands which might be useful for defining the druggable pharmacophore sites within the receptor. As no atomic level high-resolution structure of GPR84 is available, we have tried to define the ligand binding pocket(s) of GPR84 by a combination of site-directed mutagenesis and molecular modelling. For the mutational analysis, I have employed the GPR84-G α fusion

protein approach. At the beginning of this chapter the characterization of Flp-InTM T-RExTM-293 cell lines expressing human GPR84-G α_{i2} fusion proteins will be discussed followed by the detailed description of molecular homology modelling and mutagenesis studies.

4.2. Characterization of Flp-InTM T-RExTM-293 cell lines expressing hGPR84-G α_{i2} fusion proteins

The GPCR-G protein fusion protein approach is appreciated to be a suitable strategy for the characterization of pharmacological tool compounds of specific GPCRs as it was found to significantly enhance the coupling efficiency between the receptor and G α protein subunit compared to co-expressing both polypeptides as separate entities (Milligan, 2000; Milligan, 2003; Suga and Haga, 2007). As agonist-stimulated human GPR84 was found to preferentially couple to G $\alpha_{i1/2}$ and G α_{i3} over G α_o and G α_z G-proteins in BRET assays employing GPR84-SPASM sensors (see section 3.2.5) and as G α_{i2} and G α_{i3} are widely expressed while G α_{i1} shows a restricted expression pattern (Milligan and Kostenis, 2006), I generated FLAG-hGPR84-G α_{i2} and FLAG-hGPR84-G α_{i3} fusion protein constructs wherein the N-terminus of the wild type G α protein subunit is coupled in frame to the C-terminal tail of human GPR84 and a FLAG epitope was added to the N-terminus of GPR84. Two PTX-resistant mutant versions of G α_{i2} , C352G G α_{i2} and C352I G α_{i2} were also fused to the FLAG-tagged human GPR84, generating FLAG-hGPR84-G α_{i2} C352G and FLAG-hGPR84-G α_{i2} C352I receptor constructs. PTX-resistant fusion constructs were generated because the coupling to endogenous G α_i proteins could be blocked by the PTX treatment of cells expressing these constructs so that the signalling response obtained would be exclusively due to intra-molecular interactions between the exogenous GPR84 and fused G protein. All these fusion protein constructs were then stably expressed in Flp-InTM T-RExTM-293 cells at the Flp InTM locus.

4.2.1. Characterization of expression of hGPR84-G protein fusion constructs by Western blot analysis

The expression of FLAG-hGPR84-G α_{i2} , FLAG-hGPR84-G α_{i2} C352G and FLAG-hGPR84-G α_{i2} C352I receptor constructs was characterized by immunoblotting membranes prepared from Flp-InTM T-RExTM-293 cells induced with doxycycline

(100 ng/ml, 24 hours) to express the receptor of interest (Figure 4.1).

Monoclonal anti-FLAG M2 antibody was used for immunoblotting the membranes to detect the FLAG sequence which was added to the N-terminus of the receptor. A distinct band of about 84 kDa was detected in the immunoblot of membranes purified from doxycycline-treated cells which confirmed the expression of either FLAG-hGPR84-G α_{i2} , FLAG-hGPR84-G α_{i2} C352G or FLAG-hGPR84-G α_{i2} C352I receptor construct as intact polypeptides in the corresponding stable cell lines (Figure 4.1). No expression of fusion protein constructs was detected in membranes prepared from untreated cells. Another band of about 100 kDa detected in the immunoblot of membranes purified from stable cell lines expressing FLAG-hGPR84-G α_{i2} C352G and FLAG-hGPR84-G α_{i2} C352I fusion proteins might reflect N-glycosylated versions of the receptor construct.

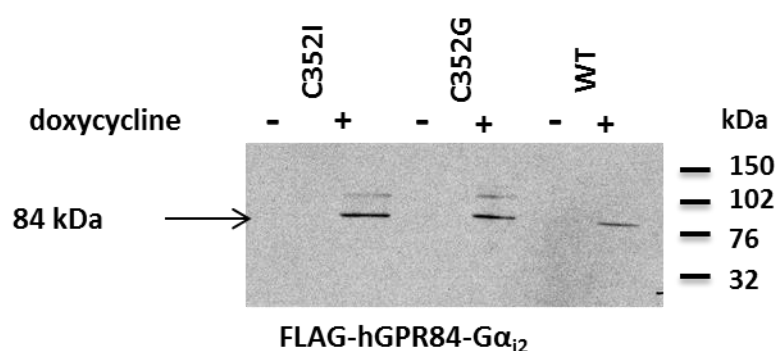


Figure 4.1 Immunoblot of FLAG-hGPR84-G α_{i2} WT, FLAG-hGPR84-G α_{i2} C352I and FLAG-hGPR84-G α_{i2} C352G fusion protein constructs probed with anti-FLAG antibody. Membranes were generated from Flp-InTM T-RExTM-293 stable cell lines either untreated (-dox) or treated (+dox) with 100 ng/ml doxycycline for 24 hours to express either FLAG-hGPR84-G α_{i2} , FLAG-hGPR84-G α_{i2} C352G or FLAG-hGPR84-G α_{i2} C352I. Samples containing 10 μ g of membrane protein were resolved by SDS-PAGE followed by immunoblotting with monoclonal M2 anti-FLAG antibody.

4.2.2. Saturation binding study

The expression level of FLAG-hGPR84-G α_{i2} and FLAG-hGPR84-G α_{i2} C352I in the corresponding Flp-InTM T-RExTM-293 stable cell lines was measured using saturation binding assays using a radiolabelled antagonist of GPR84, [³H]-G9543 which is an analogue of GPR84 antagonist compound-104, 107 and 161. [³H]-G9543 was found to bind to membranes expressing FLAG-hGPR84-G α_{i2} fusion construct with high avidity (K_d : 0.3 ± 0.01 nM; $n=3$) (Figure 4.2a_{ii} and Table 4.1). Mutation at the Cysteine 352 position of the G α_{i2} to isoleucine did not alter the binding affinity of the radiolabelled antagonist to the receptor as similar K_d

value (0.25 ± 0.02 nM; $n=7$) was obtained when membranes expressing FLAG-hGPR84-G α_{i2} C352I fusion protein was used in the binding study (Figure 4.2b_{ii} and Table 4.1). The analysis of saturation binding data also revealed that both FLAG-hGPR84-G α_{i2} and FLAG-hGPR84-G α_{i2} C352I receptor constructs were expressed effectively in the stable cell lines and their expression levels were comparable, which is evident from the similar B_{max} values (6251 ± 954 and 6538 ± 267 fmol.mg protein⁻¹, respectively).

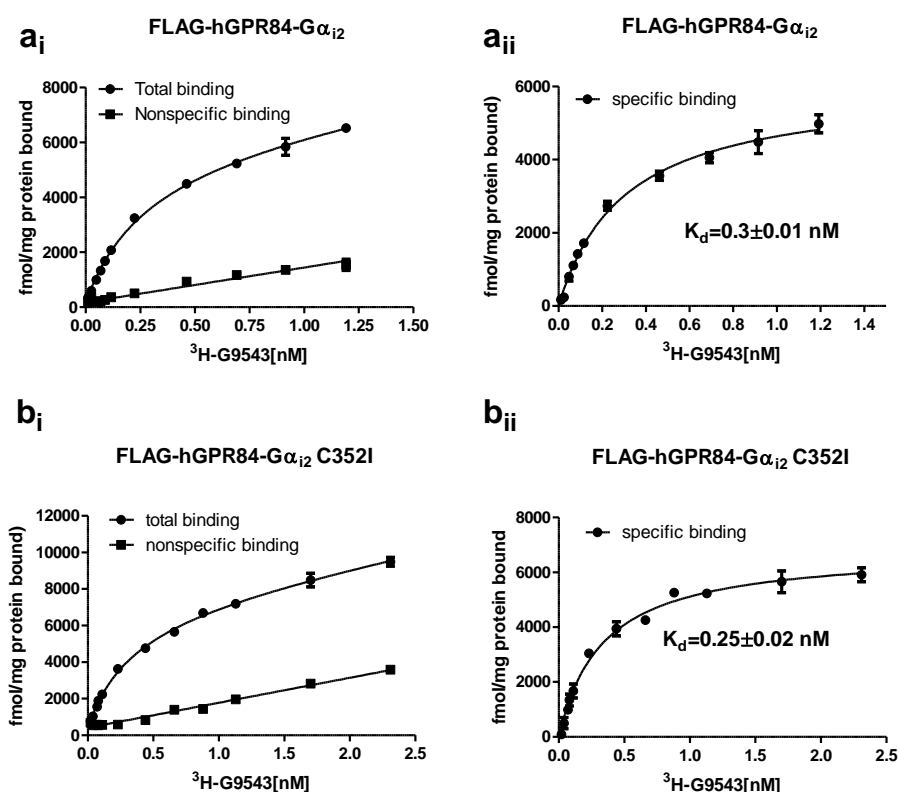


Figure 4.2 The radioligand [³H]-G9543 displayed similar binding properties at FLAG-hGPR84-G α_{i2} and FLAG-hGPR84-G α_{i2} C352I receptor constructs. Membranes were prepared from Flp-In™ T-REx™-293 cells induced with 100 ng/ml doxycycline for 24 hours to express either FLAG-hGPR84-G α_{i2} or FLAG-hGPR84-G α_{i2} C352I. The capacity of various concentrations of [³H]-G9543 to bind to membrane preparations expressing either FLAG-hGPR84-G α_{i2} (a_i, a_{ii}) or FLAG-hGPR84-G α_{i2} C352I (b_i, b_{ii}) was assessed with (nonspecific binding) or without (total binding) 1 μ M antagonist compound-104. Specific binding of the radioligand to the receptor was estimated by subtracting nonspecific binding from total binding. Data represented in (a_i and a_{ii}) and (b_i and b_{ii}) are from a representative experiment of three or seven independent experiments, respectively performed on separate membrane preparations.

4.2.3. Functional characterization of Flp-InTM T-RExTM- HEK 293 cell lines expressing FLAG-hGPR84-Gα_{i2} fusion proteins

To check the functional integrity of GPR84-G protein fusion proteins, agonist-promoted [³⁵S]-GTPγS binding assays were performed using membranes generated from Flp-InTM T-RExTM-293 cells either uninduced or induced with doxycycline (100 ng/ml, 24 hours) expressing either FLAG-hGPR84-Gα_{i2}, FLAG-hGPR84-Gα_{i2} C352I or hGPR84-Gα_{i2} C352G constructs. Decanoic acid (C-10), 3,3'-Diindolylmethane (DIM), DIM analogue PSB-16671 and compound-1 each enhanced [³⁵S]-GTPγS binding to membranes expressing the FLAG-hGPR84-Gα_{i2} fusion construct in a concentration-dependent fashion with pEC₅₀ of 4.26±0.02, 5.27±0.06, 6.28±0.05 and 7.54±0.06, respectively (Figure 4.3 a_i-a_{iii}). The potencies of decanoic acid (EC₅₀: 54±0.02 μM) and DIM (EC₅₀: 5±0.90 μM) displayed at the FLAG-hGPR84-Gα_{i2} fusion protein were about 10-fold lower than that (EC₅₀: 4.6±0.1 μM and 0.5 μM, respectively for C-10 and DIM) observed at FLAG-tagged hGPR84 estimated by Wang et al., (2006b). Similarly, the potency of PSB-16671 (EC₅₀: 524 nM) determined by this fusion protein-based [³⁵S]-GTPγS binding assay was 12.6-fold lower than that (EC₅₀: 41.3 nM) estimated in the cAMP assay using a hGPR84 expressing CHO cell line (Pillaiyar et al., 2017). The potency of compound-1 (EC₅₀: 29 nM) provided by this fusion protein was 4.4-fold lower than that (EC₅₀: 6.6 nM in cAMP assays) reported by Pillaiyar et al., (2018) but 5-fold higher than that (EC₅₀: 144 nM in cAMP assays) observed by Liu et al., (2016). Although the potency of DIM was significantly higher than decanoic acid (C-10), it acted as a weak partial agonist at FLAG-hGPR84-Gα_{i2} compared to C-10. DIM analogue PSB-16671 is more potent (10-fold) and has a greater maximal effect (about 2-fold higher response) than DIM. Compound-1 displayed the highest maximal response at the hGPR84-Gα_{i2} fusion protein, acting as a super-agonist in this assay. Noticeably, the addition of various concentrations of all these ligands to membranes generated from cells grown in the absence of doxycycline, did not result in any significant [³⁵S]-GTPγS binding, demonstrating that the enhanced binding of this guanine nucleotide analogue to membranes purified from doxycycline-treated cells was mediated by hGPR84.

The capacity of various concentrations of embelin and DIM to stimulate [³⁵S]-GTPγS incorporations into membranes purified from doxycycline-treated cells expressing either FLAG-hGPR84-Gα_{i2} C352I or FLAG-hGPR84-Gα_{i2} C352G fusion

construct was also assessed to characterize the functionality of these two PTX-resistant GPR84-G protein fusion proteins. Both of the agonists were found to promote [35 S]-GTP γ S binding to both constructs in a concentration-dependent manner (Figure 4.3b,c) while no significant incorporation of the radiolabelled nucleotide to membranes was observed when membranes were generated from cells grown in the absence of doxycycline. These results confirmed that both the PTX-resistant versions of fusion proteins were functionally active. Though DIM displayed similar potency and efficacy at hGPR84-G α_{i2} C352I and hGPR84-G α_{i2} C352G fusion constructs, potency and efficacy of embelin were decreased at the hGPR84-G α_{i2} C352G construct compared to the other constructs.

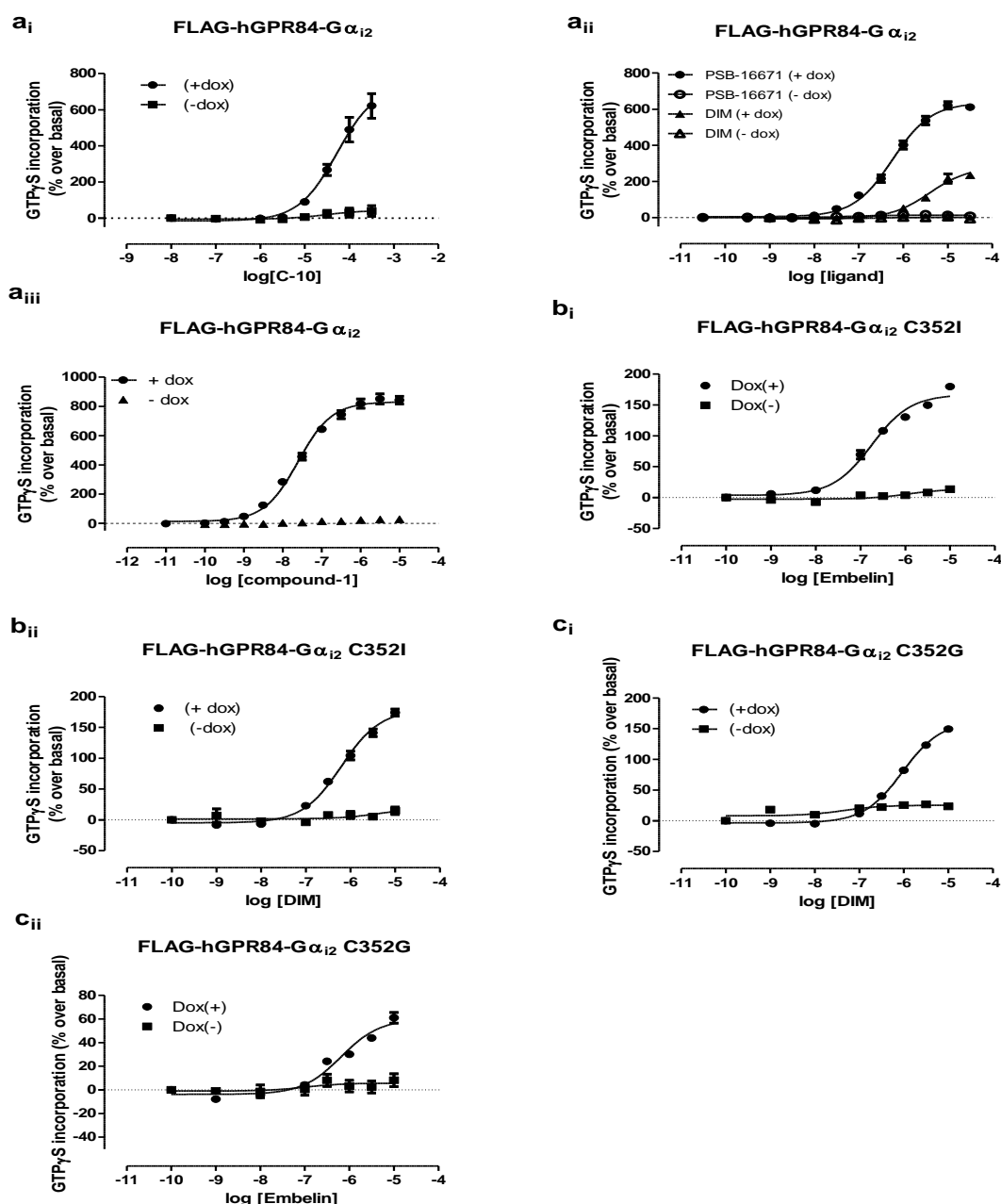


Figure 4.3 Functional characterization of Flp-In™ T-REx™-293 stable cell lines expressing either FLAG-hGPR84-Gα_{i2}, FLAG-hGPR84-Gα_{i2} C352I or FLAG-hGPR84-Gα_{i2} C352G fusion constructs. Membranes were prepared from Flp-In™ T-REx™-293 stable cell lines either uninduced (-Dox) or induced (+Dox) with 100 ng/ml doxycycline for 24 hours to express either FLAG-hGPR84-Gα_{i2}, FLAG-hGPR84-Gα_{i2} C352I or FLAG-hGPR84-Gα_{i2} C352G. The ability of various concentrations of C-10 (a_i), either DIM or DIM analogue PSB-16671 (a_{ii}) and compound-1 (a_{iii}) to stimulate binding of [³⁵S]-GTPγS to membrane preparations generated from cells harbouring the FLAG-hGPR84-Gα_{i2} fusion protein was then assessed. Equivalent studies were performed to measure the [³⁵S]-GTPγS binding to membranes purified from cells harbouring either FLAG-hGPR84-Gα_{i2} C352I (b_i, b_{ii}) or FLAG-hGPR84-Gα_{i2} C352G (c_i, c_{ii}) in response to varying concentrations of either embelin or DIM.

4.2.4. Human GPR84 couples to PTX sensitive Gα_i protein

The pre-treatment of cells expressing the FLAG-hGPR84-Gα_{i2} fusion protein with the Gα_i protein inhibitor, pertussis toxin (50 ng/ml, 24 hours) completely abolished DIM stimulated [³⁵S]-GTPγS binding to membranes (Figure 4.4a)

indicating that hGPR84 couples to PTX-sensitive $G\alpha_i$ protein. As opposed to this, DIM-induced [35 S]-GTP γ S incorporation was unaffected following PTX treatment of cells expressing the PTX insensitive mutant construct FLAG-hGPR84- $G\alpha_{i2}$ C352I (Figure 4.4b), suggesting that after PTX treatment, agonist-stimulated GPR84 exclusively interacted with the $G\alpha_{i2}$ G-protein that had been fused to the receptor rather than with any endogenous $G\alpha_i$ protein. In the case of another PTX resistant mutant construct FLAG-hGPR84- $G\alpha_{i2}$ C352G, the PTX pre-treatment of cells resulted in slightly increased binding of the [35 S]-GTP γ S to membranes compared to that prepared from untreated cells (Figure 4.4c).

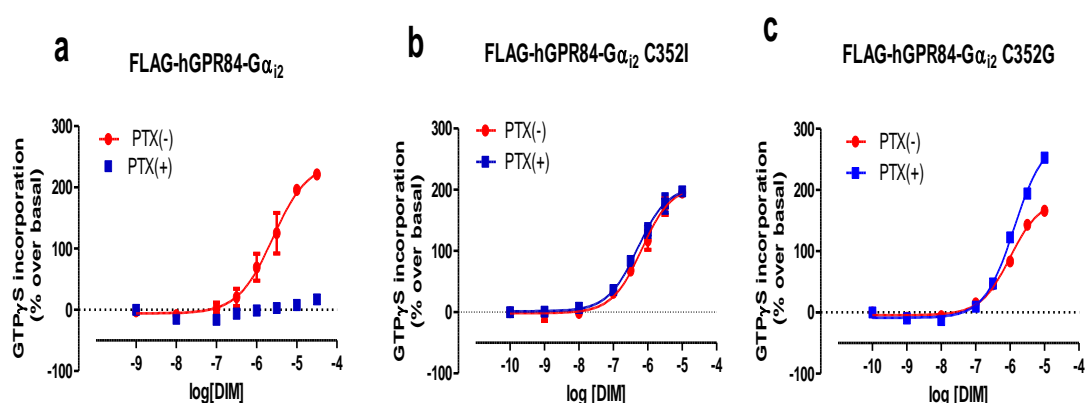


Figure 4.4 Effects of pertussis toxin (PTX) pre-treatment on DIM-induced [35 S]-GTP γ S binding to membranes purified from Flp-In™ T-REx™-293 stable cell lines expressing either FLAG-hGPR84- $G\alpha_{i2}$, FLAG- hGPR84- $G\alpha_{i2}$ C352I or FLAG-hGPR84- $G\alpha_{i2}$ C352G. Doxycycline (100 ng/ml, 24 hours) induced Flp-In™ T-REx™-293 cells expressing either FLAG-hGPR84- $G\alpha_{i2}$, FLAG- hGPR84- $G\alpha_{i2}$ C352I or FLAG-hGPR84- $G\alpha_{i2}$ C352G were either untreated (-PTX) or treated (+PTX) with 50 ng/ml of PTX for 24 hours followed by membrane generation. Using these membranes, [35 S]-GTP γ S binding assays were then performed to evaluate the function of DIM at either FLAG-hGPR84- $G\alpha_{i2}$ (a), FLAG- hGPR84- $G\alpha_{i2}$ C352I (b) or FLAG-hGPR84- $G\alpha_{i2}$ C352G (c).

4.2.5. The GPR84- $G\alpha_{i2}$ fusion protein approach enhances coupling efficiency between GPR84 and $G\alpha_i$ protein

The rationale for generating GPR84- $G\alpha$ fusion proteins was to enhance the signalling window which might be useful for the study of pharmacological properties of GPR84 ligands. In the [35 S]-GTP γ S binding assay, the magnitude of compound-1- stimulated [35 S]-GTP γ S binding obtained from the activation of FLAG-hGPR84- $G\alpha_{i2}$ C352I was 10-fold higher than that generated from the FLAG-hGPR84-eYFP (Figure 4.5a). In contrast, the potency of compound-1 was decreased by 30-fold at the fusion protein (pEC_{50} : 7.53 ± 0.07) compared to that shown at the eYFP tagged receptor (pEC_{50} : 9.0 ± 0.1). Similarly, in the case of embelin-mediated [35 S]-GTP γ S incorporation, the GPR84-G protein fusion protein

produced 5-fold higher signalling magnitude than FLAG-hGPR84-eYFP while potency was decreased by 2-fold at the FLAG-hGPR84-G α_{i2} C352I compared to that displayed by FLAG-hGPR84-eYFP (Figure 4.5b). To confirm that the higher signalling magnitude displayed by the fusion protein was not merely a reflection of higher expression level of this construct, a saturation binding study was performed using the radiolabelled antagonist [3 H-G9543] which revealed that both hGPR84-eYFP and hGPR84-G α_{i2} C352I constructs showed similar expression levels in Flp-In T-REx-293 cells as evident from their similar B_{max} values (9075 \pm 440 and 8073 \pm 619 fmol/mg protein, respectively) (Figure 4.5 c).

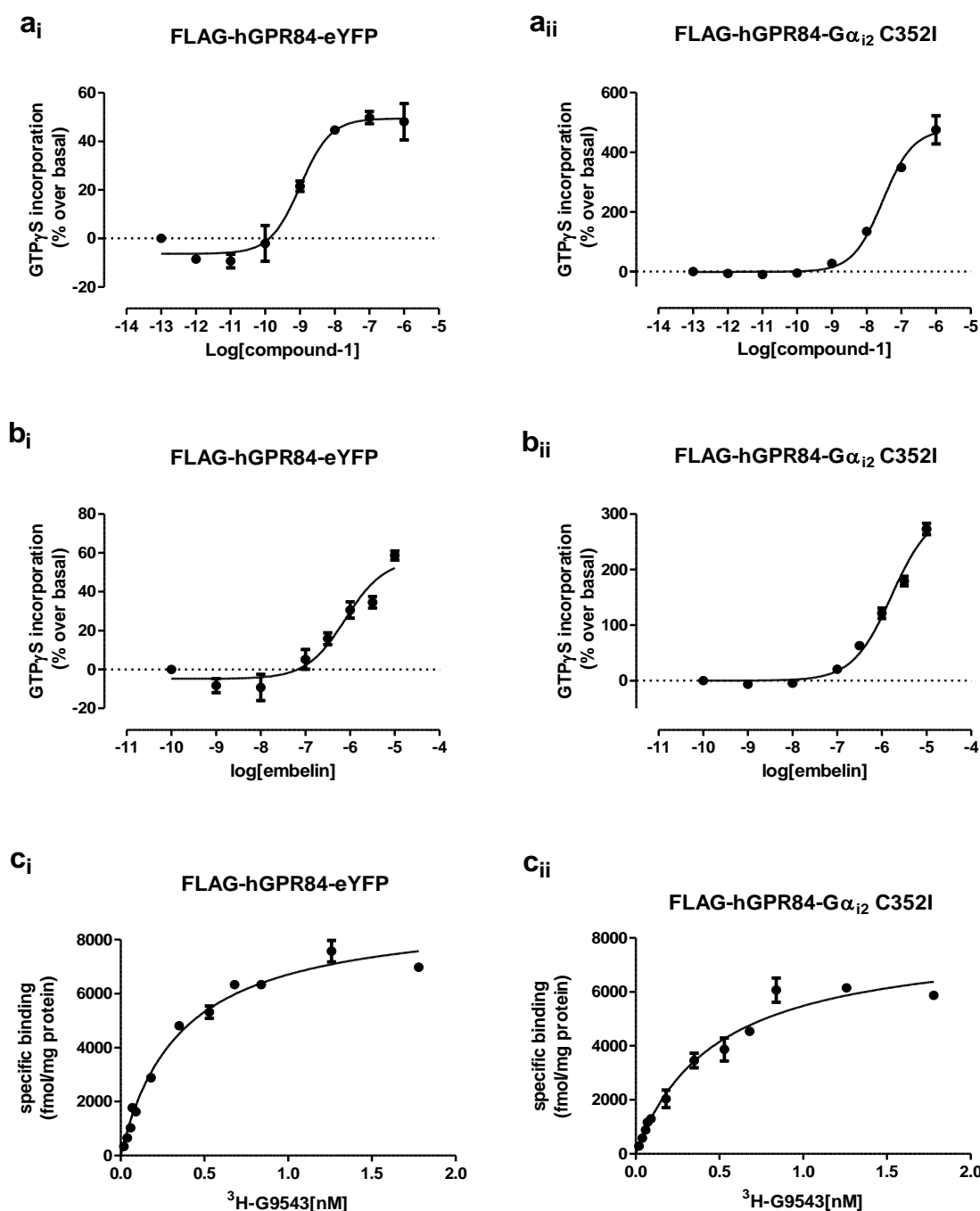


Figure 4.5 The GPR84-Gα_{i2} fusion protein approach enhances coupling efficiency between GPR84 and Gai protein compared to the eYFP tagged GPR84 construct. Flp-InTM T-RExTM-293 stable cell lines harbouring either FLAG-hGPR84-Gα_{i2} C352I or FLAG-hGPR84-eYFP were incubated with 100 ng/ml doxycycline for 24 hours to induce the expression of the receptor of interest. Membranes generated from these cells were subsequently used to perform [³⁵S]-GTPγS incorporation assays to assess the function of either compound-1 (a_i, a_{ii}) or embelin (b_i, b_{ii}). Varying concentrations of [³H]-G9543 in the absence (total binding) or presence (nonspecific binding) of 1 μM compound-104 were evaluated for their capacity to bind to membranes expressing either FLAG-hGPR84-eYFP (c_i) or FLAG-hGPR84-Gα_{i2} C352I (c_{ii}) allowing estimation of B_{max} values. Specific binding to membranes was estimated by subtracting nonspecific binding from total binding.

4.2.6. GPR84 agonists displayed similar activity at the FLAG-hGPR84-G α_{i2} and FLAG-hGPR84-G α_{i2} C352I fusion protein

GPR84 agonists displayed similar pharmacological properties at FLAG-hGPR84-G α_{i2} and FLAG-hGPR84-G α_{i2} C352I fusion constructs. In the [35 S]-GTP γ S binding assay, the potency and efficacy of embelin, compound-1, compound-51 and DIM were very similar between these two GPR84-G α fusion constructs (Figure 4.6 a) which implies that the PTX-insensitive mutant version FLAG-hGPR84-G α_{i2} C352I could be effectively employed for the pharmacological study of GPR84 ligands in place of the wild type G protein containing fusion protein. I also generated a FLAG-hGPR84-G α_{i3} C351I fusion protein in an effort to check whether this construct generates a higher signalling window compared to the FLAG-hGPR84-G α_{i2} C352I fusion construct. In the [35 S]-GTP γ S incorporation assays, potency and maximal response displayed by embelin were equivalent between FLAG-hGPR84-G α_{i2} C352I and FLAG-hGPR84-G α_{i3} C351I (Figure 4.6b).

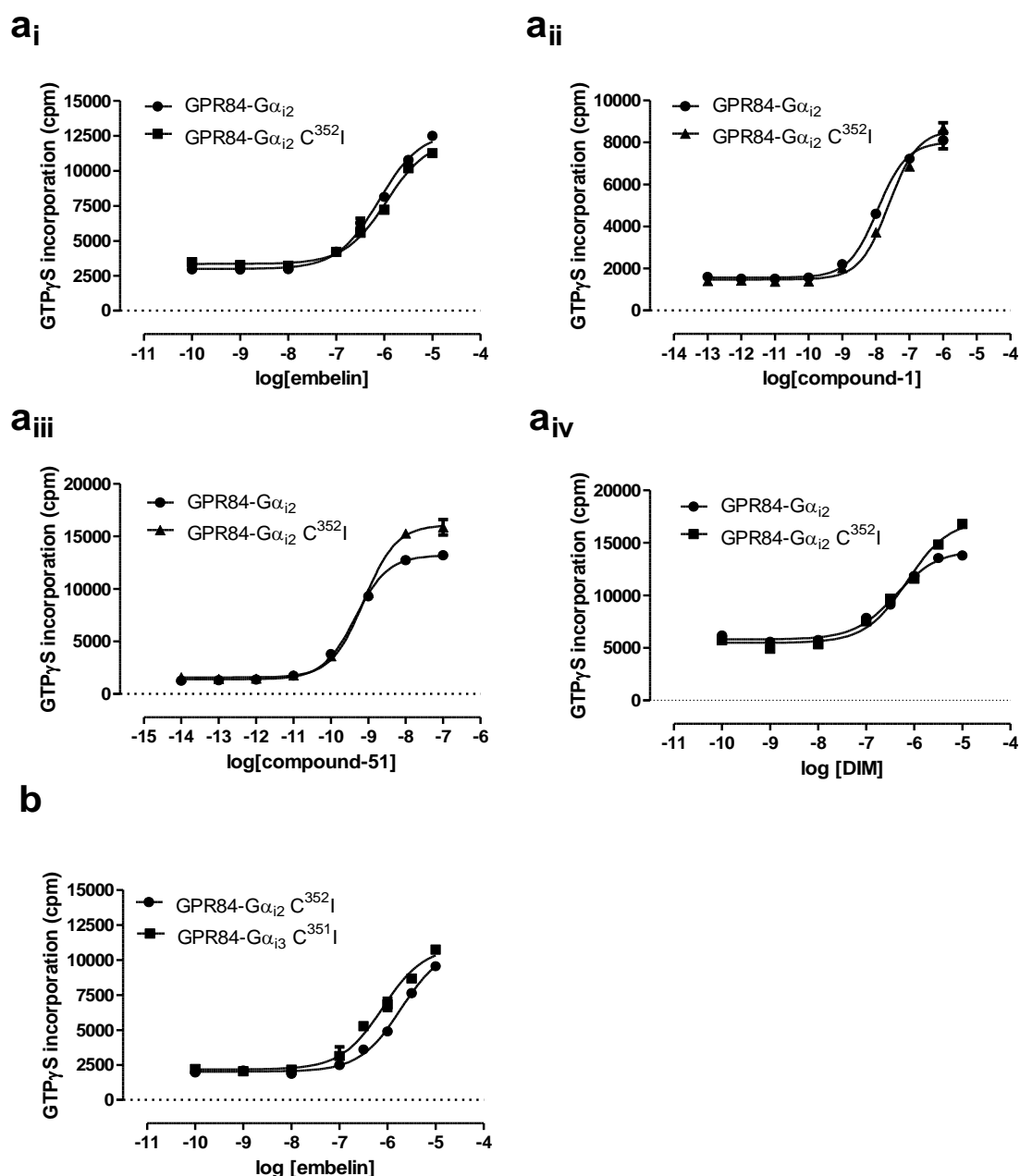


Figure 4.6 Agonists of hGPR84 display similar activity at FLAG-hGPR84-G α_{i2} and FLAG-hGPR84-G α_{i2} C352I fusion proteins. Membranes were prepared from Flp-InTM T-RExTM-293 stable cells treated with doxycycline (100 ng/ml for 24 hours) to induce the expression of either FLAG-hGPR84-G α_{i2} , FLAG-hGPR84-G α_{i2} C352I or FLAG-hGPR84-G α_{i3} C351I. The capacity of various concentrations of embelin (a_i), compound-1 (a_{ii}), compound-51 (a_{iii}) or DIM (a_{iv}) to promote [³⁵S]-GTP γ S binding to membranes expressing either FLAG-hGPR84-G α_{i2} or FLAG-hGPR84-G α_{i2} C352I was assessed. A similar study was performed to evaluate the ability of various concentrations of embelin (b) to stimulate [³⁵S]-GTP γ S incorporation into membranes expressing either FLAG-hGPR84-G α_{i2} C352I or FLAG-hGPR84-G α_{i3} C351I.

4.2.7. Functional characterization using the cAMP inhibition assay

The functional integrity of the GPR84- $G\alpha_{i2}$ fusion proteins was also assessed in cAMP inhibition assays. In these assays, DIM concentration-dependently inhibited forskolin amplified production of cAMP in cells expressing either FLAG-hGPR84- $G\alpha_{i2}$, FLAG-hGPR84- $G\alpha_{i2}$ C352I or FLAG-hGPR84- $G\alpha_{i2}$ C352G yielding pEC_{50} of 5.21 ± 0.1 , 5.47 ± 0.14 and 5.56 ± 0.14 , respectively (Figure 4.7A). This observed inhibition of cAMP production in cells by agonist-activated GPR84 is in agreement with the receptor being coupled to $G\alpha_{i/o}$ family G-proteins. Although all three fusion proteins displayed similar potency of DIM, the efficacy of DIM was decreased by two-fold at the FLAG-hGPR84- $G\alpha_{i2}$ C352G mutant construct compared to the other two fusion proteins. The reduced efficacy of DIM displayed at FLAG-hGPR84- $G\alpha_{i2}$ C352G might be due to the lower expression level of this fusion protein construct in the cell or due to the effect of cysteine to glycine mutation at 352 position of the $G\alpha_{i2}$ protein which might interrupt G protein coupling to the receptor because 352 position is located in the C terminus of the $G\alpha_i$ protein which is known to be involved in GPCR-G protein interactions. The analysis of concentration-response data obtained from the cAMP assay using the FLAG-hGPR84- $G\alpha_{i2}$ receptor construct, also revealed that potencies of DIM (5.3 ± 0.14) and embelin (6.3 ± 0.12) were higher than that of the endogenous agonist, C-10 (4.7 ± 0.1). Consistent with the results obtained from [35 S]-GTP γ S binding assays, in the cAMP assay DIM also acted as a partial agonist compared to decanoic acid (Figure 4.7B). In contrast to the BRET assay using the GPR84-SPASM- $G\alpha_{i1/2}$ biosensor wherein embelin acted as a partial agonist compared to decanoic acid (section 3.2.3), in the cAMP assay embelin showed similar efficacy, suggesting that measuring pharmacological parameters at G-protein activation level might be more useful for comparing the efficacy of ligands as less receptor reserve is associated with G-protein activation which is not/less subject to amplification of signalling or other modulatory effects that may happen in the case of downstream signalling events.

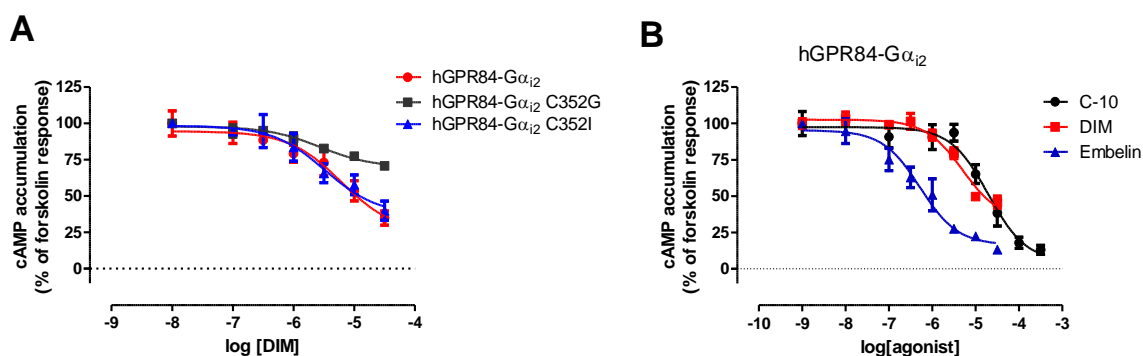


Figure 4.7 Effects of agonist-mediated GPR84 activation on intracellular cAMP accumulation. The capacity of various concentrations of DIM to inhibit forskolin-induced cAMP production in doxycycline-treated (100 ng/ml for 24 hours) Flp-InTM T-RExTM-293 cells expressing either FLAG-hGPR84-Gα_{i2}, FLAG-hGPR84-Gα_{i2} C352G or FLAG-hGPR84-Gα_{i2} C352I fusion constructs was assessed (A). A similar study was done to assess the ability of varying concentrations of either C-10, DIM or embelin to inhibit the forskolin-promoted cAMP accumulation in cells expressing the FLAG-hGPR84-Gα_{i2} fusion protein.

4.3. Investigation of the mode of binding of ligands to hGPR84

Until now, very little was known regarding the mode of binding of ligands to GPR84. A single modelling and mutagenesis study was performed by Nikaido et al., (2015) to define the molecular determinants responsible for ligand binding to GPR84. In an effort to delineate how the putative endogenous agonist decanoic acid and the synthetic agonist DIM bind to GPR84, they developed a homology model of hGPR84 using the crystal structure of human active-state β_2 -adrenergic receptor as a template. This homology model predicted that the carboxylate of the medium chain fatty acid decanoic acid was pointing towards the bottom of the binding cavity created by the transmembrane helices of GPR84. They reported that amino acid residues leucine 100^{3.32} and asparagine 104^{3.36} of transmembrane domain III (Ballesteros and Weinstein residue location number in superscript) and asparagine 357^{7.39} of transmembrane domain VII were critical for decanoic acid recognition and function since the mutations of L100D, N104Q or N357D in the context of a hGPR84-Gα_{i1} fusion protein resulted in either complete loss of function or reduced activity of decanoic acid as assessed in [³⁵S]-GTPγS incorporation assays. Importantly, response to DIM was unaffected by these mutations, demonstrating that DIM binds to another site on GPR84 that is distinct from the binding site of decanoic acid. Previously it was reported that

at least one or two arginine residues located in or near the extracellular face of fatty acid sensing receptors (FFA1-3 and FFA4) acted as charge partner to coordinate the carboxyl group of fatty acids or other synthetic ligands (Milligan et al., 2017b; Mahmud et al., 2017). For example, several groups confirmed that two arginine residues, arginine 183^{5.39} and arginine 258^{7.35} present in FFA1 coordinate the carboxyl group of long chain fatty acids or synthetic ligands (Sum et al., 2007; Tikhonova et al., 2007; Srivastava et al., 2014). Similarly, arginine 180^{5.39} and arginine 255^{7.35} located in TMD V and TMD VII, respectively of FFA2 and arginine 185^{5.39} and arginine 258^{7.35} within FFA3 were shown to anchor the negatively charged carboxylate of short-chain fatty acids (Stoddart et al., 2008a). FFA4, previously known as GPR120, which is structurally different from the three other fatty acid receptors, has only a single arginine residue R99^{2.64} which was reported to make ionic interactions with the carboxylate of long chain fatty acids (Hudson et al., 2014b; Watson et al., 2012; Sun et al., 2010). In accordance with these findings, it is expected that similar arginine or other positively charged amino acid residues within GPR84 might act as anchor(s) for the carboxylate function of medium chain fatty acid ligands. Surprisingly, Nikaido et al., (2015) failed to identify any arginine residue or other positively charged amino acid(s) of GPR84 that can coordinate the carboxylate function of the medium chain fatty acid, decanoic acid. Rather their model predicted that asparagine 104, located in the 3.36 position within GPR84 might coordinate the carboxylate moiety of the fatty acid. Recently, Yin et al., (2016) reported the crystal structure of human OX1 receptor which shares 31% of sequence identity with the transmembrane domains of human GPR84 (Tikhonova, 2017). Sequence alignment between the extracellular loop 2 (EL2) of the crystal structure of rhodopsin and EL2 of human GPR84 revealed that there was 43% sequence conservation between them, which is quite surprising because EL2 of GPCRs generally differs substantially from each other in terms of primary amino acid sequence as well as secondary structure (Tikhonova, 2017; MacKenzie et al., 2014; Wheatley et al., 2012; Costanzi, 2012). Combining the transmembrane domains of the crystal structure of OX1 receptor and EL2 from the crystal structure of rhodopsin, Tikhonova (2017) developed a hybrid template and based on this template, a novel homology model of human GPR84 was constructed in which the Arginine 172 of EL2 was directed towards the putative binding pocket created by the helical bundle (Figure 4.8A). This homology model of GPR84

predicted that Arginine 172 within the extracellular loop 2 (EL2) of the receptor might coordinate the negatively charged carboxyl group of the medium chain fatty acids or other bioisosteres of natural/synthetic agonists such as embelin, 6-OAU or compound-1. The homology model developed by Nikaido et al., (2015) failed to predict this arginine group within the EL2 of human GPR84 as it shares no sequence identity with the EL2 of the β_2 -adrenergic receptor used as the template for homology modelling. Another important thing is that the putative orientation of the decanoic acid into the binding pocket of GPR84 based on this homology model (Figure 4.8B) is opposite to that displayed by the homology model constructed by Nikaido and co-workers (2015). In the case of docking poses of decanoic acid studied by Nikaido et al., (2015) the carboxylate moiety of C-10 is directed towards the bottom of the binding cavity and the hydrophobic aliphatic chain is pointing upwards to the extracellular side whilst herein the hydrophobic chain appears to be pointed deep into the core of the helical bundle.

The homology model predicted that residues Y69, L73, Y81, L100, F101, N104, F170, R172, L182, Y186, F187, Y332, F335, N339, H352, and W360 form the putative ligand-binding pocket of GPR84 (Figure 4.8 B,C). To investigate the role of residues R172, F170, F101^{3.33}, F335^{6.51} and W360^{7.43} in the ligand recognition and/or function, aromatic residues F101^{3.33}, F170^{EL2}, F335^{6.51} and W360^{7.43} were mutated to alanine and the basic residue R172 was mutated to alanine or lysine (Figure 4.9) within the setting of the FLAG-hGPR84-G α_{i2} C352I fusion construct. All these mutant constructs of GPR84 were developed by site-directed mutagenesis and then Flp-In T-REx-293 cells stably harbouring the mutant receptor of interest at the Flp InTM locus were generated.

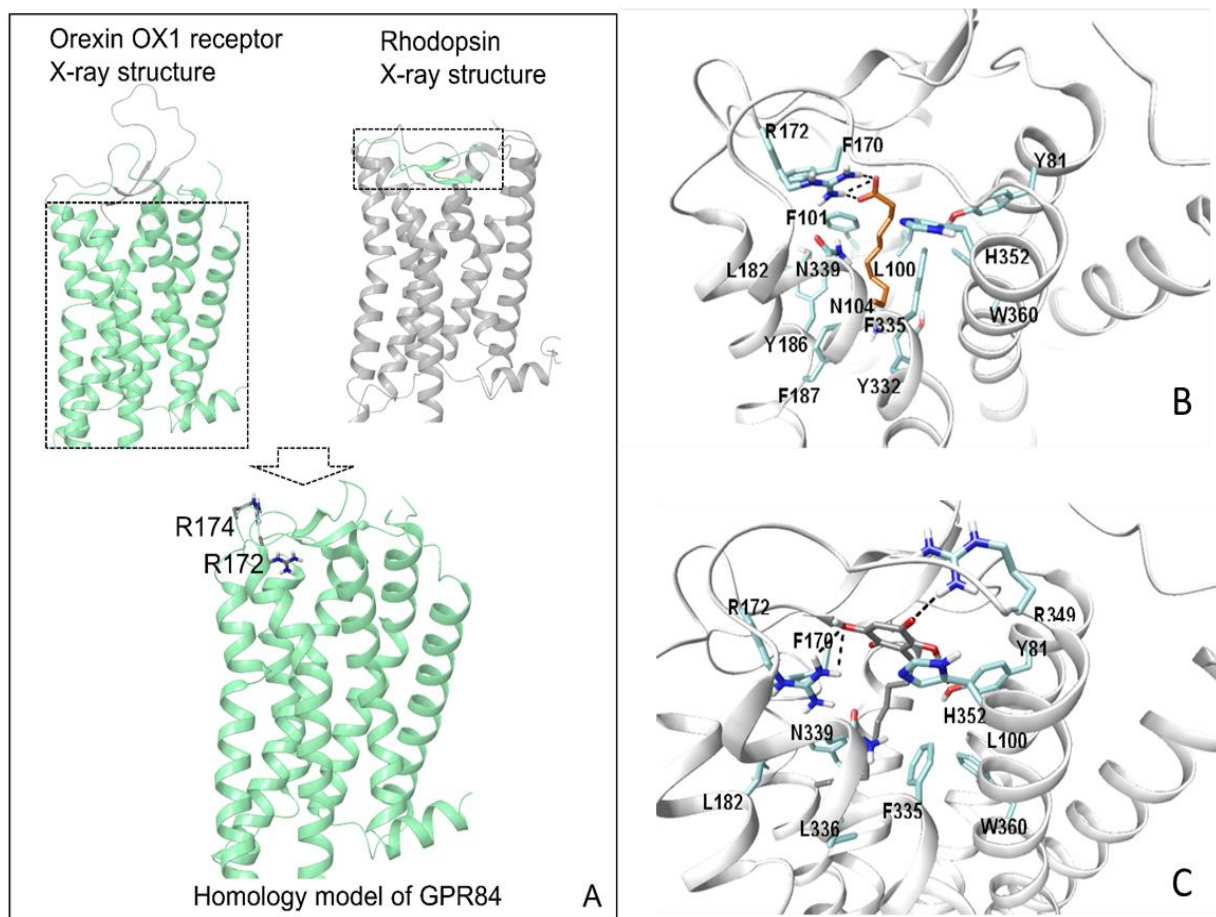


Figure 4.8 Homology model of human GPR84 and the putative ligand-binding cavity. (A) A GPR84 homology model was generated based on a hybrid template comprising the transmembrane domains of the crystal structure of the human orexin receptor (hOX1R) and the 2nd extracellular loop (EL2) of the crystal structure of rhodopsin (Mahmud et al., 2017). Two arginines, Arginine 172 and Arginine 174 located within EL2 are visualized. (B–C) The putative binding pocket(s) for decanoic acid (B) and embelin (C) are shown. Both agonists appear to be anchored at Arginine 172 of the EL2 by forming hydrogen bond/salt bridges shown as dotted black lines. Other potentially important amino acid residues were also visualized. These figures were generated by Dr Irina G. Tikhonova as part of the collaboration.

| | | | | |
|--------------------|--------------------|-------------------|--------------------|------------|
| 10 | 20 | 30 | 40 | 50 |
| MWNSSDANFS | CYHESVLGYR | YVAVSWGCVV | AVTGTGVGNVL | TLLALAIQPK |
| 60 | 70 | 80 | 90 | 100 |
| LRTRENLIIA | NLTLDLLYC | TLLQPFSSVD | YLHLHWRTGA | TFCRVFGLLL |
| 110 | 120 | 130 | 140 | 150 |
| F ASNSVSILT | LCLIALGRYL | LIAHPKLFQ | VFSAGIVLA | LVSTWVGVVA |
| 160 | 170 | 180 | 190 | 200 |
| SFAPLWPIYI | LVPVVCTCS F | D IRGRPYTT | ILMGIYFVLG | LSSVGIFYCL |
| 210 | 220 | 230 | 240 | 250 |
| IHRQVKRAAQ | ALDQYKLRQA | SIHSNHVART | DEAMPGRFQE | LDSRLASGGP |
| 260 | 270 | 280 | 290 | 300 |
| SEGISSEPV | AATTQTLEGD | SSEVGQINS | KRAQMAEKS | PPEASAKAQP |
| 310 | 320 | 330 | 340 | 350 |
| IKGARRAPDS | SSEFGKVTRM | CFAVFLCFAL | SYIP F LLLN | LDARVQAPRV |
| 360 | 370 | 380 | 390 | |
| VHMLAANLT W | LNGCINPVLY | AAMNRQFRQA | YGSILKRGP | SFHLRH |

Figure 4.9 Primary amino acid sequence of human GPR84 highlighting the residues I have mutated. Red indicates that the residue (F101^{3.33}, F170^{EL2}, F335^{6.51} and W360^{7.43}) was mutated to alanine and blue indicates that the residue (R172 of the EL2) was mutated to alanine as well as to lysine. This figure was collected from the website <https://www.uniprot.org/uniprot/Q9NQS5>.

4.3.1. Assessment of expression levels of different mutants of hGPR84

Saturation binding studies were performed using a radiolabelled form of the antagonist of GPR84, [³H]-G9543, to measure the expression level of different mutant versions of GPR84 and wild type GPR84. [³H]-G9543 bound to membranes expressing FLAG-hGPR84-Gα_{i2} C352I with high affinity yielding a K_d value of 0.25±0.02 nM (n=7) (Figure 4.10a and Table 4.1). The binding affinity of the radioligand to the receptor was unaffected by mutation of arginine 172^{EL2} to either alanine or lysine as similar K_d values (0.27±0.02 nM and 0.22±0.03 nM, respectively for GPR84 R172A-Gα_{i2} C352I and GPR84 R172K-Gα_{i2} C352I fusion constructs, n=7) were obtained when membranes expressing either FLAG-hGPR84 R172A-Gα_{i2} C352I or FLAG-hGPR84 R172K-Gα_{i2} C352I were used in the binding studies (Figure 4.10 b,c). On the other hand, mutation of phenylalanine 335^{6.51} or phenylalanine 170^{EL2} to alanine decreased the binding affinity (K_d values 2.18±0.2 and 0.93±0.2 nM, respectively for GPR84 F335A-Gα_{i2} C352I and GPR84 F170A-Gα_{i2} C352I) of the radioligand to the receptor by 8.7 and 3.7-fold, respectively. Saturation binding data also revealed that hGPR84-Gα_{i2} C352I, hGPR84 R172A-Gα_{i2} C352I, hGPR84 R172K-Gα_{i2} C352I and hGPR84 F335A-Gα_{i2} C352I fusion constructs were expressed effectively in the corresponding Flp-In T-REx cell line and there was no significant variation in their expression levels

since similar B_{max} values were observed (Table 4.1). By contrast, the expression of hGPR84 F170A-Gα_{i2} C352I (B_{max}: 1419±180 fmol/mg protein) was much lower than the wild type receptor (B_{max}: 6538±267 fmol/mg protein). No specific binding of [³H]-G9543 to either GPR84 F101A or GPR84 W360A constructs was detected (Figure 4.11).

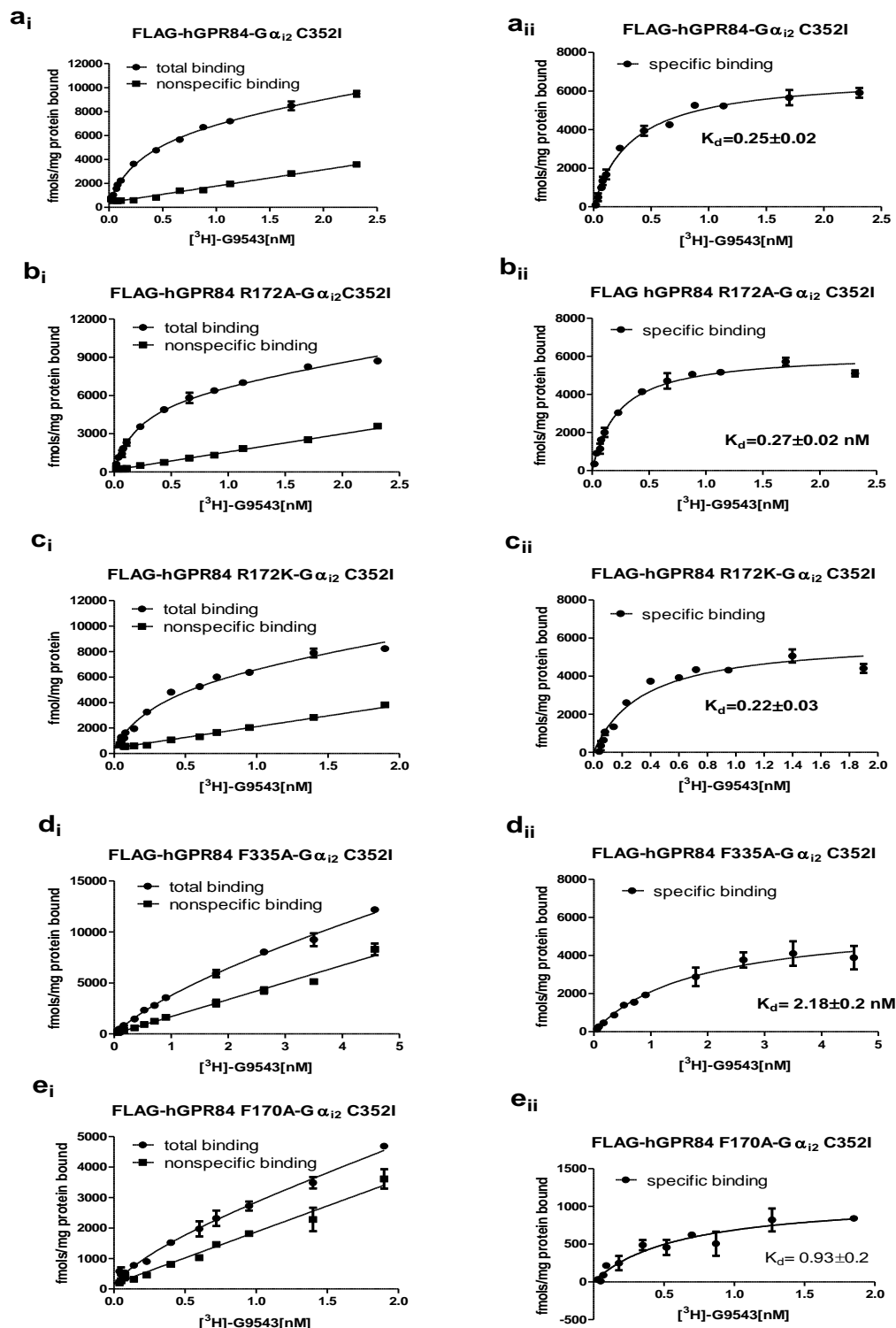


Figure 4.10 Binding properties of [³H]-G9543 at wild type and mutant versions of human GPR84. Membranes were prepared from doxycycline-induced (100 ng/ml, 24 hours) Flp-In T-Rex-293 cells expressing the receptor of interest. Various concentrations of [³H]-G259543 with (nonspecific binding) or without (total binding) 1 μ M antagonist compound-104 were assessed for their capacity to bind to membranes expressing either FLAG-hGPR84-G α_{12} C352I (a_i,a_{ii}), FLAG-hGPR84 R172A-G α_{12} C352I (b_i,b_{ii}), FLAG-hGPR84 R172K-G α_{12} C352I(c_i,c_{ii}), FLAG-hGPR84 F335A-G α_{12} C352I (d_i,d_{ii}) or FLAG-hGPR84 F170A-G α_{12} C352I (e_i,e_{ii}) constructs. Specific binding of radioligand was measured by subtracting nonspecific binding from total binding. Representative results of five (d,e) or seven(a-c) independent experiments were shown.

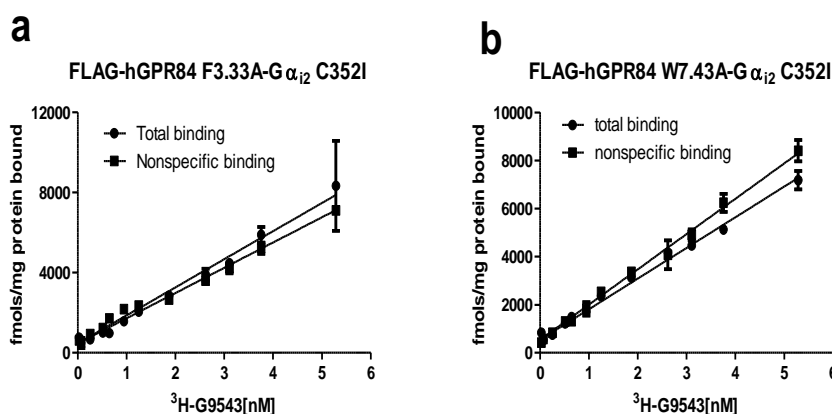


Figure 4.11 Mutation of phenylalanine 101^{3.33} or tryptophan 360^{7.43} to alanine completely eliminated the ability of the radiolabelled antagonist [³H]-G9543 to bind to human GPR84. The capacity of increasing concentrations of [³H]-G9543 to bind to membranes expressing either FLAG-hGPR84 F3.33A-Gα_{i2} C352I or FLAG-hGPR84 W7.43A-Gα_{i2} C352I was assessed in the presence (nonspecific binding) or absence (total binding) of 1 μM compound-104.

Table 4-1 Binding affinity of [³H]-G9543 to the wild type and mutant versions of hGPR84 and corresponding receptor density

| Receptor construct | Bmax (fmol/mg protein) | K _d (nM) |
|--|------------------------|---------------------|
| FLAG-hGPR84-Gα _{i2} | 6251±954 | 0.3±0.01 |
| FLAG-hGPR84-Gα _{i2} C352I | 6538±267 | 0.25±0.02 |
| FLAG-hGPR84 R172A-Gα _{i2} C352I | 7481±527 | 0.27±0.02 |
| FLAG-hGPR84 R172K-Gα _{i2} C352I | 5825±203 | 0.22±0.03 |
| FLAG-hGPR84 F335A-Gα _{i2} C352I | 5352±606 | 2.18±0.2*** |
| FLAG-hGPR84 F170A-Gα _{i2} C352I | 1419±180*** | 0.93±0.2*** |

A series of radioligand [³H]-G9543 binding assays were performed to determine the K_d of the radiolabelled antagonist and receptor density (Bmax) of the membrane preparations and data are expressed as mean±S.E.M. (n=5/7). Bmax and K_d values were analysed by one-way ANOVA followed by Dunnett's multiple comparison tests using the values displayed at the hGPR84-Gα_{i2} C352I construct as the reference. The statistical significance is presented as *P<0.05, **P<0.01, ***P<0.001

4.3.2. Arginine 172 of EL2 is a key molecular determinant of orthosteric ligand binding to hGPR84

Decylamine (Nikaido et al., 2015) and methyl decanoate (Mahmud et al., 2017) have been reported to be inactive at human GPR84, demonstrating the importance of the carboxylic acid moiety in the agonistic function of decanoic acid at hGPR84. Moreover, the homology model (shown in Figure 4.8) predicted that the carboxylate of MCFAs is anchored by arginine 172 located within EL2 of GPR84. In an effort to confirm this anchoring role of arginine 172, the effect of mutation of this amino acid residue to alanine on the agonistic function of GPR84 ligands was assessed using [³⁵S]-GTPγS binding assays. The alteration of the arginine 172 to alanine resulted in complete elimination of the activity of decanoic acid (C-10), embelin, compound-1 and 6-OAU (Figure 4.12, Table 4.2),

indicating that this residue is important for ligand recognition and function. This was not the case for DIM or the DIM analogue PSB-16671 as they were found to remain active at this mutant receptor. DIM displayed similar potency and efficacy at the R172A GPR84 mutant compared to wild type. Though the potency of PSB-16671 was decreased slightly (less than 2-fold), it displayed higher maximum response at the R172A mutant compared to the wild type receptor. The mutation of arginine 172 to lysine in the context of the FLAG-hGPR84-G α_{i2} C352I fusion protein also completely abolished responses to C-10, embelin and compound-1 (Figure 4.12). Compared to the wild type receptor this mutation also resulted in 64% reduction ($P<0.001$) of maximum response to 6-OAU while the potency of 6-OAU was decreased by 20-fold ($P<0.001$). These results demonstrated that along with maintenance, position of the positive charge is also crucial for orthosteric ligand recognition and function. Though DIM and PSB-16671 displayed similar potency at the R172K mutant, their efficacies were reduced significantly by 22 and 25%, respectively compared to that of wild type receptor. The retention of agonist function of DIM and PSB-16671 at either R172A or R172K mutant of GPR84 suggested that DIM and PSB-16671 must bind a site which is topographically distinct from the binding site shared by C-10, embelin, 6-OAU or compound-1.

The loss of orthosteric agonist function at R172A or R172K mutant receptors was not due to the loss of or reduced expression level of the mutant receptor as saturation binding studies with the radiolabelled antagonist [3 H]-G9543 revealed that there was no significant variation (Bmax: 7481 ± 527 , 5825 ± 203 and 6538 ± 267 fmol/mg protein, respectively for R172A, R172K and wild type receptor) (Figure 4.10 and Table 4.1). Moreover, the affinity of the radioligand was unaltered by the mutation at arginine 172 to either alanine or lysine since similar K_d values were obtained for both mutant receptors (Table 4.1), confirming that these mutations did not result in generation of a non-functional misfolded receptor.

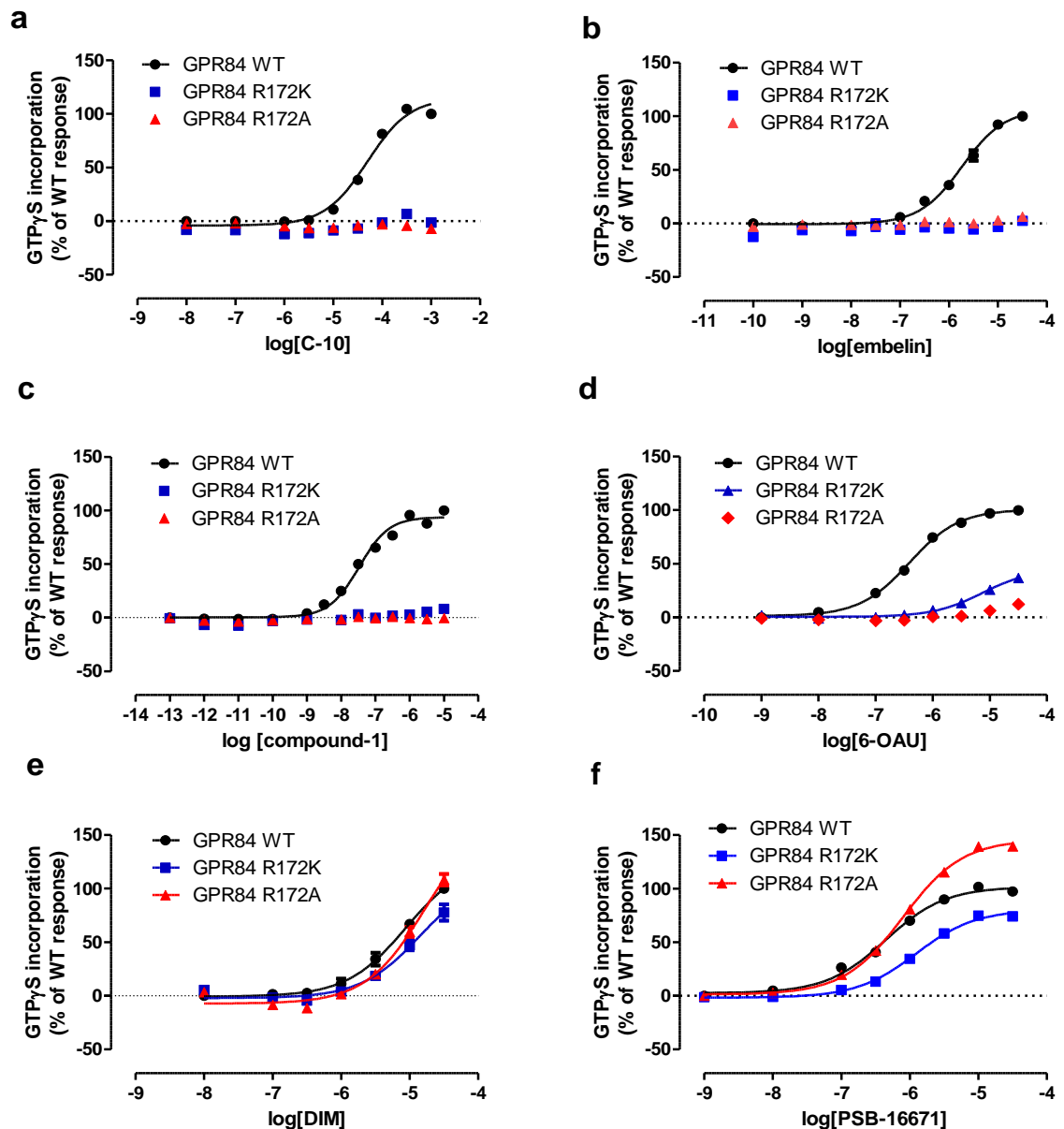


Figure 4.12 Mutation of arginine 172 of hGPR84 to either alanine or lysine abolishes the agonist function of decanoic acid, embelin, compound-1 and 6-OAU but not of DIM or PSB-16671. Membranes generated from doxycycline-treated (100 ng/ml for 24 hours) Flp-InTM T-RExTM-293 cells expressing either FLAG-hGPR84-G α_{i2} C352I, FLAG-hGPR84 R172A-G α_{i2} C352I or FLAG-hGPR84 R172K-G α_{i2} C352I were used to assess the ability of various concentrations of either C-10 (a), embelin (b), compound-1 (c), 6-OAU (d), DIM (e) or PSB-16671 (f) to promote binding of [³⁵S]-GTP γ S to the G α_{i2} G-protein associated with the fusion construct of interest. Data represent mean \pm SEM of three independent experiments performed on separate membrane preparations. To eliminate the effect of differential expression level on agonistic activity, before performing each [³⁵S]-GTP γ S binding assay, Bmax values were estimated for membrane preparations generated from Flp-InTM T-RExTM-293 cells expressing either FLAG- hGPR84-G α_{i2} C352I, FLAG-hGPR84 R172A-G α_{i2} C352I or FLAG-hGPR84 R172K-G α_{i2} C352I fusion proteins and 50 fmol per reaction was used for each receptor construct.

Table 4-2 Potency and efficacy of GPR84 ligands at wild type, R172A or R172K GPR84

| ligand | GPR84 WT | GPR84 R172A | | | GPR84 R172K | | |
|------------|-------------------|-------------------|--------------------|------------------|-------------------|--------------------|------------------|
| | pEC ₅₀ | pEC ₅₀ | ΔpEC ₅₀ | E _{max} | pEC ₅₀ | ΔpEC ₅₀ | E _{max} |
| C-10 | 4.30±0.05 | NA | NA | NR | NA | NA | NR |
| Embelin | 5.64±0.09 | NA | NA | NR | NA | NA | NR |
| Compound-1 | 7.50±0.04 | NA | NA | NR | NA | NA | NR |
| 6-OAU | 6.40±0.05 | 4.8±0.04*** | -1.6 | 12±0.8*** | 5.1±0.01*** | -1.3 | 36±4*** |
| TUG-1765 | 9.50±0.1 | NA | NA | 11±0.8*** | 6.8±0.03*** | -2.7 | 60.6±0.6*** |
| DIM | 5.20±0.1 | 4.85±0.16 | -0.35 | 108.3±5 | 4.95±0.15 | -0.25 | 78±7* |
| PSB-16671 | 6.35±0.04 | 6.1±0.01** | -0.25 | 139±2*** | 5.91±0.01** | -0.44 | 74.2±0.6*** |

A set of [³⁵S]-GTPγS binding experiments were performed to determine the potency (pEC₅₀) and efficacy (E_{max}) of the GPR84 agonists at wild type and mutant GPR84 and data are presented as mean±SEM of three independent experiments. Efficacy (E_{max}) is expressed as the percentage of wild type response. NA: not applicable; NR: no response; ΔpEC₅₀ represents mutant pEC₅₀–wild type pEC₅₀; pEC₅₀ and E_{max} values were analysed by one-way analysis of variance (ANOVA) followed by Tukey's multiple comparison tests with statistical significance denoted as *P<0.05, **P<0.01, ***P<0.001; The significance level of potency of TUG-1765 displayed at the R172K mutant compared to that of wild type receptor was determined by an unpaired two-tailed t-test.

4.3.3. Embelin, compound-1 and 6-OAU share a common binding site with MCFAs

The binding site of endogenous agonists is considered as the orthosteric site of the receptor (Smith et al., 2011a). Similar to the endogenous agonist (C-10), each of embelin, compound-1 and 6-OAU lost activity at both R172A and R172K mutants of GPR84 which suggests that embelin, compound-1 and 6-OAU share a same binding site within GPR84 which overlaps with the binding site of C-10. In all these orthosteric agonists, a hydrophilic head group (2, 5-dihydroxy-1, 4-benzoquinone in embelin; 4, 6-dihydroxypyrimidine in compound-1 and pyrimidine-2, 4-dione in 6-OAU) is attached to a long hydrophobic tail. The mutational study showed that in addition to the carboxylate group of decanoic acid, the arginine 172 also coordinated the hydrophilic polar head group of embelin, compound-1 and 6-OAU i.e these groups acted as bioisosteres of the carboxylate of MCFAs. As additional support for the fact that both embelin and compound-1 share an overlapping binding site at human GPR84 with decanoic acid, concentration-response curves for compound-1 or embelin were generated in the presence of varying fixed concentrations of C-10 employing the [³⁵S]-GTPγS incorporation assay using membranes expressing FLAG-hGPR84-Gα_{i2} fusion protein. As a direct agonist, C-10 stimulated [³⁵S]-GTPγS incorporation into membranes in the absence of either compound-1 or embelin. However, the addition of sub-maximal fixed concentrations of decanoic acid ranging from 1 μM to 100 μM to the concentration-response assay for compound-1 did not change the potency of compound-1 (Figure 4.13a). Similarly, the potency of embelin was unaffected by the co-addition of varying fixed concentrations of decanoic

acid ranging from 1 μ M to 300 μ M (Figure 4.13b). In both cases, co-addition of submaximal concentrations of C-10 to either compound-1 or embelin only produced ‘additive effect’ rather than any ‘co-operative effect’ which is consistent with the idea that embelin and compound-1 both are orthosteric with respect to decanoic acid. This conclusion is in agreement with the findings of Zhang et al., (2016) which also revealed that co-addition of increasing fixed concentrations of compound-1 ranging from 20 to 180 nM to the concentration-response assay of 3-hydroxy lauric acid in a calcium mobilization assay did not alter the measured potency of the hydroxylated MCFA suggesting that compound-1 shares a common binding site with MCFAs.

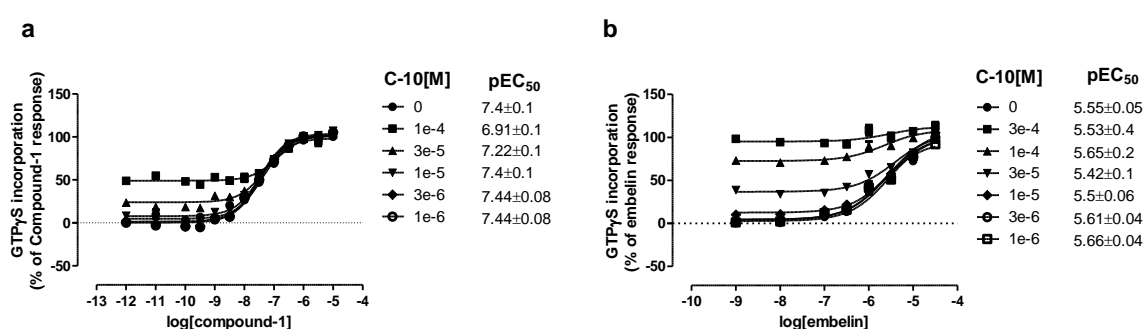


Figure 4.13 Decanoic acid, embelin and compound-1 share a common binding site in hGPR84. Membranes were prepared from Flp-In T-REx-293 cells induced with 100 ng/ml of doxycycline for 24 hours to express FLAG-hGPR84-G α_{i2} . These membranes were then employed to perform [35 S]-GTP γ S binding assays to generate concentration-response curves for compound-1 (a) or embelin (b) in the presence of increasing fixed concentrations of decanoic acid (C-10).

4.3.4. TUG-1765 and related molecules bind to the orthosteric pocket of hGPR84

In the [35 S]-GTP γ S binding assay, 6-octylpyridine-2, 4-diol (TUG-1765; designated as compound-50 by Liu et al., 2016) displayed about 92-fold higher potency (pEC₅₀: 9.5 \pm 0.1) (Figure 4.14a) than compound-1 (pEC₅₀: 7.22 \pm 0.06). Liu et al., (2016) observed similar potency of TUG-1765 (EC₅₀: 1.34 \pm 0.08 nM) in a Ca²⁺ mobilization assay. As this compound is an analogue of compound-1, it is expected that this compound would also bind to the orthosteric site of GPR84. To assess this the effect of mutation at arginine 172 to alanine or lysine on the agonistic function of TUG-1765 was examined using the [35 S]-GTP γ S binding assay. R172A mutation in the context of hGPR84-G α_{i2} C352I almost abolished the activity of TUG-1765 with only 10% of wild type response observed at 1 μ M

(Figure 4.14a). The potency of this compound was significantly reduced by some 500-fold ($P<0.001$) when this arginine residue was mutated to lysine whilst the efficacy was decreased by 40% ($P<0.001$) (Table 4.2). The almost complete loss of activity at R172A GPR84 and the large reduction of agonistic function in terms of potency and efficacy at R172K GPR84 suggested that the arginine 172 of the EL2 of GPR84 coordinated the 2,4-dihydroxypyridine moiety of TUG-1765, which therefore acted as a bioisostere of the carboxylate of MCFAs. These results suggested that TUG-1765 is also orthosteric with respect to decanoic acid.

A series of compounds structurally related to compound-1 was then assessed to define their binding modes. Among them TUG-1758, 1759, 1761, 1762, 1763 and 1764 (for structure see Figure 2.2) displayed similar efficacy to compound-1 in the [35 S]-GTP γ S binding assay. 2-nonylpyridine (TUG-1760) showed 812-fold lower potency and 5-fold lower efficacy compared to compound-1, indicating that the removal of hydroxyl groups from the heterocyclic ring is poorly tolerated. The potencies of 6-phenylethylpyridine-2,4-diol (TUG-1758) and 2-nonyl-4-pyridone (TUG-1761) were lowered by some 33-fold compared to compound-1 whilst 6-phenylbutylpyridine-2,4-diol (TUG-1759), 6-undecylpyridine-2,4-diol (TUG-1762), 6-decylpyridine-2,4-diol (TUG-1763) and 6-heptylpyridine-2,4-diol (TUG-1764) showed significantly higher potency than compound-1 affording pEC₅₀ of 8.25 ± 0.1 , 8.44 ± 0.04 , 8.20 ± 0.07 and 8.92 ± 0.02 , respectively (Figure 4.14c). Similar to compound-1, each of TUG-1758, 1759, 1762, 1763 and 1764 lacked activity at R172A GPR84 when the highest concentration of each ligand that could be practically applied was employed in the assay (Figure 4.14d). Similarly, very limited activity of these compounds was observed at R172K GPR84 when either 100 μ M of TUG-1758 or 1 μ M of TUG-1759, 1762, 1763 and 1764 were used in the assay. These findings suggest that these compounds are orthosteric agonists of human GPR84. By contrast, TUG-1761 displayed similar potency at R172A GPR84 compared to the wild type receptor and efficacy was reduced only by 33% (Figure 4.14b). However, the mutation of arginine to lysine resulted in a 5-fold reduction in potency and 80% decrease in efficacy for TUG-1761. Further studies are required to define the binding mode of TUG-1761.

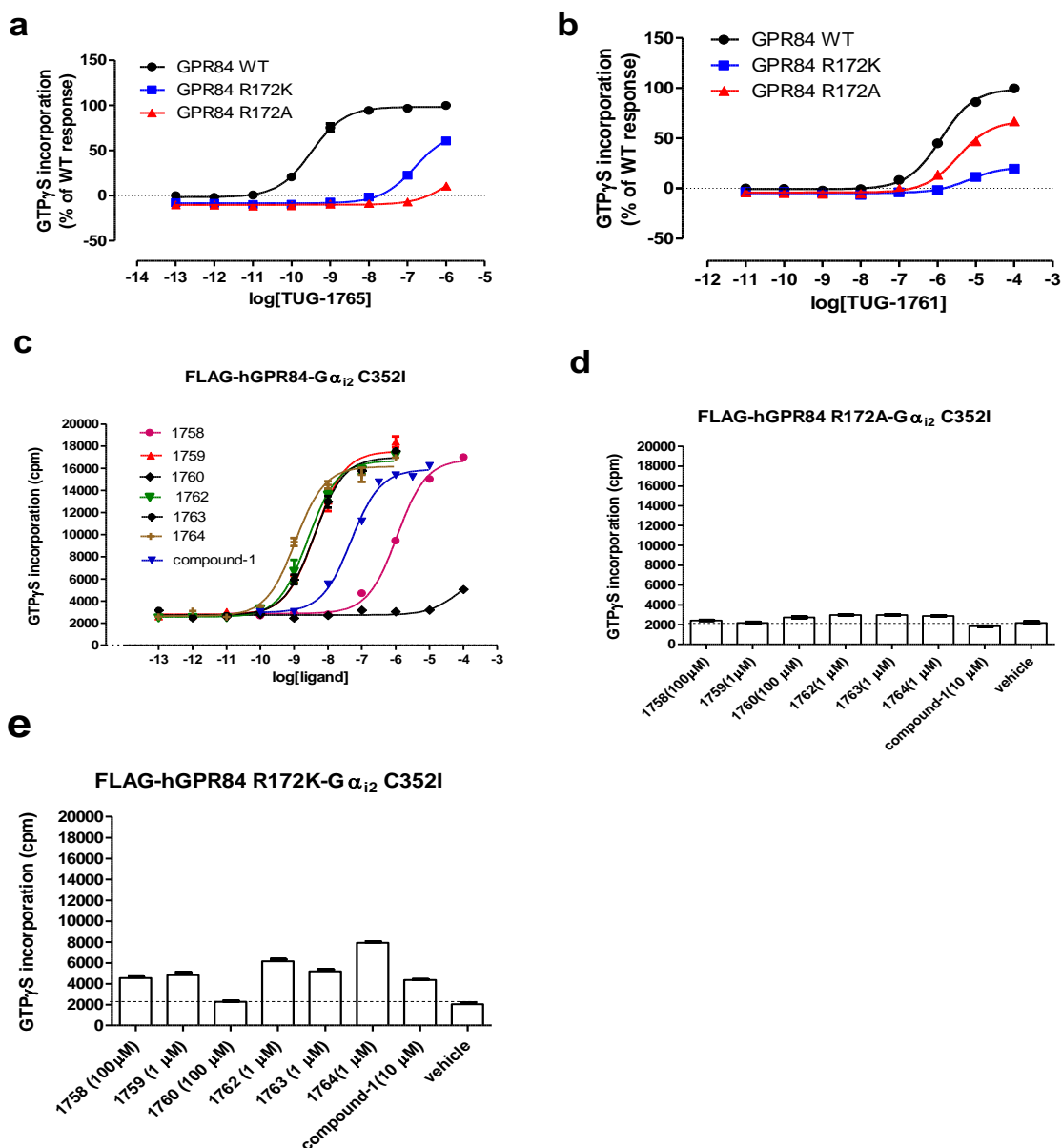


Figure 4.14 A series of compound-1 analogues are orthosteric agonists of human GPR84.

Effect of increasing concentrations of either TUG-1765 (a) or TUG-1761(b) was assessed for their ability to stimulate [35 S]-GTP γ S incorporation into membranes generated from Flp-In T-REx-293 cells induced with 100 ng/ml of doxycycline for 24 hours to express either FLAG-hGPR84-G α_{i2} C352I, FLAG-hGPR84 R172A-G α_{i2} C352I or FLAG-hGPR84 R172K-G α_{i2} C352I. Similar assays were performed to generate concentration-response curves for TUG-1758, 1759, 1760, 1762, 1763, 1764 or compound-1 using membranes expressing the FLAG-hGPR84-G α_{i2} C352I (c). Effects of the mutation of arginine 172 to alanine (d) or lysine (e) on the agonistic activity of either 100 μ M of TUG-1758 and TUG-1760, 1 μ M of TUG-1759, 1762, 1763 and 1764 or 10 μ M of compound-1 were examined by using [35 S]-GTP γ S incorporation assays.

4.3.5. Phenylalanine 335 located in TMD VI might be associated with orthosteric ligand recognition

A set of [35 S]-GTP γ S binding assays were performed to examine the potential role of phenylalanine 335^{6,51} in GPR84 ligand recognition and function. Mutation of phenylalanine 335 to alanine in the context of FLAG-hGPR84-G α_{i2} C352I largely eliminated the activity of decanoic acid, compound-1 and 6-OAU (Figure 4.15, Table 4.3). This mutation resulted in 84% reduction ($P<0.001$) in efficacy for C-10 response compared to the wild type receptor. 6-OAU showed a 38-fold ($P<0.001$) reduction in potency and 73% reduction ($P<0.001$) in efficacy at F335A GPR84. Similarly, the potency of compound-1 was decreased by 110-fold ($P<0.001$) at F335A GPR84. Another notable thing was that the response to embelin was completely abolished by the F335A mutation. This was not the case for either DIM or PSB-16671 as they retained their agonist functions at this mutated version of the receptor. This further supports that DIM and PSB-16671 bind to an allosteric site within GPR84 which is different from the binding site shared by C-10 and embelin. Although DIM showed about 3.5-fold ($P<0.05$) reduction in potency at the F335A variant, the maximum response was not statistically different ($P>0.05$). PSB-16671 displayed some 2.3-fold ($P<0.001$) higher efficacy at this mutant receptor compared to wild type GPR84 whilst potency of PSB-16671 was reduced by 2-fold ($P<0.001$).

The complete loss of activity of embelin allayed to the significant reduction in agonist function of decanoic acid, compound-1 and 6-OAU at F335A GPR84 likely not due to the decreased expression level of this construct in Flp-In T-REx-293 cells as similar expression level of the F335A mutant (Bmax: 5352 \pm 606 fmol/mg protein) was detected compared to the wild type receptor (Bmax: 6538 \pm 267 fmol/mg protein) (Figure 4.10 and Table 4.1). Moreover, membranes containing 50 fmols receptor of each construct were employed in each assay reaction. The full retention of agonist functions of DIM and PSB-16671 at F335A GPR84 indicated that the mutation of phenylalanine to alanine at this position did not produce a variant of the receptor having poor organization and folding.

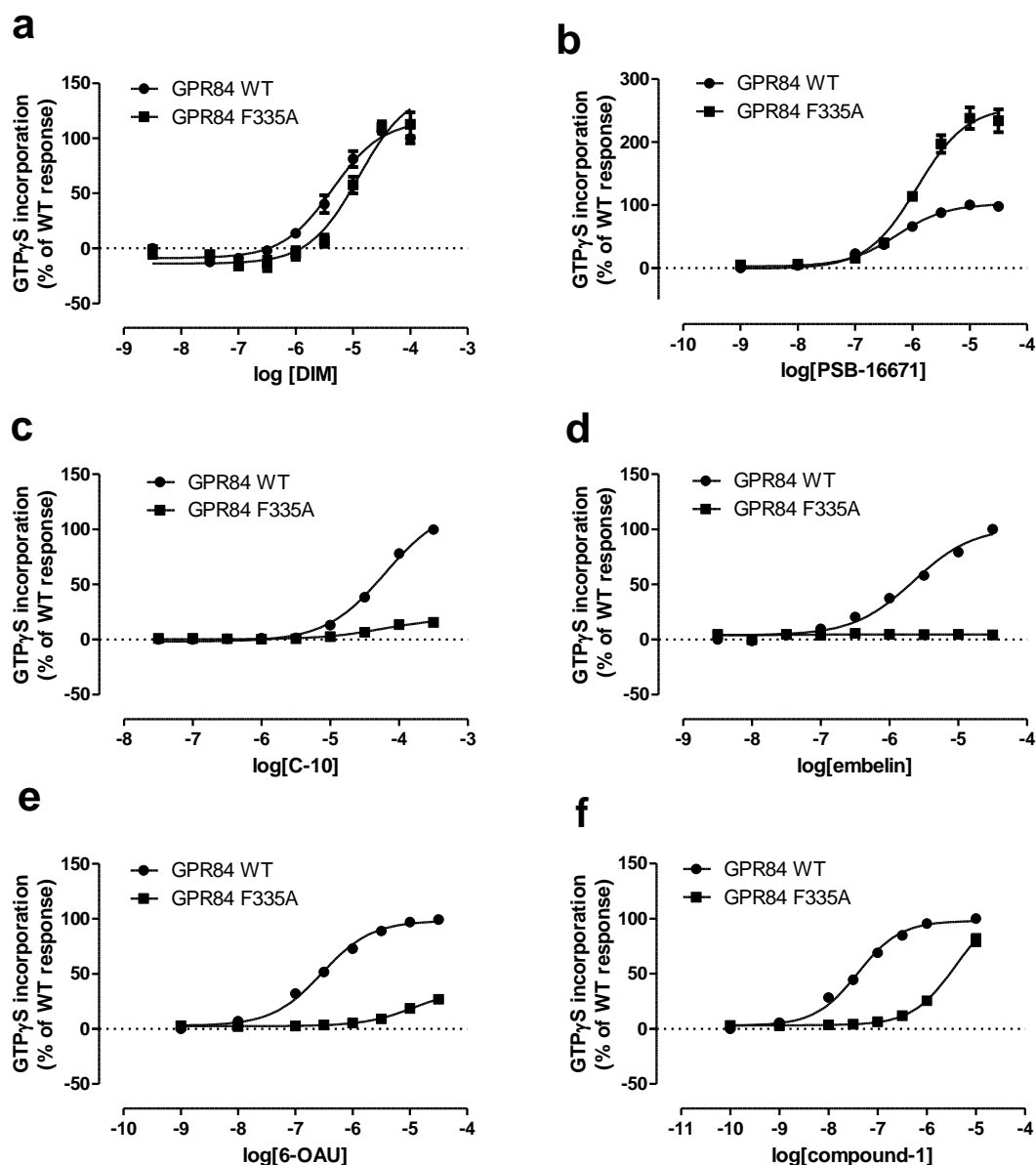


Figure 4.15 Phenylalanine 335 of human GPR84 might be part of the orthosteric ligand binding site. Increasing concentrations of DIM (a), PSB-16671 (b), C-10 (c), embelin (d), 6-OAU (e) or compound-1(f) were assessed for their ability to promote [35 S]-GTP γ S binding to membranes prepared from Flp-InTM T-RExTM-293 cells induced with 100 ng/ml doxycycline for 24 hours to express either FLAG-hGPR84-G α_{i2} C352I or FLAG-hGPR84 F335A-G α_{i2} C352I fusion constructs. Data represent means \pm SEM of combined data collected from 3 independent experiments performed on 3 different membrane preparations.

Table 4-3 Potency and efficacy of GPR84 agonists at wild type and F335^{6,51}A GPR84 in [³⁵S]-GTPγS binding assays.

| Ligand | GPR84 WT-Gα _{i2} C352I | | GPR84 F335A-Gα _{i2} C352I | | |
|------------|---------------------------------|---------------------------------|------------------------------------|--------------------|----------------------------|
| | pEC ₅₀ ±SEM | E _{max} ±SEM (% of WT) | pEC ₅₀ ±SEM | ΔpEC ₅₀ | E _{max} (% of WT) |
| C-10 | 4.3±0.01 | 99.7±0.5 | 4.3±0.05 | 0 | 15.7±2.9*** |
| Embelin | 5.64±0.07 | 100±1 | Inactive | NA | NR |
| Compound-1 | 7.40±0.04 | 100±0.3 | 5.36±0.08*** | -2.04 | 80.4±4.6*** |
| 6-OAU | 6.52±0.08 | 99.4±0.6 | 4.94±0.02*** | -1.58 | 27.0±3*** |
| DIM | 5.27±0.15 | 100±4.3 | 4.73±0.1* | -0.54 | 112.7±10 |
| PSB-16671 | 6.27±0.05 | 97.9±0.8 | 5.93±0.04** | -0.34 | 233±18*** |

A series of [³⁵S]-GTPγS binding experiments were performed to determine the potency (pEC₅₀) and efficacy (E_{max}) of the GPR84 agonists at wild type and F335A GPR84 mutant. Efficacy (E_{max}) is expressed as the percentage of wild type response. NA: not applicable; NR: no response; ΔpEC₅₀ represents mutant pEC₅₀ - wild type pEC₅₀; Analysis of pEC₅₀ and E_{max} values by two-tailed unpaired t-test was done with statistical significance denoted as *P<0.05, **P<0.01, ***P<0.001

4.3.6. Role of Phenylalanine 170 of GPR84 in ligand recognition

To assess the potential role of phenylalanine 170 in ligand recognition or function, effects of alteration of F170 to alanine on the agonistic functions of GPR84 ligands were investigated using [³⁵S]-GTPγS binding assays. Saturation [³H]-G9543 binding studies showed that the expression level of the FLAG-hGPR84 F170A-Gα_{i2} C352I mutant protein (B_{max}: 1419±180 fmol/mg protein) was some 4.6 times lower than that of the wild type receptor (B_{max}: 6538±267 fmol/mg protein) (Figure 4.10 and Table 4.1). To control for the effect of the lowered expression level of the mutant, the receptor density of each membrane preparation was estimated prior to the individual [³⁵S]-GTPγS binding assay and membranes containing 50 fmols of each fusion construct were added to each reaction. Alteration of phenylalanine 170 to alanine resulted in complete ablation of responses to either C-10 or embelin (Figure 4.16a-b). This mutation also significantly (*P*<0.01) reduced the measured potency (6.3-fold reduction) of compound-1 without affecting efficacy (Figure 4.16 d). Similarly, at F170A GPR84, 6-OAU showed a 10-fold (*P*<0.01) decrease in potency and 42.8% reduction in efficacy compared to the wild type receptor (Figure 4.16c; Table 4.4). By contrast, DIM retained its function at F170A mutant displaying a 2-fold (*P*<0.01) higher maximal response compared to the wild type receptor. Though potency of DIM was reduced by 2.8-fold, this variation was not statistically significant. PSB-16671 showed similar potency at the F170A mutant but efficacy was enhanced by 2-fold compared to wild type GPR84.

In such mutational studies, it is important to ensure that lack of or reduced activity of ligands at the mutant receptor is not due to either generation of a protein having improperly folded structure or defective cell surface trafficking (Stoddart et al., 2008a). The maintenance of agonistic functions of DIM and PSB-16671 at F170A GPR84 suggested that the mutant is functional. Moreover, the alanine replacement of the F170 did not result in a large reduction in binding affinity of the radiolabelled antagonist [^3H]-G9543. Though this mutation decreased the binding affinity of the radioligand by 3.7-fold compared to the wild type receptor, the radioligand still bind F170A GPR84 with sub-nM affinity (K_d : 0.93 ± 0.2 nM) (Figure 4.10) suggesting that alanine mutation of F170 did not generate a non-functional protein with improper folding.

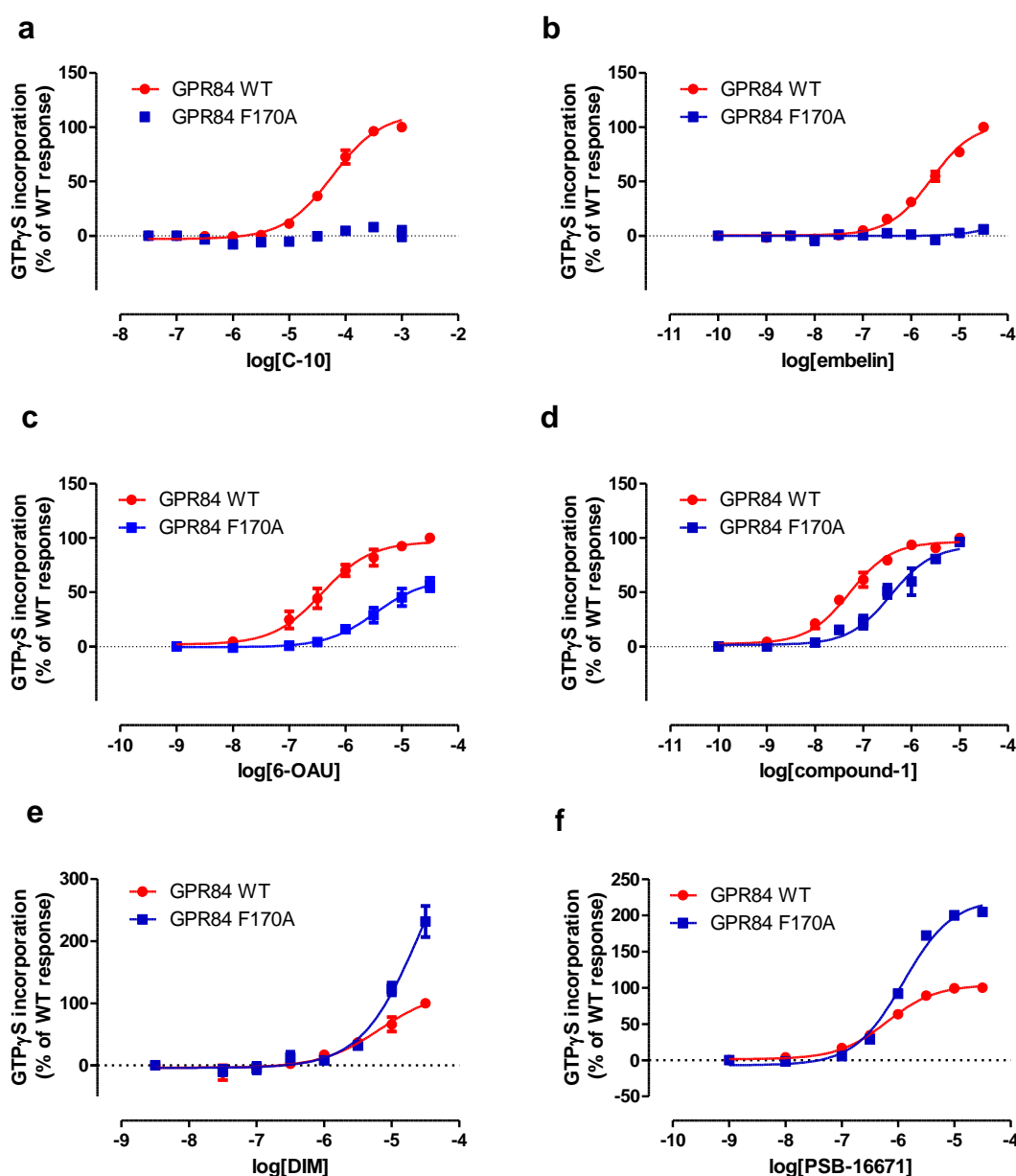


Figure 4.16 The effect of alteration of phenylalanine 170 to alanine on GPR84 ligand recognition. Membranes were generated from Flp-In T-REx-293 cells induced with 100 ng/ml of doxycycline for 24 hours to express either FLAG-hGPR84-G α_{i2} C352I or FLAG-hGPR84 F170A-G α_{i2} C352I. These membranes were then employed in [35 S]-GTP γ S incorporation assays to assess the ability of increasing concentrations of C-10 (a), embelin (b), 6-OAU (c), compound-1(d), DIM (e) or PSB-16671 (f) to promote [35 S]-GTP γ S binding to G α_{i2} G-protein associated with the fusion construct. Data represent mean \pm SEM of three independent experiments (a-e) performed on three different membrane preparations or of a single experiment (f) performed in triplicate.

Table 4-4 Potency and efficacy of GPR84 ligands at wild type and F170A GPR84

| Ligand | GPR84 WT-Gα _{i2} C352I | | GPR84 F170A-Gα _{i2} C352I | | |
|------------|---------------------------------|-----------------------|------------------------------------|--------------------|---------------------------------|
| | pEC ₅₀ ±SEM | E _{max} ±SEM | pEC ₅₀ ±SEM | ΔpEC ₅₀ | E _{max} ±SEM (% of WT) |
| C-10 | 4.2±0.04 | 100±0.9 | Inactive | NA | NR |
| Embelin | 5.52±0.06 | 100±3.9 | Inactive | NA | NR |
| Compound-1 | 7.3±0.1 | 100±6 | 6.5±0.07** | -0.8 | 96.3±1.6 |
| 6-OAU | 6.41±0.15 | 100±5.4 | 5.38±0.08** | -1.03 | 57.2±6.2* |
| DIM | 5.2±0.12 | 100±2.3 | 4.75±0.2 | -0.45 | 231±25** |
| PSB-16671 | 6.2±0.04 | 100±2.86 | 5.9 (n=1) | -0.3 | 204.7 (n=1) |

A series of [³⁵S]-GTPγS binding experiments were performed to determine the potency (pEC₅₀) and efficacy (E_{max}) of the GPR84 agonists at wild type and F170A GPR84 mutant. Efficacy (E_{max}) was expressed as the percentage of wild type response. NA: not applicable; NR: no response; ΔpEC₅₀ represents mutant pEC₅₀ - wild type pEC₅₀; pEC₅₀ and E_{max} values were analysed by two-tailed unpaired t-test with statistical significance represented as *P<0.05, **P<0.01, ***P<0.001

4.3.7. Assessment of effects of mutation of phenylalanine 101 or tryptophan 360 to alanine on agonist functions of different GPR84 ligands

To assess the potential roles of two aromatic amino acid residues, phenylalanine 101^{3,33} and tryptophan 360^{7,43} in the ligand detection or function, [³⁵S]-GTPγS binding assays were performed using membranes generated from Flp-In T-REx-293 cells expressing either FLAG-hGPR84-Gα_{i2} C352I, FLAG-hGPR84 F101A-Gα_{i2} C352I or FLAG-hGPR84 W360A-Gα_{i2} C352I. Alteration of phenylalanine 101 to alanine did not affect the agonistic activity of decanoic acid and compound-1 as they showed similar potency and efficacy at this mutant compared to the wild type receptor (Figure 4.17 a,c and Table 4.5). Similarly, the potency of embelin was unaltered at this mutant receptor. By contrast, 6-OAU showed a 6.3-fold reduction in potency (*P*<0.01) and about 27% decrease in efficacy (*P*<0.05) at the F101A mutant. Though potencies were unaffected, F101A GPR84 exhibited some 2 and 1.6-fold higher maximal responses for DIM and PSB-16671, respectively compared to the wild type receptor (Figure 4.17 e,f). Overall, this aromatic residue is not associated with ligand functions. On the other hand, mutation of tryptophan 360^{7,43} to alanine completely ablated the agonist function of embelin at GPR84 (Figure 4.17b). Though the potency of decanoic acid was enhanced by 2.4-fold (*P*<0.05), the maximum response to decanoic acid was reduced by 67% (*P*<0.001) at W360A GPR84 compared to the wild type receptor. Similarly, maximum responses to compound-1 and 6-OAU were reduced significantly (*P*<0.05) by 65% and 72%, respectively due to the alteration of tryptophan 360 to alanine. The potencies of compound-1 and 6-OAU were also decreased by 3.5-fold (*P*<0.001) and 5.6-fold (*P*<0.01), respectively. By contrast, DIM maintained

its function at W360A GPR84 displaying similar efficacy and 2.3-fold higher potency than that displayed at the wild type receptor. Though the potency of PSB-16671 was enhanced by 3.5-fold ($P<0.01$), the efficacy was reduced significantly by about 33.8% compared to wild type GPR84.

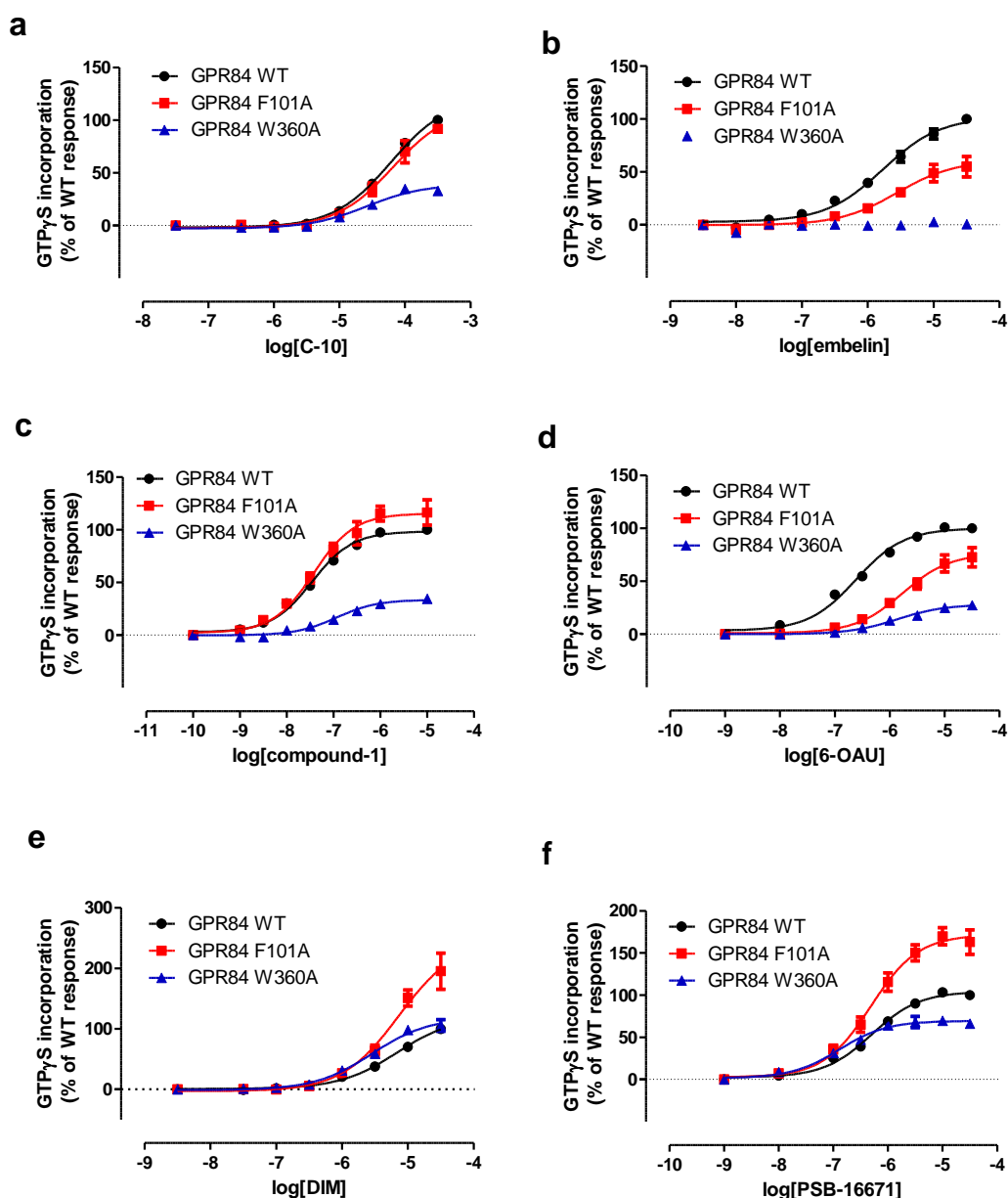


Figure 4.17 Effects of mutation of either F101 or W360 to alanine on GPR84 ligand functions.

Flp-In T-REx-293 cells harbouring either FLAG-hGPR84-G α_{i2} C352I, FLAG-hGPR84 F101A-G α_{i2} C352I or FLAG-hGPR84 W360A-G α_{i2} C352I were induced with 100 ng/ml of doxycycline for 24 hours prior to membrane preparation. These membranes were then used in [35 S]-GTP γ S incorporation assays to measure the activity of C-10 (a), embelin (b), compound-1 (c), 6-OAU (d), DIM (e) or PSB-16671 (f). Data represent mean \pm SEM of three independent experiments performed on three individual membrane preparations.

Table 4-5 Potency and efficacy of GPR84 agonists at wild type, F101A and W360A GPR84 in [³⁵S]-GTPγS binding assays

| Ligand | GPR84 WT | GPR84 F101A | | | GPR84 W360A | | |
|----------------------|-------------------|-------------------|--------------------|------------------|-------------------|--------------------|------------------|
| | pEC ₅₀ | pEC ₅₀ | ΔpEC ₅₀ | E _{max} | pEC ₅₀ | ΔpEC ₅₀ | E _{max} |
| C-10 | 4.22±0.02 | 4.14±0.15 | -0.08 | 91.7±3.7 | 4.60±0.04* | 0.38 | 33±3.7*** |
| Embelin ^a | 5.72±0.07 | 5.44±0.05* | -0.4 | 58±6.2*** | NA | NA | NR |
| Compound-1 | 7.46±0.06 | 7.40±0.03 | -0.28 | 119±7.4 | 6.91±0.07*** | -0.55 | 34.6±2.9*** |
| 6-OAU | 6.60±0.05 | 5.80±0.03** | -0.8 | 72.7±9.0* | 5.85±0.09** | -0.75 | 27.5±1.9*** |
| DIM | 5.20±0.07 | 5.14±0.07 | -0.06 | 195±30** | 5.56±0.06* | 0.36 | 106±9.5 |
| PSB-16671 | 6.35±0.04 | 6.31±0.03 | -0.04 | 163±14.5** | 6.90±0.05** | 0.55 | 66.2±2.2* |

A series of [³⁵S]-GTPγS binding experiments were performed to determine the potency (pEC₅₀) and efficacy (E_{max}) of various GPR84 agonists at wild type, F101A GPR84 and W360A GPR84 mutants and data are represented as mean±SEM of three independent experiments performed on three separate membrane preparations; NA: not applicable; NR: no response; Efficacy (E_{max}) is expressed as the percentage of wild type response. ΔpEC₅₀ represents mutant pEC₅₀– wild type pEC₅₀; pEC₅₀ and E_{max} values were analysed by one-way analysis of variance (ANOVA) followed by Tukey's multiple comparison tests with statistical significance denoted as *P<0.05, **P<0.01, ***P<0.001; ^aAnalysis of pEC₅₀ and E_{max} values for embelin was done by unpaired two-tailed t-test.

The complete elimination of agonistic action of embelin or highly reduced activity of decanoic acid, compound-1 and 6-OAU at the W360A GPR84 might be either due to loss of/lower expression of the mutant or it truly reflects the role of the amino acid in the orthosteric ligand detection. To assess whether loss of function/reduced activity of tested ligands at W360A mutant is not merely a reflection of the loss of expression of the mutant, the relative expression levels of the mutant and wild type receptor need to be estimated. The saturation binding study revealed that the radiolabelled antagonist [³H]-G9543 lost its ability to bind W360A GPR84 (Figure 4.10b) indicating either loss of expression of the mutant or change in protein structure/conformation. However, the complete retention of the agonist function of DIM at this mutant suggested that the mutant receptor was expressed effectively. As embelin activates human GPR84 with greater efficacy than DIM, the complete abolition of activity of embelin at W360A mutant whereas DIM maintained its ability to activate the receptor suggested that tryptophan 360 might be associated with embelin recognition by the receptor.

4.3.8. Potential docking poses of orthosteric agonists

Based on the mutagenesis studies described in this chapter, preliminary docking studies of GPR84 orthosteric agonists to the constructed homology model were performed. These studies showed that the binding site for decanoic acid, embelin and embelin-like ligands (6-OAU and compound-1) is likely to be at the centre of the pocket created by transmembrane helices 2, 3, 6 and 7. Docking of embelin to the homology model suggested that one carbonyl oxygen and another hydroxyl oxygen atom of the 2, 5-dihydroxy-1, 4-benzoquinone core of embelin are involved in hydrogen bonding/salt bridges with arginine 172 (Figure 4.18). This is fully consistent with the finding that embelin entirely lost ability to activate hGPR84 upon mutation of arginine 172 to either alanine or lysine. Asparagine 339 and tyrosine 81 were also predicted to form hydrogen bonds with the carbonyl oxygen of the head group of embelin. This predicted role of these two residues needs to be confirmed by further mutational analysis. Phenylalanine 170 of EL2 stabilizes arginine 172 by forming a cation- π interaction which is in agreement with the finding that R172K was not responsive to embelin and the fact that embelin lost its function at F170A GPR84. Phenylalanine 335 and tryptophan 360 might be involved in hydrophobic interactions with either the aromatic ring or aliphatic side chain of embelin. These supplemental roles of phenylalanine 335 and tryptophan 360 in the binding of embelin were evident from the mutagenesis studies wherein embelin was found to be completely inactive at both F335A and W360A mutants. These two residues might be important for the formation of the shape of the binding pocket. Leucine 100 seems to be involved in hydrophobic interactions with the aromatic ring and/or aliphatic side chain of embelin which again needs to be validated by further mutational analysis.

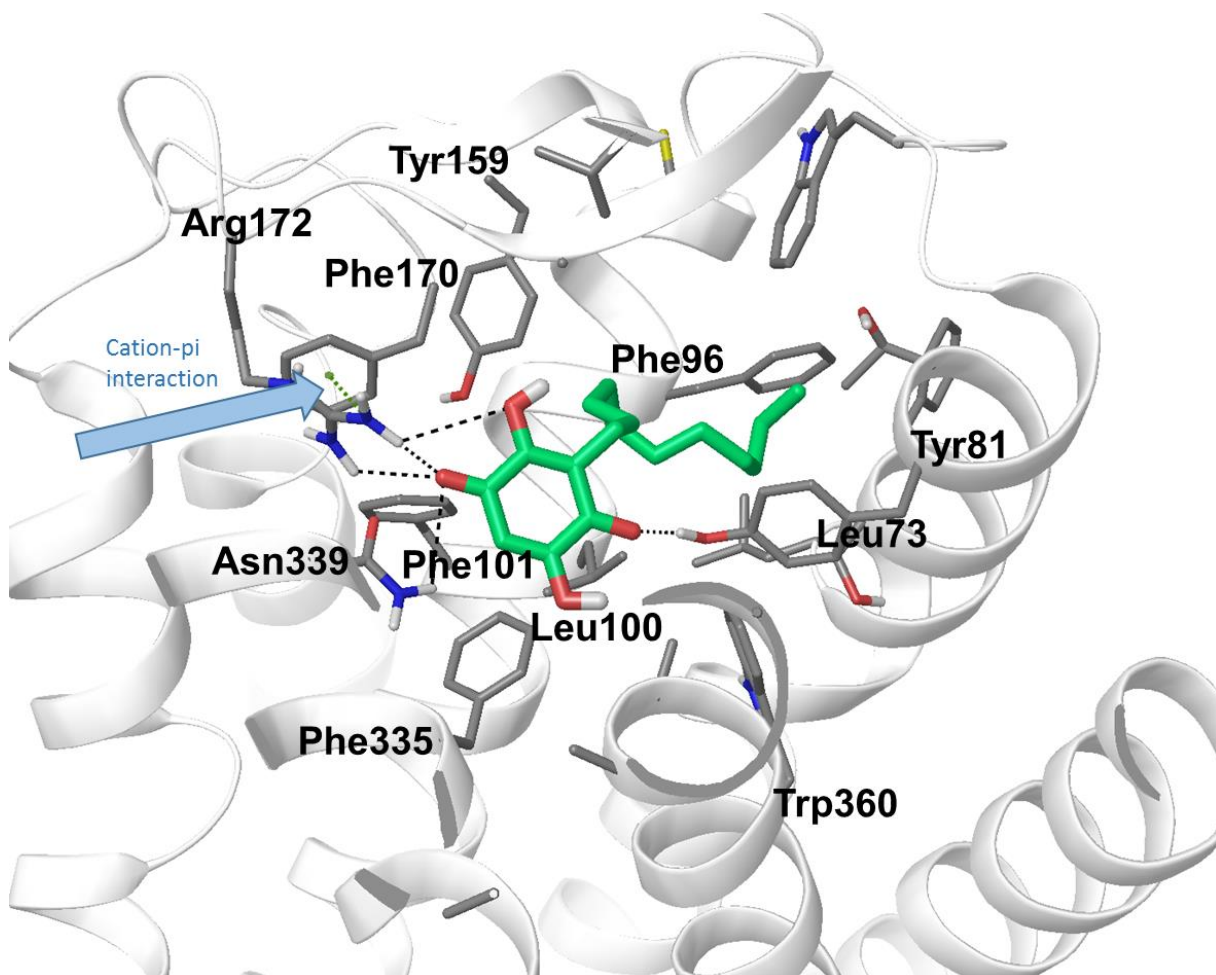


Figure 4.18 The putative binding mode of embelin in GPR84. A potential docking pose of embelin is shown. The polar head group 2, 5-dihydroxy-1, 4-benzoquinone is coordinated by arginine 172, asparagine 339 and tyrosine 81. The anchoring role of arginine 172 is in full agreement with the findings from the mutational analysis while the role of the other two residues needs to be validated. Hydrogen bonds or salt bridges are shown in dotted black lines while the cation- π interaction between F170 and R172 is depicted as a green dotted line. This figure was generated by Dr. Irina G. Tikhonova as part of collaborative work.

The docking poses of 6-OAU and compound-1 (Figure 4.19 and 4.20) are very similar to that of embelin. In both cases, one carbonyl oxygen atom of the pyrimidinedione core is coordinated by arginine 172 of EL2 which is entirely consistent with the complete ablation of agonistic functions of both ligands at R172A GPR84 and another oxygen atom is supposed to be involved in hydrogen bonding with asparagine 339. Similar to the case of embelin binding, phenylalanine 170 of EL2 is implicated in stabilizing arginine 172 by forming a cation- π interaction while phenylalanine 335 and tryptophan 360 seem to be associated with hydrophobic interactions with the heterocyclic ring or the aliphatic side chain of both 6-OAU and compound-1. These putative roles of phenylalanine 170 and 335 in the recognition of both ligands were in agreement with the significant reduction in potency of 6-OAU and compound-1 due to the

alanine replacement of either F170 or F335. Docking studies also predicted that the aliphatic amino acid leucine 100 might be important for the detection of 6-OAU and compound-1 by forming hydrophobic interaction with the heterocyclic ring or the hydrophobic tail of these ligands. To fully understand the binding modes of these embelin-like ligands, further mutational analysis with N339, Y81, L100, L73, and F96 are suggested.

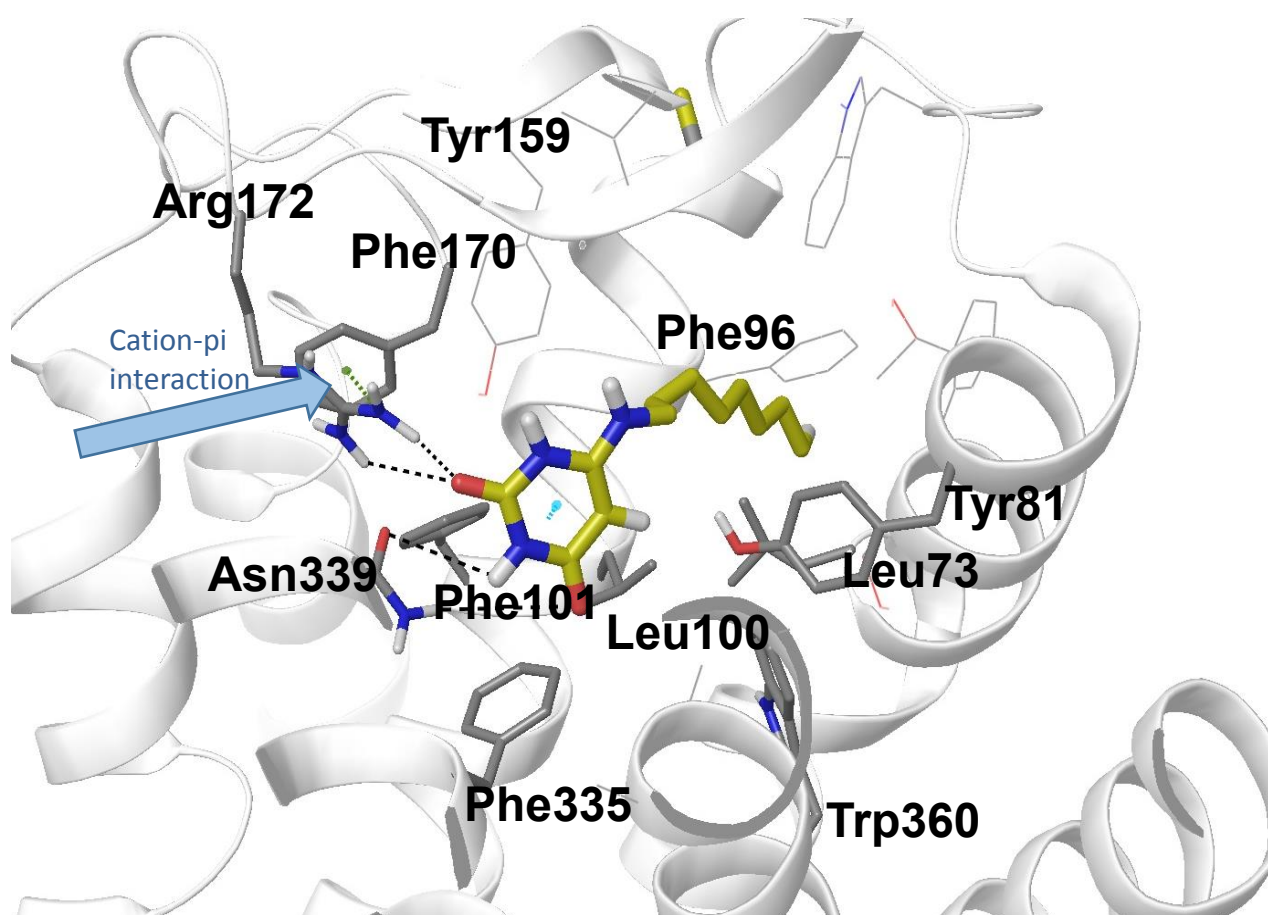


Figure 4.19 A potential docking pose of 6-OAU within GPR84.

Arginine 172 and asparagine 339 are involved in hydrogen bonding/salt bridges with the pyrimidinedione polar head group while the aliphatic hydrophobic tail is likely to be located in the inter-helical gap. Salt bridges/hydrogen bonds are depicted as black dotted lines while the dotted green line represents the cation-pi interaction between R172 and F170. This figure was from Dr. Irina G. Tikhonova as part of collaborative work.

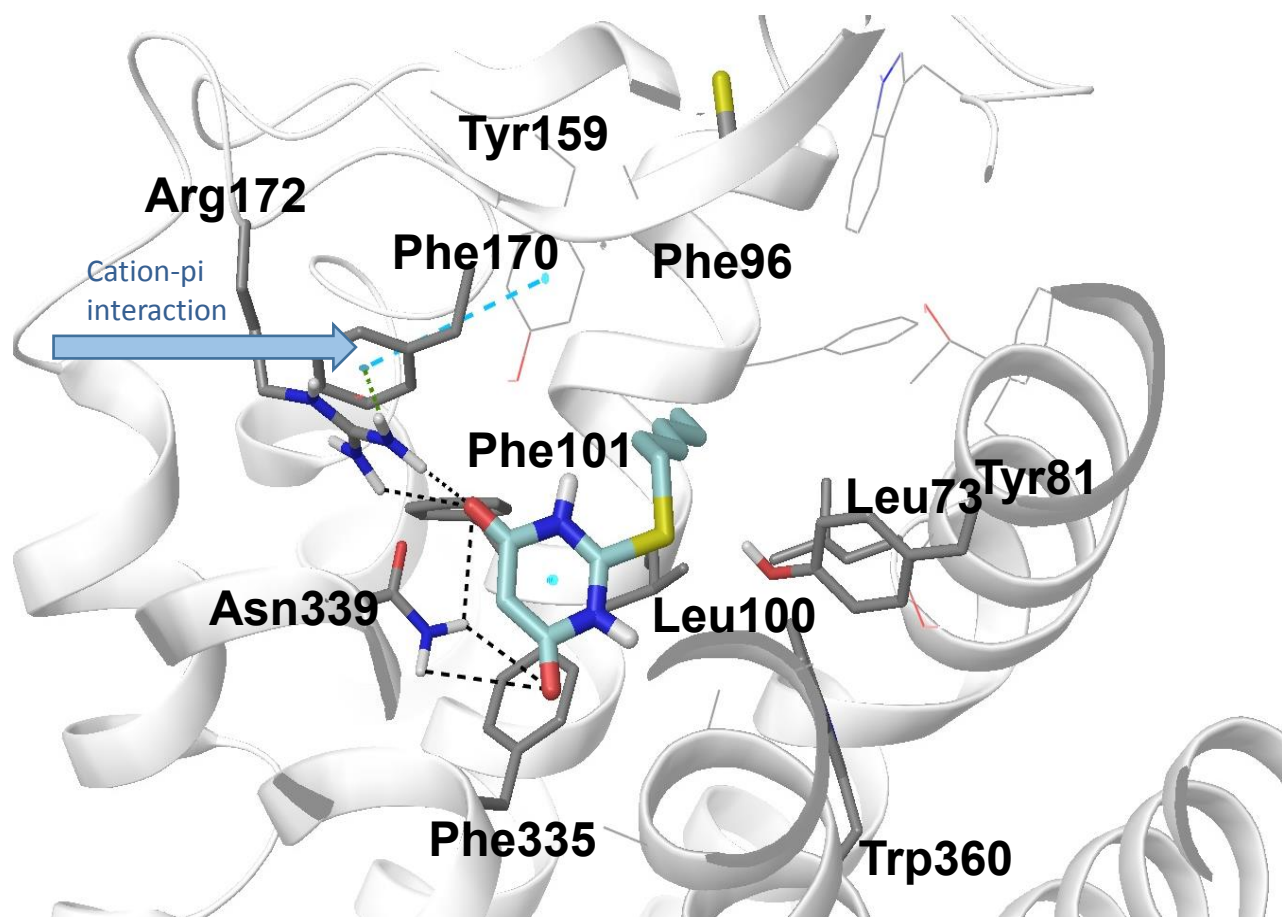


Figure 4.20 A putative binding mode of compound-1 within GPR84.

Compound-1 is likely located at the cavity involving transmembrane helices 2, 3, 6 and 7. The pyrimidinedione core structure is anchored at the centre of the binding pocket by arginine 172. Hydrogen bonds or salt bridges are represented by black dotted lines while the cation- π interaction between arginine 172 and phenylalanine 170 is shown as dotted green line. This figure was generated by Dr. Irina G. Tikhonova as part of collaborative work.

4.3.9. GPR84 antagonist compound-107 binds to a site on GPR84 which is topographically distinct from the orthosteric and allosteric agonist binding sites

Labeguere et al., (2014) reported a novel class of GPR84 antagonists containing dihydropyrimidinoisoquinolinones as the core chemical structure. Although this class of GPR84 antagonists have been considered to have potential therapeutic activity for the treatment of chronic inflammatory diseases including ulcerative colitis and inflammatory bowel diseases (Dupont et al., 2015; Vermeire et al., 2017), their modes of binding to GPR84 is still unexplored. Among this series of GPR84 antagonists, compound-104, 107 and 161 (chemical structures are shown in Table 1.4) were reported to concentration-dependently inhibit [35 S]-GTP γ S binding induced by EC₈₀ concentrations of either C-10, embelin or DIM in a non-

competitive manner (Mahmud et al., 2017) suggesting that these compounds did not bind to either the orthosteric site shared by decanoic acid and embelin or the allosteric site occupied by DIM. Saturation binding studies using the radiolabelled antagonist [^3H]-G9543, which is an analogue of compound 104, 107 and 161, revealed that the radioligand retained its ability to bind R172A GPR84- $\text{G}\alpha_{i2}$ C352I and R172K GPR84- $\text{G}\alpha_{i2}$ C352I with similar affinity (Figure 4.10 b, c) compared to the wild type receptor, indicating that this radioligand and the related compound 107 binds to a site within GPR84 which is distinct from the orthosteric binding site. Compound-107 also does not bind the allosteric site occupied by DIM, which is evident from the fact that the potency of compound-107 to block DIM stimulated [^{35}S]-GTP γ S incorporation was very similar at hGPR84 R172A- $\text{G}\alpha_{i2}$ C352I mutant (pEC_{50} : 8.05 ± 0.07) to that of WT version of the receptor (pEC_{50} : 7.97 ± 0.03) (Figure 4.21).

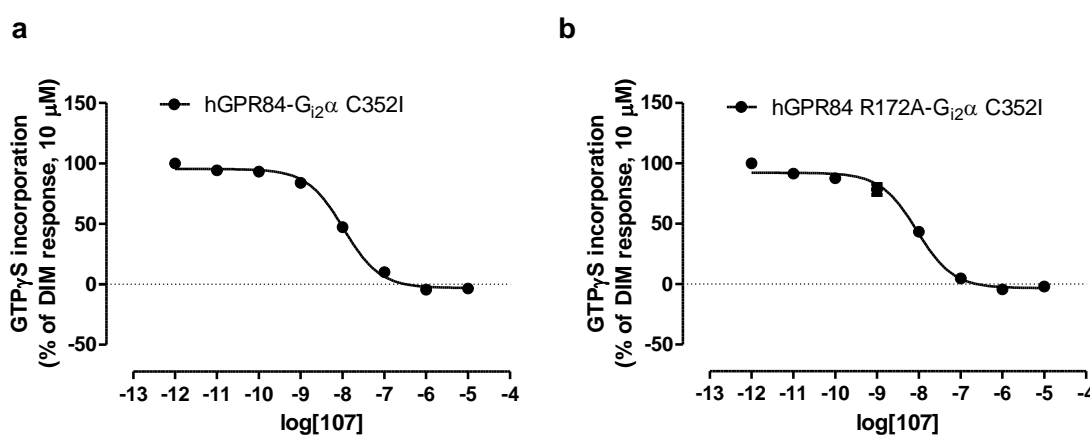


Figure 4.21 GPR84 antagonist compound-107 does not bind to the orthosteric or allosteric agonist sites within GPR84. Increasing concentrations of compound-107 were assessed for their ability to inhibit DIM-stimulated [^{35}S]-GTP γ S incorporation into membranes generated from Flp-In T-REx-293 cells induced with 100 ng/ml of doxycycline for 24 hours to express either FLAG-hGPR84- $\text{G}\alpha_{i2}$ C352I (a) or FLAG-hGPR84 R172A- $\text{G}\alpha_{i2}$ C352I (b). Data represent mean \pm S.E.M of three independent experiments performed in triplicate.

4.4. Discussion

The [35 S]-GTP γ S binding assay was employed for the characterization of pharmacological tool compounds of GPR84 as this assay is recognized to be a suitable functional assay system for measuring pharmacological parameters of $G\alpha_i$ -coupled receptors (Harrison and Traynor, 2003; Strange, 2010). The suitability of this assay for $G\alpha_i$ -coupled receptors over other G protein-coupled receptors (such as G_s -coupled and G_q -coupled receptors) stems from the fact that higher signalling window could be obtained for $G\alpha_i$ -coupled receptors owing to significantly higher expression level of $G\alpha_i$ protein in any cells/tissues as well as higher rate of exchange of guanine nucleotides at $G\alpha_i$ (Milligan, 2003; Harrison and Traynor, 2003; Strange, 2010). This assay is also appreciated to be more useful to measure relative efficacy of ligands as there would be less receptor reserve for G protein activation which is not subject to signalling amplification or other modulatory effects compared to other assays which target downstream signalling pathway such as inhibition of adenylyl cyclase (Umland et al., 2001; Engström et al., 2005; Strange, 2010).

For the study of the pharmacology of GPR84 ligands and mutational analysis, I have employed a GPR84- $G\alpha$ fusion protein approach as it is well appreciated that such a fusion protein strategy generates higher signalling window due to the enhanced coupling efficiency of GPCR and G protein interaction (see section 3.3.1). As expected, in the case of GPR84, the signalling magnitude generated by the fusion protein was 5-10 fold higher compared to that produced by eYFP-tagged GPR84 although potencies of agonists were reduced significantly compared to the other system. For example, the potency of both decanoic acid and DIM estimated at GPR84- $G\alpha_{i2}$ fusion protein was 10-fold lower than those reported by Wang et al., (2006b) measured using a FLAG-tagged GPR84. Compound-1 also displayed 30-fold decreased potency at the fusion protein compared to that showed at FLAG-hGPR84-eYFP. The 1:1 stoichiometry between GPCR and G protein in the fusion protein, which significantly increases the rate and extent of G protein coupling leading to enhanced signalling magnitude, at the same time, is responsible for reduced potency of ligands as it correlates the fraction of G protein recruitment directly to the ligand binding affinity to the receptor. So, in the GPCR-G protein fusion protein approach, the amount of interacting G protein is directly proportional to the fraction of activated

receptor which is ultimately governed by the affinity of the ligand to the receptor, implying that the functional outcome of G protein activation herein will be related to receptor occupancy. By contrast, in other systems the functional response may or may not be directly proportional to the receptor occupancy depending on the relative abundance of endogenous G proteins compared to the expressed receptor and thus there might be generation of receptor reserve.

4.4.1. Arginine 172 of EL2 is integral to orthosteric ligand recognition and functions

Though the development of crystal structures of a GPCR complexed with specific ligands is required to get accurate molecular insight into GPCR-ligand interactions, X-ray crystallography of GPCRs, especially for non-rhodopsin Class A family proteins, remains challenging and time-consuming (Kobilka and Schertler, 2008). Due to the presence of low % of polar amino acid residues compared to the largely dominant hydrophobic amino acids of the GPCR, it is always troublesome to solubilize these membrane proteins compared to the other non-membrane proteins. More importantly, the flexible and dynamic nature of the GPCR protein structure leads to exceptional instability and heterogeneity in terms of conformation, making it very difficult to get a stable conformational state of the protein for accurate crystallogenesi s (Peeters et al., 2011; Kobilka and Schertler, 2008). Due to these challenges in crystallography of GPCRs, generation of atomic-level structures of GPCRs is slow and until now crystal structures of only 43 GPCRs are available (Isberg et al., 2016), among them 25 are of rhodopsin-like Class A family. With unavailability of experimental structural information, homology modelling of a GPCR along with site-directed mutagenesis is still widely recognized to be a suitable technique for unravelling the mode of binding of ligands to a GPCR of interest (Nikaido et al., 2015; Costanzi, 2013; Costanzi, 2010; Tikhonova et al., 2007). As no crystal structure of GPR84 is available, we have applied homology modelling and site-directed mutagenesis to investigate potential binding modes of medium chain fatty acids and other orthosteric agonists. To construct an accurate homology model for any GPCR, choosing the appropriate template is crucial and this will ultimately depend on the availability of the crystal structure of other GPCRs having at least 30% sequence identity with the target GPCR (Baker and Sali, 2001; Tikhonova,

2017). For homology modelling, Nikaido et al., (2015) used the crystal structure of G-protein bound human β_2 -adrenergic receptor as the template although this shares only 20% of sequence identity with GPR84. Due to this low level of sequence conservation between the template and GPR84, this model structure of GPR84 was unable to implicate any arginine or other positively charged amino acid residue in anchoring the carboxylate function of MCFAs (Tikhonova, 2017). Stitham et al., (2003) identified Arginine-279, located in the transmembrane domain VII of the human prostacyclin receptor, as the charge partner for the carboxyl group of prostacyclin and related ligands. As it was reported that GPR84 belongs to the prostanoid receptor subfamily (Tikhonova, 2017), a similar positively charged amino acid moiety within GPR84 was expected to be involved in the ionic interaction with the carboxylate of medium chain fatty acids. More importantly, as four free fatty acid sensing receptors (FFA1-4) contain at least one arginine residue which is involved in electrostatic interaction with the carboxylate of fatty acids, a similar arginine residue within GPR84 might coordinate the carboxylate function of MCFAs. As part of a collaborative study Tikhonova (2017) developed a homology model of GPR84 using a hybrid template comprising the transmembrane architecture of crystal structure of human orexin 1 receptor (33% sequence homology with GPR84) and the 2nd extracellular loop from the crystal structure of rhodopsin (shares 43% sequence identity with EL2 of GPR84). This homology model predicted that arginine 172, located within the 2nd extracellular loop of GPR84, is the putative charge partner for the carboxylic acid group of decanoic acid. This prediction was then confirmed by mutagenesis as removal of this arginine, even with maintenance of the positive charge, completely eliminated the function of decanoic acid, embelin, compound-1 and 6-OAU, but not of DIM or PSB-16671. These results indicated that arginine 172 is integral to detection of orthosteric agonist ligands by human GPR84, whilst DIM (and analogues) binds to an allosteric site on GPR84 that is topographically distinct from the orthosteric binding site. As for decanoic acid, arginine 172 was also found to coordinate the hydrophilic head group of embelin and embelin-like compounds such as 6-OAU, compound-1 and compound-1765 indicating that these polar head groups are acting as bioisosteres of the carboxylate function of MCFAs. The complete loss of agonistic activity of decanoic acid, embelin and compound-1 and greatly reduced activity of 6-OAU at the R172K mutant demonstrated that arginine 172 could not be replaced by lysine. The homology

model predicted that arginine 172 coordinates phenylalanine 170 and asparagine 339 as well as likely forms contacts with other aromatic residues like tryptophan 360, and thereby plays a critical role in organizing the binding pocket for orthosteric ligands. This tendency of arginine to form multiple contacts with nearby aromatic residues is due to the presence of the guanidinium moiety which has the potential for forming multiple hydrogen bonds/salt bridges. Although lysine retains the positive charge of arginine, the size, shape and location of the charge are different from that of guanidine group and thus is unable to form multiple hydrogen bonds. So it is impossible for lysine to make as many interactions with other amino acid residues and thus cannot organize and stabilize the binding cavity as arginine does.

4.4.2. Phenylalanine 170 and 335 might be associated with ligand recognition

The homology modelling followed by mutational analysis also suggested that another two residues phenylalanine 170 of EL2 and phenylalanine 335 of transmembrane helix VI might play supplemental roles in ligand recognition by human GPR84. Though phenylalanine 170 is not directly involved in the detection of orthosteric agonists, the homology modelling and docking studies showed that F170 is involved in cation- π interaction with nearby arginine 172 and thus plays an important role for the stabilization of this residue. As arginine 172 is critical for ligand interaction and function (section 4.3.2), phenylalanine 170 might have a contribution in the ligand binding or function by stabilizing arginine 172. The importance of this cation- π interaction was supported by the fact that alteration of arginine 172 to lysine completely ablated responses to orthosteric agonists. The indirect role of phenylalanine 170 in the orthosteric ligand binding mode is consistent with mutagenesis studies wherein decanoic acid and embelin completely lost their agonistic functions and 6-OAU and compound-1 displayed 10 and 6.3-fold reduction in potency, respectively upon mutation of F170 to alanine. The role of amino acid residues of EL2 in the stabilization of the arginine residue which coordinates the carboxylate function of fatty acid was also observed in the case of FFA1. Tikhonova and co-workers (2007) identified an electrostatic interaction between glutamate 172 of EL2 and arginine 258^{7,35} and suggested that this interaction was important for ligand

function as evidenced from the 100-fold reduction in potency of synthetic agonist GW9508 at a R258K FFA1 mutant.

The role of EL2 of GPR84 in ligand recognition and function is not unusual as similar roles of EL2 of other GPCR have been reported by several groups (for review see Peeters et al., 2011). For example, amino acid residues, located within EL2 have been implicated in ligand binding to prostanoid receptors, including the thromboxane A2 receptor (So et al., 2003; Ruan et al., 2004) and the prostacyclin receptor (Ni et al., 2008).

The generated homology model of GPR84 also suggested that phenylalanine 335 might play an important role in the detection of ligands by forming hydrophobic interactions with either aromatic/heterocyclic ring of embelin and embelin-like ligands or the aliphatic chain of the free fatty acids. This putative role of phenylalanine 335 in ligand binding was supported by the fact that embelin was found to be totally inactive and decanoic acid displayed markedly reduced activity at the F335A mutant while 6-OAU and compound-1 showed significantly lowered potency (38 and 110-fold reduction in potency, respectively) compared to the wild type receptor. Docking studies using the constructed homology model of GPR84 also showed that tryptophan 360 is likely to be involved in hydrophobic interactions with the aromatic rings or aliphatic side chains of orthosteric agonists and stabilizes the network of interactions within the receptor. Though alteration of tryptophan 360 to alanine resulted in reduction in agonistic functions of orthosteric agonists, it was not clear whether these reduced activities were due to the lowered expression level of the mutant protein or were just reflection of the effects of mutation on protein folding and/or organization. Further work is necessary to solve these issues.

Overall, the putative binding site of orthosteric agonists within GPR84 is quite different from the other four fatty acid sensing receptors (FFA1-4). The 2nd extracellular loop of GPR84 plays the critical role in ligand binding and activation of GPR84 which is not the case for FFA1-4 receptors wherein conserved arginine residue(s) located at 5.39 and 7.35 position of TMD V and VII, respectively (FFA1-3) or at the 2.64 position of TMD II (For FFA4) are vital for ligand recognition. Though recently Srivastava and co-workers (2014) confirmed that glutamate 172 of EL2 of FFA1 is involved in recognition of the agonist by

forming a hydrogen bond with arginine 258, this role of EL2 in the ligand binding mode to FFA1 is supplemental to the anchoring role of arginine 258 and arginine 183. Another important difference is that the putative orthosteric binding site in GPR84 contains less aliphatic amino acid residues compared to other free fatty acid receptors. As GPR84 is quite different from other free fatty acid receptors in terms of sequence identity, these differences in ligand binding mode are not surprising.

4.4.3. Mutational analysis and functional studies suggested multiple distinct binding sites on human GPR84

Mutational analysis and docking of the ligands against the constructed homology model of GPR84 suggested that embelin, 6-OAU, compound-1 and compound-1 analogues, including TUG-1765, are orthosteric to decanoic acid while DIM and PSB-16671 bind to an allosteric site within human GPR84. Saturation binding studies using the radiotracer [³H]-G9543 also suggested that GPR84 antagonist compound-107 and related molecules do not bind the orthosteric binding site as it maintained the ability to bind R172A and R172K GPR84 mutants affording similar binding affinity compared to the wild type receptor. Noticeably, compound-107 also did not bind to the allosteric site shared by DIM as it displayed similar potency at R172A GPR84 mutant to inhibit the DIM-induced [³⁵S]-GTPγS binding to membranes compared to that exhibited at wild type receptor. These studies suggested three distinct binding sites within human GPR84. The presence of multiple binding sites on a GPCR is not uncommon. Srivastava et al., (2014) reported three presumed distinct binding sites on FFA1 which was evident from the crystal structure of FFA1 complexed with the partial agonist, TAK-875. The atomic-level crystal structure of FFA1 complexed with both partial agonist MK-8666 and ago-PAM AP8 also confirmed the presence of separate binding sites for the partial agonist and allosteric ligand within FFA1 (Lu et al., 2017). Based on the findings from several functional assays in conjunction with the homology modelling of FFA2 developed using the crystal structure of β₂-adrenergic receptor as the template Lee et al., (2008) also suggested that positive allosteric modulators and endogenous agonist short-chain fatty acids bind to non-overlapping distinct sites within FFA2. Similarly, functional studies together with mutational analysis revealed the possibility of

the presence of multiple binding sites for allosteric activators and short-chain fatty acids within FFA2 (Bolognini et al., 2016) and FFA3 (Hudson et al., 2014a).

5 Defining the orthologue selectivity of GPR84 ligands

5.1. Introduction

Ligands of a GPCR might display variations in pharmacology and functions among different orthologues. Investigation of this orthologue selectivity is important for the elucidation of physiological functions of orphan or enigmatic G-protein coupled receptors (Milligan, 2018; Jenkins et al., 2012). For example, although antagonist GLPG0974 and CATPB showed high affinity at human FFA2 and thus effectively inhibited short chain fatty acid-mediated responses in transfected cells expressing human FFA2 or in human-derived cells, they have been reported to be inactive at the mouse orthologue (Milligan, 2018; Sergeev et al., 2016; Pizzonero et al., 2014; Hudson et al., 2013a) which hindered the investigation of the patho-physiological role(s) of this therapeutically important drug target. Similarly, antagonists of GPR35 were shown to display species-selective pharmacology. While the antagonists CID-2745687 and ML-145 have been shown to effectively block agonist functions at human GPR35 with high potency, they were found to be inactive to antagonize the agonist effects of zaprinast or cromolyn disodium in Flp-In T-REx cells expressing rat or mouse GPR35 (Jenkins et al., 2012). Similar to FFA2 receptors, the study of the biological functions or patho-physiological roles of GPR35 remains challenging due to this reported inactivity of certain antagonists at mouse or rat orthologues. Defining the orthologue selectivity of a specific GPCR having potential therapeutic activity is also important for drug discovery programmes (Strasser et al., 2013) as murine animal models are routinely used for this purpose. The variation in the pharmacology of the potential small-molecule drugs among human and rodent orthologues needs to be explored before initiating the target validation processes performed in rodent models of human diseases.

There is 85% sequence conservation between human and mouse GPR84 (Wang et al., 2006b; Gaidarov et al., 2018) and thus mouse GPR84 is considered to be the true orthologue of human GPR84. Though mouse GPR84 was reported to respond to medium chain fatty acids (Wang et al., 2006b) and to embelin and embelin derivatives (Gaidarov et al., 2018) in a manner similar to that of human GPR84, studies with other agonists or antagonists of GPR84 to define potential species-

selective pharmacology are lacking. To explore the orthologue selectivity of GPR84 ligands, FLAG-mGPR84-eYFP, FLAG-mGPR84-G α_{i2} and FLAG-mGPR84-G α_{i2} C352I fusion constructs were generated. This chapter aimed at

- i) Defining the orthologue selectivity of GPR84 agonists and antagonists by employing both eYFP-tagged human and mouse GPR84 as well as the fusion protein approach of human and mouse GPR84
- ii) Exploring the pharmacology of GPR84 ligands in a RAW264.7 cell line which is widely used as a murine immune cell model

5.2. Characterization of cell lines expressing FLAG-mGPR84-G α_{i2} , FLAG-mGPR84-G α_{i2} C352I or FLAG-mGPR84-eYFP constructs

5.2.1. Characterization of the expression of FLAG-mGPR84-G α_{i2} or FLAG-mGPR84-G α_{i2} C352I by western blot analysis

The expression of FLAG-mGPR84-G α_{i2} or FLAG-mGPR84-G α_{i2} C352I in doxycycline-induced Flp-In T-REx-293 cells was characterized by immunoblotting membranes prepared from both uninduced and doxycycline-induced cells with an anti-ICL3-mouse GPR84 antiserum which is able to detect the 3rd intracellular loop (ICL3) of the expressed receptor. Immunoblots of membranes purified from doxycycline-induced cells revealed poorly resolved multiple bands having molecular masses between 80 and 105 kDa (Figure 5.1 A). These bands were specific as they were not detected in immunoblots of membranes generated from cells grown in the absence of doxycycline. The pre-treatment of membranes of doxycycline-treated cells with peptide N-glycosidase enzyme (PNGase F) at a final concentration of 0.05 U/ μ l converted these bands into a predominant single band having an apparent molecular mass of 80 kDa which migrated more rapidly in the gel (Figure 5.1A). These outcomes confirmed the expression of FLAG-mGPR84-G α_{i2} in Flp-In T-REx-293 cells as an intact polypeptide and revealed that multiple bands in the immunoblot of membranes of doxycycline-treated cells represented N-glycosylated forms of the receptor construct. Similarly, the detection of a diffuse band having an apparent molecular mass between 80 and 105 kDa in the immunoblot of membranes generated from doxycycline-induced Flp-In T-REx-293 cells harbouring FLAG-

mGPR84-G α_{i2} C352I confirmed the effective expression of the fusion protein in the cell line (Figure 5B).

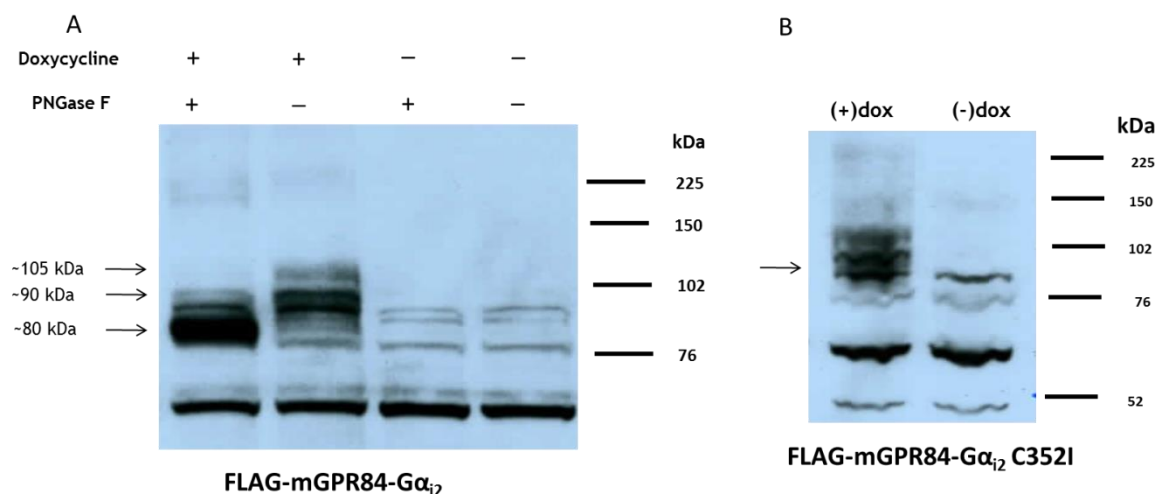


Figure 5.1 Immunoblot of FLAG-mGPR84-G α_{i2} and FLAG-mGPR84-G α_{i2} C352I probed with anti-ICL3-mouse GPR84 antiserum. Flp-In T-REx-293 cells stably harbouring FLAG-mGPR84-G α_{i2} were either uninduced (-Dox) or induced (+Dox) with 100 ng/ml of doxycycline for 24 hours prior to membrane preparation. These membranes were then either untreated (-PNGase F) or treated with N-glycosidase F (+PNGase F) at a final concentration of 0.05 units/ μ l followed by heating for 3 hours at 37°C. These samples containing 10 μ g proteins were then resolved by sodium dodecyl sulfate polyacrylamide gel electrophoresis (SDS-PAGE) followed by immunoblotting with anti-ICL3-mouse GPR84 antiserum (A). Similarly, membranes generated from uninduced (-Dox) or doxycycline-induced (100 ng/ml, 24 hours, +Dox) Flp-In T-REx -293 cells harbouring FLAG-mGPR84-G α_{i2} C352I were subjected to SDS-PAGE and subsequently immunoblotted with anti-ICL3-mouse GPR84 antiserum (B).

5.2.2. Characterization of the expression of FLAG-mGPR84-eYFP or FLAG-hGPR84-eYFP in HEK-293 cells

To characterize the expression of FLAG-mGPR84-eYFP and FLAG-hGPR84-eYFP in HEK-293 cells, membranes generated from transiently transfected HEK-293 cells were subjected to immunoblotting with either an anti-GFP antiserum which is able to detect the eYFP moiety of the expressed receptor construct or with anti-ICL3-mouse GPR84 antiserum which can recognize the 3rd intracellular loop of mouse GPR84 and potentially that of human GPR84 as well. A discrete band having an apparent molecular mass between 150 and 160 kDa representing a potential dimer of the receptor constructs and another discrete band having a molecular weight of 70 to 75 kDa corresponding to the monomeric form confirmed the expression of either FLAG-mGPR84-eYFP or FLAG-hGPR84-eYFP in the corresponding cells (Figure 5.2A). Pre-treatment of membranes with N-

glycosidase enzyme (PNGase F) resulted in greatly increased intensity of the band having a molecular weight consistent with the monomeric form (~72 kDa), suggesting the cleavage of glycan(s) from glycosylated forms of the receptor. This enzyme treatment also slightly increased the migration speed of the immunoreactive species corresponding to the monomeric form of both human and mouse GPR84. Importantly, the band having molecular mass between 150 and 160 kDa was also detected in the immunoblot following treatment with the N-glycosidase enzyme, suggesting that the deglycosylation process did not significantly affect the dimerization of GPR84. The presence of the other three specific bands having a molecular mass greater than 225 kDa in the immunoblots might reflect aggregates or oligomeric forms of the receptor construct.

Similar to the immunoblot performed using anti-GFP antiserum, immunoblots with anti-ICL3-mouse GPR84 antiserum confirmed the expression of FLAG-mGPR84-eYFP or FLAG-hGPR84-eYFP in transiently transfected HEK-293 cells which was evidenced from the detection of a specific band having a molecular mass of about 150 kDa, probably corresponding to a dimeric form of the receptor construct (Figure 5.2B). The intensity of this band having a molecular mass of about 150 kDa in the immunoblot of membranes generated from cells transfected with FLAG-hGPR84-eYFP was substantially reduced compared to that of FLAG-mGPR84-eYFP, indicating that the anti-ICL3-mouse GPR84 antiserum was less sensitive to detect the 3rd intracellular loop of human GPR84. Another band having a molecular mass of some 70 kDa appeared in the immunoblot of membranes following treatment with the N-glycosidase enzyme which was not detected in the blot of untreated membranes, further supporting the N-glycosylation of mouse GPR84.

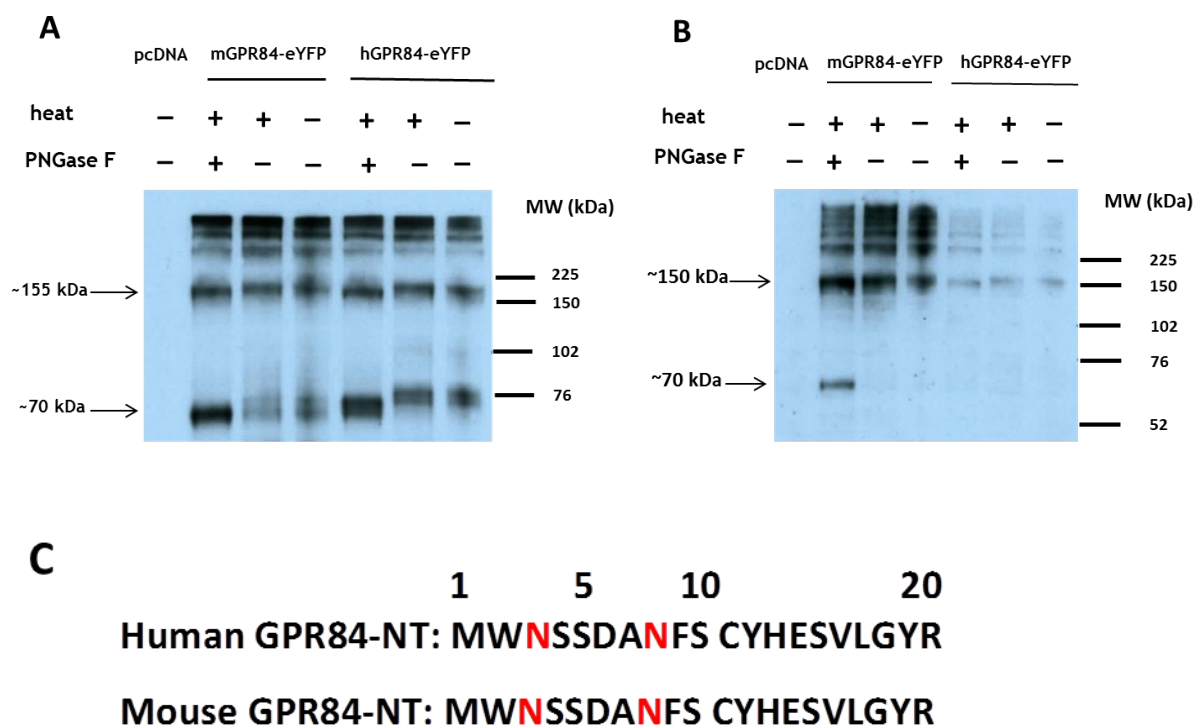


Figure 5.2 Immunoblot of FLAG-mGPR84-eYFP and FLAG-hGPR84-eYFP probed with anti-GFP (A) or anti-ICL3-mouse GPR84 antiserum (B). HEK-293 cells were transiently transfected with FLAG-hGPR84-eYFP, FLAG-mGPR84-eYFP or empty vector pcDNA5 and membranes were generated after 36 hours of transfection. Membranes purified from cells transfected with FLAG-hGPR84-eYFP or FLAG-mGPR84-eYFP were then either untreated (-PNGase F) or treated (+PNGase F) with N-glycosidase enzyme (PNGase F) followed by incubating for 2 hours at 37°C (+heat). These samples containing 8 µg of proteins were subsequently subjected to SDS-PAGE to resolve the proteins. To assess the effect of the application of heat on degradation/migration of protein, membranes which were not (-heat) incubated at 37°C were also run in the gel. The resolved proteins were then immunoblotted with either an anti-GFP antiserum (A) or with the anti-ICL3-mouse GPR84 antiserum (B). Possible N-glycosylation sites within the N-terminus of human and mouse GPR84 are highlighted in red (C).

5.2.3. Functional characterization using [³⁵S]-GTPγS binding assays

I generated doxycycline-inducible Flp-In T-REx-293 cell lines stably harbouring FLAG-mGPR84-Gα_{i2}, FLAG-mGPR84-Gα_{i2} C352I or FLAG-mGPR84-eYFP receptor constructs. To check the functionality of these mouse GPR84 receptor constructs, agonist-induced [³⁵S]-GTPγS incorporation assays were performed using membranes prepared from both uninduced (no doxycycline added) and doxycycline-induced (100 ng/ml, 24 hours) cells expressing FLAG-mGPR84-Gα_{i2}, FLAG-mGPR84-Gα_{i2} C352I or FLAG-mGPR84-eYFP constructs. Compound-1, embelin, PSB-16671 and DIM each enhanced [³⁵S]-GTPγS binding to membranes generated from cells induced with doxycycline to express FLAG-mGPR84-Gα_{i2} in a concentration-dependent fashion with pEC₅₀ of 7.51±0.10, 5.54±0.04, 6.50±0.10 and 5.36±0.01, respectively (Figure 5.3 a_i,a_{ii}). These results confirmed

that FLAG-mGPR84-G α_{i2} expressed in Flp-In T-REx-293 cells is functionally active. Each of ligands did not promote any significant [35 S]-GTP γ S incorporation into membranes generated from Flp-In T-REx-293 cells which were not induced with doxycycline, implying that agonist-promoted binding of [35 S]-GTP γ S into membranes purified from doxycycline-induced cells was mediated by activation of mouse GPR84. Consistent with the results observed at FLAG-hGPR84-G α_{i2} (see section 4.2.3), PSB-16671 also displayed substantially higher potency (about 13-fold) and efficacy (about 2.6-fold) than parent compound DIM at FLAG-mGPR84-G α_{i2} , indicating that DIM also acted as a partial agonist at mouse orthologue. Contrary to the result observed at FLAG-hGPR84-G α_{i2} wherein PSB-16671 displayed lower efficacy than compound-1 (section 4.2.3), at FLAG-mGPR84-G α_{i2} both agonists showed an equivalent maximal response (Figure 5.3 a_i, a_{ii}).

Compound-1 and embelin also concentration-dependently promoted binding of [35 S]-GTP γ S into membranes generated from doxycycline-induced Flp-In T-REx-293 cells expressing FLAG-mGPR84-G α_{i2} C352I whilst no significant binding of radiolabelled guanine nucleotide was observed when membranes prepared from cells grown in the absence of doxycycline were employed (Figure 5.3 b_i, b_{ii}). These results demonstrated the functional integrity of the FLAG-mGPR84-G α_{i2} C352I construct. Compound-1 and embelin displayed similar potency at FLAG-mGPR84-G α_{i2} and FLAG-mGPR84-G α_{i2} C352I, implying that mutation of cysteine 352 of G α_{i2} to isoleucine did not alter the pharmacology of GPR84 agonists.

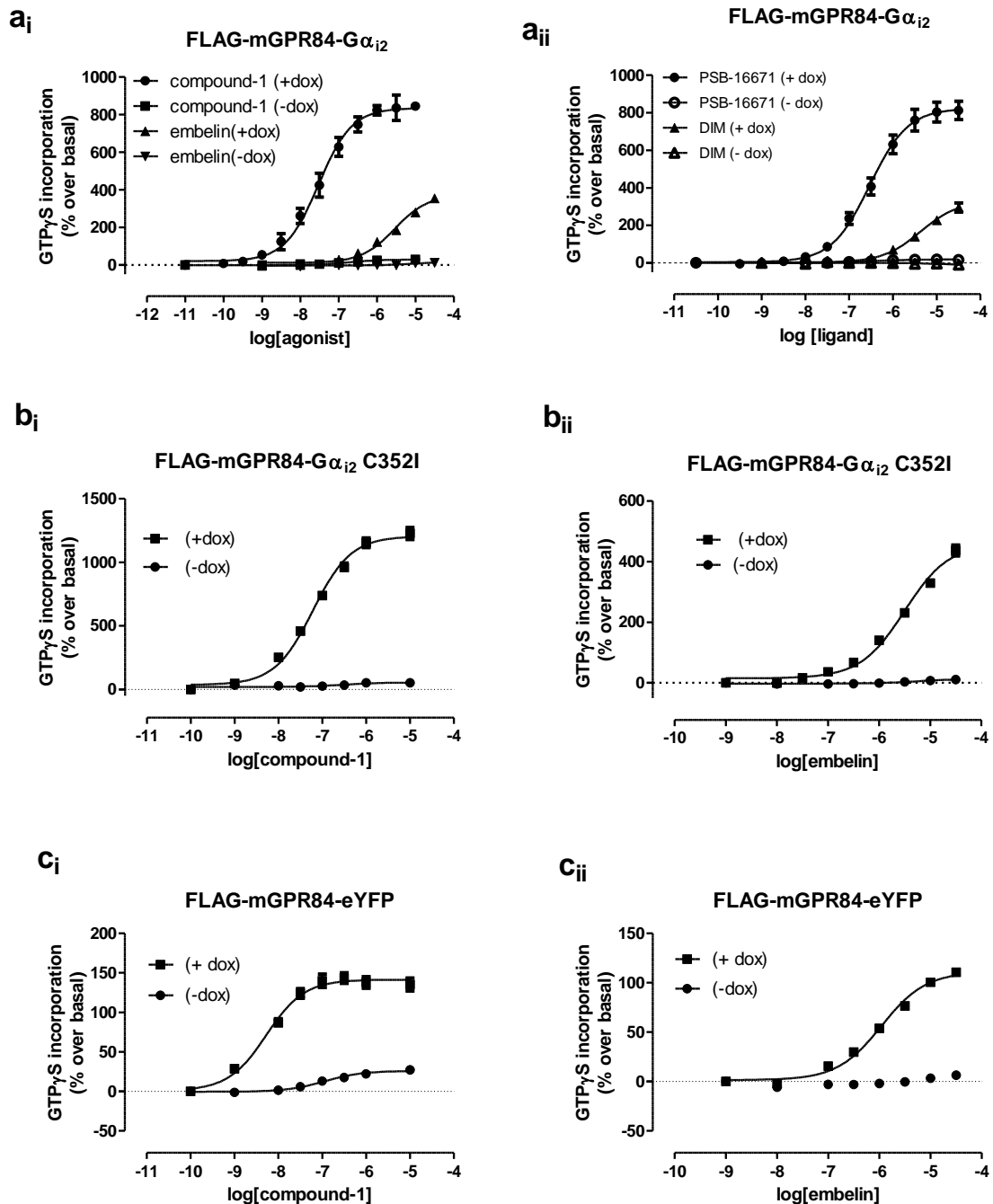


Figure 5.3 FLAG-mGPR84-Gα_{i2}, FLAG-mGPR84-Gα_{i2} C352I and FLAG-mGPR84-eYFP are functionally active in [³⁵S]-GTPγS binding assays. Flp-In T-REx-293 cells stably harbouring FLAG-mGPR84-Gα_{i2}, FLAG-mGPR84-Gα_{i2} C352I or FLAG-mGPR84-eYFP were either uninduced (-Dox) or induced (+Dox) with 100 ng/ml of doxycycline for 24 hours prior to membrane preparation. Various concentrations of either compound-1 or embelin (a_i) and PSB-16671 or DIM (a_{ii}) were then assessed for their ability to stimulate [³⁵S]-GTPγS binding to membranes prepared from either untreated or doxycycline-treated cells harbouring FLAG-mGPR84-Gα_{i2}. Equivalent studies were performed to evaluate the capacity of increasing concentrations of compound-1 (b_i) or embelin (b_{ii}) to induce promotion of [³⁵S]-GTPγS incorporation into membranes generated from cells harbouring FLAG-mGPR84-Gα_{i2} C352I. Similarly, the effects of mouse GPR84 activation on [³⁵S]-GTPγS incorporation into membranes purified from cells harbouring FLAG-mGPR84-eYFP were evaluated following addition of increasing concentrations of compound-1 (c_i) or embelin (c_{ii}).

Compound-1 and embelin also concentration-dependently stimulated incorporation of [35 S]-GTP γ S into membranes prepared from doxycycline-induced cells expressing FLAG-mGPR84-eYFP (Figure 5.3 c_i, c_{ii}) displaying pEC₅₀ of 8.3 \pm 0.08 and 6.0 \pm 0.08, respectively. Though compound-1 and embelin displayed higher potency (about 6.5 and 3-fold increased potencies, respectively) at FLAG-mGPR84-eYFP compared to that displayed at FLAG-mGPR84-G α_{i2} , the signalling magnitudes generated by FLAG-mGPR84-eYFP were much lower than the fusion protein construct. While embelin did not promote any significant binding of [35 S]-GTP γ S to membranes generated from cells which were not treated with doxycycline to allow expression of FLAG-mGPR84-eYFP, compound-1 was found to promote some [35 S]-GTP γ S incorporations into same membrane preparations perhaps indicating some degree of leaky expression.

5.2.4. Mouse GPR84 couples to PTX-sensitive G α_i G proteins

The pre-treatment of cells expressing FLAG-mGPR84-G α_{i2} fusion protein with the G α_i protein inhibitor, pertussis toxin (50 ng/ml, 24 hours) either completely or largely (80% reduction compared to untreated cells) inhibited [35 S]-GTP γ S binding to G α_{i2} protein induced by embelin or compound-1, respectively (Figure 5.4 a_i, a_{ii}) which is in agreement with the fact that mouse GPR84 couples to PTX-sensitive G α_i . In contrast, agonist-induced [35 S]-GTP γ S incorporation was not altered substantially following the PTX treatment of cells expressing PTX-insensitive fusion protein FLAG-mGPR84-G α_{i2} C352I (Figure 5.4 b_i, b_{ii}), implying that after addition of PTX to cells, most of the [35 S]-GTP γ S incorporation into membranes reflected binding of the radiolabelled guanine nucleotide into the fused exogenous G α_{i2} G protein while contribution from the endogenous G α_i protein was marginal.

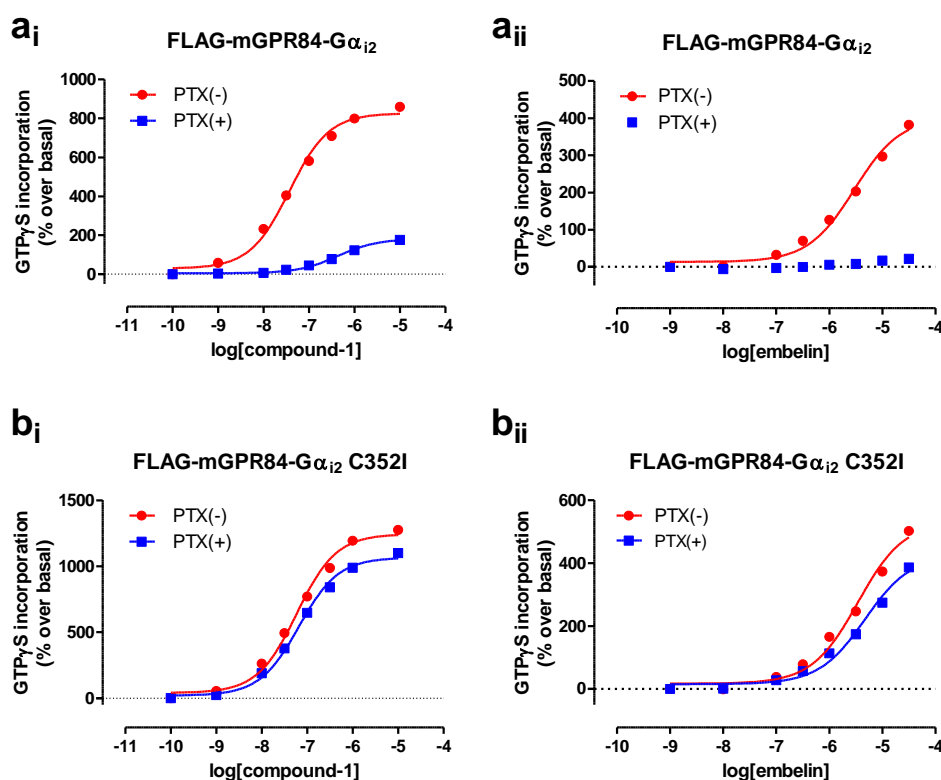


Figure 5.4 Mouse GPR84 couples to pertussis toxin-sensitive $G\alpha_i$ G proteins. Flp-In T-REx-293 cells stably harbouring FLAG-mGPR84- $G\alpha_{i2}$ or FLAG-mGPR84- $G\alpha_{i2}$ C352I were induced with 100 ng/ml doxycycline to express the receptor of interest. These cells were then either untreated (PTX-) or treated (PTX+) with 50 ng/ml of PTX for 24 h prior to membrane preparation. Various concentrations of compound-1 (a_i) or embelin (a_{ii}) were then assessed for their capacity to stimulate binding of [³⁵S]-GTPγS into membranes expressing FLAG-mGPR84- $G\alpha_{i2}$. Equivalent experiments were performed to assess the ability of increasing concentrations of compound-1 (b_i) or embelin (b_{ii}) to promote [³⁵S]-GTPγS binding to $G\alpha_{i2}$ associated with FLAG-mGPR84- $G\alpha_{i2}$ C352I.

5.3. Orthosteric and allosteric agonists display similar activities at human and mouse orthologues of GPR84

In a preliminary study, [³⁵S]-GTPγS binding assays were performed using membranes prepared from HEK-293 cells transiently transfected with FLAG-mGPR84-eYFP, FLAG-hGPR84-eYFP or the empty vector pcDNA5. In this assay, decanoic acid(C-10), undecanoic acid(C-11), embelin, DIM, compound-1 and 6-OAU displayed similar potencies at both human GPR84 and mouse GPR84 (Figure 5.5 and Table 5.1). The variation in efficacy of these ligands found in the assay might reflect differential expression levels of mouse and human GPR84 in transiently transfected cells. Agonist functions of all these ligands were also evaluated by performing equivalent [³⁵S]-GTPγS binding assays using membranes prepared from HEK-293 cells transiently transfected with FLAG-hGPR84- $G\alpha_{i2}$ C352I or FLAG-mGPR84- $G\alpha_{i2}$ C352I fusion constructs. In these assays, orthosteric

agonists decanoic acid(C-10), undecanoic acid(C-11), embelin, 6-OAU and compound-1 as well as both the allosteric agonists DIM and PSB-16671 concentration-dependently promoted [³⁵S]-GTPγS binding to membranes displaying similar potencies and efficacies at human and mouse orthologues of GPR84 (Figure 5.6 and Table 5.1). Potencies of C-10, embelin, compound-1, 6-OAU, DIM or PSB-16671 were also indistinguishable between human and mouse GPR84 when membranes prepared from doxycycline-induced (100 ng/ml, 24 hours) Flp-In T-REx-293 cells stably harbouring FLAG-hGPR84-Gα_{i2} C352I or FLAG-mGPR84-Gα_{i2} C352I were used in [³⁵S]-GTPγS binding assays (Figure 5.7 and Table 5.2). The similar rank order of potency of tested agonists was observed between FLAG-hGPR84-Gα_{i2} C352I and FLAG-mGPR84-Gα_{i2} C352I which is as follows:

Compound-1>6-OAU=PSB-16671>Embelin>DIM>C-10.

The FLAG-mGPR84-Gα_{i2} C352I also maintained the similar rank order of efficacy of agonists compared to that displayed at FLAG-hGPR84-Gα_{i2} C352I (Figure 5.7 g,h): **Compound-1>6-OAU>PSB-16671>C-10> embelin=DIM**

Embelin, compound-1, DIM and PSB-16671 also showed similar functions at FLAG-hGPR84-Gα_{i2} and FLAG-mGPR84-Gα_{i2} when membranes prepared from Flp-In T-REx-293 cells induced with 100 ng/ml doxycycline for 24 hours were employed in the assay (Figure 5.8 and Table 5.2).

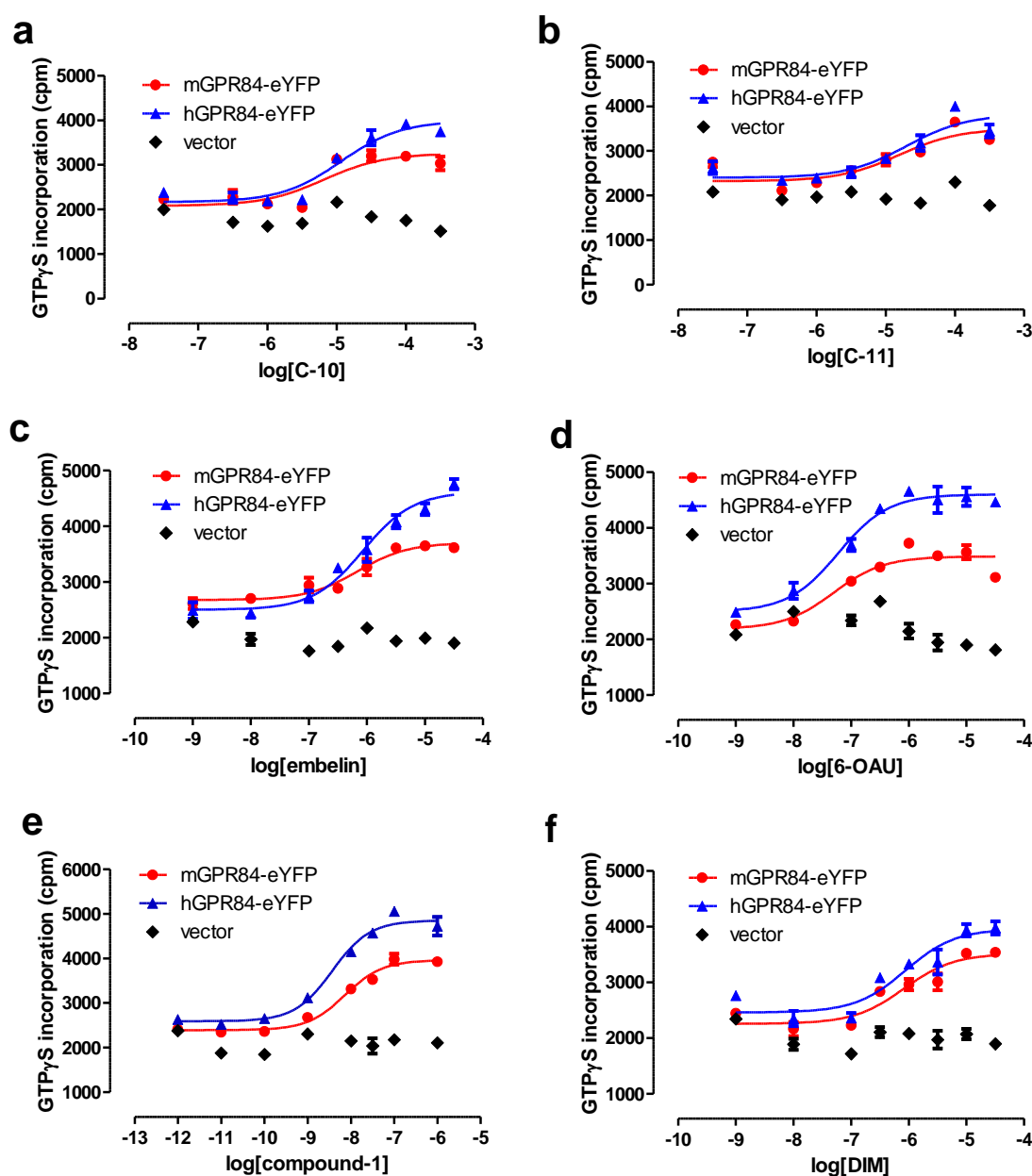


Figure 5.5 Agonists of human GPR84 display very similar activity at mouse GPR84.

Membranes were purified from HEK-293 cells transiently transfected with FLAG-hGPR84-eYFP, FLAG-mGPR84-eYFP or empty vector pcDNA5. $[^{35}\text{S}]\text{-GTP}\gamma\text{S}$ binding assays were then performed using these membranes to assess the ability of increasing concentrations of C-10 (a), C-11 (b), embelin (c), 6-OAU (d), compound-1 (e) or DIM (f) to induce $[^{35}\text{S}]\text{-GTP}\gamma\text{S}$ incorporation into membranes.

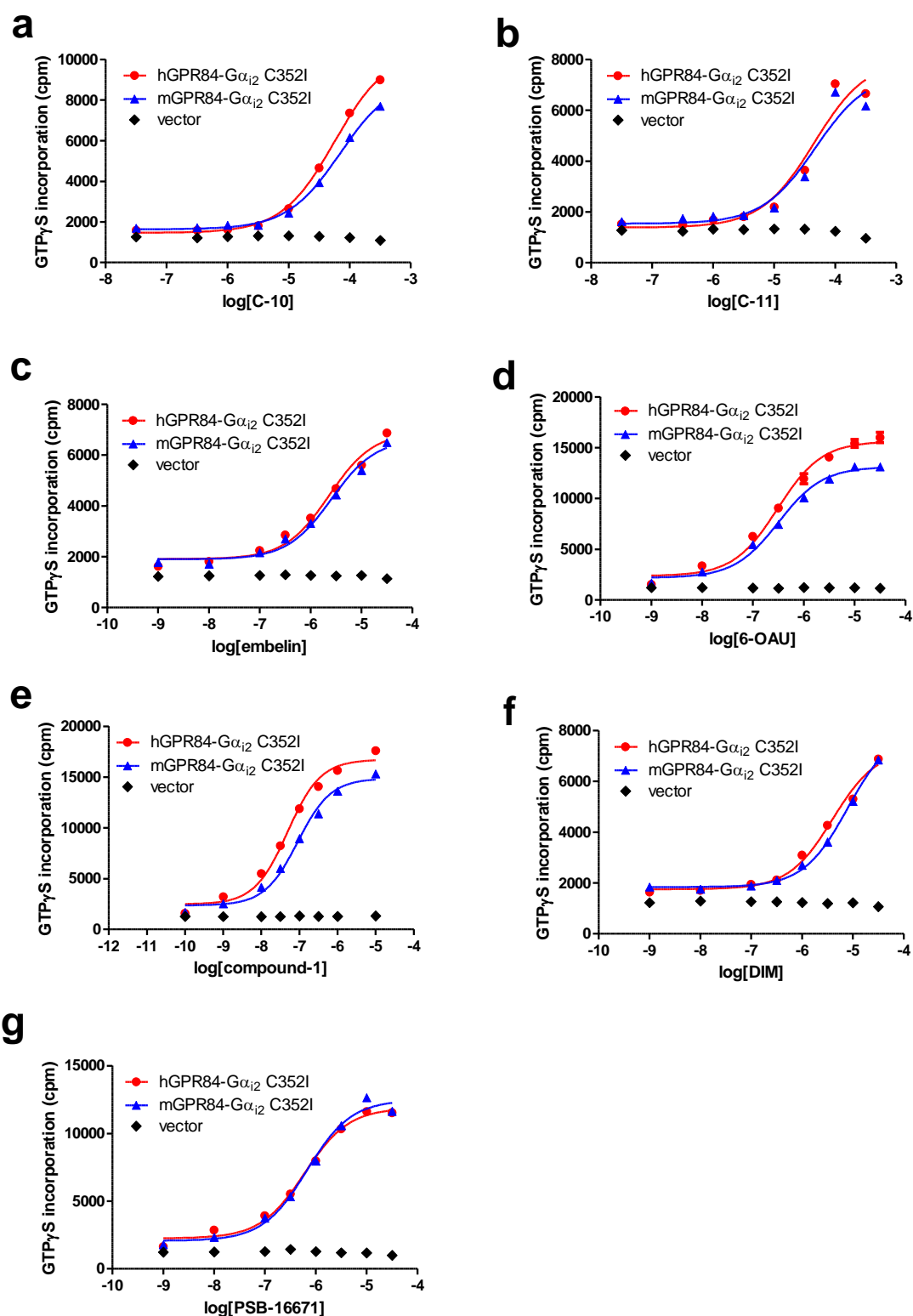


Figure 5.6 Human and mouse GPR84 showed similar responsiveness to orthosteric and allosteric ligands in HEK-293 cells. Increasing concentrations of C-10 (a), C-11 (b), embelin (c), 6-OAU(d), compound-1 (e), DIM (f) or PSB-16671 (g) were evaluated for their ability to promote binding of [35 S]-GTP γ S to membranes generated from HEK-293 cells transiently transfected with FLAG-hGPR84-G α_{i2} C352I, FLAG-mGPR84-G α_{i2} C352I or empty vector pcDNA5.

Table 5-1 Potency of different GPR84 agonists at human and mouse GPR84 observed in transiently transfected HEK-293 cells

| Ligand | Human GPR84 | | Mouse GPR84 | |
|-------------------|-------------------------------|-------------|-------------------------------|-------------|
| | hGPR84-Gα _{i2} C352I | hGPR84-eYFP | mGPR84-Gα _{i2} C352I | mGPR84-eYFP |
| C-10 | 4.24±0.04 | 5.00±0.20 | 4.15±0.04 | 5.13±0.40 |
| C-11 | 4.34±0.20 | 4.05±0.28 | 4.32±0.25 | 4.24±0.50 |
| Embelin | 5.63±0.12 | 6.10±0.10 | 5.58±0.10 | 6.20±0.20 |
| Compound-1 | 7.31±0.10 | 8.38±0.10 | 7.04±0.08 | 8.14±0.10 |
| 6-OAU | 6.51±0.08 | 7.20±0.10 | 6.50±0.07 | 7.16±0.16 |
| DIM | 5.40±0.10 | 6.00±0.30 | 5.10±0.04 | 6.04±0.30 |
| PSB-16671 | 6.21±0.08 | | 6.16±0.10 | |

A series of [³⁵S]-GTPγ assays were performed using membranes generated from transiently transfected HEK-293 cells expressing FLAG tagged human and mouse GPR84 and human and mouse GPR84 fused to Gα_{i2} C352I as described in Figure 5.5 and 5.6 and potencies of different ligands were determined. Data (pEC₅₀) are expressed as mean±S.E.M.

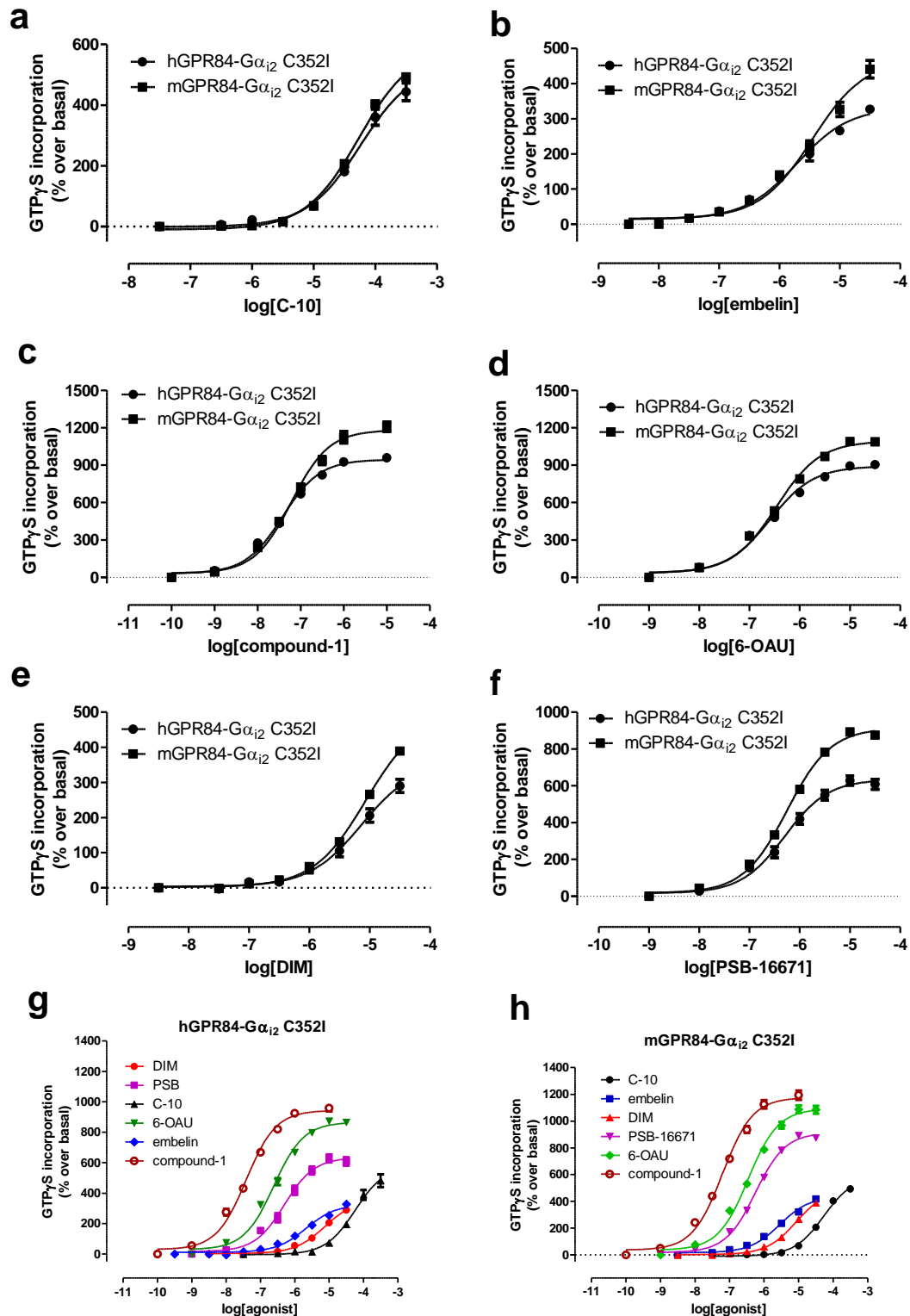


Figure 5.7 Mouse GPR84 responds to different GPR84 agonists in a manner very similar to human orthologue. Flp-In T-REx-293 cells stably harbouring FLAG-hGPR84-G α_{i2} C352I or FLAG-mGPR84-G α_{i2} C352I were incubated with 100 ng/ml of doxycycline for 24 hours followed by generation of membranes. Using these membranes, [35 S]-GTP γ S binding to G α_{i2} associated with FLAG-hGPR84-G α_{i2} C352I or FLAG-mGPR84-G α_{i2} C352I were measured in response to varying concentrations of C-10 (a), embelin (b), compound-1 (c), 6-OAU (d), DIM (e) or PSB-16671 (f). Data for all the agonists from (a-f) are shown again in (g) and (h) to compare their relative efficacy at FLAG-hGPR84-G α_{i2} C352I or FLAG-mGPR84-G α_{i2} C352I, respectively.

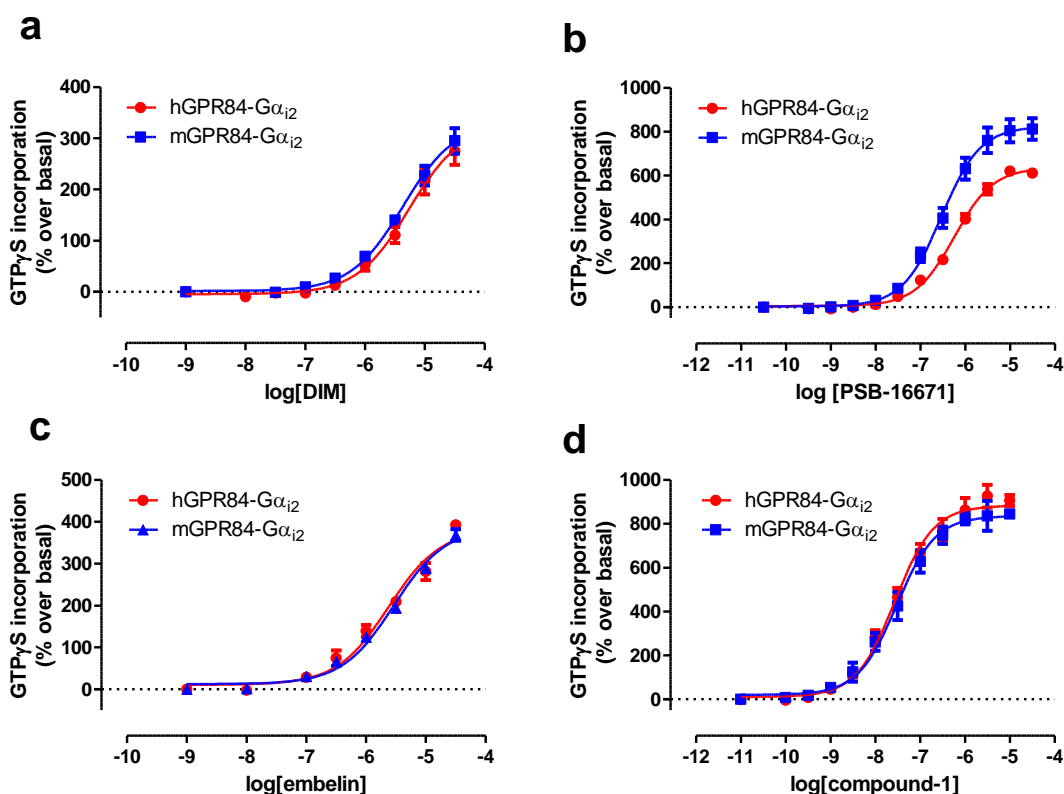


Figure 5.8 Comparison of GPR84 agonist functions between human and mouse GPR84. Flp-In T-Rex-293 cells stably harbouring FLAG-hGPR84-G α_{i2} or FLAG-mGPR84-G α_{i2} were incubated with 100 ng/ml of doxycycline for 24 hours prior to membrane preparation. These membranes were then employed to assess the ability of increasing concentrations of DIM (a), PSB-16671 (b), embelin (c) or compound-1 (d) to stimulate [35 S]-GTP γ S binding to the G α_{i2} associated with FLAG-hGPR84-G α_{i2} or FLAG-mGPR84-G α_{i2} . Data represent mean \pm SEM of three independent experiments performed on three individual membrane preparations.

Table 5-2 Potency of different agonists at human and mouse GPR84 observed in doxycycline-inducible Flp-In T-Rex-293 cells expressing human or mouse GPR84 as fusion protein constructs

| Ligand | Human GPR84 | | Mouse GPR84 | |
|------------|------------------------|------------------------------|------------------------|------------------------------|
| | hGPR84-G α_{i2} | hGPR84-G α_{i2} C352I | mGPR84-G α_{i2} | mGPR84-G α_{i2} C352I |
| C-10 | | 4.24 \pm 0.01 | | 4.26 \pm 0.06 |
| Embelin | 5.72 \pm 0.12 | 5.67 \pm 0.06 | 5.54 \pm 0.04 | 5.55 \pm 0.03 |
| Compound-1 | 7.54 \pm 0.06 | 7.46 \pm 0.06 | 7.51 \pm 0.10 | 7.21 \pm 0.01 |
| 6-OAU | | 6.60 \pm 0.05 | | 6.46 \pm 0.06 |
| DIM | 5.30 \pm 0.07 | 5.20 \pm 0.07 | 5.36 \pm 0.01 | 5.06 \pm 0.03 |
| PSB-16671 | 6.28 \pm 0.05 | 6.35 \pm 0.04 | 6.50 \pm 0.10 | 6.25 \pm 0.04 |

A set of [35 S]-GTP γ S incorporation assays were conducted using membranes prepared from doxycycline induced stable cell lines expressing human or mouse GPR84 as fusion protein construct with either G α_{i2} or pertussis toxin resistant G α_{i2} C352I as described in Figure 5.7 and 5.8. Data (pEC $_{50}$) are expressed as mean \pm S.E.M of three (for h/mGPR84-G α_{i2}) or two (for PTX-insensitive fusion proteins h/mGPR84-G α_{i2} C352I) independent experiments performed on separate membranes isolated from doxycycline-treated Flp-In T-Rex-293 cells.

5.4. Defining the pharmacology of GPR84 ligands in RAW 264.7 cells

5.4.1. Orthosteric and allosteric agonists of GPR84 display similar pharmacology in RAW 264.7 cells to those observed in transfected cells expressing FLAG-mGPR84-eYFP

It is well established that GPR84 is expressed in the mouse monocyte-macrophage cell line RAW 264.7 and the expression is upregulated following treatment with the TLR4 agonist, lipopolysaccharide (Wang et al., 2006b; Recio et al., 2018; Mancini et al., 2019). To investigate the pharmacological properties of GPR84 ligands in a more relevant physiological setting, I used RAW 264.7 cells as a model murine cell line. In an attempt to investigate whether LPS treatment leads to enhanced functional responses to GPR84 ligands, [35 S]-GTP γ S binding assays were performed using membranes generated from untreated (LPS-) or LPS-treated (100 ng/ml) RAW 264.7 cells. The synthetic GPR84 agonist compound-1 concentration-dependently enhanced [35 S]-GTP γ S incorporation into membranes generated from RAW 264.7 cells both untreated or treated with LPS for 5 hours and 11 hours exhibiting pEC₅₀ of 7.3 \pm 0.15, 7.66 \pm 0.06 and 7.57 \pm 0.02, respectively (Figure 5.9a,b). Although the LPS pre-treatment for 5 and 11 hours increased the maximal response of compound-1 by 32 and 20%, respectively compared to untreated cells (Figure 5.9a), no statistically significant ($P>0.05$) enhancement of potency of compound-1 was observed, which implies that LPS treatment of RAW 264.7 cells did not produce any significant receptor reserve for GPR84. The allosteric agonist PSB-16671 was also found to promote [35 S]-GTP γ S binding to membranes purified from RAW 264.7 cells treated with 100 ng/ml of LPS for 5 and 11 hours displaying pEC₅₀ of 6.78 \pm 0.13 and 6.75 \pm 0.10, respectively (Figure 5.9b). Decanoic acid, embelin and DIM also concentration-dependently enhanced [35 S]-GTP γ S binding to membranes from LPS-treated (100 ng/ml, 11hours) RAW 264.7 cells with pEC₅₀ of 4.36 \pm 0.06, 6.5 \pm 0.20 and 6.50 \pm 0.25, respectively (Figure 5.9c). Potencies of decanoic acid, embelin, compound-1, DIM and PSB-16671 displayed at RAW264.7 cells were very similar to those estimated at transfected HEK-293 cells expressing mouse GPR84-eYFP (Table 5.1 and Table 5.3). By contrast, although potencies of C-10, compound-1 and PSB-16671 were indistinguishable between RAW 264.7 cells and Flp-In T-REx-293 cells expressing FLAG-mGPR84-G α_{i2} , both embelin and DIM displayed about 9

and 13-fold higher potencies, respectively at RAW 264.7 cells compared to stably transfected Flp-In T-REx cells (Table 5.2 and 5.3). In contrast to transfected cells expressing mouse GPR84, wherein compound-1 and PSB-16671 displayed similar efficacy, in RAW 264.7 cells compound-1 showed about 30% higher maximal response than PSB-16671 (Figure 5.9 b). Whereas C-10 displayed similar efficacy to PSB-16671, maximal responses of DIM and embelin were substantially lower than those of PSB-16671, compound-1 or C-10 (Figure 5.9b,c) which implies that DIM and embelin acted as partial GPR84 agonists at RAW 264.7 cells in [³⁵S]-GTPγS binding assays which is consistent with the results observed in transfected cells expressing mouse GPR84.

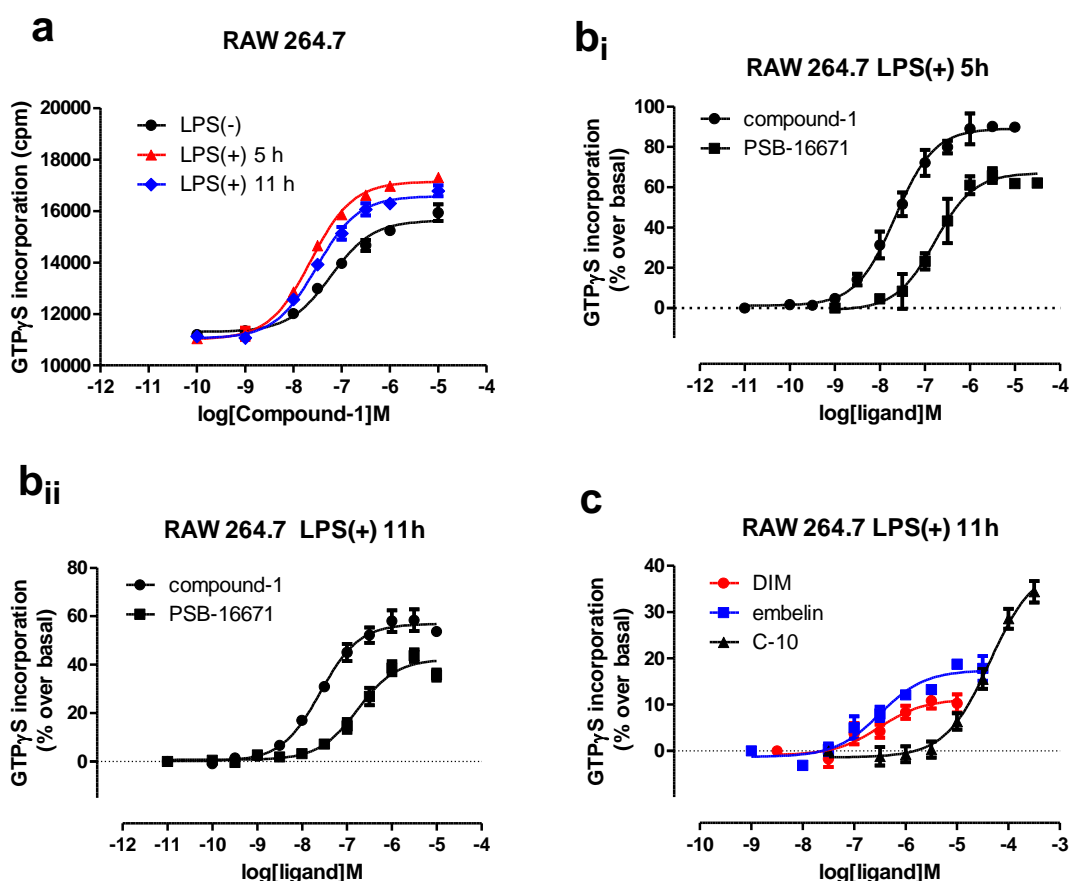


Figure 5.9 RAW 264.7 cells respond to GPR84 orthosteric and allosteric agonists in a manner equivalent to transfected cells expressing mouse GPR84. The effect of increasing concentrations of compound-1 to induce stimulation of [35 S]-GTP γ S binding to membranes prepared from RAW 264.7 cells either untreated (LPS-) or treated (LPS+) with 100 ng/ml of LPS for 5 or 11 hours is shown (a). Similarly, the capacity of varying concentrations of compound-1 or PSB-16671 to enhance binding of [35 S]-GTP γ S to membranes purified from RAW 264.7 cells induced with LPS for 5 hours (b_i) or 11 hours (b_{ii}) was assessed. Effects of various concentrations of C-10, embelin or DIM in promoting binding of [35 S]-GTP γ S to membranes generated from RAW264.7 cells treated with LPS for 11 hours are also shown (c). Data presented in (a) and (c) are from a representative experiment of three and two independent experiments, respectively and data shown in (b_i) and (b_{ii}) are expressed as mean \pm S.E.M. of three and five independent experiments, respectively performed on separate membrane preparations.

Table 5-3 Potencies of GPR84 orthosteric and allosteric agonists in LPS-treated RAW 264.7 cells

| Ligand | pEC ₅₀ (mean±S.E.M.) | |
|------------|---------------------------------|-------------|
| | LPS (+) 5 h | LPS(+) 11 h |
| C-10 | | 4.36±0.06 |
| Embelin | | 6.50±0.20 |
| Compound-1 | 7.66±0.06 | 7.57±0.02 |
| DIM | | 6.50±0.25 |
| PSB-16671 | 6.78±0.13 | 6.75±0.10 |

A set of [³⁵S]-GTPγS binding studies were performed using membranes generated from LPS-induced RAW264.7 cells as described in Figure 5.9 and potencies of different GPR84 agonists were determined. Data are expressed as mean±S.E.M. of three independent experiments performed using separate membrane preparations isolated from RAW 264.7 cells treated with 100 ng/ml of LPS for 5 and 11 hours.

5.4.2. GPR84 antagonists showed reduced potency in RAW 264.7 cells compared to human GPR84 expressing THP-1 cells

Though the maintenance of similar potency values of orthosteric and allosteric agonists at RAW 264.7 cells to those observed at transfected cells expressing cloned mouse GPR84 suggested that effects of these ligands in RAW264.7 cells might be mediated in a GPR84-specific manner, to confirm this in more detail, the capacity of the established GPR84 antagonists compound-104, 107, 161 or GLPG1205 to block ligand-mediated [³⁵S]-GTPγS binding to membranes of RAW 264.7 cells was examined. GPR84 antagonist compound-104, compound-107 and GLPG1205 completely inhibited compound-1-induced binding of [³⁵S]-GTPγS to membranes generated from LPS-treated RAW 264.7 cells in a concentration-dependent manner with pIC₅₀ of 6.44±0.16, 6.52±0.07 and 6.22±0.05, respectively (Figure 5.10a). In contrast, compound-837 was inactive at RAW 264.7 cells in inhibiting the response to compound-1 (Figure 5.10a). Compound-107, compound-161 and GLPG1205 also effectively and concentration-dependently blocked PSB-16671-stimulated incorporation of [³⁵S]-GTPγS into membranes from LPS-treated RAW 264.7 cells displaying pIC₅₀ of 6.82±0.08, 6.35±0.28 and 6.44±0.06, respectively (Figure 5.10b). Similarly, in [³⁵S]-GTPγS binding assays, response to an EC₈₀ concentration of decanoic acid (C-10) was also concentration-dependently antagonized by compound-104, compound-161 and GLPG1205 with pIC₅₀ of 6.92±0.12, 5.70±0.15 and 6.43±0.08, respectively whilst compound-837 was inactive in suppressing the C-10-induced [³⁵S]-GTPγS binding (Figure 5.10c). Moreover, GPR84 antagonist GLPG1205 completely and

concentration-dependently inhibited embelin or DIM-induced [^{35}S]-GTP γ S binding to membranes of RAW264.7 cells displaying pIC₅₀ of 6.55 \pm 0.04 and 6.52 \pm 0.17, respectively (Figure 5.10 d,e). These studies confirmed that compound-1, decanoic acid, PSB-16671, embelin or DIM-induced promotion of [^{35}S]-GTP γ S incorporation into membranes isolated from LPS-stimulated RAW 264.7 cells were mediated in a GPR84-specific manner.

GPR84 antagonist compound-107 displayed some 20 to 30-fold decreased potency at RAW 264.7 cells in inhibiting the agonistic function of compound-1 and PSB-16671, respectively compared to that displayed at LPS-induced THP-1 cells estimated by Mancini et al., (2019). Moreover, potencies of compound-104 and 161 to block agonist function of C-10 displayed in RAW 264.7 cells were some 5 and 12.6-fold lower, respectively than those estimated at FLAG-hGPR84-eYFP reported by Mahmud et al., (2017). These substantial reductions in potencies of compound-107, 104 and 161 at RAW 264.7 cells in comparison with cells expressing human GPR84 suggested substantially lower affinity of this series of antagonists for mouse GPR84. While the radiolabelled antagonist [^3H]-G9543 has been reported to bind membranes purified from LPS-treated THP-1 cells with sub-nM affinity (Mancini et al., 2019), this radioligand did not show any significant specific binding to membranes generated from LPS-treated RAW 264.7 cells (Figure 5.9 f), implying that [^3H]-G9543 and potentially the related antagonist compounds-104, 107 or 161 displayed greatly reduced affinity for mouse GPR84. This result is consistent with the decreased potency of compound-107 and related molecules at mouse GPR84 compared to the human orthologue.

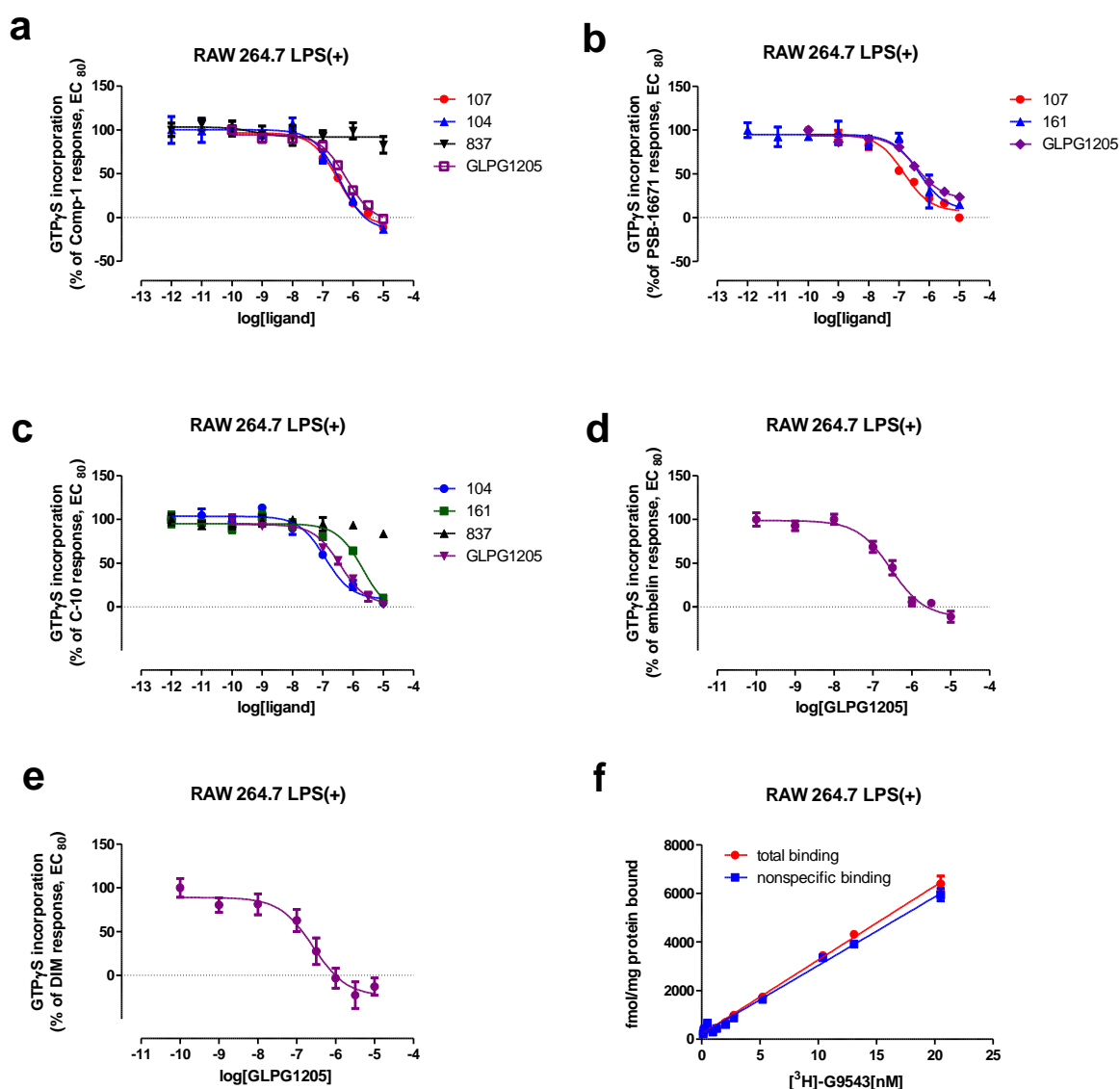


Figure 5.10 GPR84 antagonists compound-104, 107, 161 and GLPG1205 but not compound-837 effectively blocked agonist-induced responses in RAW 264.7 cells. Membranes were generated from RAW 264.7 cells which were treated with LPS (100 ng/ml for 5 hours) to allow upregulation of GPR84 expression. Membranes containing 5 μ g of proteins were then employed to assess the ability of varying concentrations of compound-104, 107, 837 or GLPG1205 to inhibit [³⁵S]-GTP γ S binding induced by an EC₈₀ concentration of compound-1 (a). Effects of various concentrations of compound-107, 161 or GLPG1205 in blocking PSB-16671-stimulated binding of [³⁵S]-GTP γ S were also examined (b). Similar studies were performed assessing the capacity of increasing concentrations of compound-104, 161, 837 or GLPG1205 to block [³⁵S]-GTP γ S incorporation into membranes mediated by an EC₈₀ concentration of C-10 (c). Increasing concentrations of GLPG1205 were also assayed for their ability to block [³⁵S]-GTP γ S binding to membranes stimulated by an EC₈₀ concentration of either embelin (d) or DIM (e). Increasing concentrations (ranging from 0.13 nM to 20.5 nM) of radioligand [³H]-G9543 with (nonspecific binding) or without (total binding) 1 μ M compound-104 were assessed for their ability to bind to membranes purified from LPS-treated RAW 264.7 cells (f).

Table 5-4 Potencies of GPR84 antagonists to inhibit the response to an EC₈₀ concentration of various agonists at LPS-induced RAW264.7 cells

| Antagonist | Agonist | | | | |
|--------------|------------|-----------|-----------|-----------|-----------|
| | Compound-1 | PSB-16671 | C-10 | Embelin | DIM |
| Compound-104 | 6.44±0.16 | | 6.92±0.12 | | |
| Compound-107 | 6.52±0.07 | 6.82±0.08 | | | |
| Compound-161 | | 6.35±0.28 | 5.70±0.15 | | |
| GLPG1205 | 6.22±0.05 | 6.44±0.06 | 6.43±0.08 | 6.55±0.04 | 6.52±0.17 |
| Compound-837 | Inactive | | Inactive | | |

A series of [³⁵S]-GTPγS incorporation assays were performed using membranes prepared from LPS-induced RAW264.7 cells as described in Figure 5.10 to determine the potencies of different GPR84 antagonist in inhibiting response to different GPR84 agonists. Data are expressed as pIC₅₀ (mean±S.E.M, n=3).

5.4.3. GLPG1205 displays differential modes of action in antagonizing the effect of compound-1 and PSB-16671 in RAW264.7 cells

In an attempt to investigate the mode of action of GPR84 antagonist GLPG1205 (designated as compound-122 in the patent literature (Labeguere et al. 2014; <http://www.guidetopharmacology.org/GRAC/LigandDisplayForward?ligandId=10171>), effects of addition of increasing fixed concentrations of GLPG1205 on the position of concentration-response curves of compound-1 were analysed by employing [³⁵S]-GTPγS binding assay using membranes generated from naïve RAW264.7 cells. Though increasing fixed concentrations of GLPG1205 progressively decreased the potency of compound-1, the effect of antagonism was not fully surmounted when higher concentrations of the antagonist were applied (Figure 5.11a); this implies that antagonism of GLPG1205 in blocking compound-1-mediated effect did not follow classical simple competitive antagonism. However, global fitting of dataset with Gaddam/Schild EC₅₀ shift analysis revealed that the Schild slope factor is close to 1.0, suggesting that GLPG1205 antagonized the agonist function of compound-1 in RAW264.7 cells in a competitive manner. The global analysis also estimated the pA₂ affinity value for the antagonist to be 7.23. Similarly, increasing fixed concentrations of GLPG1205 also caused a progressive right-shift of the position of concentration-response curves for compound-1 (Figure 5.11b) when membranes generated from Flp-In T-REx-293 cells expressing FLAG-mGPR84-Gα_{i2} were employed in [³⁵S]-GTPγS incorporation assay. Once again, though antagonism mediated by higher concentrations (3 and 10 μM) of GLPG1205 was not surmounted fully, the global fitting of data with Gaddam/Schild EC₅₀ shift analysis revealed that the slope factor is 1.04 which is consistent with the competitive mode of antagonism. The

estimated pA_2 affinity value of GLPG1205 for FLAG-mGPR84- $G\alpha_{i2}$ was 6.90 which is similar to that observed in RAW264.7 cells. By contrast, addition of varying fixed concentrations of GLPG1205 to the concentration-response assays for PSB-16671 did not significantly affect the potency of PSB-16671 rather resulted in progressive decrease in maximal response (Figure 5.11c), indicating that in RAW264.7 cells, GLPG1205 antagonized the effect of PSB-16671 in a non-competitive manner i.e GLPG1205 binds to a site on GPR84 that is distinct from the binding site shared by PSB-16671.

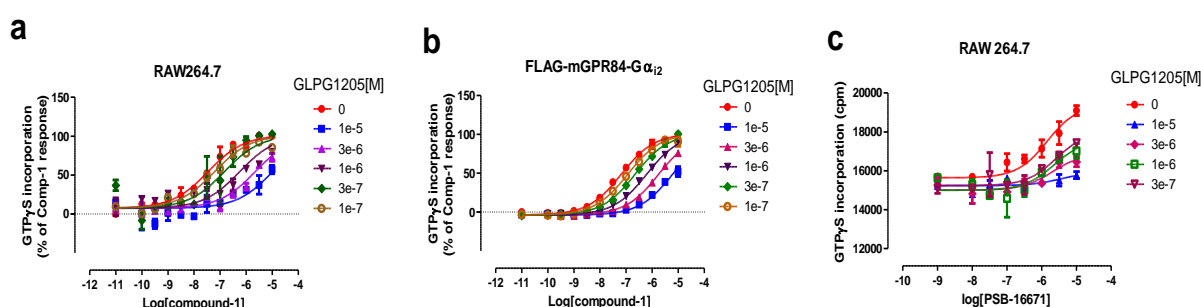


Figure 5.11 GLPG1205 antagonizes effect of compound-1 in a competitive manner while it is non-competitive with PSB-16671 in blocking effect of PSB-16671 in RAW264.7 cells.

Concentration-response curves for compound-1 were generated in the presence or absence of varying fixed concentrations (ranging from 100 nM to 10 μ M) of antagonist GLPG1205 using [35 S]-GTP γ S binding assays employing membranes prepared from naïve RAW264.7 cells (a) or Flp-In T-REx-293 cells (b) induced with 100 ng/ml doxycycline for 24 hours to express FLAG-mGPR84- $G\alpha_{i2}$. Data shown in (a) and (b) are from globally fitted data with Gaddam/Schild EC_{50} shift analysis. Similarly, [35 S]-GTP γ S incorporation assays were performed using membranes of naïve RAW264.7 cells in which increasing fixed concentrations of antagonist GLPG1205 ranging from 300 nM to 10 μ M were added to concentration-response assays for PSB-16671(c). In all these assays, membranes were pre-incubated with fixed concentrations of antagonist GLPG1205 for 15 minutes at room temperature followed by addition of agonist.

5.5. Antagonist 107 and 104 display reduced potency at mouse GPR84 compared to the human orthologue while antagonist 837 was inactive at mouse GPR84

In the case of blockade of the agonist function of compound-1 and PSB-16671 as assessed by [35 S]-GTP γ S incorporation assays, GPR84 antagonist compound-107 showed reduced potency at RAW 264.7 cells compared to the human monocytic cell line THP-1 (section 5.4.2). As further support for this variation in the pharmacology of GPR84 antagonists between mouse and human orthologues, transfected cells expressing cloned mouse and human GPR84 were employed. HEK-293 cells were transiently transfected with FLAG-hGPR84- $G\alpha_{i2}$ C352I and

FLAG-mGPR84-G α_{i2} C352I fusion constructs and membranes were generated after 36 hours of transfection. In [35 S]-GTP γ S binding assays using these membranes, both compound-104 and 107 effectively inhibited response to EC $_{80}$ concentrations of orthosteric agonist compound-1 in a concentration-dependent manner at both human and mouse GPR84-G α_{i2} fusion proteins, affording pIC $_{50}$ of 7.65 \pm 0.03 and 6.5 \pm 0.08 (human vs mouse GPR84) and 8.05 \pm 0.14 and 6.68 \pm 0.05 (human vs mouse GPR84), respectively (Figure 5.12 a,b). Moreover, potencies of compound-104 and 107 were decreased by about 15 and 23-fold, respectively at FLAG-mGPR84-G α_{i2} C352I compared to FLAG-hGPR84-G α_{i2} C352I. Although compound-837 effectively and concentration-dependently blocked compound-1-promoted binding of [35 S]-GTP γ S to G α_i protein associated with human GPR84 with pIC $_{50}$ of 7.96 \pm 0.04, it was totally inactive at FLAG-mGPR84-G α_{i2} C352I (Figure 5.12c).

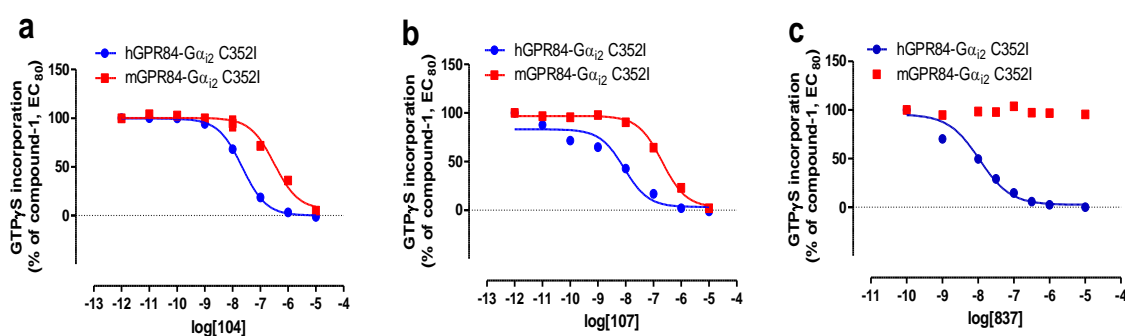


Figure 5.12 Antagonist compounds -104 and 107 are more potent at human GPR84 than the mouse orthologue while compound 837 is inactive at mouse GPR84. Concentration-response curves for compound-104 (a) or compound-107 (b) inhibiting compound-1-stimulated [35 S]-GTP γ S binding to membranes generated from HEK-293 cells transiently transfected with FLAG-hGPR84-G α_{i2} C352I or FLAG-mGPR84-G α_{i2} C352I are shown. Similar studies were performed assessing the ability of varying concentrations of compound-837 to block compound-1-mediated [35 S]-GTP γ S binding to membranes of HEK-293 cells (c).

More intense variations in potencies of compound-104 and 107 between human and mouse GPR84 were observed when membranes purified from doxycycline-induced Flp-In T-REx-293 cells expressing FLAG-hGPR84-G α_{i2} or FLAG-mGPR84-G α_{i2} were used in [35 S]-GTP γ S binding assays. While compound-104 and compound-107 completely reversed compound-1-mediated [35 S]-GTP γ S binding to G α_{i2} associated with both FLAG-hGPR84-G α_{i2} and FLAG-mGPR84-G α_{i2} , potencies to do that were decreased by some 68 and 48-fold, respectively at the FLAG-mGPR84-G α_{i2} compared to the equivalent form of human GPR84 (Figure 5.13 a,c; Table 5.5). In comparison with FLAG-hGPR84-G α_{i2} , FLAG-mGPR84-G α_{i2}

also displayed some 43 and 50-fold reduction in potencies for compound-104 and 107, respectively in inhibiting the response to an EC_{80} concentration of PSB-16671 (Figure 5.13 b,d; Table 5.5). Another notable thing was that while both compound-104 and 107 were able to completely block the PSB-16671-induced [35 S]-GTP γ S binding to membranes expressing FLAG-hGPR84-G α_{i2} , both antagonists failed to block fully agonist function of PSB-16671 mediated by FLAG-mGPR84-G α_{i2} . Saturation binding studies with the radiolabelled antagonist [3 H]-G9543 also revealed the marked differences in affinity of this class of antagonists between human and mouse GPR84. While [3 H]-G9543 bound to FLAG-hGPR84-G α_{i2} with high affinity (K_d : 0.3 ± 0.01 nM), it did not display any significant specific binding to FLAG-mGPR84-G α_{i2} (Figure 5.14) at concentrations up to 30 nM. Consistent with the results obtained from HEK-293 cells transiently transfected with PTX-insensitive fusion proteins, compound-837 entirely blocked agonist effects of both compound-1 and PSB-16671 in Flp-In T-REx-293 cells expressing FLAG-hGPR84-G α_{i2} with pIC_{50} of 8.00 ± 0.02 in both cases whilst it was inactive in cells expressing FLAG-mGPR84-G α_{i2} (Figure 5.13 e,f).

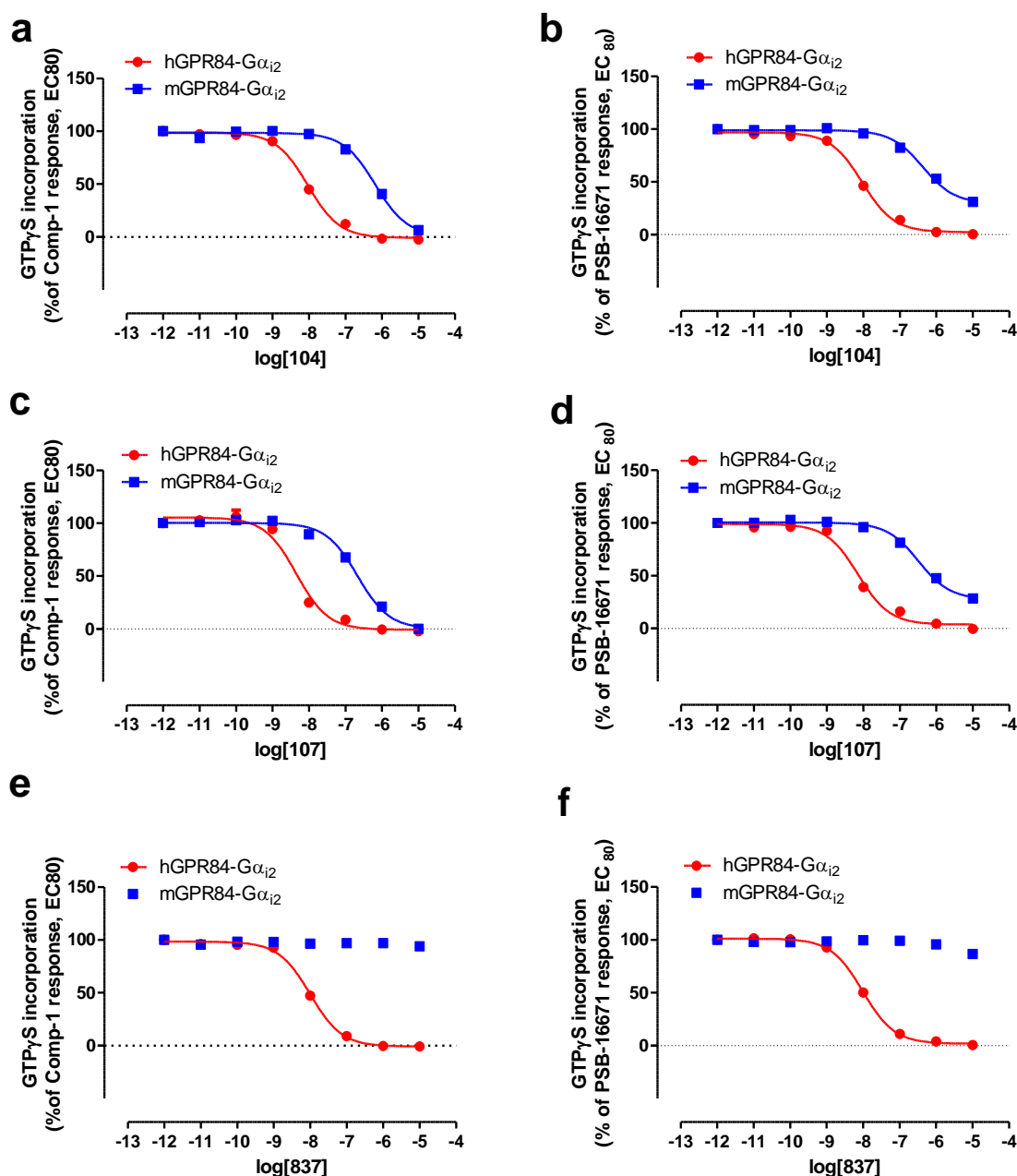


Figure 5.13 Compound-104 and 107 display markedly lower potency at mouse GPR84 compared to the human orthologue while compound-837 is inactive at mouse GPR84. Flp-In T-REx-293 cells stably harbouring FLAG-hGPR84-G α_{i2} or FLAG-mGPR84-G α_{i2} were induced with 100 ng/ml of doxycycline for 24 hours prior to membrane preparation. These membranes were then employed to assess the ability of varying concentrations of compound-104 (a), 107 (c) or 837 (e) to inhibit [³⁵S]-GTP γ S incorporation induced by an EC₈₀ concentration of compound-1. Similar studies were performed to assess the capacity of increasing concentrations of compound-104 (b), 107 (d) or 837 (f) to block [³⁵S]-GTP γ S binding stimulated by an EC₈₀ concentration of PSB-16671. Data represented are pooled from three independent experiments performed on three individual membrane preparations.

Table 5-5 Potencies of compounds-104, 107 and 837 to inhibit the response to an EC₈₀ concentration of compound-1 or PSB-16671 at FLAG-hGPR84-Gα_{i2} or FLAG mGPR84-Gα_{i2}.

| Antagonist | Agonist | | | |
|--------------|------------|--------------|-----------|--------------|
| | Compound-1 | | PSB-16671 | |
| | hGPR84 | mGPR84 | hGPR84 | mGPR84 |
| Compound-104 | 8.04±0.02 | 6.20±0.04*** | 8.03±0.02 | 6.40±0.03*** |
| Compound-107 | 8.35±0.04 | 6.67±0.02*** | 8.20±0.04 | 6.50±0.07** |
| Compound-837 | 8.00±0.02 | Inactive | 8.01±0.02 | Inactive |

[³⁵S]-GTPγS binding assays were conducted using membranes generated from doxycycline-treated stable cells expressing human or mouse GPR84 as fusion protein constructs to determine the potency of different antagonists in inhibiting agonist functions of compound-1 or PSB-16671 as described in Figure 5.13. Data (pIC₅₀) are expressed as mean±S.E.M of three independent experiments performed using three separate membrane preparations generated from doxycycline induced Flp-In T-REx cells stably harbouring FLAG-hGPR84-Gα_{i2} or FLAG-mGPR84-Gα_{i2}. pIC₅₀ values were analysed by two-tailed unpaired t-test. Statistical significance between human and mouse GPR84 are represented as *P<0.05, **P<0.01 and ***P<0.001.

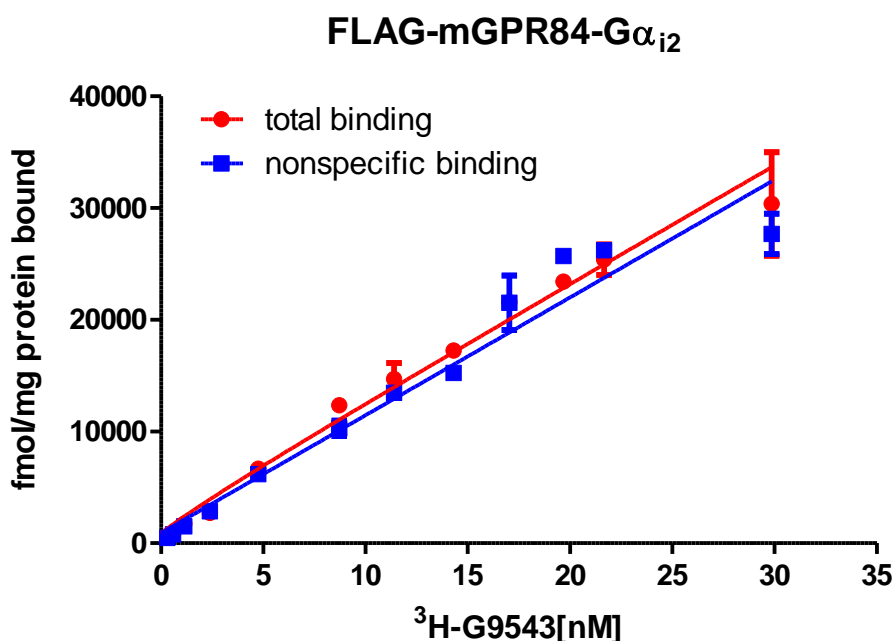


Figure 5.14 The radiolabelled antagonist [³H]-G9543 did not display significant binding to mouse GPR84. Various concentrations (ranging from 0.3 to 30 nM) of radioligand antagonist [³H]-G9543 in the presence (nonspecific binding) or absence (total binding) of 1μM compound-104 were assessed for their ability to bind to membranes generated from Flp-In T-REx cells treated with 100 ng/ml of doxycycline for 24 hours to induce expression of FLAG-mGPR84-Gα_{i2}.

5.6. Discussion

5.6.1. Human and mouse GPR84 can exist as N-glycosylated forms

Glycosylation is a common post-translational phenomenon which has been implicated in regulation and functions of GPCRs (Li et al., 2017). Depending on the type of GPCR, glycosylation has been implicated in protein folding, receptor expression, cell surface trafficking, ligand binding, internalization, desensitization, dimerization and even in signalling bias. For example, Min et al., (2015) reported that N-linked glycosylations are involved in cell surface trafficking and internalization of D2 and D3 receptors and desensitization of D3 receptors. Glycosylations on asparagine 5 and asparagine 15 of the N-terminus were reported to contribute to the dimerization of the β_2 adrenergic receptor (Li et al., 2017). Recently Soto et al., (2015) reported that glycosylations on asparagine 250 and asparagine 259 within the EL2 of the protease-activated receptor-1 (PAR1) were responsible for the $G_{\alpha_{12/13}}$ selectivity of thrombin-activated PAR1 over G_q G protein. Being a very poorly characterized receptor little is known about the regulation of GPR84 and no studies have been performed regarding the roles or extent of glycosylation of this receptor. Herein for the first time I have demonstrated that both human and mouse GPR84 are N-glycosylated. The pre-treatment of membranes generated from cells expressing FLAG-mGPR84- $G_{\alpha_{12}}$ with peptide N-glycosidase (PNGase F) converted poorly resolved multiple bands on SDS-PAGE into predominantly a single band with apparent molecular mass of some 80 kDa, consistent with the monomeric form of the fusion protein construct and confirming differentially N-glycosylated forms of mouse GPR84. Similarly, pre-treatment of membranes of cells expressing FLAG-mGPR84-eYFP or FLAG-hGPR84-eYFP with PNGase F enhanced the intensity of the band having a molecular mass of some 70 kDa which confirmed the cleavage of N-glycans from the glycosylated form of both human and mouse GPR84. PNGase treatment also resulted in slight enhancement of electrophoretic mobility of the protein band having a molecular mass consistent with the monomeric form. These studies confirmed that both human and mouse GPR84 exist as N-glycosylated forms. Asparagine 3 and asparagine 8 of the N-terminus of GPR84 might be the possible N-glycosylation sites because both of these asparagine residues within human and mouse GPR84 are present in the Asn-Xaa-

Ser/Thr motif (where Xaa is not proline) which is known to be the consensus sequence for N-glycosylation of Class A GPCRs (Li et al., 2017; Min et al., 2015; Soto et al., 2015; Landolt-Marticorena and Reithmeier, 1994). Deglycosylation by PNGase treatment also preserved the band having molecular mass of some 155 kDa, corresponding potentially to the dimeric form in the immunoblot of membranes of cells expressing FLAG-hGPR84-eYFP or FLAG-mGPR84-eYFP, suggesting that removal of N-glycans might not affect the dimerization of human or mouse GPR84.

5.6.2.Characterization of orthosteric and allosteric activators of GPR84 in RAW 264.7 cells

The mouse monocyte/macrophage cell line RAW 264.7 is widely employed as an immune cell model to characterize the physiological functions of certain GPCRs having immuno-modulatory effects (Han et al., 2018; Han et al., 2017; Liu et al., 2014; Hudson et al., 2013b; Oh et al., 2010; Wang et al., 2006b). Though previously it was shown that GPR84 mRNA is upregulated in RAW 264.7 cells by pre-treatment with the toll-like receptor 4 (TLR4) agonist LPS, very little was known regarding the functional consequences of LPS treatment and detailed study of the pharmacology of GPR84 ligands in RAW 264.7 cells was also lacking. Only a single study performed by Wang et al., (2006b) reported that the GPR84 agonists decanoic acid, undecanoic acid, lauric acid and DIM enhanced secretion of the pro-inflammatory cytokine IL-12 p40 from LPS-stimulated RAW 264.7 cells in a concentration-dependent manner, while addition of these ligands resulted in no significant release of this cytokine from untreated cells. Though these studies suggested the potential role of GPR84 to control inflammatory processes, it was not confirmed whether these responses of MCFAs or DIM in promoting release of cytokine from RAW 264.7 cells were mediated exclusively by GPR84 as no GPR84 antagonist was available at that time to be used as tool compound to characterize the cellular functions of GPR84. Herein I have characterized the pharmacology of orthosteric and allosteric GPR84 agonists in RAW 264.7 cells and confirmed at least partly that the agonist functions of these ligands were mediated by GPR84 activation in RAW 264.7 cells which were evidenced from the complete blockade of agonist-stimulated effects by established GPR84 antagonists. Herein I have found that in [³⁵S]-GTPγS binding assay, LPS treatment of RAW 264.7 cells led to higher signalling magnitude than in untreated cells,

suggesting increased G protein activation due to the upregulation of GPR84 following LPS stimulation. Despite this, no statistically significant increase in potency for compound-1 was observed following LPS treatment of RAW 264.7 cells, suggesting that upregulation of GPR84 by LPS treatment failed to produce any significant receptor reserve for GPR84. The orthosteric agonists decanoic acid, compound-1, embelin and allosteric agonists DIM and PSB-16671 were found to produce a robust and concentration-dependent enhancement of [35 S]-GTP γ S incorporation into membranes generated from LPS-induced RAW 264.7 cells. These responses to compound-1, PSB-16671 or decanoic acid in RAW 264.7 cells were exerted by GPR84 activation as such effects were effectively and concentration-dependently antagonized by the GPR84 antagonists compound-104 and 107, which displayed similar potencies to those shown at Flp-In T-REx cells expressing mouse GPR84-G α_{i2} . The responses to embelin or DIM in RAW264.7 cells were also mediated by GPR84 activation which was evidenced from the complete blockade of responses to an EC $_{80}$ concentration of DIM or embelin by the GPR84 antagonist GLPG1205. Another important outcome was that in [35 S]-GTP γ S incorporation assays employing membranes of LPS-treated RAW264.7 cells, DIM and embelin functioned as partial agonists of GPR84 compared to decanoic acid and PSB-16671, while compound-1 displayed the highest maximal response. These results are in agreement with those observed in transfected cells expressing cloned mouse GPR84. Compared to decanoic acid, DIM was also found to act as a partial agonist in inducing secretion of IL-12 p40 from LPS-stimulated RAW 264.7 cells (Wang et al., 2006b). Yin et al., (2009) explored that DIM behaved as a partial agonist at the G $_i$ -coupled receptor cannabinoid receptor type 2 (CB $_2$) and functioned as a weak inverse agonist at CB $_1$ receptor. They also reported that DIM-induced inhibition of upregulation of the pro-inflammatory cytokine IL1- β in LPS-stimulated RAW264.7 cells was partially exerted by CB $_2$ receptor as evident from the partial blockade of effect of DIM by a CB $_2$ antagonist. These results indicated that effect of DIM-induced G protein activation in RAW264.7 cells as assessed by [35 S]-GTP γ S assay might not be exclusively mediated by GPR84. However, herein I found that DIM-induced enhanced G protein activation was mediated by GPR84 as DIM-stimulated [35 S]-GTP γ S incorporation into membranes of LPS-induced RAW264.7 cells was completely and effectively inhibited by the GPR84 antagonist GLPG1205.

The potency of embelin measured in RAW 264.7 cells (EC_{50} : 316 nM) was similar to that (EC_{50} : 220 nM in cAMP assays) displayed in HEK-293 cells expressing mouse GPR84 estimated by Gaidarov et al., (2018). While the potency of compound-1 in promoting [35 S]-GTP γ S binding to membranes of LPS-induced RAW 264.7 cells was very similar to that observed at mouse bone marrow-derived neutrophils (pEC_{50} : 7.89 ± 0.12) estimated by Mancini et al., (2019), the potency of PSB-16671 displayed at RAW 264.7 cells was some 15-fold higher than that showed in mouse neutrophils, suggesting that GPR84 might not be the primary target for PSB-16671 in mouse neutrophils. However, measured potencies of compound-1 and PSB-16671 at RAW 264.7 cells were similar to those estimated at LPS-treated THP-1 cells (pEC_{50} : 7.79 ± 0.08 and 6.94 ± 0.07 , respectively) which is in agreement with the maintenance of similar pharmacology of GPR84 agonists between human and mouse orthologue. Further support to this, the potency of compound-1 (EC_{50} : 21 nM) estimated in LPS-induced RAW 264.7 cells was highly similar to that displayed in human neutrophils (EC_{50} : 42 nM in intracellular calcium mobilization assay, Sundqvist et al., 2018).

5.6.3. Antagonists but not agonists of GPR84 display significant variations in pharmacology between human and mouse orthologues

Mouse GPR84 was found to respond to orthosteric and allosteric agonists of GPR84 in a manner very similar to human orthologue, implying that they can be used for translating the pharmacology of GPR84 observed in transfected cells to in-vivo mouse models designed to study the pathophysiological role of GPR84. This maintenance of similar pharmacology of GPR84 agonists between human and mouse GPR84 was observed in both cases when eYFP-tagged receptor or the fusion-protein approach was employed. By contrast, GPR84 antagonists displayed marked variations in potency or affinity between human and mouse orthologues. Though compound-837 was found to effectively antagonize the responses to compound-1 or PSB-16671 at human GPR84 with high potency (IC_{50} : 10 nM), it lacked activity at mouse GPR84 both in Flp-In T-REx cells expressing FLAG-mGPR84-G α_{i2} and in LPS-treated RAW 264.7 cells, implying that this antagonist could not be employed in murine models for the elucidation of physiological functions of GPR84. Though the non-competitive GPR84 antagonist compound-104 displayed high potency (IC_{50} : 10 nM) in blocking the agonist

functions of compound-1 or PSB-16671 at FLAG-hGPR84-G α_{i2} , the potency of this ligand was reduced by 68 and 43-fold, respectively at the equivalent fusion protein of mouse GPR84. Similarly, as estimated by the [35 S]-GTP γ S binding assay, compound-107 displayed very high potency (IC₅₀: 4.5 nM vs compound-1; 6.3 nM vs PSB-16671) in inhibiting the agonist effect of compound-1 or PSB-16671 at FLAG-hGPR84-G α_{i2} whereas mouse versions of the fusion construct showed 48 and 50-fold lower potency, respectively. These lowered potencies of this class of antagonists in blocking effects of GPR84 agonists were also maintained in LPS-treated RAW264.7 mouse monocytes. For example, compared to human monocytes THP-1, RAW 264.7 cells displayed some 23 and 30-fold reductions in potency for compound-107 in inhibiting compound-1 and PSB-16671-mediated G-protein activation, respectively. Similarly, while the GPR84 antagonist GLPG1205 displayed an IC₅₀ of 15 nM in blocking compound-1-promoted increased production of reactive oxygen species (ROS) in TNF α -stimulated human neutrophils (Sundqvist et al., 2018), the measured IC₅₀ value for blocking compound-1-mediated [35 S]-GTP γ S incorporation into membranes of LPS-induced RAW264.7 cells was 600 nM. Though variation in potency between two different assays is not unusual, a 40-fold reduction in potency for GLPG1205 in mouse macrophage compared to human neutrophil suggested that this large variation stems from the species difference. The greatly reduced potencies of this class of antagonists at the mouse orthologue were consistent with the finding that modest concentrations of radiolabelled antagonist [3 H]-G9543 did not show significant specific binding to membranes generated from LPS-treated RAW264.7 cells or transfected cells expressing FLAG-mGPR84-G α_{i2} , indicating substantially lowered affinity of the radioligand or related antagonists to mouse GPR84. These results imply that care should be taken in the case of utilization of these antagonists as GPR84 tool compounds either in mouse disease models or murine cell lines.

Though GLPG1205 failed to generate therapeutic efficacy in phase II clinical trial in ulcerative colitis patients (Vermiere et al., 2017), currently it is under investigation in phase II clinical trial for idiopathic pulmonary fibrosis (IPF) (<https://www.glpg.com/IPF>; Saniere et al., 2019). Despite being considered as a promising therapeutic candidate, mode of binding or mechanism of antagonism of GLPG1205 had not been available in scientific literature. Herein I have found

that GLPG1205 displays varying modes of antagonism in blocking agonist effect of compound-1 and PSB-16671 at mouse GPR84. While GLPG1205 was found to antagonize the agonist function of PSB-16671 in naïve RAW264.7 mouse monocytes in a non-competitive manner, the antagonism of GLPG1205 in blocking the effect of compound-1 in RAW264.7 cells seems to follow a competitive mode of action, displaying a pA_2 affinity value of 7.23. GLPG1205 was also found to be competitive with compound-1 in Flp-In T-REx-293 cells expressing FLAG-mGPR84- $G\alpha_{i2}$ showing a pA_2 affinity value of 6.9. These results suggested that GLPG1205 is likely to bind to a site on mouse GPR84 which is overlapping with the compound-1 binding site but distinct from the site occupied by PSB-16671. Further studies are required to confirm the binding mode of this therapeutically important antagonist.

Though the species-selectivity of ligands of a GPCR poses a great challenge for the biological characterization of the receptor, the elucidation of molecular insight into orthologue selectivity of ligands of specific GPCRs might be helpful to define ligand-binding modes and thus might be utilized for the development of more selective and/potent ligands (Strasser et al., 2013; Milligan, 2011). For example, by applying sequence alignment, homology modelling, mutagenesis studies and radioligand binding assays, Sergeev et al., (2017) identified a single amino acid residue, lysine 65 located within the transmembrane domain II of FFA2 receptor which defined the human-selectivity of the antagonists GLPG0974 and CATPB over rodent orthologues. Similarly, the determination of the molecular basis of human-selectivity of GPR84 antagonist compound-837 over the mouse orthologue might help define the binding mode of this highly potent antagonist. Moreover, defining the molecular determinant(s) responsible for reduced affinity of antagonist compounds-104, 107, 161 or GLPG1205 for mouse GPR84 compared to human orthologue might be helpful for the elucidation of their binding modes and these pieces of information could be used for the generation of more potent antagonist(s). In this context, investigations of molecular basis of species differences in pharmacology of GPR84 antagonists is required for the development of tool compounds to be applied in the translation of in-vitro pharmacology to in-vivo animal disease models.

6 Allosteric modulation of GPR84

6.1. Introduction

Recently allosteric modulation of GPCRs has attracted great interest as this property can be exploited for the development of more selective and safer drug candidates compared to classical drugs which act on orthosteric sites of GPCRs (Hudson et al., 2013c). Drug development programmes based on targeting the orthosteric sites of GPCRs which display high degrees of sequence homology among sub-types face great challenges due to potential off-target effects leading to adverse drug reactions. For example, due to the high sequence homology across orthosteric sites of different sub-types of muscarinic acetylcholine receptors (M_1 , M_2 , M_3 , M_4 and M_5 mAChR), the development of sub-type selective drugs remains challenging (Korczynska et al., 2018; Christopoulos, 2014; Suratman et al., 2011; Chan et al., 2008). In this context, targeting allosteric sites of muscarinic receptors is currently considered to be an effective therapeutic strategy to limit Alzheimer's disease and other neurodegenerative disorders (Korczynska et al., 2018; Moran et al., 2018; Bradley et al., 2017). As allosteric sites are often more divergent than orthosteric sites, allosteric modulators of GPCRs frequently have more sub-type selectivity (Christopoulos, 2014; Wooten et al., 2013; Keov et al., 2011). The sub-type selectivity might also be obtained from selective cooperativity wherein despite having similar binding affinity for different sub-types, allosteric modulators may display cooperativity with the orthosteric agonist only at one sub-type of the receptor. For example, though thiochrome and LY2033298 bind to the allosteric sites of all the mAChR sub-types, they only act as PAMs of function of acetylcholine at M_4 mAChR whilst displaying neutral cooperativity at other subtypes (Suratman et al., 2011; Chan et al., 2008; Lazareno et al., 2004). Moreover, allosteric modulators have been considered to be safer in the case of overdose (Hudson et al., 2013c). This low risk of overdose-mediated toxicity arises from the saturability of the allosteric effect of modulators on orthosteric agonist affinity or efficacy which is limited by the extent of cooperativity between the two ligands (Keov et al., 2011; Wooten et al., 2013). This ceiling effect of allosteric interaction will lead to decreased side effects or toxicity (Christopoulos, 2014) in cases where the drug target (metabotropic glutamate receptors, muscarinic receptor, GABA_A receptor etc.) is associated with highly regulated physiological

function wherein overstimulation can cause adverse drug reactions. One classic example is that benzodiazepines including diazepam, which allosterically enhance the binding affinity of GABA for the GABA_A ionotropic receptor resulting in enhanced opening of the chloride ion channel. This is considered to be safe because the cooperativity between benzodiazepines and GABA is limited (Christopoulos, 2014) which means that after all the allosteric binding sites on the receptor have been occupied by the benzodiazepine, no further enhancement in GABA-mediated signalling will occur irrespective of the concentration of the benzodiazepine in the tissue compartment. Though allosteric modulation of GPCRs has been considered to be a novel therapeutic strategy, only four allosteric modulators (cinacalcet, evocalcet, etelcalcitide and maraviroc) have yet approved for clinical applications (Trinh et al., 2018; Fukagawa et al., 2018; Fukagawa et al., 2017; Dorr et al., 2005; Lindberg et al., 2005).

Recently 3,3'-diindolylmethane (DIM) and the DIM analogue PSB-16671 have been identified as allosteric modulators of human GPR84 (Nikaido et al., 2015; Pillaiyar et al., 2017). Though Pillaiyar and colleagues (2017) reported that both ligands acted as positive allosteric modulators (PAM) of potency and efficacy of decanoic acid at human GPR84 in cAMP accumulation assays, information on the allosteric interaction of DIM or PSB-16671 with other orthosteric GPR84 agonist is lacking. Moreover, no studies have been performed to assess the allosteric effects of DIM or DIM analogues on orthosteric agonist affinity or efficacy at other species orthologues of GPR84. Recently, Gaidarov et al., (2018) reported that GPR84 activation might be exploited for the development of therapeutics to treat atherosclerosis. Though the putative endogenous agonists MCFAs can activate GPR84 with moderate potency, the actions of MCFAs or other synthetic orthosteric agonists at GPR84 could potentially be substantially enhanced by PAM agonists such DIM and it is plausible to exploit such allosteric modulation of GPR84 to develop novel combination therapies against atherosclerosis. In this context, further studies on allosteric modulation of GPR84 are required. Herein I have performed detailed characterization of allosteric interactions between DIM and DIM analogues and orthosteric GPR84 agonists at both human and mouse GPR84.

6.2. DIM analogues 6a and 3a are activators of human GPR84

In [35 S]-GTP γ S binding assays employing membranes purified from Flp-In T-REx-293 cells expressing FLAG-hGPR84-G α_{i2} , two DIM analogues 5,5'-dinitro-3,3'-diindolylmethane (6a) and 5,5'-dimethoxy-3,3'-diindolylmethane (3a) displayed GPR84 agonism whilst three further DIM analogues 5,5'-diiodo-3,3'-diindolyl-(4-methylphenyl)methane (2b), 5,5'-dimethoxy-3,3'-diindolyl-(4-methylphenyl)methane (3b) and 5,5'-dimethoxy-3,3'-diindolyl-(3,5-difluorophenyl)methane (3c) were found to be inactive (Figure 6.1). Though 6a displayed similar potency (pEC_{50} : 5.3 ± 0.9) as DIM (pEC_{50} : 5.3 ± 0.08), the maximal response to 6a ($143 \pm 9.0\%$ of DIM response) was significantly higher than that of DIM. DIM analogue 3a showed reduced potency (pEC_{50} : 4.7 ± 0.10) and efficacy ($80 \pm 6.3\%$ of DIM response) than DIM at FLAG-hGPR84-G α_{i2} (Figure 6.1). In mutagenesis studies it was found that DIM and the DIM analogue PSB-16671 bind to an allosteric site on human GPR84 that is topographically distinct from the orthosteric binding site (section 4.3). Small molecule agonists binding to the allosteric site distinct from that shared by orthosteric agonists frequently affect the potency or efficacy of orthosteric agonists i.e they act as ago-PAMs (Hudson et al., 2014a; Smith et al., 2011b). To assess whether DIM and DIM analogues display any allosteric effects on orthosteric agonist binding affinity or efficacy, interaction studies were performed using [35 S]-GTP γ S binding assays.

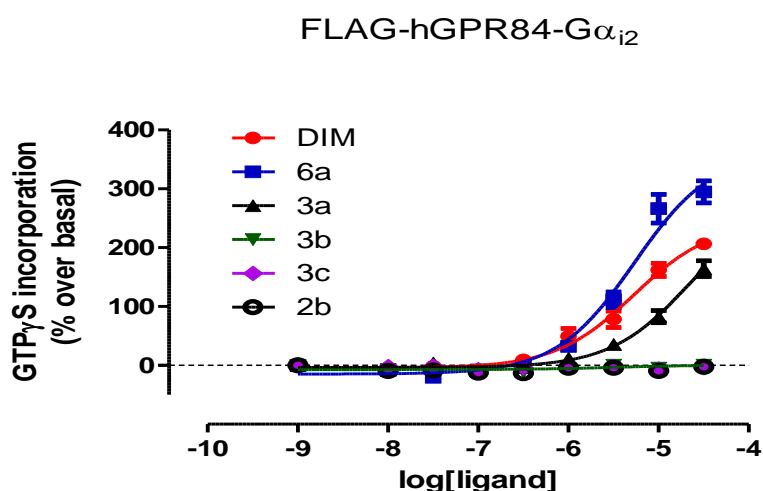


Figure 6.1 DIM analogues 6a and 3a retain the ability to activate human GPR84 while 2b, 3b and 3c lack agonist function. Membranes were purified from doxycycline-induced (100 ng/ml, 24 hours) Flp-In T-REx-293 cells stably harbouring FLAG-hGPR84-G α_{i2} and were subsequently employed in [35 S]-GTP γ S incorporation assays to evaluate the functions of DIM and DIM analogues 2b, 3a, 3b, 3c and 6a.

6.3. DIM is a potent PAM agonist at human GPR84

6.3.1. DIM is a potent PAM of potency and efficacy of decanoic acid

The potential allosteric interaction between DIM and the presumed endogenous agonist decanoic acid (C-10) was evaluated using [35 S]-GTP γ S binding assays employing membranes of Flp-In T-REx-293 cells expressing FLAG-hGPR84-G α_{i2} . In this assay co-addition of increasing fixed concentrations of DIM resulted in progressive increase in potency and efficacy of decanoic acid (Figure 6.2a) indicating that DIM acted as a positive allosteric modulator (PAM) of both affinity and efficacy of C-10. DIM-induced enhancement in potency and efficacy of C-10 approached a saturating level at higher concentrations of DIM (Figure 6.2a) which is consistent with the anticipated saturability of the allosteric effect (Kenakin, 2010; May et al., 2007). Global analysis of the data sets using an operational model of allosterism (Ehlert, 2005; Leach et al., 2007) revealed that DIM showed a high positive cooperativity with C-10 displaying an affinity cooperativity factor, (α value) of 28 ($\log\alpha$: 1.45 ± 0.09) but a more limited activation cooperativity factor, β value of 2.32 ($\log\beta$: 0.36 ± 0.06) (Table 6.1). In reciprocal interaction studies where the protocol was reversed, co-incubation of increasing defined concentrations of C-10 was found to progressively enhance the potency and maximal response of DIM (Figure 6.2b) with estimated affinity cooperativity factor (α value) of 20 ($\log\alpha$: 1.30 ± 0.09) and activation cooperativity factor, β value of 16 ($\log\beta$: 1.20 ± 0.05). These results are broadly consistent with the expected reciprocity of ligand allosteric effects (May et al., 2007) as similar affinity cooperativity values were obtained when the experimental protocol was reversed. The larger variation in the estimated activation cooperativity value (2.3 versus 16 in reciprocal assays) is due to the large difference in intrinsic agonist activity between C-10 and DIM. The estimated average τ value (0.2) for DIM was much lower than that for C-10 (average τ value 1.58) which is consistent with DIM acting as a partial agonist of GPR84 compared to C-10. The extent of allosteric effect on modulation of maximal response i.e the activation cooperativity factor (β) is usually governed by the intrinsic efficacy of the modulator used (van der Westhuizen et al., 2018; Hudson et al., 2014a; Keov et al., 2011). Due to some 8-fold higher intrinsic activity of C-10 than DIM, 7-fold higher activation cooperativity was obtained

when C-10 was employed as the modulator in the reciprocal assay compared to the value observed when DIM was utilized as the modulator. The net affinity/efficacy cooperativity factor ($\alpha\beta$) combining the allosteric effects of allosteric modulator on both affinity and efficacy of orthosteric agonist can also be used for quantifying the magnitude of cooperativity between the two ligands (Hudson et al., 2014a; Smith et al., 2011b; Langmead, 2011). The high net cooperativity value ($\alpha\beta$: 66 and 297 in reciprocal experiment) estimated by the mathematical analysis of allosteric interactions between DIM and C-10 revealed that these ligands strongly modulate the function of each other at human GPR84.

Global fitting of the experimental data obtained from the interaction study between DIM and C-10 using an operational model of allosterism also provided estimates of the binding affinities of DIM and C-10 for the FLAG-hGPR84-G α_{i2} fusion protein. The measured affinity of DIM (K_A : 5.6 to 6.9 μ M) for FLAG-hGPR84-G α_{i2} was about 100 fold higher than for decanoic acid (K_A : 0.18 to 0.50 mM).

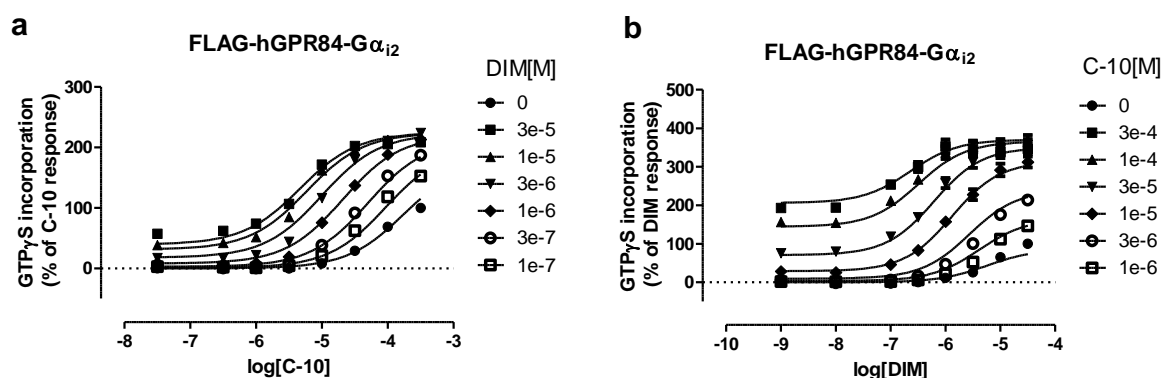


Figure 6.2 DIM and C-10 display strong positive cooperativity in modulating function of each other at human GPR84. Membranes purified from doxycycline-treated (100 ng/ml, 24 hours) Flp-In T-REx-293 cells expressing FLAG-hGPR84-G α_{i2} were employed in [35 S]-GTP γ S incorporation assays to evaluate effects of co-addition of increasing fixed concentrations (ranging from 100 nM to 10 μ M) of DIM on the concentration-response curves for C-10 (a). In reciprocal experiments, various defined concentrations of C-10 ranging from 1 μ M to 300 μ M were assessed for their ability to modulate concentration-response curves for DIM (b). Data shown in (a) and (b) represent mean \pm SEM of three individual experiments performed on three separate membrane preparations carried out in triplicate and curves displayed are best fit curves obtained from global analysis of datasets with an operational model of allosterism. The best fit values of allosteric parameters for the interaction between C-10 and DIM are shown in Table 6.1.

Table 6-1 Allosteric parameters for the interaction between DIM and C-10 at FLAG-hGPR84-G α_{i2} .

| Agonist ^a | C-10 | DIM |
|------------------------------|------------------|------------------|
| Modulator ^b | DIM | C-10 |
| log α | 1.45 \pm 0.09 | 1.30 \pm 0.09 |
| log β | 0.36 \pm 0.06 | 1.20 \pm 0.05 |
| log τ_A | 0.30 \pm 0.058 | -0.66 \pm 0.05 |
| log τ_B | -0.70 \pm 0.02 | 0.08 \pm 0.04 |
| pK _A ^c | 3.30 \pm 0.08 | 5.16 \pm 0.056 |
| pK _B ^d | 5.25 \pm 0.03 | 3.75 \pm 0.066 |
| α | 28.34 | 20.0 |
| β | 2.32 | 15.87 |
| $\alpha\beta$ | 65.74 | 297.2 |

^a Agonist is the compound used to generate concentration-response curve

^b Modulator is the compound used in fixed concentrations

^c pK_A are values estimated for the agonist

^d pK_B are values estimated for the modulator

[³⁵S]-GTP γ S binding studies were performed using membranes generated from doxycycline-induced Flp-In T-REx-293 cells expressing FLAG-hGPR84-G α_{i2} as described in Figure 6.2 to estimate the cooperativity parameters. Data are means \pm SEM of three individual experiments performed on three separate membrane preparations carried out in triplicate.

6.3.2. DIM displays strong allosteric interactions with other orthosteric agonists of human GPR84

To assess whether DIM displays any allosteric effects on binding affinity or efficacy of other orthosteric agonists of GPR84, a set of [³⁵S]-GTP γ S binding assays were performed using membranes expressing FLAG-hGPR84-G α_{i2} . Co-incubation of increasing fixed concentrations of DIM ranging, from 100 nM to 30 μ M, was found to progressively increase the potency of compound-1 without altering the maximal response (Figure 6.3 a_i), displaying an affinity cooperativity factor, α value of 120 (log α 2.08 \pm 0.04) (Table 6.2) which indicates that DIM behaved as a very strong PAM of potency of compound-1. The effect of DIM on binding affinity modulation approached a limit as the potentiation of the potency reached a saturating point at higher concentrations of DIM. In reciprocal assays, increasing defined concentrations of compound-1 ranging from 0.3 nM to 100 nM also progressively enhanced the potency and maximal response of DIM (Figure 6.3 a_{ii}) with an affinity cooperativity factor, α value of 63 (log α : 1.80 \pm 0.1) and activation cooperativity factor, β value of 25 (log β : 1.40 \pm 0.04). Though the magnitude of allosteric effect of compound-1 on binding affinity of DIM was 1.9-fold higher than that of DIM on compound-1, the difference did not reach statistical significance level (P value>0.05, two-tailed unpaired t test).

The large variation in the activation cooperativity value (0.9 vs 25 in the reciprocal assays) was not unexpected as it stems from the substantial difference in intrinsic agonist activity between compound-1 (average τ value 6.8) and DIM (average τ value 0.43). Global analysis of the experimental data with an operational model of allosterism revealed that compound-1 (average K_A : 100 nM) binds FLAG-hGPR84-G α_{i2} with 50-fold higher affinity than DIM (average K_A : 5.0 μ M).

DIM also acted as a highly effective PAM of potency of 6-OAU as increasing defined concentrations of DIM progressively enhanced the potency of 6-OAU (Figure 6.3 c_i) with the binding affinity cooperativity factor, α value, of 126 ($\log\alpha$: 2.1 ± 0.14) (Table 6.2) without altering the maximal response. Equivalent outcomes were obtained in reciprocal assays wherein various concentrations of 6-OAU ranging from 10 nM to 3 μ M gradually increased the potency as well as maximal response of DIM (Figure 6.3 c_{ii}) with the affinity cooperativity factor, α value of 68 ($\log\alpha$: 1.83 ± 0.1) and activation cooperativity factor, β value of 8.0. As 6-OAU (average τ value: 3.41) displayed some 8.3-fold higher intrinsic agonist activity than DIM (average τ value 0.41), proportionally 8-fold higher activation cooperativity value was obtained when 6-OAU was used as the modulator in the allosteric interaction study than in the case when DIM was employed as the modulator. Mathematical analysis of allosteric interaction between 6-OAU and DIM estimated the binding affinity of the two ligands to be 1.3 μ M and 8.9 μ M, respectively.

DIM acted as a PAM of potency and efficacy of embelin as increasing fixed concentrations of DIM was found to increase the potency as well as maximal response of the embelin (Figure 6.3 b_i) with an affinity cooperativity factor, α value of 16 and activation cooperativity factor, β value of 7.6 (Table 6.2). Similar outcomes were obtained in the reciprocal assay, where various fixed concentrations of embelin also caused a large leftward and upward shifting of the concentration-response curves of DIM (Figure 6.3 b_{ii}) with affinity cooperativity factor, α value of 13.0 and activation cooperativity factor, β value of 11.4. Embelin (average τ value: 0.57) displayed 1.78-fold higher intrinsic efficacy than DIM (average τ value: 0.32) and thus a 1.5-fold higher magnitude of allosteric effect on efficacy was observed when embelin was employed as the modulator in reciprocal allosteric experiments. The net affinity/efficacy

cooperativity factor, $\alpha\beta$ value of 122 and 148 (for the reciprocal assay) revealed that the magnitude of cooperativity between embelin and DIM was very high and in contrast to allosteric effects between DIM and compound-1/6-OAU, allosteric effects of DIM on embelin were governed by both affinity and efficacy modulation. Global analysis of allosteric effects of embelin on DIM and vice versa also estimated the binding affinities of two ligands. Embelin (average K_A : 2.6 μM) was found to bind human GPR84 with 2.7-fold higher avidity than DIM (average K_A : 7.1 μM).

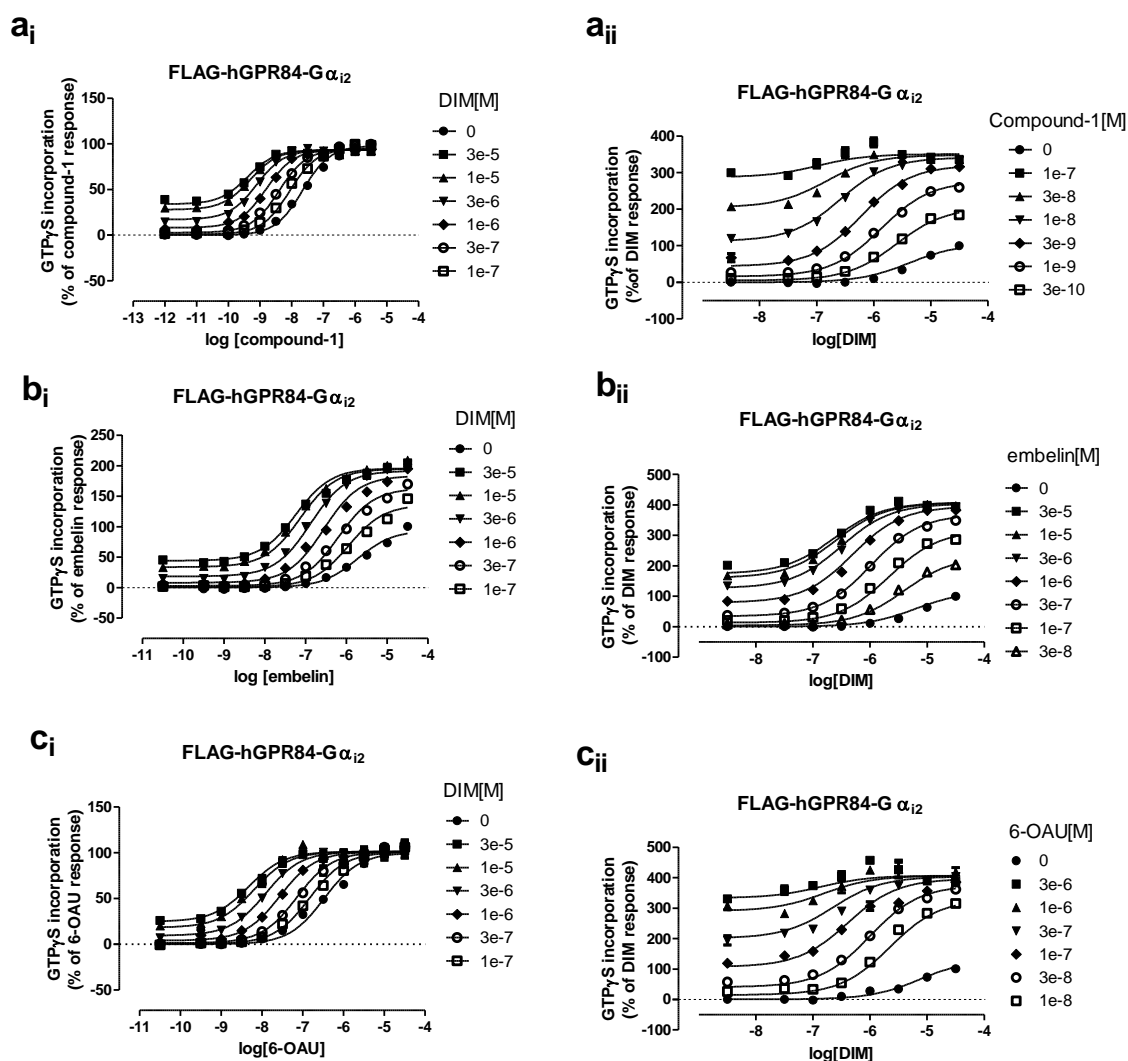


Figure 6.3 DIM is a potent PAM of potency of compound-1 and 6-OAU at human GPR84 while it modulates both the potency and efficacy of embelin. Membranes prepared from doxycycline-induced (100 ng/ml, 24 hours) Flp-In T-REx-293 cells stably harbouring FLAG-hGPR84-G α_{i2} were used in [35 S]-GTP γ S incorporation assays wherein increasing fixed concentrations of DIM ranging from 100 nM to 30 μ M were co-added to concentration-response assays for compound-1 (**a_i**), embelin (**b_i**) or 6-OAU (**c_i**) to assess their capacity to modulate the function of the corresponding orthosteric agonist. Similar co-addition studies assessing the effect of various increasing concentrations of compound-1 (**a_{ii}**), embelin (**b_{ii}**) or 6-OAU (**c_{ii}**) on concentration-response curves for DIM were performed. Data are means \pm SEM of three independent experiments performed on three separate membrane preparations carried out in duplicate (**a_i**, **b_i**, **c_i**) or triplicate (**a_{ii}**, **b_{ii}**, **c_{ii}**). Fitted curves displayed are from global analysis of datasets fitted with an operational model of allosterism. The best fit values of allosteric parameters of interaction between DIM and corresponding orthosteric agonist are shown in Table 6.2.

Table 6-2 Allosteric parameters for the interactions between DIM and different orthosteric agonists in [³⁵S]-GTPγS binding assays at FLAG-hGPR84-Gα_{i2}.

| Agonist ^a | Compound-1 | DIM | Embelin | DIM | 6-OAU | DIM |
|------------------------------|------------|------------|-----------|-----------|------------|------------|
| Modulator ^b | DIM | Compound-1 | DIM | Embelin | DIM | 6-OAU |
| logα | 2.08±0.04 | 1.80±0.10 | 1.20±0.05 | 1.11±0.04 | 2.10±0.14 | 1.83±0.10 |
| logβ | -0.06±0.01 | 1.4±0.04 | 0.88±0.03 | 1.06±0.03 | -0.03±0.07 | 0.91±0.2 |
| logτ _A | 0.73±0.10 | -0.43±0.03 | -0.2±0.02 | -0.5±0.03 | 0.61±0.07 | -0.28±0.15 |
| logτ _B | -0.31±0.01 | 0.91±0.10 | -0.5±0.02 | -0.3±0.01 | -0.52±0.06 | 0.44±0.04 |
| pK _A ^c | 7.21±0.03 | 5.24±0.04 | 5.5±0.04 | 5.1±0.03 | 5.76±0.1 | 5.05±0.05 |
| pK _B ^d | 5.31±0.03 | 6.72±0.10 | 5.2±0.04 | 5.7±0.02 | 5.1±0.01 | 6.00±0.10 |
| α | 120 | 63 | 16 | 13 | 126 | 68 |
| β | 0.9 | 25 | 7.6 | 11.4 | 0.93 | 8.0 |
| αβ | 108 | 1575 | 122 | 148 | 117 | 544 |

^a Agonist is the compound used to generate concentration-response curve

^b Modulator is the compound used in defined concentrations

^c pK_A are values estimated for the agonist

^d pK_B are values estimated for the modulator

A set of [³⁵S]-GTPγS binding studies were performed using membranes generated from doxycycline-induced Flp-In T-REx-293 cells expressing FLAG-hGPR84-Gα_{i2} as described in Figure 6.3 to estimate the allosteric parameters for the interaction between DIM and GPR84 orthosteric agonists. Data are means ± SEM of three independent experiments performed on three separate membrane preparations.

6.3.3. DIM displays probe dependence in allosteric modulation of potency of orthosteric agonists

DIM displayed probe dependence in enhancing the potency of orthosteric GPR84 agonists (Figure 6.4 a). The greatest increment of the potency was observed for compound-1 and 6-OAU (affinity cooperativity values of 120 and 126, respectively). This enhancement in potency of compound-1 and 6-OAU was significantly higher ($P < 0.001$) than DIM-promoted potentiation (α value of 28) of the potency of the putative endogenous agonist, C-10. Moreover, the DIM-induced increase (16-fold) in potency of embelin was significantly ($P < 0.05$) lower than that for C-10 (28-fold increase). These results indicated that the magnitude of positive affinity cooperativity between DIM and various potential orthosteric agonists depends on the nature of the orthosteric agonist and strongly correlates with the efficacy of the orthosteric agonist. The higher the maximal response of the orthosteric agonist used as the probe for GPR84 function, the higher was the affinity modulation exerted by DIM. This feature of probe dependence of DIM-promoted allosteric modulation of GPR84 orthosteric agonist functions indicated that allosteric interaction of DIM with human GPR84 might follow the two-state Monod-Wyman-Changeux (MWC) model which has been implicated for the mechanism of probe-dependence of allosteric ligands (Canals et al., 2012). However, little probe dependence was observed when net affinity/efficacy cooperativity (αβ) displayed by the allosteric interaction of DIM with orthosteric

agonists was considered (Figure 6.4 b). Similar net positive cooperativity ($\alpha\beta=122$) was observed with a low efficacy agonist i.e. embelin compared to those displayed when full agonist compound-1 ($\alpha\beta=108$) or 6-OAU ($\alpha\beta=117$) was used as the modulator. Though, the net positive cooperativity ($\alpha\beta=67$) obtained from the allosteric interaction of DIM with C-10 was some 1.6-fold lower than that for compound-1, the difference was not statistically significant.

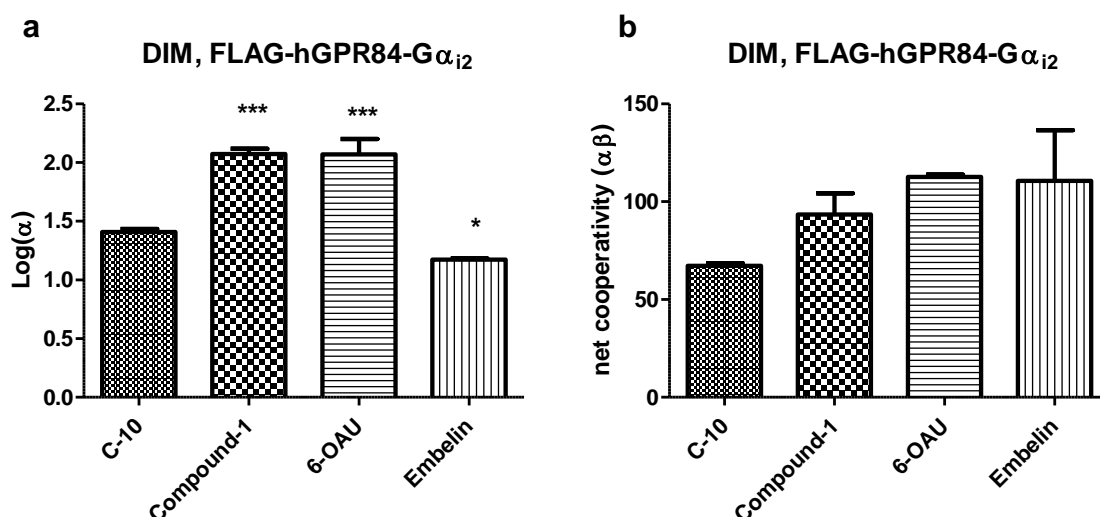


Figure 6.4 Probe dependence of DIM-promoted affinity modulation of different GPR84 orthosteric agonists at FLAG-hGPR84-G α_{i2} . Logarithm of the binding affinity cooperativity ($\log\alpha$) or net affinity/efficacy cooperativity ($\alpha\beta$) were determined by fitting data obtained from allosteric interaction studies between DIM and orthosteric agonists to the operational model of allosterism. $\log\alpha$ or $\alpha\beta$ values were analysed by one-way ANOVA followed by Dunnett's multiple comparison tests using value for C-10 as the control. Statistical significance between values for C-10 and other orthosteric agonist was expressed as * $P<0.05$, ** $P<0.01$, *** $P<0.001$

6.3.4. DIM acts as a moderately potent PAM of potency of compound-1 and C-10 at mouse GPR84 while it behaves as a potent PAM of potency but weak NAM of efficacy of compound-1 in LPS-treated RAW264.7 cells

To see whether DIM displays any orthologue selectivity in terms of cooperativity with compound-1, allosteric interaction studies were performed assessing effects of increasing fixed concentrations of DIM on the ability of compound-1 to stimulate [35 S]-GTP γ S binding to membranes purified from doxycycline-induced Flp-In T-REx-293 cells expressing FLAG-mGPR84-G α_{i2} or from LPS-treated RAW264.7 cells. DIM was also found to act as a PAM of potency of compound-1 at FLAG-mGPR84-G α_{i2} as increasing concentrations of DIM caused a progressive left-

ward shift of concentration-response curve of compound-1 (Figure 6.5a).

However a marked decrease in cooperativity between DIM and compound-1 was observed at FLAG-mGPR84-G α_{i2} compared to FLAG-hGPR84-G α_{i2} . DIM displayed 7.5-fold lower binding affinity cooperativity (α : 16 vs 120, for FLAG-mGPR84-G α_{i2} and FLAG-hGPR84-G α_{i2} , respectively) and approximately 4-fold lower net affinity/efficacy cooperativity ($\alpha\beta$: 26 vs 108) at mouse GPR84 than the human orthologue. The estimated binding affinities of compound-1 and DIM for FLAG-mGPR84-G α_{i2} (K_A : 181 nM and 4.8 μ M, respectively) were very similar to those for FLAG-hGPR84-G α_{i2} (K_A : 100 nM and 5.0 μ M, respectively) which is in good agreement with the maintenance of similar potency values of compound-1 and DIM between human and mouse GPR84 (section 5.3).

In LPS-treated RAW264.7 cells DIM behaved as a potent PAM of potency but weak NAM of efficacy of compound-1, displaying a binding affinity cooperativity factor, α , value of 129 and efficacy cooperativity factor, β , value of 0.22 (Figure 6.5b, Table 6.3). Though DIM caused a 4.5-fold (β : 0.22) decrease in maximal response to compound-1, this effect was outcompeted by high positive binding cooperativity (α : 129) leading to an overall affinity/efficacy cooperativity value, $\alpha\beta$ of 28 which is equivalent to that displayed at FLAG-mGPR84-G α_{i2} . By contrast, DIM acted as a moderately potent PAM of potency of C-10 (Figure 6.5c) displaying affinity cooperativity factor, α , value of 16.3 while the effect of DIM on efficacy of C-10 was marginal (β : 0.74). These results demonstrated that DIM also displayed probe dependence in modulating function of orthosteric agonists of GPR84 in RAW264.7 cells as it showed 7.9-fold lower affinity cooperativity and 2.4-fold lower net affinity/efficacy cooperativity with C-10 than those exhibited with compound-1. This higher cooperativity with compound-1 than C-10 was due to the higher intrinsic agonist activity of compound-1 (τ : 8.7) than C-10 (τ : 3.2) in RAW264.7 cells which is consistent with the fact that degree of cooperativity tracks with the intrinsic efficacy of the orthosteric probe (van der Westhuizen et al., 2018).

Similar to the results observed at FLAG-hGPR84-G α_{i2} and FLAG-mGPR84-G α_{i2} , DIM acted as a weak partial agonist (operational efficacy, τ : 0.32) at RAW264.7 cells compared to compound-1 (τ : 8.7) or C-10 (τ : 3.2). Similarly, equivalent binding affinities of compound-1 and DIM for mouse GPR84 were observed at RAW264.7

cells (K_A : 190 nM and 6.0 μ M, respectively) and transfected cells expressing FLAG-mGPR84-G α_{i2} .

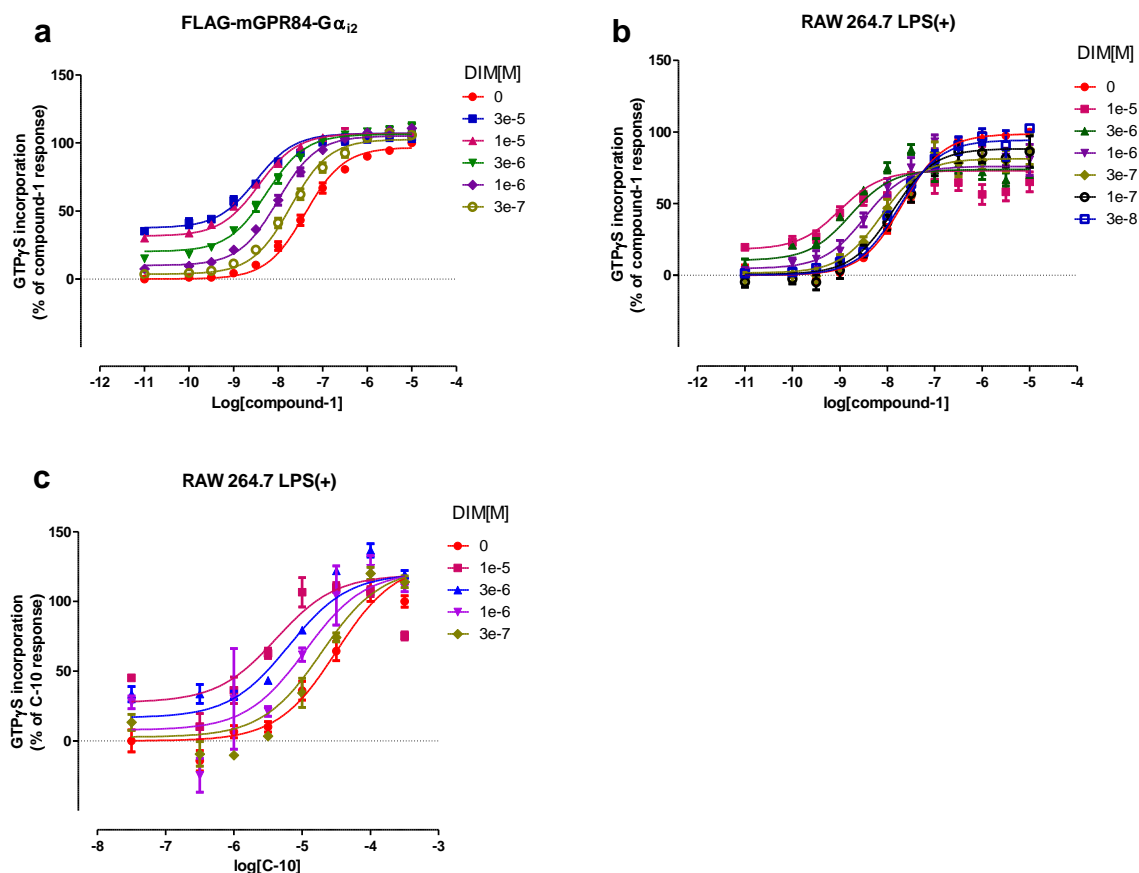


Figure 6.5 DIM acts as a PAM of potency of compound-1 at FLAG-mGPR84-G α_{i2} while it behaves as a PAM of affinity and NAM of efficacy of compound-1 at LPS-treated RAW264.7 cells. Membranes were generated from doxycycline-induced (100 ng/ml, 24 hours) Flp-In T-REx-293 cells stably harbouring FLAG-mGPR84-G α_{i2} or from LPS-treated (100 ng/ml, 5 hours) RAW264.7 cells. Effects of co-incubation of increasing fixed concentrations of DIM on compound-1-mediated [35 S]-GTP γ S incorporation into membranes expressing FLAG-mGPR84-G α_{i2} were then evaluated (a). Similarly, interaction studies were performed using membranes of LPS-treated RAW264.7 cells wherein effects of various increasing fixed concentrations of DIM on potency and efficacy of compound-1(b) or C-10 (c) were assessed. Data are mean \pm SEM of two (a, c) or three (b) independent experiments performed on separate membrane preparations carried out in duplicate (a,b) or in triplicate (c). Curves displayed are from fitting datasets with an operational model of allosterism and allosteric parameters of interaction between DIM and compound-1/C-10 are shown in Table 6.3.

Table 6-3 Allosteric parameters for the interaction between compound-1/C-10 and DIM at mouse GPR84.

| | FLAG-mGPR84-G α_{i2} | RAW264.7 | |
|------------------------------|-----------------------------|------------------|------------------|
| Agonist ^a | Compound-1 | Compound-1 | C-10 |
| Modulator ^b | DIM | DIM | DIM |
| log α | 1.20 \pm 0.10 | 2.11 \pm 0.23 | 1.21 \pm 0.38 |
| log β | 0.20 \pm 0.09 | -0.65 \pm 0.10 | -0.13 \pm 0.20 |
| log τ_A | 0.51 \pm 0.18 | 0.94 \pm 0.10 | 0.50 \pm 0.17 |
| log τ_B | -0.32 \pm 0.08 | -0.5 \pm 0.10 | -0.53 \pm 0.17 |
| pK _A ^c | 6.74 \pm 0.01 | 6.72 \pm 0.10 | 3.88 \pm 0.26 |
| pK _B ^d | 5.32 \pm 0.01 | 5.22 \pm 0.20 | 5.30 \pm 0.30 |
| α | 16 | 129 | 16.3 |
| β | 1.6 | 0.22 | 0.74 |
| $\alpha\beta$ | 25.44 | 28.4 | 12.0 |

^a Agonist is the compound used to generate concentration-response curve

^b Modulator is the compound used in fixed concentrations

^c pK_A are values estimated for the agonist

^d pK_B are values estimated for the modulator

A series of [³⁵S]-GTP γ S binding studies were performed using membranes generated from doxycycline-induced Flp-In T-REx-293 cells expressing FLAG-mGPR84-G α_{i2} or from LPS-treated RAW264.7 cells as described in Figure 6.5 and the allosteric parameters for the interaction between DIM and GPR84 orthosteric agonists were then measured using an operational model of allosterism. Data are means \pm SEM of two (for FLAG-mGPR84-G α_{i2}) or three (for RAW264.7 cells) individual experiments performed on separate membrane preparations.

6.4. DIM analogue 3a is a PAM agonist at human GPR84

6.4.1. DIM analogue 3a is a potent PAM of potency of compound-1 and 6-OAU

As for DIM, the DIM analogue 3a (5,5'-dimethoxy-3,3'-diindolylmethane) was also found to act as a strong positive allosteric modulator at human GPR84 as increasing concentrations of 3a increased the potency of compound-1 (Figure 6.6 a_i) and 6-OAU (Figure 6.6 b_i) yielding affinity cooperativity factor, α , values of 56 and 100, respectively. When the allosteric assay protocol was reversed, both compound-1 and 6-OAU also potentiated the function of 3a by modulating both potency and maximal response (Figure 6.6 a_{ii} and b_{ii}) with affinity cooperativity factor, α , value of 25.1 and 29.5, respectively and activation cooperativity factor, β , value of 19.5 and 14, respectively (Table 6.4). Though the allosteric effect of 6-OAU on binding affinity of 3a for hGPR84 was not statistically different ($P > 0.05$) from that of 3a on 6-OAU, the magnitude of affinity modulation of 3a by compound-1 was statistically different ($P < 0.001$) from that of compound-1 by 3a, which is not consistent with the maintenance of similar value in reciprocal allosteric interaction studies. The operational efficacy value,

τ for 3a (average τ : 0.26 and 0.35, respectively for interaction with compound-1 and 6-OAU) was 16 and 11-fold lower than that for compound-1 (average τ : 4.1) and 6-OAU (average τ : 3.81), respectively; indicating that 3a is a weak partial agonist compared to compound-1 and 6-OAU. Owing to this marked variation in intrinsic agonist activity between 3a and compound-1/6-OAU, 19.5 and 11-fold higher magnitudes of efficacy modulation were obtained when compound-1 or 6-OAU was employed as the modulator than when 3a was used as the modulator in the allosterism experiments. Application of an operational model of allosterism to the global analysis of allosterism data revealed that 3a binds FLAG-hGPR84- $G\alpha_{i2}$ with modest affinity (average K_A : 12.5 μ M and 29 μ M, respectively for interaction with compound-1 and 6-OAU) while the binding affinity of compound-1 and 6-OAU was estimated to be 86 nM and 1.0 μ M, respectively. These are very similar to measured binding affinity values obtained from the mathematical analysis of allosteric interaction of DIM with compound-1/6-OAU (section 6.3.2).

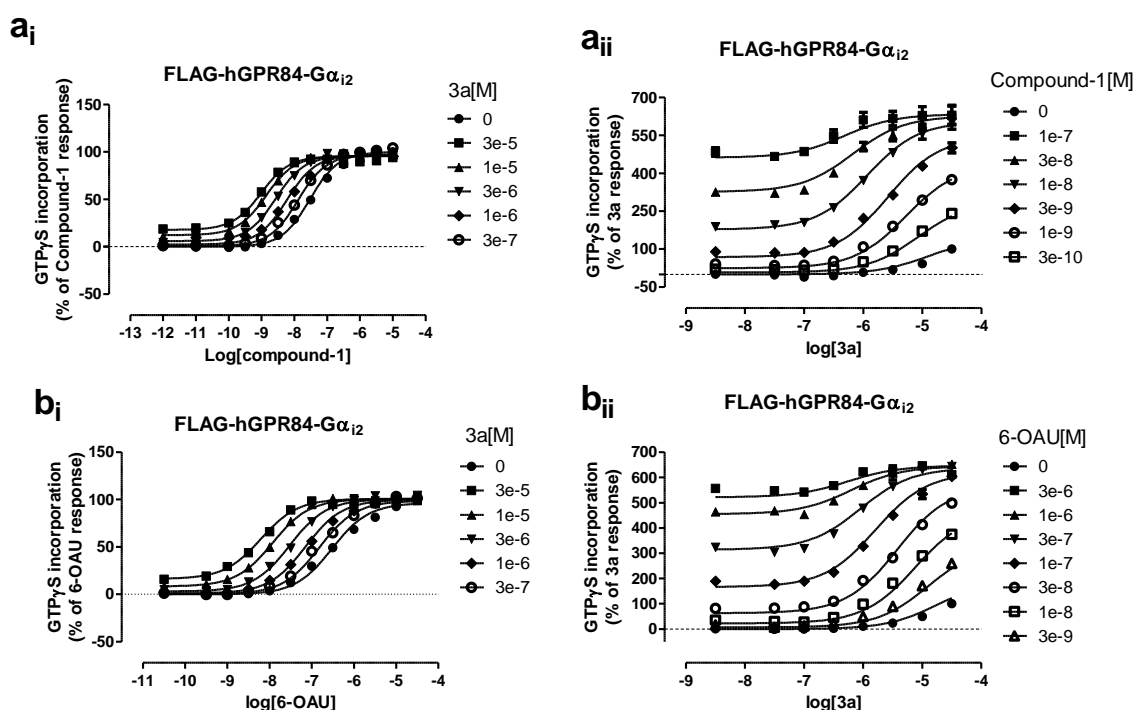


Figure 6.6 DIM analogue 3a is a potent PAM of potency of compound-1 and 6-OAU at human GPR84. Effects of co-incubation of increasing fixed concentrations of 3a ranging from 300 nM to 30 μ M on the concentration-response assays of compound-1 (a_i) or 6-OAU (b_i) were evaluated using [³⁵S]-GTP γ S incorporation assays employing membranes of Flp-In T-REx-293 cells expressing FLAG-hGPR84- $G\alpha_{i2}$. Equivalent co-addition studies were performed assessing the effects of increasing fixed concentrations of compound-1 (a_{ii}) or 6-OAU (b_{ii}) on the concentration-response curves for 3a. Data represent means \pm SEM of five (a_i), three (a_{ii}, b_i) or two (b_{ii}) independent experiments performed on separate membrane preparations. Curves displayed are from global fitting of datasets with operational model of allosterism and best fit values of allosteric parameters are shown in Table 6.4.

6.4.2. DIM analogue 3a is a moderately potent PAM of potency and efficacy of decanoic acid

DIM analogue 3a and C-10 also displayed effective positive cooperativity in modulating function of each other at FLAG-hGPR84-G α_{i2} and this cooperativity was governed by both affinity and efficacy modulation. Co-incubation of various defined concentrations of 3a ranging from 300 nM to 30 μ M resulted in progressive enhancement of potency as well as maximal response to C-10 (Figure 6.7a), yielding an affinity cooperativity factor, α , value of 6.84 ($\log \alpha$: 0.65 ± 0.2) and activation cooperativity factor, β value of 4.5 (Table 6.4). Equivalent outcomes were obtained in reciprocal assays wherein increasing defined concentrations of C-10 also enhanced the potency and efficacy of 3a (Figure 6.7b) with affinity cooperativity factor, α , value of 3.4 ($\log \alpha$: 0.53 ± 0.13) and activation cooperativity factor, β , value of 82.7. The 18-fold increase in the magnitude of efficacy modulation in such reciprocal assays reflected similar degrees of increase in intrinsic agonist activity of C-10 (average τ : 2.0) compared to that of 3a (average τ : 0.1) which is consistent with the dependence of the efficacy modulation on the intrinsic activity of the modulator used. The estimated binding affinities of C-10 and 3a for FLAG-hGPR84-G α_{i2} obtained from fitting data with an operational model of allosterism were 0.38 mM and 7 μ M, respectively, which are similar to the values obtained in the allosteric interaction studies between C-10 and DIM (section 6.3.1) and between 3a and compound-1 (section 6.4.1).

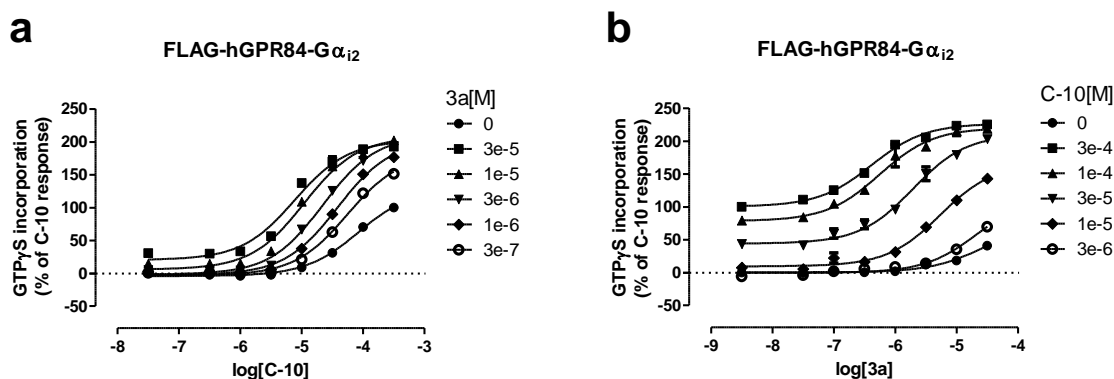


Figure 6.7 DIM analogue 3a is a moderately potent PAM of potency and efficacy of C-10 at human GPR84. Membranes isolated from doxycycline-treated (100 ng/ml, 24 hours) Flp-In T-REx-293 cells expressing FLAG-hGPR84-G α_{i2} were employed in [35 S]-GTP γ S binding assays in which increasing fixed concentrations of DIM analogue 3a, ranging from 300 nM to 30 μ M, were assessed for their ability to affect concentration-response curves for C-10 (a). In reciprocal interaction studies, increasing fixed concentrations of C-10 ranging from 3 μ M to 0.3 mM were co-incubated with concentration-response assays for 3a to evaluate their effects on potency and efficacy of 3a. Curves shown in (a) and (b) are from global fitting of datasets with an operational model of allosterism and best fit values of allosteric parameters are shown in Table 6.4.

Table 6-4 Operational model parameters of allosteric interactions between 3a and different orthosteric agonists at FLAG-hGPR84-G α_{i2}

| Agonist ^a | Compound-1 | 3a | 6-OAU | 3a | C-10 | 3a |
|------------------------|------------------|-------------------|------------------|------------------|-----------------|------------------|
| Modulator ^b | 3a | Compound-1 | 3a | 6-OAU | 3a | C-10 |
| log α | 1.75 \pm 0.05 | 1.4 \pm 0.09*** | 2.0 \pm 0.14 | 1.47 \pm 0.06 | 0.83 \pm 0.2 | 0.53 \pm 0.13 |
| log β | -0.06 \pm 0.02 | 1.3 \pm 0.06 | 0.1 \pm 0.05 | 1.15 \pm 0.04 | 0.65 \pm 0.16 | 1.92 \pm 0.12 |
| log τ_A | 0.70 \pm 0.13 | -0.62 \pm 0.01 | 0.65 \pm 0.1 | -0.45 \pm 0.04 | 0.46 \pm 0.1 | -1.07 \pm 0.12 |
| log τ_B | -0.54 \pm 0.13 | 0.51 \pm 0.1 | -0.46 \pm 0.03 | 0.5 \pm 0.02 | -1.1 \pm 0.08 | 0.05 \pm 0.04 |
| pK $_A^c$ | 7.01 \pm 0.04 | 4.82 \pm 0.06 | 5.9 \pm 0.07 | 4.62 \pm 0.05 | 3.24 \pm 0.14 | 5.2 \pm 0.07 |
| pK $_B^d$ | 5.0 \pm 0.05 | 7.12 \pm 0.05 | 4.46 \pm 0.14 | 6.1 \pm 0.03 | 5.1 \pm 0.06 | 3.71 \pm 0.07 |
| α | 56 | 25.1 | 100 | 29.5 | 6.84 | 3.4 |
| β | 0.9 | 19.5 | 1.25 | 14.0 | 4.5 | 82.7 |
| $\alpha\beta$ | 50.4 | 490 | 125 | 413 | 31 | 281 |

^a Agonist is the compound used to generate concentration-response curve

^b Modulator is the compound used in defined concentrations

^c pK $_A$ are values estimated for the agonist

^d pK $_B$ are values estimated for the modulator

A series of [35 S]-GTP γ S binding studies were performed using membranes generated from doxycycline-induced Flp-In T-REx-293 cells expressing FLAG-hGPR84-G α_{i2} as described in Figure 6.6 and 6.7 and the allosteric parameters for the interaction between DIM analogue 3a and different GPR84 orthosteric agonists were then estimated using an operational model of allosterism. Data are means \pm SEM. Log α values were analysed by unpaired two-tailed t test with statistical significance expressed as ***P<0.001.

6.4.3. DIM analogue 3a displays probe dependence in modulating function of GPR84 orthosteric agonists

DIM analogue 3a displayed probe-dependence in potentiating function of orthosteric agonists in human GPR84. In [35 S]-GTP γ S binding assays, the extent of 3a-mediated binding affinity modulation for compound-1 or 6-OAU was

significantly higher than for C-10 (Figure 6.8) which correlated with the higher efficacy of compound-1/6-OAU (average τ : 4.1 and 3.8, respectively) than C-10 (average τ : 2.0). Though the degree of potentiation of binding affinity of 6-OAU for human GPR84 was 2.4-fold higher than that for compound-1, the difference did not reach statistical significance level ($P > 0.05$, two-tailed unpaired t test). Another important thing to be noted was that 3a significantly enhanced the maximal response of C-10 by a factor of 4.5 whereas no significant efficacy modulation was obtained from the allosteric interaction between 3a and compound-1 or 6-OAU (β : 0.9 and 1.25, respectively). The greatest extent of overall positive cooperativity ($\alpha\beta$: 125) was obtained for 6-OAU which was significantly higher than those displayed in the interaction study when C-10 ($\alpha\beta$: 31) or compound-1 ($\alpha\beta$: 51) was used to probe the function of human GPR84.

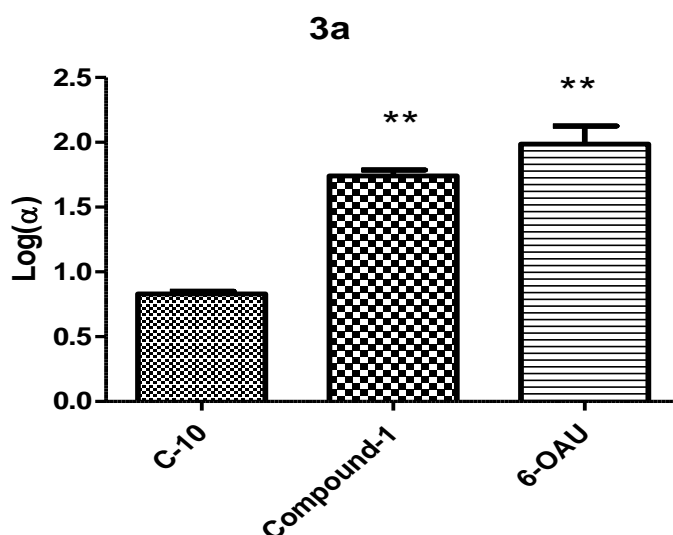


Figure 6.8 DIM analogue 3a exhibits probe-dependence in modulating binding affinity of orthosteric agonists at human GPR84 in [35 S]-GTP γ S binding assays. $\text{Log}\alpha$ values were determined by applying an operational model of allosterism to data obtained from the interaction study between 3a and defined orthosteric agonists and were analysed by one way-ANOVA followed by Tukey's multiple comparison tests. Statistical significance is expressed as * $P < 0.05$, ** $P < 0.01$ and *** $P < 0.001$.

6.5. DIM analogue 6a is a weak NAM of efficacy of compound-1 at human GPR84

DIM analog 5,5'-dinitro-3,3'-diindolylmethane (6a) is a weak negative allosteric modulator (NAM) of the efficacy of compound-1 at FLAG-hGPR84-G α_{i2} as co-addition of different increasing concentrations of 6a resulted in decrease in maximal response to compound-1 with activation cooperativity factor, β value of 0.12, without altering the potency of compound-1 (Figure 6.9 and Table 6.5). The application of an operational model of allosterism for analysis of experimental data estimated the binding affinity of compound-1 for FLAG-hGPR84-G α_{i2} to be 125 nM which is equivalent to values measured from the analysis of allosteric effects of DIM on compound-1 (section 6.3.2). The estimated binding affinity of 6a (K_A : 9.0 μ M) was very similar to that of parent compound DIM (K_A : 5 μ M) which is in agreement with their equivalent potency values at FLAG-hGPR84-G α_{i2} (Figure 6.1)

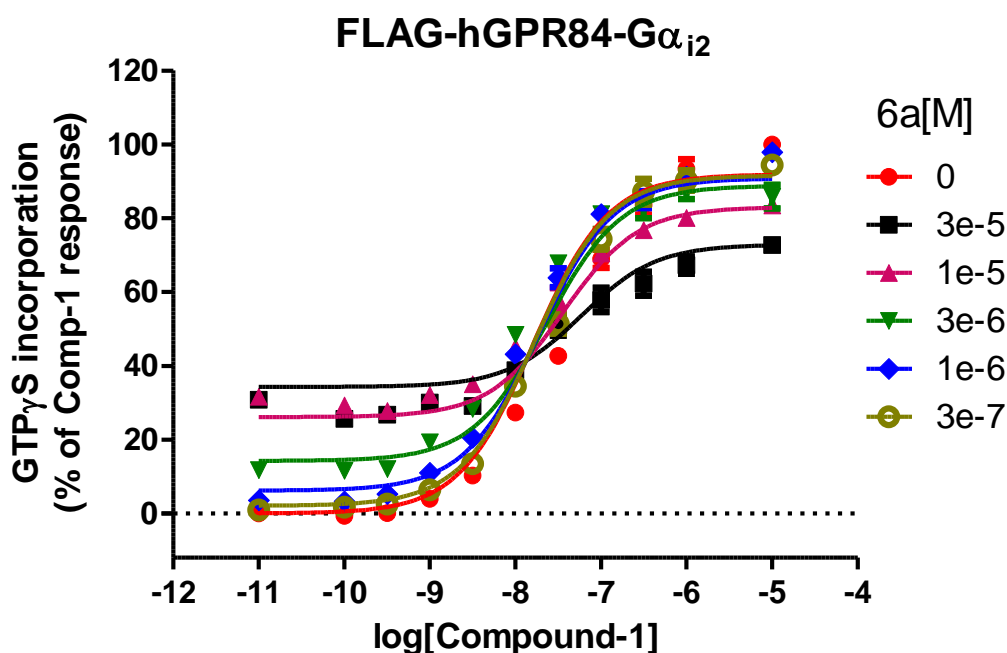


Figure 6.9 DIM analogue 6a acts as a weak NAM of efficacy of compound-1 at human GPR84. Effects of various fixed concentrations of 6a, ranging from 300 nM to 30 μ M, on the ability of compound-1 to induce promotion of [35 S]-GTP γ S incorporation into membranes of Flp-In T-REx cells expressing FLAG-hGPR84-G α_{i2} were evaluated. Data are expressed as mean \pm SEM of three independent experiments performed on three separate membrane preparations carried out in duplicate. Curves are from data fitted to an operational model of allosterism where the $\log\alpha$ value was constrained to 1 as the potency of compound-1 was unaltered by co-addition of increasing fixed concentrations of 6a. The allosteric parameters are shown in Table 6.5.

Table 6-5 Allosteric parameters for interaction between 6a and compound-1 at FLAG-hGPR84-Gα_{i2}

| Agonist ^a | Modulator ^b | logβ | logτ _A | logτ _B | pK _A ^c | pK _B ^d | β |
|----------------------|------------------------|------------|-------------------|-------------------|------------------------------|------------------------------|------|
| Compound-1 | 6a | -0.92±0.17 | 0.84±0.03 | -0.2±0.03 | 6.9±0.04 | 5.04±0.07 | 0.12 |

^a Agonist is the compound used to generate concentration-response curve

^b Modulator is the compound used in defined concentrations

^c pK_A are values estimated for the agonist

^d pK_B are values estimated for the modulator

Allosteric parameters for interaction between DIM analogue 6a and compound-1 were extracted from the data generated from [³⁵S]-GTPγS binding study using membranes prepared from doxycycline-treated Flp-In T-REx cells expressing FLAG-hGPR84-Gα_{i2} as described in Figure 6.9. Data are means ± SEM (n=3).

6.6. DIM analogues 2b and 3c lack affinity at human GPR84

In [³⁵S]-GTPγS incorporation assays, DIM analog 2b (5,5'-diiodo-3,3'-diindolyl(4-methylphenyl)methane) and 3c (5,5'-dimethoxy-3,3'-diindolyl(3,5-difluorophenyl)methane) were found to be inactive at hGPR84 (Figure 6.1). To assess whether these inactive small molecules displayed any potential allosteric interaction with orthosteric agonists of GPR84, a set of co-addition studies were performed where various fixed concentrations of 2b or 3c were added to the concentration-response assay of decanoic acid (Figure 6.10 a_i and b_i) or compound-1 (Figure 6.10 a_{ii} and b_{ii}). In all these experiments, both the potency and efficacy of C-10 and compound-1 were unaffected by co-addition of defined concentrations of both 2b and 3c which indicated that these DIM analogues lacked ability to bind to hGPR84. Both these DIM analogues contain a bulky substitution on the linker between two indole rings. The lack of affinity of 2b and 3c for human GPR84 implies that the bulky substitution on the linker is intolerable for receptor binding. Pillaiyar et al. (2017) reported that any aryl or alkyl substitution on the linker between two indole rings diminishes the potency of the DIM analogue. Further SAR studies with a broader range of these DIM analogues might explore the potential binding pocket of such allosteric ligands.

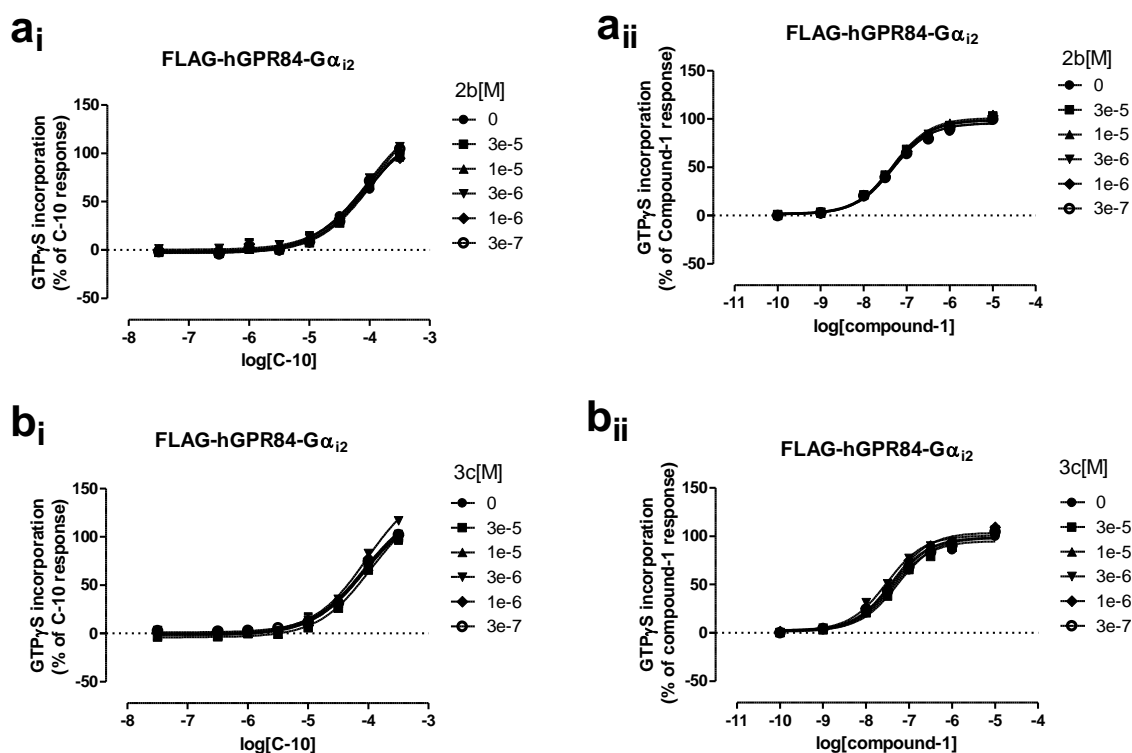


Figure 6.10 DIM analogues 2b and 3c lack ability to bind human GPR84. Membranes were prepared from Flp-In T-REx-293 cells induced with 100 ng/ml of doxycycline for 24 hours to express FLAG-hGPR84-Gα_{i2}. Using these membranes, [³⁵S]-GTPγS binding assays were performed in which increasing fixed concentrations of 2b were co-added to the concentration-response curve for C-10 (a_i) or compound-1 (a_{ii}) to assess their ability to affect the function of the respective orthosteric agonist. Equivalent studies were performed assessing the ability of various increasing fixed concentrations of 3c to affect the concentration-response curves for C-10 (b_i) or compound-1 (b_{ii}).

6.7. DIM analogue PSB-16671 is a potent PAM agonist at both human and mouse GPR84

6.7.1. PSB-16671 is more effective than DIM in enhancing the potency of decanoic acid

Though DIM displays strong cooperativity with orthosteric agonists of GPR84 (section 6.3), the affinity of DIM for human GPR84 is modest (average K_A : 6.3 μ M) which necessitates the development of new PAM agonists having higher affinity for GPR84. Recently Pillaiyar et al., (2017) reported a more potent and efficacious DIM analogue PSB-16671 which has 10-fold higher potency and 2-fold higher efficacy than DIM (section 4.2.3). Compared to DIM, PSB-16671 was reported to be more effective in potentiating the function C-10 in cAMP accumulation assays (Pillaiyar et al., 2017). To investigate whether PSB-16671 also displayed a higher magnitude of positive cooperativity than DIM in [35 S]-GTP γ S binding assays which measure the signalling effect immediately downstream of GPCR activation, concentration-response assays for C-10 were conducted in the absence or presence of various increasing fixed concentrations of PSB-16671 (Figure 6.11a). Indeed, in this assay PSB-16671 was found to be more effective than DIM in the function of C-10 as a significantly higher magnitude of binding affinity modulation of C-10 ($\log\alpha$: 2.37 ± 0.22 , $\alpha=232$) was obtained than that produced by DIM ($\log\alpha$: 1.45 ± 0.09 ; $\alpha=26$). When the experimental protocol was reversed, increasing concentrations of decanoic acid increased both the potency and efficacy of PSB-16671 (Figure 6.11b) with affinity cooperativity factor, α , value of 41 ($\log\alpha$: 1.61 ± 0.13) and activation cooperativity factor, β value of 6.7 (Table 6.5). Though theoretically it is expected that the magnitude of allosteric modulation of binding affinity obtained from the reciprocal assay should be similar to that yielded in the allosteric interaction study, the extent of the binding affinity modulation ($\log\alpha$: 1.61 ± 0.13 , $\alpha=41$) of PSB-16671 exerted by C-10 was significantly lower than that of C-10 by PSB-16671. This discrepancy in maintaining similar binding affinity modulation in reciprocal allosteric experiments is not unusual as Lee et al., (2008) also reported similar inconsistency in observing similar binding cooperativity in reciprocal allosteric interaction studies in which the PAM agonist phenylacetamide 1 potentiated the function of acetate at FFA2 in calcium mobilization assays, displaying a 89-fold increase in potency of acetate ($\log\alpha$:

1.95; $\alpha=89$) whilst acetate-induced enhancement of the potency of phenylacetamide 1 was significantly lower ($\log\alpha$: 1.38; $\alpha=24$). However, in the reciprocal experiments equivalent outcomes were obtained in terms of net affinity/efficacy cooperativity factor ($\alpha\beta$) (292 vs 272 in reciprocal assays). Operational model analysis of these datasets revealed that PSB-16671 (average K_A : 1.5 μM) binds human GPR84 with 240-fold higher affinity than decanoic acid (average K_A : 0.36 mM) while compared to DIM (average K_A : 6.3 μM , Table 6.1), the affinity of PSB-16671 is 4.2 times higher.

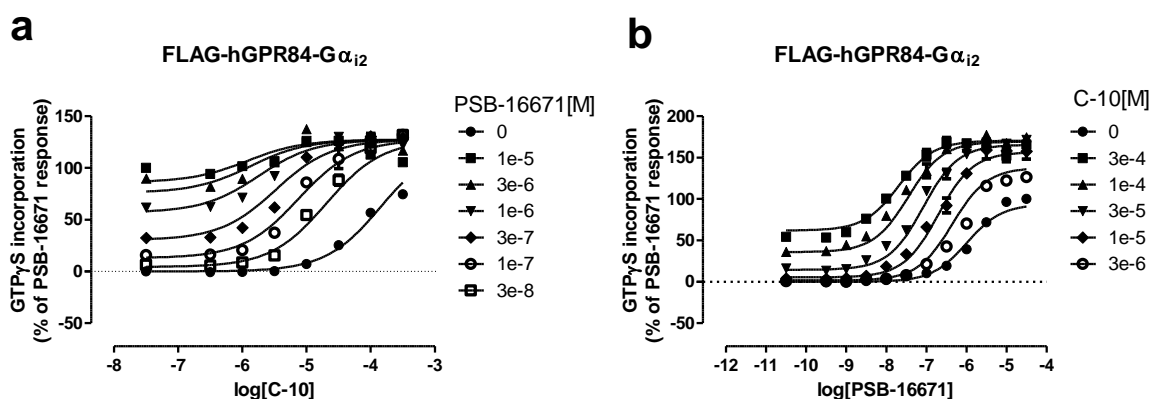


Figure 6.11 PSB-16671 is a PAM of potency of C-10 at human GPR84. Effects of co-addition of increasing concentrations of PSB-16671, ranging from 30 nM to 0.1 μM , on the ability of C-10 to stimulate $[^{35}\text{S}]\text{-GTP}\gamma\text{S}$ incorporation into membranes of Flp-In T-REx-293 cells expressing FLAG-hGPR84- $\text{G}\alpha_{i2}$ were assessed (a). Equivalent studies were conducted assessing the effects of co-incubation of increasing concentrations (ranging from 3 μM to 30 mM) of C-10 on PSB-16671-mediated $[^{35}\text{S}]\text{-GTP}\gamma\text{S}$ binding to FLAG-hGPR84- $\text{G}\alpha_{i2}$ (b). Data are mean \pm SEM of three independent experiments performed on separate membrane preparations. The curves displayed are from global fitting of the experimental data with the operational model of allosterism and the estimated allosteric parameters are shown in Table 6.6.

6.7.2. PSB-16671 is more effective than DIM in potentiating function of compound-1 and embelin at human GPR84

To investigate whether PSB-16671 displays any probe-dependence in modulating functions of GPR84 orthosteric agonists, a series of interaction studies were conducted assessing the effects of increasing fixed concentrations of PSB-16671 on concentration-response assays for compound-1 and embelin (Figure 6.12). PSB-16671 also displayed very strong allosteric interaction with compound-1 at human GPR84 as the potency of compound-1 was progressively enhanced by the co-addition of increasing concentrations of PSB-16671 (Figure 6.12a_i) affording an affinity cooperativity factor, α , value of 257 ($\log\alpha$: 2.41 ± 0.17). This allosteric modulation of potency of compound-1 reached a saturating limit at higher

concentrations of PSB-16671. Though PSB-16671 caused a small reduction in the maximal response to compound-1 (activation cooperativity factor, β value of 0.71), it was greatly outweighed by the high degree of binding affinity modulation, ultimately led to a high net affinity/efficacy cooperativity ($\alpha\beta$) value of 182.5. In reciprocal experiments, equivalent outcomes were obtained where compound-1 increased the potency and efficacy of PSB-16671 (Figure 6.12a_{ii}) with an affinity cooperativity factor, α value of 105 ($\log\alpha$: 2.02 ± 0.11) and activation cooperativity factor, β value of 2.34 (Table 6.6). Mathematical analysis of the allosteric interaction between PSB-16671 and compound-1 also estimated the binding affinity of PSB-16671 and compound-1 for FLAG-hGPR84-G α_{i2} fusion protein as being 0.9 μ M and 69 nM, respectively. Again PSB-16671 was found to be more effective than DIM (α : 120) in enhancing the measured potency of compound-1 although this higher degree (2-fold) of binding affinity modulation exerted by PSB-16671 compared to DIM did not reach the statistical significance level ($P>0.05$, two tailed unpaired t-test).

PSB-16671 was also found to strongly potentiate the function of embelin at human GPR84 (Figure 6.12b) by positively modulating both potency and efficacy of embelin, yielding an affinity cooperativity factor, α value of 16.4 and activation cooperativity factor, β value of 15.5. Though PSB-16671-induced enhancement of the potency of embelin was equivalent to that produced by DIM ($\log\alpha$: 1.22 ± 0.08 vs 1.20 ± 0.05 , respectively for PSB-16671 and DIM), PSB-16671 displayed 2-fold higher magnitude of positive modulation of efficacy of embelin than that generated by DIM (β : 15.5 vs 7.6) which is correlated with the higher intrinsic agonist activity of PSB-16671 (average τ : 0.91) than that of DIM (average τ : 0.32). Application of an operational model of allosterism to the global analysis of experimental data revealed that PSB-16671 and embelin bind FLAG-hGPR84-G α_{i2} with similar avidity (average K_A : 1.4 vs 1.5 μ M, respectively).

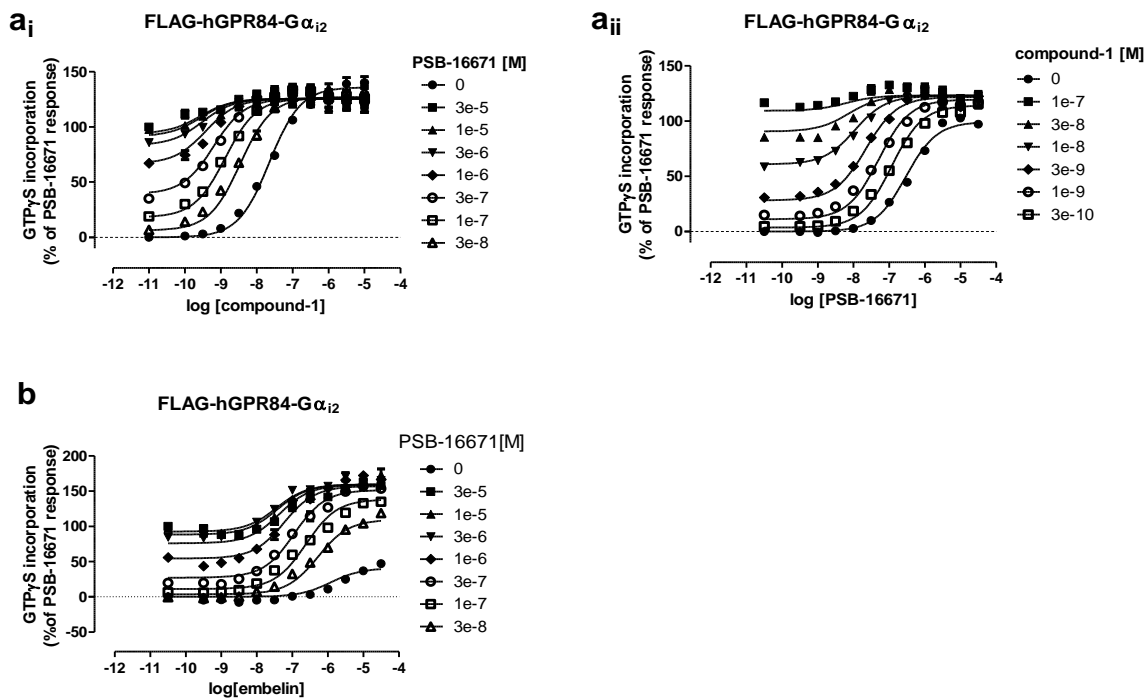


Figure 6.12 PSB-16671 acts as a PAM of potency of compound-1 while it behaves as a strong PAM of potency and efficacy of embelin at human GPR84. A [35 S]-GTP γ S binding assay was performed using membranes purified from Flp-In T-REx cells expressing FLAG-hGPR84-G α_{i2} in which increasing fixed concentrations of PSB-16671 ranging from 30 nM to 30 μ M were evaluated for their ability to modulate compound-1-induced [35 S]-GTP γ S binding (a_i). Equivalent co-addition studies were performed assessing the effects of various fixed concentrations of compound-1 ranging from 0.3 nM to 100 nM on PSB-16671-mediated [35 S]-GTP γ S incorporation into membranes (a_{ii}). Similarly, concentration-response assays for embelin were also performed with or without increasing fixed concentrations of PSB-16671 ranging from 30 nM to 30 μ M (b). Data are expressed as mean \pm SEM of four (a_i, a_{ii}) or two (b) individual experiments performed on separate membrane preparations carried out in duplicate. Curves displayed are from experimental data best fit to the operational model of allosterism and estimates of allosteric parameters are shown in Table (6.6).

Table 6-6 Operational model parameters of allosteric interactions between PSB-16671 and orthosteric agonists at FLAG-hGPR84-G α_{i2}

| Agonist ^a | C-10 | PSB-16671 | Compound-1 | PSB-16671 | Embelin |
|------------------------------|-----------------|-------------------|------------------|-----------------|------------------|
| Modulator ^b | PSB-16671 | C-10 | PSB-16671 | Compound-1 | PSB-16671 |
| log α | 2.37 \pm 0.22 | 1.61 \pm 0.13 | 2.41 \pm 0.17 | 2.02 \pm 0.11 | 1.22 \pm 0.08 |
| log β | 0.1 \pm 0.20 | 0.82 \pm 0.04 | -0.15 \pm 0.06 | 0.37 \pm 0.12 | 1.2 \pm 0.05 |
| log τ_A | 0.67 \pm 0.2 | -0.002 \pm 0.03 | 0.86 \pm 0.05 | 0.28 \pm 0.1 | -0.59 \pm 0.05 |
| log τ_B | 0.2 \pm 0.02 | 0.15 \pm 0.07 | 0.22 \pm 0.05 | 0.65 \pm 0.1 | -0.04 \pm 0.02 |
| pK _A ^c | 3.41 \pm 0.2 | 5.72 \pm 0.06 | 7.0 \pm 0.2 | 6.1 \pm 0.1 | 5.82 \pm 0.06 |
| pK _B ^d | 5.95 \pm 0.06 | 3.47 \pm 0.1 | 6.02 \pm 0.13 | 7.42 \pm 0.07 | 5.85 \pm 0.04 |
| α | 232 | 40.6 | 257 | 104.7 | 16.4 |
| β | 1.26 | 6.7 | 0.71 | 2.34 | 15.5 |
| $\alpha\beta$ | 292 | 272 | 182.5 | 245 | 254.2 |

^a Agonist is the compound used to generate concentration-response curve

^b Modulator is the compound used in defined concentrations

^c pK_A are values estimated for the agonist

^d pK_B are values estimated for the modulator

Allosteric parameters for interaction between PSB-16671 and GPR84 orthosteric agonists were extracted from the data generated from [35 S]-GTP γ S binding study using membranes prepared from doxycycline-treated Flp-In T-REx cells expressing FLAG-hGPR84-G α_{i2} as described in Figure 6.11 and 6.12. Data are means \pm SEM (n=3).

6.7.3. PSB-16671 displays little probe-dependence in allosteric modulation of orthosteric agonists at human GPR84

Though compound-1 displayed higher intrinsic activity than C-10 (average τ : 5.85 vs 3.04, respectively), equivalent magnitude of PSB-16671-induced binding affinity modulation of compound-1 and C-10 (α : 257 vs 232, respectively) was observed at FLAG-hGPR84-G α_{i2} in [35 S]-GTP γ S incorporation assays, which indicates that PSB-16671 displayed little probe-dependence in allosteric modulation of human GPR84. However, the PSB-16671-promoted increase in the potency of embelin (16.4 fold) was significantly lower in comparison with those obtained from the allosteric interaction between PSB-16671 and compound-1/C-10, which is consistent with the significantly lower intrinsic activity of embelin (τ : 0.26). Another notable thing is that while allosteric efficacy modulation of compound-1 exerted by PSB-16671 was marginal, PSB-16671 generated some 15.5-fold increase in the efficacy of embelin. However, PSB-16671 generated equivalent net affinity/efficacy cooperativity factor ($\alpha\beta$: 292, 182.5, 254.2; respectively with C-10, compound-1 and embelin) in allosteric interaction studies with C-10, compound-1 or embelin, suggesting that in [35 S]-GTP γ S binding assays, PSB-16671 exhibited no overall probe-dependence in displaying positive cooperativity with orthosteric agonists of GPR84.

6.7.4. PSB-16671 is also a potent PAM of activity of orthosteric agonists at mouse GPR84

There might be differences among species orthologues of a GPCR in terms of magnitude and direction or probe-dependence of cooperativity between an allosteric agonist and orthosteric agonist (Christopoulos, 2014; Wooten et al., 2013). To investigate whether PSB-16671 displays any variation between human and mouse orthologues of GPR84 in terms of cooperativity with orthosteric agonists, a set of interaction studies were performed using membranes expressing FLAG-mGPR84-G α_{i2} wherein the effects of increasing fixed concentrations of PSB-16671 on concentration-response assays for compound-1, C-10 or embelin were evaluated (Figure 6.13). Similar patterns of allosteric interactions between PSB-16671 and compound-1 was observed at mouse GPR84 in which co-addition of increasing concentrations of PSB-16671 ranging from 30 nM to 10 μ M resulted in progressive increase in the potency of compound-1 (Figure 6.13a_i) with binding affinity cooperativity factor, α value of 105 ($\log\alpha$:

2.02±0.11) indicating that PSB-16671 is also a strong PAM agonist at mouse GPR84. Similar magnitude of positive binding affinity cooperativity between PSB-16671 and compound-1 was observed ($\log\alpha$: 2.15±0.1; α : 141) in reciprocal experiments when increasing concentrations of compound-1 ranging from 0.3 nM to 100 nM were added to the concentration-response assay for PSB-16671 (Figure 6.13 a_{ii}), which is in full agreement with the reciprocity of the allosteric effect. In both cases, no efficacy modulation was observed and effect of PSB-16671 on the binding affinity of compound-1 vice versa approached a saturable limit at higher concentrations of the modulator. In comparison with DIM, PSB-16671 exhibited 6.5-fold higher binding affinity cooperativity and 4.5-fold higher net affinity/efficacy cooperativity with compound-1 at FLAG-mGPR84-G α_{i2} . Though compared to mouse GPR84, human GPR84 displayed some 2.4-fold higher magnitude of binding affinity cooperativity and 1.5-fold higher net affinity/efficacy cooperativity between PSB-16671 and compound-1 in [³⁵S]-GTP γ S binding assays, these differences were not statistically significant ($P>0.05$; two-tailed unpaired t-test).

Global analysis of these datasets using an operational model of allosterism showed that estimated binding affinity of PSB-16671 (average K_A : 0.94 μ M) and compound-1 (average K_A : 81.5 nM) for FLAG-mGPR84-G α_{i2} was equivalent to that observed at the fusion protein version of human GPR84, which is also consistent with the fact that both the ligands displayed no variation in potency between human and mouse orthologues (section 5.3). Compared to DIM (K_A : 4.8 μ M, Table 6.3), PSB-16671 has a 5-fold higher affinity for mouse GPR84.

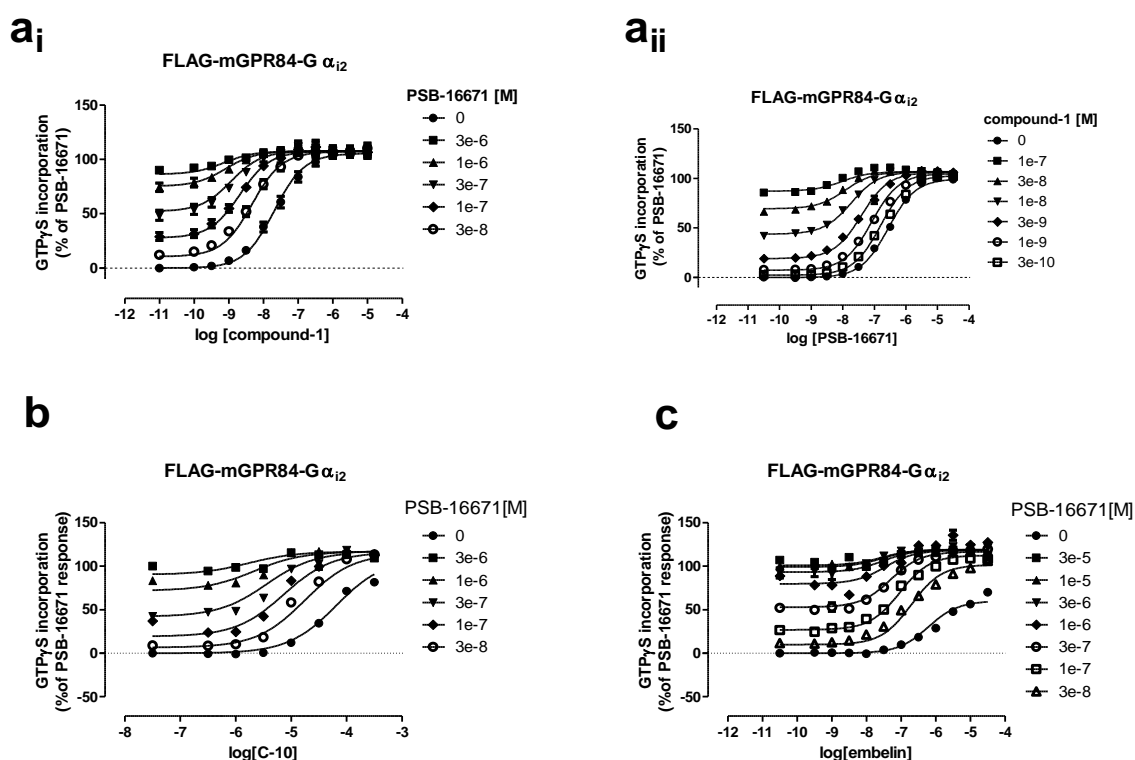


Figure 6.13 PSB-16671 displays strong positive cooperativity with different orthosteric agonists of GPR84 at FLAG-mGPR84-G α_{i2} . The ability of increasing fixed concentrations of PSB-16671 to affect compound-1-induced [35 S]-GTP γ S binding to membranes purified from Flp-In T-REx-293 cells expressing FLAG-mGPR84-G α_{i2} was evaluated (a_i). In reciprocal interaction studies, various concentrations of compound-1 were evaluated for their capacity to modulate PSB-16671-promoted binding of [35 S]-GTP γ S into G α_{i2} associated with FLAG-mGPR84-G α_{i2} (a_{ii}). Equivalent co-addition studies were performed assessing the effects of increasing concentrations of PSB-16671 on concentration-response curves for C-10 (b) or embelin (c). Data represent mean \pm SEM of four (a_i, a_{ii}) or two (b,c) individual experiments performed using separate membrane preparations. Curves displayed are from global fitting of experimental data with operational model of allosterism; the allosteric parameters are shown in Table 6.7.

Table 6-7 Operational model parameters of allosteric interactions between PSB-16671 and different orthosteric agonists at FLAG-mGPR84-G α_{i2}

| Agonist ^a | Compound-1 | PSB-16671 | C-10 | Embelin |
|------------------------------|-----------------|-----------------|-----------------|------------------|
| Modulator ^b | PSB-16671 | Compound-1 | PSB-16671 | PSB-16671 |
| log α | 2.02 \pm 0.11 | 2.15 \pm 0.1 | 2.1 \pm 0.2 | 1.33 \pm 0.08 |
| log β | 0.05 \pm 0.09 | 0.12 \pm 0.04 | 0.16 \pm 0.1 | 0.9 \pm 0.03 |
| log τ_A | 0.68 \pm 0.1 | 0.46 \pm 0.02 | 0.58 \pm 0.1 | -0.12 \pm 0.03 |
| log τ_B | 0.42 \pm 0.02 | 0.54 \pm 0.06 | 0.48 \pm 0.06 | 0.43 \pm 0.02 |
| pK _A ^c | 6.98 \pm 0.17 | 5.96 \pm 0.08 | 3.51 \pm 0.2 | 5.97 \pm 0.06 |
| pK _B ^d | 6.1 \pm 0.13 | 7.2 \pm 0.07 | 5.75 \pm 0.08 | 6.0 \pm 0.03 |
| α | 104.7 | 141.2 | 125.4 | 21.3 |
| β | 1.12 | 1.3 | 1.45 | 7.9 |
| $\alpha\beta$ | 117 | 183 | 182.4 | 168.3 |

^a Agonist is the compound used to generate concentration-response curve

^b Modulator is the compound used in defined concentrations

^c pK_A are values estimated for the agonist

^d pK_B are values estimated for the modulator

Allosteric parameters for interaction between PSB-16671 and GPR84 orthosteric agonists were extracted from the data generated from [35 S]-GTP γ S binding study using membranes prepared from doxycycline-treated Flp-In T-REx cells expressing FLAG-mGPR84-G α_{i2} as described in Figure 6.13. Data are means \pm SEM.

PSB-16671 also displayed very high positive cooperativity with C-10 (Figure 6.13b) or embelin (Figure 6.13c) at FLAG-mGPR84-G α_{i2} in [35 S]-GTP γ S binding assays, exhibiting affinity cooperativity factor, α , values of 125.4 and 21.3, respectively (Table 6.7). Though approximately 1.9-fold lower affinity cooperativity between PSB-16671 and C-10 was obtained at the FLAG-mGPR84-G α_{i2} than displayed at FLAG-hGPR84-G α_{i2} , this variation was not statistically significant. In the case of allosteric interaction between PSB-16671 and embelin, similar magnitude of affinity modulation of embelin by PSB-16671 was observed between human and mouse GPR84 (α : 16.4 vs 21.3) whilst human GPR84 displayed 2-fold higher degrees of efficacy modulation of embelin by PSB-16671 than that exhibited at mouse GPR84 (β : 15.5 vs 7.9). Application of an operational model of allosterism for the global analysis of datasets obtained from the allosteric interaction between PSB-16671 and C-10 predicted the estimated binding affinities of PSB-16671 and C-10 for FLAG-mGPR84-G α_{i2} to be 1.7 μ M and 0.3 mM, respectively which were very similar to those measured by similar studies at FLAG-hGPR84-G α_{i2} (average K_A : 1.5 μ M and 0.36 mM, respectively for PSB-16671 and C-10). Similarly, mathematical analysis of datasets from interaction studies between PSB-16671 and embelin revealed that both agonists bind mouse GPR84 with similar avidity (K_A : 1.0 μ M) and there was no variation in binding affinities of PSB-16671 and embelin between mouse and human (K_A : 1.4 and 1.5 μ M, respectively) orthologues of GPR84. This maintenance of binding affinities of PSB-16671, C-10 and embelin between human and mouse GPR84 are in good agreement with the equivalent potencies of these agonists at human and mouse GPR84 (section 5.3).

Consistent with the results obtained from the interaction studies using FLAG-hGPR84-G α_{i2} , PSB-16671 potentiated the binding affinity of compound-1 and C-10 for mouse GPR84 to a similar extent (α : 105 vs 125). Though PSB-16671-promoted enhancement (21.3 fold) of potency of embelin was significantly lower than that observed when compound-1 or C-10 was used to probe the function of mouse GPR84, PSB-16671 caused some 8-fold increase in efficacy for embelin whilst no significant modulation of efficacy was observed for compound-1 (β =1.12) or C-10 (β = 1.45). However, equivalent magnitude of net affinity/efficacy cooperativity was obtained whether compound-1, C-10 or embelin ($\alpha\beta$: 117, 182 and 168, respectively) was used as a probe for receptor

function, suggesting little probe-dependence of allosteric interaction of PSB-16671 with orthosteric GPR84 agonists in [35 S]-GTP γ S incorporation assays.

6.7.5. PSB-16671 is a potent PAM agonist of the function of orthosteric agonists of mouse GPR84 in RAW 264.7 cells

To study the allosteric interaction between PSB-16671 and orthosteric GPR84 agonists in a more physiological setting, the mouse monocyte-macrophage cell line RAW264.7 was employed. Membranes were prepared from both LPS-treated (100 ng/ml, 5 hours) and untreated (LPS-) RAW 264.7 cells and subsequently employed in [35 S]-GTP γ S binding assays to investigate the effects of varying fixed concentrations of PSB-16671 on concentration-response curve for compound-1 (Figure 6.14 a, b_i). In both cases, progressive increases in measured potency of compound-1 was observed upon co-addition of increasing concentrations of PSB-16671 with affinity cooperativity factor, α value of 219 and 251, respectively (Table 6.8) for LPS untreated and treated cells, which indicates that PSB-16671 is a potent PAM of potency of compound-1 at RAW 264.7 cells. This is consistent with the results obtained in transfected cells expressing FLAG-mGPR84-G α_{i2} . Though co-addition of PSB-16671 resulted in a small reduction in maximal response to compound-1 (β : 0.63 and 0.83, for LPS-treated and untreated cells, respectively), this effect was completely outweighed by high affinity cooperativity values which led to high net affinity/efficacy cooperativity factor, $\alpha\beta$ value of 159 and 182, respectively for LPS-treated and untreated RAW264.7 cells. These results suggested that LPS-treatment of RAW264.7 cells did not alter the magnitude of cooperativity between compound-1 and PSB-16671. In reciprocal allosterism experiments, co-incubation of increasing concentrations of compound-1 caused both leftward and upward shifts of the concentration-response curve for PSB-16671 (Figure 6.14 b_{ii}), yielding an affinity cooperativity factor, α value of 87 and activation cooperativity factor, β value of 2.14 (Table 6.8). Though the extent of modulation of binding affinity ($\log\alpha$: 1.94 ± 0.03) of PSB-16671 by compound-1 obtained in reciprocal assays was significantly lower ($P<0.001$) than that for compound-1 by PSB-16671 ($\log\alpha$: 2.4 ± 0.04), similar net affinity/efficacy cooperativity value ($\alpha\beta$: 159 vs 186.4 in reciprocal assays) was maintained between both assays whether PSB-16671 or compound-1 was used as the modulator. The degree of potentiation of binding affinity of compound-1 by PSB-16671 observed in RAW264.7 cells was significantly ($P<0.05$, two-tailed

unpaired t test) higher than that displayed in Flp-In T-REx-293 cells expressing FLAG-mGPR84-G α_{i2} (log α : 2.4 ± 0.04 vs 2.02 ± 0.11 , respectively). However, similar affinity cooperativity was observed between RAW264.7 cells and transfected cells expressing the cloned mouse receptor (log α : 1.94 ± 0.03 vs 2.15 ± 0.09 , respectively, $P > 0.05$) when the ability of increasing concentrations of compound-1 to modulate the potency and efficacy of PSB-16671 was investigated. Moreover, no significant variation ($P > 0.05$) in net affinity/efficacy cooperativity ($\alpha\beta$: 159 vs 117) was observed between RAW264.7 cells and transfected cells expressing FLAG-mGPR84-G α_{i2} . Similar estimated binding affinities of PSB-16671 (average $K_A = 0.5 \mu\text{M}$) and compound-1 (average $K_A = 79 \text{ nM}$) for mouse GPR84 were observed at RAW 264.7 cells compared to those displayed at Flp-In T-REx-293 cells expressing FLAG-mGPR84-G α_{i2} .

Marked variation in allosteric interaction with compound-1 was observed between DIM and PSB-16671 at LPS-treated RAW-264.7 cells. Compared to DIM, PSB-16671 displayed 2-fold higher binding affinity cooperativity (128 vs 251) with compound-1 although this variation did not reach statistical significance level ($P > 0.05$, two-tailed unpaired t test). Though DIM caused a 4.5-fold (β : 0.22) decrease in maximal response to compound-1, acting as a weak NAM of efficacy, PSB-16671-mediated efficacy modulation of compound-1 was marginal (β : 0.63, 1.6-fold decrease in efficacy). However, PSB-16671 displayed some 5.7-fold higher net affinity/efficacy cooperativity ($\alpha\beta$: 159 vs 28) than DIM in modulating the function of compound-1 at LPS-treated RAW264.7 cells.

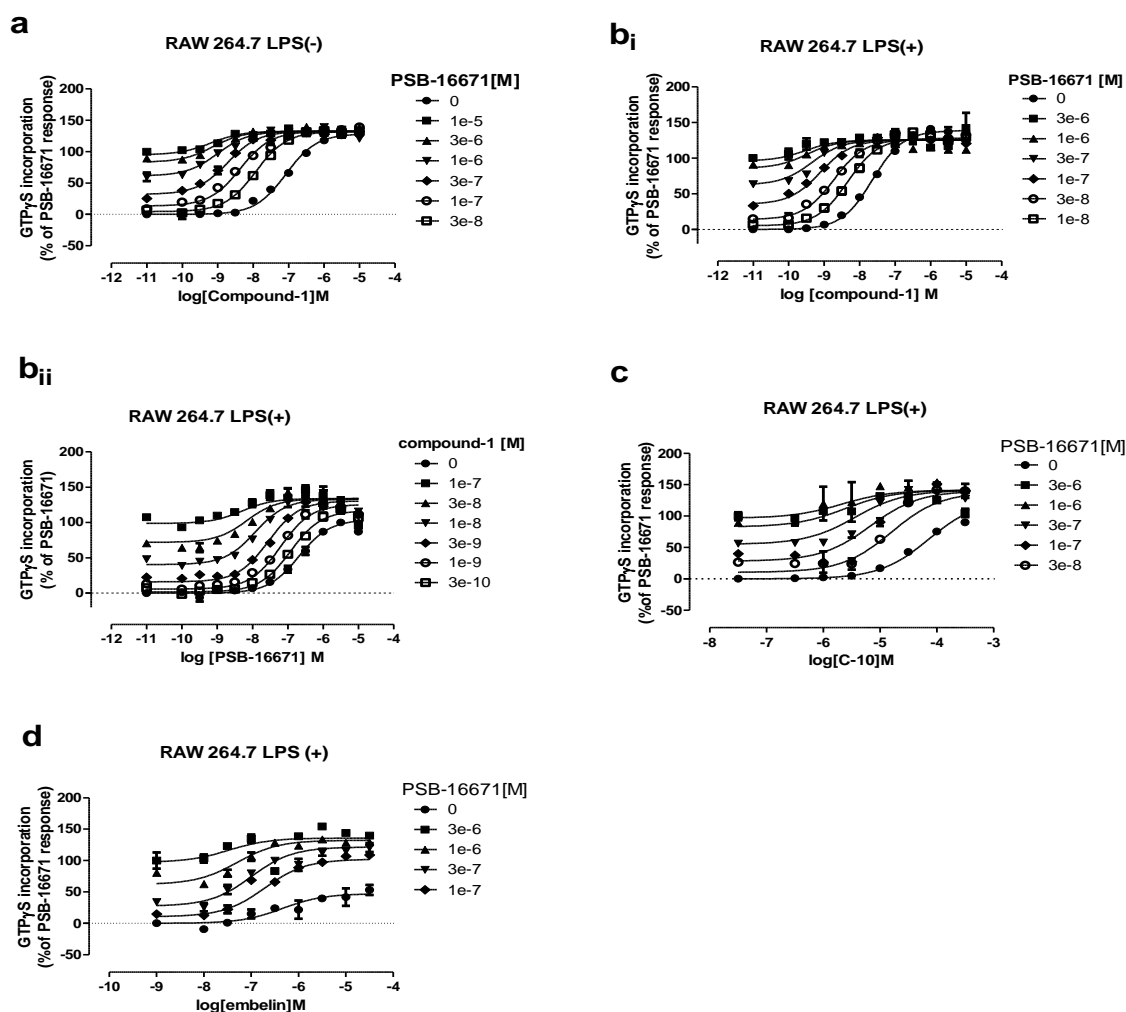


Figure 6.14 PSB-16671 displays high positive cooperativity in modulating function of compound-1, C-10 and embelin in [35 S]-GTP γ S binding assays in RAW 264.7 cells. Increasing fixed concentrations of PSB-16671 ranging from 30 nM to 10 μ M were assessed for their ability to affect compound-1-mediated [35 S]-GTP γ S incorporation into membranes purified from naïve (-LPS) RAW264.7 cells (a). Similar interaction study was performed to evaluate the effect of increasing defined concentrations of PSB-16671 on the ability of various concentrations of compound-1 to stimulate [35 S]-GTP γ S binding to membranes generated from LPS-induced (100 ng/ml, 5 hours) RAW264.7 cells (bi). In reciprocal experiment, the capacity of increasing fixed concentrations of compound-1 to modulate the potency and efficacy of PSB-16671 were investigated (bii). Equivalent allosteric interaction studies were performed using membranes of LPS-treated (LPS+) RAW264.7 cells in which concentration-response assays for C-10 (c) or embelin (d) were conducted with or without increasing fixed concentrations of PSB-16671. Data represented in (bi) and (bii) are mean \pm SEM of four and three independent experiments performed on separate membrane preparations while data presented in (a), (c) and (d) are representative of two individual experiments. Curves drawn are from fitting the datasets with operational model of allosterism and the allosteric parameters quantified from these analyses are shown in Table 6.8.

Table 6-8 Operational model parameters of allosteric interactions between PSB-16671 and different orthosteric agonists at RAW 264.7 cells.

| Agonist ^a | Compound-1 | Compound-1 | PSB-16671 | C-10 | Embelin |
|------------------------------|------------------------|------------------------|-------------------------|------------------------|------------------------|
| Modulator ^b | PSB-16671 ^e | PSB-16671 ^f | Compound-1 ^f | PSB-16671 ^f | PSB-16671 ^f |
| log α | 2.34±0.13 | 2.4±0.04 | 1.94±0.03*** | 1.81±0.4 | 1.36±0.2 |
| log β | -0.1±0.14 | -0.20±0.05 | 0.33±0.08 | 0.25±0.2 | 0.8±0.06 |
| log τ_A | 0.62±0.2 | 0.53±0.05 | 0.14±0.02 | 0.50±0.24 | -0.56±0.05 |
| log τ_B | 0.11±0.02 | 0.15±0.03 | 0.3±0.03 | 0.24±0.07 | 0.21±0.1 |
| pK _A ^c | 6.54±0.05 | 7.0±0.1 | 6.3±0.15 | 3.51±0.3 | 6.2±0.1 |
| pK _B ^d | 6.26±0.43 | 6.3±0.1 | 7.24±0.05 | 6.12±0.13 | 5.5±0.2 |
| α | 219 | 251.2 | 87.1 | 64 | 23 |
| β | 0.83 | 0.63 | 2.14 | 1.8 | 6.3 |
| $\alpha\beta$ | 182 | 159 | 186.4 | 115.2 | 145 |

^a Agonist is the compound used to generate concentration-response curve

^b Modulator is the compound used in defined concentrations

^c pK_A are values estimated for the agonist

^d pK_B are values estimated for the modulator

^e experiment performed with membranes generated from naïve RAW264.7 cells

^f experiments performed with membranes generated from LPS-treated RAW264.7 cells. Allosteric parameters for interaction between PSB-16671 and different GPR84 orthosteric agonists were extracted from the data generated from [³⁵S]-GTPγS binding study using membranes prepared from naïve or LPS-treated RAW264.7 cells as described in Figure 6.14. Data are means±SEM.

To assess whether PSB-16671 exhibited any probe-dependence in allosteric interaction with orthosteric agonists of GPR84 at RAW264.7 cells, interaction studies were performed using [³⁵S]-GTPγS binding assays whereby effects of increasing defined concentrations of PSB-16671 on the potency and efficacy of C-10 (Figure 6.14 c) or embelin (Figure 6.14 d) were evaluated. PSB-16671 also acted as a strong PAM of potency and efficacy of C-10 or embelin at LPS-treated RAW264.7 cells and the allosteric effects reached a limit at higher concentrations of the modulator. Though PSB-16671-mediated potentiation of C-10 binding affinity for mouse GPR84 was 2-fold lower in RAW264.7 cells compared to that displayed at FLAG-mGPR84-Gα_{i2} (α : 64 vs 125), the magnitude of binding affinity cooperativity with embelin was equivalent between RAW264.7 cells and transfected cells expressing FLAG-mGPR84-Gα_{i2} (α : 23 vs 21.3). Similar to the results obtained from FLAG-hGPR84-Gα_{i2}, PSB-16671 was found to be more effective than DIM in potentiating the function of C-10 in RAW264.7 cells displaying 4-fold higher affinity cooperativity (α : 64 vs 16.3) and 9.5-fold higher net affinity/efficacy cooperativity ($\alpha\beta$: 115 vs 12) with C-10 which strongly correlates with some 6-fold higher intrinsic agonist activity of PSB-16671 (τ : 1.74) than DIM (τ : 0.3) in RAW264.7 cells.

Mathematical analysis of allosteric interaction between PSB-16671 and C-10 revealed that PSB-16671(K_A: 0.76 μ M) binds mouse GPR84 with 400-fold higher

affinity than C-10 (K_A : 0.31 mM). Similarly global fitting of datasets obtained from interaction studies between PSB-16671 and embelin with an operational model of allosterism estimated binding affinity of PSB-16671 and embelin for mouse GPR84 to be 3 μ M and 0.63 μ M, respectively, which are very similar to those measured at transfected cells expressing FLAG-mGPR84-G α_{i2} .

6.7.6. PSB-16671 exhibits probe-dependence in modulating function of orthosteric agonists of GPR84 in RAW264.7 cells

PSB-16671 exhibited probe-dependence in modulating the binding affinity of orthosteric agonists for mouse GPR84 in LPS-induced RAW264.7 cells as evidenced from the findings that greatest magnitude of affinity modulation was observed for compound-1 (α : 251) followed by for C-10 (α : 64) and lowest binding affinity modulation (α : 23) was generated when embelin was used to probe the receptor function. These results are in good agreement with the correlation of magnitude of affinity modulation with the efficacy of the orthosteric agonist used in the allosteric interaction study. While the cooperativity with compound-1 was solely governed by the affinity modulation, the cooperativity with C-10 or embelin incorporated both the affinity and efficacy modulation. The highest potentiation of efficacy by PSB-16671 was observed for embelin (β : 6.3) which was 3.5-fold higher than that for C-10. However, no significant variation in overall affinity/efficacy cooperativity was observed irrespective of the nature of the orthosteric agonist used as a probe for the receptor function ($\alpha\beta$: 159, 115, and 145, respectively for compound-1, C-10 and embelin).

6.8. Discussions

6.8.1. Orthosteric and allosteric ligand act co-operatively to greatly enhance the function of GPR84 which may be a therapeutic strategy to limit atherosclerosis

Though DIM was reported to be a PAM agonist at GPR84 (Nikaido et al., 2015) based on the additive effects of DIM and MCFAs in double stimulation assay performed using [35 S]-GTP γ S binding assay, the mechanism of allosteric effect was unexplored at that time. Recently Pillaiyar et al., (2017) have studied allosteric interaction between DIM or DIM analogue PSB-16671 and the putative endogenous agonist C-10 using forskolin-induced cAMP accumulation assays in CHO cells expressing human GPR84 and reported that DIM and PSB-16671 both acted as PAM of potency and efficacy of C-10 at human GPR84. Though this study revealed that allosteric effect of DIM or PSB-16671 on C-10 is governed by both potency and efficacy modulation, other allosteric features including ‘reciprocity of the allosteric effect’ and ‘probe dependence’ of allosteric interaction were not studied. Moreover, allosteric interaction of DIM or DIM derivatives in mouse GPR84 was lacking. In this context, detailed studies of allosteric modulation of GPR84 are required. To assess whether combinations of orthosteric and allosteric ligands enhance the function of GPR84 substantially, I have performed detailed studies of allosteric interactions of DIM and DIM analogues with a series of orthosteric GPR84 agonists, C-10, compound-1, embelin or 6-OAU using [35 S]-GTP γ S binding assays employing membranes of transfected cells expressing FLAG-hGPR84-G α_{i2} . Moreover, to assess whether DIM and PSB-16671 exhibit any species selectivity in displaying cooperativity with orthosteric agonists, interaction studies were also performed using transfected cells expressing FLAG-mGPR84-G α_{i2} and the mouse monocyte-macrophage cell line RAW264.7. In these assays, DIM, DIM analogue 3a and particularly PSB-16671 acted as highly effective positive allosteric modulator of function of orthosteric GPR84 agonists, implying that DIM and DIM analogues could be used with MCFAs or synthetic orthosteric agonist as a combination therapy to limit atherosclerosis as recently Gaidarov et al., (2018) suggested that stimulation of GPR84 could be a potential therapeutic strategy to treat atherosclerosis. Recently several groups reported that PAM or ago-PAMs including BQCA and BQZ-12 which displayed selectivity on M $_1$ mAChR over other muscarinic receptor subtypes could be an effective

therapeutic candidate to treat cognitive decline associated with Alzheimer's disease or other neurodegenerative disorders as these allosteric modulators will greatly potentiate function of endogenous agonist acetylcholine at M_1 mAChR concomitantly will preserve the spatiotemporal physiological signalling of acetylcholine (Bradley et al., 2017; Dallagnol et al., 2018). Similarly, application of ago-PAM of GPR84 including DIM or PSB-16671 might be an effective therapeutic strategy to treat atherosclerosis as it will greatly enhance the function of putative endogenous agonist MCFAs at GPR84. The plasma concentration of decanoic acid in human healthy volunteers is below μM concentration (Nagasaki et al., 2012). Shrestha et al., (2015) estimated the plasma concentration of C-10 in healthy Japanese volunteers to be below $0.5 \mu\text{M}$ although this concentration might be higher in the community who routinely take coconuts or coconuts oil in their diet including south Indian. The very low potency of decanoic acid ($57 \mu\text{M}$ at FLAG-hGPR84- $\text{G}\alpha_{i2}$ C352I and FLAG-mGPR84- $\text{G}\alpha_{i2}$ C352I, $10 \mu\text{M}$ at FLAG-hGPR84-eYFP and $43 \mu\text{M}$ at RAW264.7 cells), as well as low affinity to human and mouse GPR84 (average K_A : $300 \mu\text{M}$) are not in good agreement with the physiological relevance of GPR84-MCFAs pairing. This lower affinity of decanoic acid at GPR84 indicates that concentrations in the blood are too low in isolation to activate the receptor significantly which suggests that MCFAs might not be the true endogenous activators of GPR84. However, this may be overcome in the presence of an allosteric agonist, DIM or DIM-like molecules. DIM was found to enhance the potency of decanoic acid by a factor of 28 while in reciprocal assay C-10 displayed a 20-fold increase in the potency of DIM. Due to this high cooperativity between DIM and C-10, it is expected that decanoic acid will be able to activate GPR84 at a concentration much lower than the plasma concentration in the presence of DIM. As such, in the presence of $10 \mu\text{M}$ allosteric agonist DIM, the plasma concentration of C-10 might be able to produce half-maximal effects of GPR84 which would not be possible for C-10 in isolation. The potentiation of action of C-10 at GPR84 in the presence of PSB-16671 will be much more pronounced as PSB-16671 was found to enhance the potency of C-10 by more than 200-fold. High cooperativity between C-10 and DIM or DIM derivatives also predicted that similar endogenous molecules might enhance the function of C-10 at GPR84 resulting in lower concentrations of C-10 required for the activation of GPR84 (Mahmud et al., 2017).

Recently allosteric interaction across dimer (homodimer or heterodimer) or even oligomer of GPCR has been proposed as a mean to generate the cooperativity between two interacting ligands (Burford et al., 2015; Lane et al., 2014; Wootten et al., 2013; Smith and Milligan, 2010; Springael et al., 2007; May et al., 2007) wherein binding of an allosteric or orthosteric ligand to their corresponding binding site(s) on one protomer (homomer or heteromer) can either alter the binding affinity of the same ligand or other ligand for the interacting protomer and/or affect the maximal signalling response generated from the second protomer. For example, Lane et al., (2014) reported that bitopic ligand SB269652, which is a NAM of affinity of dopamine at D₂R, displayed negative cooperativity with orthosteric agonist dopamine across a D₂R homodimer. Considering this possibility, the observed high positive cooperativity between DIM or PSB-16671 and orthosteric GPR84 agonists might be generated due to the allosteric interaction across GPR84 dimer in which binding of DIM or PSB-16671 on the allosteric site within one protomer of GPR84 might result in either enhancement in binding affinity of the orthosteric agonists for the orthosteric binding site on the second protomer of the receptor and/or increase in maximal response of this ligand generated from the opposing homomer. However, retention of agonist function of DIM or PSB-16671 at both R172A GPR84 and R172K GPR84 (section 4.3.2) suggested that DIM or PSB-16671 and orthosteric agonists bind to the same monomer of GPR84 to modulate the function of each other.

6.8.2. MCFAs may act as endogenous allosteric modulators of GPR84 rather than acting as orthosteric agonists

DIM is produced in vivo from the metabolism of indole-3-carbinol which is present in the cruciferous vegetables including broccoli, kale, cauliflower (Reed et al., 2006; Maciejewska et al., 2009). Following an oral dose of 1000 mg indole-3-carbinol, the peak plasma level of DIM in healthy women was estimated to be 607 ng/ml which is equivalent to 2.5 μ M (Reed et al., 2006). Considering the potency of DIM to be 1 to 5 μ M estimated at eYFP tagged human or mouse GPR84 and human or mouse GPR84-G α_{i2} fusion protein, respectively and the affinity of DIM for GPR84 to be 5 μ M, this peak level of DIM will be able to activate GPR84 partially. However, as C-10 was found to enhance the potency of DIM by 20 fold when co-bound to GPR84, in the presence of high plasma levels of

decanoic acid or other MCFAs, significantly much lower concentration of DIM will be sufficient to activate GPR84 than in the absence of MCFAs. So it is possible for DIM to activate GPR84 even at lower concentrations produced from lower dosing of indole-3-carbinol. As such C-10 or other MCFAs might act as endogenous allosteric modulators of GPR84 rather than acting as orthosteric agonists (Mahmud et al., 2017). As several lipids or lipid-derived molecules including cholesterol, endocannabinoids, lipoxin A4, pregnenolone have been reported to behave as endogenous allosteric modulators of different GPCRs (see van der Westhuizen et al., 2015; Christopoulos and Kenakin, 2002 for review), this will not be unusual that MCFAs may act as endogenous allosteric regulator of GPR84.

6.8.3. The relative contribution of affinity and efficacy modulation to the functional cooperativity between DIM or PSB-16671 and orthosteric GPR84 agonists

In the case of allosteric interaction studies performed using [35 S]-GTP γ binding assays, a general trend was that DIM or PSB-16671-promoted enhancement in efficacy was significantly higher for partial agonist embelin than for C-10 whilst the efficacy modulation of compound-1 or 6-OAU appeared to be marginal. This conclusion is based on the mathematical analysis of allosterism data with an operational model of allosterism and needs to be validated by direct binding assays. Unfortunately, to date, no radioligand is available which targets the binding sites of these ligands. Both DIM and PSB-16671 potentiated the maximal response to embelin to a greater extent displaying efficacy cooperativity factor, β of 7.6 and 15.5, respectively in Flp-In T-REx-293 cells expressing FLAG-hGPR84-G α_{i2} . PSB-16671 also enhanced the efficacy of embelin by a factor of 8 and 6.3 in transfected cells expressing FLAG-mGPR84-G α_{i2} and LPS-treated RAW264.7 cells, respectively. These results demonstrated that DIM and PSB-16671-mediated allosteric effects on embelin were governed by both affinity and efficacy modulation. Though DIM enhanced the maximal response of C-10 by 2.3-fold in transfected cells expressing FLAG-hGPR84-G α_{i2} which is consistent with the result reported by Pillaiyar et al., (2017) in cAMP accumulation assays, no significant modulation of efficacy (β : 0.74) was observed in LPS-treated RAW264.7 cells, indicating species variation in allosteric effect of DIM on C-10. In the case of high positive cooperativity between PSB-16671 and C-10, contribution from efficacy modulation was insignificant compared to potency

modulation as evidenced from the finding that PSB-16671 enhanced maximal response to C-10 displaying efficacy cooperativity factor, β value of 1.3, 1.45 and 1.8 at FLAG-hGPR84-G α_{i2} , FLAG-mGPR84-G α_{i2} and in LPS-treated RAW264.7 cells, respectively whereas the net affinity/efficacy cooperativity factor, $\alpha\beta$ values were 292,182 and 115, respectively.

In the case of study of allosteric interaction between the modulator and full agonist in functional assays, detection of efficacy modulation is quite challenging as full agonist can elicit signalling response which might reach maximal system response with or without the modulator used (Berizzi et al., 2016). Though DIM displayed very high net cooperativity factor, $\alpha\beta$ of 108 and 117 with compound-1 and 6-OAU, respectively in human GPR84, the efficacy cooperativity factor, β values were 0.9 and 0.93, respectively. This was also the case for allosteric interaction of 3a with compound-1 or 6-OAU in human GPR84. As 6-OAU and compound-1 both are full agonists at human GPR84, it is difficult to quantify relative efficacy modulation if any without performing direct binding assays. In the case of allosteric interaction of DIM with compound-1 in transfected cells expressing FLAG-mGPR84-G α_{i2} wherein although some degrees of increase in maximal response to compound-1 was obtained (β : 1.6), the exact quantification of the contribution of efficacy modulation remains challenging due to the full agonism of compound-1 at the FLAG-mGPR84-G α_{i2} . By contrast, DIM was found to decrease the maximal response to compound-1 by some 4.5-fold (β : 0.22) in LPS-induced RAW264.7 cells. On the other hand, the high positive cooperativity between PSB-16671 and compound-1 obtained from allosteric interaction studies in transfected cells expressing FLAG-hGPR84-G α_{i2} or in LPS-treated RAW264.7 cells appeared to be solely governed by the binding affinity modulation as PSB-16671 decreased the maximal response of compound-1 by 1.4-fold (β : 0.71) and 1.6-fold (β : 0.63), respectively.

6.8.4. Probe-dependence of allosteric effects of DIM and DIM analogues

DIM displayed probe-dependence in exhibiting positive affinity cooperativity with orthosteric agonists of GPR84 including C-10, embelin, compound-1 and 6-OAU in a manner that degree of affinity cooperativity strongly correlates with the efficacy of the orthosteric agonist used as a probe for receptor function which is

consistent with the postulate of two states MWC model (Canals et al., 2012). The rank order of positive affinity cooperativity with orthosteric agonists was as follows: compound-1=6-OAU>> C-10>embelin. A similar correlation between the extent of positive cooperativity and orthosteric agonist efficacy in allosteric interaction at M₁ mAChR were reported by Canals et al., (2012) and van der Westhuizen et al., (2018). In contrast, little probe-dependence in allosteric interaction between DIM and orthosteric agonists was observed in human GPR84 when net affinity/efficacy cooperativity was considered. In transfected cells expressing FLAG-hGPR84-Gα_{i2} or FLAG-mGPR84-Gα_{i2}, PSB-16671 potentiated binding affinity of compound-1 and C-10 for human or mouse GPR84 to the similar extent (α: 257 vs 232 and 105 vs 125, respectively for compound-1 and C-10 at human and mouse GPR84, respectively) despite compound-1 (average τ: 5.85 and 4.8) displayed higher operational efficacy than C-10 (average τ: 3.04 and 3.8) at both human and mouse GPR84. This result indicates little probe-dependence of PSB-16671 in modulating the function of compound-1 and C-10. In contrast, PSB-16671 showed some 15-fold (for human GPR84) and 5-fold (for mouse GPR84) lower affinity cooperativity with embelin than that displayed with compound-1 or C-10 which is strongly linked with the significantly lower intrinsic agonist activity of embelin (τ: 0.26 and 0.76, respectively for human and mouse GPR84) than either compound-1 or C-10. However, equivalent net positive affinity/efficacy cooperativity (αβ) values were obtained whether C-10, compound-1 or embelin was used as the probe for GPR84 function, suggesting little probe-dependence of PSB-16671 in allosteric interaction with orthosteric agonists. On the other hand, PSB-16671 displayed strong probe-dependence in modulating binding affinity of orthosteric agonists in mouse monocyte-macrophage cell line RAW264.7 cells which was evidenced from some 11 and 2.8-fold higher positive affinity cooperativity with compound-1 and C-10, respectively than with embelin. However, once again similar net affinity/efficacy cooperativity was maintained in allosteric interaction of PSB-16671 with orthosteric agonist, C-10, embelin or compound-1.

6.8.5. Relative to DIM or 3a, PSB-16671 displays markedly higher positive cooperativity with orthosteric GPR84 agonists

Estimates of operational efficacy (τ) values for DIM and PSB-16671 obtained from the global analysis of datasets of allosteric interaction between DIM/PSB-16671 with compound-1 by an operational model of allosterism showed that relative to DIM, PSB-16671 has 4.2, 5.8 and 4.4-fold higher intrinsic agonist activity (τ) in FLAG-hGPR84-G α_{i2} , FLAG-mGPR84-G α_{i2} and RAW264.7 cells, respectively which is fully consistent with the finding that DIM acts as a partial agonist compared to PSB-16671 (section 4.2.3, 5.2.3 and 5.4). Owing to this higher intrinsic agonist activity of PSB-16671 than DIM, in comparison with DIM, PSB-16671 displayed higher degrees of positive affinity cooperativity (2.0 and 6.5-fold higher in RAW264.7 cells or at FLAG-hGPR84-G α_{i2} and at FLAG-mGPR84-G α_{i2} , respectively) with compound-1 which is consistent with the correlation between degrees of affinity cooperativity and operational efficacy (τ) of the modulator used (Canals et al., 2012; Keov et al., 2011). A similar correlation between the magnitude of positive affinity cooperativity and operational efficacy of allosteric modulator was observed among human M₁ mAChR PAMs in modulating the function of orthosteric agonist acetylcholine wherein higher efficacy modulator MIPS1780 (τ : 6) and MIPS1745 (τ : 1.1) showed 7.5 and 3.2-fold higher positive binding cooperativity with acetylcholine than that displayed by BQCA (τ : 0.3) in IP1 accumulation assays (van der Westhuizen et al., 2018). Relative to DIM, PSB-16671 displayed some 1.7, 4.6 and 5.6-fold higher net affinity/efficacy cooperativity ($\alpha\beta$) with compound-1 at FLAG-hGPR84-G α_{i2} , FLAG-mGPR84-G α_{i2} and RAW264.7 cells, respectively. Similarly, consistent with significantly higher intrinsic efficacy of PSB-16671 than 3a, PSB-16671 exhibited 3.7 and 9.4-fold higher composite cooperativity ($\alpha\beta$) with compound-1 and C-10, respectively in human GPR84. This strong correlation between observed functional cooperativity and degrees of intrinsic efficacy of modulator suggests that allosteric interaction of DIM or DIM analogues with orthosteric agonists of GPR84 likely follow two-state MWC model of action (Dallagnol et al., 2018). PSB-16671 also exhibited markedly higher positive affinity cooperativity than DIM when C-10 was used to probe the GPR84 function which is consistent with the finding reported by Pillaiyar et al., (2017). Compared to DIM, PSB-16671 showed some 8 and 4-fold higher affinity cooperativity with C-10 in transfected cells expressing FLAG-

hGPR84-G α_{i2} and LPS-treated RAW264.7 cells, respectively which is strongly correlated with the variation in intrinsic agonist activity between PSB-16671 and DIM in respective cells. Though DIM and PSB-16671 exhibited similar affinity cooperativity with embelin at human GPR84, PSB-16671 showed 2-fold higher efficacy modulation of embelin than DIM. These results demonstrated that PSB-16671 is much more effective than DIM in potentiating the function of orthosteric GPR84 agonists in both transfected cells expressing human and mouse GPR84 and in RAW264.7 cells implying that PSB-16671 appears to be more effective to be used as a potential therapeutic candidate or lead compound to develop further potent allosteric drug to treat atherosclerosis.

6.8.6. DIM but not PSB-16671 displays marked variation between human and mouse GPR84 in modulating the function of orthosteric agonists

As compared to orthosteric sites, allosteric sites of GPCRs are likely to display more variation in amino acid sequences between species orthologues (Lindsley et al., 2016), it is expected that allosteric modulators might exhibit species selectivity in displaying cooperativity with orthosteric agonists which might pose a great challenge for the translation of pharmacology of allosteric modulators observed in transfected cells into animal disease models (Christopoulos, 2014; Suratman et al., 2011; Smith and Milligan, 2010). However, in interaction studies using [35 S]-GTP γ S binding assays, PSB-16671 showed no significant variation ($P>0.05$; two-tailed unpaired t-test) in displaying positive cooperativity with orthosteric GPR84 agonists between human and mouse GPR84. Though PSB-16671 displayed 2.4-fold higher affinity cooperativity and 1.5-fold higher net affinity/efficacy cooperativity with compound-1 at FLAG-hGPR84-G α_{i2} than at FLAG-mGPR84-G α_{i2} , these variations did not reach statistical significance. Moreover, equivalent affinity cooperativity (257 vs 251) and net affinity/efficacy cooperativity (182 vs 159) between PSB-16671 and compound-1 were observed between transfected cells expressing FLAG-hGPR84-G α_{i2} and mouse monocyte-macrophage cell line RAW264.7. Similarly, no significant variations in binding affinity modulation or net affinity/efficacy modulation were observed between human and mouse orthologues when C-10 or embelin was used to probe the GPR84 function. By contrast, DIM displayed marked variation in cooperativity

with compound-1 or C-10 between human and mouse GPR84. In comparison with FLAG-hGPR84-G α_{i2} , FLAG-mGPR84-G α_{i2} showed significantly lower affinity cooperativity (α : 120 vs 16) and net affinity/efficacy cooperativity ($\alpha\beta$: 108 vs 25.4) between DIM and compound-1. Though equivalent magnitudes of binding affinity modulation of compound-1 (120 vs 129) or C-10 (28 vs 16) by DIM were observed between transfected cells expressing cloned human GPR84 and LPS-treated RAW264.7 cells, DIM showed some 4 and 5.5-fold lower net affinity/efficacy cooperativity with compound-1 and C-10, respectively at LPS-treated RAW264.7 cells relative to Flp-In T-REx-293 cells expressing FLAG-hGPR84-G α_{i2} . Global analysis of datasets with an operational model of allosterism yielded similar estimates of binding affinity of DIM for human and mouse GPR84 (average K_A : 5 μ M for both human and mouse GPR84), implying that the observed species variation in allosteric effect of DIM on compound-1 or C-10 between human and mouse orthologues was due to differential cooperativity rather than affinity. Suratman et al., (2011) also reported an ago-PAM, LY2033298 which has identical affinity for human and mouse M_4 mAChR but displayed significantly lower positive cooperativity with acetylcholine at mouse M_4 mAChR than human orthologue. As relative to DIM, PSB-16671 has 5-fold higher affinity for human and mouse GPR84 and was found to be more effective in potentiating function of orthosteric GPR84 agonists both in human and mouse GPR84 without displaying any significant species selectivity, PSB-16671 has more potential to be used as a tool compound to characterize the allosteric site(s) of GPR84 and biological function of the receptor.

6.8.7. Complex allosterism between DIM and compound-1 in LPS-treated RAW264.7 cells

While allosteric interaction between DIM and orthosteric agonists displayed in transfected cells expressing FLAG-hGPR84-G α_{i2} could be explained by two state MWC model as the probe-dependence of DIM in modulating binding affinity of orthosteric agonists followed the postulate of this two state model that higher efficacy agonist will be potentiated to greater extent than the lower efficacy agonist, the allosteric interaction between DIM and compound-1 in RAW264.7 cells could not be explained by this two state scheme. DIM displayed higher affinity cooperativity with compound-1 than with C-10 which is consistent with

the two state MWC model according to which, the degree of cooperativity will be strongly correlated with the intrinsic efficacy of orthosteric probe. By contrast, DIM was found to behave as a potent PAM of affinity but a weak NAM of efficacy (4.5-fold decrease in maximal response) of compound-1 in LPS-induced RAW264.7 cells. This opposing effect of DIM on compound-1 affinity and efficacy cannot be explained by the two states MWC model as according to this model allosteric ligand which enhances the binding affinity of the orthosteric ligand will also potentiate the maximal response to orthosteric agonist (Keov et al., 2011) and thus a multi-state model would be required to explore the mechanistic insight into the complex allosterism between DIM and compound-1 in RAW264.7 cells. This complex allosteric modulation wherein the allosteric modulator enhances the binding affinity of orthosteric agonist but decreases the efficacy was also observed in CB1 receptor and FFA3 receptor. Price et al., (2005) reported that Org27569 and PSNCBAM-1 both acted as a strong NAM of efficacy and simultaneously enhanced the binding affinity of the orthosteric CB1 receptor agonist. Similarly, Hudson et al., (2014a) reported that compound 6, an analogue of hexahydroquinolone-3-carboxamide behaved as a potent NAM of efficacy of FFA3 agonist propionate (C3) while it displayed positive binding cooperativity with C3. In both cases, these allosteric modulators acted as PAM antagonists ($\alpha\beta < 1$). In contrast, DIM did not act as a PAM antagonist as it showed high net affinity/efficacy cooperativity, $\alpha\beta$ of 28.

6.8.8. Orthosteric and allosteric ligands bind human and mouse GPR84 with similar affinity

Though binding affinity of antagonist 104 or 107 for human GPR84 can be estimated using the radiolabelled antagonist [^3H]-G9543 (section 4.3.1; Mancini et al., 2019; Mahmud et al., 2017), no other radioligand targeting other binding sites within GPR84 is available which makes it very challenging to estimate the binding affinity of different orthosteric and allosteric ligands. Moreover, the measured potency values of GPR84 ligands estimated in different heterologous expression systems cannot be used as surrogate measures of affinity due to the existence of receptor reserve generated from the higher expression level of the receptor. The application of an operational model of allosterism (Leach et al., 2007; Ehlert, 2005) for global analysis of datasets obtained from the interaction studies between DIM or DIM analogues and orthosteric agonists of GPR84

provided estimates of binding affinity of both ligands to the receptor. As expected, these estimates of binding affinity of the ligand for GPR84 were found to be constant for different combinations of orthosteric and allosteric agonists. For example, the estimated binding affinity of decanoic acid (C-10) for FLAG-hGPR84-G α_{i2} remains constant (average K_A : 0.34, 0.38 and 0.36 mM, respectively) whether DIM, 3a or PSB-16671 was used as the allosteric modulator in the interaction study. Similarly, the mathematical analysis of allosteric interaction between C-10 and DIM, 3a or PSB-16671 yielded the binding affinity of DIM, 3a or PSB-16671 for the human GPR84 to be 6.2, 7.0 and 1.5 μ M, respectively. The estimated binding affinities of compound-1, 6-OAU and embelin for FLAG-hGPR84-G α_{i2} were 69-100 nM, 1-1.3 μ M and 1.5-2.6 μ M, respectively. Equivalent estimates of binding affinities of DIM (K_A : 5.0-8.9 μ M), 3a (K_A : 12.5- 29 μ M) and PSB-16671 (K_A : 0.9-1.4 μ M) for human GPR84 were obtained when compound-1, 6-OAU or embelin was used to probe the receptor function. The rank order of affinity of these ligands for FLAG-hGPR84-G α_{i2} is as follows:

Compound-1>> 6-OAU=PSB-16671=embelin>DIM>3a>>C-10

Based on these estimates of binding affinities, PSB-16671 has 360 and 5-fold higher affinity for human GPR84 than C-10 and DIM, respectively while compound-1 binds human GPR84 with 14 times higher avidity than PSB-16671. The binding affinities of C-10, DIM, PSB-16671, embelin and compound-1 for FLAG-mGPR84-G α_{i2} were estimated to be 0.3 mM, 4.8 μ M, 1.2 μ M, 1.0 μ M and 130 nM which were very similar to those obtained from the allosteric interaction studies performed in LPS-treated RAW264.7 cells and in transfected cells expressing FLAG-hGPR84-G α_{i2} . These results demonstrated that orthosteric and allosteric ligands bind human and mouse GPR84 with similar affinity which is consistent with the maintenance of equivalent potencies of these ligands between human and mouse GPR84 (section 5.3). These results imply that mathematical analysis of the effect of allosteric agonist on the activity of orthosteric agonist by an operational model of allosterism can provide estimates of binding affinity of each ligand to the receptor and this is particularly useful in the case of unavailability of direct binding assays for poorly characterized receptor like GPR84. Gregory et al., (2012) found that estimates of binding affinities of a series of allosteric modulators for mGlu₅ receptor obtained from

the analysis of the allosteric effect of allosteric modulators on orthosteric agonist by an operational model of allosterism were very similar to those derived from radioligand binding assays. Bolognini et al., (2016) also validated the use of this approach for estimation of binding affinity of allosteric ligand AZ1729 and reported no variation in measured affinity between operational model analysis and radioligand binding assays. Another notable thing was that the estimated binding affinities of DIM and embelin for GPR84 were equivalent to their measured potency values in [35 S]-GTP γ S binding assays employing FLAG-hGPR84-G α_{i2} . Moreover, no large variation between affinity for GPR84 and potency to do G protein activation for PSB-16671, compound-1 and 6-OAU were observed wherein potency values were 2.3, 3 and 3.5-times higher than the corresponding affinity value, respectively. This was not the case for C-10 for which affinity was found to be 6.7 times lower than the potency value. Despite this, these outcomes suggested that the measured potencies of GPR84 ligands using [35 S]-GTP γ S binding assay employing GPR84-G α_i fusion protein could be used as surrogate measures of binding affinity of the corresponding ligand for GPR84.

7 Final discussion

G protein-coupled receptor 84 (GPR84), a member of the rhodopsin-like Class A GPCR family, recently has received considerable interest as a novel target for drug development against inflammation-associated diseases (ulcerative colitis, IBD, rheumatoid arthritis, chronic neuropathic pain, esophagitis, atherosclerosis) and fibrosis-associated diseases (idiopathic pulmonary fibrosis, pulmonary hypertension associated with heart failure with reduced ejection fraction (HFrEF), diabetic nephropathy, non-alcoholic steatohepatitis) due to the potential role of GPR84 signalling in promoting or exacerbating inflammation and/or fibrosis (Vermiere et al., 2017; Nicol et al., 2015; Gaidarov et al., 2018; Gagnon et al., 2018; Saniere et al., 2019; Li et al., 2018; Puengel et al., 2018; Nguyen et al., 2019). Based on its restricted and lower basal expression in immune cells with strong upregulation in the diseased conditions, therapeutics targeting GPR84 are predicted to be more selective and less toxic compared to currently available anti-inflammatory or anti-fibrotic agents. Despite these potentials for being a therapeutic target, GPR84 still remains poorly characterized in terms of signal transduction pathways, biological functions and mode of ligand-GPR84 interactions and is still officially considered as an ‘orphan’ receptor as the proposed endogenous agonists, MCFAs possess poor potency/affinity in activating the receptor, with a lack of consensus among the scientific community whether the concentration of these putative endogenous agonists under physiological conditions will reach the level required for activation of the receptor. Though recent years have seen synthesis of some potent and selective synthetic agonists including 6-OAU, compound-1 and its derivatives and the allosteric agonist PSB-16671, as well as a series of potent and selective GPR84 antagonists including the clinically trialled GLPG1205, their mode of binding to GPR84 as well as mode of pharmacological actions are unclear, which has hindered detailed characterization of the receptor. In this context, in an attempt to uncover the therapeutic potential of GPR84, this thesis aimed at elucidating the G protein selectivity of the receptor, defining ligand-GPCR interactions and characterizing the pharmacological profiles of currently available tool compounds along with their potential orthologue selectivity. The major experimental findings of this thesis are as follows:

- Using a series of BRET-based GPR84 SPASM biosensors, agonist-activated human GPR84 was found to couple to $G\alpha_{i/o}$ G protein family members (Figure 3.5 and 3.6). Within the $G\alpha_{i/o}$ G protein family, $G\alpha_{i1/2}$ and $G\alpha_{i3}$ were found to be preferentially recruited to agonist-activated human GPR84 over $G\alpha_z$ and $G\alpha_o$ (Figure 3.7).
- In BRET assays using SPASM-based GPR84 biosensors, DIM and embelin were found to behave as partial agonists compared to the presumed endogenous agonist decanoic acid (C-10) while compound-1 and TUG-1765 acted as super-agonists at human GPR84 (Figure 3.4). Similar trends of the relative efficacy of these GPR84 agonists were also observed in [^{35}S]-GTP γ S binding assays employing membranes generated from transfected cells expressing FLAG-hGPR84- $G\alpha_{i2}$ (Figure 5.7g) or from LPS-induced RAW264.7 cells (Figure 5.9).
- An integral role of arginine 172 of EL2 in orthosteric ligand detection and function was predicted by homology modelling (Figure 4.8) and subsequently confirmed in site-directed mutagenesis studies (Figure 4.12 and 4.14) in which arginine 172 coordinates the carboxylate function of MCFAs and the bioisosteres of carboxylate i.e. hydrophilic head groups of embelin and embelin-like molecules including 6-OAU, compound-1 and TUG-1765.
- Homology modelling, site-directed mutagenesis and ligand docking to constructed homology model also suggested that in addition to arginine 172, phenylalanine 170 of EL2, phenylalanine 335^{6,51} and tryptophan 360^{7,43} are likely to play important roles in orthosteric ligand recognition (Figure 4.15, 4.16 and 4.17).
- Mutagenesis studies suggest that embelin, 6-OAU, compound-1 and TUG-1765 bind human GPR84 at a site that is overlapping with the binding site of the presumed endogenous agonist, decanoic acid i.e they are orthosteric to C-10 whilst DIM and its analogue PSB-16671 bind to hGPR84 on a site that is topographically distinct from the orthosteric binding site (Chapter 4).

- Functional studies and radioligand saturation binding studies with a radiolabelled antagonist [^3H]-G9543, which is an analogue of GPR84 antagonists compound-104, 107, 161, revealed that [^3H]-G9543 and the related antagonists are likely to bind to a site which is distinct from the orthosteric and allosteric binding sites on human GPR84 (Figure 4.10 and 4.21). Despite no atomic-level structure of GPR84 being available to date, mutational analysis and functional studies suggest at least three binding sites on human GPR84 which are spatiotemporally distinct from each other.
- The pharmacology of orthosteric agonists including C-10, embelin, compound-1 and allosteric agonists including DIM and PSB-16671 as well as antagonists of GPR84 observed in RAW264.7 cells was similar to those displayed in transfected cells expressing mouse GPR84 (Figure 5.9 and 5.10).
- In [^{35}S]-GTP γ S binding assays, antagonists but not agonists of GPR84 displayed significant variation in pharmacology between the human and mouse orthologues as evidenced from either loss of activity of competitive antagonist compound-837 or markedly reduced potencies of non-competitive GPR84 antagonists including compound-104, 107 and 161 at mouse GPR84 (Figure 5.13 and 5.10).
- DIM and DIM analogue PSB-16671 acted as highly effective positive allosteric modulators (PAM) of function of GPR84 orthosteric agonists including C-10, embelin, 6-OAU and compound-1 at both human and mouse GPR84 through a mechanism which incorporates both affinity and efficacy modulation of embelin and C-10 or through predominantly modulating binding affinity of full agonist (6-OAU/compound-1) (Figure 6.2, 6.3, 6.5, 6.11, 6.12, 6.13).
- DIM and PSB-16671 displayed PAM activity at human and mouse GPR84 in a 'probe-dependent' manner wherein the positive binding affinity cooperativity tracks with the intrinsic efficacy of the orthosteric agonist (Figure 6.4a, Table 6.6 and 6.7). However, no significant probe-dependence was observed in allosteric interaction between DIM/DIM

analogues and orthosteric agonists at human/mouse GPR84 when net affinity/efficacy cooperativity was considered (Figure 6.4b, Table 6.6 and 6.7).

- Compared to DIM, PSB-16671 displayed significantly higher positive binding affinity cooperativity and higher net affinity/efficacy cooperativity with C-10/compound-1 at human and mouse GPR84, implying that the functional cooperativity with orthosteric GPR84 agonists tracks with the intrinsic efficacy of the modulator used (Chapter 6).
- Mathematical analysis of allosteric interaction between DIM/DIM analogues and GPR84 orthosteric agonists showed that the estimated binding affinities of GPR84 ligands for mouse GPR84 were equivalent to those observed for the human GPR84 (Chapter 6).

In summary, throughout this thesis, I characterized GPR84 orthosteric and allosteric ligands in terms of their binding modes and mechanism of pharmacological actions. These research efforts would have a broader implication in generating therapeutics targeting GPR84. GPR84 antagonists including GLPG1205 in isolation or in combination with other anti-inflammatory or anti-fibrotic agent would be potential therapeutics for the treatment of idiopathic pulmonary fibrosis, chronic neuropathic pain, pulmonary hypertension associated with heart failure with reduced ejection fraction (HFrEF), diabetic nephropathy etc. while GPR84 agonists such as compound-1 and its derivatives or a combination of orthosteric and allosteric agonist (PSB-16671) would be a potential therapy for atherosclerosis although further research is required to validate the role of GPR84 signalling in the pathogenesis of atherosclerosis.

Although compound-1 and its derivatives, including TUG-1765/compound-51 are highly potent and selective agonists of the receptor, the predicted modes of ligand-GPR84 interaction described in this thesis will accelerate the structure-based drug design (SBDD) and thus will lead to the development of further improved ligands which can be employed as tool compounds or future therapeutics.

Despite being a potential therapeutic target, little is known regarding the biological roles of this receptor hindering the target validation process of the receptor. Although recombinant heterologous expression systems are widely employed for the study of pharmacology of GPCRs owing to their simplicity and ubiquity, the observed pharmacology might not be truly representative of physiological function of a receptor (Croston, 2017) and thus GPR84 research should now be focussed on the translation of the observed pharmacology in transfected cells into primary human and murine cell lines including lymphocytes, neutrophils, dendritic cells etc. and on the elucidation of pathophysiological roles of the receptor by employing animal disease models including mouse models of atherosclerosis, Alzheimer's disease, Type II diabetes, diabetic nephropathy and different fibrosis models.

As the availability of potent and selective tool compounds with a defined mode of action is required for the success in the target validation process, the characterization of GPR84 orthosteric and allosteric ligands described in this thesis might be useful for the translational research on GPR84. Based on the findings from the pharmacological characterization of GPR84 ligands in transfected cells expressing human and mouse GPR84 and murine macrophage cell line RAW264.7 cells, compound-1 and its derivatives TUG-1765 can be used as potent and selective tool compound to characterize the orthosteric site of GPR84 whilst DIM analogue PSB-16671 instead of DIM can be employed as a tool compound to characterize the allosteric site of GPR84 or as a lead compound to develop further improved allosteric ligand as PSB-16671 was found to be more effective in enhancing the function of orthosteric GPR84 agonists with higher affinity for GPR84 displaying no species selectivity between human and mouse orthologues. Potent and selective agonists compound-1, TUG-1765 and PSB-16671 can also be fluorescently labelled which might be useful in the biological and pharmacological characterization of GPR84.

In the context of ongoing debate on the physiological agonist of the receptor, investigation of role of GPR84 signalling in the pathogenesis of human and mouse atherosclerosis or neuro-inflammatory diseases might inform true endogenous agonist of the receptor as GPR84 was reported to be associated with progression of atherosclerotic plaque formation (Recio et al., 2018) and with microglial motility and ruffling in response to neuronal injury (Wei et al., 2017).

As there might be substantial variation in the pharmacology of GPCR ligands between different species orthologues, which can hinder the translation of in vitro pharmacology into in-vivo animal disease models, I investigated the potential orthologue selectivity of GPR84 ligands using transfected cells expressing either human and mouse GPR84 and the mouse monocyte-macrophage cell line RAW264.7. The maintenance of similar pharmacology of GPR84 orthosteric and allosteric agonists between human and mouse GPR84 implies that these ligands can be utilized as tool compounds in mouse-derived cell lines or mouse disease models.

The observed selectivity of GPR84 antagonist compound-837 for human GPR84 over mouse orthologue implicates that compound-837 could not be employed for in vivo mouse disease models and the observed significant reduction in potency of a series of non-competitive antagonists (compound-104, 107) at mouse GPR84 implies that cautions should be taken in the use of these antagonists in mouse models/cell lines. Further studies are required to investigate the molecular basis of human selectivity of compound-837 over the mouse orthologue employing the humanized mouse GPR84 and to define the molecular determinants responsible for the reduced affinity of non-competitive GPR84 antagonists at mouse GPR84 compared to the human orthologue. Such structural information might be useful for defining their binding modes which can then be utilized to design and develop further improved ligands. In terms of defining the orthologue selectivity of GPR84 ligands, future research should include investigation of GPR84 signalling in a broader range of species orthologues including rat, bovine, guinea pig, sheep receptor.

As elucidation of signal transduction pathways of a GPCR is necessary to find out the specific biological function(s) of the receptor, future study with GPR84 should also focus on the extensive investigation of downstream signalling pathways as current scientific literature shows conflicting information on the GPR84 signalling pathways. For example, though Recio et al., (2018) reported that 6-OAU-activated GPR84 promotes NF κ B translocation to the nucleus resulting in enhanced expression of pro-inflammatory mediators in LPS-induced macrophages, GPR84 was found to be associated with inhibition of NF κ B signalling pathways in osteoclast precursor cells, BMDMs (Park et al., 2018). Similarly, Park et al., (2018) reported that GPR84 activation inhibits ERK

signalling pathways in BMDM which is in sharp contrast with the finding reported by Recio et al., (2018) and other groups that GPR84 activates ERK1/2 signalling. Moreover, though Gaidarov et al., (2018) reported that embelin-induced GPR84 activation results in coupling to $G\alpha_{12/13}$ -induced Rho-Rac signalling pathways, no interaction between compound-1/TUG-1765-activated human GPR84 and $G\alpha_{12/13}$ G protein was found using the SPASM sensor-based BRET assay (Figure 3.5 and 3.6) which is in agreement with findings reported by Gagnon et al., (2018). Further studies are required to investigate this discrepancy. In this context, employing the CRISPR/Cas9 engineered cells lacking G protein(s) or GPR84 receptor might be an effective strategy to elucidate the signalling pathways and associated biological functions of this poorly characterized receptor.

As signalling outcome of a GPCR in a specific cell is also dependent on the 'phosphorylation barcodes' of the receptor, future research should be directed towards the investigation of phosphorylation profile(s) of GPR84. Recently biased agonists of GPCR have attracted considerable interests due to their potential to display fewer side effects compared to the conventional unbiased agonists and thus the biased agonism if any at GPR84 in terms of G protein versus β -arrestin-mediated signalling needs to be investigated.

The research efforts presented in this thesis provides new insights into mechanisms of allosteric interactions of GPR84 with detailed pharmacology of such allosteric interactions including 'probe-dependence' and potential orthologue variation of allosteric effects between human and mouse GPR84. These characterizations of allosteric pharmacology might accelerate drug development program targeting the allosteric sites of this receptor. However, to validate the allosteric modulation at GPR84 as a potential therapeutic strategy to treat diseases like atherosclerosis, further research is required to uncover the binding modes of these allosteric ligands to the receptor and to translate the allosteric pharmacology observed in in vitro cell lines into in vivo animal models.

Similar to the allosteric ligands for FFA3 (Hudson et al., 2014a) and for metabotropic glutamate receptors (Wood et al., 2011), the DIM derivatives were also found to be characterized by the presence of the so-called 'molecular switches' i.e small chemical modifications that can alter the allosteric effects dramatically in a series of allosteric ligands which was evidenced from the

observed differential modes of allosteric interactions such as ago-PAM (DIM, analogue 3a and PSB-16671), weak NAM (analogue 6a), PAM/NAM (DIM in RAW264.7 cells) activity and loss of allosteric modulation and agonism (analogue 2b and 3c). Although the existence of these types of molecular switches represents a shallow SAR for GPR84 allosteric ligands, thereby posing a challenge for lead optimization, this also can be exploited for the generation of diverse ligands with differential modes of allosteric pharmacology. The PAM/NAM activity of DIM on compound-1 in RAW264.7 cells suggests that there is a possibility to design allosteric agonists acting as PAM antagonists at GPR84 which might have improved target coverage and longer half-life compared to the currently available orthosteric antagonists (Kenakin and Strachan, 2018).

References

- Abdel-Aziz, H., Schneider, M., Neuhuber, W., Meguid Kassem, A., Khailah, S., Müller, J., Gamal Eldeen, H., Khairy, A., T Khayyal, M., Shcherbakova, A., Efferth, T. and Ulrich-Merzenich, G. (2016) GPR84 and TREM-1 Signaling Contribute to the Pathogenesis of Reflux Esophagitis. *Mol Med.* 21(1):1011-24.
- Ahn, K.S., Sethi, G. and Aggarwal, B.B. (2007) Embelin, an inhibitor of X chromosome-linked inhibitor-of-apoptosis protein, blocks nuclear factor-kappaB (NF-kappaB) signaling pathway leading to suppression of NF-kappaB-regulated antiapoptotic and metastatic gene products. *Mol Pharmacol.* 71(1):209-19.
- Aiello, R.J., Bourassa, P.A., Lindsey, S., Weng, W., Natoli, E., Rollins, B.J. and Milos, P.M. (1999) Monocyte chemoattractant protein-1 accelerates atherosclerosis in apolipoprotein E-deficient mice. *Arterioscler Thromb Vasc Biol.* 19(6):1518-25.
- Alexander, S.P., Christopoulos, A., Davenport, A.P., Kelly, E., Marrion, N.V., Peters, J.A., Faccenda, E., Harding, S.D., Pawson, A.J., Sharman, J.L., Southan, C., Davies, J.A. and CGTP Collaborators. (2017) THE CONCISE GUIDE TO PHARMACOLOGY 2017/18: G protein-coupled receptors. *Br J Pharmacol.* 174 (Suppl 1):S17-S129.
- Alexander, S.P., Davenport, A.P., Kelly, E., Marrion, N., Peters, J.A., Benson, H.E., Faccenda, E., Pawson, A.J., Sharman, J.L., Southan, C., Davies, J.A. and CGTP Collaborators. (2015) The Concise Guide to PHARMACOLOGY 2015/16: G protein-coupled receptors. *Br J Pharmacol.* 172(24):5744-869.
- Altenbach, C., Kusnetzow, A.K., Ernst, O.P., Hofmann, K.P. and Hubbell, W.L. (2008) High-resolution distance mapping in rhodopsin reveals the pattern of helix movement due to activation. *Proc Natl Acad Sci.* 105(21):7439-44.
- Alvarez-Curto, E. and Milligan, G. (2016) Metabolism meets immunity: The role of free fatty acid receptors in the immune system. *Biochem Pharmacol.* 114:3-13.

Araç, D., Boucard, A.A., Bolliger, M.F., Nguyen, J., Soltis, S.M., Südhof, T.C. and Brunger, A.T. (2012) A novel evolutionarily conserved domain of cell-adhesion GPCRs mediates autoproteolysis. *EMBO J.* 31(6):1364-78.

Asagiri, M. and Takayanagi, H. (2007) The molecular understanding of osteoclast differentiation. *Bone.* 40(2):251-64.

Audet, M. and Bouvier, M. (2012) Restructuring G-protein- coupled receptor activation. *Cell.* 151(1):14-23.

Audoy-Rémus, J., Bozoyan, L., Dumas, A., Filali, M., Lecours, C., Lacroix, S., Rivest, S., Tremblay, M.E. and Vallières, L. (2015) GPR84 deficiency reduces microgliosis, but accelerates dendritic degeneration and cognitive decline in a mouse model of Alzheimer's disease. *Brain Behav Immun.* 46:112-20.

Baker, D. and Sali, A. (2001) Protein structure prediction and structural genomics. *Science.* 294:93-6.

Bédard, A., Tremblay, P., Chernomoretz, A. and Vallières, L. (2007) Identification of genes preferentially expressed by microglia and upregulated during cuprizone-induced inflammation. *Glia.* 55(8):777-89.

Berizzi, A.E., Gentry, P.R., Rueda, P., Den Hoedt, S., Sexton, P.M., Langmead, C.J. and Christopoulos, A. (2016) Molecular Mechanisms of Action of M5 Muscarinic Acetylcholine Receptor Allosteric Modulators. *Mol Pharmacol.* 90(4): 427-36.

Bertin, B., Freissmuth, M., Jockers, R., Strosberg, A.D., and Marullo, S. (1994) Cellular signaling by an agonist-activated receptor/Gs alpha fusion protein. *Proc Natl Acad Sci.* 91(19):8827-31.

Bolognini, D., Moss, C.E., Nilsson, K., Petersson, A.U., Donnelly, I., Sergeev, E., König, G.M., Kostenis, E., Kurowska-Stolarska, M., Miller, A., Dekker, N., Tobin,

A.B. and Milligan, G. (2016) A Novel Allosteric Activator of Free Fatty Acid 2 Receptor Displays Unique Gi-functional Bias. *J Biol Chem.* 291(36):18915-31.

Bouchard, C., Page, J., Bedard, A., Tremblay, P., and Vallieres, L. (2007) G protein-coupled receptor 84, a microglia-associated protein expressed in neuroinflammatory conditions. *Glia.* 55(8):790-800.

Bradley, S.J., Bourgognon, J.M., Sanger, H.E., Verity, N., Mogg, A.J., White, D.J., Butcher, A.J., Moreno, J.A., Molloy, C., Macedo-Hatch, T., Edwards, J.M., Wess, J., Pawlak, R., Read, D.J., Sexton, P.M., Broad, L.M., Steinert, J.R., Mallucci, G.R., Christopoulos, A., Felder, C.C. and Tobin, AB. (2017) M1 muscarinic allosteric modulators slow prion neurodegeneration and restore memory loss. *J Clin Invest.* 127(2):487-99.

Brown, A.J., Goldsworthy, S.M., Barnes, A.A., Eilert, M.M., Tcheang, L., Daniels, D., Muir, A.I., Wigglesworth, M.J., Kinghorn, I., Fraser, N.J., Pike, N.B., Strum, J.C., Steplewski, K.M., Murdock, P.R., Holder, J.C., Marshall, F.H., Szekeres, P.G., Wilson, S., Ignar, D.M., Foord, S.M., Wise, A. and Dowell, S.J. (2003) The Orphan G protein-coupled receptors GPR41 and GPR43 are activated by propionate and other short chain carboxylic acids. *J Biol Chem.* 278(13):11312-9.

Brueggemeier, U., Geerts, A., Golz, S., and Summer, H. (2005). Diagnostics and therapeutics for diseases associated with g protein-coupled receptor 84 (gpr84). WO2005050225 A2.

Brys, R. C., and Dupont, S. (2013) Screening methods to identify compounds useful in the prevention and/or treatment of inflammatory conditions. WO 2013092793 A1.

Bunnage, M.E., Chekler, E.L. and Jones, L.H. (2013) Target validation using chemical probes. *Nat Chem Biol.* 9(4):195-9.

Burford, N.T., Traynor, J.R. and Alt, A. (2015) Positive allosteric modulators of the μ -opioid receptor: a novel approach for future pain medications. *Br J Pharmacol.* 172(2):277-86.

- Canals, M., Lane, J.R., Wen, A., Scammells, P.J., Sexton, P.M. and Christopoulos, A. (2012) A Monod-Wyman-Changeux mechanism can explain G protein-coupled receptor (GPCR) allosteric modulation. *J Biol Chem.* 287(1): 650-9.
- Chan, W.Y., McKinzie, D.L., Bose, S., Mitchell, S.N., Witkin, J.M., Thompson, R.C., Christopoulos, A., Lazareno, S., Birdsall, N.J., Bymaster, F.P. and Felder, C.C. (2008) Allosteric modulation of the muscarinic M4 receptor as an approach to treating schizophrenia. *Proc Natl Acad Sci.* 105(31):10978-83.
- Christiansen, E., Watterson, K.R., Stocker, C.J., Sokol, E., Jenkins, L., Simon, K., Grundmann, M., Petersen, R.K., Wargent, E.T., Hudson, B.D., Kostenis, E., Ejlsing, C.S., Cawthorne, M.A., Milligan, G. and Ulven, T. (2015) Activity of dietary fatty acids on FFA1 and FFA4 and characterisation of pinolenic acid as a dual FFA1/FFA4 agonist with potential effect against metabolic diseases. *Br J Nutr.* 113(11):1677-88.
- Christopoulos, A. (2014) Advances in G protein-coupled receptor allostery: from function to structure. *Mol Pharmacol.* 86(5):463-78.
- Christopoulos, A. and Kenakin, T. (2002) G protein-coupled receptor allostery and complexing. *Pharmacol Rev.* 54(2):323-74.
- Christopoulos, A., Changeux, J.P., Catterall, W.A., Fabbro, D., Burris, T.P., Cidlowski, J.A., Olsen, R.W., Peters, J.A., Neubig, R.R., Pin, J.P., Sexton, P.M., Kenakin, T.P., Ehlert, F.J., Spedding, M. and Langmead, C.J. (2014) International Union of Basic and Clinical Pharmacology. XC. multisite pharmacology: recommendations for the nomenclature of receptor allostery and allosteric ligands. *Pharmacol Rev.* 66(4):918-47.
- Chung, S., Funakoshi, T. and Civelli, O. (2008) Orphan GPCR research. *Br J Pharmacol.* 153 (Suppl 1):S339-46.

Clegg, M.A., Tomkinson, N.C., Prinjha, R.K. and Humphreys, P.G. (2017) Small molecules and their role in effective preclinical target validation. *Future Med Chem.* 9(14):1579-82.

Conklin, B.R., Herzmark, P., Ishida, S., Voyno-Yasenetskaya, T.A., Sun, Y., Farfel, Z., Bourne, H.R.(1996) Carboxyl-terminal mutations of Gq alpha and Gs alpha that alter the fidelity of receptor activation. *Mol Pharmacol.* 50(4):885-90.

Costanzi, S. (2010) Modeling G Protein-Coupled Receptors: a Concrete Possibility. *Chim Oggi.* 28(3):26-31.

Costanzi, S. (2012) Homology modeling of class A G protein-coupled receptors. *Methods Mol Biol.* 857:259-79.

Costanzi, S. (2013) Modeling G protein-coupled receptors and their interactions with ligands. *Curr Opin Struct Biol.* 23:185-190.

Croston, G.E. (2017) The utility of target-based discovery. *Expert Opin Drug Discov.* 12(5):427-9.

Dallagnol, J.C.C., Khajehali, E., van der Westhuizen, E.T., Jörg, M., Valant, C., Gonçalves, A.G., Capuano, B., Christopoulos, A. and Scammells, P.J. (2018) Synthesis and Pharmacological Evaluation of Heterocyclic Carboxamides: Positive Allosteric Modulators of the M1 Muscarinic Acetylcholine Receptor with Weak Agonist Activity and Diverse Modulatory Profiles. *J Med Chem.* 61(7):2875-94.

Davenport, A.P., Alexander, S.P., Sharman, J.L., Pawson, A.J., Benson, H.E., Monaghan, A.E., Liew, W.C., Mpamhanga, C.P., Bonner, T.I., Neubig, R.R., Pin, J.P., Spedding, M. and Harmar, A.J. (2013) International Union of Basic and Clinical Pharmacology. LXXXVIII. G protein-coupled receptor list: recommendations for new pairings with cognate ligands. *Pharmacol Rev.* 65(3):967-86.

- Dawson, J., Miltz, W., Mir, A.K. and Wiessner, C. (2003) Targeting monocyte chemoattractant protein-1 signalling in disease. *Expert Opin Ther Targets*. 7(1):35-48.
- DeWire, S.M., Ahn, S., Lefkowitz, R.J. and Shenoy, S.K. (2007) Beta-arrestins and cell signaling. *Annu Rev Physiol*. 69:483-510.
- Dietrich, P.A., Yang, C., Leung, H.H., Lynch, J.R., Gonzales, E., Liu, B., Haber, M., Norris, M.D., Wang, J. and Wang, J.Y. (2014) GPR84 sustains aberrant β -catenin signaling in leukemic stem cells for maintenance of MLL leukemogenesis. *Blood*. 124(22):3284-94.
- Díez, J.J. and Iglesias, P. (2003) The role of the novel adipocyte-derived hormone adiponectin in human disease. *Eur J Endocrinol*. 148(3):293-300.
- Divorty, N., Mackenzie, A.E., Nicklin, S.A. and Milligan, G. (2015) G protein-coupled receptor 35: an emerging target in inflammatory and cardiovascular disease. *Front Pharmacol*. 6:41.
- Divorty, N., Milligan, G., Graham, D. and Nicklin, S.A. (2018) The Orphan Receptor GPR35 Contributes to Angiotensin II-Induced Hypertension and Cardiac Dysfunction in Mice. *Am J Hypertens*. 31(9):1049-58.
- Dorr, P., Westby, M., Dobbs, S., Griffin, P., Irvine, B., Macartney, M., Mori, J., Rickett, G., Smith-Burchnell, C., Napier, C., Webster, R., Armour, D., Price, D., Stammen, B., Wood, A. and Perros, M. (2005) Maraviroc (UK-427,857), a potent, orally bioavailable, and selective small-molecule inhibitor of chemokine receptor CCR5 with broad-spectrum anti-human immunodeficiency virus type 1 activity. *Antimicrob Agents Chemother*. 49(11):4721-32.
- Dorsam, R.T. and Gutkind, J.S. (2007) G-protein-coupled receptors and cancer. *Nat Rev Cancer*. 7(2):79-94.
- Dupont, S., Arijs, I., Blanque, R., Laukens, D., Nys, K., Ceccotti, M.C., Merciris, D., De Vos, S., Mate, O., Parent, I., De Vriendt, V., Labeguere,

- F., Galien, R., Devos, M., Rutgeerts, P., Vandeghinste, N., Vermeire, S., and Brys, R. (2015) GPR84 inhibition as a novel therapeutic approach in IBD: mechanistic and translational studies. *J Crohns Colitis*. 9 (suppl 1):S92-S93.
- Eder, J., Sedrani, R. and Wiesmann, C. (2014) The discovery of first-in-class drugs: origins and evolution. *Nat Rev Drug Discov*. 13(8):577-87.
- Ehlert, F.J. (2005) Analysis of allosterism in functional assays. *J Pharmacol Exp Ther*. 315(2):740-54.
- Eichel, K., Jullié, D. and von Zastrow, M. (2016) β -Arrestin drives MAP kinase signalling from clathrin-coated structures after GPCR dissociation. *Nat Cell Biol*. 18(3):303-10.
- Engström, M., Tomperi, J., El-Darwish, K., Ahman, M., Savola, J.M. and Wurster, S. (2005) Superagonism at the human somatostatin receptor subtype 4. *J Pharmacol Exp Ther*. 312(1):332-8.
- Fang, Y., Kenakin, T., and Liu, C. (2015) Editorial: Orphan GPCRs as emerging drug targets. *Front Pharmacol*. 6:295.
- Fredriksson, R., Lagerström, M.C., Lundin, L.G. and Schiöth, H.B. (2003) The G-protein-coupled receptors in the human genome form five main families. Phylogenetic analysis, paralogon groups, and fingerprints. *Mol Pharmacol*. 63(6):1256-72.
- Fredriksson, R., and Schioth, H. B. (2005) The Repertoire of G-Protein-Coupled Receptors in Fully Sequenced Genomes. *Mol Pharmacol*. 67(5):1414-25.
- Friesner, R.A., Murphy, R.B., Repasky, M.P., Frye, L.L., Greenwood, J.R., Halgren, T.A., Sanschagrin, P.C. and Mainz, D.T. (2006) Extra precision glide: docking and scoring incorporating a model of hydrophobic enclosure for protein-ligand complexes. *J Med Chem*. 49(21):6177-96.

Fukagawa, M., Shimazaki, R. and Akizawa, T. (2018) Head-to-head comparison of the new calcimimetic agent evocalcet with cinacalcet in Japanese hemodialysis patients with secondary hyperparathyroidism. *Kidney Int.* 94:818-25.

Fukagawa, M., Yokoyama, K., Shigematsu, T., Akiba, T., Fujii, A., Kuramoto, T., Odani, M. and Akizawa, T. (2017) A phase 3, multicentre, randomized, double-blind, placebo-controlled, parallel-group study to evaluate the efficacy and safety of etelcalcetide (ONO-5163/AMG 416), a novel intravenous calcimimetic, for secondary hyperparathyroidism in Japanese haemodialysis patients. *Nephrol Dial Transplant.* 32(10):1723-30.

Fukuhara, S., Chikumi, H. and Gutkind, J.S. (2000) Leukemia-associated Rho guanine nucleotide exchange factor (LARG) links heterotrimeric G proteins of the G(12) family to Rho. *FEBS Lett.* 485(2-3):183-8.

Fukuhara, S., Murga, C., Zohar, M., Igishi, T. and Gutkind JS. (1999) A novel PDZ domain containing guanine nucleotide exchange factor links heterotrimeric G proteins to Rho. *J Biol Chem.* 274(9):5868-79.

Gagnon, L., Leduc, M., Thibodeau, J.F., Zhang, M.Z., Grouix, B., Sarra-Bournet, F., Gagnon, W., Hince, K., Tremblay, M., Geerts, L., Kennedy, C.R.J., Hébert, R.L., Gutsol, A., Holterman, C.E., Kamto, E., Gervais, L., Ouboudinar, J., Richard, J., Felton, A., Laverdure, A., Simard, J.C., Létourneau, S., Cloutier, M.P., Leblond, F.A., Abbott, S.D., Penney, C., Duceppe, J.S., Zacharie, B., Dupuis, J., Calderone, A., Nguyen, Q.T., Harris, R.C. and Laurin, P. (2018) A Newly Discovered Antifibrotic Pathway Regulated by Two Fatty Acid Receptors: GPR40 and GPR84. *Am J Pathol.* 188(5):1132-48.

Gaidarov, I., Anthony, T., Gatlin, J., Chen, X., Mills, D., Solomon, M., Han, S., Semple, G. and Unett, D.J. (2018) Embelin and its derivatives unravel the signaling, proinflammatory and antiatherogenic properties of GPR84 receptor. *Pharmacol Res.* 13:185-98.

Geetha, V. R., Vamshi, K. T., Joseph, A. D., and Vinay, S. B. (2007) Fatty acid receptors as new therapeutic targets for diabetes. *Expert Opin Ther Targets*. 11:661-71.

Gentry, P.R., Sexton, P.M. and Christopoulos, A. (2015) Novel Allosteric Modulators of G Protein-coupled Receptors. *J Biol Chem*. 290(32):19478-88.

Gilman, A.G. (1987) G proteins: transducers of receptor-generated signals. *Annu Rev Biochem*. 56:615-49.

Gregory, K.J., Noetzel, M.J., Rook, J.M., Vinson, P.N., Stauffer, S.R., Rodriguez, A.L., Emmitte, K.A., Zhou, Y., Chun, A.C., Felts, A.S., Chauder, B.A., Lindsley, C.W., Niswender, C.M. and Conn, P.J. (2012) Investigating metabotropic glutamate receptor 5 allosteric modulator cooperativity, affinity, and agonism: enriching structure-function studies and structure-activity relationships. *Mol Pharmacol*. 82(5):860-75.

Gurevich, V.V. and Gurevich, E.V. (2018) GPCRs and Signal Transducers: Interaction Stoichiometry. *Trends Pharmacol Sci*. 39(7):672-84.

Hakak, Y., Unett, D.J., Gatlin, J., Liaw, C.W. and Inc, A.P. (2007) Human G protein-coupled receptor and modulators thereof for the treatment of atherosclerosis and atherosclerotic disease and for the treatment of conditions related to MCP-1 expression. WO Patent 2007/027661 (A2)

Hamann, J., Aust, G., Araç, D., Engel, F.B., Formstone, C., Fredriksson, R., Hall, R.A., Harty, B.L., Kirchhoff, C., Knapp, B., Krishnan, A., Liebscher, I., Lin, H.H., Martinelli, D.C., Monk, K.R., Peeters, M.C., Piao, X., Prömel, S., Schöneberg, T., Schwartz, T.W., Singer, K., Stacey, M., Ushkaryov, Y.A., Vallon, M., Wolfrum, U., Wright, M.W., Xu, L., Langenhan, T. and Schiöth, H.B. (2015) International Union of Basic and Clinical Pharmacology. XCIV. Adhesion G protein-coupled receptors. *Pharmacol Rev*. 67(2):338-67.

- Han, L., Song, S., Niu, Y., Meng, M. and Wang, C. (2017) Eicosapentaenoic Acid (EPA) Induced Macrophages Activation through GPR120-Mediated Raf-ERK1/2-IKK β -NF- κ B p65 Signaling Pathways. *Nutrients*. 9(9):937.
- Han, L., Yu, J., Chen, Y., Cheng, D., Wang, X. and Wang, C. (2018) Immunomodulatory Activity of Docosahexenoic Acid on RAW264.7 Cells Activation through GPR120-Mediated Signaling Pathway. *J Agric Food Chem*. 66(4):926-34.
- Hara, T., Kimura, I., Inoue, D., Ichimura, A., and Hirasawa, A. (2013) Free Fatty Acid Receptors and Their Role in Regulation of Energy Metabolism. *Rev Physiol Biochem Pharmacol*. 164:77-116
- Harrison, C. and Traynor, J.R. (2003) The [35S]GTPgammaS binding assay: approaches and applications in pharmacology. *Life Sci*. 74(4):489-508.
- Hart, M.J., Jiang, X., Kozasa, T., Roscoe, W., Singer, W.D., Gilman, A.G., Sternweis, P.C. and Bollag, G. (1998) Direct stimulation of the guanine nucleotide exchange activity of p115 RhoGEF by G α 13. *Science*. 280(5372):2112-4.
- Hauser, A.S., Attwood, M.M., Rask-Andersen, M., Schiöth, H.B. and Gloriam, D.E. (2017) Trends in GPCR drug discovery: new agents, targets and indications. *Nat Rev Drug Discov*. 16(12):829-42.
- Hirasawa, A., Tsumaya, K., Awaji, T., Katsuma, S., Adachi, T., Yamada, M., Sugimoto, Y., Miyazaki, S. and Tsujimoto, G. (2005) Free fatty acids regulate gut incretin glucagon-like peptide-1 secretion through GPR120. *Nat Med*. 11(1):90-4.
- Hofmann, K.P., Scheerer, P., Hildebrand, P.W., Choe, H.W., Park, J.H., Heck, M. and Ernst, O.P. (2009) A G protein-coupled receptor at work: the rhodopsin model. *Trends Biochem Sci*. 34(11):540-52.

Holliday, N.D., Watson, S.J. and Brown, A.J. (2012) Drug discovery opportunities and challenges at G protein coupled receptors for long chain free Fatty acids. *Front Endocrinol (Lausanne)*. 2:112.

Hopkins, A. L., and Groom, C. R. (2002) The druggable genome. *Nat Rev Drug Discov*. 1:727-30.

Hu, R., Zhu, K., Li, Y., Yao, K., Zhang, R., Wang, H., Yang, W. and Liu, Z. (2011) Embelin induces apoptosis through down-regulation of XIAP in human leukemia cells. *Med Oncol*. 28(4):1584-8.

Huang, W., Manglik, A., Venkatakrishnan, A.J., Laeremans, T., Feinberg, E.N., Sanborn, A.L., Kato, H.E., Livingston, K.E., Thorsen, T.S., Kling, R.C., Granier, S., Gmeiner, P., Husbands, S.M., Traynor, J.R., Weis, W.I., Steyaert, J., Dror, R.O. and Kobilka, B.K. (2015) Structural insights into μ -opioid receptor activation. *Nature*. 524(7565):315-21.

Hudson, B.D., Christiansen, E., Murdoch, H., Jenkins, L., Hansen, A.H., Madsen, O., Ulven, T. and Milligan, G. (2014a) Complex pharmacology of novel allosteric free fatty acid 3 receptor ligands. *Mol Pharmacol*. 86(2):200-10.

Hudson, B.D., Due-Hansen, M.E., Christiansen, E., Hansen, A.M., Mackenzie, A.E., Murdoch, H., Pandey, S.K., Ward, R.J., Marquez, R., Tikhonova, I.G., Ulven, T. and Milligan, G. (2013a) Defining the molecular basis for the first potent and selective orthosteric agonists of the FFA2 free fatty acid receptor. *J Biol Chem*. 288(24):17296-312.

Hudson, B.D., Shimpukade, B., Mackenzie, A.E., Butcher, A.J., Pediani, J.D., Christiansen, E., Heathcote, H., Tobin, A.B., Ulven, T., and Milligan, G. (2013b). The pharmacology of TUG-891, a potent and selective agonist of the free fatty acid receptor 4 (FFA4/GPR120), demonstrates both potential opportunity and possible challenges to therapeutic agonism. *Mol Pharmacol*. 84(5):710-25.

Hudson, B.D., Shimpukade, B., Milligan, G. and Ulven, T. (2014b) The molecular basis of ligand interaction at free fatty acid receptor 4 (FFA4/GPR120). *J Biol Chem.* 289(29):20345-58.

Hudson, B.D., Smith, N.J. and Milligan, G. (2011) Experimental challenges to targeting poorly characterized GPCRs: uncovering the therapeutic potential for free fatty acid receptors. *Adv Pharmacol.* 62:175-218.

Hudson, B.D., Ulven, T. and Milligan, G. (2013c) The therapeutic potential of allosteric ligands for free fatty acid sensitive GPCRs. *Curr Top Med Chem.* 13(1): 14-25.

Hughes, J.P., Rees, S., Kalindjian, S.B. and Philpott, K.L. (2011) Principles of early drug discovery. *Br J Pharmacol.* 162(6):1239-49.

Husted, A.S., Trauelsen, M., Rudenko, O., Hjorth, S.A. and Schwartz, T.W. (2017) GPCR-Mediated Signaling of Metabolites. *Cell Metab.* 25(4):777-96.

Isberg, V., Mordalski, S., Munk, C., Rataj, K., Harpsoe, K., Hauser, A. S., Vroling, B., Bojarski, A. J., Vriend, G. and Gloriam, D. E. (2016) 'GPCRdb: an information system for G protein-coupled receptors'. *Nucleic Acids Res.* 44(D1):D356-64.

Itoh, Y., Kawamata, Y., Harada, M., Kobayashi, M., Fujii, R., Fukusumi, S., Ogi, K., Hosoya, M., Tanaka, Y., Uejima, H., Tanaka, H., Maruyama, M., Satoh, R., Okubo, S., Kizawa, H., Komatsu, H., Matsumura, F., Noguchi, Y., Shinohara, T., Hinuma, S., Fujisawa, Y. and Fujino, M. (2003) Free fatty acids regulate insulin secretion from pancreatic beta cells through GPR40. *Nature.* 422(6928):173-6.

Jacobson, M.P., Pincus, D.L., Rapp, C.S., Day, T.J., Honig, B., Shaw, D.E. and Friesner, R.A. (2004) A hierarchical approach to all-atom protein loop prediction. *Proteins.* 55(2):351-67.

Jenkins, L., Alvarez-Curto, E., Campbell, K., de Munnik, S., Canals, M., Schlyer, S. and Milligan, G. (2011) Agonist activation of the G protein-coupled receptor

GPR35 involves transmembrane domain III and is transduced via $G\alpha_{13}$ and β -arrestin-2. *Br J Pharmacol*. 162(3):733-48.

Jenkins, L., Harries, N., Lappin, J.E., MacKenzie, A.E., Neetoo-Isseljee, Z., Southern, C., McIver, E.G., Nicklin, S.A., Taylor, D.L. and Milligan, G. (2012) Antagonists of GPR35 display high species ortholog selectivity and varying modes of action. *J Pharmacol Exp Ther*. 343(3):683-95.

Jones, L.H. (2016) An industry perspective on drug target validation. *Expert Opin Drug Discov*. 11(7):623-5.

Juneja, J. and Casey, P.J. (2009) Role of G12 proteins in oncogenesis and metastasis. *Br J Pharmacol*. 158(1):32-40.

Kaku, K., Enya, K., Nakaya, R., Ohira, T. and Matsuno, R. (2015) Efficacy and safety of fasiglifam (TAK-875), a G protein-coupled receptor 40 agonist, in Japanese patients with type 2 diabetes inadequately controlled by diet and exercise: a randomized, double-blind, placebo-controlled, phase III trial. *Diabetes Obes Metab*. 17(7):675-81.

Katritch, V., Cherezov, V. and Stevens, R.C. (2013) Structure-function of the G protein-coupled receptor superfamily. *Annu Rev Pharmacol Toxicol*. 53:531-56.

Kenakin, T. (2001) Inverse, protean, and ligand-selective agonism: matters of receptor conformation. *FASEB J*. 15(3):598-611.

Kenakin, T. (2002) Efficacy at G-protein-coupled receptors. *Nat Rev Drug Discov*. 1(2):103-10.

Kenakin, T. (2011) Functional selectivity and biased receptor signaling. *J Pharmacol Exp Ther*. 336(2):296-302.

Kenakin, T. (2013) New concepts in pharmacological efficacy at 7TM receptors: IUPHAR review 2. *Br J Pharmacol*. 168(3):554-75.

Kenakin, T. (2017) Theoretical Aspects of GPCR-Ligand Complex Pharmacology. *Chem Rev.* 117(1):4-20.

Kenakin, T. and Miller, L.J. (2010) Seven transmembrane receptors as shapeshifting proteins: the impact of allosteric modulation and functional selectivity on new drug discovery. *Pharmacol Rev.* 62(2):265-304.

Kenakin, T. and Strachan, R.T. (2018) PAM-Antagonists: A Better Way to Block Pathological Receptor Signaling? *Trends Pharmacol Sci.* 39(8):748-65.

Kenakin, T.P. (2010) Ligand detection in the allosteric world. *J Biomol Screen.* 15(2):119-30.

Keov, P., Sexton, P.M. and Christopoulos, A. (2011) Allosteric modulation of G protein-coupled receptors: a pharmacological perspective. *Neuropharmacology.* 60(1):24-35.

Khalil, N., Manganas, H., Ryerson, C.J., Shapera, S., Cantin, A.M., Hernandez, P., Turcotte, E.E., Parker, J.M., Moran, J.E., Albert, G.R., Sawtell, R., Hagerimana, A., Laurin, P., Gagnon, L., Cesari, F. and Kolb M. (2019) Phase 2 clinical trial of PBI-4050 in patients with idiopathic pulmonary fibrosis. *Eur Respir J.* 53(3). pii: 1800663. doi: 10.1183/13993003.00663-2018.

Khan, S.M., Sleno, R., Gora, S., Zylbergold, P., Laverdure, J.P., Labbé, J.C., Miller, G.J. and Hébert, T.E. (2013) The expanding roles of G $\beta\gamma$ subunits in G protein-coupled receptor signaling and drug action. *Pharmacol Rev.* 65(2):545-77.

Kim, H.J., Yoon, H.J., Kim, B.K., Kang, W.Y., Seong, S.J., Lim, M.S., Kim, S.Y. and Yoon, Y.R. (2016) G Protein-Coupled Receptor 120 Signaling Negatively Regulates Osteoclast Differentiation, Survival, and Function. *J Cell Physiol.* 231(4):844-51.

Kim, J.H. and Kim, N. (2014) Regulation of NFATc1 in Osteoclast Differentiation. *J Bone Metab.* 21(4):233-41.

Kobilka, B.K. and Deupi, X. (2007) Conformational complexity of G-protein-coupled receptors. *Trends Pharmacol Sci.* 28(8):397-406.

Kobilka, B. and Schertler, G.F. (2008) New G-protein-coupled receptor crystal structures: insights and limitations. *Trends Pharmacol Sci.* 29(2):79-83.

Kobilka, B.K. (2007) G protein coupled receptor structure and activation. *Biochim Biophys Acta.* 1768(4):794-807.

Korczynska, M., Clark, M.J., Valant, C., Xu, J., Moo, E.V., Albold, S., Weiss, D.R., Torosyan, H., Huang, W., Kruse, A.C., Lyda, B.R., May, L.T., Baltos, J.A., Sexton, P.M., Kobilka, B.K., Christopoulos, A., Shoichet, B.K. and Sunahara, R.K. (2018) Structure-based discovery of selective positive allosteric modulators of antagonists for the M2 muscarinic acetylcholine receptor. *Proc Natl Acad Sci.* 115(10):E2419-E2428.

Kozasa, T., Jiang, X., Hart, M.J., Sternweis, P.M., Singer, W.D., Gilman, A.G., Bollag, G. and Sternweis, P.C. (1998) p115 RhoGEF, a GTPase activating protein for Galpha12 and Galpha13. *Science.* 280(5372):2109-11.

Krishnamurthy, N. and Kurzrock, R. (2018) Targeting the Wnt/beta-catenin pathway in cancer: Update on effectors and inhibitors. *Cancer Treat Rev.* 62:50-60.

Kruse, A.C., Ring, A.M., Manglik, A., Hu, J., Hu, K., Eitel, K., Hübner, H., Pardon, E., Valant, C., Sexton, P.M., Christopoulos, A., Felder, C.C., Gmeiner, P., Steyaert, J., Weis, W.I., Garcia, K.C., Wess, J. and Kobilka, B.K. (2013) Activation and allosteric modulation of a muscarinic acetylcholine receptor. *Nature.* 504(7478):101-6.

Labeguere, F.G., Newsome, G.J.R., Alvey, L.J., Saniere, L.R.M. and Flethcer, S.R. (2014) Novel dihydropyrimidinoisoquinolinones and pharmaceutical compositions thereof for the treatment of inflammatory disorders. WO 2013/092791A1.

- Lagerström, M.C. and Schiöth, H.B. (2008) Structural diversity of G protein-coupled receptors and significance for drug discovery. *Nat Rev Drug Discov.* 7(4):339-57.
- Landolt-Marticorena, C. and Reithmeier, R.A. (1994) Asparagine-linked oligosaccharides are localized to single extracytosolic segments in multi-span membrane glycoproteins. *Biochem J.* 302(1):253-60.
- Lane, J.R., Donthamsetti, P., Shonberg, J., Draper-Joyce, C.J., Dentry, S., Michino, M., Shi, L., López, L., Scammells, P.J., Capuano, B., Sexton, P.M., Javitch, J.A. and Christopoulos, A. (2014) A new mechanism of allostery in a G protein-coupled receptor dimer. *Nat Chem Biol.* 10(9):745-52.
- Langmead, C.J. (2011) Determining allosteric modulator mechanism of action: integration of radioligand binding and functional assay data. *Methods Mol Biol.* 746:195-209.
- Lattin, J. E., Schroder, K., Su, A. I., Walker, J. R., Zhang, J., Wiltshire, T., Saijo, K., Glass, C. K., Hume, D. A., Kellie, S., and Sweet, M. J. (2008) Expression analysis of G protein-coupled receptors in mouse macrophages. *Immunome Res.* 4:5.
- Lazareno, S., Dolezal, V., Popham, A. and Birdsall, N.J. (2004) Thiochrome enhances acetylcholine affinity at muscarinic M4 receptors: receptor subtype selectivity via cooperativity rather than affinity. *Mol Pharmacol.* 65(1):257-66.
- Le Poul, E., Loison, C., Struyf, S., Springael, J.Y., Lannoy, V., Decobecq, M.E., Brezillon, S., Dupriez, V., Vassart, G., Van Damme, J., et al. (2003) Functional characterization of human receptors for short chain fatty acids and their role in polymorphonuclear cell activation. *J Biol Chem.* 278:25481-9.
- Leach, K., Sexton, P.M. and Christopoulos, A. (2007) Allosteric GPCR modulators: taking advantage of permissive receptor pharmacology. *Trends Pharmacol Sci.* 28(8):382-9.

Leach, K., Wen, A., Cook, A.E., Sexton, P.M., Conigrave, A.D. and Christopoulos, A. (2013) Impact of clinically relevant mutations on the pharmacoregulation and signaling bias of the calcium-sensing receptor by positive and negative allosteric modulators. *Endocrinology*. 154(3):1105-16.

Lebon, G., Warne, T., Edwards, P.C., Bennett, K., Langmead, C.J., Leslie, A.G. and Tate, C.G. (2011) Agonist-bound adenosine A2A receptor structures reveal common features of GPCR activation. *Nature*. 474(7352):521-5.

Lee, T., Schwandner, R., Swaminath, G., Weiszmann, J., Cardozo, M., Greenberg, J., Jaeckel, P., Ge, H., Wang, Y., Jiao, X., Liu, J., Kayser, F., Tian, H. and Li, Y. (2008) Identification and functional characterization of allosteric agonists for the G protein-coupled receptor FFA2. *Mol Pharmacol*. 74(6):1599-1609.

Leff, P. (1995) The two-state model of receptor activation. *Trends Pharmacol Sci*. 16(3):89-97.

Lefkowitz, R.J. and Shenoy, S.K. (2005) Transduction of receptor signals by beta-arrestins. *Science*. 308(5721):512-7.

Li, X., Zhou, M., Huang, W. and Yang, H. (2017) N-glycosylation of the B2 adrenergic receptor regulates receptor function by modulating dimerization. *FEBS J*. 284(13):2004-18.

Li, Y., Chung, S., Li, Z., Overstreet, J.M., Gagnon, L., Grouix, B., Leduc, M., Laurin, P., Zhang, M.Z. and Harris, R.C. (2018) Fatty acid receptor modulator PBI-4050 inhibits kidney fibrosis and improves glycemic control. *JCI Insight*. 3(10). pii: 120365.

Liang, Y.L., Khoshouei, M., Radjainia, M., Zhang, Y., Glukhova, A., Tarrasch, J., Thal, D.M., Furness, S.G.B., Christopoulos, G., Coudrat, T., Danev, R., Baumeister, W., Miller, L.J., Christopoulos, A., Kobilka, B.K., Wootten, D., Skiniotis, G. and Sexton, P.M. (2017) Phase-plate cryo-EM structure of a class B GPCR-G-protein complex. *Nature*. 546(7656):118-23.

Lindberg, J.S., Culleton, B., Wong, G., Borah, M.F., Clark, R.V., Shapiro, W.B., Roger, S.D., Husserl, F.E., Klassen, P.S., Guo, M.D., Albizem, M.B. and Coburn, J.W. (2005) Cinacalcet HCl, an oral calcimimetic agent for the treatment of secondary hyperparathyroidism in hemodialysis and peritoneal dialysis: a randomized, double-blind, multicenter study. *J Am Soc Nephrol.* 16(3):800-7.

Lindsley, C.W., Emmitte, K.A., Hopkins, C.R., Bridges, T.M., Gregory, K.J., Niswender, C.M. and Conn P.J. (2016) Practical Strategies and Concepts in GPCR Allosteric Modulator Discovery: Recent Advances with Metabotropic Glutamate Receptors. *Chem Rev.* 116(11):6707-41.

Liu, Y., Chen, L.Y., Sokolowska, M., Eberlein, M., Alsaaty, S., Martinez-Anton, A., Logun, C., Qi, H.Y. and Shelhamer, J.H. (2014) The fish oil ingredient, docosahexaenoic acid, activates cytosolic phospholipase A₂ via GPR120 receptor to produce prostaglandin E₂ and plays an anti-inflammatory role in macrophages. *Immunology.* 143(1):81-95.

Liu, Y., Zhang, Q., Chen, L.H., Yang, H., Lu, W., Xie, X. and Nan, F.J. (2016) Design and synthesis of 2-alkylpyrimidine-4,6-diol and 6-alkylpyridine-2,4-diol as potent GPR84 agonists. *ACS Med Chem Lett.* 7(6):579-83.

Lu, H., Wang, J., Wang, Y., Qiao, L. and Zhou, Y. (2016) Embelin and Its Role in Chronic Diseases. *Adv Exp Med Biol.* 928:397-418.

Lu, J., Byrne, N., Wang, J., Bricogne, G., Brown, F.K., Chobanian, H.R., Colletti, S.L., Di Salvo, J., Thomas-Fowlkes, B., Guo, Y., Hall, D.L., Hadix, J., Hastings, N.B., Hermes, J.D., Ho, T., Howard, A.D., Josien, H., Kornienko, M., Lumb, K.J., Miller, M.W., Patel, S.B., Pio, B., Plummer, C.W., Sherborne, B.S., Sheth, P., Souza, S., Tummala, S., Vornrhein, C., Webb, M., Allen, S.J., Johnston, J.M., Weinglass, A.B., Sharma, S. and Soisson, S.M. (2017) Structural basis for the cooperative allosteric activation of the free fatty acid receptor GPR40. *Nat Struct Mol Biol.* 24(7):570-7.

- Luttrell, L.M. and Lefkowitz, R.J. (2002) The role of beta-arrestins in the termination and transduction of G-protein-coupled receptor signals. *J Cell Sci.* 115(Pt 3):455-65.
- Ma, L. and Pei, G. (2007) Beta-arrestin signaling and regulation of transcription. *J Cell Sci.* 120(Pt 2):213-8.
- Maciejewska, D., Rasztawicka, M., Wolska, I., Anuszewska, E. and Gruber, B. (2009) Novel 3,3'-diindolylmethane derivatives: synthesis and cytotoxicity, structural characterization in solid state. *Eur J Med Chem.* 44(10):4136-47.
- MacKenzie, A.E., Caltabiano, G., Kent, T.C., Jenkins, L., McCallum, J.E., Hudson, B.D., Nicklin, S.A., Fawcett, L., Markwick, R., Charlton, S.J. and Milligan, G. (2014) The antiallergic mast cell stabilizers lodoxamide and bufrolin as the first high and equipotent agonists of human and rat GPR35. *Mol Pharmacol.* 85(1):91-104.
- Mackenzie, A.E., Quon, T., Lin, L.C., Hauser, A.S., Jenkins, L., Inoue, A., Tobin, A.B., Gloriam, D.E., Hudson, B.D., and Milligan, G. (2019) Receptor selectivity between the G proteins Gα12 and Gα13 is defined by a single leucine-to-isoleucine variation. *FASEB J.* doi: 10.1096/fj.201801956R.
- Mahmud, Z.A., Jenkins, L., Ulven, T., Labéguère, F., Gosmini, R., De Vos, S., Hudson, B.D., Tikhonova, I.G. and Milligan, G. (2017) Three classes of ligands each bind to distinct sites on the orphan G protein-coupled receptor GPR84. *Sci Rep.* 7(1):17953.
- Malik, R. U., Ritt, M., DeVree, B. T., Neubig, R. R., Sunahara, R. K., and Sivaramakrishnan, S. (2013) Detection of G protein-selective G protein-coupled receptor (GPCR) conformations in live cells. *J Biol Chem.* 288(24):17167-78.
- Malik, R.U., Dysthe, M., Ritt, M., Sunahara, R.K., Sivaramakrishnan, S. (2017) ER/K linked GPCR-G protein fusions systematically modulate second messenger response in cells. *Sci Rep.* 7(1):7749.

Mancini, S.J., Mahmud, Z.A., Jenkins, L., Bolognini, D., Newman, R., Barnes, M., Edye, M.E., McMahon, S.B., Tobin, A.B. and Milligan, G. (2019) On-target and off-target effects of novel orthosteric and allosteric activators of GPR84. *Sci Rep.* 9(1):1861.

Marium, N., Grainne, D. and Alex, W. (2018) A comparison of pirfenidone versus nintedanib for the management of idiopathic pulmonary fibrosis. *Eur Respir J.* 52: PA4791.

Marques, M., Laflamme, L., Benassou, I., Cissokho, C., Guillemette, B. and Gaudreau, L. (2014) Low levels of 3,3'-diindolylmethane activate estrogen receptor α and induce proliferation of breast cancer cells in the absence of estradiol. *BMC Cancer.* 14:524.

Mason, J.S., Bortolato, A., Congreve, M. and Marshall, F.H. (2012) New insights from structural biology into the druggability of G protein-coupled receptors. *Trends Pharmacol Sci.* 33(5):249-60.

May, L.T., Leach, K., Sexton, P.M. and Christopoulos, A. (2007) Allosteric modulation of G protein-coupled receptors. *Annu Rev Pharmacol Toxicol.* 47:1-51.

McArdle, M.A., Finucane, O.M., Connaughton, R.M., McMorrow, A.M. and Roche, H.M. (2013) Mechanisms of obesity-induced inflammation and insulin resistance: insights into the emerging role of nutritional strategies. *Front Endocrinol (Lausanne).* 4:52.

Menzaghi, F., Behan, D. P., and Chalmers, D. T. (2002) Constitutively activated G protein-coupled receptors: A novel approach to CNS drug discovery. *Curr Drug Targets CNS Neurol Disord.* 1:105-21.

Milligan, G. (2000) Insights into ligand pharmacology using receptor-G-protein fusion proteins. *Trends Pharmacol Sci.* 21(1):24-8.

- Milligan, G. (2002) Construction and analysis of function of G protein-coupled receptor-G protein fusion proteins. *Methods Enzymol.* 343:260-73.
- Milligan, G. (2003) Principles: extending the utility of [³⁵S]GTP gamma S binding assays. *Trends Pharmacol Sci.* 24(2):87-90.
- Milligan, G. (2011) Orthologue selectivity and ligand bias: translating the pharmacology of GPR35. *Trends Pharmacol Sci.* 32(5):317-25.
- Milligan, G. (2018) G protein-coupled receptors not currently in the spotlight: free fatty acid receptor 2 and GPR35. *Br J Pharmacol.* 175(13):2543-53.
- Milligan, G. and Kostenis, E. (2006) Heterotrimeric G-proteins: a short history. *Br J Pharmacol.* 147 (Suppl 1):S46-55.
- Milligan, G., Alvarez-Curto, E., Hudson, B.D., Prihandoko, R. and Tobin, A.B. (2017a) FFA4/GPR120: Pharmacology and Therapeutic Opportunities. *Trends Pharmacol Sci.* 38(9):809-21.
- Milligan, G., Shimpukade, B., Ulven, T. and Hudson, B.D. (2017b) Complex Pharmacology of Free Fatty Acid Receptors. *Chem Rev.* 117(1):67-110.
- Min, C., Zheng, M., Zhang, X., Guo, S., Kwon, K.J., Shin, C.Y., Kim, H.S., Cheon, S.H. and Kim, K.M. (2015) N-linked Glycosylation on the N-terminus of the dopamine D2 and D3 receptors determines receptor association with specific microdomains in the plasma membrane. *Biochim Biophys Acta.* 1853(1):41-51.
- Minihane, A. M., Vinoy, S., Russell, W. R., Baka, A., Roche, H. M., Tuohy, K. M., Teeling, J. L., Blaak, E. E., Fenech, M., Vauzour, D., McArdle, H. J., Kremer, B. H., Sterkman, L., Vafeiadou, K., Benedetti, M. M., Williams, C. M., and Calder, P. C. (2015) Low-grade inflammation, diet composition and health: current research evidence and its translation. *Br J Nutr.* 114:999-1012.
- Moran, S.P., Cho, H.P., Maksymetz, J., Remke, D.H., Hanson, R.M., Niswender, C.M., Lindsley, C.W., Rook, J.M. and Conn, P.J. (2018) PF-06827443 Displays

Robust Allosteric Agonist and Positive Allosteric Modulator Activity in High Receptor Reserve and Native Systems. *ACS Chem Neurosci*. 9(9):2218-24.

Morgan, P., Van Der Graaf, P.H., Arrowsmith, J., Feltner, D.E., Drummond, K.S., Wegner, C.D. and Street, S.D. (2012) Can the flow of medicines be improved? Fundamental pharmacokinetic and pharmacological principles toward improving Phase II survival. *Drug Discov Today*. 17(9-10):419-24.

Mori, T., Doi, R., Kida, A., Nagai, K., Kami, K., Ito, D., Toyoda, E., Kawaguchi, Y. and Uemoto, S. (2007) Effect of the XIAP inhibitor Embelin on TRAIL-induced apoptosis of pancreatic cancer cells. *J Surg Res*. 142(2):281-6.

Müller, M.M., Lehmann, R., Klassert, T.E., Reifenstein, S., Conrad, T., Moore, C., Kuhn, A., Behnert, A., Guthke, R., Driesch, D. and Slevogt, H. (2017) Global analysis of glycoproteins identifies markers of endotoxin tolerant monocytes and GPR84 as a modulator of TNF α expression. *Sci Rep*. 7(1):838.

Muredda, L., Kępczyńska, M.A., Zaibi, M.S., Alomar, S.Y. and Trayhurn, P. (2018) IL-1 β and TNF α inhibit GPR120 (FFAR4) and stimulate GPR84 (EX33) and GPR41 (FFAR3) fatty acid receptor expression in human adipocytes: implications for the anti-inflammatory action of n-3 fatty acids. *Arch Physiol Biochem*. 124(2):97-108.

Nagasaki, H., Kondo, T., Fuchigami, M., Hashimoto, H., Sugimura, Y., Ozaki, N., Arima, H., Ota, A., Oiso, Y. and Hamada, Y. (2012) Inflammatory changes in adipose tissue enhance expression of GPR84, a medium-chain fatty acid receptor: TNF α enhances GPR84 expression in adipocytes. *FEBS Lett*. 586(4): 368-72.

Naor, Z., Benard, O and, Seger, R. (2000) Activation of MAPK cascades by G-protein-coupled receptors: the case of gonadotropin-releasing hormone receptor. *Trends Endocrinol Metab*. 11(3):91-9.

Nawrocki, A.R. and Scherer, P.E. (2004) The delicate balance between fat and muscle: adipokines in metabolic disease and musculoskeletal inflammation. *Curr Opin Pharmacol.* 4(3):281-9.

Ngo, T., Kufareva, I., Coleman, J.L.J., Graham, R.M., Abagyan, R. and Smith, N.J. (2016) Identifying ligands at orphan GPCRs: current status using structure-based approaches. *Br J Pharmacol.* 173(20):2934-51.

Nguyen, Q.T., Jalloul Nsaibia, M., Sirois, M.G., Calderone, A., Tardif, J.C., Fen Shi, Y., Ruiz, M., Daneault, C., Gagnon, L., Grouix, B., Laurin, P. and Dupuis, J. (2019) PBI-4050 Reduces Pulmonary Hypertension, Lung fibrosis and Right Ventricular Dysfunction in Heart Failure. *Cardiovasc Res.* doi: 10.1093/cvr/cvz034.

Ni, F., So, S.P., Cervantes, V. and Ruan, K.H. (2008) A profile of the residues in the second extracellular loop that are critical for ligand recognition of human prostacyclin receptor. *FEBS J.* 275(1):128-37.

Nicol, L.S., Dawes, J.M., La Russa, F., Didangelos, A., Clark, A.K., Gentry, C., Grist, J., Davies, J.B., Malcangio, M. and McMahon, S.B. (2015) The role of G-protein receptor 84 in experimental neuropathic pain. *J Neurosci.* 35(23):8959-69.

Nikaido, Y., Koyama, Y., Yoshikawa, Y., Furuya, T. and Takeda, S. (2015) Mutation analysis and molecular modeling for the investigation of ligand-binding modes of GPR84. *J Biochem.* 157(5):311-20.

Nikolovska-Coleska, Z., Xu, L., Hu, Z., Tomita, Y., Li, P., Roller, P.P., Wang, R., Fang, X., Guo, R., Zhang, M., Lippman, M.E., Yang, D. and Wang, S. (2004) Discovery of embelin as a cell-permeable, small-molecular weight inhibitor of XIAP through structure-based computational screening of a traditional herbal medicine three-dimensional structure database. *J Med Chem.* 47(10):2430-40.

- Oh, D.Y. and Lagakos, W.S. (2011) The role of G-protein-coupled receptors in mediating the effect of fatty acids on inflammation and insulin sensitivity. *Curr Opin Clin Nutr Metab Care*. 14(4):322-7.
- Oh, D.Y., Talukdar, S., Bae, E.J., Imamura, T., Morinaga, H., Fan, W., Li, P., Lu, W.J., Watkins, S.M. and Olefsky, J.M. (2010) GPR120 is an omega-3 fatty acid receptor mediating potent anti-inflammatory and insulin-sensitizing effects. *Cell*. 142(5):687-98.
- Oldham, W.M. and Hamm, H.E. (2008) Heterotrimeric G protein activation by G-protein-coupled receptors. *Nat Rev Mol Cell Biol*. 9(1):60-71.
- Overington, J. P., Al-Lazikani, B., and Hopkins A. L. (2006) How many drug targets are there? *Nat Rev Drug Discov*. 5:993-6.
- Park, J.W., Yoon, H.J., Kang, W.Y., Cho, S., Seong, S.J., Lee, H.W., Yoon, Y.R. and Kim, H.J. (2018) G protein-coupled receptor 84 controls osteoclastogenesis through inhibition of NF- κ B and MAPK signaling pathways. *J Cell Physiol*. 233(2): 1481-9.
- Park, P.S., Lodowski, D.T. and Palczewski, K. (2008) Activation of G protein-coupled receptors: beyond two-state models and tertiary conformational changes. *Annu Rev Pharmacol Toxicol*. 48:107-41.
- Peeters, M.C., van Westen, G.J., Li, Q. and IJzerman, A.P. (2011) Importance of the extracellular loops in G protein-coupled receptors for ligand recognition and receptor activation. *Trends Pharmacol Sci*. 32(1):35-42.
- Pillaiyar, T., Köse, M., Namasivayam, V., Sylvester, K., Borges, G., Thimm, D., von Kügelgen, I., and Müller, C.E. (2018) 6-(Ar)Alkylamino-Substituted Uracil Derivatives: Lipid Mimetics with Potent Activity at the Orphan G Protein-Coupled Receptor 84 (GPR84). *ACS Omega*. 3(3):3365-83.
- Pillaiyar, T., Köse, M., Sylvester, K., Weighardt, H., Thimm, D., Borges, G., Förster, I., von Kügelgen, I. and Müller, C.E. (2017) Diindolylmethane

Derivatives: Potent Agonists of the Immunostimulatory Orphan G Protein-Coupled Receptor GPR84. *J Med Chem.* 60(9):3636-55.

Pizzonero, M., Dupont, S., Babel, M., Beaumont, S., Bienvenu, N., Blanqué, R., Cherel, L., Christophe, T., Crescenzi, B., De Lemos, E., Delerive, P., Deprez, P., De Vos, S., Djata, F., Fletcher, S., Kopiejewski, S., L'Ebraly, C., Lefrançois, J.M., Lavazais, S., Manioc, M., Nelles, L., Oste, L., Polancec, D., Quénéhen, V., Soulas, F., Triballeau, N., van der Aar, E.M., Vandeghinste, N., Wakselman, E., Brys, R. and Saniere, L. (2014) Discovery and optimization of an azetidine chemical series as a free fatty acid receptor 2 (FFA2) antagonist: from hit to clinic. *J Med Chem.* 57(23):10044-57.

Price, M.R., Baillie, G.L., Thomas, A., Stevenson, L.A., Easson, M., Goodwin, R., McLean, A., McIntosh, L., Goodwin, G., Walker, G., Westwood, P., Marrs, J., Thomson, F., Cowley, P., Christopoulos, A., Pertwee, R.G. and Ross, R.A. (2005) Allosteric modulation of the cannabinoid CB1 receptor. *Mol Pharmacol.* 68(5): 1484-95.

Puengel, T., De Vos, S., Krenkel, O., Pujuguet, P., Auberval, M., Marsais, F., Shoji, K.F., Saniere, L., Trautwein, C., Brys, R. and Tacke, F. (2018) Pharmacological inhibition of the medium chain fatty acid receptor GPR84 reduces myeloid cell infiltration into injured liver and ameliorates steatohepatitis and fibrosis. *J hepatol.* 68(suppl_1):S338.

Radhika, V., Onesime, D., Ha, J.H. and Dhanasekaran, N. (2004) Galpha13 stimulates cell migration through cortactin-interacting protein Hax-1. *J Biol Chem.* 279(47):49406-13.

Rask-Andersen, M., Almén, M.S. and Schiöth, H.B. (2011) Trends in the exploitation of novel drug targets. *Nat Rev Drug Discov.* 10(8):579-90.

Rask-Andersen, M., Masuram, S. and Schiöth, H.B. (2014) The druggable genome: Evaluation of drug targets in clinical trials suggests major shifts in molecular class and indication. *Annu Rev Pharmacol Toxicol.* 54:9-26.

Rasmussen, S.G., Choi, H.J., Fung, J.J., Pardon, E., Casarosa, P., Chae, P.S., Devree, B.T., Rosenbaum, D.M., Thian, F.S., Kobilka, T.S., Schnapp, A., Konetzki, I., Sunahara, R.K., Gellman, S.H., Pautsch, A., Steyaert, J., Weis, W.I. and Kobilka, B.K. (2011) Structure of a nanobody-stabilized active state of the $\beta(2)$ adrenoceptor. *Nature*. 469(7329):175-80.

Recio, C., Lucy, D., Purvis, G.S.D., Iveson, P., Zeboudj, L., Iqbal, A.J., Lin, D., O'Callaghan, C., Davison, L., Griesbach, E., Russell, A.J., Wynne, G.M., Dib, L., Monaco, C. and Greaves, D.R. (2018) Activation of the Immune-Metabolic Receptor GPR84 Enhances Inflammation and Phagocytosis in Macrophages. *Front Immunol*. 9:1419.

Reed, G.A., Arneson, D.W., Putnam, W.C., Smith, H.J., Gray, J.C., Sullivan, D.K., Mayo, M.S., Crowell, J.A. and Hurwitz, A. (2006) Single-dose and multiple-dose administration of indole-3-carbinol to women: pharmacokinetics based on 3,3'-diindolylmethane. *Cancer Epidemiol Biomarkers Prev*. 15(12):2477-81.

Reiter, E. and Lefkowitz, R.J. (2006) GRKs and beta-arrestins: roles in receptor silencing, trafficking and signaling. *Trends Endocrinol Metab*. 17(4):159-65.

Rhee, S.G. (2001) Regulation of phosphoinositide-specific phospholipase C. *Annu Rev Biochem*. 70:281-312.

Ring, A.M., Manglik, A., Kruse, A.C., Enos, M.D., Weis, W.I., Garcia, K.C. and Kobilka, B.K. (2013) Adrenaline-activated structure of β_2 -adrenoceptor stabilized by an engineered nanobody. *Nature*. 502(7472):575-9.

Rosenbaum, D.M., Rasmussen, S.G. and Kobilka, B.K. (2009) The structure and function of G-protein-coupled receptors. *Nature*. 459(7245):356-63.

Ross, E.M. and Wilkie, T.M. (2000) GTPase-activating proteins for heterotrimeric G proteins: regulators of G protein signaling (RGS) and RGS-like proteins. *Annu Rev Biochem*. 69:795-827.

- Rossi, A.M. and Taylor, C.W. (2011) Analysis of protein-ligand interactions by fluorescence polarization. *Nat Protoc.* 6(3):365-87.
- Ruan, K.H., Wu, J., So, S.P., Jenkins, L.A. and Ruan, C.H. (2004) NMR structure of the thromboxane A₂ receptor ligand recognition pocket. *Eur J Biochem.* 271: 3006-16.
- Saito, Y., Kitamura, H., Hijikata, A., Tomizawa-Murasawa, M., Tanaka, S., Takagi, S., Uchida, N., Suzuki, N., Sone, A., Najima, Y., Ozawa, H., Wake, A., Taniguchi, S., Shultz, L.D., Ohara, O. and Ishikawa, F. (2010) Identification of therapeutic targets for quiescent, chemotherapy-resistant human leukemia stem cells. *Sci Transl Med.* 2(17):17ra9.
- Sanier, L., Marsais, F., Jagerschmidt, C., Meurisse, S., Cuzic, S., Shoji, K., Clement-Lacroix, P., Van Osselaer, N. and De Vos, S. (2019) 'Characterization of GLPG1205 in Mouse Fibrosis Models: A Potent and Selective Antagonist of GPR84 for Treatment of Idiopathic Pulmonary Fibrosis', American Thoracic Society 2019 International Conference, *Less idiopathic: structural and functional abnormalities in IPF*, May 17-22, 2019 - Dallas, TX, ATS Journals.
- Santos, R., Ursu, O., Gaulton, A., Bento, A.P., Donadi, R.S., Bologa, C.G., Karlsson, A., Al-Lazikani, B., Hersey, A., Oprea, T.I. and Overington, J.P. (2017) A comprehensive map of molecular drug targets. *Nat Rev Drug Discov.* 16(1):19-34.
- Scheerer, P., Park, J.H., Hildebrand, P.W., Kim, Y.J., Krauss, N., Choe, H.W., Hofmann, K.P. and Ernst, O.P. (2008) Crystal structure of opsin in its G-protein-interacting conformation. *Nature.* 455(7212):497-502.
- Schenone, M., Dančák, V., Wagner, B.K. and Clemons, P.A. (2013) Target identification and mechanism of action in chemical biology and drug discovery. *Nat Chem Biol.* 9(4):232-40.

- Schiöth, H.B. and Fredriksson, R. (2005) The GRAFS classification system of G-protein coupled receptors in comparative perspective. *Gen Comp Endocrinol.* 142(1-2):94-101.
- Schrodinger, LLC, New York, NY, USA (2014) MacroModel 10.6.
- Schulte, G. (2010) International Union of Basic and Clinical Pharmacology. LXXX. The class Frizzled receptors. *Pharmacol Rev.* 62(4):632-67.
- Seifert, R., Wenzel-Seifert, K. and Kobilka, B.K. (1999) GPCR-Galpa fusion proteins: molecular analysis of receptor-G-protein coupling. *Trends Pharmacol Sci.* 20(9):383-9.
- Semack, A., Sandhu, M., Malik, R.U., Vaidehi, N. and Sivaramakrishnan, S. (2016) Structural Elements in the Gas and Gαq C Termini That Mediate Selective G Protein-coupled Receptor (GPCR) Signaling. *J Biol Chem.* 291(34):17929-40.
- Sergeev, E., Hansen, A.H., Bolognini, D., Kawakami, K., Kishi, T., Aoki, J., Ulven, T., Inoue, A., Hudson, B.D. and Milligan, G. (2017) A single extracellular amino acid in Free Fatty Acid Receptor 2 defines antagonist species selectivity and G protein selection bias. *Sci Rep.* 7(1):13741.
- Sergeev, E., Hansen, A.H., Pandey, S.K., MacKenzie, A.E., Hudson, B.D., Ulven, T. and Milligan, G. (2016) Non-equivalence of Key Positively Charged Residues of the Free Fatty Acid 2 Receptor in the Recognition and Function of Agonist Versus Antagonist Ligands. *J Biol Chem.* 291(1):303-17.
- Shaner, N.C., Lambert, G.G., Chamma, A., Ni, Y., Cranfill, P.J., Baird, M.A., Sell, B.R., Allen, J.R., Day, R.N., Israelsson, M., Davidson, M.W. and Wang, J. (2013) A bright monomeric green fluorescent protein derived from *Branchiostoma lanceolatum*. *Nat Methods.* 10(5):407-9.
- Shenoy, S.K. and Lefkowitz, R.J. (2003) Multifaceted roles of beta-arrestins in the regulation of seven-membrane-spanning receptor trafficking and signalling. *Biochem J.* 375(Pt 3):503-15.

- Sherman, W., Day, T., Jacobson, M.P., Friesner, R.A. and Farid, R. (2006) Novel procedure for modeling ligand/receptor induced fit effects. *J Med Chem.* 49(2):534-53.
- Shrestha, R., Hui, S.P., Imai, H., Hashimoto, S., Uemura, N., Takeda, S., Fuda, H., Suzuki, A., Yamaguchi, S., Hirano, K. and Chiba, H. (2015) Plasma capric acid concentrations in healthy subjects determined by high-performance liquid chromatography. *Ann Clin Biochem.* 52(Pt 5):588-96.
- Shukla, A.K., Xiao, K. and Lefkowitz, R.J. (2011) Emerging paradigms of β -arrestin-dependent seven transmembrane receptor signaling. *Trends Biochem Sci.* 36(9):457-69.
- Siehl, S. (2007) G12/13-dependent signaling of G-protein-coupled receptors: disease context and impact on drug discovery. *Expert Opin Drug Discov.* 2(12):1591-604.
- Siehl, S. (2009) Regulation of RhoGEF proteins by G12/13-coupled receptors. *Br J Pharmacol.* 158(1):41-9.
- Simon, M.I., Strathmann, M.P. and Gautam, N. (1991) Diversity of G proteins in signal transduction. *Science.* 252(5007):802-8.
- Sivaramakrishnan, S., and Spudich, J. A. (2011) Systematic control of protein interaction using a modular ER/K α -helix linker. *Proc Natl Acad Sci.* 108:20467-72.
- Small-Molecule Drug Discovery Suite v. 2014-4 Schrödinger, LLC, New York, NY (2014).
- Smith, J.S. and Rajagopal, S. (2016) The β -Arrestins: Multifunctional Regulators of G Protein-coupled Receptors. *J Biol Chem.* 291(17):8969-77.
- Smith, N.J. (2012) Low affinity GPCRs for metabolic intermediates: challenges for pharmacologists. *Front Endocrinol (Lausanne).* 3:1.

Smith, N.J. and Milligan, G. (2010) Allostery at G protein-coupled receptor homo- and heteromers: uncharted pharmacological landscapes. *Pharmacol Rev.* 62(4):701-25.

Smith, N.J., Bennett, K.A. and Milligan, G. (2011a) When simple agonism is not enough: emerging modalities of GPCR ligands. *Mol Cell Endocrinol.* 331(2):241-7.

Smith, N.J., Ward, R.J., Stoddart, L.A., Hudson, B.D., Kostenis, E., Ulven, T., Morris, J.C., Tränkle, C., Tikhonova, I.G., Adams, D.R. and Milligan, G. (2011b) Extracellular loop 2 of the free fatty acid receptor 2 mediates allostery of a phenylacetamide ago-allosteric modulator. *Mol Pharmacol.* 80(1):163-73.

So, S.P., Wu, J., Huang, G., Huang, A., Li, D. and Ruan, K.H. (2003) Identification of residues important for ligand binding of thromboxane A₂ receptor in the second extracellular loop using the NMR experiment-guided mutagenesis approach. *J Biol Chem.* 278:10922-7.

Soto, A.G., Smith, T.H., Chen, B., Bhattacharya, S., Cordova, I.C., Kenakin, T., Vaidehi, N. and Trejo, J. (2015) N-linked glycosylation of protease-activated receptor-1 at extracellular loop 2 regulates G-protein signaling bias. *Proc Natl Acad Sci.* 112(27):E3600-8.

Southern, C., Cook, J.M., Neetoo-Isseljee, Z., Taylor, D.L., Kettleborough, C.A., Merritt, A., Bassoni, D.L., Raab, W.J., Quinn, E., Wehrman, T.S., Davenport, A.P., Brown, A.J., Green, A., Wigglesworth, M.J. and Rees, S. (2013) Screening β -arrestin recruitment for the identification of natural ligands for orphan G-protein-coupled receptors. *J Biomol Screen.* 18(5):599-609.

Sprang, S.R., Chen, Z. and Du, X. (2007) Structural basis of effector regulation and signal termination in heterotrimeric G α proteins. *Adv Protein Chem.* 74:1-65.

Springael, J.Y., Urizar, E., Costagliola, S., Vassart, G. and Parmentier, M. (2007) Allosteric properties of G protein-coupled receptor oligomers. *Pharmacol Ther.* 115(3):410-8.

- Sriram, K. and Insel, P.A. (2018) G Protein-Coupled Receptors as Targets for Approved Drugs: How Many Targets and How Many Drugs? *Mol Pharmacol.* 93(4):251-8.
- Srivastava, A., Yano, J., Hirozane, Y., Kefala, G., Gruswitz, F., Snell, G., Lane, W., Ivetac, A., Aertgeerts, K., Nguyen, J., Jennings, A. and Okada, K. (2014) High-resolution structure of the human GPR40 receptor bound to allosteric agonist TAK-875. *Nature.* 513(7516):124-7.
- Stitham, J., Stojanovic, A., Merenick, B.L., O'Hara, K.A. and Hwa, J. (2003) The unique ligand-binding pocket for the human prostacyclin receptor. Site-directed mutagenesis and molecular modeling. *J Biol Chem.* 278:4250-7.
- Stockert, J.A. and Devi, L.A. (2015) Advancements in therapeutically targeting orphan GPCRs. *Front Pharmacol.* 6:100.
- Stoddart, L. A., Smith, N. J., Jenkins, L., Brown, A. J., and Milligan, G. (2008a) Conserved polar residues in transmembrane domains V, VI, and VII of free fatty acid receptor 2 and free fatty acid receptor 3 are required for the binding and function of short chain fatty acids. *J Biol Chem.* 283:32913-24.
- Stoddart, L.A., Smith, N.J. and Milligan, G. (2008b) International Union of Pharmacology. LXXI. Free fatty acid receptors FFA1, -2, and -3: pharmacology and pathophysiological functions. *Pharmacol Rev.* 60(4):405-17.
- Strange, P.G. (2010) Use of the GTP γ S ([³⁵S]GTP γ S and Eu-GTP γ S) binding assay for analysis of ligand potency and efficacy at G protein-coupled receptors. *Br J Pharmacol.* 161(6):1238-49.
- Strasser, A., Wittmann, H.J., Buschauer, A., Schneider, E.H. and Seifert, R. (2013) Species-dependent activities of G-protein-coupled receptor ligands: lessons from histamine receptor orthologs. *Trends Pharmacol Sci.* 34(1):13-32.

- Suga, H. and Haga, T. (2007) Ligand screening system using fusion proteins of G protein-coupled receptors with G protein alpha subunits. *Neurochem Int.* 51: 140-64.
- Sum, C.S., Tikhonova, I.G., Neumann, S., Engel, S., Raaka, B.M., Costanzi, S. and Gershengorn, M.C. (2007) Identification of residues important for agonist recognition and activation in GPR40. *J Biol Chem.* 282(40):29248-55.
- Sun, L. and Ye, R.D. (2012) Role of G protein-coupled receptors in inflammation. *Acta Pharmacol Sin.* 33(3):342-50.
- Sun, Q., Hirasawa, A., Hara, T., Kimura, I., Adachi, T., Awaji, T., Ishiguro, M., Suzuki, T., Miyata, N., and Tsujimoto, G. (2010) Structure-activity relationships of GPR120 agonists based on a docking simulation. *Mol Pharmacol.* 78(5):804-10.
- Sundqvist, M., Christenson, K., Holdfeldt, A., Gabl, M., Mårtensson, J., Björkman, L., Dieckmann, R., Dahlgren, C. and Forsman, H. (2018) Similarities and differences between the responses induced in human phagocytes through activation of the medium chain fatty acid receptor GPR84 and the short chain fatty acid receptor FFA2R. *Biochim Biophys Acta Mol Cell Res.* 1865(5):695-708.
- Suratman, S., Leach, K., Sexton, P., Felder, C., Loiacono, R. and Christopoulos, A. (2011) Impact of species variability and 'probe-dependence' on the detection and in vivo validation of allosteric modulation at the M4 muscarinic acetylcholine receptor. *Br J Pharmacol.* 162(7):1659-70.
- Suzuki, N., Hajicek, N. and Kozasa, T. (2009) Regulation and physiological functions of G12/13-mediated signaling pathways. *Neurosignals.* 17(1):55-70.
- Suzuki, M., Takaishi, S., Nagasaki, M., Onozawa, Y., Iino, I., Maeda, H., Komai, T. and Oda, T. (2013) Medium-chain fatty acid-sensing receptor, GPR84, is a proinflammatory receptor. *J Biol Chem.* 288(15):10684-91.
- Swinney, D.C. and Anthony, J. (2011) How were new medicines discovered? *Nat Rev Drug Discov.* 10(7):507-19.

Syrovatkina, V., Alegre, K.O., Dey, R. and Huang, X.Y. (2016) Regulation, Signaling, and Physiological Functions of G-Proteins. *J Mol Biol.* 428(19):3850-68.

Takayanagi, H., Kim, S., Koga, T., Nishina, H., Isshiki, M., Yoshida, H., Saiura, A., Isobe, M., Yokochi, T., Inoue, J., Wagner, E.F., Mak, T.W., Kodama, T. and Taniguchi, T. (2002) Induction and activation of the transcription factor NFATc1 (NFAT2) integrate RANKL signaling in terminal differentiation of osteoclasts. *Dev Cell.* 3(6):889-901.

Takeda, S., Yamamoto, A., Okada, T., Matsumura, E., Nose, E., Kogure, K., Kojima, S. and Haga, T. (2003) Identification of surrogate ligands for orphan G protein-coupled receptors. *Life Sci.* 74(2-3):367-77.

Takeuchi, H., Noguchi, O., Sekine, S., Kobayashi, A. and Aoyama, T. (2006) Lower weight gain and higher expression and blood levels of adiponectin in rats fed medium-chain TAG compared with long-chain TAG. *Lipids.* 41:207-12

Talukdar, S., Olefsky, J. M., and Osborn, O. (2011) Targeting GPR120 and other fatty acid-sensing GPCRs ameliorates insulin resistance and inflammatory diseases. *Trends Pharmacol Sci.* 32(9):543-50.

Tikhonova, I.G. (2017) Application of GPCR Structures for Modelling of Free Fatty Acid Receptors. *Handb Exp Pharmacol.* 236:57-77.

Tikhonova, I.G., Sum, C.S., Neumann, S., Thomas, C.J., Raaka B.M., Costanzi, S. and Gershengorn, M.C. (2007) Bidirectional, iterative approach to the structural delineation of the functional ‘chemoprint’ in GPR40 for agonist recognition. *J Med Chem.* 50(13):2981-9.

Trayhurn, P. and Denyer, G. (2012) Mining microarray datasets in nutrition: expression of the GPR120 (n-3 fatty acid receptor/sensor) gene is down-regulated in human adipocytes by macrophage secretions. *J Nutr Sci.* 1:e3.

Trinh, P.N.H., May, L.T., Leach, K. and Gregory K.J. (2018) Biased agonism and allosteric modulation of metabotropic glutamate receptor 5. *Clin Sci (Lond)*. 132(21):2323-38.

Umland, S. P., Wan, Y., Shah, H., Billah, M., Egan, R. W. and Hey, J. A. (2001) Receptor Reserve Analysis of the Human $\alpha 2C$ -Adrenoceptor Using [35S]GTP γ S and cAMP Functional Assays. *Eur J Pharmacol*. 411:211-21.

van der Westhuizen, E.T., Spathis, A., Khajehali, E., Jörg, M., Mistry, S.N., Capuano, B., Tobin, A.B., Sexton, P.M., Scammells, P.J., Valant, C. and Christopoulos, A. (2018) Assessment of the Molecular Mechanisms of Action of Novel 4-Phenylpyridine-2-One and 6-Phenylpyrimidin-4-One Allosteric Modulators at the M1 Muscarinic Acetylcholine Receptors. *Mol Pharmacol*. 94(1):770-83.

Van der Westhuizen, E.T., Valant, C., Sexton, P.M. and Christopoulos, A. (2015) Endogenous allosteric modulators of G protein-coupled receptors. *J Pharmacol Exp Ther*. 353(2):246-60.

Van Eck, M., Singaraja, R.R., Ye, D., Hildebrand, R.B., James, E.R., Hayden, M.R. and Van Berkel, T.J. (2006) Macrophage ATP-binding cassette transporter A1 overexpression inhibits atherosclerotic lesion progression in low-density lipoprotein receptor knockout mice. *Arterioscler Thromb Vasc Biol*. 26(4):929-34.

Vanhoutte, F., Dupont, S., Van Kaem, T., Gouy, M. H., Blanque, R., Brys, R., Vandeghinste, N., Gheyle, L., Haazen, W., van 't Klooster, G. and Beetens, J. (2015) Human Safety, Pharmacokinetics and Pharmacodynamics of the GPR84 Antagonist GLPG1205, a Potential New Approach to Treat IBD. *J Crohn's Colitis*. 9:S387– S387.

Venkatakrisnan, A.J., Deupi, X., Lebon, G., Tate, C.G., Schertler, G.F. and Babu, M.M. (2013) Molecular signatures of G-protein-coupled receptors. *Nature*. 494(7436):185-94.

- Venkataraman, C and Kuo, F. (2005) The G-protein coupled receptor, GPR84 regulates IL-4 production by T lymphocytes in response to CD3 crosslinking. *Immunol Lett.* 101(2):144-53.
- Vermiere, S., Reinisch, W., Wasko-Czopnik, D., Van Kaem, T., Desrivot, J., Vanhoutte, F. and Beets, J. (2017) Efficacy and safety of GLPG1205, a GPR84 antagonist, in ulcerative colitis: multi-centre proof-of-concept study. *J Crohns Colitis.* 11(suppl_1):S390-S391.
- Wacker, D., Stevens, R.C. and Roth, B.L. (2017) How Ligands Illuminate GPCR Molecular Pharmacology. *Cell.* 170(3):414-27.
- Wada, T., Nakashima, T., Hiroshi, N. and Penninger, J.M. (2006) RANKL-RANK signaling in osteoclastogenesis and bone disease. *Trends Mol Med.* 12(1):17-25.
- Wang, J., Simonavicius, N., Wu, X., Swaminath, G., Reagan, J., Tian, H. and Ling, L. (2006a) Kynurenic acid as a ligand for orphan G protein-coupled receptor GPR35. *J Biol Chem.* 281(31):22021-8.
- Wang, J., Wu, X., Simonavicius, N., Tian, H., and Ling, L. (2006b) Medium chain fatty acids as ligands for orphan G protein-coupled receptor GPR84. *J Biol Chem.* 281(45):34457-64.
- Wang, M., Zhang, X., Zhang, S. and Liu, Z. (2019) Zebrafish fatty acids receptor Gpr84 enhances macrophage phagocytosis. *Fish Shellfish Immunol.* 84:1098-9.
- Ward, R.J., Alvarez-Curto, E. and Milligan, G. (2011) Using the Flp-In™ T-Rex™ system to regulate GPCR expression. *Methods Mol Biol.* 746:21-37.
- Watson, S.J., Brown, A.J. and Holliday, N.D. (2012) Differential signaling by splice variants of the human free fatty acid receptor GPR120. *Mol Pharmacol.* 81(5):631-42.

- Watterson, K.R., Hudson, B.D., Ulven, T. and Milligan, G. (2014) Treatment of type 2 diabetes by free Fatty Acid receptor agonists. *Front Endocrinol (Lausanne)*. 5:137.
- Wauquier, F., Philippe, C., Léotoing, L., Mercier, S., Davicco, M.J., Lebecque, P., Guicheux, J., Pilet, P., Miot-Noirault, E., Poitout, V., Alquier, T., Coxam, V. and Wittrant, Y. (2013) The free fatty acid receptor G protein-coupled receptor 40 (GPR40) protects from bone loss through inhibition of osteoclast differentiation. *J Biol Chem*. 288(9):6542-51.
- Wei, L., Tokizane, K., Konishi, H., Yu, H.R. and Kiyama, H. (2017) Agonists for G-protein-coupled receptor 84 (GPR84) alter cellular morphology and motility but do not induce pro-inflammatory responses in microglia. *J Neuroinflammation*. 14(1):198.
- Weis, W.I. and Kobilka, B.K. (2018) The Molecular Basis of G Protein-Coupled Receptor Activation. *Annu Rev Biochem*. 87:897-919.
- Wettschureck, N. and Offermanns, S. (2005) Mammalian G proteins and their cell type specific functions. *Physiol Rev*. 85(4):1159-204.
- Wheatley, M., Wootten, D., Conner, M.T., Simms, J., Kendrick, R., Logan, R.T., Poyner, D.R. and Barwell, J. (2012) Lifting the lid on GPCRs: the role of extracellular loops. *Br J Pharmacol*. 165(6):1688-1703.
- Wise, A., Sheehan, M., Rees, S., Lee, M., and Milligan, G. (1999) Comparative Analysis of the Efficacy of A1 Adenosine Receptor Activation of Gi/oα G Proteins following Coexpression of Receptor and G Protein and Expression of A1 Adenosine Receptor–Gi/oα Fusion Proteins. *Biochemistry*. 38(8):2272-8.
- Wittenberger, T., Schaller, H. C., and Hellebrand, S. (2001) An expressed sequence tag (EST) data mining strategy succeeding in the discovery of new G-protein coupled receptors. *J Mol Biol*. 307:799-813.

- Wood, M.R., Hopkins, C.R., Brogan, J.T., Conn, P.J. and Lindsley, C.W. (2011) "Molecular switches" on mGluR allosteric ligands that modulate modes of pharmacology. *Biochemistry*. 50(13):2403-10.
- Wootten, D., Christopoulos, A. and Sexton, P.M. (2013) Emerging paradigms in GPCR allostery: implications for drug discovery. *Nat Rev Drug Discov*. 12(8):630-44.
- Xu, F., Wu, H., Katritch, V., Han, G.W., Jacobson, K.A., Gao, Z.G., Cherezov, V. and Stevens, R.C. (2011) Structure of an agonist-bound human A2A adenosine receptor. *Science*. 332(6027):322-7.
- Yao, X., Parnot, C., Deupi, X., Ratnala, V.R., Swaminath, G., Farrens, D. and Kobilka, B. (2006) Coupling ligand structure to specific conformational switches in the beta2-adrenoceptor. *Nat Chem Biol*. 2(8):417-22.
- Ye, N., Li, B., Mao, Q., Wold, E.A., Tian, S., Allen, J.A. and Zhou, J. (2019) Orphan Receptor GPR88 as an Emerging Neurotherapeutic Target. *ACS Chem Neurosci*. 10(1):190-200.
- Yin, H., Chu, A., Li, W., Wang, B., Shelton, F., Otero, F., Nguyen, D.G., Caldwell, J.S. and Chen, Y.A. (2009) Lipid G protein-coupled receptor ligand identification using beta-arrestin PathHunter assay. *J Biol Chem*. 284(18):12328-38.
- Yin, J., Babaoglu, K., Brautigam, C.A., Clark, L., Shao, Z., Scheuermann, T.H., Harrell, C.M., Gotter, A.L., Roecker, A.J., Winrow, C.J., Renger, J.J., Coleman, P.J. and Rosenbaum, D.M. (2016) Structure and ligand-binding mechanism of the human OX1 and OX2 orexin receptors. *Nat Struct Mol Biol*. 23(4):293-9.
- Yin, X.F., Chen, J., Mao, W., Wang, Y.H. and Chen, M.H. (2012) A selective aryl hydrocarbon receptor modulator 3,3'-Diindolylmethane inhibits gastric cancer cell growth. *J Exp Clin Cancer Res*. 31:46.

- Yona, S., Lin, H.H., Siu, W.O., Gordon, S. and Stacey, M. (2008) Adhesion-GPCRs: emerging roles for novel receptors. *Trends Biochem Sci.* 33(10):491-500.
- Yonezawa T, Kurata R, Yoshida K, Murayama MA, Cui X, Hasegawa A. (2013) Free fatty acids-sensing G protein-coupled receptors in drug targeting and therapeutics. *Curr Med Chem.* 20(31):3855-71.
- Yousefi, S., Cooper, P. R., Potter, S. L., Mueck, B., and Jarai, G. (2001) Cloning and expression analysis of a novel G-protein-coupled receptor selectively expressed on granulocytes. *J Leukoc Biol.* 69(6):1045-52.
- Zhang, Q., Yang, H., Li, J. and Xie, X. (2016) Discovery and Characterization of a Novel Small-Molecule Agonist for Medium-Chain Free Fatty Acid Receptor G Protein-Coupled Receptor 84. *J Pharmacol Exp Ther.* 357(2):337-44.
- Zhang, Y., Sun, B., Feng, D., Hu, H., Chu, M., Qu, Q., Tarrasch, J.T., Li, S., Sun Kobilka, T., Kobilka, B.K. and Skiniotis, G. (2017) Cryo-EM structure of the activated GLP-1 receptor in complex with a G protein. *Nature.* 546(7657):248-53.
- Zheng, W., Thorne, N. and McKew, J.C. (2013) Phenotypic screens as a renewed approach for drug discovery. *Drug Discov Today.* 18(21-22):1067-73.

Appendices

SCIENTIFIC REPORTS

OPEN

Three classes of ligands each bind to distinct sites on the orphan G protein-coupled receptor GPR84

Zobaer Al Mahmud¹, Laura Jenkins¹, Trond Ulven², Frédéric Labéguère^{3,6}, Romain Gosmini³, Steve De Vos⁴, Brian D. Hudson¹, Irina G. Tikhonova⁵ & Graeme Milligan¹

Received: 12 September 2017

Accepted: 5 December 2017

Published online: 20 December 2017

Medium chain fatty acids can activate the pro-inflammatory receptor GPR84 but so also can molecules related to 3,3'-diindolylmethane. 3,3'-Diindolylmethane and decanoic acid acted as strong positive allosteric modulators of the function of each other and analysis showed the affinity of 3,3'-diindolylmethane to be at least 100 fold higher. Methyl decanoate was not an agonist at GPR84. This implies a key role in binding for the carboxylic acid of the fatty acid. Via homology modelling we predicted and confirmed an integral role of arginine¹⁷², located in the 2nd extracellular loop, in the action of decanoic acid but not of 3,3'-diindolylmethane. Exemplars from a patented series of GPR84 antagonists were able to block agonist actions of both decanoic acid and 3,3'-diindolylmethane at GPR84. However, although a radiolabelled form of a related antagonist, [³H]G9543, was able to bind with high affinity to GPR84, this was not competed for by increasing concentrations of either decanoic acid or 3,3'-diindolylmethane and was not affected adversely by mutation of arginine¹⁷². These studies identify three separable ligand binding sites within GPR84 and suggest that if medium chain fatty acids are true endogenous regulators then co-binding with a positive allosteric modulator would greatly enhance their function in physiological settings.

GPR84 is designated officially as an 'orphan' G protein-coupled receptor (GPCR)¹. This terminology indicates that the endogenous ligands that activate the receptor remain unidentified or that suggested ligands are not accepted with unanimity by the research community. Further work is needed, therefore, to validate suggested pairings. Despite this, the ability of medium chain fatty acids (MCFAs) to act as activators of GPR84 was first reported more than 10 years ago². A number of subsequent studies have confirmed the ability of MCFAs, and also of hydroxylated MCFAs, to activate GPR84^{3–6}, although this has not been observed in all studies⁷. The most potent of the MCFAs in activating GPR84 are generally decanoic (also called capric) acid (C10) (Fig. 1) and undecanoic acid (C11). Lack of full acceptance of MCFAs as the key endogenous activators of GPR84 may reflect that the mode of interaction of the MCFAs with GPR84 is poorly defined^{3,8,9} and that the reported potency of these ligands at GPR84, particularly in cells natively expressing this receptor, is very modest².

All GPCRs that are currently accepted by the International Union of Basic and Clinical Pharmacology to be receptors for fatty acids contain either a single, (free fatty acid receptor 4, FFA4)^{10–12}, or a pair, (free fatty acid receptors 1–3, FFA1–3)^{13,14}, of arginine residues that act to co-ordinate the carboxylate function of the fatty acid. It is well appreciated that in each of these cases the carboxylate is key to ligand function because equivalent fatty acid esters and amides are not activators of the corresponding receptor⁸. To date only a single study has reported on significant efforts to define the mode of binding of MCFAs to GPR84³. Surprisingly, given that all currently recognised free fatty acid receptors contain a suitable charge partner for the carboxylate of the fatty acid, this study³ failed to identify an equivalent arginine or other positively charged residue that might play a similar role in GPR84, instead suggesting that the MCFA carboxylate may reach deep within the core of the receptor to interact

¹Centre for Translational Pharmacology, Institute of Molecular, Cell and Systems Biology, College of Medical, Veterinary and Life Sciences, University of Glasgow Glasgow, G12 8QQ, Scotland, United Kingdom. ²Department of Physics, Chemistry and Pharmacy, University of Southern Denmark, Campusvej 55, DK-5230, Odense M, Denmark. ³Galapagos SASU, 102 Avenue Gaston Roussel, 93230, Romainville, France. ⁴Galapagos NV, Generaal De Wittelaan L11 A3, 2800, Mechelen, Belgium. ⁵School of Pharmacy, Medical Biology Centre, Queen's University Belfast, Belfast, BT9 7BL, United Kingdom. ⁶Present address: Evotec, 195 Route d'Espagne, 31100, Toulouse, France. Zobaer Al Mahmud and Laura Jenkins contributed equally to this work. Correspondence and requests for materials should be addressed to G.M. (email: Graeme.Milligan@glasgow.ac.uk)

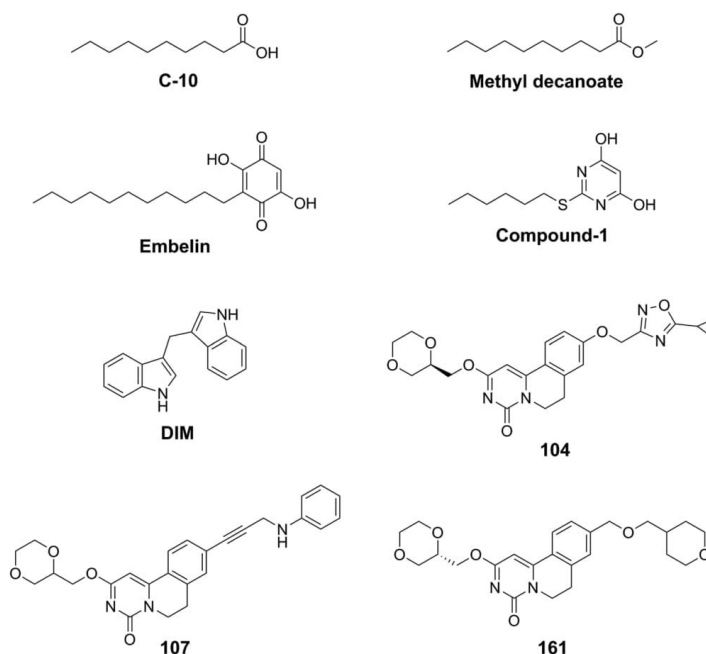


Figure 1. Structures of GPR84 ligands used in the studies. Chemical structures of the MCFA C10, the equivalent methyl ester, a pair of synthetic GPR84 orthosteric agonists (embelin, compound-1), the allosteric GPR84 agonist DIM and three exemplar GPR84 antagonists (compounds 104, 107 and 161) are shown.

with asparagine 104 (residue position 3.36)³. For orphan receptors to be formally paired with their endogenous ligand(s) requires not only that the suggested ligand(s) can activate the receptor but also that the ligands are able to do so at concentrations commensurate with their circulating or local tissue concentrations¹⁵. For example, it has been suggested that the orphan receptor GPR35 is a functional receptor for kynurenic acid¹⁶. However, the very low potency of this ligand at human GPR35 has led commentators to question the physiological relevance of this proposed pairing^{17,18}. Although MCFAs are reported to activate GPR84 with micromolar potency² there remain questions about whether such levels of MCFAs are generally present within the body. Moreover, measures of the potency of MCFAs derive generally from experiments performed following heterologous expression of GPR84^{2,4}. Such experiments often overestimate true ligand affinity at a receptor due to features of receptor reserve and direct measures of affinity of the MCFAs for GPR84 are lacking.

Across the group of GPCRs activated by free fatty acids there is substantial evidence for multiple binding sites for both endogenously produced and synthetic ligands. Recent studies on FFA1 showed co-operative effects between a fatty acid and the synthetic, clinically-trialled partial agonist TAK-875¹⁹ and multiple binding pockets on this receptor have been confirmed in atomic level X-ray structures of the receptor²⁰. Furthermore, although no equivalent crystal structures are yet available, functional studies have identified synthetic small molecule ligands that appear to bind to locations distinct from the short chain fatty acid binding sites on both FFA2^{21,22} and FFA3²³, see⁸ for review. Finally, although limited in detailed characterisation, there are also studies consistent with the presence of multiple binding pockets in GPR84^{3,24}.

Herein we address these issues for the purported MCFA-GPR84 pairing and in so doing demonstrate that, as expected for a free fatty acid receptor, an arginine residue, here located within the 2nd extracellular loop (ECL2) of GPR84, acts as the putative charge partner for MCFAs to allow their recognition by the receptor. We also show that a series of other GPR84 agonist ligands with long hydrophobic tails and carboxylate bioisostere head groups^{4,25,26} bind the receptor in a manner overlapping with the MCFAs and, as such, these each act as 'orthosteric' agonists. By contrast, 3,3'-diindolylmethane (DIM)^{3,24,27} (Fig. 1), previously shown to be an 'allosteric' activator of GPR84^{4,25,24}, does not appear to bind to the GPR84 orthosteric site. DIM, and certain related molecules produce extensive increases in the measured potency of both MCFAs and other orthosteric agonists and this suggests that endogenously produced molecules acting in a similar way may result in significantly lower concentrations of MCFA being required to activate GPR84 than would have previously been predicted. Finally, we demonstrate that a group of GPR84 antagonist ligands²⁸, although able to block signalling by both orthosteric and allosteric agonist ligands, do so non-competitively by binding at a location that is distinct from either of these agonist sites.

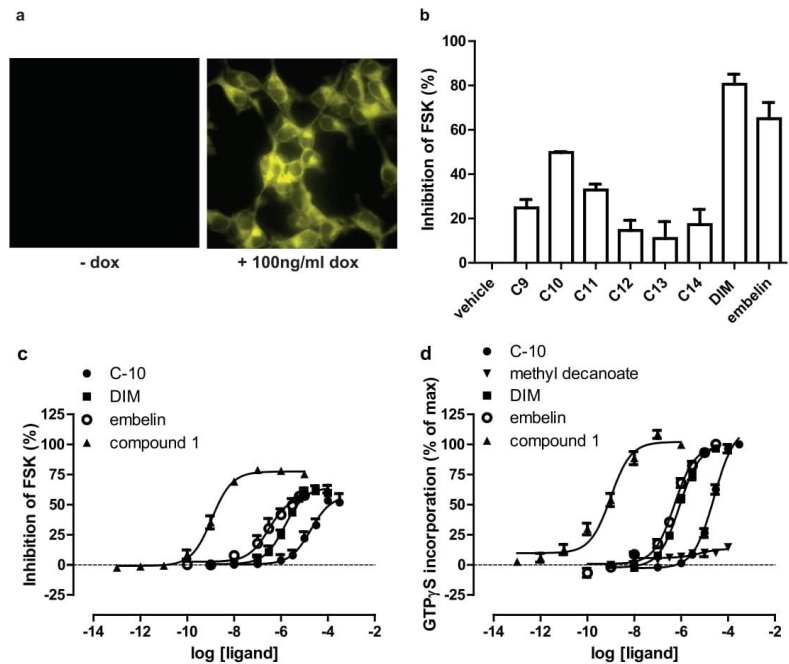


Figure 2. C10 and other ligands can activate GPR84. Flp-In T-REx 293 cells harboring FLAG-hGPR84-eYFP at the Flp-In T-REx locus were untreated (– dox) or maintained in the presence of doxycycline (100 ng/ml) for 24 hours. Such cells were imaged to detect the eYFP tag linked to the receptor (a). The capacity of fatty acids of chain length 9–14 (100 μ M) to inhibit forskolin-stimulated cAMP levels in doxycycline-induced cells was assessed and compared to effects of embelin and DIM (b). C10, embelin, DIM and compound 1 each regulate cAMP levels in a concentration-dependent manner (c). Membrane preparations generated from doxycycline-induced cells were also used in [35 S]GTP γ S binding assays and each of C10, embelin, DIM and compound-1 promoted binding of [35 S]GTP γ S in a concentration-dependent manner (d). By contrast methyl decanoate was without effect (d).

Results

Decanoic acid is an endogenous ligand that can activate GPR84. We expressed a form of human (h)GPR84 (FLAG-hGPR84-eYFP) that incorporated both an N-terminal FLAG epitope-tag sequence and C-terminal enhanced Yellow Fluorescent Protein (eYFP) in Flp-In T-REx 293 cells. In such cells addition of the antibiotic doxycycline allows induced expression of DNA constructs in the Flp-In T-REx locus²⁹. Imaging of such cells showed that the FLAG-hGPR84-eYFP construct was expressed effectively (Fig. 2a). GPR84 is recognized to interact selectively with pertussis toxin-sensitive, G_i-family G proteins^{4,8}. In the initial de-orphanization study on GPR84 Wang and colleagues² showed MCFAs with chain length C9–C14 were able to activate GPR84. Initially, we used this same group of fatty acids and demonstrated that when using 100 μ M of each MCFAs, decanoic acid (C10) produced the largest effect as assessed by measuring the capacity of the ligands to inhibit forskolin-amplified levels of cAMP in cells expressing FLAG-hGPR84-eYFP (Fig. 2b). As positive controls in these studies we used two further ligands recognized to be agonists of GPR84; 2,5-dihydroxy-3-undecyl-2,5-cyclohexadiene-1,4-dione (embelin)³ (Fig. 1) and DIM (Fig. 1). Concentration-response studies showed both embelin ($pEC_{50} = 6.7 \pm 0.3$) and DIM ($pEC_{50} = 5.9 \pm 0.1$) to be substantially more potent than C10 ($pEC_{50} = 4.7 \pm 0.2$) (Fig. 2c). G_i-coupled receptors are frequently highly effective in promoting binding of the guanine nucleotide analog [35 S]GTP γ S to receptor-associated G proteins³⁰. Using this as an alternate end-point both embelin ($pEC_{50} = 6.2 \pm 0.1$) and DIM ($pEC_{50} = 6.0 \pm 0.1$) also promoted enhanced binding of [35 S]GTP γ S to membrane preparations of cells induced to express FLAG-hGPR84-eYFP (Fig. 2d). Once more these were both considerably more potent than C10 ($pEC_{50} = 4.6 \pm 0.1$). We also assessed a more recently reported GPR84 agonist, 2-(hexylthio)pyridine-4,6 diol (designated compound-1²⁵, or ZQ16²⁶, in previous reports) (Fig. 1). This was substantially more potent as an agonist in both the inhibition of cAMP ($pEC_{50} = 9.0 \pm 0.1$) (Fig. 2c) and [35 S]GTP γ S binding ($pEC_{50} = 9.1 \pm 0.2$) (Fig. 2d) assays. Importantly, methyl decanoate (Fig. 1), lacking the carboxylate function of C10, was completely inactive at GPR84 (Fig. 2d).

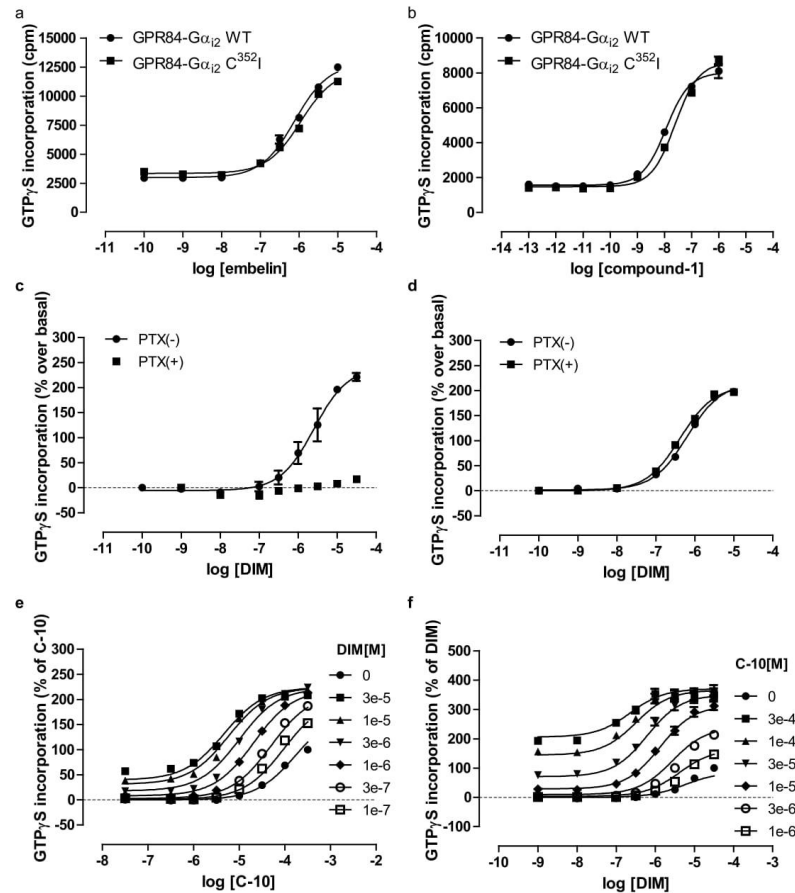


Figure 3. C10 and DIM display allosteric interactions in activating GPR84. Either a GPR84-G α_{12} fusion protein, or a pertussis toxin-resistant variant, GPR84-Cys^{352Ile} G α_{12} , was expressed in Flp-In T-REx 293 cells. Membrane preparations were then generated and used to assess the effect of varying concentrations of embelin (a) or compound-1 (b) on binding of [³⁵S]GTP γ S. Cells as above expressing (c), GPR84-G α_{12} or (d), GPR84-Cys^{352Ile} G α_{12} were treated with or without pertussis toxin (PTX) for 24 h prior to membrane production. The effects of varying concentrations of DIM were then measured. How fixed concentrations of DIM affected the concentration-dependence of C10-induced stimulation of binding of [³⁵S]GTP γ S (e) and *vice versa* (f) was assessed. Details of fitting datasets akin to the examples shown in (e) and (f) to an operational model of allosteric modulation⁴⁶ is provided in Table 1.

DIM is a positive allosteric modulator of the potency of decanoic acid. The only previous study³ designed to explore the mode of binding of ligands to GPR84 employed a fusion protein^{31,32} in which the G protein G α_{11} was linked in-frame to the C-terminal tail of GPR84. Therefore, we also generated a pair of related GPCR-G protein fusion constructs in which, because G α_{11} displays a restricted distribution pattern whilst G α_{12} is expressed ubiquitously, either wild type G α_{12} or a pertussis toxin-resistant variant of this, Cys^{352Ile} G α_{12} ³³, was linked in-frame to the C-terminal tail of GPR84. Following expression of either of the GPR84-G α_{12} fusion proteins in Flp-In T-REx 293 cells and membrane preparation the measured potency of each of embelin and compound-1 was indistinguishable between the two GPR84-G protein fusion constructs (Fig. 3a,b). Response to DIM was all but eliminated when using membranes generated from cells that had been induced to express the wild type GPR84-G α_{12} fusion protein and then pre-treated with pertussis toxin (Fig. 3c). In contrast, response to DIM was unaffected following pertussis toxin treatment of cells induced to express the pertussis toxin-resistant

| Agonist ^a | Modulator ^b | log α | log β | pK _A ^c | pK _B ^d |
|----------------------|------------------------|--------------|-------------|------------------------------|------------------------------|
| compound-1 | DIM | 2.1 ± 0.07 | -0.2 ± 0.05 | 6.7 ± 0.06 | 5.2 ± 0.04 |
| DIM | compound-1 | 1.8 ± 0.08 | 1.14 ± 0.03 | 5.3 ± 0.04 | 6.9 ± 0.07 |
| compound-1 | 3a | 1.75 ± 0.05 | -0.1 ± 0.02 | 6.8 ± 0.03 | 5 ± 0.04 |
| 3a | compound-1 | 1.43 ± 0.08 | 1.2 ± 0.06 | 4.83 ± 0.06 | 7.2 ± 0.05 |
| C-10 | DIM | 1.4 ± 0.1 | 0.4 ± 0.07 | 3.3 ± 0.08 | 5.2 ± 0.03 |
| DIM | C-10 | 1.3 ± 0.1 | 1.2 ± 0.05 | 5.2 ± 0.06 | 3.8 ± 0.06 |
| embelin | DIM | 1.22 ± 0.05 | 0.8 ± 0.02 | 5.5 ± 0.03 | 5.15 ± 0.03 |
| DIM | embelin | 1.12 ± 0.04 | 1.0 ± 0.03 | 5.1 ± 0.03 | 5.7 ± 0.02 |

Table 1. Estimation of binding affinities and the allosteric characteristics of pairs of GPR84 agonists. ^aAgonist is the compound used to generate concentration-response curve. ^bModulator is the compound used in defined concentrations. ^cpK_A are values estimated for the agonist. ^dpK_B are values estimated for the modulator. Data are means ± SEM.

GPR84-Cys³⁵²Ile G α_{12} fusion protein (Fig. 3d). These studies indicate that following pertussis toxin treatment of cells expressing the GPR84-Cys³⁵²Ile G α_{12} fusion protein all agonist-induced binding of [³⁵S]GTP γ S reflects incorporation of nucleotide into the receptor-linked G protein α subunit. Using this system the ability of various concentrations of C10 to stimulate binding of [³⁵S]GTP γ S was enhanced by co-addition of increasing concentrations of DIM (Fig. 3e). As such, as well as a direct agonist, DIM acted as a positive allosteric modulator (PAM) of the potency of C10 (Fig. 3e, Table 1). As anticipated for such an allosteric effect, equivalent outcomes were also observed when the experimental protocol was reversed and effects of increasing concentrations of C10 on the potency of DIM were assessed (Fig. 3f, Table 1). Importantly, as well as defining that C10 and DIM likely bind to topographically distinct sites on GPR84, mathematical analysis of these datasets provided estimates of the binding affinity of the ligands to the GPR84-G α_{12} fusion protein. These predicted C10 to bind with very modest affinity (K_A range 0.17–0.53 mM), whilst DIM (K_A range 5.6–6.9 μ M) was predicted to bind with more than 200 times greater affinity (Table 1).

We next assessed whether DIM would also affect the measured functional potency of either embelin or compound-1. For both pairings this was the case, with increasing concentrations of DIM enhancing the measured potency of compound-1 (Fig. 4a) and embelin (Fig. 4b) and *vice versa* (Fig. 4a,b). This demonstrated that both compound-1 and embelin also most likely bind to GPR84 at a different site(s) than DIM. Moreover, the binding affinity of DIM calculated from the PAM effects of each of embelin and compound-1 on potency of DIM is anticipated to be independent of the identity of the second ligand used in such studies and, indeed, in both these cases mathematical analysis of the datasets once more allowed assessment of affinity of DIM for the GPR84-G α_{12} fusion protein as being between 5 and 10 μ M (Table 1). By contrast, co-addition studies using C10 with either compound-1 (Fig. 4c) or embelin (Fig. 4d) did not result in modulation of the potency of the ligands, and these results are consistent with C10, compound-1 and embelin sharing a single, common binding site.

Analogues of DIM lose functional activity. We next studied a series of analogues of DIM²⁷ (Fig. 5a). Although some of these, including compounds '3a' and '6a' also showed direct agonism of GPR84 (Fig. 5b) others, including '2b', '3b' and '3c' (Fig. 5b) were inactive. Each of the inactive ligands tested contains a bulky substitution on the linker between the indole groups. Whilst compound '3a' produced as large positive allosteric effects on the potency of the orthosteric agonist ligands as did DIM (Fig. 5c), increasing concentrations of either '2b' (Fig. 5d) or '3c' (Fig. 5e) were unable to effect the position of the concentration-response curves for the orthosteric agonists of GPR84, including compound-1. These data suggest that unlike compound '3a', compounds '2b' and '3c' lack affinity for GPR84. Studies with a broader range of such analogues²⁴ may help define the allosteric agonist binding pocket.

Defining an orthosteric binding mode. We selected, *a priori*, to designate the C10 binding site as the 'orthosteric' site because C10 is an endogenously produced ligand. To try to identify how a MCFA might interact with GPR84 we turned to homology modelling studies. Although GPR84 is not closely related to the other GPCRs that respond to either short chain (FFA2, FFA3) or long chain (FFA1, FFA4) fatty acids^{8,9}, in each of the other cases the carboxylate of the fatty acid is co-ordinated by one or more arginine residues located at or near the extracellular surface^{12–14}. A previous effort to model the structure of GPR84 and to predict the mode and orientation of binding of C10 developed a receptor homology model based on the atomic level, active-state structure of the β_2 -adrenoceptor³. These studies, however, did not identify a potential charge partner for the carboxylate of the fatty acid near the extracellular surface and, indeed, concluded that the carboxylate of C10 was pointing downwards, deep into the cleft of the seven transmembrane domain core of the receptor and interacting with an asparagine located at position 104 in the primary amino acid sequence³. As we have highlighted recently⁹ GPR84 and the β_2 -adrenoceptor are only distantly related whilst, of the currently available atomic level GPCR structures, the orexin OX₁ receptor³⁴ has highest overall sequence identity (31%) with GPR84. We, therefore, generated and employed a new homology model of GPR84 based on the transmembrane domain architecture of the OX₁ receptor (Fig. 6). However, because ECL2 of GPR84 is very similar in sequence to that of rhodopsin (Fig. 6a), with 43% residue identity over this region, we incorporated this knowledge into the modelling process. In the resulting hybrid model (Fig. 6a) Arg¹⁷² within ECL2 is pointing into the potential binding cavity within the helical bundle. This was not the case when Nikaido *et al.*³ employed the β_2 -adrenoceptor-based model, probably because the ECL2 sequences of the β_2 -adrenoceptor and GPR84 have no relatedness. This new model, therefore, provided the

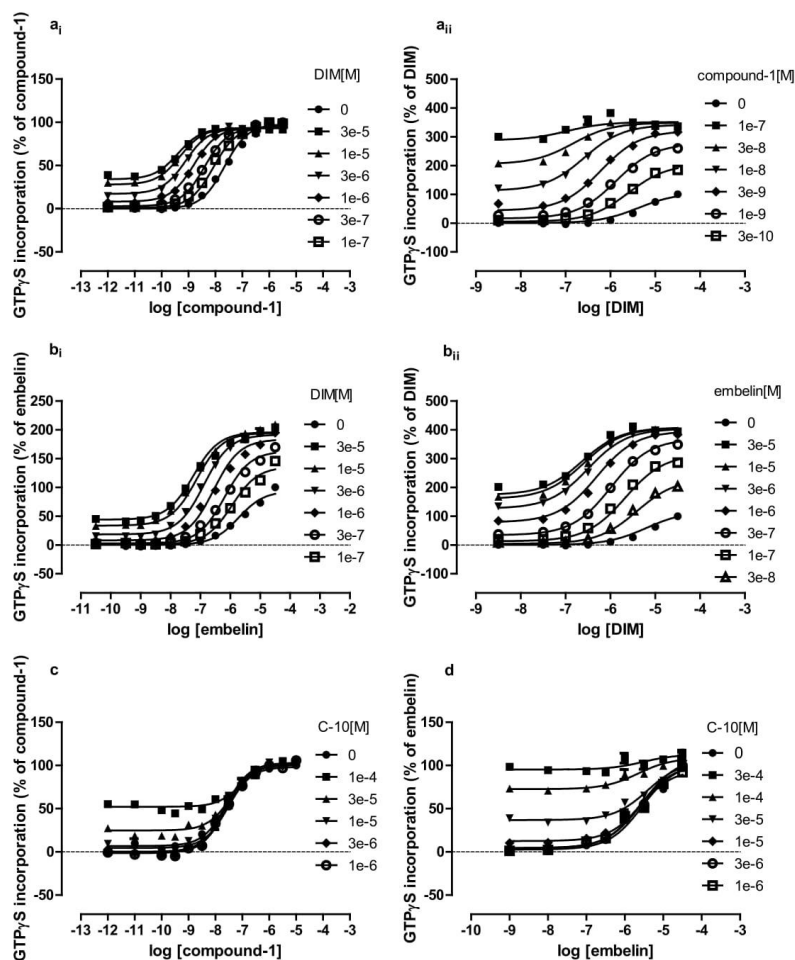


Figure 4. DIM also displays allosteric interactions with other orthosteric GPR84 agonists. Experiments were performed as in Fig. 3 to assess potential positive allosteric effects between DIM and compound-1 (a_i,a_{ii}) and embelin (b_i,b_{ii}). Similar studies assessed potential allosteric effects between C10 and either compound-1 (c) or embelin (d). Table 1 provides quantitative outcomes of fitting datasets akin to those shown in (a) and (b) to an operational model of allostery.

hypothesis that Arg¹⁷² might co-ordinate the carboxylate moiety of MCFAs, as well as the bioisosteric headgroups of embelin and compound-1. To assess this we mutated Arg¹⁷² to Ala within the setting of the GPR84-Cys³⁵²Ile G α_{12} fusion protein. Now, although the allosteric agonist DIM retained full activity at this mutant (Fig. 7a_i), no response was produced by C10, embelin or compound-1 (Fig. 7a_{ii}–iv). Retention of positive charge at this position by generating an Arg¹⁷²Lys mutation within the GPR84-Cys³⁵²Ile G α_{12} fusion protein also eliminated response to each of C10, embelin and compound-1 without affecting response to DIM (Fig. 7a). Equivalent results were obtained in studies in which the Arg¹⁷²Ala mutation was introduced into the FLAG-hGPR84-eYFP construct (Fig. 7b). By contrast, mutation to Ala of Arg¹⁷⁴, located only 2 amino acids away from Arg¹⁷², but instead predicted to point away from the binding cavity (Fig. 6a), did not affect function or potency of any of DIM, C10, embelin or compound-1 (Fig. 7b). Based on these studies, we explored potential docking poses of each of C10, embelin and compound-1. These studies suggest that the hydrophobic tail of each of these ligands projects downwards towards and into the core of the receptor (Fig. 6B–D).

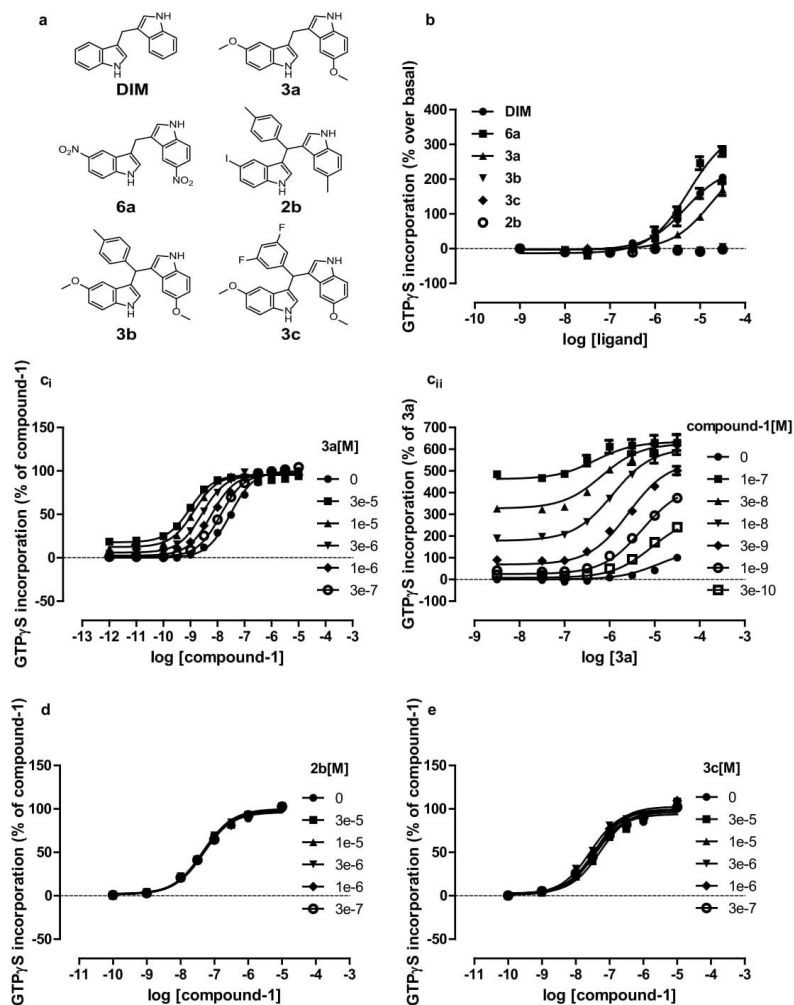


Figure 5. Certain DIM analogs lack affinity at GPR84. The ability of DIM and various analogs of DIM, (structures in **a**) to promote binding of [³⁵S]GTP-γS to membranes of Flp-In T-REx 293 cells expressing the GPR84-G_{o12} fusion protein was assessed (**b**). The effect of compound 3a on the concentration-response curve to compound-1 (**c_i**) and *vice versa* (**c_{ii}**) and the lack of effect of compounds 2b (**d**) and 3c (**e**) on the concentration-response curve to compound-1 are displayed.

Studies with GPR84 antagonists. Although the maintenance of agonist activity of DIM at Arg¹⁷²Ala and Arg¹⁷²Lys GPR84 provided confidence that these alterations did not simply generate a poorly organized and folded form of this receptor, we wished to explore this more fully. Labeguere *et al.*,³⁵ have reported a series of compounds able to functionally antagonize GPR84. We explored the ability of three closely related exemplars from this series to limit [³⁵S]GTP-γS binding induced by EC₈₀ concentrations of each of C10, embelin and DIM in membranes of cells expressing FLAG-hGPR84-eYFP. Compounds 104, 107 and 161 (9-(5-cyclopropyl-1,2,4-oxadiazol-3-ylmethoxy)-2-((R)-1-[1,4]dioxan-2-ylmethoxy)-6,7-dihydro-pyrimido[6,1-a]isoquinolin-4-one; 2-((1,4)dioxan-2-ylmethoxy)-9-(3-phenylamino-prop-1-ynyl)-6,7-dihydro-pyrimido[6,1-a]isoquinolin-4-one; 2-((S)-1-[1,4]dioxan-2-ylmethoxy)-9-(tetrahydro-pyran-4-yl-methoxymethyl)-6,7-dihydro-pyrimido[6,1-a]isoquinolin-4-one, respectively) (Fig. 1) each did so, and in a concentration-dependent fashion, with 104 and

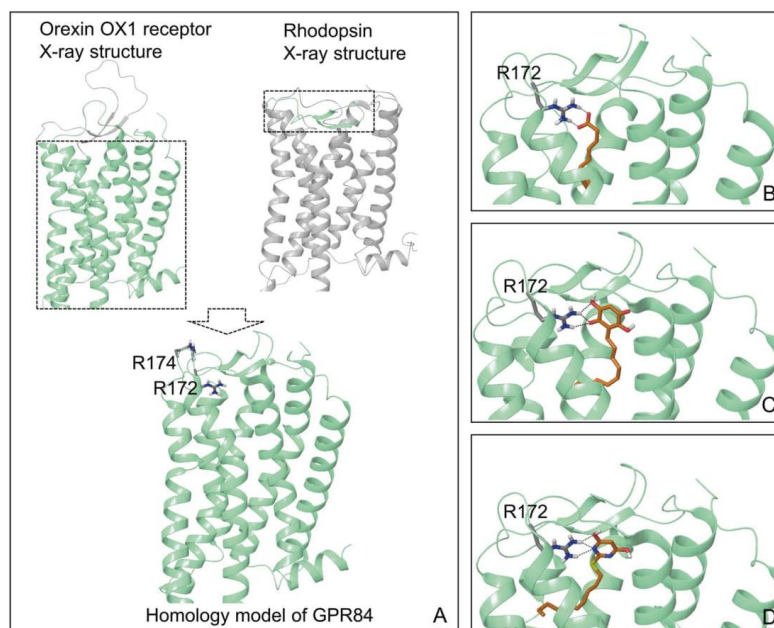


Figure 6. Homology model of GPR84 and the putative binding modes of orthosteric GPR84 agonists. (A) A GPR84 homology model was constructed based on a hybrid template involving the crystal structure of the helical bundle of the OX₁ orexin receptor and the crystal structure of ECL2 of rhodopsin. Two arginines, Arg¹⁷² and Arg¹⁷⁴ located within ECL2 are visualized. (B–D) The putative docking pose of C10 (B), embelin (C) and compound-1 (D), respectively is shown. The anchoring R¹⁷² within ECL2 is visualized. Hydrogen bonds or salt bridges are in dotted black lines.

107 being more potent than 161 (Fig. 8a–c). Although able to block function of embelin, analysis of the effects of increasing concentrations of compound 107 on the position of the concentration–response curve for embelin showed that the antagonist decreased measured maximal effects of this agonist (Fig. 8d) rather than moving the measured EC₅₀ of the agonist to higher concentrations as would be anticipated for a competitive and reversible receptor blocker. These features indicate that compound 107 blocks the effects of embelin in a non-competitive manner, likely by binding to a distinct site on GPR84. Moreover, at higher concentrations of 107 the maximal effect of DIM at GPR84 was also reduced (Fig. 8e), once more indicating a non-competitive mode of blockade of the agonism produced by DIM. Further support to define that compound 107 does not bind to the orthosteric agonist binding site was that compound 107 had equal potency to block DIM-stimulated binding of [³⁵S]GTPγS to GPR84-Cys³⁵²Ile Gα₁₂ and to the Arg¹⁷²Ala GPR84-Cys³⁵²Ile Gα₁₂ fusion proteins (Fig. 8f).

We next studied the binding characteristics of a radiolabelled form of a GPR84 antagonist [³H]G9543 that is chemically related to compounds 104, 107 and 161 (Fig. 9). [³H]G9543 bound to membranes expressing FLAG-hGPR84-eYFP with high affinity ($K_d = 0.24 \pm 0.07$ nM) and in a manner consistent with a single binding site (Fig. 9a). This was also the case for the GPR84-Cys³⁵²Ile Gα₁₂ fusion protein ($K_d = 0.26 \pm 0.02$ nM). Binding of [³H]G9543 to the GPR84-Cys³⁵²Ile Gα₁₂ fusion protein was competed fully and effectively by the antagonist compound 104 (Fig. 9b) with pK_i of compound 104 assessed as 8.73 ± 0.1 . By contrast, neither C10 nor DIM was able to compete effectively with [³H]G9543 to bind GPR84 (Fig. 9b), and this was also the case for embelin (Fig. 9b). This suggests that [³H]G9543 and, by extension, compound 104 binds to a further site that is topographically distinct from that occupied by C10 and embelin and also from that occupied by DIM. This further indicates separation of the agonist and antagonist binding sites and that these GPR84 antagonists block agonist function at GPR84 in a non-competitive fashion. In further support for this model, binding affinity of [³H]G9543 was not altered substantially at the Arg¹⁷²Ala GPR84-eYFP ($K_d = 0.15 \pm 0.01$ nM) (Fig. 9c) or, indeed, the Arg¹⁷⁴Ala GPR84-eYFP ($K_d = 0.25 \pm 0.06$ nM) (Fig. 9d) variants.

Discussion

Potential endogenous activating ligands have been suggested for a number of GPCRs that officially remain designated as ‘orphans’^{1,57}. However, in many of these cases the suggested ligands have previously been paired with more certainty with other members of the GPCR superfamily, and/or the reported potency of the suggested

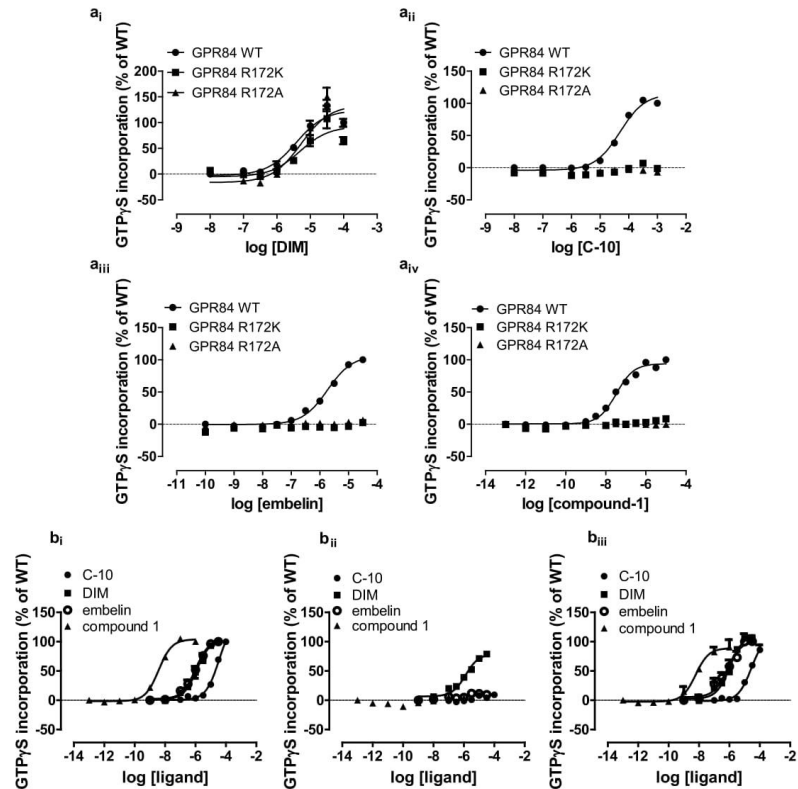


Figure 7. Conversion of arginine¹⁷² to alanine or lysine eliminates agonism of orthosteric agonists but not of DIM. (a) Membranes expressing either GPR84-Cys³⁵²IleGo₁₂, Arg¹⁷²Ala GPR84-Cys³⁵²IleGo₁₂ or Arg¹⁷²Lys GPR84-Cys³⁵²IleGo₁₂ were used in [³⁵S]GTPγS binding studies to assess function of (a*i*) DIM, (a*ii*), C10, (a*iii*) embelin and (a*iv*) compound-1. (b) Similar studies were performed on membrane of cells induced to express FLAG-hGPR84-eYFP (b*i*), FLAG-Arg¹⁷²Ala hGPR84-eYFP (b*ii*), FLAG-Arg¹⁷⁴Ala hGPR84-eYFP (b*iii*) to assess activity of C10, DIM, embelin and compound-1.

ligand is modest at the receptor in question¹. Moreover, in such cases there is generally also little known about the predicted mode of binding of the ligand to the receptor. Clearly such issues do not exclude the possibility that a physiologically relevant pairing has been uncovered, but does highlight that further and more detailed studies are generally required to provide further support or confirmation.

GPR84 is not closely related to either of the groups of previously defined free fatty acid-responsive GPCRs, FFA1-3 and FFA4. However, a feature shared by FFA1-4 is that each possesses at least one arginine residue located close to the extracellular face of the receptor that acts as the charge partner for the carboxylate moiety of fatty acid ligands^{8,9}. Earlier studies showed that wild type GPR84 failed to respond to decylamine³ and herein we confirm the importance of the carboxylate of C10 to activation of the receptor because methyl decanoate was also unable to act as an agonist at GPR84. Previous mutational studies³ did not identify a positively charged amino acid that could act to co-ordinate the carboxylate of MCFAs, but instead suggested that the carboxylate might interact with an asparagine residue which modelling studies indicated to be deep within the central pocket created by the architecture of the seven transmembrane helices³. The homology model developed in these studies³ was based on the atomic level structure of a G protein-bound, active state of the β_2 -adrenoceptor. However, the β_2 -adrenoceptor has very limited sequence similarity to GPR84. In recent times the expansion of available atomic level structures of different GPCRs means that potentially better starting points for homology modelling can be selected from receptors that have higher levels of sequence similarity. Of the currently available structures, the orexin OX₁ receptor³⁴ is most closely related to GPR84, and using this as a template to model the transmembrane domain architecture, in concert with recognition that the sequence of ECL2 of GPR84 is highly homologous to that of rhodopsin, for

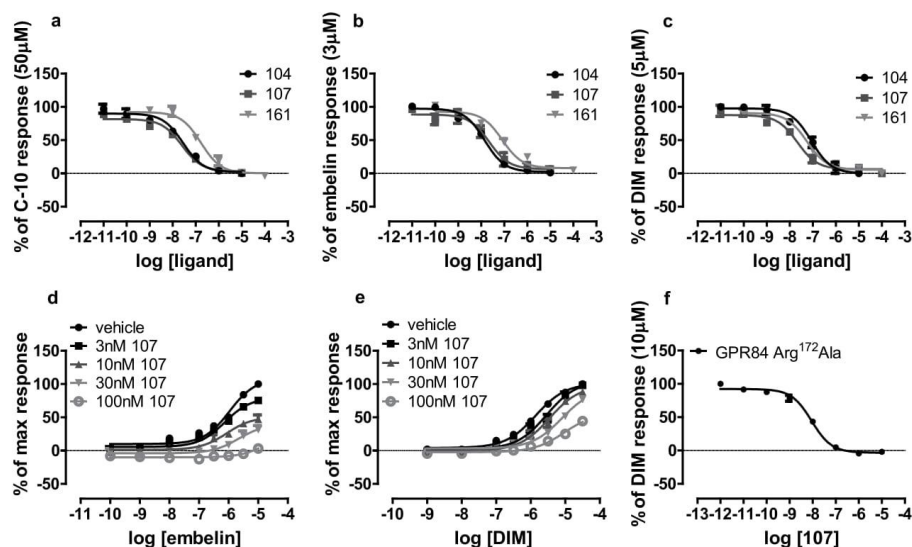


Figure 8. A number of GPR84 antagonists block agonist effects of both orthosteric and allosteric agonists. The ability of increasing concentrations of compounds 104, 107 and 161 to block agonism induced by EC₅₀ concentrations of C10 (50 μ M) (a), embelin (3 μ M) (b) and DIM (5 μ M) (c) were assessed. The ability of compound 107 to block activation of GPR84 by varying concentrations of embelin (d) or DIM (e) was also assessed. (f) Compound 107 inhibited DIM-induced binding of [³⁵S]GTP- γ S in membranes of cells induced to Arg¹⁷²Ala GPR84-Cys³⁵²IleG α_{12} .

which atomic level structures are known, allowed us to build a novel homology model⁹ that predicted that Arg¹⁷², within ECL2, might provide a charge partner for the fatty acid carboxylate. Indeed, this prediction was supported. Alteration of this residue to alanine completely eliminated receptor activation by C10. Moreover, a number of other GPR84 agonists in which an extended alkyl chain is linked to a head group that can be considered as a bioisostere of the fatty acid carboxylate all also lacked ability to activate Arg¹⁷²Ala GPR84. Interestingly, all of these agonists also lost detectable activity when Arg¹⁷² was converted to Lys, indicating that the position of the positive charge is just as vital as its preservation. The size and shape of the positive charge of Lys is quite different to Arg and the modelling studies also suggested the Arg to be engaged in a network of interactions with close-by aromatic residues that help define the conformation and location of the amino acid side chain. Hence, as Lys would be unlikely to form the same contacts and therefore organize the binding pocket in an equivalent manner, it is not surprising that it is unable to substitute in this regard.

GPR84 antagonist ligands have, to date, been described in detail only in the patent literature³⁵, but the antagonist GLPG1205 did enter a clinical trial for the treatment of ulcerative colitis³⁸. Despite being safe and tolerable GLPG1205 did not show efficacy in patients with ulcerative colitis after 12 weeks of chronic dosing. Whilst antagonist compounds 104, 107 and 161, that derive from the same patented series as GLPG1205, were able to inhibit the function of both C10 and embelin in a concentration-dependent manner, binding studies performed using a further related radiolabelled antagonist [³H]G9543 indicated that affinity for this ligand was not lost by mutation of Arg¹⁷². Moreover, C10 was unable to effectively compete with [³H]G9543 for binding to GPR84. This suggests that rather than acting as orthosteric competitive antagonists these compounds block agonist function at GPR84 in a non-competitive fashion. Indeed, direct analysis indicated this to be the case in that whilst orthosteric agonist EC₅₀ was little affected by increasing concentrations of compound 107, ongoing reduction in maximal agonist effects were observed with increasing concentrations of this antagonist.

As recently indicated by others²⁴, DIM acted as an allosteric agonist at GPR84, and retained full function as an agonist at both Arg¹⁷²Ala and Arg¹⁷²Lys GPR84, where responses to C10 and other orthosteric agonists were lost. Moreover, as well as an allosteric agonist DIM acted as a highly effective PAM of the agonist actions of each of C10 and other orthosteric GPR84 agonists including embelin and compound-1. As anticipated from this, C10 and the other orthosteric agonists produced reciprocal effects on the potency of DIM. This may be important in relation to activation of GPR84 *in vivo*. Affinity estimates for DIM at GPR84, based on mathematical analysis of the positive allosteric effects of C10 and other orthosteric ligands on DIM, were in the region of 5–10 μ M. This approach can provide estimates of ligand affinity at a GPCR whereas direct measures of agonist potency are often difficult to relate directly to ligand affinity if the target receptor is expressed heterologously in a cell line due to the potential for high level receptor expression resulting in a receptor reserve for function.

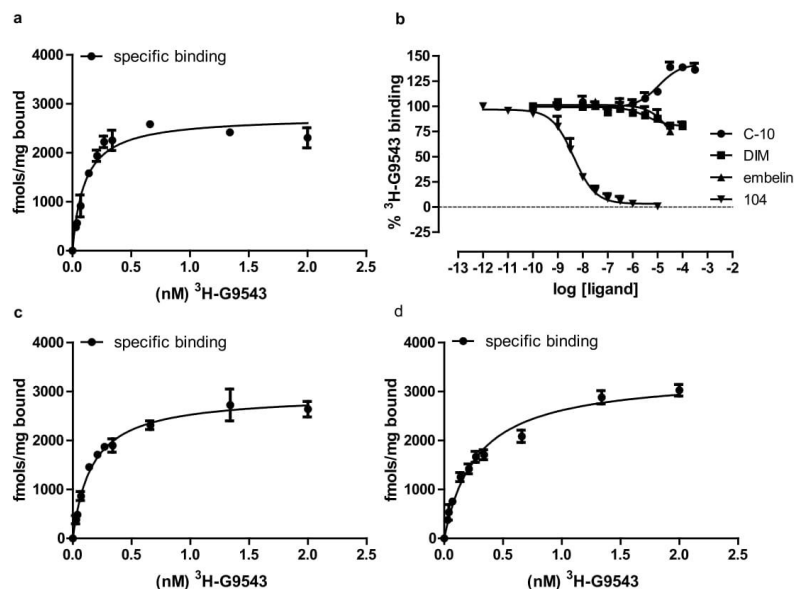


Figure 9. The antagonist [³H]G9543 binds GPR84 with high affinity but not at the orthosteric or allosteric agonist binding sites. Increasing concentrations of [³H]G9543 in the absence or presence of 1 μ M compound 104 were assessed for their ability to bind to membrane preparations expressing wild type GPR84 (a). Specific binding of [³H]G9543, i.e. total binding minus that detected in the presence of 1 μ M compound 104 is shown. Similar experiments were performed on membranes expressing Arg¹⁷²Ala GPR84 (c) or Arg¹⁷⁴Ala GPR84 (d). The ability of varying concentrations of compound 104, C10, embelin, and DIM to compete for binding of [³H]G9543 to GPR84 was also assessed (b).

DIM can be produced *in vivo* by metabolism of the natural product indole-3-carbinol and following oral dosing to women of up to 1000 mg of indole-3-carbinol, plasma levels of DIM peaked within 2 hours at between 500–600 ng/ml (approximately 2 μ M). However, this is rapidly cleared³⁶. At peak levels, this is a sufficiently high level of DIM to partially activate GPR84 directly. Potentially of importance, however, the substantial positive allosteric effects of C10 on the observed potency of DIM indicated that at high levels of C10 or other MCFAs the potency of DIM to activate GPR84 would be some 20 fold higher than in the absence of C10. An effect of DIM could be manifest, therefore, at much lower concentrations, either arising from lower dosing with indole-3-carbinol or that the period of time before clearance of DIM to a level below that required for activation of GPR84 would be extended significantly. Perhaps more directly relevant to the *in vivo* situation, the detected low potency of MCFAs when studied in isolation would be increased into a range more akin to circulating concentrations of MCFAs. Although present in high levels in tropical oils such as coconut oil and palm kernel oil, levels of C10 in human plasma are generally low³⁷, routinely below 0.5 μ M. This is towards the limit of the range anticipated to be able to activate GPR84 when added in isolation. However, in the presence of 10 μ M DIM this concentration of C10 would be anticipated to be sufficient to cause half-maximal activation of GPR84.

The concept that endogenously produced molecules may act as allosteric regulators of GPCRs, rather than uniquely acting as orthosteric ligands, is not entirely novel. Indeed, this concept has been reviewed recently³⁸. Clearly many specific ions can act as allosteric regulators of agonist function at a broad range of GPCRs but, generally, concentrations of key ions are controlled within very strict limits. More interesting examples of endogenous allosteric regulators noted by³⁸ include a variety of lipids and lipid-derived mediators, and thus it remains possible that MCFAs are acting at GPR84 as allosteric regulators rather than the true orthosteric activators of this receptor. While other means to generate the observed allosteric interactions between C10 and DIM can be envisaged, including the potential existence of dimeric forms of GPR84³⁹, the most simple explanation for this and for maintenance of agonist function of DIM at Arg¹⁷²Ala GPCR is that these two classes of agonists bind to distinct sites on a single receptor molecule. Similar reasoning supports that DIM must also bind at a site distinct from the GPR84 antagonists used herein. As for C10, agonist function of DIM was blocked by the GPR84 antagonists in a concentration-dependent manner and in a manner consistent with non-competitive interactions. Moreover, as for C10, DIM was unable to compete effectively with [³H]G9543 for binding to GPR84. These results are entirely consistent with the hypothesis that at least three spatiotemporally distinct ligand binding sites can be identified on GPR84. Recent structural studies suggest that this should not be entirely surprising. For example a recent atomic

level structure of the protease activated receptor 2 (PAR-2) indicated ways in which multiple chemical series of blockers of a receptor may bind to non-overlapping sites⁴⁰, whilst intracellular binding sites for antagonists of a number of chemokine receptor subtypes have recently been identified^{41,42}. Clearly an atomic level structure of GPR84 is not available, but even without such information, mutagenesis studies should now start to help unravel the likely modes of binding of these distinct classes of pharmacological regulators of GPR84. Although the GPR84 antagonist GLPG1205 did not show efficacy in patients suffering from ulcerative colitis²⁸ there remains considerable interest in targeting GPR84 in conditions that range from reflux esophagitis⁴³, via cognitive decline⁴⁴, to neuropathic pain⁴⁵. Greater insights into the biology and pharmacological behaviour of ligands at GPR84 will assist in efforts to do so.

Methods

Materials. Medium chain fatty acids, methyl decanoate, embelin and DIM were from Sigma-Aldrich. Compound-1 and the GPR84 antagonist compounds 104 (9-(5-cyclopropyl-[1,2,4]oxadiazol-3-ylmethoxy)-2-((R)-1-[1,4]dioxan-2-ylmethoxy)-6,7-dihydro-pyrimido[6,1-a]isoquinolin-4-one), 107 (2-((1,4)dioxan-2-ylmethoxy)-9-(3-phenylamino-prop-1-ynyl)-6,7-dihydro-pyrimido[6,1-a]isoquinolin-4-one) and 161 (2-((S)-1-[1,4]dioxan-2-ylmethoxy)-9-(tetrahydro-pyran-4-yl-methoxymethyl)-6,7-dihydro-pyrimido[6,1-a]isoquinolin-4-one) (Fig. 1) were synthesized as in^{25,35}. The analogs of DIM (Fig. 5) were a gift from Dorota Maciejewska, Department of Organic Chemistry, Medical University of Warsaw, Poland. [³⁵S]GTPγS was from PerkinElmer Life Sciences. Tissue culture reagents were from Invitrogen and molecular biology enzymes and reagents from New England BioLabs. Polyethylenimine (PEI) [linear poly(vinyl alcohol) (MW-25000)] was from Polysciences (Warrington, PA). All other experimental reagents were from Sigma-Aldrich unless indicated otherwise.

Plasmids and mutagenesis. A FLAG epitope (amino acid sequence DYKDDDDK) was introduced at the N-terminal end of human GPR84 cDNA by PCR using the following primers: sense, 5' GCGGGATCCGCCACCA TGGACTACAAGGACGACGATGATAAGTGTGGAACAGCTCTGACGCC 3', and antisense: 5' GTGGCGGCC GCGATGGAGCCTATGGAACTCC 3'. The resulting cDNA was subsequently cloned in-frame into the BamHI and NotI sites of an eYFP-pcDNA5/FRT/TO plasmid yielding the final N-terminal epitope and C-terminal fluorescent protein-tagged construct FLAG-humanGPR84-eYFP-pcDNA5/FRT/TO.

FLAG-humanGPR84-G_{α12} fusion proteins were constructed by replacing eYFP within the FLAG-humanGPR84-eYFP-pcDNA5/FRT/TO construct with sequence corresponding to G_{α12} or Cys³⁵²Ile G_{α12} using NotI and XhoI restriction enzymes. Site-directed mutagenesis to generate point mutants of GPR84 was performed according to the QuikChange method (Stratagene, Cheshire, UK). The identity of all constructs was verified by nucleotide sequencing.

Cell culture, transfection and generation of cell lines. Flp-In TREx 293 cells (Invitrogen) were maintained in Dulbecco's modified Eagle's medium without sodium pyruvate (Invitrogen), supplemented with 10% (v/v) fetal calf serum, 1% penicillin/streptomycin mixture, and 10 µg/ml blasticidin at 37 °C in a 5% CO₂ humidified atmosphere. To generate Flp-In TREx 293 cells able to inducibly express the various GPR84 receptor constructs the cells were transfected with a mixture containing the desired cDNA in pcDNA5/FRT/TO vector and pOG44 vector (1:9) by using 1 mg/ml PEI (MW-25000). Cells were grown until 60 to 80% confluent then transfected with 8 µg of required plasmid DNA and PEI (ratio 1:6 DNA/PEI), diluted in 150 mM NaCl, pH 7.4. After incubation at room temperature for 10 min, the mixture was added to cells. After 48 h the medium was changed to medium supplemented with 200 µg/ml hygromycin B to initiate the selection of stably transfected cells. After isolation of resistant cells, expression of the appropriate construct from the Flp-In TREx locus was induced by treatment with up to 100 ng/ml doxycycline for 24 h.

HTRF-based cAMP inhibition assays. All cAMP experiments were performed using Flp-In TREx HEK293 cells induced to express the receptor of interest. Experiments were carried out using a homogenous time-resolved FRET-based detection kit (CisBio Bioassays; CisBio, Codolet, France) according to the manufacturer's protocol. For the assay cells were plated at 5000 cells/well in low-volume 384-well plates. The ability of agonists to inhibit 1 µM forskolin-induced cAMP production was assessed following a co-incubation for 30 min with agonist compounds. Reactions were stopped according to the manufacturer's instructions and the output was measured by with a PHERAstar FS plate reader (BMGLabtech, Aylesbury, UK).

Membrane preparation. Membranes were generated from Flp-In TREx HEK293 cells treated with 100 ng/mL doxycycline to induce expression of the receptor construct of interest. Cells were washed with ice-cold phosphate-buffered saline, removed from dishes by scraping and centrifuged at 3000 rpm for 5 min at 4 °C. Pellets were resuspended in TE buffer (10 mM Tris-HCl, 0.1 mM EDTA; pH 7.5) containing a protease inhibitor mixture (Roche Applied Science, West Sussex, UK) and homogenized with a 5 ml hand-held homogenizer. This material was centrifuged at 1500 rpm for 5 min at 4 °C and the supernatant was further centrifuged at 50000 rpm for 45 min at 4 °C. The resulting pellet was resuspended in TE buffer and protein content was assessed using a BCA protein assay kit (Pierce, Fisher Scientific, Loughborough, UK).

[³⁵S]GTPγS incorporation assay. Initially, 5 µg of generated membrane protein was pre-incubated for 15 min at 25 °C in assay buffer (20 mM HEPES, 5 mM MgCl₂, 160 mM NaCl; 1 µM GDP; 0.05% fatty acid-free bovine serum albumin; pH 7.5) containing the indicated ligand concentrations. In experiments designed to assess potential allosteric interactions between DIM and related molecules and either C10 or the other 'orthosteric'

agonist the compounds were added at the same time to the membrane preparation. The reaction was then initiated with addition of [35 S]GTP- γ S (50 nCi per tube), and the reaction was terminated after 45 minutes incubation at 30 °C by rapid filtration through GF/C glass filters using a 24-well Brandel cell harvester (Alpha Biochem, Glasgow, UK). Unbound radioligand was removed from filters by three washes with ice-cold phosphate buffered saline (pH 7.4) and filters were dried for 2–3 h at room temperature. Dried filters were added to 3 mL of Ultima GoldTM XR (PerkinElmer Life Sciences, Beaconsfield, UK) and [35 S]GTP- γ S binding was determined by liquid scintillation spectrometry.

Radioligand binding assay. [3 H]G9543 is an analog of compounds 104, 107 and 161 with the same characteristic 2-(substituted-alkoxy)-9-substituted-6,7-dihydro-pyrimido[6,1-a]isoquinolin-4-one chemotype. Assays were carried out either with increasing concentrations (for saturation binding) or respective K_d concentrations (for displacement assays) of [3 H]G9543, binding buffer (phosphate-buffered saline with 0.5% fatty acid free bovine serum albumin; pH 7.4), and the indicated concentrations of test compounds (for displacement assays) in a total assay volume of 500 μ L in glass tubes. Binding was initiated by the addition of membranes (5 μ g of protein per tube). All assays were performed at 25 °C for 1 h before termination by the addition of ice-cold phosphate-buffered saline and vacuum filtration through GF/C glass filters using a 24-well Brandel cell harvester (Alpha Biochem, Glasgow, UK). Each reaction tube was washed three times with ice-cold PBS. The filters were allowed to dry for 2–3 h and then placed in 3 mL of Ultima GoldTM XR. Radioactivity was quantified by liquid scintillation spectrometry. Specific binding was defined as the difference between binding detected in the presence and absence of 1 μ M compound 104.

Data analysis. All data are presented as means \pm SEM of at least three independent experiments. Data analysis and curve fitting was carried out using the GraphPad Prism software package version 5.0b (GraphPad, San Diego). For functional assays the concentration-response data were plotted on a log axis, with the untreated vehicle control plotted at 1 log unit lower than the lowest ligand concentration, and fitted to a three parameter sigmoidal curve with the Hill slope constrained to equal 1. In case of inhibition experiments with antagonists an equivalent analysis was followed to fit an inverse sigmoidal curve. To perform the statistical analysis of curve parameters, data from multiple experiments were fitted independently and resulting curve fit values were analysed with indicated tests. For radioligand binding data, saturation binding curves were generated by fitting the specific binding, which was obtained by subtracting non-specific from total binding, to a one site specific binding model that allows calculation of K_d values for the radioligand at wild type and mutant receptors. To determine affinity of unlabelled ligands, data obtained in displacement assays were fit to an inverse three parameter sigmoidal curve constrained by radioligand affinity and concentration to allow for K_i calculation.

To quantify the extent of allosteric interaction between pairs of ligands, data were analysed using an operational model of allosteric modulation described previously⁴⁶. The general version of this model can be depicted by the following equation:

$$E = \frac{E_m(\tau_A[A](K_B + \alpha\beta[B]) + \tau_B[B]K_A)^n}{([A]K_B + K_AK_B + [B]K_A + \alpha[A][B])^n + (\tau_A[A](K_B + \alpha\beta[B]) + \tau_B[B]K_A)^n}$$

where, E is the pharmacological effect, [A] and [B] are the orthosteric and allosteric compound concentrations at equilibrium, respectively; K_A and K_B are the equilibrium dissociation constants of the orthosteric and allosteric ligands respectively, denoting the binding affinities of the two ligands to the receptor; α is the binding cooperativity factor denoting the magnitude and direction of the allosteric effect on binding affinity of the orthosteric agonist to the receptor, β is the activation cooperativity factor representing the measure of the allosteric effect on orthosteric efficacy. τ_A and τ_B represent the intrinsic activity of the orthosteric and allosteric ligand, respectively. E_m is the maximal possible system response and n denotes the slope factor of the transducer function. In case of global fitting of the allosterism data through this equation, E_m and n values were always constrained and other parameters (K_A , K_B , τ_A , τ_B , α , β) were estimated.

Molecular modelling. The OX₁ receptor and rhodopsin crystal structures with the PDB codes of 4ZJ8 and 2Z73, respectively, were used as templates to create a hybrid model of GPR84. In particular, the helical bundle from the OX₁ receptor crystal structure was assembled with the second extracellular loop from the rhodopsin crystal structure and the combined template was used in modelling of GPR84. The homology model of GPR84 was generated with the Prime 3.8 module of the Schrodinger software⁴⁷ with the default energy-based method⁴⁸. The obtained homology model was refined in the MacroModel 10.6 module of the Schrodinger software package⁴⁷ using short molecular mechanics and dynamics optimization. Molecular docking to the GPR84 model was conducted using the InducedFit module^{49,50} of the Schrodinger software⁴⁷. The receptor grid was defined around Arg¹⁷². The side chain trimming was applied for Tyr⁶⁹ and Phe³³⁵ that largely occluded the binding cavity. The best docking pose was chosen based on the docking energy and interactions with Arg¹⁷². Figures of the molecular models were generated with Maestro 9.9 of the Schrodinger software package⁴⁷.

Data availability. The datasets generated and analysed during the current study are available from the corresponding author on reasonable request.

References

- Davenport, A. P. *et al.* International Union of Basic and Clinical Pharmacology. LXXXVIII. G protein-coupled receptor list: recommendations for new pairings with cognate ligands. *Pharmacol Rev.* **65**, 967–986 (2013).
- Wang, J., Wu, X., Simonavicius, N., Tian, H. & Ling, L. Medium-chain fatty acids as ligands for orphan G protein-coupled receptor GPR84. *J Biol Chem.* **281**, 34457–34464 (2006).
- Nikaido, Y., Koyama, Y., Yoshikawa, Y., Furuya, T. & Takeda, S. Mutation analysis and molecular modeling for the investigation of ligand-binding modes of GPR84. *J Biochem.* **157**, 311–320 (2015).
- Suzuki, M. *et al.* Medium-chain fatty acid-sensing receptor, GPR84, is a proinflammatory receptor. *J Biol Chem.* **288**, 10684–10691 (2013).
- Southern, C. *et al.* Screening β -arrestin recruitment for the identification of natural ligands for orphan G-protein-coupled receptors. *J Biomol Screen.* **18**, 599–609 (2013).
- Kaspersen, M. M., Jenkins, L., Dunlop, J., Milligan, G. & Ulven, T. Succinct synthesis of saturated hydroxy fatty acids and *in vitro* evaluation of all hydroxylauric acids at FFA1, FFA4 and GPR84. *Med ChemComm* **8**, 1360 (2017).
- Yin, H. *et al.* Lipid G protein-coupled receptor ligand identification using beta-arrestin PathHunter assay. *J Biol Chem.* **284**, 12328–12338 (2009).
- Milligan, G., Shimpukade, B., Ulven, T. & Hudson, B. D. Complex Pharmacology of Free Fatty Acid Receptors. *Chem Rev.* **117**, 67–110 (2017).
- Tikhonova, I. G. Application of GPCR Structures for Modelling of Free Fatty Acid Receptors. *Handb Exp Pharmacol.* **236**, 57–77 (2017).
- Watson, S. J., Brown, A. J. & Holliday, N. D. Differential signaling by splice variants of the human free fatty acid receptor GPR120. *Mol Pharmacol.* **81**, 631–642 (2012).
- Shimpukade, B., Hudson, B. D., Hovgaard, C. K., Milligan, G. & Ulven, T. Discovery of a potent and selective GPR120 agonist. *J Med Chem.* **55**, 4511–4515 (2012).
- Hudson, B. D. *et al.* The pharmacology of TUG-891, a potent and selective agonist of the free fatty acid receptor 4 (FFA4/GPR120), demonstrates both potential opportunity and possible challenges to therapeutic agonism. *Mol Pharmacol.* **84**, 710–725 (2013).
- Sum, C. S. *et al.* Identification of residues important for agonist recognition and activation in GPR40. *J Biol Chem.* **282**, 29248–29255 (2007).
- Stoddart, L. A., Smith, N. J., Jenkins, L., Brown, A. J. & Milligan, G. Conserved polar residues in transmembrane domains V, VI, and VII of free fatty acid receptor 2 and free fatty acid receptor 3 are required for the binding and function of short chain fatty acids. *J Biol Chem.* **283**, 32913–32924 (2008).
- Husted, A. S., Traelsen, M., Rudenko, O., Hjorth, S. A. & Schwartz, T. W. GPCR-Mediated Signaling of Metabolites. *Cell Metab.* **25**, 777–796 (2017).
- Wang, J. *et al.* Kynurenic acid as a ligand for orphan G protein-coupled receptor GPR35. *J Biol Chem.* **281**, 22021–8 (2006).
- Milligan, G. Orthologue selectivity and ligand bias: translating the pharmacology of GPR35. *Trends Pharmacol Sci* **32**, 317–325 (2011).
- Divorcy, N., Mackenzie, A. E., Nicklin, S. A. & Milligan, G. G protein-coupled receptor 35: an emerging target in inflammatory and cardiovascular disease. *Front Pharmacol.* **6**, 41 (2015).
- Yabuchi, C. *et al.* A novel anti-diabetic drug, fasiglafam/TAK-875, acts as an ago-allosteric modulator of FFAR1. *PLoS One.* **8**, e76280 (2013).
- Lu, J. *et al.* Structural basis for the co-operative allosteric activation of the free fatty acid receptor GPR40. *Nat Struct Mol Biol.* **24**, 570–577 (2017).
- Lee, T. *et al.* Identification and functional characterization of allosteric agonists for the G protein-coupled receptor FFA2. *Mol Pharmacol.* **74**, 1599–1609 (2008).
- Bolognini, D. *et al.* A novel allosteric activator of Free Fatty Acid 2 receptor displays unique Gi-functional bias. *J Biol Chem.* **291**, 18915–18931 (2016).
- Hudson, B. D. *et al.* Complex pharmacology of novel allosteric free fatty acid 3 receptor ligands. *Mol Pharmacol.* **86**, 200–210 (2014).
- Pillaiyar, T. *et al.* Diindolylmethane Derivatives: Potent Agonists of the Immunostimulatory Orphan G Protein-Coupled Receptor GPR84. *J Med Chem.* **260**, 3636–3655 (2017).
- Liu, Y. *et al.* Design and Synthesis of 2-Alkylpyrimidine-4,6-diol and 6-Alkylpyridine-2,4-diol as Potent GPR84 Agonists. *ACS Med Chem Lett.* **7**, 579–583 (2016).
- Zhang, Q., Yang, H., Li, J. & Xie, X. Discovery and Characterization of a Novel Small-Molecule Agonist for Medium-Chain Free Fatty Acid Receptor G Protein-Coupled Receptor 84. *J Pharmacol Exp Ther.* **357**, 337–344 (2016).
- Maciejewska, D., Rasztawicka, M., Wolska, I., Anuszevska, E. & Gruber, B. Novel 3,3'-diindolylmethane derivatives: synthesis and cytotoxicity, structural characterization in solid state. *Eur J Med Chem.* **44**, 4136–4147 (2009).
- Vermiere, S. *et al.* Efficacy and safety of GLPG1205, a GPR84 antagonist, in ulcerative colitis: multi-centre proof-of-concept study. *J Crohns Colitis* **11** (suppl_1), S390–S391 (2017).
- Ward, R. J., Alvarez-Curto, E. & Milligan, G. Using the Flp-InTM T-RexTM system to regulate GPCR expression. *Methods Mol Biol.* **746**, 21–37 (2011).
- Milligan, G. Principles: extending the utility of [35S]GTP gamma S binding assays. *Trends Pharmacol Sci.* **24**, 87–90 (2003).
- Milligan, G. *et al.* G protein-coupled receptor fusion proteins in drug discovery. *Curr Pharm Des.* **10**, 1989–2001 (2004).
- Milligan, G., Parenty, G., Stoddart, L. A. & Lane, J. R. Novel pharmacological applications of G-protein-coupled receptor-G protein fusions. *Curr Opin Pharmacol.* **7**, 521–526 (2007).
- Lane, J. R., Powney, B., Wise, A., Rees, S. & Milligan, G. Protean agonism at the dopamine D2 receptor: (S)-3-(3-hydroxyphenyl)-N-propylpiperidine is an agonist for activation of Go1 but an antagonist/inverse agonist for Gi1, Gi2, and Gi3. *Mol Pharmacol.* **71**, 1349–1359 (2007).
- Yin, J. *et al.* Structure and ligand-binding mechanism of the human OX1 and OX2 orexin receptors. *Nat Struct Mol Biol.* **23**, 293–299 (2016).
- Labeguere, F. *et al.* Novel dihydropyrimidinoisoquinolinones and pharmaceutical compositions thereof for the treatment of inflammatory disorders. WO 2013/092791A1 (2014).
- Reed, G. A. *et al.* Single-dose and multiple-dose administration of indole-3-carbinol to women: pharmacokinetics based on 3,3'-diindolylmethane. *Cancer Epidemiol Biomarkers Prev.* **15**, 2477–2481 (2006).
- Shrestha, R. *et al.* Plasma capric acid concentrations in healthy subjects determined by high-performance liquid chromatography. *Ann Clin Biochem.* **52**, 588–596 (2015).
- van der Westhuizen, E. T., Valant, C., Sexton, P. M. & Christopoulos, A. Endogenous allosteric modulators of G protein-coupled receptors. *J Pharmacol Exp Ther.* **353**, 246–260 (2015).
- Smith, N. J. & Milligan, G. Allostery at G protein-coupled receptor homo- and heteromers: uncharted pharmacological landscapes. *Pharmacol Rev.* **62**, 701–725 (2010).
- Cheng, R. K. Y. *et al.* Structural insight into allosteric modulation of protease-activated receptor 2. **545**, 112–115 (2017).
- Oswald, C. *et al.* Intracellular allosteric antagonism of the CCR9 receptor. *Nature.* **540**, 462–465 (2016).
- Zheng, Y. *et al.* Structure of CC chemokine receptor 2 with orthosteric and allosteric antagonists. *Nature* **540**, 458–461 (2016).

43. Abdel-Aziz, H. *et al.* GPR84 and TREM-1 signaling contribute to the pathogenesis of reflux esophagitis. *Mol Med.* **21**, 1011–1024 (2015).
44. Audoy-Rémus, J. *et al.* GPR84 deficiency reduces microgliosis, but accelerates dendritic degeneration and cognitive decline in a mouse model of Alzheimer's disease. *Brain Behav Immun.* **46**, 112–120 (2015).
45. Nicol, L. S. *et al.* The role of G-protein receptor 84 in experimental neuropathic pain. *J Neurosci.* **35**, 8959–8969 (2015).
46. Ehlert, F. J. Analysis of allosterism in functional assays. *J Pharmacol Exp Ther.* **315**, 740–754 (2005).
47. Small-Molecule Drug Discovery Suite v. 2014-4 Schrödinger, LLC, New York, NY (2014).
48. Jacobson, M. P. *et al.* A hierarchical approach to all-atom protein loop prediction. *Proteins.* **55**, 351–367 (2004).
49. Friesner, R. A. *et al.* Extra precision glide: Docking and scoring incorporating a model of hydrophobic enclosure for protein-ligand complexes. *J Med Chem.* **49**, 6177–619 (2006).
50. Sherman, W. *et al.* Novel procedure for modeling ligand/receptor induced fit effects. *J Med Chem.* **49**, 534–553 (2006).

Acknowledgements

We thank Dorota Maciejewska, Department of Organic Chemistry, Medical University of Warsaw, Poland for providing the analogs of DIM. ZAM thanks the Commonwealth Scholarship Commission for financial support.

Author Contributions

G.M. developed and co-ordinated the project, Z.A.M. and L.J. performed the experiments, F.L., R.G., S.D.V., and T.U. provided ligands, chemical support and insight, B.D.H. performed data analysis, I.G.T. developed the homology models. G.M. wrote the manuscript with assistance and input from all other authors.

Additional Information

Competing Interests: RG, SDV are, and FL was, employed by Galapagos. The other authors declare no competing financial interests.

Publisher's note: Springer Nature remains neutral with regard to jurisdictional claims in published maps and institutional affiliations.



Open Access This article is licensed under a Creative Commons Attribution 4.0 International License, which permits use, sharing, adaptation, distribution and reproduction in any medium or format, as long as you give appropriate credit to the original author(s) and the source, provide a link to the Creative Commons license, and indicate if changes were made. The images or other third party material in this article are included in the article's Creative Commons license, unless indicated otherwise in a credit line to the material. If material is not included in the article's Creative Commons license and your intended use is not permitted by statutory regulation or exceeds the permitted use, you will need to obtain permission directly from the copyright holder. To view a copy of this license, visit <http://creativecommons.org/licenses/by/4.0/>.

© The Author(s) 2017

SCIENTIFIC REPORTS

OPEN

On-target and off-target effects of novel orthosteric and allosteric activators of GPR84

Received: 9 October 2018
Accepted: 20 December 2018
Published online: 12 February 2019

Sarah J. Mancini¹, Zobaer Al Mahmud¹, Laura Jenkins¹, Daniele Bolognini¹, Robert Newman², Matt Barnes², Michelle E. Edye³, Stephen B. McMahon³, Andrew B. Tobin¹ & Graeme Milligan¹

Many members of the G protein-coupled receptor family, including examples with clear therapeutic potential, remain poorly characterised. This often reflects limited availability of suitable tool ligands with which to interrogate receptor function. In the case of GPR84, currently a target for the treatment of idiopathic pulmonary fibrosis, recent times have seen the description of novel orthosteric and allosteric agonists. Using 2-(hexylthiol)pyrimidine-4,6 diol (2-HTP) and di(5,7-difluoro-1H-indole-3-yl) methane (PSB-16671) as exemplars of each class, in cell lines transfected to express either human or mouse GPR84, both ligands acted as effective on-target activators and with high co-operativity in their interactions. This was also the case in lipopolysaccharide-activated model human and mouse immune cell lines. However in mouse bone-marrow-derived neutrophils, where expression of GPR84 is particularly high, the capacity of PSB-16671 but not of 2-HTP to promote G protein activation was predominantly off-target because it was not blocked by an antagonist of GPR84 and was preserved in neutrophils isolated from GPR84 deficient mice. These results illustrate the challenges of attempting to study and define functions of poorly characterised receptors using ligands that have been developed via medicinal chemistry programmes, but where assessed activity has been limited largely to the initially identified target.

Although a substantial number of G protein-coupled receptors (GPCRs) are the targets of therapeutic medicines and have been extensively studied¹, this is not the case for many other family members. More than 100 GPCRs remain 'orphans' in that the endogenously produced ligands that activate them are either unknown or are not fully accepted² and many more are lacking well-characterised ligands that can be used to help define their function and physiological roles. Despite this, based on links to disease³, or phenotypes associated with 'knock-out' of the corresponding gene in mouse models, a number of these poorly defined GPCRs are currently considered to offer potential therapeutic opportunities. A case in point is GPR84, where blockade may be effective in idiopathic pulmonary fibrosis⁴ and other fibrotic indications, and where previous studies have assessed whether antagonism of this receptor might be effective in the treatment of ulcerative colitis⁵. Moreover, it has also been suggested that activation of GPR84 may result in effects beneficial for treatment of atherosclerosis⁶.

Shown more than 10 years ago to be activated by medium chain length fatty acids (MCFAs)⁷, this receptor officially remains an orphan². This reflects that the potency/affinity of MCFAs at this receptor is low and that concentrations of circulating MCFAs may not routinely reach levels sufficient to occupy the receptor effectively. In recent times a number of more potent activators of GPR84 have been described. These include 2,5-dihydroxy-3-undecyl-2,5-cyclohexadiene-1,4-dione (embelin)⁸, 6-(octylamino) pyrimidine-2,4(1H,3H)-dione (6-*n*-octylaminouracil, 6-OAU)^{9–10} and 2-(hexylthiol)pyrimidine-4,6 diol (2-HTP), which has previously been designated either as 'compound 1'^{11,12} or ZQ-16^{13,14}. Because agonist actions of each of MCFAs, embelin and 2-HTP at human GPR84 are prevented by mutation of arginine172 of the receptor¹¹ that acts to co-ordinate the carboxylate of MCFAs, both embelin and 2-HTP are classified as orthosteric agonists, i.e. they bind at the same site as the MCFAs that are notionally the endogenous activators of the receptor. As with many other GPCRs, GPR84 can also be activated by ligands that bind at a distinct site(s). The best studied of these is 3,3'-diindolylmethane

¹Centre for Translational Pharmacology, Institute of Molecular, Cell and Systems Biology, University of Glasgow, Glasgow, G12 8QQ, United Kingdom. ²Sosei Heptares, Steinmetz Building, Granta Park, Great Abington, Cambridge, CB21 6DG, United Kingdom. ³Wolfson Centre for Age-Related Diseases, King's College London, London, SE1 1UL, United Kingdom. Sarah J. Mancini, Zobaer Al Mahmud and Laura Jenkins contributed equally. Correspondence and requests for materials should be addressed to G.M. (email: Graeme.Milligan@glasgow.ac.uk)

(DIM)^{11,15,16} which is generated *in vivo* by metabolism of indole-3-carbinol. The effects of DIM are not attenuated by mutation of arginine172¹¹ and, therefore, DIM and related molecules are described as allosteric agonists at GPR84. Although not considered as an endogenous agonist, it has been calculated that DIM binds human GPR84 with substantially higher affinity than do MCFAs such as decanoic acid¹¹. Progress in generating ligands related to DIM but with higher potency has recently been reported by Pillaiyar *et al.*¹⁶, with di(5,7-difluoro-1H-indole-3-yl)methane (PSB-16671) the most potent analogue generated¹⁶. Antagonists of GPR84 are particularly limited, with GLPG1205 and related molecules, including compound 107 (2-((1,4)dioxan-2-ylmethoxy)-9-(3-phenylamino-prop-1-ynyl)-6,7-dihydro-pyrimido[6,1-a]isoquinolin-4-one), being the only reported and studied examples^{11,14}. These act as high affinity, but non-competitive, blockers of the actions of both orthosteric and allosteric agonists of GPR84¹¹ and GLPG1205 has been used to block effects of GPR84 activation in human phagocytes¹⁴.

Herein, we set out to establish the detailed pharmacology and usefulness of 2-HTP and PSB-16671 to characterise and define the biology and function of GPR84 in both human and mouse. PSB-16671 produced activation and co-operativity effects that were mediated directly by GPR84 both in cells transfected to express either human or mouse GPR84, and in human and mouse-derived immune cell models. However the ability of PSB-16671 to activate G-proteins in mouse bone marrow-derived neutrophils was instead largely 'off-target' and not mediated by GPR84. These conclusions are based on the inability of a GPR84 antagonist that blocked effects of PSB-16671 at mouse GPR84 in both transfected cells and in the macrophage-like RAW264.7 cell line to do so in bone marrow-derived neutrophils, and because the activity of PSB-16671 is preserved in neutrophils from GPR84 knock-out mice. These studies indicate the challenges and dangers of simply transferring outcomes from medicinal chemistry programmes into physiological studies and outcomes for poorly characterised receptors where little is known about the mode of binding of ligands that are described to have potency and affinity at that specific target. Doing so may result in incorrect assignment of functions to such a receptor.

Results

Human and mouse GPR84 display similar responsiveness to both orthosteric and allosteric agonists. 2-(hexylthiol)pyrimidine-4,6 diol (2-HTP) is a potent agonist of human GPR84^{11,13,14}. This ligand has been shown to share an overlapping binding site on human GPR84 with MCFAs such as decanoic acid (C10) that are considered the likely endogenous ligands of the receptor. This is based on effects of both 2-HTP and C10 being eliminated following mutation of arginine172 in the receptor¹¹ and because, when added concurrently at submaximal concentrations, these two ligands produce additive, rather than co-operative, responses^{11,12}. By contrast, 3,3'-diindolylmethane (DIM) and related activators of GPR84 bind to a different site as their function is unaffected by mutation of arginine172¹¹ and at sub-maximal concentrations they produce co-operative effects with either MCFAs or 2-HTP¹¹. Recently Pillaiyar *et al.*¹⁶ identified di(5,7-difluoro-1H-indole-3-yl)methane (PSB-16671) as a more potent analogue of DIM at human GPR84.

GPR84 couples selectively to members of the pertussis toxin-sensitive G_i-G protein family^{7,8,11}. Activation of these G proteins is particularly amenable to analysis by measuring regulation of binding of guanine nucleotides and their analogues¹⁷. Initially, therefore, we examined the ability of 2-HTP to promote the binding of [³⁵S]GTP-γS in membranes of Flp-In T-REx 293 cells that had been induced to express a human GPR84-Gα₁₂ fusion protein¹¹. 2-HTP promoted binding of [³⁵S]GTP-γS in a concentration-dependent manner with pEC₅₀ = 7.54 ± 0.06 (Fig. 1a). Addition of a range of concentrations of PSB-16671 to cell membranes expressing human GPR84-Gα₁₂ showed that this ligand can also activate human GPR84 with, in this case, pEC₅₀ = 6.28 ± 0.05 (Fig. 1b). Equivalent studies using DIM confirmed the higher potency of PSB-16671 as originally reported by¹⁶ (Fig. 1b), but noticeably PSB-16671 also displayed markedly greater efficacy, i.e. greater effect at maximally effective concentrations, than DIM (Fig. 1b). Importantly, no significant stimulation of binding of [³⁵S]GTP-γS was produced by either 2-HTP or PSB-16671 when these were added to membranes of cells harbouring human GPR84-Gα₁₂ but in which expression of the construct had not been induced (Fig. 1a,b). This demonstrates that both ligands act in an 'on-target' manner to directly activate human GPR84. When sub-maximal concentrations of PSB-16671 were co-added with 2-HTP to membranes expressing human GPR84-Gα₁₂, this resulted in enhanced potency of 2-HTP (Fig. 1c), and fitting of such data to an operational model of allostery¹⁸ indicated that the extent of co-operativity (α) was greater than 200 fold (log α 2.41 ± 0.17) (Table 1), whilst effects on ligand efficacy were marginal (log β was close to zero) (Table 1). Such data sets also allowed estimation of the binding affinity of 2-HTP at human GPR84 (pK_a = 7.0 ± 0.2) and of PSB-16671 (pK_a = 6.02 ± 0.13). Reciprocal experiments in which the effects of increasing concentrations of 2-HTP on the potency of PSB-16671 were assessed (Fig. 1d) resulted in similar conclusions and highly similar estimates of the binding affinities of the two ligands (Table 1).

As mouse models of GPR84 function and various mouse-derived immune cell lines are central to studies on this receptor we cloned mouse GPR84 from RAW264.7 cells. Following construction into an equivalent Gα₁₂ fusion protein, stable integration into Flp-In T-REx 293 cells, and doxycycline-induced expression of the construct, membrane preparations were again tested for response to, and co-operativity between, 2-HTP and PSB-16671 (Fig. 2). Outcomes were very similar to those observed when using the human orthologue of GPR84, pEC₅₀ 2-HTP: 7.52 ± 0.11, PSB-16671: 6.53 ± 0.07, DIM: 5.37 ± 0.08 (Fig. 2, Table 2), and once again DIM acted as a partial agonist when compared to PSB-16671 (Fig. 2).

LPS promotes upregulation of the expression and function of GPR84 protein as well as corresponding mRNA. GPR84 is often described as a pro-inflammatory receptor⁸ and is expressed by a range of white cell types and cell lines^{7,8,10}. With underpinning pharmacological characterisation in place we turned to explore potential effects of these ligands in human THP-1 monocytes. These cells are known to upregulate expression of mRNA encoding GPR84 in response to activation of toll-like receptor 4 (TLR4) by lipopolysaccharide (LPS)^{7,19}. Although this has been suggested to imply a pivotal role of GPR84 in monocyte/macrophage activation and host immune response, nothing is known about how this may reflect or be related to changes in

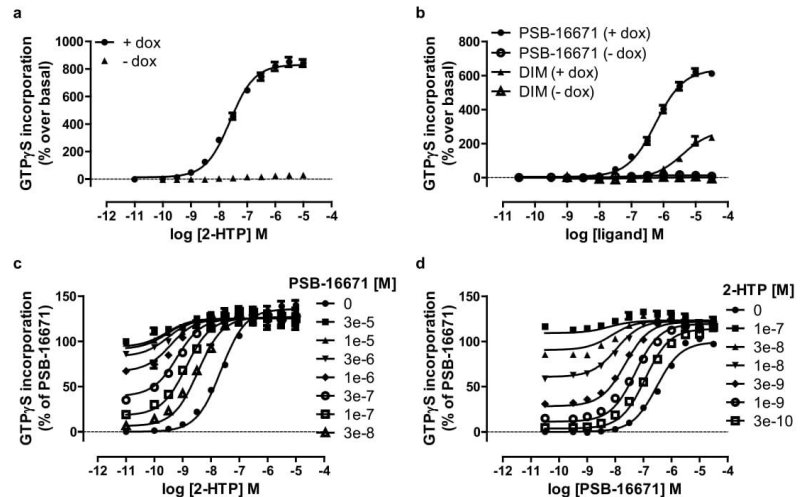


Figure 1. Characterisation of orthosteric and allosteric activators of human GPR84. Flp-In T-REx 293 cells harbouring a human GPR84- $G_{\alpha_{12}}$ fusion protein were either untreated (–) or treated with doxycycline (100 ng. ml⁻¹, 24 h) (+) to induce expression of the fusion construct. Membranes from these cells were then used to measure binding of [³⁵S]GTPγS in response to varying concentrations of 2-HTP (a) and either PSB-16671 or DIM (b). Equivalent studies measured the effects of various concentrations of PSB-16671 on the potency and efficacy of 2-HTP (c) or *vice versa* (d). Data represent means ± S.E.M. of combined data from experiments performed on 4 individual membrane preparations. See Table 1 for quantitative analysis.

| Agonist ^a | Modulator ^b | log _{0.5} | log ₃ | pK _A ^c | pK _B ^d |
|----------------------|------------------------|--------------------|------------------|------------------------------|------------------------------|
| 2-HTP | PSB-16671 | 2.41 ± 0.17 | −0.15 ± 0.06 | 7.0 ± 0.2 | 6.02 ± 0.13 |
| PSB-16671 | 2-HTP | 2.02 ± 0.11 | 0.37 ± 0.12 | 6.1 ± 0.1 | 7.42 ± 0.07 |

Table 1. Binding affinity and co-operativity of ligands as activators of human GPR84. ^aAgonist is the compound used to generate concentration-response curve. ^bModulator is the compound used in defined concentrations. ^cpK_A are values estimated for the agonist. ^dpK_B are values estimated for the modulator. Data are means ± SEM, n = 4. Flp-In T-REx 293 cells harbouring a human GPR84- $G_{\alpha_{12}}$ fusion protein were treated with doxycycline (100 ng. ml⁻¹, 24 h) to induced expression of the fusion protein. [³⁵S]GTPγS binding studies were then performed as described in Fig. 1 and binding affinity and cooperativity factors extracted from such data.

actual expression levels of the receptor. The radiolabelled GPR84 antagonist [³H]9543 binds human GPR84 with sub-nM affinity¹¹. Saturation [³H]9543 binding studies performed on membranes from LPS-treated THP-1 cells confirmed this ($K_d = 0.18 \pm 0.02$ nM, (n = 4)) (Fig. 3a). Using a concentration of [³H]9543 close to 10 times K_d and subsequent correction for predicted receptor occupancy allowed estimation of B_{max} across a range of individual membrane preparations. Membranes prepared from untreated THP-1 cells specifically bound 47 ± 7.5 fmol.mg protein⁻¹ [³H]9543, whilst after exposure to LPS for 24 hours this increased to 167 ± 22 fmol.mg protein⁻¹ (means ± S.E.M., n = 7) (Fig. 3b(i)). This 3.5 fold increase in receptor density compared to a more extensive 10.0 ± 2.5 fold (mean ± S.E.M., n = 6) increase in GPR84 mRNA levels at this time point as assessed using q-RT-PCR (Fig. 3b(ii)). To assess if upregulation of expression of GPR84 in LPS-stimulated THP-1 cells had functional consequences we measured the ability of both 2-HTP and PSB-16671 to promote binding of [³⁵S]GTPγS in membranes from these cells. A notable feature in each separate preparation studied was that treatment with LPS resulted in a higher level of basal, ligand-independent binding of [³⁵S]GTPγS (Fig. 3c). Moreover, for 2-HTP, the extent of stimulation of binding of [³⁵S]GTPγS was markedly higher in membranes derived from LPS-pretreated THP-1 cells than those that were not treated with LPS (Fig. 3d), consistent with the higher measured expression of GPR84 receptor protein. Despite this, no significant increase in potency of 2-HTP was observed (pEC_{50} vehicle = 7.89 ± 0.21 , LPS treated = 7.79 ± 0.08) (Fig. 3e), suggesting that even after LPS induced up-regulation no substantial receptor reserve was generated for GPR84. Similar results were observed for PSB-16671 (pEC_{50} vehicle = 6.82 ± 0.12 , LPS treated = 6.94 ± 0.07) (Fig. 3f,g). Although these outcomes were consistent with both 2-HTP and PSB-16671 mediating effects via GPR84 in these cells, both ligands are experimental tool compounds with limited broader current characterisation. To further determine if the effects of these ligands

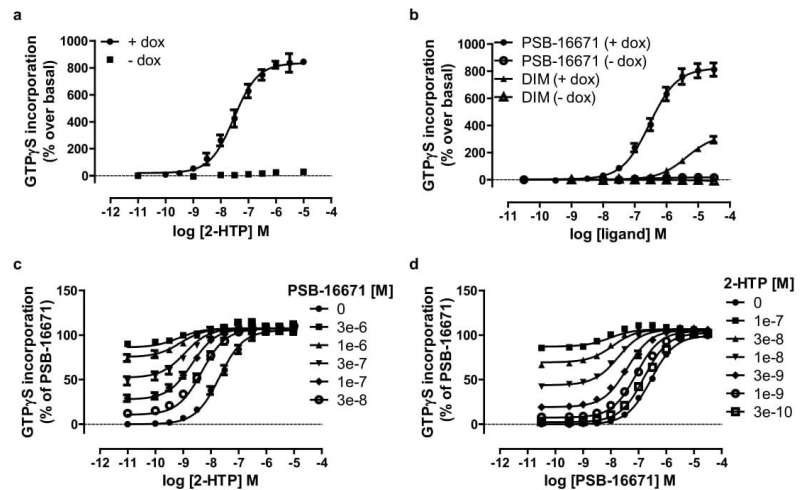


Figure 2. Characterisation of orthosteric and allosteric activators of mouse GPR84. Flp-In T-Rex 293 cells harbouring a mouse GPR84-G α_{12} fusion protein were either untreated (–) or treated with doxycycline (100 ng. ml⁻¹, 24 h) (+) to induce expression of the fusion construct. Membranes from these cells were then used to measure binding of [³⁵S]GTPγS in response to varying concentrations of 2-HTP (a) and either PSB-16671 or DIM (b). Equivalent studies measured the effects of various concentrations of PSB-16671 on the potency and efficacy of 2-HTP (c) or *vice versa* (d). Data represent means \pm S.E.M. of combined data from experiments performed on 4 (a) or 5 (b) individual membrane preparations. See Table 2 for quantitative outcomes.

| | Mouse GPR84-G α_{12} | | RAW264.7 | |
|------------------------------|-----------------------------|-----------------|------------------|-----------------|
| Agonist ^a | 2-HTP | PSB-16671 | 2-HTP | PSB-16671 |
| Modulator ^b | PSB-16671 | 2-HTP | PSB-16671 | 2-HTP |
| log α | 2.02 \pm 0.11 | 2.15 \pm 0.1 | 2.4 \pm 0.04 | 1.94 \pm 0.03 |
| log β | 0.05 \pm 0.09 | 0.12 \pm 0.04 | -0.17 \pm 0.05 | 0.33 \pm 0.08 |
| pK _A ^c | 6.98 \pm 0.17 | 5.96 \pm 0.08 | 7.0 \pm 0.1 | 6.3 \pm 0.15 |
| pK _B ^d | 6.1 \pm 0.13 | 7.2 \pm 0.07 | 6.3 \pm 0.1 | 7.24 \pm 0.05 |

Table 2. Binding affinity and co-operativity of ligands as activators of mouse GPR84. ^aAgonist is the compound used to generate concentration-response curve. ^bModulator is the compound used in defined concentrations. ^cpK_A are values estimated for the agonist. ^dpK_B are values estimated for the modulator. Data are means \pm SEM, n = 4. Either Flp-In T-Rex 293 cells harbouring a mouse GPR84-G α_{12} fusion protein were treated with doxycycline (100 ng.ml⁻¹, 24 h) to induce expression of the fusion protein or membranes were prepared from RAW264.7 cells. [³⁵S]GTPγS binding studies were then performed as described in Fig. 2 (mouse GPR84-G α_{12} fusion protein) or Fig. 5 (RAW264.7 cells) and estimated binding affinity and cooperativity factors extracted.

in LPS-activated THP-1 cells were actually mediated via GPR84, we assessed if their effects could be blocked by compound 107, which has previously been shown to act as a non-competitive antagonist of human GPR84¹¹. For both the activating ligands compound 107 fully blocked their ability to stimulate binding of [³⁵S]GTPγS in a concentration-dependent fashion (pIC₅₀ versus 2-HTP = 7.86 \pm 0.02, versus PSB-16671 = 8.32 \pm 0.07) (Fig. 4a,b).

The macrophage cell line RAW 264.7 is also a popular model to study immune cell-controlled release of pro-inflammatory mediators. It is, however, a murine-derived cell line, and differences in production of cytokines such as TNF α and IL-1 β have been noted compared to human leukocytes²⁰. Expression of mRNA encoding mouse GPR84 was clearly detected in these cells using RT-PCR (Fig. 5a) and indeed, as described earlier, we cloned mouse GPR84 from these cells. As expected from the similar calculated binding affinities and G protein activation characteristics of 2-HTP and PSB-16671 at the cloned human and mouse orthologues of GPR84 (Tables 1 and 2) both ligands were able to stimulate binding of [³⁵S]GTPγS in membranes of LPS-treated RAW 264.7 cells (pEC₅₀ 2-HTP = 7.58 \pm 0.08, PSB-16671 = 6.75 \pm 0.10) (Fig. 5b) with similar potency as noted for the human GPR84 expressing systems. Moreover, marked co-operative effects were also generated by co-addition of the two ligands (Fig. 5c,d) and estimation of co-operativity and affinity values from these studies were also very similar to those for mouse GPR84 expressed in the Flp-In T-Rex 293 cells (Table 2).

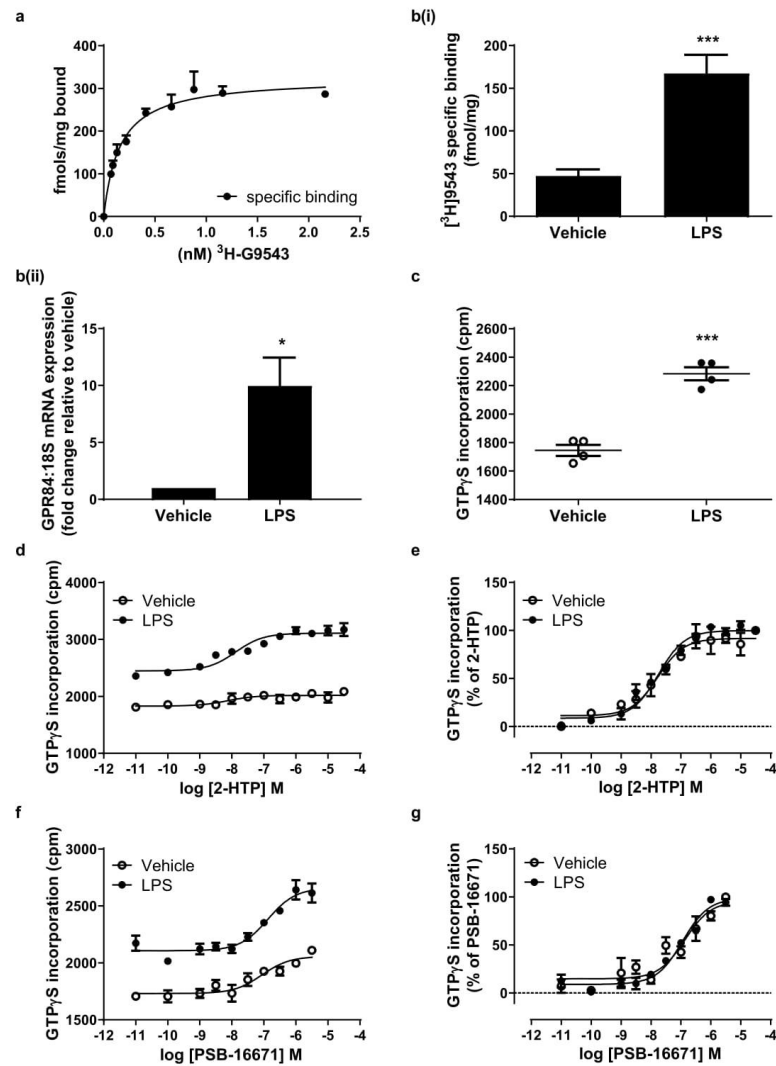


Figure 3. Expression and function of GPR84 in human THP-1 monocytes. THP-1 monocytes were treated with or without LPS ($100 \text{ ng} \cdot \text{ml}^{-1}$) for 24 h. After membrane preparation the specific binding of either varying concentrations of the GPR84 antagonist ^3H 9543 was measured in membranes from LPS-treated THP-1 cells to allow estimation of both K_d and B_{max} (a) or the specific binding of a single concentration of ^3H 9543 that was close to 10 times the estimated K_d was measured in membranes from both vehicle and LPS-treated cells (b(i)). Data in a are from a representative experiment of four separate studies in which $B_{\text{max}} = 293 \pm 55$ and $K_d = 0.18 \pm 0.02 \text{ nM}$, whilst in b(i) they are means \pm S.E.M. ($n = 7$). LPS-treated cells expressed significantly higher amounts of the receptor *** $p < 0.001$ (two-tail t-test). Equivalent assessments of levels of GPR84 mRNA were conducted (b(ii)). Data are means \pm S.E.M. ($n = 6$) * $p < 0.05$ (two-tail t-test). (c) LPS treatment was associated with increased levels of basal binding of ^{35}S GTP γ S ($n = 4$) *** $p < 0.001$ (two-tail t-test). The ability of varying concentration of 2-HTP (d,e) and PSB-16671 (f,g) to promote binding of ^{35}S GTP γ S was measured in membranes of both untreated (vehicle) and LPS-treated cells. In (d,f) data are shown from representative experiments and illustrates the enhanced efficacy of the ligand following LPS treatment, whilst in e and g data pooled from multiple experiments were normalised and illustrate that the potency of the ligands was not affected by the upregulation of GPR84.

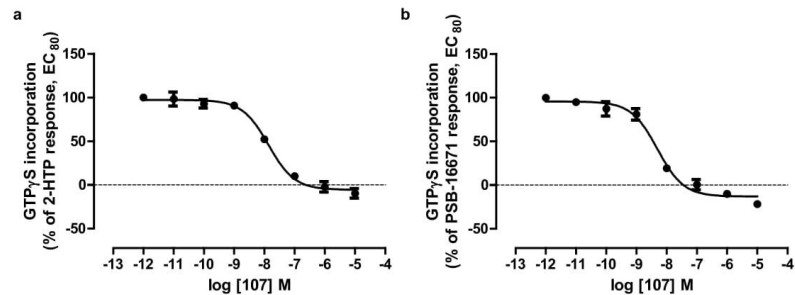


Figure 4. The effects of activators of GPR84 in THP-1 cells are on-target. Membranes were generated from LPS-treated THP-1 cells as in Fig. 3. The ability of varying concentrations of compound 107 to inhibit binding of [35 S]GTP γ S induced by EC $_{80}$ concentrations of either 2-HTP (a) and PSB-16671 (b) were then measured. Data represent means \pm S.E.M. of combined data from experiments performed on 4 individual membrane preparations.

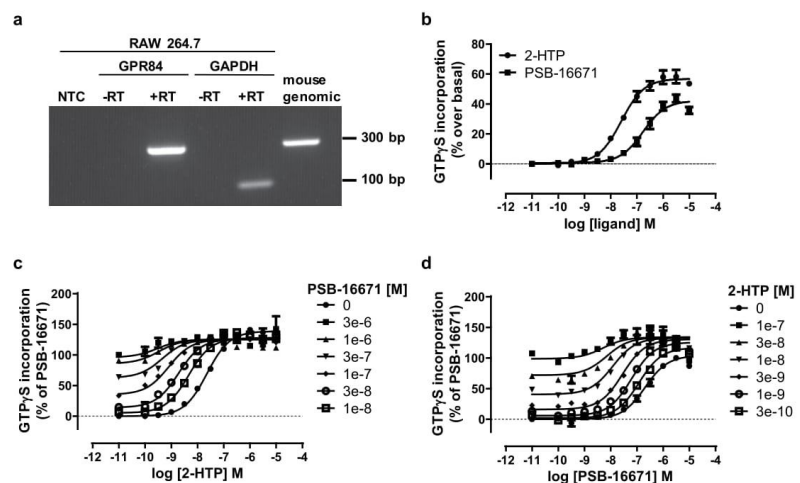


Figure 5. Expression and function of GPR84 in murine RAW264.7 cells. Expression of mRNA encoding GPR84 in RAW 264.7 cells was detected by RT-PCR and compared to amplification of GPR84 from mouse genomic DNA (a) (+RT = reverse transcribed, -RT = without reverse transcription, NTC = no template control). Detection of GAPDH was used as a control (predicted amplicon 110bp). RAW 264.7 cells were treated with LPS (100 ng·ml $^{-1}$, 5 h) and membranes subsequently prepared. The ability of varying concentrations of 2-HTP and PSB-16671 to promote binding of [35 S]GTP γ S were assessed (b), as were the effects of various concentrations of PSB-16671 on the potency and efficacy of 2-HTP (c) or *vice versa* (d). Data represent means \pm S.E.M. of combined data from experiments performed on 5 (b), 4 (c) or 3 (d) individual membrane preparations. See Table 2 for quantitative analysis.

The non-competitive GPR84 antagonist compound 107 has lower affinity at mouse than at human GPR84. Compound 107 was able to fully block stimulation produced by both 2-HTP and PSB-16671 in membranes from RAW 264.7 cells in a concentration-dependent manner (pIC $_{50}$ versus 2-HTP = 6.50 ± 0.06 and versus PSB-16671 = 6.84 ± 0.09) (Fig. 6a,b). It was also noticeable however that the potency of compound 107 was substantially lower in membranes from RAW 264.7 cells than in equivalent preparations from THP-1 cells. This suggested that compound 107 might have lower affinity at mouse GPR84 compared to the human orthologue. Indeed, when we compared directly the potency of compound 107 to inhibit effects of either 2-HTP or PSB-16671 at cloned human and mouse GPR84 in membranes from Flp-In T-REX 293 cells expressing either human or mouse GPR84-G α_{12} fusion proteins compound 107 was between 20 and 75 fold less potent at the

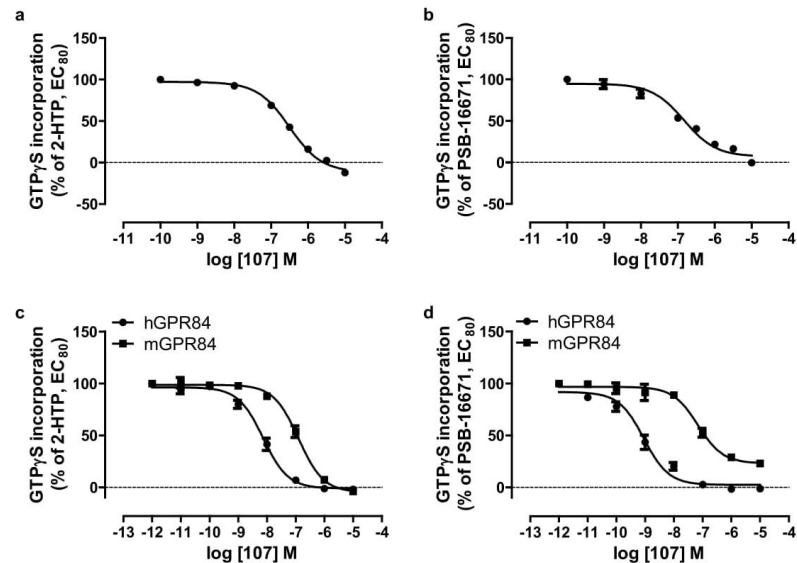


Figure 6. The effects of activators of GPR84 in RAW264.7 cells are on-target. Membranes were generated from LPS-treated RAW264.7 cells (a,b). These were used in [35 S]GTP γ S binding studies in which the effect of varying concentrations of compound 107 was used to block effects of EC₈₀ concentrations of either 2-HTP (a) or PSB-16671 (b). The ability of compound 107 to block effects of either 2-HTP (c) or PSB-16671 (d) to promote binding of [35 S]GTP γ S to either human or mouse GPR84-G α_{12} fusion proteins expressed in Flp-In T-REx 293 cells is also displayed. Data represent means \pm S.E.M. of combined data from experiments performed on 7 (a) or 5 (b–d) individual membrane preparations.

mouse orthologue (pIC₅₀ human = 8.14 ± 0.06 , mouse = 6.90 ± 0.05 versus 2-HTP, and 9.05 ± 0.10 (human) and 7.17 ± 0.10 (mouse) against PSB-16671 respectively) (Fig. 6c,d). As compound 107 is closely related to [3 H]9543¹¹ this lower affinity at mouse GPR84 likely explains why we were unable to obtain direct measures of binding affinity of [3 H]9543 at mouse GPR84 and, as such, it was not possible, unlike in THP-1 cells, to quantify GPR84 expression levels in RAW 264.7 cells using this radioligand.

In mouse bone marrow-derived neutrophils G α_i activation by PSB-16671 is largely independent of GPR84. Despite this limitation we moved forward to assess function of GPR84 in mouse bone marrow-derived neutrophils because the Immunological Genome Project (Immgen) database (<http://www.immgen.org/databrowser/index.html>) indicates expression of GPR84 mRNA to be highest in these cells. 2-HTP again acted to stimulate binding of [35 S]GTP γ S in membranes isolated from such cells (Fig. 7a). The potency of 2-HTP (pEC₅₀ = 7.89 ± 0.12) (Fig. 7a(i)) was similar to those observed in RAW 264.7 cell membrane preparations and this was potentially consistent with its major target in mouse bone marrow-derived neutrophils also being GPR84. However, the potency of PSB-16671 (pEC₅₀ = 5.54 ± 0.09) (Fig. 7a(ii)) was some 10 fold lower than in RAW 264.7 cell membrane preparations, suggesting that this was not an effect transduced by GPR84. Moreover, although PSB-16671 was not more efficacious than 2-HTP in membranes of either cells transfected to express the mouse GPR84-G α_{12} fusion protein (Fig. 2) or in mouse RAW 264.7 cells (Fig. 5), now in membranes from mouse bone marrow-derived neutrophils stimulation of binding of [35 S]GTP γ S by PSB-16671 was much greater than produced by a maximally effective concentration of 2-HTP (Fig. 7a(i)). Although the effect of 2-HTP was completely blocked by compound 107 (Fig. 7a(ii)) the effect of PSB-16671 by contrast was only slightly inhibited by compound 107 (Fig. 7a(ii)). Interestingly, although the parent compound of PSB-16671, DIM, was only able to produce a small fraction of the response generated by PSB-16671, this was instead fully blocked by co-addition of compound 107 (Fig. 7a(ii)).

This combination of observations suggested that a large proportion of the effect of PSB-16671 in mouse bone marrow-derived neutrophils must be an 'off-target' effect that is not mediated by GPR84. To test this directly we also isolated bone marrow-derived neutrophils from GPR84 deficient mice (Fig. 7b) and generated membrane preparations. Here, although 2-HTP was unable to stimulate binding of [35 S]GTP γ S (Fig. 7c(i)), PSB-16671 maintained capacity to promote a large increase in [35 S]GTP γ S binding (Fig. 7c(ii)) and this was unaffected by the presence of compound 107 (Fig. 7c(ii)). In contrast, the effect of DIM observed in wild type bone marrow-derived neutrophils was lacking in those derived from the GPR84 knock-out animals (Fig. 7c(i)), consistent with

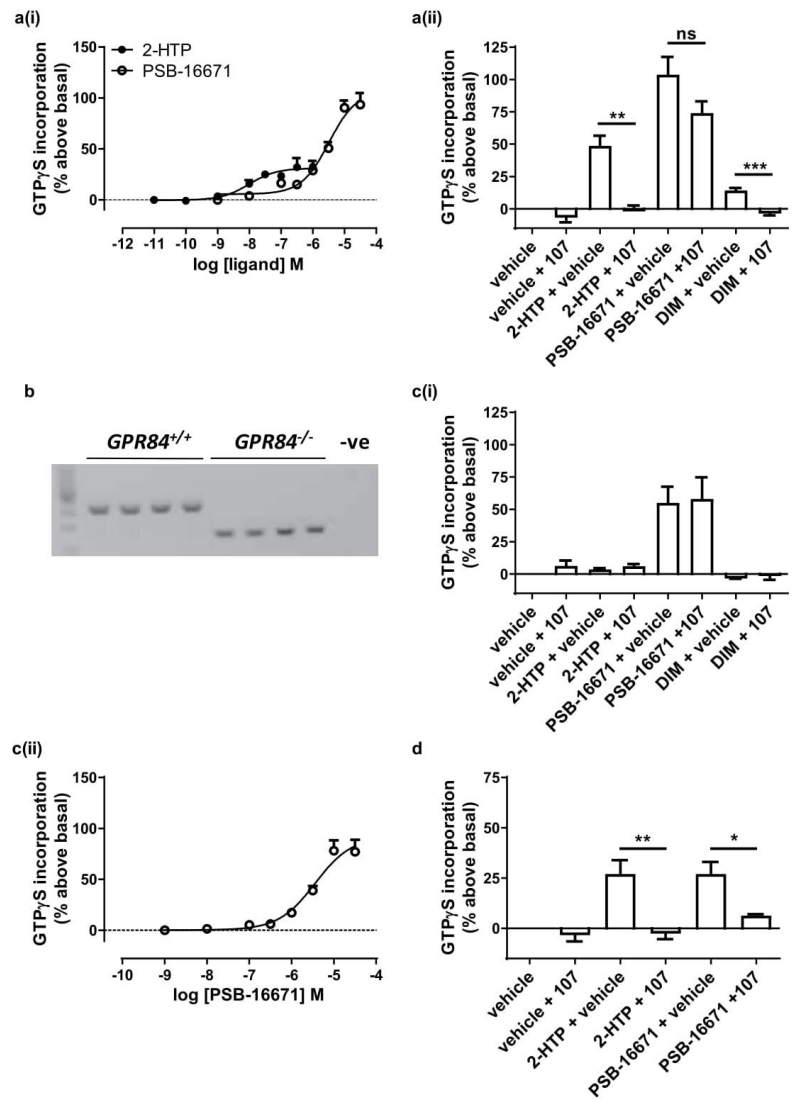


Figure 7. PSB-16671 acts in an off-target, non-GPR84 mediated fashion in mouse bone marrow derived but not human neutrophils. Neutrophils were generated from mouse femur bone marrow taken from wild type (a) or GPR84 deficient (c) animals. PCR analysis shows genotyping from 4 wild type and 4 GPR84 knock-out mice (b). Membranes prepared from these cells were used in [35 S]GTP γ S binding studies to measure effects of varying concentrations of either 2-HTP or PSB-16671 (a(i), c(ii)). The ability of compound 107 (10 μ M) to block the effects of 2-HTP (1 μ M), PSB-16671 (10 μ M) or DIM (30 μ M) were also assessed (a(ii), c(i)). Neutrophil membranes prepared from human whole blood were used in [35 S]GTP γ S binding studies to assess the ability of compound 107 to block the effects of 2-HTP or PSB-16671 (d). Data represents means \pm S.E.M. of combined data from experiments performed on membrane preparations from 3 individual donors. *p < 0.05, **p < 0.01, ***p < 0.001 relative to agonist only (two-tail t-test).

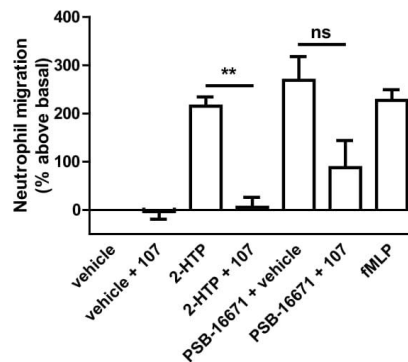


Figure 8. PSB-16671 promotes chemotaxis of mouse bone marrow-derived neutrophils via GPR84. Neutrophils were isolated from wild type mouse femur bone marrow and used in migration studies where the effect of both 2-HTP (100 nM) and PSB-16671 (10 μ M), as well as the capacity of pre-treatment with compound 107 (10 μ M) to block the effects of these agonists was assessed and compared to the effect of chemotactic agonist fMLP (10 μ M). Data represent means \pm S.E.M. of combined data from experiments performed on 3 individual membrane preparations. ** $p < 0.01$ relative to agonist only (two-tail t-test).

being mediated by GPR84. Moreover, PSB-16671 stimulated binding of [35 S]GTP γ S in membranes of bone marrow-derived neutrophils of GPR84 deficient mice with potency ($pEC_{50} = 5.44 \pm 0.14$) highly similar to preparations from wild type mice (Fig. 7c(ii)).

Effects of PSB-16671 in human neutrophils are mediated predominantly by GPR84. Based on these observations we also assessed if PSB-16671 might display non-GPR84 mediated effects in human neutrophils. We isolated such cells, generated membrane preparations and again performed a series of [35 S]GTP γ S binding studies. Here both 2-HTP and PSB-16671 were able to promote [35 S]GTP γ S binding, and to a similar extent (Fig. 7d). Moreover, for both the orthosteric and the allosteric agonist their effects were prevented by co-addition of compound 107 (Fig. 7d), consistent with being mediated via GPR84. Finally, although PSB-16671 generated a substantial GPR84-independent increase in binding of [35 S]GTP γ S in mouse bone marrow-derived neutrophils there was potentially a component of this that was sensitive to blockade by the GPR84 antagonist compound 107 (Fig. 7a(ii)). We thus explored if activation of GPR84 promoted migration of these cells. Interestingly, both 2-HTP and PSB-16671 did so (Fig. 8) and to an extent similar to that produced by the chemotactic peptide fMLP (Fig. 8). In this assay compound 107 fully blocked the effect of 2-HTP. By contrast, although compound 107 largely prevented migration in response to PSB-16671 a proportion was not blocked by compound 107 (Fig. 8). This suggests that in mouse bone marrow-derived neutrophils activation of GPR84 does indeed promote cell migration. However, there is also a component of the effect of PSB-16671 on cell migration that is GPR84-independent.

The effect of PSB-16671 in mouse bone marrow-derived neutrophils is not via GPR35. Because GPR84 is phylogenetically related to the receptor GPR35 we assessed whether either PSB-16671 or 2-HTP could also activate mouse GPR35. To do so we used a β -arrestin-2 recruitment assay as this has been the mostly widely used approach to explore the pharmacology of GPR35^{21–23}. It has previously been noted that PSB-16671 is unable to activate human GPR35¹⁶. We confirmed this and that 2-HTP was also unable to activate human GPR35, whilst the GPR35 agonist Iodexamide²¹ did so (Fig. 9a), and with high potency ($pEC_{50} = 8.33 \pm 0.03$). Similarly, neither PSB-16671 nor 2-HTP was able to activate mouse GPR35 (Fig. 9b). However, although Iodexamide was able to activate mouse GPR35, it did so with some 500 fold lower potency ($pEC_{50} = 5.67 \pm 0.01$) than at the human orthologue (Fig. 9b).

Conclusions

Such outcomes illustrate effectively the challenges in efforts to extrapolate the use of ligands that have received limited characterisation during medicinal chemistry structure-activity studies¹⁶ into broader cell and tissue studies and, potentially, between species orthologues.

Discussion

Studies on poorly characterised GPCRs, including those activated by fatty acids of varying chain length, are frequently restricted by the limited tool box of pharmacological ligands that are available²⁴. This has, for example, greatly hindered efforts to better understand roles of free fatty acid receptor 3²⁴. Equally, roles of other GPCRs that have few available pharmacological tool compounds, such as members of the adhesion class of receptors, are poorly understood despite many being potentially interesting targets in areas such as cancer²⁵. Even within the numerically predominant, class A family of receptors that are related to rhodopsin a substantial number remain as ‘orphans’² or have been the subject of a limited number of studies. Whilst such areas of ligand deficit can offer

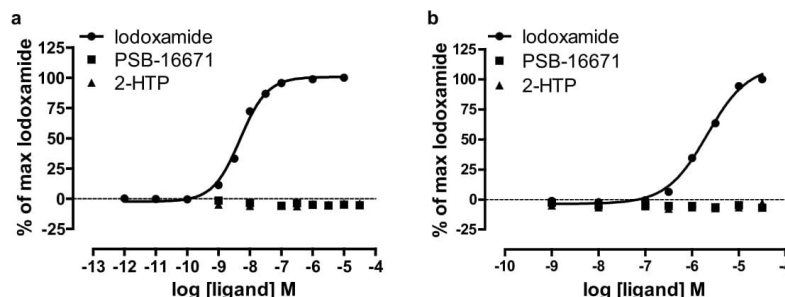


Figure 9. The effect of PSB-16671 in mouse bone marrow-derived neutrophils is not via GPR35. Interactions between eYFP-tagged forms of human GPR35a (a) or mouse GPR35 (b) and a luciferase-tagged form of β -arrestin 2 was assessed following co-transfection into HEK293 cells and the addition of the indicated concentrations of the GPR35 agonist lodoxamide, 2-HTP or PSB-16671. Results are taken from three independent experiments.

many opportunities for medicinal chemists to produce improved ligands when initial chemical starting points become available, a major challenge is then to understand ligand selectivity and potential 'off-target' effects before such compounds can be used with confidence in physiological settings. In recent studies designed to develop analogues of 3-3'-diindolylmethane, Pillaiyar *et al.*¹⁶, showed that the higher potency ligand di(5,7-difluoro-1H-indole-3-yl)methane (PSB-16671) was selective for GPR84 in that it did not activate the long chain free fatty acid receptors FFA1 and FFA4 or the phylogenetically related receptor GPR35. Moreover, although DIM is known to have effects at the arylhydrocarbon receptor, PSB-16671 lacked activity at this target¹⁶.

It is clearly impractical to randomly investigate all possible 'off-target' effects of a small molecule ligand, but we were alerted to the possibility that PSB-16671 might produce certain non-GPR84-mediated effects in studies using mouse bone marrow-derived neutrophils. In membranes derived from both Flp-In T-REx 293 cells transfected to express a form of mouse GPR84 and, more importantly, in murine RAW264.7 cells, PSB-16671 and the orthosteric GPR84 agonist 2-HTP appeared to have similar efficacy, because at maximally effective concentrations these two compounds increased levels of [³⁵S]GTP γ S binding to similar levels. However, in mouse bone marrow-derived neutrophils the stimulation produced by PSB-16671 was markedly higher than produced by 2-HTP. To examine this more directly we assessed whether effects of both 2-HTP and PSB-16671 would be blocked by the non-competitive GPR84 antagonist compound 107, which has previously been shown to antagonise effects of both the MCEFA decanoic acid and of DIM at human GPR84¹¹. However, although compound 107 did block the effect of 2-HTP almost completely at 10 μ M it only marginally inhibited the effect of PSB-16671 in membranes of mouse bone marrow-derived neutrophils. In previous studies we have shown that compound 107 has high affinity at human GPR84 but this has not previously been assessed at the mouse orthologue. When we compared directly the potency of compound 107 to antagonise effects of either 2-HTP or PSB-16671 at human versus mouse GPR84 in cells in which the receptor was expressed as the corresponding G α_{12} fusion protein, it was clear that although compound 107 is, indeed, an effective antagonist of the mouse receptor, it is substantially less potent than at the human orthologue. Moreover, although some 20 fold less potent in blocking effects mediated by the orthosteric agonist 2-HTP at the mouse receptor this was even more extensive when considering PSB-16671 which, as an allosteric agonist at both human and mouse GPR84, binds at a different site than 2-HTP. These were important observations and require consideration because antagonists at certain poorly characterised receptors can display very marked selectivity between species orthologues. For example, CID-2745687 (methyl-5-[(tert butylcarbamothioylhydrazinylidene)methyl]-1-(2,4-difluorophenyl)pyrazole-4-carboxylate) is described in both academic publications and supplier catalogues as an 'antagonist of GPR35'. However, although it is indeed a high affinity antagonist of human GPR35²⁴ it has been shown to lack activity at both the rat and mouse orthologues²³. Similarly, although the clinically trialed FFA2 receptor antagonist GLPG0974 is a high affinity antagonist of the human receptor, this compound also lacks significant activity at rodent orthologues²⁶.

To further validate the non-GPR84 mediated effect of PSB-16671 in mouse bone marrow-derived neutrophils we isolated such cells and generated membranes from a GPR84 knock-out mouse line²⁷. Here, although 2-HTP lacked activity, PSB-16671 produced stimulation of [³⁵S]GTP γ S binding almost as effectively as in samples from wild type mice and, once more, this effect was not blocked by compound 107. It was also notable that the potency of PSB-16671 in membranes of bone marrow-derived neutrophils from both wild type and GPR84 deficient mice was almost 10 fold lower than in membranes from RAW264.7 cells, suggesting that it has a further molecular target at which it displays somewhat lower affinity than at mouse GPR84. This illustrates the importance of performing careful pharmacological studies in which the effects of poorly characterised ligands are measured across a range of concentrations, and not simply at a single high concentration. The non-GPR84 molecular target of PSB-16671 in mouse bone marrow-derived neutrophils remains unclear. As the [³⁵S]GTP γ S binding assay reports on activation of heterotrimeric G proteins, and predominantly on members of the G $_i$ -subfamily¹⁷, the site is likely to be a highly expressed G $_i$ -coupled GPCR. Database information, e.g. the Immgen database (<http://www.immgen.org/databrowser/index.html>) indicates that such cells express a wide range of GPCRs, with various chemokine

receptors, e.g. CXCR4, CXCR2 and CCR1, as well as other receptors associated with chemotaxis e.g. formyl peptide receptor 1 (FPR1) and the complement component 5a receptor 1 (C5a₁), being particularly highly expressed. However, a number of orphan GPCRs including GPR27, GPR64, GPR107 and GPR141 are also highly expressed at the mRNA level. In time it will be interesting to explore whether PSB-16671 is able to activate one of more of these receptors, either as an orthosteric or an allosteric agonist.

Similarly, efforts have been made to catalogue GPCR expression in RAW264.7 cells²⁸ and phorbol ester-stimulated THP-1 cells²⁹ and assessment of such profiles may help define the range of potential targets for activation by PSB-16671 that should be prioritised.

A further key feature of these studies was the ability to measure directly levels of expression of GPR84 in human tissues and human-derived cells. Although it is well appreciated that treatment of cell lines such as THP-1 monocytes with TLR4 receptor activators such as LPS results in a time-dependent upregulation of mRNA encoding GPR84^{7,10} it has not previously been possible to assess how this might relate to altered levels of expression of the receptor itself. Herein, by using the specific binding of [³H]9543 we were able to do so. Interestingly, although levels of GPR84 receptor protein were upregulated some 3.5 fold and this resulted in higher G protein activation in response to maximally effective concentrations of either 2-HTP or PSB-16671, such treatment did not enhance the potency of either of these ligands. One potential means to improve biological function of an agonist ligand is to increase levels of its receptor in response to a challenge or stress such that a maintained concentration of the endogenous agonist now produces greater effect. However, these results indicate that the LPS-induced upregulation did not generate a marked GPR84 receptor reserve in THP-1 cells. As such, whilst the effect of LPS is likely to allow greater levels of maximal signal from endogenous activators of the receptor, it will not result in improved sensitivity of the cell to such activators.

Recently, clinical trials with ligands that have affinity at GPR84 have explored the potential of blocking this receptor for the treatment of both ulcerative colitis³ and idiopathic pulmonary fibrosis^{4,30}. Furthermore, suggestions that activation of GPR84 might have beneficial effects in atherosclerotic conditions⁶ have begun to provide greater focus on this receptor. In recent times a number of distinct compounds with agonist^{6,12,13,31} or positive allosteric modulator (PAM)-agonist¹⁶ activation of GPR84 have been described and substantial structure-activity relationships of some of these compounds have been illustrated^{6,12,13,16,31}. However, before using compounds from such series to claim direct evidence on further roles for GPR84 and its potential therapeutic indications, a better understanding of potential off- target effects are clearly required.

Methods

Materials. PSB-16671¹⁶, compound 104 (9-(5-cyclopropyl-[1,2,4]oxadiazol-3-ylmethoxy)-2-((R)-1-[1,4]dioxan-2-ylmethoxy)-6,7-dihydro-pyrimido[6,1-a]isoquinolin-4-one), compound 107 (2-([1,4]dioxan-2-ylmethoxy)-9-(3-phenylamino-prop-1-ynyl)-6,7-dihydro-pyrimido[6,1-a]isoquinolin-4-one)¹¹ and [³H]9543¹¹ were provided by Laurent Sanier (Galapagos NV). 2-(hexylthiol)pyrimidine-4,6 diol (2-HTP) was provided by Trond Ulven, University of Copenhagen.

GPR84 knock-out mice. GPR84 (GenBank accession number NM_030720, Ensembl identification number ENSMUSG00000063234) KO mice²⁷ were provided by Deltagen under a GlaxoSmithKline license agreement. Targeting replaced 257 bp of coding sequence with an IRES³²LacZ³³poly(A) expression cassette and a positive selection cassette that contains the neomycin phosphotransferase gene driven by the PGK promoter (Neo). The insertion of the LacZ IRESLacZ introduces a premature translational stop signal that deletes the first three predicted transmembrane domain sequences. Disruption of the GPR84 gene was confirmed using PCR and standard agarose gel electrophoresis using the following primers: gene specific (endogenous), 5'-CAGATGCCAAGTCTCTCTGCTA-3'; gene specific (targeted, endogenous), 5'-GAGGTAGCGTCCTAGAGCAAT-3'; and Neo (targeted), 5'-GCCTCTGTTCACATACA-3'.

Mice forming the initial breeding pairs were supplied by GlaxoSmithKline, which consisted of heterozygous (HET) F1 offspring from WT and KO breeding. HET pairs were bred in-house from 8 weeks old to produce litters of mixed genotypes according to Mendelian genetics.

Animal maintenance. Both wild type C57BL/6 (Glasgow) and GPR84 knock out (London) mice were fed *ad libitum* with a standard mouse chow diet. Male and female animals at 8–15 weeks old were used. Animals were cared for in accordance with national guidelines on animal experimentation. All animal experiments were conducted under appropriate home office licences. Experiments were conducted under Establishment licence number (PEL) 70/2901 (Kings College) and 70/8473 (Glasgow).

Cloning of mouse GPR84. Mouse GPR84 was cloned from the mouse leukaemic macrophage cell line RAW 264.7. RNA was extracted from RAW 264.7 cells using RNeasy mini Kit (Qiagen) followed by cDNA synthesis using QuantiTect Reverse Transcription Kit (Qiagen) according to the manufacturer's instructions. Using this cDNA as template, the FLAG epitope tag (amino acid sequence DYKDDDDK) was incorporated at the N-terminus of mouse GPR84 by PCR reaction using the following primers:

Mouse GPR84 sense: 5' CAT GTT GGA TCC GCC ACC ATG GAC TAC AAG GAC GAC GAT GAT AAG TGG AAC AGC TCA GAT GCC AAC 3'.

Mouse GPR84 antisense: 5' CAT GTT GCG GCC GC G ATG GAA CCG GCG GAA ACT CTG 3'.

The sequences corresponding to BamHI and NotI sites required for cloning are underlined.

The resulting PCR amplified product, FLAG-mouse (m)GPR84 was then subcloned in-frame between the BamHI and NotI sites of an eYFP-pcDNA5/FRT/TO plasmid ultimately generating FLAG-mGPR84-eYFP-pcDNA5/FRT/TO construct. The identity of the construct was then confirmed by DNA sequencing. The FLAG-human (h)GPR84-G_{α12} fusion protein construct was cloned in pcDNA5/FRT/TO

expression vector as described previously¹¹. For generation of the FLAG-mGPR84-G α_{12} fusion construct, at first the internal BamHI site of G α_{12} of FLAG-hGPR84-G α_{12} was silently mutated by site directed mutagenesis using the QuikChange method (Stratagene, Cheshire, UK) using the following primers:

C636T G α_{12} Forward: 5' GAGCGAAGAAGTGGATTCACTGCTTTGAGGGTG 3'.

C636T G α_{12} Reverse: 5' CACCCTCAAAGCAGTGAATCCACTTCTTCCGCTC 3'.

The FLAG-mGPR84-G α_{12} fusion protein construct was then generated by replacing human GPR84 of FLAG-hGPR84-C636TG α_{12} pcDNA5/FRT/TO plasmid with the sequence corresponding to mouse GPR84 using BamHI and NotI restriction enzymes.

RNA extraction and gene expression analysis. RNA was extracted from THP-1 cells using an RNeasy kit (Qiagen). Between 1000–2000 ng of RNA was reverse-transcribed using the High Capacity cDNA Reverse Transcription kit (Applied Biosystems). qPCR was performed with an Applied Biosystems ABI-PRISM 7900HT Sequence Detection System. Gene expression was normalised to eukaryotic 18 S ribosomal RNA using qPCR master mix (Applied Biosystems) and the following TaqMan[®] Gene Expression Assays (Applied Biosystems): GPR84 (Hs00220561_m1) and eukaryotic 18 S rRNA (Hs99999901_s1). GPR84 expression in RAW 264.7 cells was confirmed by RT-PCR using the primers F-5'-AGGTGACCCGTATGTGCTTC-3' and R-5'-ACTCTGGTTCCGGATGTTT-3'. For GAPDH the primers used for RT PCR were: F-5'-TTGATGGCAACAATCTCCAC-3' and R-5'-CGTCCCGTAGACAAAATGGT-3'.

Anticipated cDNA amplicon size: 110 bp. Images shown in Fig. 7 were acquired using Gene Genius Bio Imaging System from Syngene and GeneSnap v7.12.

Expression of human and mouse GPR84-G α_{12} fusion proteins. Doxycycline inducible Flp-In T-REx-293 stable cell lines expressing FLAG-hGPR84-G α_{12} and FLAG-mGPR84-G α_{12} constructs were generated by co-transfection of the receptor construct of interest and integration plasmid pOG44(1:9) into Flp-In T-REx-293 cells using 1 mg/ml of cationic DNA complexing agent polyethyleneimine (PEI, MW-25000). Flp-In T-REx-293 cells were maintained in Dulbecco's modified Eagle's Medium (DMEM) without sodium pyruvate (Invitrogen) supplemented with 10% fetal bovine serum (FBS), 1% penicillin/streptomycin and 10 μ g/ml blasticidin at 37 °C in 5% CO₂ humidified atmosphere. The cells were transfected at 60 to 80% confluency with a total of 8 μ g DNA (0.8 μ g receptor of interest in pcDNA5/FRT/TO vector and 7.2 μ g of pOG44 plasmid vector) and PEI (ratio 1:6 DNA/PEI), each diluted in 150 mM sterile NaCl, pH 7.4. The mixture of DNA complexes and PEI were incubated at room temperature for 10 minutes and then added to the cells. Stably transfected cells were selected by changing medium to medium containing 200 μ g/ml hygromycin B 48 hours after transfection. After isolation of stable transfectants, expression of the receptor construct was induced on demand by treating the cells with 100 ng/ml of doxycycline for 24 hours.

Cell culture. THP-1 monocytes were maintained at a density of between 1×10^5 – 8×10^5 cells/ml in RPMI-1640 (Invitrogen) supplemented with 10% (v/v) heat inactivated FBS, 1% penicillin/streptomycin mixture and 2 mM L-glutamine at 37 °C in a 5% CO₂ humidified atmosphere. Cells seeded at a density of 4×10^5 cells/ml were exposed to lipopolysaccharide (LPS) (100 ng/ml) (Sigma, Dorset, UK) for 24 h prior to RNA extraction or membrane preparation. RAW 264.7 mouse macrophages were maintained in DMEM (with 4.5 g/L D-glucose, 0.11 g/L sodium pyruvate) supplemented with 10% heat inactivated FBS, 1% penicillin/streptomycin and 2 mM L-glutamine at 37 °C and 5% CO₂ humidified atmosphere. To upregulate GPR84 expression, RAW 264.7 cells were treated with 100 ng/ml of LPS for 5 h prior to membrane preparation. Flp-In[™] T-REx[™]-293 cells (Invitrogen) were maintained in Dulbecco's modified Eagle's medium without sodium pyruvate (Invitrogen), supplemented with 10% (v/v) heat inactivated FBS, 1% penicillin/streptomycin mixture, and 10 μ g/ml blasticidin at 37 °C in a 5% CO₂ humidified atmosphere. Expression of the appropriate construct from the Flp-In[™] T-REx[™] locus was induced by treatment with 100 ng/ml doxycycline for 24 h.

Membrane preparation. Membranes were generated from THP-1 or RAW 264.7 cells in the presence or absence of LPS stimulation or Flp-In[™] T-REx[™]-293 cells following doxycycline treatment to induce receptor expression. Cells were centrifuged at 3000 rpm for 5 min at 4 °C. Pellets were resuspended in TE buffer (10 mM Tris-HCl, 0.1 mM EDTA; pH 7.5) containing a protease inhibitor mixture (Roche, Applied Science, West Sussex, UK) and homogenised with a 5 ml hand-held homogeniser. This material was centrifuged at 1500 rpm for 5 min at 4 °C and the supernatant was further centrifuged at 50000 rpm for 45 min at 4 °C. The resulting pellet was resuspended in TE buffer and protein content assessed using a BCA protein assay kit (Pierce, Fisher Scientific, Loughborough, UK).

Isolation of neutrophils from mouse bone marrow. Tibiae and femurs of GPR84 knock-out and wild type mice were removed and freed of soft tissue. Both epiphyses were removed using sterile scissors and bones were flushed with a syringe filled with ice-cold RPMI 1640. Bone marrow suspension was passed through a 100 μ m cell strainer and collected in a sterile 15 mL polypropylene tube for centrifugation at 300 g for 5 min at 4 °C. The resulting pellet was resuspended in PBS containing 1% FBS and 2 mM EDTA. Neutrophils were isolated using the EasySep[™] Mouse Neutrophil Enrichment Kit according to manufacturer's instructions (STEMCELL Technologies UK Ltd, Cambridge, UK).

Isolation of neutrophils from human whole blood. Peripheral blood samples were obtained from normal healthy donors following protocols approved by the University of Glasgow, College of Medical, Veterinary and Life Sciences ethics committee. Donors provided written informed consent. Neutrophils were then isolated

from human whole blood using the MACSxpress[®] Neutrophil Isolation Kit according to the manufacturer's instructions (Miltenyi Biotec, Bergisch Gladbach, Germany).

Neutrophil migration assay. After isolation, neutrophils were immediately resuspended in RPMI 1640 containing 0.5% fatty acid-free bovine serum albumin. Test compounds were prepared at the indicated concentrations in the same buffer and added at the bottom of a 96-well plate (Sigma-Aldrich). Inserts were then mounted to the plate and neutrophils were added (3000 cells/ μ L). Cells were incubated at 37 °C for 1.5 h and migrated cells were then collected and ATP content was assessed using ATPlite Luminescence Assay System[®] according to manufacturer instructions (Perkin Elmer, Buckinghamshire, UK).

Preparation of neutrophil membranes. Neutrophils were resuspended in 50 mM Tris HCl, 10 mM MgCl₂, pH 7.4, and centrifuged at 11,000 g for 15 min at 4 °C. The supernatant was discarded and pellet was resuspended in 50 mM Tris HCl, pH 7.4 and centrifuged at 11,000 g for 15 min at 4 °C. The resulting pellet was resuspended in 50 mM Tris-HCl and the protein concentration was determined using a BCA protein assay kit (Expediton, Cambridge, UK).

Radioligand binding assay. [³H]G9543 is an analogue of compounds 104 and 107 as previously described¹¹. Because [³H]G9543 binds to human GPR84 with sub nM affinity¹¹ most assays were carried out using a close to saturating concentration (2 nM) of [³H]G9543, binding buffer (PBS with 0.5% fatty-acid free bovine serum albumin; pH 7.4) in a total assay volume of 500 μ L in glass tubes. Binding was initiated by the addition of THP-1 membranes (5 μ g of protein per tube). Assays were performed at 25 °C for 1 h before termination by the addition of ice-cold PBS and vacuum filtration through GF/C glass filters using a 24-well Brandel cell harvester (Alpha Biotec, Glasgow, UK). Each reaction tube was washed 3 times with ice-cold PBS. The filters were allowed to dry and then placed in 3 ml of Ultima Gold[™] XR (PerkinElmer Life Sciences, Beaconsfield, UK). Radioactivity was quantified by liquid scintillation spectroscopy. Specific binding was defined as the difference between binding detected in the presence and absence of 1 μ M compound 104¹¹. Correction for occupancy allowed calculation of B_{max}. In some studies a range of concentrations of [³H]G9543 was used to allow estimation of K_d of the ligand and direct measurement of B_{max}.

[³⁵S]GTP γ S incorporation assay. Prepared membrane protein (5 μ g THP-1, RAW-264.7, 3 μ g Flp-In T-REx 293 cells) was incubated in assay buffer (20 mM HEPES, 5 mM MgCl₂, 160 mM NaCl, 0.05% fatty-acid-free bovine serum albumin; pH 7.5) containing the indicated ligand concentrations. In experiments designed to assess inhibition of agonist stimulation, membrane preparations were pre-incubated with antagonist compound 107 for 15 min at room temperature prior to addition of 2-HTP or PSB-16671. In experiments designed to assess potential allosteric interactions between PSB-16671 and 2-HTP, both ligands were added at the same time to the membrane preparation. The reaction was initiated by addition of [³⁵S]GTP γ S (50 nCi per reaction) with 1 μ M GDP, and incubated at 30 °C for 60 min. The reaction was terminated by rapid vacuum filtration through GF/C glassfibre filter-bottom 96-well microplates (PerkinElmer Life Sciences, Beaconsfield, UK) using a UniFilter FilterMate Harvester (PerkinElmer Life Sciences, Beaconsfield, UK). Unbound radioligand was removed from filters by three washes with ice-cold PBS. MicroScint-20 (PerkinElmer Life Sciences, Beaconsfield, UK) was added to dried filters, and [³⁵S]GTP γ S binding was quantified by liquid scintillation spectroscopy.

β -arrestin-2 interaction assays. To assess potential agonist effects of GPR84 ligands at the phylogenetically related receptor GPR35, C-terminally enhanced yellow fluorescent protein (eYFP)-tagged forms of either human GPR35a or mouse GPR35 were co-transfected with a luciferase tagged form of β -arrestin-2 into HEK293 cells as described previously²¹. 24 hours later cells were treated with varying concentrations of the GPR35 agonist lodoxamine²¹ or with 2-HTP or PSB-16671. Bioluminescence resonance energy transfer was then measured 5 minutes after addition of the luciferase substrate coelenterazine-h as in²¹.

Analysis of ligand affinity/co-operativity. To calculate the allosteric parameters data obtained from allostereism experiments were analysed using an operational model of allosteric modulation described previously^{18,32}. The general version of this model is denoted by the following equation:

$$E = \frac{E_m(\tau_A[A](K_B + \alpha\beta[B] + \tau_B[B]K_A)^n}{([A]K_B + K_AK_B + [B]K_A + \alpha[A][B]^n + (\tau_A[A(K_B + \alpha\beta[B]) + \tau_B[B]K_A)^n}$$

where, E is the measured response, [A] and [B] are the orthosteric and allosteric ligand concentration at equilibrium, respectively; K_A and K_B represent the binding affinities of the two ligands to the receptor; α is the binding cooperativity factor reflecting the allosteric effect on binding affinity of the orthosteric agonist to the receptor, β is the activation cooperativity factor denoting the empirical measure of the allosteric effect on orthosteric efficacy. The values of τ_A and τ_B measure the ability of the orthosteric and allosteric ligand, respectively to directly activate the receptor. E_m is the maximum system response and n denotes the slope factor of the transducer function. To fit the allostereism data globally through this equation, E_m and n values were always constrained and other parameters (K_A, K_B, α , β , τ_A and τ_B) were estimated.

Data Availability

The datasets generated and analysed during the current study are available from the corresponding author on reasonable request.

References

1. Hauser, A. S., Attwood, M. M., Rask-Andersen, M., Schiöth, H. B. & Gloriam, D. E. Trends in GPCR drug discovery: new agents, targets and indications. *Nat Rev Drug Discov.* **16**, 829–842 (2017).
2. Davenport, A. P. *et al.* International Union of Basic and Clinical Pharmacology. LXXXVIII. G protein-coupled receptor list: recommendations for new pairings with cognate ligands. *Pharmacol Rev.* **65**, 967–986 (2013).
3. Hauser, A. S. *et al.* Pharmacogenomics of GPCR Drug Targets. *Cell.* **172**, 41–54 (2018).
4. Gagnon, L. *et al.* Newly discovered antifibrotic pathway regulated by two fatty acid receptors: GPR40 and GPR84. *Am J Pathol.* **188**, 1132–1148 (2018).
5. Vermeire, S. *et al.* Efficacy and safety of GLPG1205, a GPR84 antagonist, in ulcerative colitis: multi-centre proof-of-concept study. *J Crohn's Colit.* **11** Issue suppl_1, S390–S391 (2017).
6. Gaidarov, I. *et al.* Embelin and its derivatives unravel the signaling, proinflammatory and antiatherogenic properties of GPR84 receptor. *Pharmacol Res.* **131**, 185–198 (2018).
7. Wang, J., Wu, X., Simonavicius, N., Tian, H. & Ling, L. Medium-chain fatty acids as ligands for orphan G protein-coupled receptor GPR84. *J Biol Chem.* **281**, 34457–34464 (2006).
8. Suzuki, M. *et al.* Medium-chain fatty acid-sensing receptor, GPR84, is a proinflammatory receptor. *J Biol Chem.* **288**, 10684–10691 (2013).
9. Wei, L., Tokizane, K., Konishi, H., Yu, H. R. & Kiyama, H. Agonists for G-protein-coupled receptor 84 (GPR84) alter cellular morphology and motility but do not induce pro-inflammatory responses in microglia. *J Neuroinflammation.* **14**, 198 (2017).
10. Recio, C. *et al.* Activation of the immune-metabolic receptor GPR84 enhances inflammation and phagocytosis in macrophages. *Front Immunol.* **9**, 1419 (2018).
11. Mahmud, Z. A. *et al.* Three classes of ligands each bind to distinct sites on the orphan G protein-coupled receptor GPR84. *Sci Rep.* **7**, 17953 (2017).
12. Liu, Y. *et al.* Design and synthesis of 2-alkylpyrimidine-4,6-diol and 6-alkylpyridine-2,4-diol as potent GPR84 agonists. *ACS Med Chem Lett.* **7**, 579–583 (2016).
13. Zhang, Q., Yang, H., Li, J. & Xie, X. Discovery and characterization of a novel small-molecule agonist for medium-chain free fatty acid receptor G Protein-Coupled Receptor 84. *J Pharmacol Exp Ther.* **357**, 337–344 (2016).
14. Sundqvist, M. *et al.* Similarities and differences between the responses induced in human phagocytes through activation of the medium chain fatty acid receptor GPR84 and the short chain fatty acid receptor FFA2R. *Biochim Biophys Acta.* **1865**, 695–708 (2018).
15. Nikaïdo, Y., Koyama, Y., Yoshikawa, Y., Furuya, T. & Takeda, S. Mutation analysis and molecular modeling for the investigation of ligand-binding modes of GPR84. *J Biochem.* **157**, 311–320 (2015).
16. Pillaiyar, T. *et al.* Diindolylmethane derivatives: potent agonists of the immunostimulatory orphan G Protein-Coupled Receptor GPR84. *J Med Chem.* **60**, 3636–3655 (2017).
17. Milligan, G. Principles: extending the utility of [35S]GTP gamma S binding assays. *Trends Pharmacol Sci.* **24**, 87–90 (2003).
18. Ehlert, F. J. Analysis of allosterism in functional assays. *J Pharmacol Exp Ther.* **315**, 740–754 (2005).
19. Müller, M. M. *et al.* Global analysis of glycoproteins identifies markers of endotoxin tolerant monocytes and GPR84 as a modulator of TNF α expression. *Sci Rep.* **7**, 838 (2017).
20. Merly, L. & Smith, S. L. Murine RAW 264.7 cell line as an immune target: are we missing something? *Immunopharmacol Immunotoxicol.* **39**, 55–58 (2017).
21. Mackenzie, A. E. *et al.* The antiallergic mast cell stabilizers lodoxamide and bufrolin as the first high and equipotent agonists of human and rat GPR35. *Mol Pharmacol.* **85**, 91–104 (2014).
22. Zhao, P. *et al.* Targeting of the orphan receptor GPR35 by pamoic acid: a potent activator of extracellular signal-regulated kinase and β -arrestin2 with antinociceptive activity. *Mol Pharmacol.* **78**, 560–568 (2010).
23. Jenkins, L. *et al.* Antagonists of GPR35 display high species ortholog selectivity and varying modes of action. *J Pharmacol Exp Ther.* **343**, 683–695 (2012).
24. Milligan, G., Shimpukade, B., Ulven, T. & Hudson, B. D. Complex pharmacology of free fatty acid receptors. *Chem Rev.* **117**, 67–110 (2017).
25. Aust, G., Zhu, D., Van Meir, E. G. & Xu, L. Adhesion GPCRs in tumorigenesis. *Handb Exp Pharmacol.* **234**, 369–396 (2016).
26. Sergeev, E. *et al.* Non-equivalence of key positively charged residues of the free fatty acid 2 receptor in the recognition and function of agonist versus antagonist ligands. *J Biol Chem.* **291**, 303–317 (2016).
27. Nicol, L. S. *et al.* The role of G-protein receptor 84 in experimental neuropathic pain. *J Neurosci.* **35**, 8959–8969 (2015).
28. Lattin, J. E. *et al.* Expression analysis of G Protein-Coupled Receptors in mouse macrophages. *Immunome Res.* **4**, 5 (2008).
29. Groot-Kormelink, P. J., Fawcett, L., Wright, P. D., Gosling, M. & Kent, T. C. Quantitative GPCR and ion channel transcriptomics in primary alveolar macrophages and macrophage surrogates. *BMC Immunol.* **13**, 57 (2012).
30. Parker, J. *et al.* PBI-4050 is safe and well tolerated and shows evidence of benefit in Idiopathic Pulmonary Fibrosis. *AJRCCM* **195**, A7606 (2017).
31. Pillaiyar, T. *et al.* 6-(Ar)Alkylamino-substituted uracil derivatives: lipid mimetics with potent activity at the orphan G Protein-Coupled Receptor 84 (GPR84). *ACS Omega.* **3**, 3365–3383 (2018).
32. Keov, P., Sexton, P. M. & Christopoulos, A. Allosteric modulation of G protein-coupled receptors: a pharmacological perspective. *Neuropharmacol.* **60**, 24–35 (2011).

Acknowledgements

SM is funded by the Heptares Therapeutics sponsored Opportunities in Receptor Biology for Industrial Translation (ORBIT) scheme. We thank ZAM thanks the Commonwealth Scholarship Commission for financial support. We thank Dr Laurent Sanier (Galapagos NV) for provision of PBS-16671, compounds 104, 107 and [3H]9543 and Dr Trond Ulven for provision of 2-HTP.

Author Contributions

G.M., A.B.T., S.B.M., R.N. and M.B. developed and co-ordinated the project, S.J.M., Z.A.M., L.J., D.B. and M.E. performed the experiments and analysed data. G.M. and S.J.M. wrote the manuscript with assistance and input from all other authors.

Additional Information

Supplementary information accompanies this paper at <https://doi.org/10.1038/s41598-019-38539-1>.

Competing Interests: RN and MB are employed by Sosei Heptares. The other authors declare no competing interests.

Publisher's note: Springer Nature remains neutral with regard to jurisdictional claims in published maps and institutional affiliations.



Open Access This article is licensed under a Creative Commons Attribution 4.0 International License, which permits use, sharing, adaptation, distribution and reproduction in any medium or format, as long as you give appropriate credit to the original author(s) and the source, provide a link to the Creative Commons license, and indicate if changes were made. The images or other third party material in this article are included in the article's Creative Commons license, unless indicated otherwise in a credit line to the material. If material is not included in the article's Creative Commons license and your intended use is not permitted by statutory regulation or exceeds the permitted use, you will need to obtain permission directly from the copyright holder. To view a copy of this license, visit <http://creativecommons.org/licenses/by/4.0/>.

© The Author(s) 2019